Deciphering Structure-Functional Relationship of Heparan Sulfate using Iduronic Acid Glycans

A Thesis

Submitted in partial fulfilment of the requirements

for the degree of

Doctor of Philosophy

By

Chethan D. Shanthamurthy

ID: 20143293

Under the Guidance of

Dr. Raghavendra Kikkeri

Indian Institute of Science Education and Research, Pune

Dedicated to

My Family and Teachers

CERTIFICATE

This is to certify that the work incorporated in this thesis entitled **"Deciphering Structure-Functional Relationship of Heparan Sulfate using Iduronic Acid Glycans"** submitted by Chethan D. Shanthamurthy carried out at Indian Institute of Science Education and Research (IISER), Pune, under my supervision. The work presented here or any part of it has not been included in any other thesis submitted previously for the award of any degree or diploma from any other University or institution.

Jan 11th, 2021

Dr. Raghavendra Kikkeri
(Research Supervisor)
Associate Professor
IISER Pune

DECLARATION

I hereby declare that the thesis entitled **"Deciphering Structure-Functional Relationship of Heparan Sulfate using Iduronic Acid Glycans"** submitted for Doctor of Philosophy in Chemistry at Indian Institute of Science Education and Research (IISER), Pune, has not been submitted by me to any other University or Institution. This work presented here was carried out at the, Indian Institute of Science Education and Research, Pune, India under the supervision of Dr. Raghavendra Kikkeri.

Chethan .D.S

Jan 11th, 2021

Chethan D. Shanthamurthy
ID- 20143293

Acknowledgments

The journey of my Ph.D has been a wonderful rollercoaster ride with many highs and lows. Throughout this journey there are many people who stood by me so that I could complete this colossal task.

First and foremost, I would like to express my sincere gratitude to my supervisor Dr. Raghavendra Kikkeri. Without him the journey would be unimaginable. Throughout the research career I have received relentless advice, support, guidance, encouragement and moral support. It is his belief in me during all those arduous moments that helped me to move forward and achieve my goal. His energy and enthusiasm for research made me to focus more. His passion towards research is at pinnacle which motivated me each and every day of my past 7 years to become a good research fellow. His interaction with me is more than that of student and supervisor relation. Apart from research he has provided guidance even in my personal life which became a constant support till today. I could have not asked for better supervisor than him. It's my privilege to have been worked under him which made my journey gratifying.

I would like to thank all my collaborators, Dr. Vered Padler-Karavani and Shani (Tel-Aviv University, Israel), Prof. Jesús Jiménez-Barbero (CIC bioGUNE), Prof. Israel Vlodavsky (Haifa, Israel), Dr. Vito Ferro (University of Queensland, Australia) for their time and efforts. Collaborating with them has immensely enriched my research work. I would also like to thank my RAC members, Prof. Ramkrishna. G. Bhat (IISER, Pune), Dr. H. V. Thulasiram (NCL, Pune) for their valuable suggestions during my course of research.

I would like to thank IISER, Pune for providing financial support. My heartfelt thanks to Prof. K. N. Ganesh and Prof. Jayant Udgaonkar (Director IISER Pune) for enabling research friendly environment. Special thanks to Prof. V. G. Anand, Prof. H. N. Gopi, Dr. T. S. Mahesh and all faculty and Technical teams of IISER, Pune for their moral support.

I would like to thank Prof. Kendagannaswamy and Basappa Sir (JSS College, Mysusu) who inculcated in me the interest towards chemistry in the initial days. I would express

my gratitude to Dr. B.K. Bettadaiah (Senior Scientist, CFTRI, Mysuru) and Dr. Manjunath (CFTRI, Mysuru) without whom I would have not be in IISER, Pune.

My friends from college handheld me throughout my journey right from clearing the CSIR exam to making up my mind to join Ph.D in IISER, Pune. I am indebted to Guru, Santhosh, Rajendra, Vijendra, Vishwa, Chandru and Pradeep. They all stood by me and believed in me which gave confidence to move towards goal. Without their selfless support this would have not been possible. Words are falling short to express my gratitude for them.

To achieve this colossal task, support from lab mates play a very important role. I am grateful to have wonderful lab mates. Special thanks to Sivakoti for making the research life and personal life easy. I would like to thank Rohan, Madhuri, Harikrishna, Preeti ma'am for guiding me during my initial stages and helping me to take baby steps in my research. I would like to specially thank Bala and Prashant for their constant support which helped me sail through the difficult times. Their knowledge and passion towards work encouraged me to keep going. A big thanks to Suraj, Sandya, Rakesh, Trimbak, Saurabh, Amol, Sharath and Deepak for their generous support. Special thanks to Phani, Catherine, Keerthana, Chinmay, Haritha, Teja, Saurav, Reshma, Ramya and Liya for their fun filled energy.

Friends in IISER played a great role in this journey. My heartfelt thanks to Neelesh, Dinesh, Yatish, Udaya, Madhu, Ashok, Punith, Vinayak, Sharvani, Konaya Shiva and Radical cricket team for making the IISER moments memorable.

Having moral support played a pivotal role during past years. I would like to take this opportunity to thank my dear friends Chetan Kumar, Vinay, Dinesh, Rashmi, Bindu and al my M.Sc friends. I would also like to thank Vinod, Prakash, Nagbhushan, Mahendra, Guruji, Hemaraj, Loki, Nagesh and all my friends for their constant support.

This thesis remains incomplete without mentioning the blessings and love of my family. My heartfelt gratitude to my father Shanthamurthy, mother Gowramma and siblings Lavanya, Praveen and Sushma. There are no better words to express my gratitude for their unconditional love, gracious understanding and life time support.

Last but not the least I express my appreciation to my wife Shilpa for her persistent support for being with me right from the initial days. Being my better half, she has stood by me throughout all the ups and downs. It is because of her motivation which made me to pursue Ph.D work.

Finally, I pray to almighty Lord 'Shree Devanur Gurumalleshwara' whose blessings made me able to complete the research work and submit this thesis for Ph. D degree.

Chethan D. Shanthamurthy

Contents

Chapter 2: Linear Synthesis of De novo Oligo-Iduronic Acid

Chapter 3: Sulfation Patterns of the L-iduronic acid Homo-oligosaccharides Encode Conformation Plasticity and Molecular Recognition

Chapter 4: Heparan Sulfate Mimics Unravel Structure-Activity Relationship of Homologus Chemokines and thereby Attenuate Cancer Development

Chapter 5: Discovery of Antiviral Heparan Sulfate Mimics

Abbreviations

Ac = acetyl

AcOH = Acetic acid

Ac_2O = Aceticanhydride

AgOTf = Silver trifluoromethanesulfonate

AM = Aectoxymethyl

AT = Antithrombin

BAIB = Bis(acetoxy)iodobenzene

BMP-2 = Bone Morphogenetic Protein-2

$BF_3.Et_2O$ = Boron trifluoride diethyl etherate

BnBr = Benzylbromide

CD_3OD = Deuterated methanol

$CDCl_3$ = Deuterated chloroform

CH_3 = methyl

CH_3CN = Acetonitrile

$CHCl_3$ = Chloroform

CLR= C-type lectin receptor

CS = Chondroitin Sulfate

D_2O = Deuterium oxide

DCM = Dichloromethane

DCC = *N*,*N*-Dicyclohexylcarbodiimide

DDR = Discoid in Domain Rectors

DMF = *N*,*N*-Dimethylformamide

DMAP = 4-Dimethylaminopyridine

ECM = Extracellular Matrix

EGF = Epidermal Growth Factor

Et_3N = Triethylamine

EtOAc = Ethylacetate

EtOH = Ethanol

FGF = Fibroblast Growth Factor

FGFR = Fibroblast Growth Factor Recepor

GAGs =Glycosaminoglycans

GDF = Growth Differentiation Factor

GlcA = Glucuronic Acid

GlcNAc = *N*-acetylglucosamine

GPC = Glypican

GPI = Glycosylphosphatidylinositol

H = Hydrogen

HB-EGF = Heparin Binding EGF like Growth Factor

HCC = Heptocellular Carcinomas

HCl = Hydrochloric Acid

HRP = Horseradish Peroxidase

H_2SO_4 = Sulfuric Acid

HPLC = High-Performance Liquid Chromatography

HP = Heparin

HRMS = High resolution mass spectroscopy

HS = Heparan Sulfate

HMBC = Heteronuclear Multiple Quantum Coherence

HRMS = High Resolution Mass Spectroscopy

HSPG = Heparan Sulfate Proteoglycan

HSQC = Heteronuclear Single Quantum Coherence

HUVECs = Human Umbilical Vein Endothelial Cells

IC_{50} = Inhibitory concentration

J = Coupling constan

IdoA = Iduronic Acid

LevOH = Levulinic Acid

LMWH = Low Molecular Weight Heparin

m/z = Mass to charge ratio

MALDI = Matrix-Assisted Laser Desorption Ionization

MeOH = Methanol

MHz = Mega Hertz

mL = Mille Liter

mM = Millimolar

MAPK = Mitogen Activated Protein Kinase

M.S = Molecular Sives

Mw = Molecular weight

NaCl = Sodium chloride

NIS = *N*-Iodosuccinimide

NaOH = Sodium hydroxide

NaOMe = Sodium methoxide

NDST = *N*-deacetylase/*N*-sulfotrasnferase

NRP-1 = Neuropilin-1

ng = Nano gram

NIS = *N*-Iodosuccinimide

nm = Nano meter

NMR = Nuclear magnetic resonance

NOESY = Nuclear Overhauser Effect spectroscopy

ppm = parts per million

PVDF =Polyvinylidene Fluoride

Py = Pyridine

P-TsOH = *Para*-tolunesulfonic acid

RFU = Relative Florescence Unit

RMS = Rhabdomyosarcoma

ROSEY = Rotating frame Overhause Effect Spectroscop

R.T = room temperature

SEM = Scanning electron microscope

$SO_3.Et_3N$ = Sulfertrioxide triethylamine

SPR = Surface Plasmon resonance

TBAI = Tetrabutylammonium iodide

TEMPO = (2,2,6,6-Tetramethylpiperidin-1-yl)oxyl

TGF = Transforming Growth Factor

THF = Tetrahydrofuran

TLC = Thin Layer Chromatography

TfOH = Trifluoromethanesulfonic Acid

TMSOTf = Trimethylsilyltrifluoromethanesulfonate

TMSSPh = Trimethyl(thiophenol)silane

UFH = Unfractionated Heparin

VEGF = Vascular Endothelial Growth Factor

ZnI_2 = Zinc Iodide

δ = chemical shift

μM = Micromolar

TMSSPh = Trimethyl(thiophenol)silane

UFH = Unfractionated Heparin

VEGF = Vascular Endothelial Growth Factor

ZnI_2 = Zinc Iodide

δ = chemical shif

μM = Micromolar

Synopsis

Heparan Sulfate (HS), a member of the glycosaminoglycan family, is composed of repeating units of α(1-4) linked D-glucosamine and uronic acid residues (L-iduronic acid and D-glucuronic acid) having diverse *N*-sulfation and *O*-sulfation patterns. Their complex structure enables binding to a great number of proteins and facilitates the modulation of numerous biological processes. Despite rapid progress in the synthesis of structurally defined HS oligosaccharides, how conformation plasticity of L-IdoA directly contributes HS biological functions remains largely obscure. In my thesis, I have explored the role of L-Iduronic acid in conformation plasticity, molecular recognition and its biological activity.

Chapter 1 highlights the structure-functional relationship of heparan sulfate in physiological and pathological conditions. More specifically, we discuss HS's structural diversity and emphasize their binding affinity to various proteins, including growth factors, chemokines, anticoagulants, and viral proteins. Finally, we also discuss modern techniques like HS microarray to profile HS-protein interactions.

Chapter 2 deals with linear approach for the synthesis of oligo-iduronic acid (oligo-IdoA) derivative using IdoA-thiophenol as the donor and a *β*-L-idopyranosyl derivative as the acceptor. Sequential modifications of the L-Idose residue yielded oligo-IdoA derivatives in moderate overall yields. We have also discussed different strategy to synthesize the oligo-IdoA and its drawback in more details. We anticipate that the new set of HS mimics will enable systematic study of the role of IdoA conformation plasticity and, oligosaccharide secondary structures, thereby developing the ability to modulate their biological functions.

Chapter 3 demonstrate tailor-made HS mimics to probe conformation plasticity of IdoA and to unravel regulatory sites of growth factors. NOE and vicinal ^{3}JH-H coupling constants analysis of HS mimics, confirmed that 4-*O*-sulfation enhances the population of the $^{1}C_{4}$ geometry at the corresponding ring. Interestingly, the $^{1}C_{4}$ conformer becomes almost exclusive upon additional 2-*O*-sulfation, whereas the non-sulfated IdoA rings display the conformation equilibrium between the $^{1}C_{4}$-, $^{4}C_{1}$- and $^{2}S_{0}$-forms. The HS mimics microarray data with various growth factors revealed key sulfation code, oligosaccharide chain length and conformation plasticity important to modulate the

binding affinity. Notably, HB-EGF displayed strong binding affinity to highly sulfated Iduronic acid trisaccharides (**I-34**), whereas 4-*O*-sulfated mono and di-iduronic acid (**I-11** and **I-21**) showed clear difference in binding affinity with $VEGF_{165}$.Furthermore, *invitro* assay showed marked difference in the blockage of endothelial cell proliferation. Taken together, sulfated oligo-Iduronic acids present encouraging consideration for therapeutic applications.

Chapter 4 reports exhaustive microarray and SPR analysis of HS mimics with chemokines. Our data revealed that homeostatic and inflammatory chemokines displayed several cryptic binding pockets for HS mimics, which is significantly differ from one other and could be potential selective inhibitors for chemokines. Notably, **I-45** turned out to be a potential small molecule inhibitor for CCR2/CCL2 mediated cancer cell invasion and metastasis. Taken together, HS mimics offer new therapeutic molecule for cancer and immuno-therapy.

Chapter 5 reports the synthesis of novel amphiphilic heparan sulfate mimics in which highly sulfated L-Idose and L-Iduronic acid units are connected to cholestanol moiety with different oligosaccharide chain length. These molecules displayed strong binding to spike protein of SARS-CoV-2 and inhibited SARS-CoV-2 infection, making it possible to acts as a potential antiviral drug.

Publications and Patent

1. **Chethan D. Shanthamurthy,** Shani Leviatan Ben-Arye, N. Vijendra Kumar, Vered Padler-Karavani, Raghavendra Kikkeri. - "Heparan sulfate mimetics Differentially Affect Homologous Chemokines and Attenuate Cancer Development". *J Med. Chem*., **2021**, *(In press*).
2. Prashant Jain**, Chethan D. Shanthamurthy*,** Shani Leviatan Ben-Arye, N. Vijendra Kumar, Vered Padler-Karavani, Raghavendra Kikkeri. - "Discovery of Rare Sulfated *N*-unsubstituted Glucosamine Based Heparan Sulfate Analogues Selectively Activating Chemokines". *Chem. Sci.*, **2021**, Advance Article. ***(*Equal Contribution).***
3. Prashant Jain, **Chethan D. Shanthamurthy*,** Preeti Chaudhary, Raghavendra Kikkeri. - "Rational Designing of Glycol-nanovehicles to Target Cellular Heterogeneity". *Chem. Sci.,* **2021**, Advance Article. ***(*Equal Contribution).***
4. Saurabh Anand, Sandhya mardhekar, Rakesh Raigawali, Nirmala Mohanta, Prashanth Jain, **Chethan D. Shanthamurthy,** Boopathy Gnanaprakasam and Raghavendra Kikkeri. - "Continuous Flow Accelerated Sulfation of Heparan Sulfate Intermediates" *Org. Lett*. **2020**, 22, 3402-3406.
5. **Chethan D. Shanthamurthy,** Raghavendra Kikkeri. - "Linear synthesis of *de novo* Oligo-iduronic acid". *Eur. J. Org. Chem*. **2019**, 2950-2953.
6. Balamurgan Subramani, **Chethan D. Shanthamurthy*,** Parag Maru, Menakshi Belakar, Sandhya Mardekar, Dhanasekaran Shanmugam, Raghavendra Kikkeri. - "Demystifying a Hexuronic Acid Ligand that Recognizes Toxoplasma Gondii and Blocks its Invasion into Host Cells". *Org. Bio. Chem*. **2019**, 17, 4535-4542. ***(*Equal Contribution)***
7. **Chethan D. Shanthamurthy**, Prashant Jain, S. Yehuda, J. T. Monteiro, S. L. Ben-Arye, Vered Padler-karavani, Bernd Lepenies, Raghavendra Kikkeri. - "ABO Antigens Active Tri and Disaccharides Microarray to Evaluate C-type Lectin Receptor Binding Preference". *Scientific reports*. **2018**, 26, 6603.
8. **Chethan D. Shanthamurthy,** Ana Gimeno, Shani Leviatan Ben-Arye, N. Vijendra Kumar, Vered Padler-Karavani, Jesus Jimenez-Barbero, Raghavendra Kikkeri. - "The Next Generation Hepran Sulfate Mimics for Modulating Biological Activity". **2021**, Submitted.

9. Prashant Jain**, Chethan D. Shanthamurthy*,** Shani Leviatan Ben-Arye, N. Vijendra Kumar, Vered Padler-Karavani, Raghavendra Kikkeri. - "Synthetic Heparan Sulfate Ligands for Vascular Endothelial Growth Factor to Modulate Angiogenesis". **2021**, Submitted. ***(*Equal Contribution)*.**
10. R Kikkeri, **Chethan D. Shanthamurthy,** Prashant Jain**,** Well-defined Heparan sulfate and their Mimics Useful as Chemokine Inhibitors for Cancer Therapeutics. PCT patent submitted.

CHAPTER 1

Structural Micro-Heterogeneity of Heparan Sulfate

1.1 Introduction

Glycans are 'dark matters' of the biological system, for their structure and functions are highly challenging to elucidate.[1-4] Structural complexity of Glycans stems from the unique template-independent biosynthetic pathway resulting in highly heterogeneous and numerous modifications on core structures[5,6] (**Fig. 1**). Recent developments in chemical and enzymatic glycans synthesis have drawn increasing scientific interaction trying to evaluate the structure-functional relationship in glycans.[7-11] Among the many cell surface glycans, heparan sulfates (HS) have uncommon polysaccharide structure. They belong to the glycosaminoglycan (GAGs) family and are usually part of cell surfaces, and extracellular matrices. In contrast to other GAGs members, HS displays exceeding modifications than other polysaccharides and is evolutionally conserved.[12,13] The biosynthesis of HS starts with glycosylation of D-xylose residue to the prescribed serine residue of proteoglycans, followed by glycosylation of galactose and glucuronic acid residues, leads to the formation of the tetrasaccharide linkage region. In the Golgi complex region, the linkage regions undergo further sequential chain elongation by attaching N-acetyl-D-glucosamine (GlcNAc) and D-glucuronic acid (GlcA) and eventually produce polymers of 50 to 200 disaccharide repeating units. At the same time, HS undergoes structural modifications by *N*-deacetylase and *N*-sulfotransferase enzymes, resulting in deprotection of certain acetyl groups from GlcNAc cluster and attachment of sulfate residue. Furthermore, epimerase enzyme changes some of the D-glucuronic acid into the L-iduronic acid and O-sulfotransferase enzyme family by incorporating sulfate groups in C-2, C-6 or C-3 positions of glucosamine or C-2 of glucuronic/iduronic acid residues, respectively[14,15] (**Fig. 2**). Finally, HSPGs on cell surfaces undergo one additional modification by the enzymes endosulfatase and endogenous heparinase, which cleave some of the 6-*O*-sulfate groups and trim the HS polymeric length resulting in crispy HS structures that interact with multiple proteins and cell-signaling molecules and regulate biological processes.[16,17]

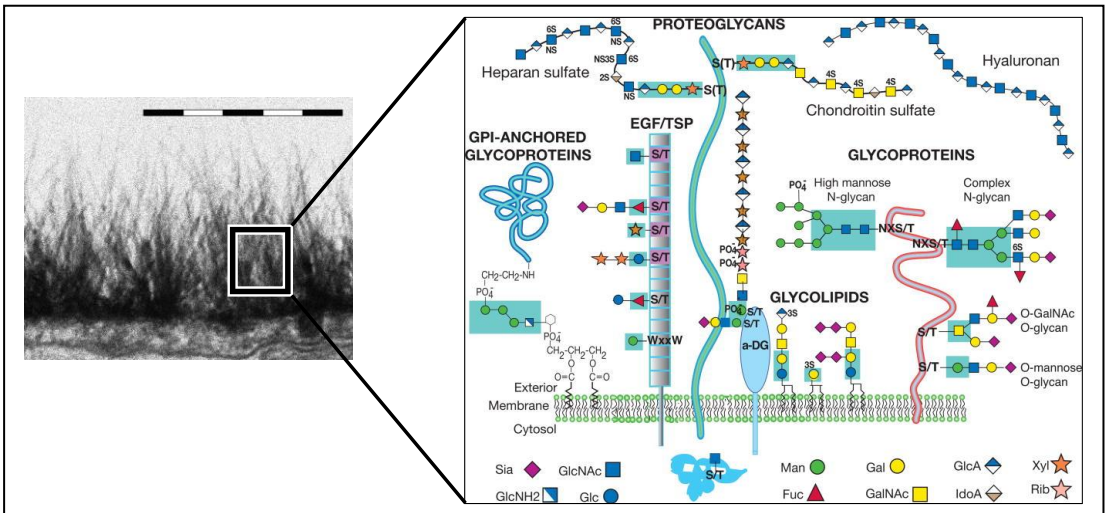

Figure 1: Cell surface representing different classes of mammalian glycans. (Adopted with permission from the ref. 5 and 6).

1.2 Heparan Sulfate Proteoglycans

Nearly 17 proteoglycans were identified to have one or more HS polysaccharide scaffolds. These HS proteoglycans (HSPGs) are ubiquitous in pericellular (basement membrane), cell surfaces and intracellular domains in tissues.[18-20] The basement membrane HSPGs contains Perlecan, Agrin and collagen XVIII proteoglycans **(Fig. 3).** These HSPGs are composed of 1-4 HS polysaccharide chains and they are typically found along with laminins and collagen type IV polymeric networks. The HSPGs in BM promote various cellular functions, such as cell-survival, cell division, migration and proliferation by binding to a wide range of growth factors, such as vascular endothelial growth factors (VEGF), transforming growth factor-β (TGF-β) and fibroblast growth factors (FGF).[21-23] Laminin and collagen IV networks regulate cell signaling by binding with integrin family receptors and discoid in domain rectors 1(DDR).[24-26] Perlecan is found in both, vascular and avascular tissues, interacts with various protein ligands. It is involved in regulating cell adhesion, thrombosis and cell death.[27,28] The HS on Perlecan regulates vascular biology and tumor angiogenesis by binding and presenting various growth factors to their cognate receptor.[29-33]

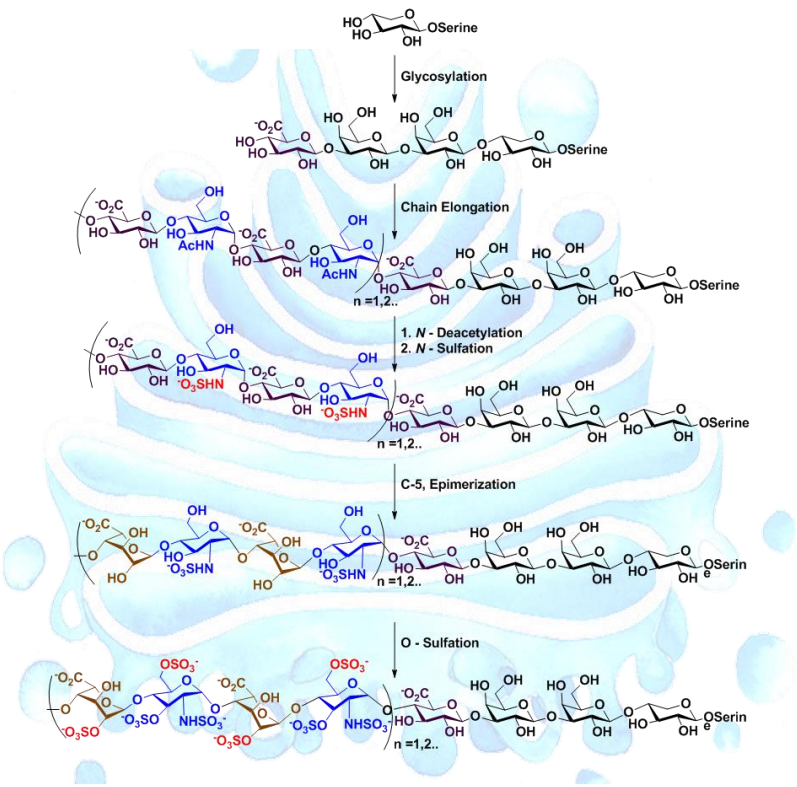

Figure 2: Biosynthesis of Heparan sulfate polysaccharide

Agrin, which has HS and CS-GAGs sequences, is an extracellular proteoglycan highly expressed in nervous tissues and functions as a co-receptor for neurite roles.[34,35] The HS in agrin binds to FGF2, thrombospondin, beta-amyloid peptide, N-CAM and protein tyrosine phosphatase.[36]

Collagen XVIII is another HSPG. It is a homo trimer, containing three identical α1 chains. The HS are attached to a serine-glycine chains, have a triple helix structure and are abundantly expressed in all vascular and epithelial basement membrane.[37-39] Collagen XVIII is a negative regulator of angiogenesis and directly implicate in the generation of adipose tissue and hyperlipidemia associated with visceral obesity and fatty liver.[40]

The transmembrane PGs are composed of five HSPGs units, namely, syndecan, glypican, betaglycan, neuropilin-1 and CD44 **(Fig. 4)**. Syndecan is one of the more abundant cell surface HSPGs and found in almost all cells and tissue types. In vertebrates, there are four types of syndecan isomers (syn-1 to4). Syndecans 1 to 3 are expressed in a tissue-specific manner, while syndecan-4 is widely distributed. Their structure consists of a variable ectodomain and a highly conserved cytoplasmic domain.

The structural and functional diversity of syndecans relies on GAG compositions and structures. The GAGs chains alter as per tissue and species of origin.[41,42]

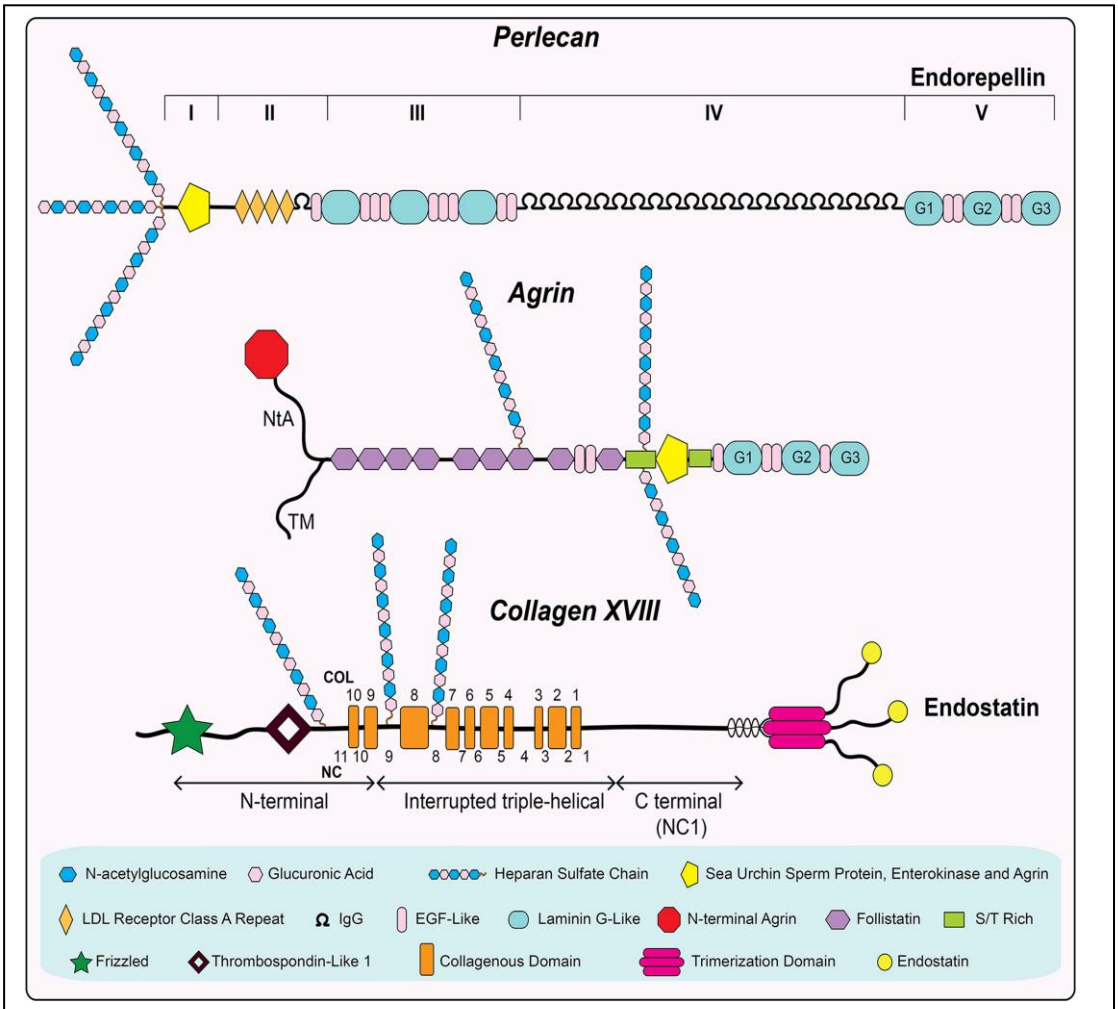

Figure 3: Pericellular proteoglycans, which comprise perlecan agrin, and collagens XVIIIand XV. (Adopted with permission from the ref. 18)

Syndecan-1 and syndecan-3 contain additional chondroitin sulfate (CS) chains to alter structural diversity.[43,44] Recent advances in structural and functional studies suggest that syndecans act as co-receptors for several cell signaling, i.e., HS chains of syn-4 recruit soluble FGF to the cell membrane and cluster with FGFR thus forming ternary structure to stimulate its activity. Syndecans participate in a variety of physiological and pathological processes. Syndecans bind to many ligands of diverse protein families including growth factors, cytokines, chemokines, fibrillin-1, fibronectin, collagen, tenascins, vitronectin etc. In addition, syndecans possess a unique binding affinity with pathogens including HIV-1, -2, herpes simplex virus, dengue virus, hepatitis C virus. Several bacterial pathogens, notably, staphylococcus aureus, Pseudomonas aeruginosa Neisseria gonorrhoeae binds to syndecans.[19,45-48]

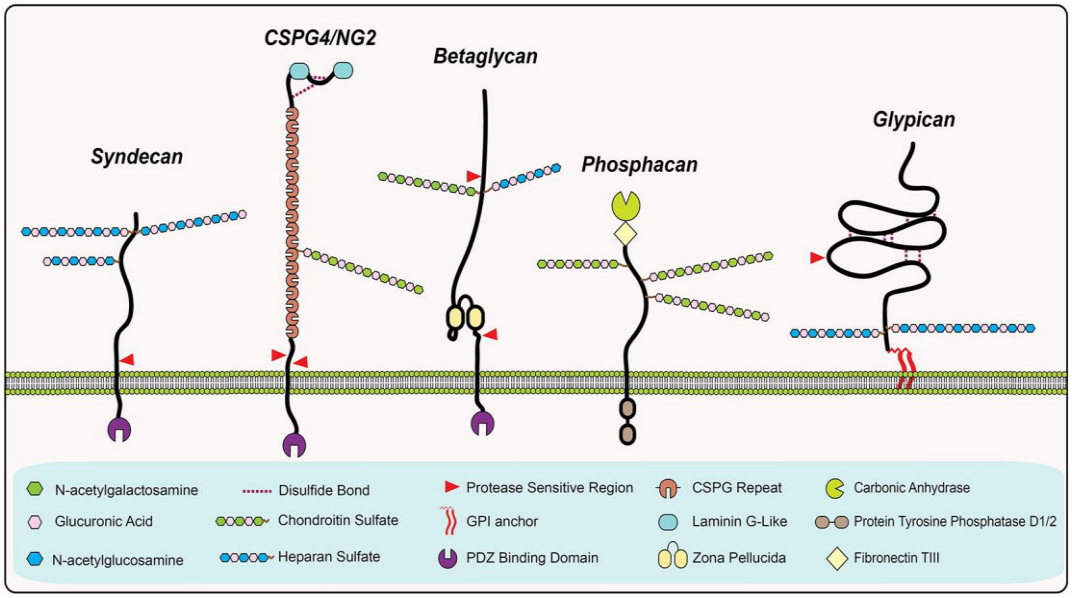

Figure 4: Cell surface proteoglycans, which comprise transmembrane type 1, Proteoglycans (four syndecans, CSPG4/NG2, betaglycan and phosphacan) and six GPI-anchored proteoglycans, glypicans 1–6.(Adopted with permission from the ref. 18).

Glypicans are another family of transmembrane proteoglycans, commonly expressed with glycosyl phosphatidylinositol-linked (GPI-linked) in the proteoglycan chain. According to the literature, six glypicans (GPC1 to GPC6) are found in mammalian cell surface, and they are predominantly expressed during embryonic developments. Glypicans isoforms do not display homology domains, suggesting that these HSPGs have unique functions. They composed of 1 to 5 HS chains per proteoglycan, but GPC5 produced by rhabdomyosarcoma cells also exhibit chondroitin sulfate (CS) domain. Glypicans regulate a variety of growth and survival factors during cell differentiation and apoptosis.[49,50] The abnormal expression of glypicans modulatesseveral signaling pathways (Wnt and hedgehog) and propagates tumor progression.[51,52] Anti-glypicans are believed to be the next generation antibody for cancer treatment. GPC1 overexpressed in breast cancer and upregulate the heparin binding growth factors interactions, resulting in proliferation, angiogenesis and metastasis of cancer cells.[53] GPC2 is overexpressed in brain, heart, lung and kidney cancer tissues and undetectable in normal tissues, indicating that GPC2 is a tumor antigen for several cancer types. Since GPC3 is overexpressed in hepatocellular carcinomas (HCCs)[54,55] and was not detected in nonmalignant tissues, it is used as a tumor marker for HCC for therapy. GPC4 overexpresses in pancreatic cancer.[56] GPC5 expression was found in rhabdomyosarcoma (RMS)[57] cells. However, its level decreased in breast and prostate

cancer, indicating that GPC5 display distinct role in different cancer types. GPC6 overexpress in ovarian cancer and gastric cancer tissues. All these results suggest that glypicans are new group of therapeutic antigens for cancer therapy.[58]

Beta-glycan is a cell surface proteoglycan that functions as a co-receptor for TGFβ and is also named TGFb type III receptor.[59] It is mainly involved in modulating reproduction and fetal growth. The ectodomain of beta-glycans composed 1-2 HS GAGs sequences and binds to all isoform of TGFb proteins, which include activins, inhibin, GDFs and BMPs.[60]

Neuropilin-1 (NRP1), a transmembrane protein and coreceptor for various proteins, such as semaphorins and VEGFs, regulates endocytosis and transport to a number of cell surface receptors from cytoplasm to cell surface and vice versa.[61,62]

In summary, HSPGs are widely dispersed over cell surfaces and pericellular space. The HS structures on PGs are substrates and tissue specific and have a role in regulating biological activities. For example, beta-glycan, with its specific HS sequences, controls TGFb activities, that are missing in basement membrane HSPGs. Similarly, syndecans, glypicans, parlecan and agrin probably have common HS domains to bind various growth factors. Neuropilin-1 is having 3-*O*-sulfated HS essential for neurite growth factors binding. Hence, demystifying HS micro heterogeneity is critical to understand and regulate specific biological functions.

1.3 Structural Diversity of Heparan Sulfate

1.3.1 The Diversity of Uronic Acids Composition and Conformation

The two core uronic acidsin HS structures are D-glucuronic acid and L-Iduronic acid, wherein L-Iduronic acid is around 20-50% of the structure. In heparin's composition, iduronic acid exceeds 80%.[63] The epimerase enzyme generally activates right after the deacetylation and *N*-sulfation of GlcNAc. Hence, L-IdoA is more abundant at NS (N-sulfate) region than NAc (N-acetyl) and NH (amine) region of HS chain. In HS oligosaccharides, all possible sulfated IdoA-GlcNS disaccharide patterns are found, excluding IdoA-GlcNS3S/GlcNS3S6S disaccharides. In another example, GlcA is rich with uronic acid residues in NH/NAc regions, indicating that the biosynthetic pathway restricts the uronic acid composition next in NS/NH/NAc regions. Around four different sulfated GlcA-GlcNH/GlcNAc disaccharides are present in the HS chain.[64,65]

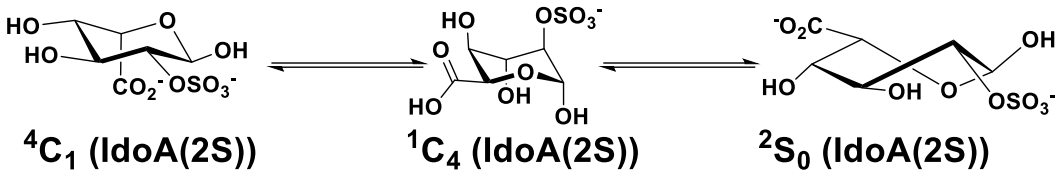

Figure 5: Different Conformation of Iduronic Acid

L-IdoA preferentially adopts $^{1}C_{4}$-boat and $^{2}S_{0}$-skew boat conformations and only rarely the $^{4}C_{1}$-boat conformation while D-GlcA normally adapts as $^{4}C_{1}$-chair conformation.[66,67](Fig. 5) The flexible conformation of L-IdoA allows repositioning of sulfate and carboxylic acid residues and plays a crucial role in some of the protein binding. The interaction between fondaparinux (a penta-saccharide heparin mimetic) and antithrombin is one of the best studied examples of conformation plasticity of L-IdoA and explains its critical role in inhibiting blood coagulation.[68,69] Moreover, the HP tri-saccharides and hexa-saccharide library reveals that 6-*O*-, 3-*O*-sulfated and *N*-sulfated GlcN significantly contribute to shift conformation equilibrium of IdoA from $^{1}C_{4}$ to $^{2}S_{0}$ geometry.[70,71]

1.3.2 Diversity of 2-*O*-Sulfation of L-IdoA and D-GlcA

D-IdoA and D-GlcA undergo sulfation at C-2 position and nearly 50-90 % of L-IdoA in HS chain is sulfated. The 2-*O*-sulfation of L-IdoA at NA/NS domain can be compared to the NAc domain while, in contrast, 2-*O*-sulfation of D-GlcA is widely distributed.[63]

1.3.3 Diversity of 6-O-Sulfated and 3-O-Sulfated GlcN

At least three 6-*O*-[72] and five 3-*O*-[73]sulfotransferases have been identified, but little is known about their preferential substrates. 6-*O*-GlcN is widely distributed in NH/NS/NAc domain, whereas, 3-*O*-sulfate GlcN is rarely found in HS chain. They are mainly present in NS domain next to IdoA2S and GlcA residue (Fig. 6). The biodistribution of 3OST and 6OST isoform enzymes are highly irregular throughout body, indicating that the HS structures of same proteoglycans might be different at tissue levels.[74,75]

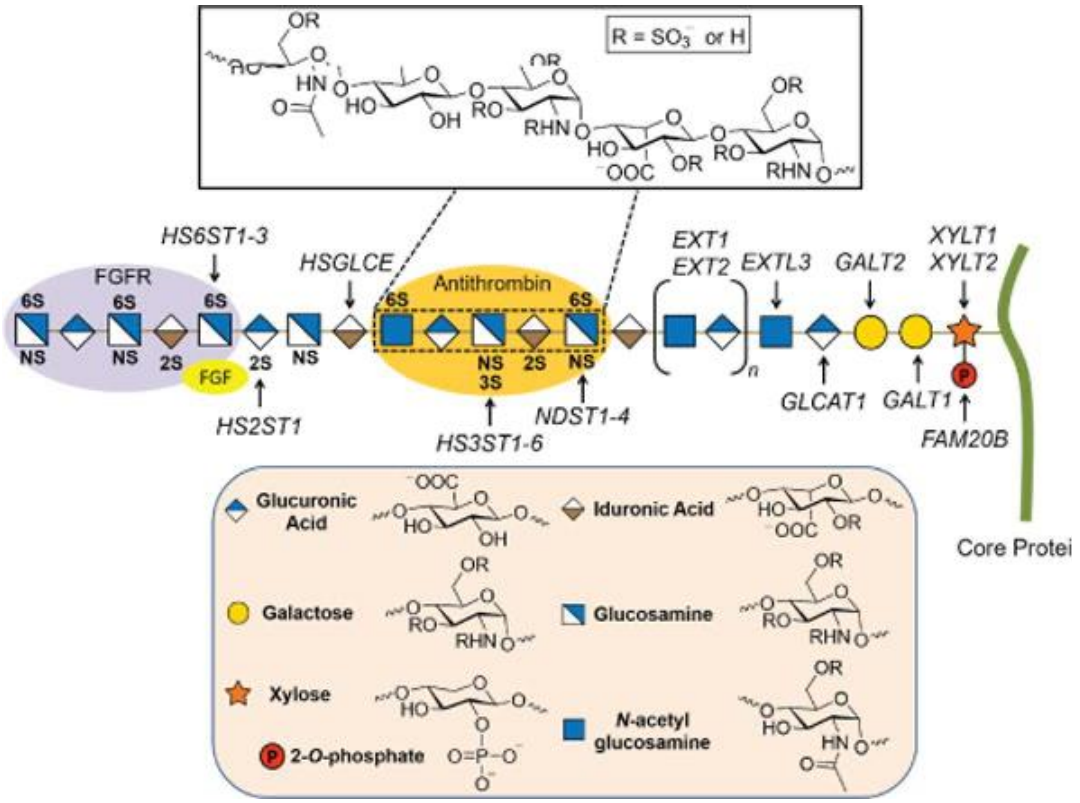

Figure 6: Molecular diversity of Heparan Sulfate. (Adopted with permission from the ref. 74)

1.3.4 Diversity of N-Deacetylated/N-Sulfated GlcN

Four isoforms of GlcNAc *N*-deacetylase/*N*-sulfotrasnferase (NDST) enzymes with different activities are known.[76] The active site of these enzymes contains *N*-sulfation and *N*-deacetylation sites which are tightly coupled for activating the two reactions simultaneously, i.e., NDST2 is highly active in *N*-deacetylation and *N*-sulfation as compared to NDST1.[77] Whereas, NDST3 has high activity of *N*-deacetylation compared to *N*-sulfation and *vice versa* for NDST4. The biodistribution of NDST and the difference in NDST isoforms activities alter the expression level of NS/NH region in the HS chain at diverse organs.[75,76]

1.4 Heparan Sulfate Binding Proteins

The inherent negative charges on HS bind to the plethora of proteins via ionic and hydrogen bond network. The negatively charged species, such as sulfate and carboxyl group on HS mediate ionic bonding with lysine and arginine residues in the proteins. Polar residues, such as asparagine, glutamine, and histidine of proteins bind to HS by hydrogen binding. The HSBPs are mainly classified based on their functions, which

include blood coagulation factors; growth factors, chemokines and cytokines; extracellular proteins; transmembrane signaling receptors and cell adhesion proteins (Fig. 7). Given the structural similarities between HS and other GAGs family members, such as chondroitin sulfate and dermatan sulfate, HSBPs can also bind to CS and DS, with a binding affinity that is lower than that of HS. Typically, the binding affinity of HS with proteins is in the range of μM to nM concentration.[15,21,47,78-80]

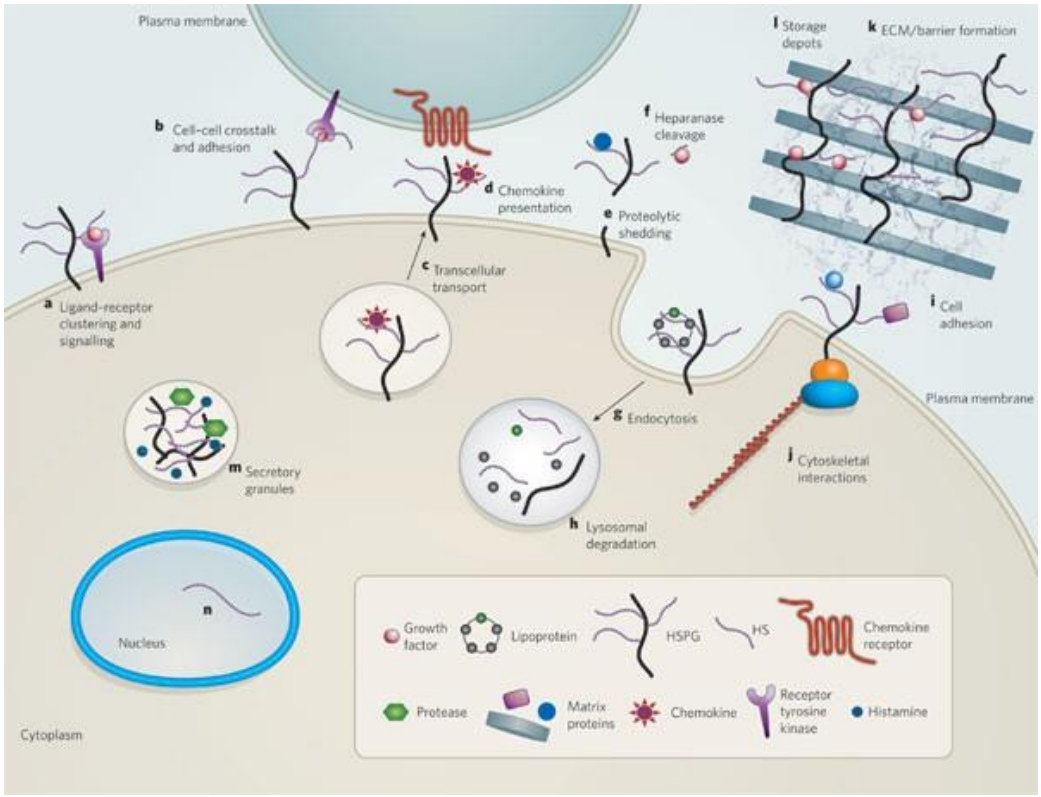

Figure 7. Hepran Sulfate or Heparin interact with plethora of protein present on cell surface and in Extracellularmatrix (ECM). (Adopted with permission from the ref. 78).

1.4.1 Blood Coagulation Factors

The role of heparin as an anticoagulant is known for a long time. Heparin binds to antithrombin III and regulates serine protease inhibitors, commonly named as serpins, modulating the enzymatic activities of thrombin.[68,69,81] The 18-mer HS was found to have the optimum scaffold length that maximize the rate of thrombin activity.[82,83] Later it has been found the pentasaccharide HS is sufficient for AT binding and regulates factor Xa and IIa protease activation.[84] Co-crystallization of HS with AT revealed that *N*-sulfation and 6-*O*-sulfation of GlcN in pentasaccharide sequence is essential for AT binding.[85-87] Moreover, the $^{2}S_{0}$-conformation of IdoA was also found to be essential for

modulating the activity of AT binding.[68,88] The interaction of ATIII and pentasaccharide resulted in a ternary complex formation between HS-ATIII-thrombin and accelerated factor Xa inhibition.[89] In addition to ATIII, blood coagulation also takes place via protein C inhibition and heparin cofactor II binding with HS.[90] Hence, deciphering the HS structure that selectively binding to these serpins is essential to study their activities. The structure of PCI is similar to AT, but the HS-binding domain of PCI is entirely different from that of AT. Recent studies showed that 14-mer HS of NS domain has PCI activity compared to 18-mer HS for AT activity.[91] However, the exact sequence has not fully explored yet.

Heparin cofactor II is another serine protease inhibitor and thrombin inactivator.[90] The rate of inhibition of thrombin by HCII is accelerated by dermatan sulfate and heparan sulfate, whereas, AT and HS chains normally activate PCI, demonstrating the unique pathway of activation.[92] HCII, which is synthesized by the liver, circulates in human plasma and was detected in the intima of human arteries. However, its tissue distribution is not clear. During pregnancy, DS in placenta activates HCII locally to inhibit coagulation in the placenta.[93] Though HCII is isostructural to AT. Their binding site of DS and HS ligands and their protease inhibition activity is not fully evaluated. Synthetic HS and DS libraries allow the study of structure-functional relation of blood coagulants and few drug molecules as an anticoagulant.

1.4.2 Growth factors

Growth factors are a large class of proteins that regulate cell-physiological properties, such as cell proliferation, migration, differentiation and survival/apoptosis. Most of the growth factors bind heparan sulfates on HSPGs and mediate cell signaling.[23,94-97] For instance, Fibroblast growth factor-2 binds to HS and activates its tyrosine kinase receptors by forming a ternary complex with FGF-HS-FGFR.[98] Similarly, HS binds to epidermal growth factors and vascular endothelial growth factors and modulates the cell signaling.[99,100] Among the various growth factors, the interaction between FGF-1 and FGF-2 was studied using NMR spectra and X-ray crystallography.[101,102] It was shown that HS-tetra and hexa-mers are optimum ligands for FGFs binding, but higher oligosaccharides are required for dimerization and activation of FGFs. IdoA2S and GlcNS are critical composition of HS for FGF-1 and FGF-2 binding. 6-*O*-sulfation has been shown to be essential for FGF-1 binding, but not for FGF-2. FGF-4 predominantly

requires both 2-*O*- and 6-*O*-sulfated HS for specific binding.[103-107] Though nearly 18 mammalian FGFs and five VEGF are reported in the literature, their HS binding patterns is not fully understood. Synthetic HS library with various sulfation code, uronic acid composition and oligosaccharide length could be ideal platform for deciphering the HS code of these growth factors.

1.4.3 Interaction with Chemokines and Cytokines

One of the most important biological functions of HS is to regulate cytokines and chemokines activity. HS functions as co-receptors between cytokines and cell surface receptors. HS oligosaccharides regulate around 50 different chemokines through specific active domains.[108-110] Among these BMP (bone morphogenic proteins), and TGF-β family of proteins, have important functions during animal development and tumorigenesis. BMPs stimulate osteogenesis and bone formation during development.[111,112] HS acts as a coreceptor for BMP dimerization and cell signaling. However, the structure-functions of BMP-HS is not fully explored. Previous studies have shown that lack of *N*-sulfation and IdoA residue in HS chain reduces BMP binding.[113] Synthesis of different sulfation pattern of NS domain containing L-IdoA may be used to reveal molecular level details of these interactions.

Chemokines are family of 40 isostructural glycoproteins that regulate leukocyte migration, angiogenesis, and breast cancer metastasis and leukocyte degranulation (Fig. 8). In response to external stimuli, such as bacterial or virus infection, chemokines that are released by a wide range of cells to recruit leukocytes to the damage site and induce immune responses, and thereby kill the parasite.[114-118] At normal conditions, chemokines are in monomeric form. HS binds to chemokines during inflammatory response, polymerizes and increases its activity. Understanding structure-function relationship between HS and chemokines allows the design of novel anti-inflammatory active scaffolds, which have the minimal side effects.

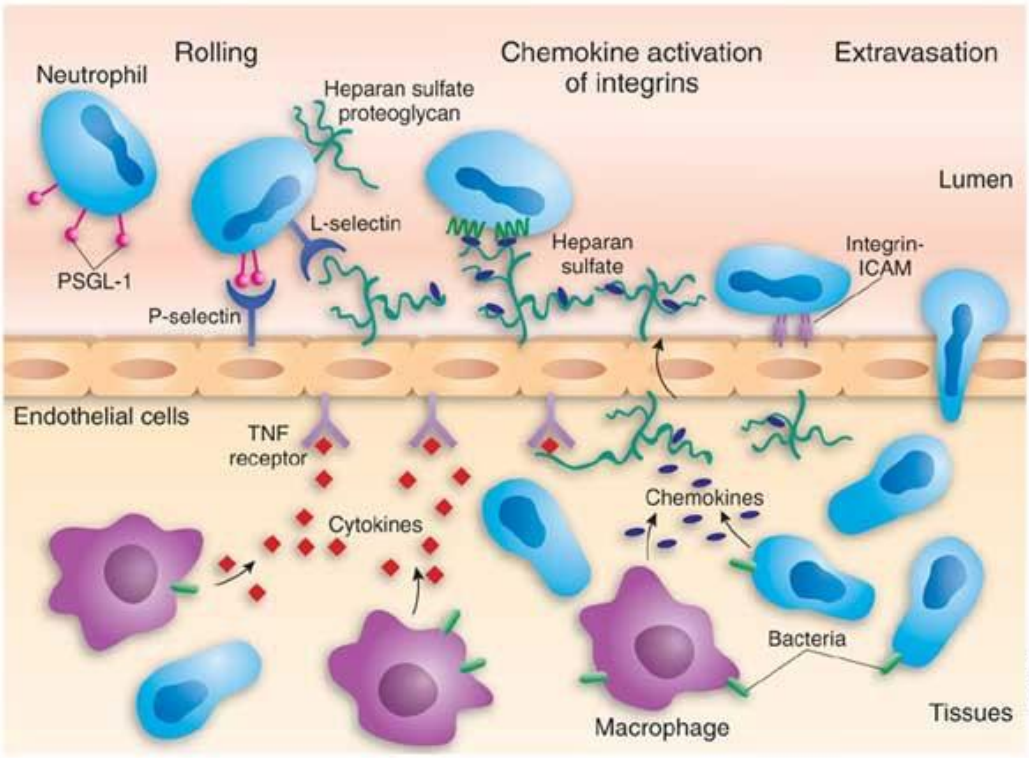

Figure 8: Role of the Heparan Sulfate during the Inflammation. (Adopted with permission from the ref. 115)

1.5 Chemical Synthesis of Heparan Sulfate

Synthesis of HS oligosaccharide is a highly challenging goal, because of the variability in sulfation and glycosylation patterns and of uronic acid compositions. Recent developments in one-pot syntheses protocols as well as in *de novo* syntheses of building blocks improve the prospect of synthesizing HS chains.[75,119-121] The preparation of IdoA building blocks starting from 1,2-*O*-isopropylidene-6,3-glycuronolactone, D-xylose and D-glucuronic acid resulted in bulk quantities of L-IdoA derivatives for HS oligosaccharide synthesis.[122-127] The efficient synthesis of the glucuronic acid donor with PivOAc esters at C-2 positions turned out to be an efficient donor for GlcA composed HS oligosaccharide synthesis.[128]

As HS exhibits diverse sulfation patterns, the synthesis of these molecules requires different protecting – deprotecting steps and different techniques, donor-acceptors strategies were employed and brought to success the α-glycosylation of GlcN and uronic acid.[129-131] Among the techniques, the nickel catalyzed *N*-benzylidene glucosamine tricholoroacetimidate yielded highly selective α-glycosylation of the

glucosamine donor with a wide number of acceptors.[132] The synthesis of 1,6-anhydroidopyranose derivative as acceptor, starting from 1,2:5,6-di-*O*-isopropylidene-α-D-glucofuranose, gave high yield and good α-selectivity. The synthesis of HS oligosaccharides was conducted successfully by convergent [2+2]n glycosylation approaches; by careful choice of donor and promoter, it was possible to overcome the inherent low reactivity of *N*-acetyl acceptors to yield only the desired α-linked oligosaccharide in good yield.[133-136] The *N*, *N*-diacetyl glucosamine proved to be the most effective one.[137] A fluorous supported modular synthesis of HS was recently reported in which the presence of perfluoro decyl group at the reducing end of HS protected chain resulted in fluorous solid-phase extraction.[138] HS oligosaccharide was also prepared using a linear glycosylation strategy. The successful application of 1-hydroxyl glucosamine donor and 1-thiophenyl acceptor resulted in excellent stereo selection and the formation of α(1-4) and β(1-4) linkage between the GlcN and GlcA residues. Fondaparinux, an anticoagulant drug was synthesized in 0.63% of the overall yield of 22 steps.[139-142]

1.6 Analysis of Heparan Sulfate-Protein Interactions using Microarray

Microarray is a sensitive, robust and reliable technique to detect biological binding events. It has advantages over other sensor techniques, such as the ability to measure binding interactions in real time, and the capacity for multiple binding events, examined simultaneously up to 1000 of parallel arrays. Display of carbohydrates on a microarray surface mimics the presentation of carbohydrates on cell surfaces and allows multivalent binding interactions that strengthen the often-weak individual carbohydrate binding events. In contrast to most comparable technologies, using this technology, only small amounts of receptor and analyte are needed for the binding studies.[143-147] Carbohydrate microarrays were used for studying binding affinities of proteins, antibodies, cytokines, bacteria and viruses. We used this technique to investigate the sulfation patterns and oligosaccharide lengths, crucial for protein binding. The high-throughput format enables to screen a large number of binding sites in parallel and decipher critical carbohydrate epitopes essential to fine-tune the protein binding.

1.7 References

1. Krasnova, L. & Wong, C. H. *Understanding the Chemistry and Biology of Glycosylation with Glycan Synthesis*. *Annual Review of Biochemistry* **85**, (2016).

2. Wang, L. X. & Davis, B. G. Realizing the promise of chemical glycobiology. *Chem. Sci.* **4**, 3381–3394 (2013).

3. Varki, A. Biological roles of glycans. *Glycobiology* **27**, 3–49 (2017).

4. Prescher, J. A. & Bertozzi, C. R. Chemistry in Living Systems. *Nat. Chem. Biol.* **1**, 13–21 (2005).

5. Stanley, P. What Have We Learned from Glycosyltransferase Knockouts in Mice? *J. Mol. Biol.* **428**, 3166–3182 (2016).

6. Reines, B. P. & Ninham, B. W. Structure and function of the endothelial surface layer: unraveling the nanoarchitecture of biological surfaces. *Q. Rev. Biophys.* **52**, e13 (2019).

7. Zhu, X. & Schmidt, R. R. New principles for glycoside-bond formation. *Angew. Chemie - Int. Ed.* **48**, 1900–1934 (2009).

8. Zhang, X., Lin, L., Huang, H. & Linhardt, R. J. Chemoenzymatic Synthesis of Glycosaminoglycans. *Acc. Chem. Res.* **53**, 333-346 (2019).

9. Kulkarni, S. S. *et al.* 'One-Pot' Protection, Glycosylation, and Protection-Glycosylation Strategies of Carbohydrates. *Chem. Rev.* **118**, 8025–8104 (2018).

10. Hunter, C. D., Guo, T., Daskhan, G., Richards, M. R. & Cairo, C. W. Synthetic Strategies for Modified Glycosphingolipids and Their Design as Probes. *Chem. Rev.* **118**, 8188–8241 (2018).

11. Boltje, T. J., Buskas, T. & Boons, G. J. Opportunities and challenges in synthetic oligosaccharide and glycoconjugate research. *Nat. Chem.* **1**, 611–622 (2009).

12. Dulaney, S. B. & Huang, X. *Strategies in Synthesis of Heparin/Heparan Sulfate Oligosaccharides. 2000-Present. Advances in Carbohydrate Chemistry and Biochemistry* **67**, 96-136 (2012).

13. Esko, J. D. & Lindahl, U. Molecular diversity of heparan sulfate. *J. Clin. Invest.*

108, 169–173 (2001).

14. Kreuger, J. & Kjellén, L. Heparan Sulfate Biosynthesis: Regulation and Variability. *J. Histochem. Cytochem.* **60**, 898–907 (2012).

15. Whitelock, J. M. & Iozzo, R. V. Heparan sulfate: A complex polymer charged with biological activity. *Chem. Rev.* **105**, 2745–2764 (2005).

16. Masola, V., Bellin, G., Gambaro, G. & Onisto, M. Heparanase: A Multitasking Protein Involved in Extracellular Matrix (ECM) Remodeling and Intracellular Events. *Cells* **7**, 236 (2018).

17. Pye, D. A., Vives, R. R., Turnbull, J. E., Hyde, P. & Gallagher, J. T. Heparan sulfate oligosaccharides require 6-O-sulfation for promotion of basic fibroblast growth factor mitogenic activity. *J. Biol. Chem.* **273**, 22936–22942 (1998).

18. Iozzo, R. V. & Schaefer, L. Proteoglycan form and function: A comprehensive nomenclature of proteoglycans. *Matrix Biol.* **42**, 11–55 (2015).

19. Bernfield, M. *et al.* F Unctions of C Ell S Urface. *Structure* 729–777 (1999).

20. Ruoslahti, E. STRUCTURE AND BIOLOGY OF PROTEOGLYCAN. *Ann. Rev. Cell Bioi.* **4**, 229-55 (1988)

21. Xu, D. & Esko, J. D. Demystifying heparan sulfate-protein interactions. *Annu. Rev. Biochem.* **83**, 129–157 (2014).

22. Iozzo, R. V. Basement membrane proteoglycans: From cellar to ceiling. *Nat. Rev. Mol. Cell Biol.* **6**, 646–656 (2005).

23. Raman, R., Venkataraman, G., Ernst, S., Sasisekharan, V. & Sasisekharan, R. Structural specificity of heparin binding in the fibroblast growth factor family of proteins. *Proc. Natl. Acad. Sci. U. S. A.* **100**, 2357–2362 (2003).

24. Staudinger, L. A. *et al.* Interactions between the discoidin domain receptor 1 and β1 integrin regulate attachment to collagen. *Biol. Open* **2**, 1148–1159 (2013).

25. Yeh, Y. C., Lin, H. H. & Tang, M. J. A tale of two collagen receptors, integrin β_1 and discoidin domain receptor 1, in epithelial cell differentiation. *Am. J. Physiol. - Cell Physiol.* **303**, C1207–C1217 (2012).

26. Theos, A. C. *et al.* Functions of adaptor protein (AP)-3 and AP-1 in tyrosinase

sorting from endosomes to melanosomes. *Mol. Biol. Cell* **16**, 5356–5372 (2005).

27. Gubbiotti, M. A., Neill, T. & Iozzo, R. V. A current view of perlecan in physiology and pathology: A mosaic of functions. *Matrix Biol.* **57**–**58**, 285–298 (2017).

28. Laplante, P. *et al.* Perlecan proteolysis induces an α2β1 integrin- and Src family kinase-dependent anti-apoptotic pathway in fibroblasts in the absence of focal adhesion kinase activation. *J. Biol. Chem.* **281**, 30383–30392 (2006).

29. Jiang, X. & Couchman, J. R. Perlecan and Tumor Angiogenesis. *J. Histochem. Cytochem.* **51**, 1393–1410 (2003).

30. Aviezer, D. *et al.* Perlecan, basal lamina proteoglycan, promotes basic fibroblast growth factor-receptor binding, mitogenesis, and angiogenesis. *Cell* **79**, 1005–1013 (1994).

31. Whitelock, J. M., Melrose, J. & Iozzo, R. V. Diverse cell signaling events modulated by Perlecan. *Biochemistry* **47**, 11174–11183 (2008).

32. Iozzo, R. V. & San Antonio, J. D. Heparan sulfate proteoglycans: heavy hitters in the angiogenesis arena. *J. Clin. Invest.* **108**, 349–355 (2001).

33. Iozzo, R. V. & Sanderson, R. D. Proteoglycans in cancer biology, tumour microenvironment and angiogenesis. *J. Cell. Mol. Med.* **15**, 1013–1031 (2011).

34. Yu, P., Pearson, C. S. & Geller, H. M. Flexible Roles for Proteoglycan Sulfation and Receptor Signaling. *Trends Neurosci.* **41**, 47–61 (2018).

35. Baerwald-De La Torre, K., Winzen, U., Halfter, W. & Bixby, J. L. Glycosaminoglycan-dependent and -independent inhibition of neurite outgrowth by agrin. *J. Neurochem.* **90**, 50–61 (2004).

36. Burgess, R. W., Dickman, D. K., Nunez, L., Glass, D. J. & Sanes, J. R. Mapping sites responsible for interactions of agrin with neurons. *J. Neurochem.* **83**, 271–284 (2002).

37. Fukai, N. *et al.* Lack of collagen XVIII/endostatin results in eye abnormalities. *EMBO J.* **21**, 1535–1544 (2002).

38. Rehn, M., Hintikka, E. & Pihlajaniemi, T. Primary structure of the α1 chain of

mouse type XVIII collagen, partial structure of the corresponding gene, and comparison of the α1 (XVIII) chain with its homologue, the α1(XV) collagen chain. *J. Biol. Chem.* **269**, 13929–13935 (1994).

39. Oh, S. P. *et al.* Isolation and sequencing of cDNAs for proteins with multiple domains of Gly-Xaa-Yaa repeats identify a distinct family of collagenous proteins. *Proc. Natl. Acad. Sci. U. S. A.* **91**, 4229–4233 (1994).

40. Aikio, M. *et al.* Specific collagen XVIII isoforms promote adipose tissue accrual via mechanisms determining adipocyte number and affect fat deposition. *Proc. Natl. Acad. Sci. U. S. A.* **111**, (2014).

41. Couchman, J. R. Transmembrane signaling proteoglycans. *Annu. Rev. Cell Dev. Biol.* **26**, 89–114 (2010).

42. Sarrazin, S., Lamanna, W. C. & Esko, J. D. Heparan sulfate proteoglycans. *Cold Spring Harb. Perspect. Biol.* **3**, 1–33 (2011).

43. Deepa, S. S., Yamada, S., Zako, M., Goldberger, O. & Sugahara, K. Chondroitin sulfate chains on syndecan-1 and syndecan-4 from normal murine mammary gland epithelial cells are structurally and functionally distinct and cooperate with heparan sulfate chains to bind growth factors.. *J. Biol. Chem.* **279**, 37368–37376 (2004).

44. Zhang, Y. *et al.* Targeting of heparanase-modified syndecan-1 by prosecretory mitogen lacritin requires conserved core GAGAL plus heparan and chondroitin sulfate as a novel hybrid binding site that enhances selectivity. *J. Biol. Chem.* **288**, 12090–12101 (2013).

45. Addi, C. *et al.* The Flemmingsome reveals an ESCRT-to-membrane coupling via ALIX/syntenin/syndecan-4 required for completion of cytokinesis. *Nat. Commun.* **11**, 1–15 (2020).

46. Tumova, S., Woods, A. & Couchman, J. R. Heparan sulfate proteoglycans on the cell surface: Versatile coordinators of cellular functions. *Int. J. Biochem. Cell Biol.* **32**, 269–288 (2000).

47. Karamanos, N. K. *et al.* Proteoglycan chemical diversity drives multifunctional cell regulation and therapeutics. *Chem. Rev.* **118**, 9152–9232 (2018).

48. Afratis, N. A. *et al.* Syndecans – key regulators of cell signaling and biological functions. *FEBS J.* **284**, 27–41 (2017).

49. Theocharis, A. D. & Karamanos, N. K. Proteoglycans remodeling in cancer: Underlying molecular mechanisms. *Matrix Biol.* **75**–**76**, 220–259 (2019).

50. Theocharis, A. D., Skandalis, S. S., Tzanakakis, G. N. & Karamanos, N. K. Proteoglycans in health and disease: Novel roles for proteoglycans in malignancy and their pharmacological targeting. *FEBS J.* **277**, 3904–3923 (2010).

51. Filmus, J. & Capurro, M. The role of glypicans in Hedgehog signaling. *Matrix Biol.* **35**, 248–252 (2014).

52. Capurro, M., Martin, T., Shi, W. & Filmus, J. Glypican-3 binds to Frizzled and plays a direct role in the stimulation of canonical Wnt signaling. *J. Cell Sci.* **127**, 1565–1575 (2014).

53. Matsuda, K. *et al.* Glypican-1 is overexpressed in human breast cancer and modulates the mitogenic effects of multiple heparin-binding growth factors in breast cancer cells. *Cancer Res.* **61**, 5562–5569 (2001).

54. Saad, A. *et al.* Role of Glycanation and Convertase Maturation of Soluble Glypican-3 in Inhibiting Proliferation of Hepatocellular Carcinoma Cells. *Biochemistry* **57**, 1201–1211 (2018).

55. Wang, L., Yao, M., Pan, L. H., Qian, Q. & Yao, D. F. Glypican-3 is a biomarker and a therapeutic target of hepatocellular carcinoma. *Hepatobiliary Pancreat. Dis. Int.* **14**, 361–366 (2015).

56. Cao, J. *et al.* Targeting glypican-4 overcomes 5-FU resistance and attenuates stem cell–like properties via suppression of Wnt/β-catenin pathway in pancreatic cancer cells. *J. Cell. Biochem.* **119**, 9498–9512 (2018).

57. Williamson, D. *et al.* Role for amplification and expression of Glypican-5 in rhabdomyosarcoma. *Cancer Res.* **67**, 57–65 (2007).

58. Li, N., Gao, W., Zhang, Y. F. & Ho, M. Glypicans as Cancer Therapeutic Targets. *Trends in Cancer* **4**, 741–754 (2018).

59. López-Casillas, F. *et al.* Structure and expression of the membrane proteoglycan betaglycan, a component of the TGF-β receptor system. *Cell* **67**, 785–795 (1991).

60. Elderbroom, J. L. *et al.* Ectodomain shedding of TβRIII is required for TβRIII-mediated suppression of TGF-β signaling and breast cancer migration and invasion. *Mol. Biol. Cell* **25**, 2320–2332 (2014).

61. Chaudhary, B., Khaled, Y. S., Ammori, B. J. & Elkord, E. Neuropilin 1: Function and therapeutic potential in cancer. *Cancer Immunol. Immunother.* **63**, 81–99 (2014).

62. Mercurio, A. M. VEGF/neuropilin signaling in cancer stem cells. *Int. J. Mol. Sci.* **20**, 1-12 (2019).

63. Hook, M., Lindahl, U. & Iverius, P. H. Distribution of sulphate and iduronic acid residues in heparin and heparan sulphate. *Biochem. J.* **137**, 33–43 (1974).

64. Rabenstein, D. L. Heparin and heparan sulfate: Structure and function. *Nat. Prod. Rep.* **19**, 312–331 (2002).

65. Lindahl, U. & Kjellen, L. Heparin or heparan sulfate - What is the difference? *Thromb. Haemost.* **66**, 44–48 (1991).

66. Torri, G. *et al*. Controversial glycosaminoglycan. *Nature* **322**, 215-216 (1986).

67. Ferro, D. R. *et al.* Evidence for Conformational Equilibrium of the Sulfated L-Iduronate Residue in Heparin and in Synthetic Heparin Mono- and Oligosaccharides: NMR and Force-Field Studies. *J. Am. Chem. Soc.* **108**, 6773–6778 (1986).

68. Cram, D. J. International Edition in English. *Angew. Chemie Int. Ed. English* **24**, 799–810 (1985).

69. Petitou, M. & Van Boeckel, C. A. A. A synthetic antithrombin III binding pentasaccharide is now a drug! What comes next? *Angew. Chemie - Int. Ed.* **43**, 3118–3133 (2004).

70. Muñoz-García, J. C. *et al.* Effect of the substituents of the neighboring ring in the conformational equilibrium of iduronate in heparin-like trisaccharides.

Chem. - A Eur. J. **18**, 16319–16331 (2012).

71. Hsieh, P. H., Thieker, D. F., Guerrini, M., Woods, R. J. & Liu, J. Uncovering the Relationship between Sulphation Patterns and Conformation of Iduronic Acid in Heparan Sulphate. *Sci. Rep.* **6**, 1–8 (2016).

72. Habuchi, H. *et al.* The occurrence of three isoforms of heparan sulfate 6-O-sulfotransferase having different specificities for hexuronic acid adjacent to the targeted N- sulfoglucosamine. *J. Biol. Chem.* **275**, 2859–2868 (2000).

73. Shworak, N. W. *et al.* Multiple Isoforms of Heparan Sulfate d-Glucosaminyl 3-O -Sulfotransferase . *J. Biol. Chem.* **274**, 5170–5184 (1999).

74. Weiss, R. J., Esko, J. D. & Tor, Y. Targeting heparin and heparan sulfate protein interactions. *Org. Biomol. Chem.* **15**, 5656–5668 (2017).

75. Lindahl, U., Kusche-Gullberg, M. & Kjellen, L. Regulated diversity of heparan sulfate. *J. Biol. Chem.* **273**, 24979–24982 (1998).

76. Aikawa, J. I. & Esko, J. D. Molecular cloning and expression of a third member of the heparan sulfate/heparin GlcNac N-deacetylase/N-sulfotransferase family. *J. Biol. Chem.* **274**, 2690–2695 (1999).

77. Kusche-Gullberg, M., Eriksson, I., Pikas, D. S. & Kjellén, L. Identification and expression in mouse of two heparan sulfate glucosaminyl N-deacetylase/N-sulfotransferase genes. *J. Biol. Chem.* **273**, 11902–11907 (1998).

78. Bishop, J. R., Schuksz, M. & Esko, J. D. Heparan sulphate proteoglycans fine-tune mammalian physiology. *Nature* **446**, 1030–1037 (2007).

79. Raman, R., Sasisekharan, V. & Sasisekharan, R. Structural Insights into biological roles of protein-glycosaminoglycan interactions. *Chem. Biol.* **12**, 267–277 (2005).

80. Dreyfuss, J. L. *et al.* Heparan sulfate proteoglycans: Structure, protein interactions and cell signaling. *An. Acad. Bras. Cienc.* **81**, 409–429 (2009).

81. Rosenberg, D. R., Hichs, M. and Damus S. P. Anticoagulant Action of Haprin. Frens. *Natutre* **246**, 355-357 (1973).

82. Chon-, M. Synthesis of thrombin- inhibiting heparin mimetics without side

effects. **398**, 417–422 (1999).

83. Bray, B., Lane, D. A., Freyssinet, J. M., Pejler, G. & Lindahl, U. Anti-thrombin activities of heparin. Effect of saccharide chain length on thrombin inhibition by heparin cofactor II and by antithrombin. *Biochem. J.* **262**, 225–232 (1989).

84. Herbert, J. M. *et al.* SR 90107A/Org 31540, a novel anti-factor Xa antithrombotic agent. *Cardiovasc. Drug Rev.* **15**, 1–26 (1997).

85. Van Boeckel, C. A. A. *et al*. Rational design of synthetic haparin analogues with tailor-made coagulation factor inhibitory activity. *Nat. Struct. Biol*. **2**, 736-739 (1995).

86. Dementiev, A., Petitou, M., Herbert, J. M. & Gettins, P. G. W. The ternary complex of antithrombin-anhydrothrombin-heparin reveals the basis of inhibitor specificity. *Nat. Struct. Mol. Biol.* **11**, 863–867 (2004).

87. Visser, A., Grootenhius P. D. J. and Van Boeckel, C. A. A. A mechanism of haparin indused potentiation of antithrombin III. *Nat. Struct. Biol.* **1**, 423-425 (1994).

88. Demeter, F. *et al.* Replacement of the L-iduronic acid unit of the anticoagulant pentasaccharide idraparinux by a 6-deoxy-L-talopyranose – Synthesis and conformational analysis. *Sci. Rep.* **8**, 2–11 (2018).

89. Li, W., Johnson, D. J. D., Esmon, C. T. & Huntington, J. A. Structure of the antithrombin-thrombin-heparin ternary complex reveals the antithrombotic mechanism of heparin. *Nat. Struct. Mol. Biol.* **11**, 857–862 (2004).

90. Pratt, C. W. & Church, F. C. General features of the heparin-binding serpins antithrombin, heparin cofactor II and protein C inhibitor. *Blood Coagulation and Fibrinolysis* **4**, 479–490 (1993).

91. Baglin, T. P., Carrell, R. W., Church, F. C., Esmon, C. T. & Huntington, J. A. Crystal structures of native and thrombin-complexed heparin cofactor II reveal a multistep allosteric mechanism. *Proc. Natl. Acad. Sci. U. S. A.* **99**, 11079–11084 (2002).

92. Raghuraman, A., Mosier, P. D. & Desai, U. R. Understanding dermatan sulfate-heparin cofactor II interaction through virtual library screening. *ACS Med.*

Chem. Lett. **1**, 281–285 (2010).

93. Giri, T. K. & Tollefsen, D. M. Placental dermatan sulfate: Isolation, anticoagulant activity, and association with heparin cofactor II. *Blood* **107**, 2753–2758 (2006).

94. Beenken, A. & Mohammadi, M. The FGF family: Biology, pathophysiology and therapy. *Nat. Rev. Drug Discov.* **8**, 235–253 (2009).

95. Turner, N. & Grose, R. Fibroblast growth factor signalling: From development to cancer. *Nat. Rev. Cancer* **10**, 116–129 (2010).

96. Yun, Y. R. *et al.* Fibroblast growth factors: Biology, function, and application for tissue regeneration. *J. Tissue Eng.* **1**, 1–18 (2010).

97. Pellegrini, L. Role of heparan sulfate in fibroblast growth factor signaling: a structural view. *Curr. Opin. Struct. Biol.* **11**, 629-634 (2001).

98. Moodie, Z. *et al.* Letters To Nature. *Nature* **420**, 812–817 (2002).

99. Raab, G. & Klagsbrun, M. Heparin-binding EGF-like growth factor. *Biochim. Biophys. Acta - Rev. Cancer* **1333**, (1997).

100. Sznol, M. *et al.* for the Treatment of Cancer. **105**, 1027–1030 (2000).

101. Faham, S., Linhardtt, R. J. & Rees, D. C. Diversity does make a difference: fibroblast growth factor-heparin interactions Salem Faham*, Robert J Linhardtt and Douglas C Rees. *Curr. Opin. Struct. Biol.* **8**, 578–586 (1998).

102. Pellegrini, L., Burke, D. F., Von Delft, F., Mulloy, B. & Blundell, T. L. Crystal structure of fibroblast growth factor receptor ectodomain bound to ligand and heparin. *Nature* **407**, 1029–1034 (2000).

103. Allen, B. L., Filla, M. S. & Rapraeger, A. C. Role of heparan sulfate as a tissue-specific regulator of FGF-4 and FGF receptor recognition. *J. Cell Biol.* **155**, 845–857 (2001).

104. Ashikari-Hada, S. *et al.* Characterization of Growth Factor-binding Structures in Heparin/Heparan Sulfate Using an Octasaccharide Library. *J. Biol. Chem.* **279**, 12346–12354 (2004).

105. Turnbull, J. E., Fernig, D. G., Ke, Y., Wilkinson, M. C. & Gallagher, J. T.

Identification of the basic fibroblast growth factor binding sequence in fibroblast heparan sulfate. *J. Biol. Chem.* **267**, 10337–10341 (1992).

106. Faham, S., Hileman, R. E., Fromm, J. R., Linhardt, R. J. & Rees, D. C. Heparin structure and interactions with basic fibroblast growth factor. *Science (80-.).* **271**, 1116–1120 (1996).

107. Noti, C., De Paz, J. L., Polito, L. & Seeberger, P. H. Preparation and use of microarrays containing synthetic heparin oligosaccharides for the rapid analysis of heparin-protein interactions. *Chem. - A Eur. J.* **12**, 8664–8686 (2006).

108. RALF P AUS , M.D., AND G EORGE C OTSARELIS, M. D. & H. T He B Iology of H Air F Ollicles. *New Engl. J. Med. Fig.* **341**, 491–497 (2004).

109. Lortat-Jacob, H., Grosdidier, A. & Imberty, A. Structural diversity of heparan sulfate binding domains in chemokines. *Proc. Natl. Acad. Sci. U. S. A.* **99**, 1229–1234 (2002).

110. Lortat-Jacob, H. The molecular basis and functional implications of chemokine interactions with heparan sulphate. *Curr. Opin. Struct. Biol.* **19**, 543–548 (2009).

111. Lin, X. Functions of heparan sulfate proteoglycans in cell signaling during development. *Development* **131**, 6009–6021 (2004).

112. Bach, D. H., Park, H. J. & Lee, S. K. The Dual Role of Bone Morphogenetic Proteins in Cancer. *Mol. Ther. - Oncolytics* **8**, 1–13 (2018).

113. Smith, R. A. A. *et al.* Minimum structural requirements for BMP-2-binding of heparin oligosaccharides. *Biomaterials* **184**, 41–55 (2018).

114. Sallusto, F. & Baggiolini, M. o v e Rv I e w Chemokines and leukocyte traffic. *Online* **9**, 949–952 (2008).

115. Parish, C. R. Heparan sulfate and inflammation. *Nat. Immunol.* **6**, 861–862 (2005).

116. Belperio, J. A. *et al.* CXC chemokines in angiogenesis. *J. Leukoc. Biol.* **68**, 1–8 (2000).

117. Handel, T. M. *et al.* Regulation of protein function by glycosaminoglycans - As exemplified by chemokines. *Annu. Rev. Biochem.* **74**, 385–410 (2005).

118. Schluger, N. W. & Rom, W. N. Early responses to infection: Chemokines as mediators of inflammation. *Curr. Opin. Immunol.* **9**, 504–508 (1997).

119. Gama, C. I. & Hsieh-Wilson, L. C. Chemical approaches to deciphering the glycosaminoglycan code. *Curr. Opin. Chem. Biol.* **9**, 609–619 (2005).

120. Polat, T. & Wong, C. H. Anomeric reactivity-based one-pot synthesis of heparin-like oligosaccharides. *J. Am. Chem. Soc.* **129**, 12795–12800 (2007).

121. Chang, K. L., Zulueta, M. M. L., Lu, X. A., Zhong, Y. Q. & Hung, S. C. Regioselective one-pot protection of d-glucosamine. *J. Org. Chem.* **75**, 7424–7427 (2010).

122. Schell, P., Orgueira, H. A., Roehrig, S. & Seeberger, P. H. Synthesis and transformations of D-glucuronic and L-iduronic acid glycals. *Tetrahedron Lett.* **42**, 3811–3814 (2001).

123. Ke, W., Whitfield, D. M., Gill, M., Larocque, S. & Yu, S. H. A short route to L-iduronic acid building blocks for the syntheses of heparin-like disaccharides. *Tetrahedron Lett.* **44**, 7767–7770 (2003).

124. Adibekian, A. *et al.* De novo synthesis of uronic acid building blocks for assembly of heparin oligosaccharides. *Chem. - A Eur. J.* **13**, 4510–4522 (2007).

125. Cao, X. *et al.* Direct C5-Isomerization Approach to l-Iduronic Acid Derivatives. *Asian J. Org. Chem.* **4**, 899–902 (2015).

126. Lee, J. C., Lu, X. A., Kulkarni, S. S., Wen, Y. S. & Hung, S. C. Synthesis of Heparin Oligosaccharides. *J. Am. Chem. Soc.* **126**, 476–477 (2004).

127. Hansen, S. U. *et al.* Scalable synthesis of L-lduronic acid derivatives via stereocontrolled cyanohydrin reaction for synthesis of heparin-related disaccharides. *Org. Lett.* **11**, 4528–4531 (2009).

128. Dhamale, O. P., Zong, C., Al-Mafraji, K. & Boons, G. J. New glucuronic acid donors for the modular synthesis of heparan sulfate oligosaccharides. *Org. Biomol. Chem.* **12**, 2087–2098 (2014).

129. Hu, Y. P. *et al.* Divergent synthesis of 48 heparan sulfate-based disaccharides and probing the specific sugar-fibroblast growth factor-1 interaction. *J. Am.*

Chem. Soc. **134**, 20722–20727 (2012).

130. Prabhu, A., Venot, A. & Boons, G. J. New Set of Orthogonal Protecting Groups for the Modular Synthesis of Heparan Sulfate Fragments. *Org. Lett.* **5**, 4975–4978 (2003).

131. Fan, R. H., Achkar, J., Hernández-Torres, J. M. & Wei, A. Orthogonal sulfation strategy for synthetic heparan sulfate ligands. *Org. Lett.* **7**, 5095–5098 (2005).

132. Mensah, E. A., Yu, F. & Nguyen, H. M. Nickel-catalyzed stereoselective glycosylation with C(2)- N-substituted benzylidene d-glucosamine and galactosamine trichloroacetimidates for the formation of 1,2-cis-2-amino glycosides. applications to the synthesis of heparin disaccharides, GPI Anchor Pseudodisaccharides and α-GalNAc. *J. Am. Chem. Soc.* **132**, 14288–14302 (2010).

133. Hansen, S. U., Miller, G. J., Cliff, M. J., Jayson, G. C. & Gardiner, J. M. Making the longest sugars: a chemical synthesis of heparin-related $[4]_n$ oligosaccharides from 16-mer to 40-mer. *Chem. Sci.* **6**, 6158–6164 (2015).

134. Jayson, G. C. *et al.* Synthetic heparan sulfate dodecasaccharides reveal single sulfation site interconverts CXCL8 and CXCL12 chemokine biology. *Chem. Commun.* **51**, 13846–13849 (2015).

135. Miller, G. J. *et al.* Efficient chemical synthesis of heparin-like octa-, deca- and dodecasaccharides and inhibition of FGF2- and VEGF165-mediated endothelial cell functions. *Chem. Sci.* **4**, 3218–3222 (2013).

136. Hansen, S. U., Miller, G. J., Jayson, G. C. & Gardiner, J. M. First Gram-Scale Synthesis of a Heparin-Related Dodecasaccharide. 2–5 (2013).

137. Castro-Palomino, J. C. & Schmidt, R. R. N,N-diacetyl-glucosamine and -galactosamine derivatives as glycosyl donors. *Tetrahedron Lett.* **36**, 6871–6874 (1995).

138. Zong, C., Venot, A., Dhamale, O. & Boons, G. J. Fluorous supported modular synthesis of heparan sulfate oligosaccharides. *Org. Lett.* **15**, 342–345 (2013).

139. Dey, S., Lo, H. J. & Wong, C. H. An Efficient Modular One-Pot Synthesis of Heparin-Based Anticoagulant Idraparinux. *J. Am. Chem. Soc.* **141**, 10309–10314

(2019).

140. Chang, C. H. *et al.* Synthesis of the heparin-based anticoagulant drug fondaparinux. *Angew. Chemie - Int. Ed.* **53**, 9876–9879 (2014).

141. Dai, X. *et al.* Formal Synthesis of Anticoagulant Drug Fondaparinux Sodium. *J. Org. Chem.* **81**, 162–184 (2016).

142. Li, T. *et al.* Total synthesis of anticoagulant pentasaccharide fondaparinux. *ChemMedChem* **9**, 1071–1080 (2014).

143. Park, S., Gildersleeve, J. C., Blixt, O. & Shin, I. Carbohydrate microarrays. *Chem. Soc. Rev.* **42**, 4310–4326 (2013).

144. Rillahan, C. D. & Paulson, J. C. Glycan microarrays for decoding the glycome. *Annu. Rev. Biochem.* **80**, 797–823 (2011).

145. Shanthamurthy, C. D. *et al.* ABO Antigens Active Tri- and Disaccharides Microarray to Evaluate C-type Lectin Receptor Binding Preferences. *Sci. Rep.* **8**, 1–7 (2018).

146. Disney, M. D. & Seeberger, P. H. The use of carbohydrate microarrays to study carbohydrate-cell interactions and to detect pathogens. *Chem. Biol.* **11**, 1701–1707 (2004).

147. Liang, P. H., Wang, S. K. & Wong, C. H. Quantitative analysis of carbohydrate-protein interactions using glycan microarrays: Determination of surface and solution dissociation constants. *J. Am. Chem. Soc.* **129**, 11177–11184 (2007).

CHAPTER 2

Linear Synthesis of *De novo* Oligo-Iduronic Acid

Abstract

L-Iduronic acid (IdoA) plays a pivotal role in glycosaminoglycan (GAG) protein interactions. However, the structural microheterogeneity of GAG appears to impede the systematic investigation of IdoA functions. Under such conditions, oligo-Iduronic acid (Oligo-IdoA) are ideal and straightforward heparin mimetics to unravel the relationship between IdoA structure and functions. We report for the first time the synthesis of oligo-IdoA precursors by screening different synthetic strategies to ensure good reactivity and high-yields.

2.1 Introduction

L-Iduronic acid (IdoA) is key hexuronic acid component of heparin (HP), heparan sulfate (HS), and dermatan sulfate (DS). It is classified under the glycosaminoglycan (GAG) family.[1-6] The biosynthesis of HS and HP is initiated by the attachment of D-xylose to the prescribed serine residue of proteoglycan core proteins, followed by glycosylation of two galactose and glucuronic acid residues, leading to the formation of a tetrasaccharide linker region. In the Golgi complex, the linker region undergoes a series of enzymatic modifications, including deacetylation, sulfation, and epimerization of D-glucuronic acid into L-iduronic acid.[7,8] This results in highly complex and diverse HS/HP structures.[9,10] NMR and theoretical studies of HP and HS oligosaccharides confirmed that IdoA is predominantly presents with $^{1}C_{4}$-chair and $^{2}S_{0}$ skew-boat geometry and less abundance as a $^{4}C_{1}$-chair conformation.[11-13] This conformation flexibility adds additional structural diversity in HP and HS active domains and thereby fine-tunes its protein interactions. The interaction between fondaparinux (a pentasaccharide heparin mimetic) and antithrombin III is a well-studied example of the conformation plasticity of IdoA and its critical role in inhibiting blood coagulation.[14-17] Nieto and coworkers synthesized an HP trisaccharides library and showed that 6-*O*-sulfated and *N*-sulfated glucosamine (GlcN) residues next to IdoA significantly contribute to $^{2}S_{0}$ conformation.[18,19]Liu and his coworkers synthesized HP hexasaccharide and proved that 2-*O*- and 3-*O*-sulfation of GlcN and 2-*O*-sulfation of IdoA are also crucial for stabilizing $^{2}S_{0}$ geometry in oligosaccharides.[20] Even though many reports have confirmed the conformational flexibility of IdoA, the considerable microheterogeneity of GAG chains has limited our in-depth knowledge of IdoA. Because of these conditions, developing the library of oligo-IdoA is envisioned as a potent model (**Fig. 1**). However, the synthesis of such oligosaccharides is highly challenging, as IdoA is not commercially available. Herein, we have succeeded developing the first synthetic protocol for fully protected oligo-IdoA precursors.

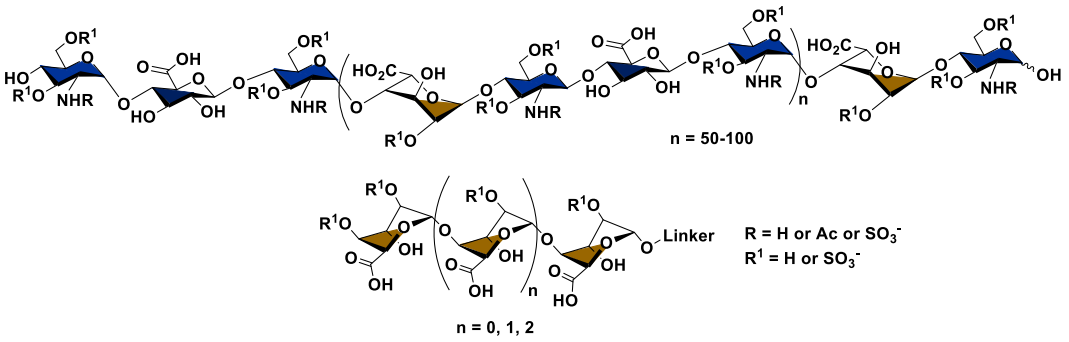

Figure 1. Chemical structures of HS/HP and Oligo-Iduronic acid derivatives.

2.2 Results and discussion

2.2.1 Synthesis of Monosaccharide Iduronic Acid Building block

Our synthetic strategy is based on identifying a suitable protocol for IdoA-disaccharides synthesis and extending the strategy for oligosaccahrides. The pioneer work from the lab of Hung, Seeberger, Boons, Liu, Gardiner, and others yielded gram scale synthesis of IdoA building blocks from one-pot and *de novo* methods.[21-30]In the present study, we employed 1,6-anhydro-*β*-L-idopyranosyl 4-alcohol (**5**) and an iduronic acid-thiophenol donor (**8a**) as important precursors to synthesize oligosaccharides. The initial synthetic strategy was based on use of IdoA derivatives **8a** and **9** as "donor" and "acceptor," circumvents the need for deprotection and oxidation steps. We used an amine-linker to block the reducing end IdoA residue for further conjugation. Compound **5** was synthesized with a total yield of 27% from 1,2:5,6-di-*O*-isopropylidene-*α*-D-glucofuranose by a six-step reaction.[31] A regioselective ring opening of **5** with trimethyl(phenylthio)silane in the presence of $ZnCI_2$ at room temperature, led to thioglycoside **6** in a 75% yield. One-pot oxidation of **6** with catalytic amounts of 2,2,6,6-tetramethyl-1-piperidinyloxyl (TEMPO) in the presence of bis(acetoxyiodo]benzene (BAIB) followed by esterification with benzyl bromide yielded **7** in 88% yield. It was further glycosylated with an azide linker to yield 78% of **9**. The C4-OH of **7** was protected with levulinic acid using DCC as a coupling agent, yielding the donor **8a** (**Scheme. 1**).

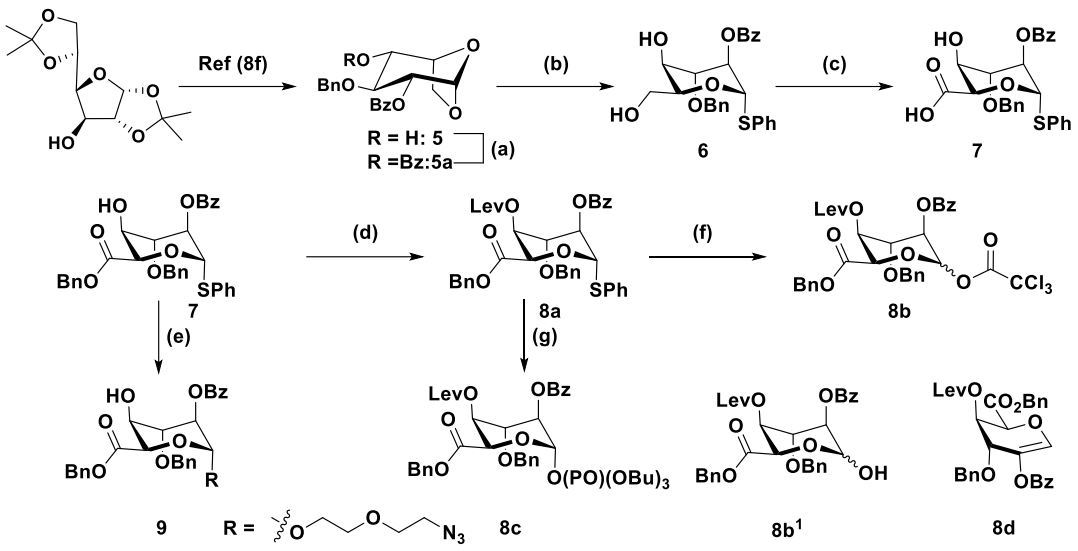

Scheme 1: Synthesis of acceptor molecules **9** and donor **8a-c**: Reagents and conditions: (a) BzCl, DCM/Py, 85%; (b) TMSSPh, $ZnCI_2$, CH_2Cl_2, RT, 75% **(6)**; (c) TEMPO, BAIB, CH_2Cl_2/H_2O (1/1); BnBr, TBAI, $NaHCO_3$, DMF, 60 °C, (2steps), 88% **(7)**; (d) LevOH, DCC, DMAP, CH_2Cl_2, 88% **(8a)**; (e)

2.2.2 Synthesis of Iduronic Acid Disaccharide

An attempt to glycosylate **8a** and **9** in the presence of *N*-iodosuccinimide (NIS) and a catalytic amount of trimethylsilyl trifluoromethanesulfonate (TMSOTf) in DCM at -20 °C ended with the lactal **8d** instead of the desired di-IdoA **I-1**. The use of a strong thiophilic promoter condition, such as NIS/trifluoromethanesulfonic acid (TfOH), in a range of temperatures and time periods failed to yield di-idoA **I-1 (Scheme 2)**. These results lead us to conclude that the neighboring 2-benzoyl substitution of donor **8a** stabilizes the benzyl oxonium-ion intermediate in the presence of a thiophilic agent and facilitates 1,2-trans glycosylation due to the weak nucleophilicity of **9**, steroselective glycosylation did not proceed and ledtolactal.

To improve the glycosylation, we have synthesized IdoA-donors with good leaving groups, such as trichloroimidate (**8b**) and phosphorimidate (**8c**). Under mild acidic conditions (catalytic amount of TMSOTf), IdoA-trichloroimidate (**8b**) yielded **I-1** in 5% yield. Encouraged by this minor step forward, we examined other trichloroacetimidate promoters, such as silver(I) triflate (AgOTf), triflic acid (TfOH), and $BF_3.Et_2O$. These, unfortunately, did not improve glycosylation yield and resulted

eliminated side-product **8d**. Similarly, IdoA-phosphorimidate (**8c**) failed to yield the desired **22** (Fig. 3). Based on these unsuccessful efforts, we concluded that the electron withdrawing C5-carboxylic ester in **9** reduced the nucleophilicity of the axial C4-OH, and that **9** is a poor nucleophile for 1,2-trans glycosylation.

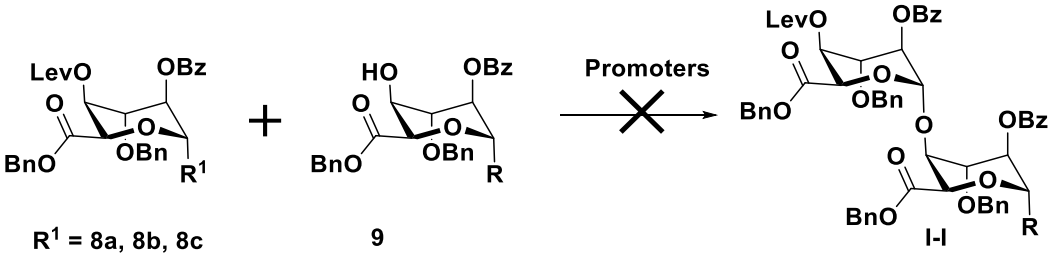

Scheme 2. Synthesis of **I-2** from **8a-c** and **9** as donors and acceptor. Promotor: **8a**: NIS/TMSOTf or NIS/TfOH; **8b**: TMSOTf or AgOTf, TfOH, $BF_3.Et_2O$; **8c**: TMSOTf.

To overcome the nucleophilicity of IdoA precursors, we proposed using strong nucleophiles **5** and **9** as donors to synthesize L-Idose disaccharide **15** and explore TEMPO oxidation of primary hydroxyl groups to yield the desired product. To achieve this, 1,2-trans L-Idose disaccharide **14** was synthesized from L-idose-tricholorimidate donor **11** and 1,6-anhydro-*β*-L-idopyranosyl 4-alcohol **5** using a catalytic amount of TMSOTf. This was, followed by acetolysis, and linker glycosylation to obtain di-L-Idose **15** in 23% (4 steps) overall yield. The removal of acyl groups of **14** by using sodium methoxide yielded di-L-Idose **16 (Scheme 3).** Finally, **16** was oxidized with TEMPO in the presence of BAIB, yielding unexpected lactonized IdoA monosaccharide **17** as a major product. Attempts with different TEMPO co-oxidants such as sodium hypochloride (NaOCl) and sodium chlorite ($NaClO_2$) met similar fate. This indicates that TEMPO/BAIB/NaOCl mediated oxidation is selective for primary alcohol, but the alkaline reaction condition and radical species formed during the oxidation resulted incleavage of the glycosidic bond, presumably by an $E1_{CB}$ elimination mechanism.[32-35] Overall, we concluded that oligo-L-Idose could be easily generated from **5**, but TEMPO oxidation of multiple primary hydroxy groups may be detrimental to the process and could result in cleavage of glycosidic bonds.

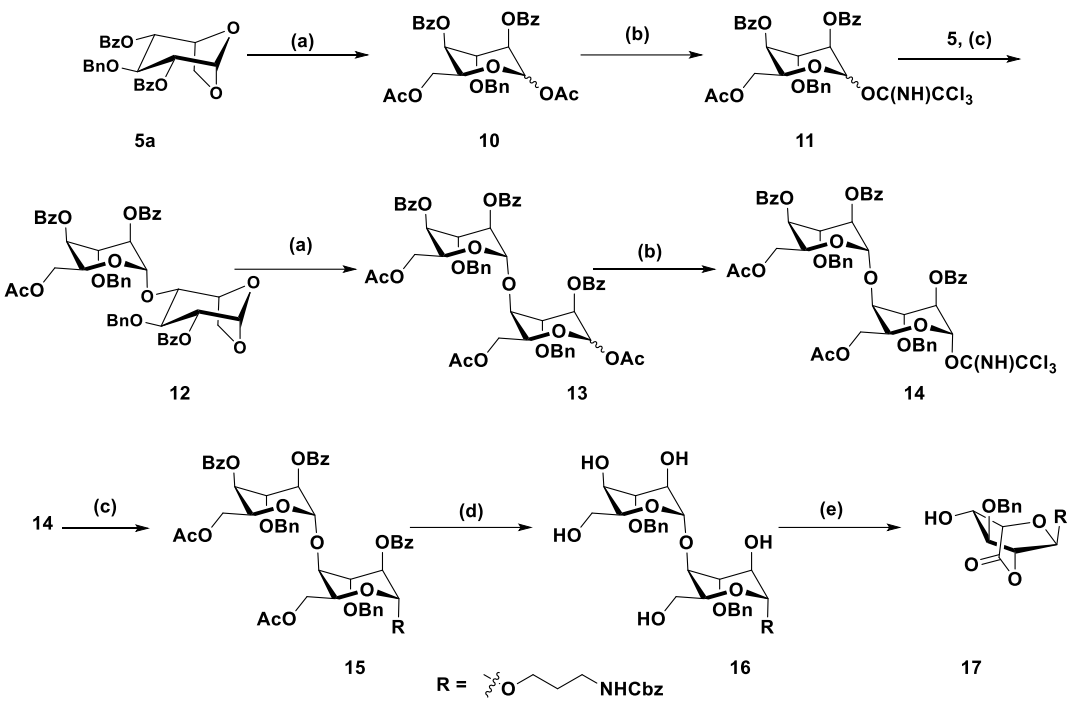

Scheme 3: Synthesis of di-L-Idose precursor (**15**): Reagents and conditions: (a) $Cu(OTf)_2$, Ac_2O, 0 °C, 82% **(10)**, 78% **(13)**; (b) Bu_2SnO, MeOH, 55 °C; $CNCCl_3$, DBU, CH_2Cl_2 53% **(11)**, 43% **(14)** (2 steps); (c) TMSOTf, CH_2Cl_2, 4 Å M.S, -78 °C 59% **(12)**, 68% **(15)**; (d) NaOMe, MeOH, 88% **(16)**; (e) TEMPO, BAIB, CH_2Cl_2/H_2O (1/1), 26% **(17)**.

2.2.3 Synthesis of Di- Tri- and TetraIduronic Acid

To tackle the TEMPO mediated oxidation-degradation of oligosaccharides, we have decided to synthesize heterogeneous L-IdoA-L-idose disaccharide **19** composition and oxidize a single primary hydroxyl moiety at a time. We started the synthesis by glycosylating **8a** and **5** with NIS and TMSOTf and obtained disaccharide **18** in 64% yield after 30 minutes **(Scheme 4).** We have corroborated the α-configuration of glycoside **18** by ^{1}H and ^{13}C-NMR, showing peaks at 5.29 and 95.17 ppm, respectively. By acetolysis of the anhydro-ring of **18**, in the presence of copper (II) trifluoromethanesulfonate [$Cu(OTf)_2$] and acetic anhydride, we have synthesized **19** in 94% yield. Successive thioglycosylation, mild deacetylation, one-pot TEMPO oxidation, and esterification of **19** yielded the target disaccharide molecule **22** in 53% (3 steps) overall yield. Glycosylation of **22** with an azide-linker yielded di-IdoA derivative **I-2** in 81% yield. Encouraged by the overall yield and stereoselectivity of the di-IdoA, we extended the protocol to synthesize different chain lengths of oligo-IdoA **(Scheme 4)**. As an example, **22** or **27** were reacted with **5** using NIS and TMSOTf. These were followed by a series of reactions, including acetolysis of the anhydro-ring,

thioglycosylation, deacetylation, oxidation, esterification, and linker glycosylation. This sequence of reactions yielded compounds **I-2** and **I-3** (tri or tetra-IdoA derivatives) in 25% (6 steps) and 20% (6 steps) yield, respectively. Based on the low nucleophilicity of L-idoA and the sensitivity of L-Idose for TEMPO oxidation, we conclude that our new convergent approach is ideal for the synthesis of moderate yields of different lengths of oligo-IdoA precursors.

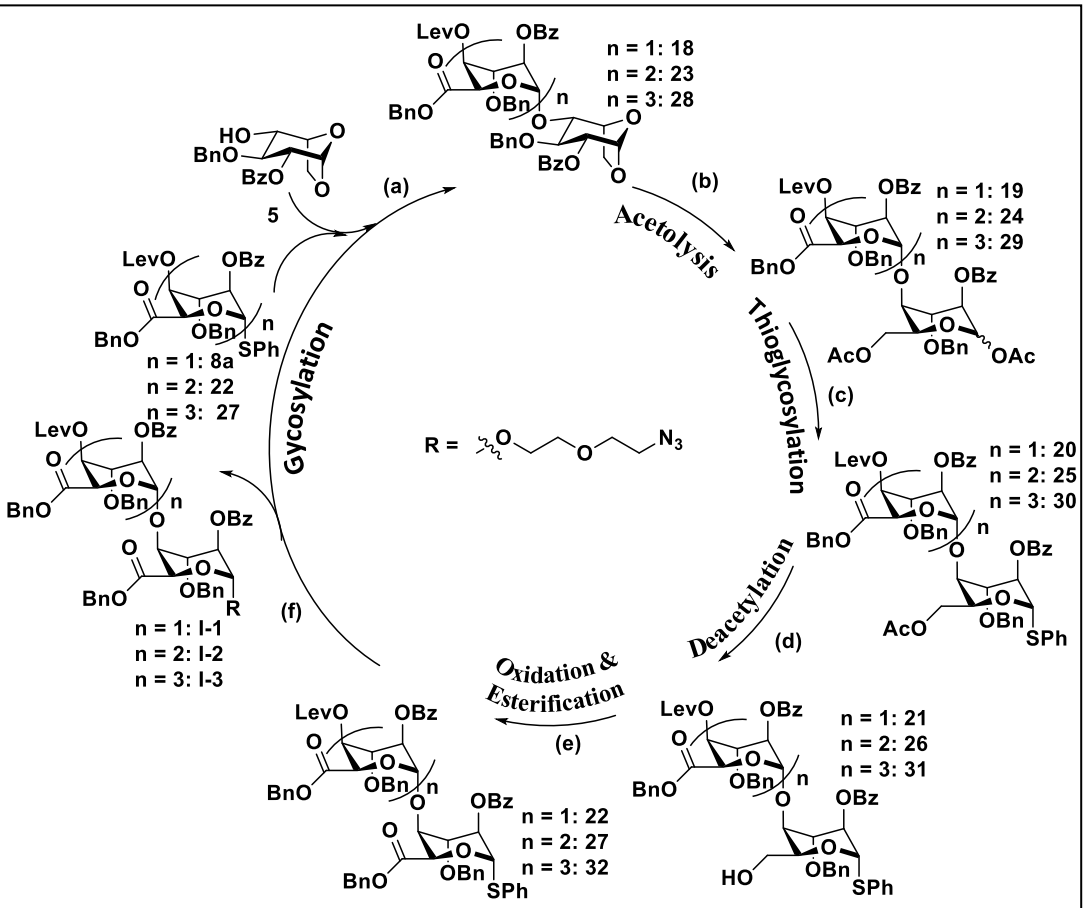

Scheme 4: Synthesis of sulfated oligo-IdoA (**I-I** to **I-3**): Reagents and conditions: a) NIS, TMSOTf, CH_2Cl_2, 4 Å M.S, -10 °C, 64% **(18)**, 62% **(23)**, 62% **(28)**; b) $Cu(OTf)_2$, AC_2O, 0 °C, 94% **(19)**, 85% **(24)**, 85% **(29)**; c) TMSSPh, ZnI_2, CH_2Cl_2, RT, 89% **(20)**, 80% **(25)**, 80% **(30)**; d) *P*-TsOH, CH_2Cl_2/MeOH(1/1), 92% **(21)**, 76% **(26)**, 66% **(31)**; e) TEMPO, BAIB, CH_2Cl_2/H_2O (1/1); BnBr, TBAI, $NaHCO_3$, DMF, 60 °C, 65% **(22)**, 63% **(27)**, 58% **(32)**; f) Azidoethoxyethanol, NIS, TfOH, 4 Å M.S, -5 °C, 81% **(I-1)**, 76% **(I-2)**, 76% **(I-3)**.

2.3 Conclusion

We report for the first time a new convergent approach for the synthesis of oligo-IdoA derivatives using an IdoA-thiophenol as the donor and a β-L-idopyranosyl derivative as the nucleophile. Sequential modifications of the L-Idose residue yielded oligo-IdoA derivatives in moderate overall yields. By using appropriate

sulfated patterns of oligo-IdoA analogues, we intend to prepare heparan sulfate mimetics that will enable systematic study of the role of IdoA conformation plasticity and, oligosaccharide secondary structures, thereby developing the ability to modulate their biological functions.

2.4 Experimental section

2.4.1 General Instructions

All chemicals were reagent grade and used as supplied except where noted. Analytical thin layer chromatography (TLC) was performed on Merck silica gel 60 F254 plates (0.25 mmol). Compounds were visualized by UV irradiation or dipping the plate in CAM/ninhydrin solution followed by heating. Column chromatography was carried out using force flow of the indicated solvent on Flukab Kieselgel 60 (230–400 mesh). ^{1}H and ^{13}C NMR spectra were recorded on Jeol 400 MHz, with cryo probe using residual solvents signals as an internal reference ($CDCl_3\delta_H$, 7.26 ppm, δ_C 77.3 ppm and CD_3OD δ_H 3.31 ppm, δ_C 49.0 ppm). The chemical shifts (δ) are reported in ppm and coupling constants (*J*) in Hz. Compound **5** was synthesized by using literature procedure. (ref. 8f).

2.5 Synthetic Procedure

2.5.1 Synthesis of Iduronic Acid Building Blocks

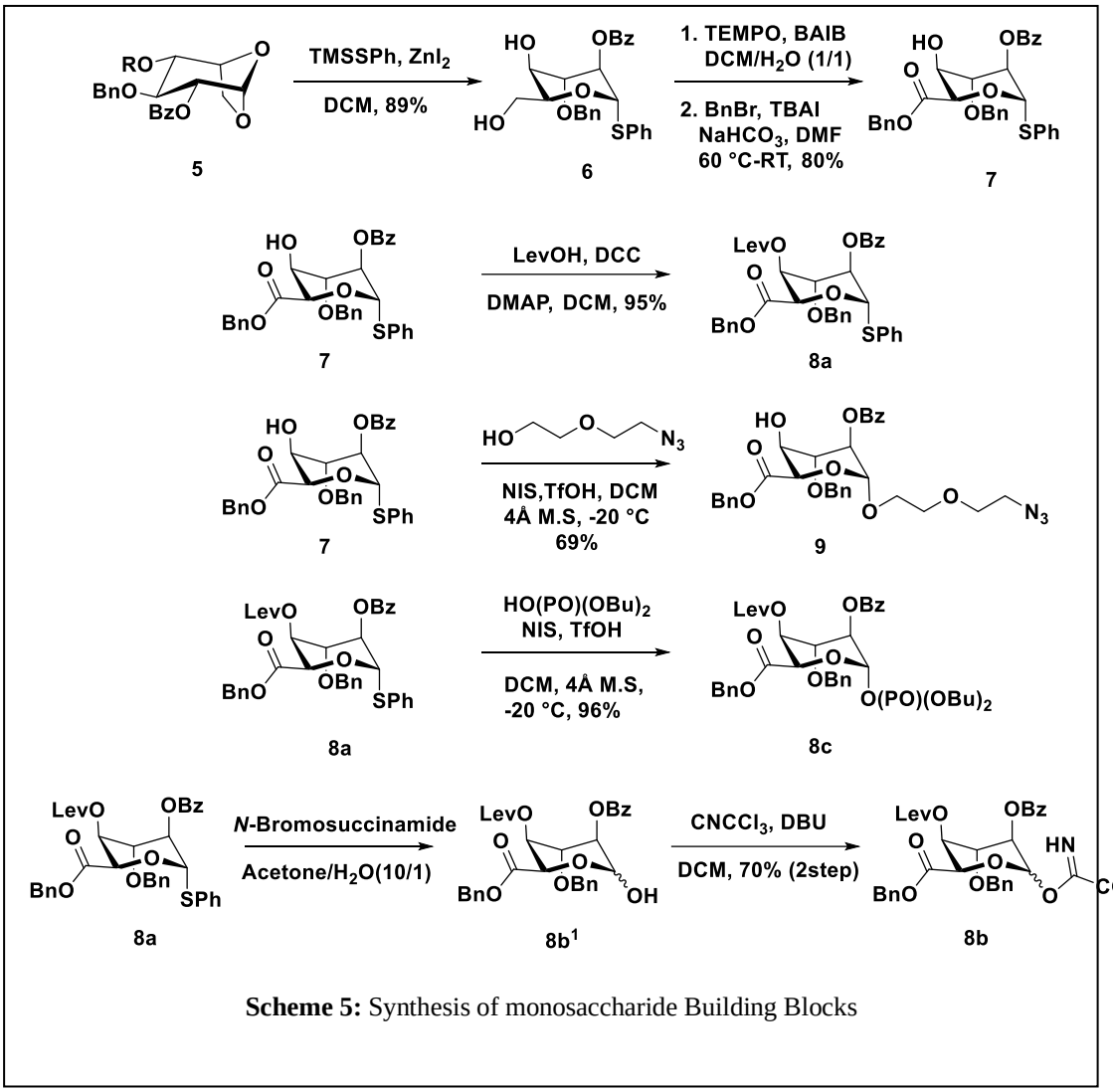

Scheme 5: Synthesis of monosaccharide Building Blocks

(2,4-O-dibenzoyl-3-O-benzyl-1,6-anhydro)-β-L-idopyranoside5a

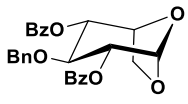

Compound **5** (2.0bg, 3.96bmmol) was dissolved in pyridine (30 mL). The reaction flask was placed in an ice. Then benzoyl chloride (2.58 ml, 2.23 mmol) was added drop wise under anhydrous condition at 0 °C. After stirring for 2h, isopropanol was added to quench the reaction. Solvents were evaporated under reduced pressure, extracted with EtOAc and 10% HCl and water. The combined organic layer washed with brine solution, dried over Na_2SO_4 and concentrated under reduced

pressure. The residue was purified by column chromatography (EtOAc/Hexane = 1/4) to afford **5a (2.2 g, 85%)** as white solid.mp 74 ºC. $[\alpha]_D^{25}$ +12.2 (*c* 1.0 $CHCl_3$); IR (cm^{-1}, $CHCl_3$): 2918, 1684, 1269, 708. ^{1}H NMR (400 MHz, Chloroform-*d*) δ 8.08 (d, *J* = 7.3 Hz, 2H), 8.01 (d, *J* = 7.2 Hz, 2H), 7.62 (q, *J* = 7.3 Hz, 2H), 7.48 (td, *J* = 7.7, 3.8 Hz, 4H), 7.17 – 7.09 (m, 5H), 5.63 (d, *J* = 1.7 Hz, 1H), 5.41 (dd, *J* = 8.4, 4.3 Hz, 1H), 5.20 (dd, *J* = 8.2, 1.8 Hz, 1H), 4.81 (t, *J* = 4.6 Hz, 1H), 4.71 (s, 2H), 4.25 (t, *J* = 8.3 Hz, 1H), 4.19 (d, *J* = 7.9 Hz, 1H), 3.80 (dd, *J* = 7.7, 5.0 Hz, 1H).^{13}C NMR (100 MHz, Chloroform-*d*) δ 165.77, 165.37, 137.66, 133.77, 133.59, 130.04, 129.88, 129.51, 129.30, 128.73, 128.62, 128.45, 127.93, 127.88, 99.52, 76.64, 74.33, 73.38, 72.90, 65.93. HRMS m/z calculated for $C_{27}H_{24}O_7H$: 461.1600**;** found**:** 461.1601.

Thiophenyl (2-O-benzoyl-3-O-benzyl)-α-L-idopyranoside6

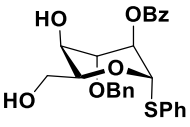

Compound **5** (9.9 g, 27.81 mmol), ZnI_2 (18.64 g, 58.39 mmol) and trimethyl(phenylthio)-silane (16.33 mL, 86.21 mmol) were dissolved in dry DCM (140 mL) under the nitrogen atmosphere and stirred at room temperature for 16 h. The reaction mixture was filtered through celite and diluted with 4N HCl, Dioxane, and water [1/1/1 (v/v/v), 60mL] mixture and stirred for 20 min. The organic layer was separated, washed with saturated $NaHCO_3$ and brine solution, dried over Na_2SO_4 and concentrated under reduced pressure. The residue was purified by flash column chromatography (EtOAc/Hexane = 1/1) to afford **6 (9.8 g, 75%)** as syrup. $[\alpha]_D^{25}$ -17.6 (*c* 1.0 $CHCl_3$); IR (cm^{-1}, $CHCl_3$): 3445, 1721, 1214.^{1}H NMR (400 MHz, Chloroform-*d*) δ 8.01 (dd, *J* = 8.3, 1.2 Hz, 3H), 7.61 – 7.55 (m, 3H), 7.47 – 7.26 (m, 10H), 5.64 (s, 1H), 5.54 (dt, *J* = 2.6, 1.3 Hz, 1H), 4.92 (d, *J* = 11.8 Hz, 1H), 4.80 (t, *J* = 5.2 Hz, 1H), 4.67 (d, *J* = 11.8 Hz, 1H), 3.99 (dd, *J* = 11.9, 6.2 Hz, 1H), 3.91 – 3.85 (m, 3H), 2.90 (d, *J* = 9.8 Hz, 1H), 2.15 (bs, 1H). ^{13}C NMR (101 MHz, Chloroform-*d*) δ 165.13, 137.33, 135.77, 133.86, 132.11, 129.86, 129.24, 128.81, 128.69, 128.19, 127.94, 127.85, 86.88, 74.11, 72.52, 70.00, 68.53, 68.33, 63.51. HRMS m/z calculated for $C_{26}H_{26}O_6SNa$:489.1348; found: 489.1342.

Benzyl(1-thiophenyl-2-O-benzoyl-3-O-benzyl)-α-L-idopyranoside uronate7

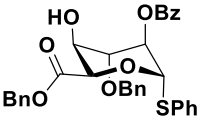

Compound **6** (9.5 g, 20.38 mmol) and [Bis(acetoxy)iodo]benzene (BAIB, 16.41g, 50.96mmol) were dissolved in mixture of water and DCM [1/1 (v/v), 180mL]. After 15 mins, 2,2,6,6-tetramethyl-1-piperidinyloxyl free

radical (TEMPO, 0.64 g, 4.07 mmol) was added at room temperature and stirred at RT for 6 h. The organic layer was washed with saturated $NH_4Cl_{(aq)}$, dried over Na_2SO_4, filtered, and concentrated under reduced pressure. The dried crude compound (9.7 g, 20.2 mmol) was dissolved in dry DMF (55 mL), benzyl bromide (4.79 mL, 40.41 mmol), tetrabutylammonium iodide (TBAI, 3.73 g, 10.10 mmol), $NaHCO_3$ (2.54 g, 30.31 mmol) were added. The reaction mixture was heated at 60°C for 4 h. Then organic layer was washed with brine solution (3x20mL), dried over Na_2SO_4, filtered, and concentrated under reduced pressure. The residue was purified by flash column chromatography (EtOAc/Hexane = 1/4) to afford **7 (10.2 g, 88%)** as syrup. $[\alpha]_D^{25}$ -39.1 (*c* 1.0 $CHCl_3$); IR (cm^{-1}, $CHCl_3$): 2919, 1725, 1453, 1215.^{1}H NMR (400 MHz, Chloroform-*d*) δ 7.98 (dd, *J* = 8.3, 1.2 Hz, 2H), 7.61 – 7.53 (m, 3H), 7.46 – 7.42 (m, 4H), 7.40 – 7.26 (m, 11H), 5.75 (s, 1H), 5.51 (dt, *J* = 2.6, 1.2 Hz, 1H), 5.46 (d, *J* = 1.7 Hz, 1H), 5.36 (d, *J* = 12.3 Hz, 1H), 5.23 (d, *J* = 12.3 Hz, 1H), 4.92 (d, *J* = 11.8 Hz, 1H), 4.69 (d, *J* = 11.8 Hz, 1H), 4.21 – 4.17 (m, 1H), 3.95 (td, *J* = 2.9, 1.2 Hz, 1H), 2.87 (d, *J* = 11.7 Hz, 1H).^{13}C NMR (101 MHz, Chloroform-*d*) δ 169.04, 164.95, 136.95, 135.46, 135.31, 133.81, 131.52, 129.78, 129.10, 128.86, 128.67, 128.63, 128.59, 128.44, 128.26, 128.15, 127.91, 127.70, 86.82, 73.70, 72.56, 69.66, 69.00, 68.25, 67.10.HRMS m/z calculated for $C_{33}H_{30}O_7SNa$:593.1610; found: 593.1604.

Benzyl (1-thiophenyl-2-O-benzoyl-3-O-benzyl-4-O-levulinoyl)-α-L- idopyranoside uronate 8a

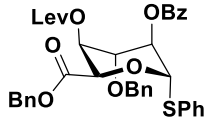

Compound **7** (8.5 g, 14.91 mmol) was dissolved in dry DCM (80 mL), levulinic acid (1.66 mL, 17.89 mmol), *N*,*N*-dicycohexylcarbodiimide (5.37 g, 26.09 mmol) and catalytic amount of 4- dimethylaminopyridine (0.91 g, 0.45 mmol) were added. The reaction mixture was stirred at room temperature for 4 h. The reaction mixture was filtered through celite and washed with saturated $NaHCO_3$ and brine solution respectively. The organic layer was dried over Na_2SO_4, filtered, and concentrated under reduced pressure. The residue was purified by flash column chromatography (EtOAc/Hexane = 1/3) to afford **8a (8.8 g, 88%)** as syrup. $[\alpha]_D^{25}$ -31.2 (*c* 1.0 $CHCl_3$); IR (cm^{-1}, $CHCl_3$): 3020, 1719, 1214.^{1}H NMR (400 MHz, Chloroform-*d*) δ 8.05 (dd, *J* = 8.4, 1.3 Hz, 2H), 7.58 – 7.52 (m, 3H), 7.47 – 7.43 (m, 3H), 7.41 – 7.34 (m, 8H), 7.33 – 7.22 (m, 5H), 5.78 (s, 1H), 5.50 (d, *J* = 2.0 Hz, 1H), 5.41 (dt, *J* = 2.4, 1.1 Hz, 2H), 5.35 – 5.32 (m, 2H), 5.15 (d, *J* = 12.0 Hz,

1H), 4.91 (d, *J* = 11.7 Hz, 1H), 4.78 (d, *J* = 11.7 Hz, 1H), 3.96 (td, *J* = 2.8, 1.1 Hz, 2H), 2.47 (t, *J* = 6.4 Hz, 2H), 2.33 – 2.25 (m, 1H), 2.23 – 2.155 (m, 1H),), 2.05 (s, 3H). ^{13}C NMR (101 MHz, Chloroform-*d*) δ 205.90, 171.63, 168.12, 165.30, 137.09, 135.59, 135.37, 133.72, 131.48, 130.01, 129.39, 129.18, 129.01, 128.71, 128.63, 128.53, 128.14, 127.81, 127.69, 86.45, 73.03, 71.94, 68.89, 67.95, 67.37, 66.99, 37.78, 29.73, 27.85. HRMS m/z calculated for $C_{38}H_{36}O_9SNa$:691.1978; found: 669.1972.

Benzyl(2-O-benzoyl-3-O-benzyl-4-O-levulinoyl)-α/β-L-idopyranoside uronate8b[1]

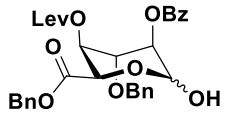

Compound **8a** (1.2 g, 1.79 mmol) was dissolved in 9:1 ratio of acetone and water (25mL). To this reaction mixture *N*-bromosuccinimide (1.59 g, 8.98 mmol) was added at 0 °C and stirred vigorously for 1h. After the completion of reaction, organic layer was washed with $Na_2S_2O_3$ solution, followed by $NaHCO_3$ solution, brine solution and dried over Na_2SO_4, then filtered and concentrated under reduced pressure. The residue was purified by column chromatography (EtOAc/Hexane = 1/2) to afford **8b[1] (0.98 g, 95%)** as syrup. $[\alpha]_D^{25}$ +129 (*c* 1.0 $CHCl_3$); IR (cm^{-1}, $CHCl_3$): 3423, 1718, 1601.^{1}H NMR (400 MHz, Chloroform-*d*) δ 8.13 – 8.05 (m, 3H), 7.57 (ddt, *J* = 7.4, 5.8, 1.3 Hz, 2H), 7.45 – 7.30 (m, 21H), 5.45 (d, *J* = 9.1 Hz, 1H), 5.32 (t, *J* = 2.7 Hz, 1H), 5.30 – 5.28 (m, 2H), 5.26 (d, *J* = 5.3 Hz, 2H), 5.21 (d, *J* = 1.9 Hz, 2H), 5.18 (d, *J* = 1.9 Hz, 1H), 5.15 – 5.13 (m, 1H), 5.07 (dt, *J* = 5.0, 1.9 Hz, 2H), 4.82 – 4.76 (m, 4H), 4.37 (dd, *J* = 23.0, 9.3 Hz, 1H), 4.09 – 4.06 (m, 2H), 3.84 – 3.66 (m, 1H), 2.43 (td, *J* = 6.7, 2.4 Hz, 2H), 2.38 (t, *J* = 6.7 Hz, 2H), 2.24 – 2.07 (m, 4H), 2.04 (s, 3H), 2.00 (d, *J* = 1.3 Hz, 2H).^{13}C NMR (101 MHz, Chloroform-*d*) δ 205.80, 205.72, 171.66, 171.58, 168.13, 167.41, 165.71, 165.29, 136.97, 136.35, 135.34, 135.28, 133.81, 133.73, 130.07, 130.02, 129.23, 129.05, 128.82, 128.67, 128.62, 128.51, 128.3, 128.15, 127.88, 93.19, 92.20, 73.81, 73.38, 73.31, 72.74, 72.37, 68.31, 67.41, 67.35, 67.14, 67.07, 66.60, 65.61, 37.69, 29.64, 29.58, 27.73..HRMS m/z calculated for $C_{32}H_{32}O_{10}Na$:599.1893; found: 599.1887.

Benzyl(2-O-benzoyl-3-O-benzyl-4-O-levulinoyl)-α/β-L-idopyranoside trichloroacetimidate 8b

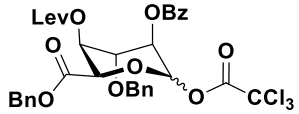

Compound **8b**[1] (0.89 g, 1.55 mmol), trichloroacetonitrile (2.32 mL, 23.17 mmol) and 1,8 diazabicyclo[5.4.0]undec-7-ene (DBU) (0.094 mL, 0.62 mmol) were dissolved in DCM (15 mL) under nitrogen atmosphere and stirred at RT for 2 h. The reaction mixture was quenched with triethylamine and solvent was evaporated under reduced pressure. The residue was purified by flash column chromatography (EtOAc/Hexane = 1/2) to afford anomeric mixture **8b (0.9 g, 81%)** as syrup. $[\alpha]_D^{25}$ +23.5 (*c* 1.0 $CHCl_3$); IR (cm^{-1}, $CHCl_3$): 3020, 1720, 1214, 745.^{1}H NMR (400 MHz, Chloroform-*d*) δ 8.73 (s, 1H), 8.09 (dd, *J* = 8.3, 1.4 Hz, 2H), 7.62 – 7.56 (m, 1H), 7.47 – 7.42 (m, 2H), 7.39 – 7.27 (m, 12H), 6.57 (s, 1H), 5.37 (dt, *J* = 2.3, 1.1 Hz, 1H), 5.35 (ddt, *J* = 3.0, 1.9, 0.9 Hz, 1H), 5.29 (d, *J* = 11.9 Hz, 1H), 5.17 (d, *J* = 12.0 Hz, 1H), 5.13 (d, *J* = 2.0 Hz, 1H), 4.85 (d, *J* = 11.6 Hz, 1H), 4.75 (d, *J* = 11.6 Hz, 1H), 3.99 (td, *J* = 2.8, 2.3, 1.4 Hz, 1H), 2.48 – 2.44 (m, 2H), 2.30 – 2.16 (m, 2H), 2.04 (s, 3H).^{13}C NMR (101 MHz, Chloroform-*d*) δ 205.78, 171.56, 167.45, 165.05, 160.15, 137.14, 135.21, 133.84, 130.04, 129.11, 129.06, 128.68, 128.65, 128.58, 128.43, 127.99, 127.78, 95.10, 72.73, 71.66, 67.84, 67.51, 67.46, 65.18, 37.72, 29.66, 27.77.HRMS m/z calculated for $C_{33}H_{30}O_7SNa$:742.0989; found: 742.0985.

Benzyl(2-O-benzoyl-3-O-benzyl-4-O-levulinoyl)-α-L-idopyranoside dibutylphosphomidate 8c

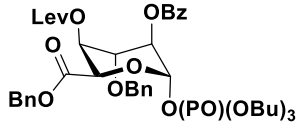

Compound **8a** (0.45 g, 0.67 mmol), dibutyl phosphate (0.41 mL, 2.02 mmol) and freshly dried 4 Å molecular sieves were dissolved in dry DCM (20 mL) and stirred at RT for 1 h. To this solution, *N*-Iodosuccinimide (0.23 g, 1.01 mmol), TfOH (11.92 µl, 0.14 mmol) was added at RT and monitored the reaction by using TLC. After the completion of reaction, the reaction mixture was quenched with triethylamine and filtered through celite. The filtrate was washed with $Na_2S_2O_3$ followed by $NaHCO_3$, brine solution, dried over Na_2SO_4 and concentrated under reduced pressure. The residue was purified by column chromatography (EtOAc/Hexane = 1/3) to afford **8c (0.47 g, 92%)** as syrup. $[\alpha]_D^{25}$ + 26.2 (*c* 1.0 $CHCl_3$); IR (cm^{-1}, $CHCl_3$): 2960, 2928, 2873, 1720, 1028. ^{1}H NMR (400 MHz, Chloroform-*d*) δ 8.06 (dd, *J* = 8.2, 1.1 Hz, 2H), 7.59l – 7.55 (m, 1H), 7.43 (t, *J* = 7.8 Hz, 2H), 7.39 – 7.27 (m, 10H), 5.96 (d, *J* = 6.9 Hz, 1H), 5.31 (s, 1H), 5.28

(d, *J* = 12.0 Hz, 1H), 5.24 (s, 1H), 5.17 (d, *J* = 11.9 Hz, 1H), 5.11 (d, *J* = 2.0 Hz, 1H), 4.83 (d, *J* = 11.6 Hz, 1H), 4.74 (d, *J* = 11.6 Hz, 1H), 4.11 – 3.96 (m, 4H), 3.94 (t, *J* = 3.0 Hz, 1H), 2.47 – 2.43 (m, 2H), 2.20 (qt, *J* = 17.1, 6.5 Hz, 2H), 2.04 (s, 3H), 1.58 (dq, *J* = 13.8, 6.7 Hz, 4H), 1.33 (dp, *J* = 14.9, 7.5 Hz, 4H), 0.90 – 0.85 (m, 2H). ^{13}C NMR (101 MHz, Chloroform-*d*) δ 205.80, 190.88, 171.54, 167.43, 164.94, 137.23, 135.22, 133.79, 129.99,129.04, 128.68, 128.65, 128.56, 128.49, 128.01, 127.71, 95.19, 95.14, 72.68, 71.83, 68.12, 67.43, 67.11, 66.40, 66.31, 37.70, 32.31 – 32.14 (m), 29.66, 27.76, 18.66, 13.65. HRMS m/z calculated for $C_{40}H_{49}O_{13}PNa$: 791.2808; found: 791.1816

Ethoxy-2-azidoethoxyl -O-(benzyl(2-O-benzoyl-3-O-benzyl))-α-L-idopyranoside uronte9

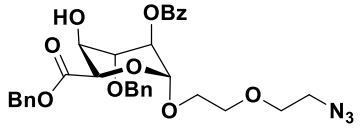

Compound **7** (1.07 g, 1.87 mmol), 2-(2-azidoethoxy)ethan-1-ol (0.29 g, 2.25 mmol) and freshly dried 4 Å molecular sieves were dissolved in dry DCM (20 mL) and stirred at RT for 1 h. Then *N*-iodosuccinimide (0.63 g, 2.81 mmol), TMSOTf (0.067 mL, 0.375 mmol) were added at -5°C and stirred for 30 min. After the completion of reaction, the reaction mixture was quenched with triethylamine and filtered through celite. The organic layer was washed with $Na_2S_2O_3$ followed by $NaHCO_3$, brine solution and dried over Na_2SO_4, then filtered and concentrated under reduced pressure. The residue was purified by column chromatography (EtOAc/Hexane = 1/4) to afford **9 (0.86 g, 78%)** as syrup. $[\alpha]_D^{25}$-5.2 (*c* 1.0 $CHCl_3$); IR (cm^{-1}, $CHCl_3$): 3020, 2010, 1724, 1214.^{1}H NMR (400 MHz, Chloroform-*d*) δ 8.00 (dd, *J* = 8.3, 1.4 Hz, 2H), 7.62 – 7.57 (m, 1H), 7.48 – 7.43 (m, 2H), 7.40 – 7.28 (m, 10H), 5.32 (d, *J* = 12.3 Hz, 1H), 5.27 – 5.26 (m, 1H), 5.24 (d, *J* = 12.3 Hz, 1H), 5.17 (s, 1H), 5.02 (d, *J* = 1.7 Hz, 1H), 4.84 (d, *J* = 11.6 Hz, 1H), 4.65 (d, *J* = 11.6 Hz, 1H), 4.16 – 4.12 (m, 1H), 3.98 – 3.93 (m, 1H), 3.89 (td, *J* = 3.0, 1.3 Hz, 1H), 3.76 – 3.67 (m, 3H), 3.63 – 3.53 (m, 2H), 3.19 (t, *J* = 5.0 Hz, 2H), 2.80 (d, *J* = 11.6 Hz, 1H). ^{13}C NMR (101 MHz, Chloroform-*d*) δ 169.54, 165.11, 137.70, 135.49, 133.84, 129.89, 129.14, 128.77, 128.73, 128.55, 128.52, 128.44, 128.02, 127.88, 99.00, 74.75, 72.16, 70.33, 70.25, 68.48, 68.29, 67.96, 67.47, 67.17, 50.83. HRMS m/z calculated for $C_{31}H_{33}N_3O_9Na$:614.2214; found: 614.2120.

2.5.2 Reaction for the Synthesis of Disaccharide

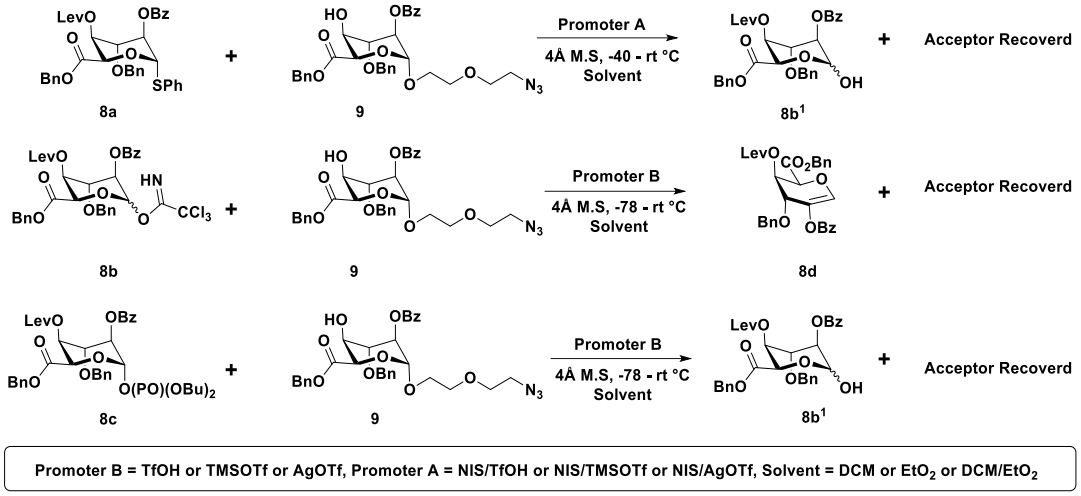

Scheme 6: Synthesis for the Disaccharide.

Benzyl (2-O-denzoyl-3-O-benzyl-4-O-levulinoyl)-1,2-dehydro-α-L-idopyranete 8d

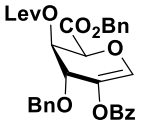

Compound **9** (0.159 g, 0,265 mmol), Compound **8c** (0.285 g, 0.372 mmol) were mixed and co-evaporated with toluene, dried over high vacuum for 2 and freshly dried 4 Å molecular sieves were added. Dissolved in dry DCM (40 mL) and stirred at RT for 1 h. Then the reaction mixture was cooled to -78 °C (different temperature -40 °C, -20 °C), TMSOTf or AgOTf (0.067 mL, 0.372 mmol) was added, and gradually increased the temperature and monitored the reaction using TLC. After the consumption of donor, the reaction was quenched with Et_3N and diluted with DCM. The molecular sieves were filtered using celite bed and organic layer was washed by $NaHCO_3$, brine solution and dried over Na_2SO_4, filtered and concentrated under reduced pressure. The residue was purified by column chromatography (EtOAc/Hexane = 1/4) to afford **8d (0.052 g, 32%)** as white solid.mp 96 ºC. $[\alpha]_D^{25}$-36.4 (*c* 1.0 $CHCl_3$); IR (cm^{-1}, $CHCl_3$): 3020, 1740, 1159. ^1H NMR (400 MHz, Chloroform-*d*) δ 7.95 – 7.92 (m, 2H), 7.61 – 7.56 (m, 1H), 7.45 – 7.34 (m, 7H), 7.26–7.24 (m, 2H), 7.08 (m, 3H), 6.90 (s, 1H), 5.45 (t, *J* = 4 Hz,1H), 5.27 (dd, *J* = 12 Hz, 2H) 4.75 (d, *J* = 12.2 Hz, 1H), 4.72 (d, *J* = 1.1 Hz, 1H), 4.66 (d, *J* = 12.3 Hz, 1H), 4.03 (d, *J* = 2.2 Hz, 1H), 2.67 (t, *J* = 6.6 Hz, 2H), 2.55 – 2.41 (m, 2H), 2.16 (s, 3H).^{13}C NMR (101 MHz, CHLOROFORM-*D*) δ 206.34, 171.66, 166.88, 165.11, 138.97, 137.42,

135.14, 133.66, 130.21, 130.17, 129.13, 128.98, 128.77, 128.54, 128.46, 128.21, 127.95, 71.58, 68.98, 68.64, 67.83, 37.97, 29.81, 28.11.HRMS m/z calculated for $C_{32}H_{30}O_9Na$:581.1788; found: 581.1785.

2.5.3 Synthesis of Iduronic Acid Disaccharide

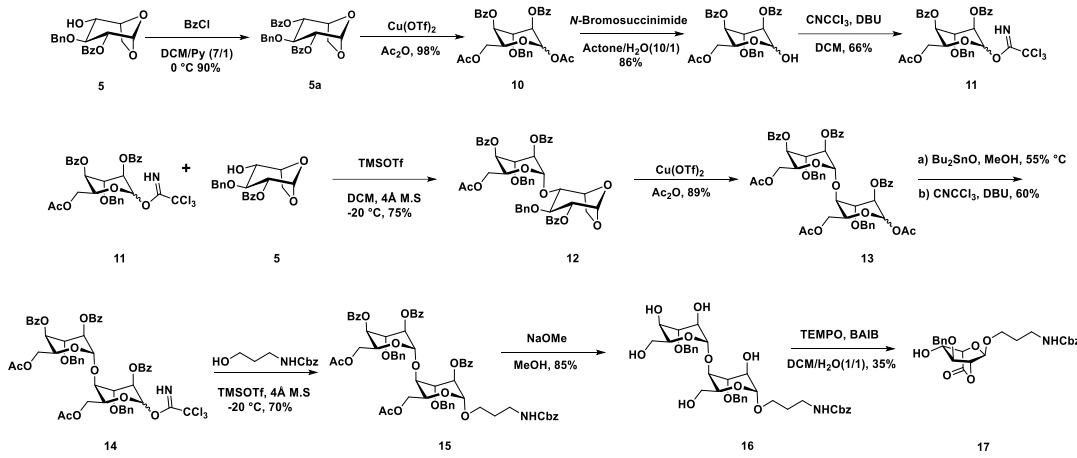

Scheme 7: Disaccharide Synthesis

(1,6-O-diacetyl-2,4-O-dibenzoyl-3-O-benzyl)-α-L-idopyranoside 10

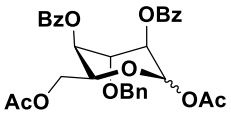

Compound **5a** (1.75 g, 4.35 mmol) was dissolved in acetic anhydride (15 mL) and stirred for few min at 0 °C, under nitrogen atmosphere. After 15 min copper trifluromethanesulfonate (0.045 g, 0.435 mmol) was added. Allow the reaction flask to stir for another 16 h, quench the reaction with $NaHCO_3$ and residue was extracted with EtOAc and the organic layer washed with water and brine solution, dried over Na_2SO_4 and concentrated under reduced pressure. The residue was purified by flash column chromatography (EtOAc/Hexane = 1/4) to afford anomeric mixture **10 (1.74 g, 82%, α:β = 1:0.5)** as syrup. $[\alpha]_D^{25}$+ 52.9 (*c* 1.0 $CHCl_3$); IR (cm^{-1}, $CHCl_3$): 1725, 1214, 726 ^{1}H NMR (400 MHz, Chloroform-*d*) δ 8.04 – 8.00 (m, 3H), 7.93 (d, *J* = 7.2 Hz, 1H), 7.84 (d, *J* = 7.2 Hz, 2H), 7.58 – 7.51 (m, 2H), 7.49 – 7.29 (m, 13H), 7.22 – 7.13 (m, 3H), 6.30 (s, 1H), 6.26 (d, *J* = 1.7 Hz, 0.5H), 5.36(s, 0.5H), 5.24 (s, 2H), 5.19 (s, 0.5), 4.90 – 4.81 (m, 3H), 4.72 (t, *J* = 6.3 Hz, 1H), 4.58 (td, *J* = 6.3, 1.7 Hz, 0.5H), 4.37 – 4.26 (m, 3H), 4.21 (t, *J* = 3.0 Hz, 0.5H), 4.11 (s, 1H), 2.14 (s, 3H), 2.09 (s, 1H), 2.03 (s, 4H). ^{13}C NMR

(100 MHz, Chloroform-*d*) δ 170.70, 170.67, 170.13, 169.50, 169.00, 168.81, 165.54, 165.04, 137.54, 137.01, 133.81, 133.66, 130.08, 129.98, 129.54, 129.27, 128.71, 128.65, 128.62, 128.56, 128.55, 128.34, 128.07, 127.94, 127.61, 91.54, 90.58, 73.75, 73.22, 72.55, 72.07, 71.91, 71.74, 66.95, 66.80, 66.53, 66.30, 66.11, 65.88, 65.76, 62.76, 62.45, 62.38, 21.06, 20.97, 20.87, 20.80. HRMS m/z calculated for $C_{31}H_{30}O_{10}Na$: 585.1737**;** found**:** 585.1736.

(6-O-diacetyl-2,4-O-dibenzoyl-3-O-benzyl)-α-L-idopyranoside tricholoroacetimidate 11

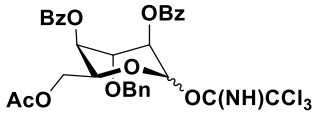

Compound **10** (1.74 g, 3.06 mmol) was dissolved in dry methanol (18mL) and dibutyltinoxide (1.54 g, 6.19 mmol) was added, under nitrogen atmosphere, the resulting solution kept at 55 °C. Allow the reaction flask stirred for another 2 h, evaporated the methanol under reduced pressure. The residue was purified by flash column chromatography (EtOAc/Hexane = 1/4) to afford anomeric deacetalated product **(1.1g, 68%, α:β = 1:0.9)** as white sticky solid. ^{1}H NMR (400 MHz, Chloroform-*d*) δ 8.00 (dd, *J* = 8.3, 1.2 Hz, 2H), 7.94 (ddd, *J* = 6.9, 5.9, 1.2 Hz, 4H), 7.84 (dd, *J* = 8.2, 1.3 Hz, 2H), 7.56 – 7.51 (m, 1H), 7.50 – 7.44 (m, 1H), 7.42-7.39 (m, 8H), 7.38 – 7.33 (m, 3H), 7.31-7.27 (m, 2H), 7.25 (s, 1H), 7.23 (d, *J* = 1.6 Hz, 1H), 7.21 (s, 1H), 7.18 (d, *J* = 7.8 Hz, 1H), 7.14 (d, *J* = 7.7 Hz, 1H), 5.37 – 5.32 (m, 2H), 5.24 – 5.23 (m, 2H), 5.15 (t, *J* = 1.7 Hz, 1H), 5.12 – 5.11 (m, 1H), 4.89 (s, 2H), 4.85 (s, 2H), 4.76 – 4.72 (m, 1H), 4.52 – 4.45 (m, 2H), 4.39 – 4.30 (m, 4H), 4.25 – 4.22 (m, 2H), 3.77 – 3.70 (m, 1H), 2.05 (s, 3H), 2.04 (s, 3H). ^{13}C NMR (100 MHz, Chloroform-*d*) δ 170.77, 170.76, 166.07, 165.79, 165.72, 165.44, 137.17, 136.48, 133.51, 133.40, 133.35, 129.96, 129.94, 129.89, 129.86, 129.13, 129.09, 129.04, 129.00, 128.83, 128.65, 128.58, 128.46, 128.34, 128.26, 128.24, 128.22, 128.14, 127.83, 92.78, 92.27, 74.03, 73.73, 73.25, 72.57, 71.59, 68.86, 67.09, 66.84, 66.59, 63.33, 63.18, 63.08, 31.64, 22.71, 20.83, 20.81, 14.20. HRMS m/z calculated for $C_{29}H_{28}O_{9}Na$: 543.1631**;** found**:** 543.1629. Anomeric deacetylated producnt (1.05 g, 3.06 mmol) was dissolved in DCM (18mL), trichloroacetonitrile (3.07 ml 30.28 mmol) and 1,8 Diazabicyclo[5.4.0]undec-7-en (DBU) (1.54 g, 6.19 mmol) were added, under nitrogen atmosphere, After stirring for 2 h, triethylamine was added to quench the reaction, evaporated the DCM under reduced pressure. The residue was purified by flash column chromatography (EtOAc/Hexane = 1/2) to afford anomeric

mixture **11 (1.07 g, 79%, α:β = 1:0.15)** as syrup. $[\alpha]_D^{25}$+28.1 (*c* 1.0 $CHCl_3$); IR (cm^{-1}, $CHCl_3$): 1720, 744, 667. ^{1}H NMR (100 MHz, Chloroform-*d*) δ 8.76 (s, 1H), 8.07 - 8.05 (m, 2H), 8.01 - 7.96 (m, 1H), 7.88 - 7.83 (m, 2H), 7.60 - 7.55 (m, 1H), 7.47 - 7.42 (m, 3H), 7.40 - 7.3 2 (m, 5H), 7.33 - 7.29 (m, 2H), 7.16 - 7.12 (m, 2H), 6.51 (s, 1H), 5.45 (dt, *J* = 2.2, 1.1 Hz, 1H), 5.27 (ddd, *J* = 2.6, 1.7, 0.9 Hz, 1H), 4.96 (d, *J* = 11.6 Hz, 1H), 4.88 - 4.85 (m, 1H), 4.82 (d, *J* = 11.6 Hz, 1H), 4.34 (d, *J* = 6.2 Hz, 2H), 4.18 - 4.16 (m, 1H), 2.00 (s, 3H). ^{13}C NMR (100 MHz, Chloroform-*d*) δ 170.60, 165.69, 165.26, 160.64, 137.36, 133.61, 133.51, 130.04, 129.92, 129.26, 128.80, 128.66, 128.56, 128.48, 128.30, 128.06, 127.98, 127.70, 94.92, 91.10, 72.61, 72.04, 67.00, 66.36, 65.92, 62.92, 20.80. HRMS m/z calculated for $C_{31}H_{28}Cl_3NO_9Na$: 686.0727**;** found**:** 686.0728.

(6-O-acetyl-2,4-O-dibenzoyl-3-O-benzyl)-α-L-idopyrosyl-α(1→4) (2-O-benzoyl-3-O-benzyl-1,6-anhydro)-β-L-idopyranose 12

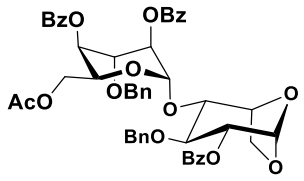

Compound **11** (0.86 g, 1.29 mmol), Compound **5** (0.46 g, 1.29 mmol), was dissolved in dry DCM (24 mL), and freshly dried 4 Å molecular sieves, were added under anhydrous conditions. After stirring for 1hr at RT, the reaction mixture was cooled to -78°C. TMSOTf (0.046 mL, 0.26 mmol) was added and monitored the reaction using TLC. After the completion of reaction, quenched with triethylamine and diluted with DCM. Filtered the molecular sieves using celite filter and washed with $NaHCO_3$, dried over Na_2SO_4, filtered and concentrated under reduced pressure. The residue was purified by column chromatography (EtOAc/Hexane = 1/4) to afford **12 (0.64 g, 59%)** as syrup. $[\alpha]_D^{25}$+ 36.7 (*c* 1.0 $CHCl_3$); IR (cm^{-1}, $CHCl_3$): 2804, 1720, 1452. ^{1}H NMR (400 MHz, Chloroform-*d*) δ 8.09 – 8.06 (m, 2H), 7.99 – 7.98 (m, 2H), 7.80 (dd, *J* = 8.4, 1.4 Hz, 2H), 7.61 – 7.55 (m, 2H), 7.48 – 7.37 (m, 9H), 7.34 – 7.30 (m, 1H), 7.15 – 7.10 (m, 5H), 7.06 – 7.03 (m, 2H), 5.55 (d, *J* = 1.8 Hz, 1H), 5.20 (s, 1H), 5.18 – 5.17 (m, 1H), 5.15 – 5.14 (m, 1H), 5.05 (dd, *J* = 8.3, 1.8 Hz, 1H), 4.89 – 4.82 (m, 2H), 4.77 (td, *J* = 6.4, 6.0, 1.5 Hz, 1H), 4.70 (t, *J* = 4.5 Hz, 1H), 4.62 (d, *J* = 11.1 Hz, 1H), 4.54 (d, *J* = 11.1 Hz, 1H), 4.28 (d, *J* = 7.8 Hz, 1H), 4.26 – 4.24 (m, 1H), 4.11 – 4.07 (m, 3H), 3.95 (t, *J* = 8.4 Hz, 1H), 3.85 (ddd, *J* = 7.8, 5.1, 1.2 Hz, 1H), 1.92 (s, 3H). ^{13}C NMR (101 MHz, $CDCl_3$) δ 170.68, 165.89, 165.80, 165.65, 138.08, 137.42, 133.60, 133.55, 133.43, 130.06, 129.97, 129.88, 129.54, 129.47, 128.97, 128.67, 128.61, 128.51, 128.35, 128.28, 128.24, 128.17, 127.95, 127.60, 99.52, 95.14, 78.10,

76.99, 75.21, 72.98, 72.94, 71.97, 67.56, 67.47, 65.72, 64.26, 63.09, 20.82. HRMS m/z calculated for $C_{49}H_{40}O_{14}Na$: 881.2785**;** found**:** 881.2785.

(6-O-acetyl-2,4-O-dibenzoyl-3-O-benzyl)-α-L-idopyranosyl-α(1→4) (1,6-O-diacetyl-2-O-benzoyl-3-O-benzyl)-α-L-idopyranoside 13

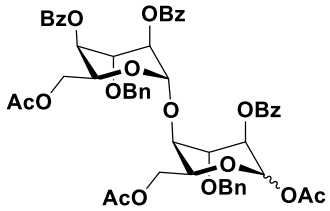

The synthetic procedure for the preparation of compound **10** was followed to obtain compound **13** (**78%, α:β = 1:0.6)** from compound **12** as syrup. $[\alpha]_D^{25}$-31.3 (*c* 1.0 $CHCl_3$); IR (cm^{-1}, $CHCl_3$): 1721, 1601, 1234. ^{1}H NMR (400 MHz, Chloroform-*d*) δ 8.03 (dd, *J* = 9.3, 7.7 Hz, 5H), 7.89 – 7.87 (m, 2H), 7.79 (ddd, *J* = 9.8, 8.2, 1.3 Hz, 3H), 7.63 – 7.60 (m, 3H), 7.58 – 7.49 (m, 4H), 7.47 – 7.21 (m, 24H), 7.12 (dt, *J* = 11.9, 7.7 Hz, 4H), 6.31 (s, 1H), 6.26 (d, *J* = 2.3 Hz, 1H), 5.54 (dd, *J* = 4.4, 2.3 Hz, 1H), 5.46 (d, *J* = 4.0 Hz, 1H), 5.28 (s, 1H), 5.22 (d, *J* = 2.2 Hz, 1H), 5.16 (s, 1H), 5.13 (s, 1H), 4.94 (dd, *J* = 11.3, 8.5 Hz, 3H), 4.81 – 4.73 (m, 5H), 4.67 (s, 2H), 4.63 – 4.54 (m, 3H), 4.50 (dd, *J* = 6.9, 2.3 Hz, 3H), 4.36 (t, *J* = 4.2 Hz, 1H), 4.23 (d, *J* = 5.9 Hz, 1H), 4.07 (d, *J* = 2.6 Hz, 1H), 4.03 (d, *J* = 3.0 Hz, 1H), 4.01 – 3.97 (m, 1H), 3.95 – 3.91 (m, 2H), 3.60 (dd, *J* = 11.7, 4.0 Hz, 1H), 3.42 (dd, *J* = 11.8, 3.9 Hz, 1H), 2.15 (s, 3H), 2.12 (s, 5H), 2.11 (s, 2H), 1.97 (s, 3H), 1.91 (s, 2H). ^{13}C NMR (101 MHz, CHLOROFORM-*D*) δ 170.93, 170.83, 170.73, 170.68, 169.16, 169.05, 166.12, 165.66, 165.51, 165.38, 165.36, 137.76, 137.32, 137.28, 137.25, 133.64, 133.49, 133.42, 130.24, 130.02, 129.85, 129.34, 129.22, 129.01, 128.83, 128.67, 128.62, 128.59, 128.49, 128.39, 128.33, 128.28, 128.20, 128.10, 128.04, 127.90, 127.53, 101.90, 100.92, 91.92, 90.77, 76.31, 75.56, 74.53, 73.68, 73.01, 72.77, 72.65, 72.40, 68.01, 67.93, 67.33, 66.99, 66.88, 66.57, 66.54, 64.44, 64.16, 63.56, 63.45, 62.87, 62.46, 21.17, 21.09, 21.02, 20.68. HRMS m/z calculated for $C_{53}H_{52}O_{17}Na$: 983.3102**;** found**:** 983.3102.

(6-O-acetyl-2,4-O-dibenzoyl-3-O-benzyl)-α-L-idopyranosyl-α(1→4) (6-O-acetyl-2-O-benzoyl-3-O-benzyl)-α-L-idopyranoside tricholoroacetimidate 14

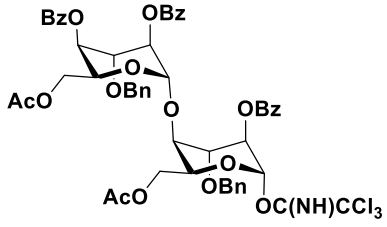

The preparation of compound **14 (78%)** was carried out from compound **13** according to the procedure for synthesizing compound **11**. Anomeric deacetylated product (**55%, α:β = 1:1)** as syrup. $[\alpha]_D^{25}$-20.8 (*c* 1.0 $CHCl_3$); IR (cm^{-1}, $CHCl_3$): 3226. 1721, 1214, 746. ^1H NMR (400 MHz, Chloroform-*d*) δ 7.95 – 7.91 (m, 4H), 7.87 – 7.84 (m, 4H), 7.70 – 7.67 (d, 4H), 7.53 – 7.44 (m, 7H), 7.43 – 7.38 (m, 3H), 7.37 – 7.27 (m, 16H), 7.25 – 7.12 (m, 14H), 7.02 (td, *J* = 8.2, 2.7 Hz, 5H), 5.33 (t, *J* = 2.4 Hz, 1H), 5.28 (t, J = 2.4 Hz, 1H), 5.24 – 5.19 (m, 2H), 5.14 – 5.12 (m, 2H), 5.00 (s, 2H), 4.82 (d, *J* = 2.6 Hz, 1H), 4.79 – 4.78 (m, 2H), 4.76 (d, *J* = 4.0 Hz, 2H), 4.69 – 4.66 (m, 2H), 4.64 (d, *J* = 3.6 Hz, 3H), 4.61 (s, 1H), 4.57 – 4.56 (s, 1H), 4.52 (td, *J* = 6.5, 2.3 Hz, 1H), 4.47 – 4.35 (m, 7H), 4.26 (dt, *J* = 5.7, 2.5 Hz, 2H), 4.21 – 4.20 (m, 1H), 4.11 – 4.09 (m, 2H), 3.92 (dt, *J* = 4.7, 2.6 Hz, 2H), 3.88 – 3.83 (m, 2H), 3.80 – 3.79 (m, 1H), 3.71 – 3.70 (m, 1H), 3.48 – 3.38 (m, 3H), 2.03 (s, 3H), 2.02 (s, 3H), 1.86 (s, 3H), 1.80 (s, 3H).^{13}C NMR (101 MHz, CHLOROFORM-*D*) δ 170.99, 170.94, 170.71, 170.64, 166.06, 165.88, 165.61, 165.34, 137.43, 137.29, 137.24, 136.83, 133.68, 133.63, 133.56, 133.43, 130.22, 130.00, 129.84, 129.31, 129.30, 129.06, 129.00, 128.87, 128.80, 128.67, 128.61, 128.47, 128.42, 128.30, 128.20, 128.09, 127.74, 101.79, 101.75, 93.09, 92.05, 76.53, 76.02, 75.00, 73.72, 73.30, 72.69, 72.56, 72.39, 68.54, 68.00, 67.61, 66.93, 64.77, 64.47, 64.39, 63.33, 63.27, 63.14, 62.90, 21.06, 20.70, 20.63.HRMS m/z calculated for $C_{51}H_{50}O_{16}Na$: 941.2997**;** found**:** 941.2985. Compound **14** as syrup. $[\alpha]_D^{25}$+246.2 (*c* 1.0 $CHCl_3$); IR (cm^{-1}, $CHCl_3$): 3020, 1720, 1610, 1214. ^1H NMR (400 MHz, Chloroform-*d*) δ 8.74 (s, 1H), 8.01 (dd, *J* = 8.4, 1.3 Hz, 2H), 7.88 – 7.86 (m, 2H), 7.75 (dd, *J* = 8.3, 1.3 Hz, 2H), 7.63 – 7.56 (m, 3H), 7.49 (tt, *J* = 7.5, 1.3 Hz, 1H), 7.43 – 7.28 (m, 11H), 7.22 – 7.18 (m, 2H), 7.08 (dd, *J* = 8.4, 7.4 Hz, 2H), 6.50 (s, 1H), 5.65 – 5.64 (m, 1H), 5.27 (dt, *J* = 2.2, 1.0 Hz, 1H), 5.15 (s, 1H), 4.97 (dd, *J* = 16.8, 11.2 Hz, 2H), 4.73 – 4.72 (m, 3H), 4.63 – 4.62 (m, 1H), 4.56 – 4.45 (m, 3H), 4.26 (dt, *J* = 3.1, 1.6 Hz, 1H), 4.08 – 4.04 (m, 1H), 3.97 – 3.92 (m, 2H), 3.35 (dd, *J* = 11.7, 3.9 Hz, 1H), 2.07 (s, 3H), 1.94 (s, 3H). ^{13}C NMR (101 MHz, $CDCl_3$) δ 170.65, 170.58, 165.53, 165.41, 165.27, 160.52, 137.51, 137.17, 133.58, 133.51, 133.29, 130.17, 129.91, 129.73, 129.22, 128.90, 128.67, 128.57, 128.49, 128.39, 128.33, 128.20, 128.16, 127.83, 127.45, 102.13, 95.68,

91.09, 74.25, 72.62, 72.42, 72.29, 67.90, 67.01, 66.44, 65.64, 64.09, 63.47, 62.67, 20.87, 20.53. HRMS m/z calculated for$C_{53}H_{50}Cl_3NO_{16}Na$: 1084.2093; found**:** 1084.2065.

Oxy-aminopropyl benzylcarbamate-O-((6-O-acetyl-2,4-O-dibenzoyl-3-O-benzyl)-α-L-idopyranosyl-α(1→4) (6-O-acetyl-2-O-benzoyl-3-O-benzyl))-α-L-idopyranoside 15

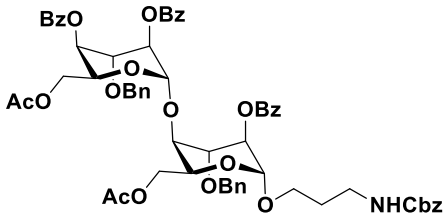

Compound **14** (0.55 g, 0.45 mmol), benzyl (3-hydroxypropyl)carbamate (0.142 g, 0.68mmol), was dissolved in dry DCM (24 mL), and freshly dried 4 Å M S, were added under anhydrous conditions. After stirring 1h at RT, the reaction flask mixture was cooled at -78 °C. TMSOTf (0.0164 ml, 0.091 mmol), was added and monitored the reaction by using TLC. After the completion of reaction, quenched with triethylamine and diluted with DCM. Filtered the molecular sieves using celite filter and washed with $NaHCO_3$, dried over Na_2SO_4, then filtered and concentrated under reduced pressure. The residue was purified by column chromatography (EtOAc/Hexane = 1/4) to afford **15 (0.34 g, 59%)** as syrup. $[\alpha]_D^{25}$-38.0 (*c* 1.0 $CHCl_3$); IR (cm^{-1}, $CHCl_3$): 3018, 1706, 1517.^{1}H NMR (400 MHz, Chloroform-*d*) δ 8.02 (dd, J = 8.3, 1.1 Hz, 2H), 7.89 (dd, J = 8.3, 1.1 Hz, 2H), 7.77 (dd, *J* = 8.3, 1.1 Hz, 2H), 7.59 – 7.56 (m, 3H), 7.48 – 7.43 (m, 2H), 7.40 (d, *J* = 7.8 Hz, 2H), 7.37 – 7.33 (m, 3H), 7.31 – 7.27 (m, 8H), 7.25 – 7.18 (m, 4H), 7.12 – 7.08 (m, 2H), 5.53 (t, *J* = 5.4 Hz, 1H), 5.35 (s, 1H), 5.23 (s, 1H), 5.09 – 5.02 (m, 3H), 4.95 – 4.91 (m, 2H), 4.77 (dd, *J* = 21.6, 11.8 Hz, 3H), 4.65 (d, *J* = 12.1 Hz, 1H), 4.57 – 4.41 (m, 5H), 4.09 (s, 1H), 4.03 (s, 1H), 3.93 – 3.83 (m, 2H), 3.74 (s, 1H), 3.60 (dt, *J* = 9.6, 4.9 Hz, 1H), 3.44 (dt, *J* = 10.2, 5.0 Hz, 2H), 3.29 (dq, *J* = 12.3, 5.3 Hz, 1H), 2.08 (s, 3H), 1.78 (s, 3H). ^{13}C NMR (101 MHz, CHLOROFORM-*D*) δ 170.89, 170.63, 165.65, 165.35, 156.61, 137.77, 137.29, 136.78, 133.60, 133.41, 130.12, 129.99, 129.83, 129.33, 129.14, 129.02, 128.58, 128.54, 128.53, 128.38, 128.35, 128.31, 128.12, 128.09, 127.93, 127.84, 101.66, 98.32, 74.50, 72.65, 72.53, 67.94, 67.70, 66.99, 66.70, 66.60, 64.98, 64.11, 63.24, 63.08, 39.64, 29.80, 29.52, 21.00, 20.49. HRMS m/z calculated for $C_{62}H_{63}NO_{18}Na$: 1132.3943**;** found**:** 1132.3942.

Oxy-aminopropyl benzylcarbamate-O-((3-O-benzyl)-α-L-idopyranosyl-α(1→4) (3-O-benzyl))-α-L-idopyranoside 16

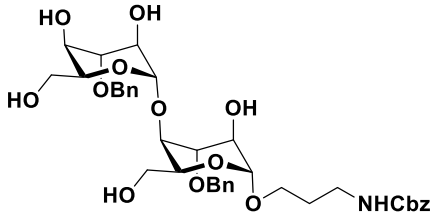

Compound **15** (0.32 g, 0.28 mmol) was dissolved in dry methanol (7 mL) and sodium methoxide (0.16 g, 2.88 mmol) was added, under nitrogen atmosphere. Allow the reaction flask stirred for another 2 h. After completion of reaction, evaporate the methanol under reduced pressure. The residue was purified by flash column chromatography (EtOAc/Hexane = 1/1) to afford **16 (0.17 g, 85%)** as syrup. $[\alpha]_D^{25}$– 2.6 (*c* 1.0 $CHCl_3$); IR (cm^{-1}, $CHCl_3$): 3453, 1517, 1214. ^1H NMR (400 MHz, Chloroform-*d*) δ 7.35 – 7.20 (m, 15H), 5.85 – 5.82 (m, 1H), 5.10 – 4.89 (m, 2H), 4.89 (s, 1H), 4.72 (s, 1H), 4.57 – 4.50 (m, 3H), 4.40 (d, *J* = 9.5 Hz, 1H), 4.20 (t, *J* = 6.6 Hz, 1H), 4.032 (s, 1H), 3.92 – 3.75 (m, 6H), 3.70 – 3.51 (m, 6H), 3.52 (dt, *J* = 9.3, 4.8 Hz, 2H), 3.38 (d, *J* = 12.2 Hz, 1H), 3.20 (dq, *J* = 13.4, 3.9, 3.5 Hz, 1H), 2.87 (d, *J* = 48.7 Hz, 2H), 2.11 (s, 1H), 1.82 – 1.78 (m, 2H).^{13}C NMR (101 MHz, $CDCl_3$) δ 156.78, 137.81, 137.06, 136.49, 128.59, 128.52, 128.41, 128.34, 128.25, 128.18, 128.04, 127.84, 127.64, 127.61, 103.40, 101.14, 74.03, 73.76, 72.98, 72.60, 71.04, 70.24, 67.21, 66.82, 66.65, 66.42, 66.19, 65.75, 64.63, 61.71, 40.04, 29.57.HRMS m/z calculated for $C_{37}H_{47}NO_{13}Na$: 736.2945**;** found**:** 736.2939

Oxy-aminopropyl benzylcarbamate-O-(2,5-Lactonyl-3-O-benzyl)-α-L-idopyranoside 17

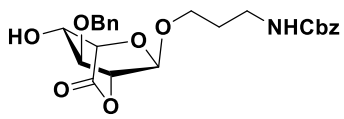

Compound **16** (0.15 g, 0.21 mmol) was dissolved in mixture of water and DCM [1/2 (v/v), 10 mL]. [Bis(acetoxy)iodo]benzene (BAIB, 0.41 g, 1.26 mmol) was added. After15 min, 2,2,6,6-tetramethyl-1-piperidinyloxyl free radical (TEMPO, 16.4 mg, 0.11 mmol) was added at RT. After stirring for 6 h, the mixture was washed with saturated NH_4Cl(aq). The organic layer was dried over Na_2SO_4, filtered, and concentrated under reduced pressure. The residue was purified by flash column chromatography (EtOAc/Hexane = 1/4) to afford **17 (0.026 g, 26%)** as syrup. $[\alpha]_D^{25}$-13.5 (*c* 1.0 $CHCl_3$); IR (cm^{-1}, $CHCl_3$): 3363, 2924, 1696, 1524. ^1H NMR (400 MHz, Chloroform-d) δ 7.375– 7.25 (m, 10H), 5.92 (bs, 1H), 5.09 (d, J = 11.9 Hz, 1H), 5.04 (dd, J = 2.4, 1.0 Hz, 1H), 5.00 (d, J = 12.1 Hz, 1H), 4.60 (s, 2H), 4.48 (t, J = 2.7 Hz, 1H), 4.24 (s, 1H), 4.13 (d, J = 3.0 Hz, 1H), 3.91 (dt, J = 8.9, 6.3 Hz, 1H), 3.66 (s, 1H),

3.59 (dt, J = 9.7, 4.9 Hz, 1H), 3.42 (dt, J = 11.3, 5.8 Hz, H), 3.30 – 3.22 (m, 1H), 2.77 (bs, 1H), 1.82 (p, J = 6.1, 5.5 Hz, 2H). 13C NMR (100 MHz, Chloroform-d) δ 168.18, 137.13, 136.67, 128.69, 128.61, 128.51, 128.36, 128.33, 128.29, 96.59, 80.83, 72.76, 71.65, 71.24, 69.32, 66.78, 40.10, 29.41. HRMS m/z calculated for $C_{24}H_{27}NO_8Na$: 480.1634; found: 480.1634.

2.5.4 Synthesis of Iduronic Acid Disaccharide Precursor

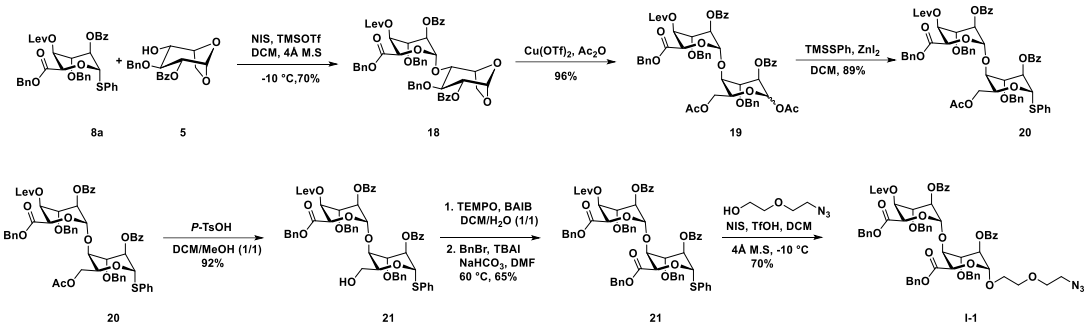

Scheme 8: Synthesis of Disaccharide

Benzyl (2-O-benzoyl-3-O-benzyl-4-O-levulinoyl)-α-L-idopyranosyluronate-α(1→4) (2-O-benzoyl-3-O-benzyl-1,6-anhydro)-β-L-idopyranose 18

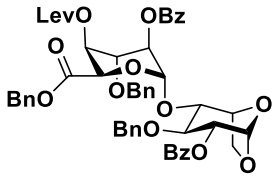

Compound **8a** (2.6 g, 3.89 mmol), Compound **5** (1.66 g, 4.67 mmol) and freshly dried 4 Å molecular sieves were dissolved in dry DCM (40 mL) and stirring at RT for 1 h. Then the reaction mixture was cooled to -10 °C and *N*-Iodosuccinimide (1.31 g, 5.84 mmol), TMSOTf (0.141 mL, 0.77 mmol) were added and monitored the reaction by using TLC. After the completion of reaction, quenched with triethylamine and diluted with DCM. The molecular sieves were filtered using celite and organic layer was washed with $Na_2S_2O_3$, followed by $NaHCO_3$, brine solution and dried over Na_2SO_4, then filtered and concentrated under reduced pressure. The residue was purified by column chromatography (EtOAc/Hexane = 1/4) to afford **18 (2.3 g, 64%)** as syrup. $[\alpha]_D^{25}$+46 (*c* 1.0 $CHCl_3$); IR (cm^{-1}, $CHCl_3$): 1720, 1452, 1268, 1106. ^{1}H NMR (400 MHz, Chloroform-*d*) δ 8.05 – 7.98 (m, 4H), 7.60 – 7.55 (m, 2H), 7.45 – 7.41 (m, 6H), 7.38 – 7.26 (m, 8H), 7.04 – 6.98 (m, 5H), 5.53 (d, *J* = 1.8 Hz, 1H), 5.31 (s, 1H), 5.22 (d, *J* = 11.9 Hz, 2H), 5.12 (dt, *J* = 2.5, 1.1 Hz, 1H), 5.10 (d, *J* = 2.3 Hz, 1H), 5.04 (dd,

J = 8.3, 1.8 Hz, 1H), 4.83 – 4.76 (m, 3H), 4.64 (t, *J* = 4.5 Hz, 1H), 4.52 (d, *J* = 10.9 Hz, 1H), 4.44 (d, *J* = 10.9 Hz, 1H), 4.25 (dd, *J* = 8.5, 4.0 Hz, 1H), 4.20 (d, *J* = 7.8 Hz, 1H), 3.94 – 3.93 (m, 1H), 3.89 (t, *J* = 8.4 Hz, 1H), 3.78 (dd, *J* = 7.4, 5.4 Hz, 1H), 2.52 – 2.39 (m, 2H), 2.35 – 2.27 (m, 1H), 2.21 – 2.09 (m, 1H), 2.05 (s, 3H). ^{13}C NMR (101 MHz, Chloroform-*d*) δ 205.87, 171.64, 167.88, 165.72, 165.45, 137.66, 137.28, 135.39, 133.83, 133.42, 129.90, 129.48, 129.16, 128.80, 128.59, 128.50, 128.43, 128.25, 128.20, 127.89, 127.52, 99.45, 95.35, 78.14, 75.08, 74.09, 72.96, 72.71, 71.92, 67.92, 67.10, 66.98, 66.15, 65.59, 37.68, 29.69, 27.77. HRMS m/z calculated for $C_{52}H_{50}O_{15}Na$:937.3047; found: 937.3042.

Benzyl (2-O-benzoyl-3-O-benzyl-4-O-levulinoyl)-α-L-idopyranosyl uronate-α(1→4) (1,6-O-diacetyl-2-O-benzoyl-3-O-benzyl)-α/β-L-idopyranoside 19

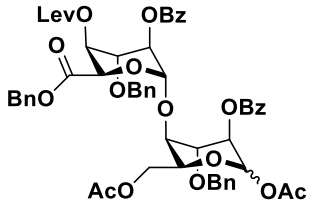

Compound **18** (2.3 g, 52 mmol) and copper trifluromethanesulfonate (0.09 g, 0.25 mmol) were dissolved in acetic anhydride (23 mL) at 0°C. The temperature of the reaction mixture was slowly increased to RT and stirred for another 16 h. Then, EtOAc (50 mL) was added and organic layer was washed with $NaHCO_3$ and brine solution, dried over Na_2SO_4 and concentrated under reduced pressure. The residue was purified by flash column chromatography (EtOAc/Hexane = 1/4) to afford anomeric mixture **19 (2.4 g, 94%, α:β = 1:1)** as syrup. $[\alpha]_D^{25}$+ 7.7 (*c* 1.0 $CHCl_3$); IR (cm^{-1}, $CHCl_3$): 1721, 1215, 1095.^{1}H NMR (400 MHz, Chloroform-*d*) δ 7.97 (ddd, *J* = 9.7, 7.7, 1.3 Hz, 6H), 7.86 (dd, *J* = 8.2, 1.1 Hz, 2H), 7.55 – 7.50 (m, 2H), 7.45 – 7.43 (m, 1H), 7.41 – 7.36 (m, 7H), 7.32 – 7.24 (m, 18H), 7.23 – 7.14 (m, 16H), 6.16 – 6.15 (m, 2H), 5.29 (dd, *J* = 4.5, 2.2 Hz, 1H), 5.26 – 5.19 (m, 3H), 5.16 – 5.11 (m, 3H), 5.07 (t, *J* = 2.9 Hz, 1H), 4.98 (t, *J* = 3.3 Hz, 1H), 4.92 (t, *J* = 3.2 Hz, 1H), 4.87 (d, *J* = 3.1 Hz, 1H), 4.84 – 4.78 (m, 3H), 4.76 – 4.71 (m, 2H), 4.69 (d, *J* = 2.0 Hz, 1H), 4.64 – 4.56 (m, 5H), 4.48 (td, *J* = 6.7, 2.2 Hz, 1H), 4.40 – 4.28 (m, 5H), 4.19 (t, *J* = 4.4 Hz, 1H), 4.06 (t, *J* = 2.7 Hz, 1H), 3.91 (q, *J* = 4.3, 3.3 Hz, 2H), 3.82 (t, *J* = 3.2 Hz, 1H), 3.79 (t, *J* = 3.4 Hz, 1H), 2.45 – 2.38 (m, 4H), 2.35 – 2.21 (m, 2H), 2.13 – 2.07 (m, 2H), 2.05 (s, 3H), 2.01 (s, 6H), 2.00 (s, 6H). ^{13}C NMR (101 MHz, CHLOROFORM-*D*) δ 205.82, 205.78, 171.44, 171.40, 170.67, 170.60, 169.08, 168.95, 167.96, 167.85, 165.91, 165.49, 165.18, 165.16, 137.82, 137.39, 137.19, 137.15, 135.19, 135.16, 133.64, 133.52, 133.41, 130.09, 129.89, 129.30, 129.26, 128.86, 128.80, 128.64,

128.61, 128.56, 128.53, 128.48, 128.42, 128.40, 128.17, 128.12, 127.99, 127.95, 127.91, 127.80, 127.63, 101.16, 100.12, 91.63, 90.63, 75.74, 75.31, 74.94, 74.21, 73.75, 73.62, 73.24, 72.78, 72.70, 68.41, 68.32, 67.81, 67.75, 67.32, 67.21, 67.18, 66.93, 66.78, 62.72, 62.15, 37.63, 29.71, 27.68, 21.08, 21.02, 20.88, 20.87.HRMS m/z calculated for $C_{56}H_{56}O_{18}Na$:1039.3364; found: 1039.3359.

Benzyl (2-O-benzoyl-3-O-benzyl-4-O-levulinoyl)-α-L-idopyranosyluronate-α(1→4) 1-thiophenyl-(6-O-acetyl-2-O-benzoyl-3-O-benzyl)-α-L-idopyranoside 20

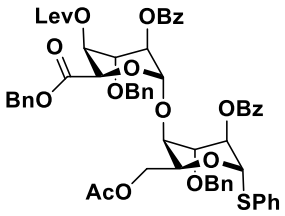

The preparation of the thioglycosylated compound **20 (89%)** was carried out from compound **19** according to the procedure for synthesizing compound **6** as syrup. $[\alpha]_D^{25}$+ 39.3 (*c* 1.0 $CHCl_3$); IR (cm^{-1}, $CHCl_3$): 1721, 1106, 1068.^{1}H NMR (400 MHz, Chloroform-*d*) δ 8.03 (d, *J* = 7.4 Hz, 2H), 7.96 (d, *J* = 7.3 Hz, 2H), 7.59 – 7.56 (m, 3H), 7.45 – 7.41 (m, 5H), 7.36 – 7.30 (m, 9H), 7.29 – 7.21 (m, 9H), 5.55 (s, 1H), 5.47 (s, 1H), 5.28 (d, *J* = 3.3 Hz, 1H), 5.18 (d, *J* = 12.0 Hz, 1H), 5.15 (t, *J* = 3.4 Hz, 1H), 4.99 (t, *J* = 3.7 Hz, 1H), 4.95 (td, *J* = 6.6, 1.9 Hz, 1H), 4.89 (d, *J* = 12.0 Hz, 1H), 4.86 – 4.82 (m, 2H), 4.75 (d, *J* = 11.5 Hz, 1H), 4.65 (d, *J* = 5.2 Hz, 1H), 4.62 (d, *J* = 5.2 Hz, 1H), 4.42 – 4.34 (m, 2H), 4.13 (t, *J* = 2.4 Hz, 1H), 3.92 (s, 1H), 3.86 (t, *J* = 3.7 Hz, 1H), 2.53 – 2.39 (m, 2H), 2.36 – 2.28 (m, 1H), 2.23 – 2.21 (m, 1H), 2.07 (s, 3H), 2.02 (s, 3H). ^{13}C NMR (101 MHz, Chloroform-*d*) δ 205.84, 171.43, 170.61, 168.01, 165.74, 165.21, 137.61, 137.23, 135.88, 135.20, 133.64, 133.43, 131.86, 130.09, 129.94, 129.34, 129.28, 129.00, 128.85, 128.69, 128.59, 128.48, 128.18, 128.04, 127.89, 127.59, 101.17, 86.08, 76.35, 74.15, 73.74, 73.09, 72.81, 69.20, 68.65, 67.99, 67.23, 65.93, 62.72, 37.67, 29.76, 27.72, 20.91. HRMS m/z calculated for $C_{60}H_{58}O_{16}SNa$:1089.3343; found: 1089.3338.

Benzyl (2-O-benzoyl-3-O-benzyl-4-O-levulinoyl)-α-L-idopyranosyluronate-α(1→4) 1-thiophenyl-(2-O-benzoyl-3-O-benzyl)-α-L-idopyranoside 21

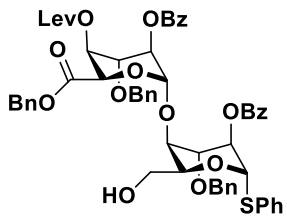

Compound **20** (1.9 g, 2.06 mmol) and *p*-toluenesulfonicacid (1.17 g, 6.19 mmol) was dissolved in equal ratio of mixture of dry DCM (15 mL) and methanol (15 mL) and stirred at RT for 3 days. The reaction mixture was quenched with triethylamine. Solvents were evaporated under reduced pressure, extracted with EtOAc and $NaHCO_3$ and water respectively. The combined organic layer washed

with brine solution, dried over Na_2SO_4 and concentrated under reduced pressure. The residue was purified by column chromatography (EtOAc/Hexane = 1/3) to afford **21 (1.60 g, 92%)** as syrup. $[\alpha]_D^{25}$-27.6 (*c* 1.0 $CHCl_3$); IR (cm^{-1}, $CHCl_3$): 3327, 1717, 1452, 1265. ^{1}H NMR (400 MHz, Chloroform-*d*) δ 8.02 (d, *J* = 7.4 Hz, 2H), 7.97 (d, *J* = 7.9 Hz, 2H), 7.59 – 7.54 (m, 3H), 7.45 – 7.39 (m, 5H), 7.37 – 7.30 (m, 8H), 7.27 – 7.21 (m, 10H), 5.58 (s, 1H), 5.47 (t, *J* = 2.2 Hz, 1H), 5.27 (d, *J* = 2.9 Hz, 1H), 5.17 (d, *J* = 12.0 Hz, 1H), 5.12 (t, *J* = 3.2 Hz, 1H), 4.99 (t, *J* = 3.5 Hz, 1H), 4.88 (d, *J* = 12.0 Hz, 1H), 4.85 – 4.79 (m, 3H), 4.72 (d, *J* = 11.6 Hz, 1H), 4.64 (dd, *J* = 11.6, 3.4 Hz, 2H), 4.12 (t, *J* = 3.1 Hz, 1H), 3.96 (s, 1H), 3.91 – 3.84 (m, 3H), 2.56 – 2.32 (m, 3H), 2.21 – 2.13 (m, 2H), 2.08 (s, 3H). ^{13}C NMR (101 MHz, Chloroform-*d*) δ 205.93, 171.46, 167.90, 165.73, 165.58, 137.63, 137.0, 135.79, 135.18, 133.77, 133.36, 131.93, 130.05, 129.91, 129.29, 129.19, 129.08, 128.81, 128.65, 128.60, 128.57, 128.50, 128.42, 128.41, 128.20, 128.12, 127.78, 127.57, 101.18, 86.13, 74.22, 73.46, 72.95, 72.82, 69.59, 68.53, 68.37, 68.01, 67.55, 67.19, 61.58, 37.63, 29.74, 27.70. HRMS m/z calculated for $C_{58}H_{56}O_{15}SNa$:1047.3238; found: 1047.3232.

Benzyl (2-O-benzoyl-3-O-benzyl-4-O-levulinoyl)-α-L-idopyranosyl uronate-α(1→4) benzyl (1-thiophenyl-2-O-benzoyl-3-O-benzyl)-α-L-idopyranoside uronate 22

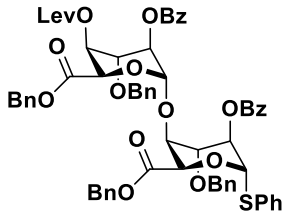

The synthetic procedure for the preparation of compound **7** was followed to obtain compound **22 (65%)** from compound **21** as syrup. $[\alpha]_D^{25}$ - 4.2 (*c* 1.0 $CHCl_3$); IR (cm^{-1}, $CHCl_3$): 2923, 1723, 1455, 1266.^{1}H NMR (400 MHz, Chloroform-*d*) δ 8.03 (d, *J* = 8.1 Hz, 2H), 7.91 (d, *J* = 8.1 Hz, 2H), 7.60 – 7.54 (m, 3H), 7.45 – 7.37 (m, 5H), 7.34 – 7.28 (m, 7H), 7.27 – 7.17 (m, 16H), 5.73 (d, *J* = 2.6 Hz, 1H), 5.41 (t, *J* = 3.0 Hz, 1H), 5.37 (d, *J* = 2.8 Hz, 1H), 5.31 (d, *J* = 2.5 Hz, 1H), 5.18 – 5.10 (m, 4H), 4.94 (t, *J* = 3.2 Hz, 1H), 4.85 (d, *J* = 2.7 Hz, 1H), 4.83 (s, 1H), 4.73 (dd, *J* = 16.3, 11.3 Hz, 2H), 4.57 (dd, *J* = 14.6, 11.3 Hz, 2H), 4.30 (t, *J* = 3.4 Hz, 1H), 4.12 (t, *J* = 3.6 Hz, 1H), 3.81 (t, *J* = 3.4 Hz, 1H), 2.40 (t, *J* = 6.4 Hz, 2H), 2.23 (dt, *J* = 17.3, 6.9 Hz, 1H), 2.11 (dt, *J* = 17.3, 6.6 Hz, 1H), 2.03 (s, 3H). ^{13}C NMR (101 MHz, Chloroform-*d*) δ 205.83, 171.38, 168.92, 167.78, 165.69, 164.92, 137.41, 137.12, 135.24, 135.20, 133.66, 133.45, 131.74, 130.14, 130.03, 129.44, 129.06, 128.78, 128.62, 128.58, 128.53, 128.43, 128.06, 127.92, 127.87, 127.65, 101.55, 86.01, 74.99,

73.39, 72.89, 72.50, 69.22, 69.09, 68.64, 67.31, 67.25, 67.19, 37.68, 29.70, 27.74. HRMS m/z calculated for $C_{65}H_{60}O_{16}SNa$:1151.3500; found: 1151.3494.

Ethoxy-2-azidoethoxyl -O-(Benzyl (2-O-benzoyl-3-O-benzyl-4-O-levulinoyl)-α-L-idopyranosyluronate-α(1→4) benzyl (2-O-benzoyl-3-O-benzyl))-α-L-idopyranoside uronate I-1

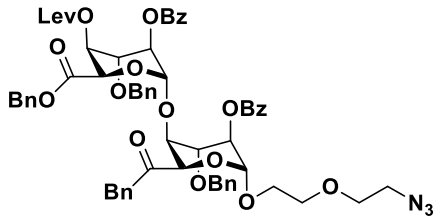

The synthetic procedure for the preparation of compound **9** was followed to obtain compound **I-1 (81%)** from compound **22** as syrup. $[\alpha]_D^{25}$ – 3.2 (*c* 1.0 $CHCl_3$); IR (cm^{-1}, $CHCl_3$): 1721, 1457, 1214, 1106. ^{1}H NMR (400 MHz, Chloroform-*d*) δ 8.04 (dd, *J* = 8.3, 1.2 Hz, 2H), 7.91 (dd, *J* = 8.3, 1.2 Hz, 2H), 7.62 – 7.57 (m, 1H), 7.48 – 7.42 (m, 5H), 7.35 – 7.26 (m, 13H), 7.24 – 7.17 (m, 8H), 5.31 (d, *J* = 12.2 Hz, 1H), 5.27 – 5.21 (m, 4H), 5.18 – 5.12 (m, 3H), 5.00 (d, *J* = 3.3 Hz, 1H), 4.98 (t, *J* = 2.8 Hz, 1H), 4.93 (d, *J* = 2.3 Hz, 1H), 4.80 (d, *J* = 11.1 Hz, 1H), 4.73 (d, *J* = 11.7 Hz, 2H), 4.59 (dd, *J* = 23.1, 11.2 Hz, 2H), 4.29 (t, *J* = 3.7 Hz, 1H), 4.04 (t, *J* = 3.6 Hz, 1H), 4.0q – 3.96 (m, 1H), 3.85 (t, *J* = 2.5 Hz, 1H), 3.75 – 3.64 (m, 3H), 3.57 (qdd, *J* = 10.3, 5.5, 4.5 Hz, 2H), 3.15 (ddd, *J* = 5.9, 4.4, 1.4 Hz, 2H), 2.40 (t, *J* = 6.5 Hz, 2H), 2.27 – 2.08 (m, 2H), 2.04 (s, 3H). ^{13}C NMR (101 MHz, Chloroform-*d*) δ 205.80, 171.46, 169.26, 167.68, 165.64, 164.95, 137.85, 137.17, 135.24, 135.21, 133.68, 133.41, 130.05, 130.00, 129.39, 129.05, 128.73, 128.63, 128.59, 128.58, 128.53, 128.49, 128.47, 128.45, 128.37, 128.30, 128.10, 127.89, 127.72, 101.40, 98.95, 75.72, 72.97, 72.50, 72.40, 70.26, 70.24, 68.76, 68.63, 68.60, 68.32, 67.31, 67.14, 66.57, 66.52, 50.78, 37.69, 29.68, 27.75. HRMS m/z calculated for $C_{63}H_{63}O_{18}Na$:1172.4004; found: 1172.3994.

2.5.5 Synthesis of Iduronic Acid Trisaccharide Precursor

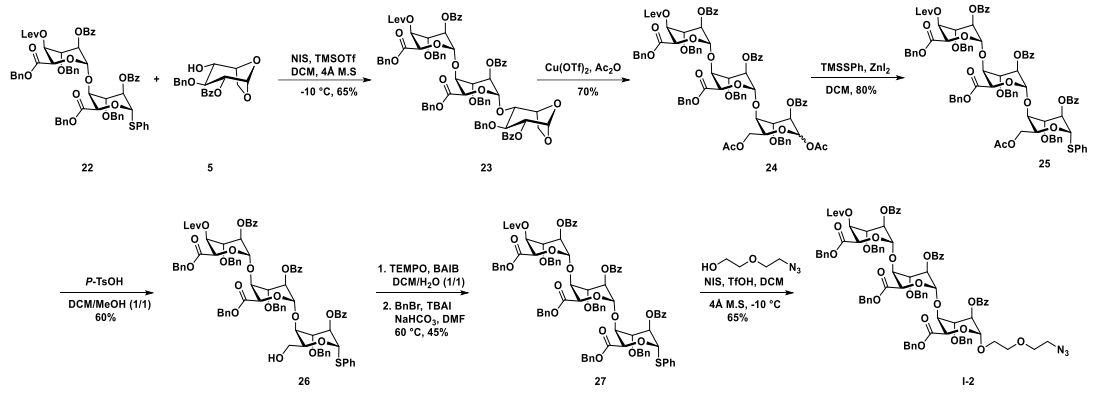

Scheme 9: Synthesis of Trisaccharide

Benzyl (2-O-benzoyl-3-O-benzyl-4-O-levulinoyl)-α-L-idopyranosyl uronate-α(1→4) benzyl (2-O-benzoyl-3-O-benzyl)-α-L-idopyranosyluronate-α(1→4) (2-O-benzoyl-3-O-benzyl-1,6-anhydro)-β-L-idopyranose 23

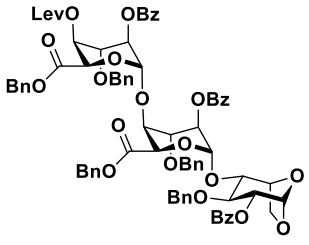

The synthetic procedure for the preparation of compound **18** was followed to obtain compound **23 (62%)** from compound **22** and **5** as syrup. $[\alpha]_D^{25}$+23.6 (*c* 1.0 $CHCl_3$); IR (cm^{-1}, $CHCl_3$): 1720, 1214, 743. ^{1}H NMR (400 MHz, Chloroform-*d*) δ 7.99 (ddd, *J* = 14.4, 8.4, 1.3 Hz, 4H), 7.88 (dd, *J* = 8.3, 1.2 Hz, 2H), 7.60 – 7.54 (m, 2H), 7.46 – 7.36 (m, 7H), 7.32 – 7.27 (m, 5H), 7.25 – 7.14 (m, 15H), 7.04 (s, 5H), 5.49 (d, *J* = 1.8 Hz, 1H), 5.39 (d, *J* = 3.6 Hz, 1H), 5.26 (s, 1H), 5.19 (t, *J* = 4.1 Hz, 1H), 5.17 – 5.07 (m, 3H), 5.06 – 5.04 (m, 1H), 5.01 – 4.98 (m, 3H), 4.94 (d, *J* = 2.3 Hz, 1H), 4.78 (d, *J* = 12.1 Hz, 1H), 4.72 (d, *J* = 11.2 Hz, 1H), 4.65 (d, *J* = 11.2 Hz, 1H), 4.62 – 4.58 (m, 3H), 4.54 (d, *J* = 4.3 Hz, 1H), 4.51 (d, *J* = 11.3 Hz, 1H), 4.28 (t, *J* = 4.6 Hz, 1H), 4.25 – 4.21 (m, 1H), 4.05 – 4.02 (m, 2H), 3.87 – 3.82 (m, 2H), 3.51 – 3.47 (m, 1H), 2.38 (t, *J* = 6.7 Hz, 2H), 2.23 – 2.05 (m, 2H), 2.01 (s, 3H). ^{13}C NMR (101 MHz, Chloroform-*d*) δ 205.77, 171.46, 169.04, 167.76, 165.85, 165.59, 164.86, 137.97, 137.55, 137.12, 135.25, 135.07, 133.70, 133.65, 133.39, 130.02, 129.98, 129.93, 129.59, 129.39, 128.88, 128.75, 128.67, 128.61, 128.59, 128.56, 128.54, 128.51, 128.46, 128.43, 128.39, 128.25, 128.23, 128.16, 127.97, 127.89, 127.54, 100.30, 99.41, 96.57, 77.84, 76.71, 75.83, 75.80, 75.77, 74.96, 73.79 , 72.64,

72.43, 72.34, 69.64, 69.22, 68.34, 67.34, 67.21, 66.58, 65.41, 37.71, 29.68, 27.78.HRMS m/z calculated for $C_{79}H_{74}O_{22}Na$:1397.4569; found: 1397.4566.

Benzyl (2-O-benzoyl-3-O-benzyl-4-O-levulinoyl)-α-L-idopyranosyl uronate-α(1→4) benzyl (2-O-benzoyl-3-O-benzyl)-α-L-idopyranosyl uronate-α(1→4) (1,6-O-diacetyl-2-O-benzoyl-3-O-benzyl)-α/β-L-idopyranoside 24

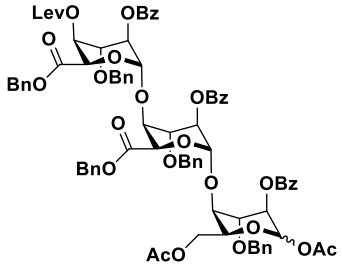

The synthetic procedure for the preparation of compound **19** was followed to obtain compound **24 (85%, α:β = 1:0.7)** from compound **23** as syrup. $[\alpha]_D^{25}$-5.6 (*c* 1.0 $CHCl_3$); IR (cm^{-1}, $CHCl_3$): 1722, 1452, 1265, 1095. ^1H NMR (400 MHz, Chloroform-*d*) δ 8.05 – 8.03 (m, 2H), 7.98 – 7.93 (m, 10H), 7.56 (t, *J* = 7.4 Hz, 2H), 7.42 (tt, *J* = 16.4, 8.0 Hz, 13H), 7.34 – 7.27 (m, 23H), 7.26 – 711 (m, 29H), 6.17 (s, 1H), 6.15 (d, *J* = 1.8 Hz, 1H), 5.30 (t, *J* = –4.3 Hz, 3H), 5.25 – 5.16 (m, 4H), 5.13 – 5.01 (m, 12H), 4.94 (dd, *J* = 10.0, 2.2 Hz, 2H), 4.78 – 4.72 (m, 5H), 4.69 – 4.60 (m, 6H), 4.55 (d, *J* = 12.0 Hz, 1H), 4.46– 4.41 (m, 3H), 4.35 (t, *J* = 3.6 Hz, 1H), 4.22 (ddd, *J* = 23.8, 14.2, 6.0 Hz, 4H), 4.03 (dtd, *J* = 21.3, 11.4, 5.1 Hz, 3H), 3.92 (dq, *J* = 13.2, 4.6 Hz, 3H), 3.82 – 3.79 (m, 4H), 2.35 (q, *J* = 6.4, 5.9 Hz, 4H), 2.22 – 2.14 (m, 2H), 2.08 (s, 4H), 2.02 (s, 3H), 2.01 (s, 3H), 2.00 (s, 2H), 1.93 (s, 2H), 1.91 (s, 3H). ^{13}C NMR (101 MHz, Chloroform-*d*) δ 205.80, 205.75, 171.46, 170.45, 169.13, 169.03, 168.95, 167.55, 167.49, 166.81, 166.03, 165.60, 165.34, 165.30,164.88, 164.83, 138.15, 137.70, 137.48, 137.45, 137.19, 137.15, 135.21, 135.08, 135.02, 133.72, 133.51, 133.49, 133.37, 130.21, 130.16, 129.98, 128.71, 128.66, 128.60, 128.53, 128.48, 128.42, 128.38, 128.31, 128.28, 128.21, 128.15, 128.11, 127.97, 127.87, 127.78, 127.58, 101.31, 100.65, 100.58, 91.81, 90.68, 76.51 , 76.38 , 75.66 , 75.33 , 75.07 , 73.46 , 73.29 , 73.20 , 73.15 , 72.75 , 72.62 , 72.53 , 72.41 , 71.12 , 71.01, 70.29, 70.19, 68.1, 67.97, 67.35, 67.30, 67.22, 67.11, 67.03, 66.73, 66.58, 66.50, 66.43, 66.38, 63.17, 62.66, 37.67, 29.83, 29.68, 27.71, 21.14, 21.06, 20.82.HRMS m/z calculated for $C_{83}H_{80}O_{25}Na$:1499.4886; found: 1499.4879.

Benzyl (2-O-benzoyl-3-O-benzyl-4-O-levulinoyl)-α-L-idopyranosyluronate-α(1→4) benzyl (2-O-benzoyl-3-O-benzyl)-α-L-idopyranosyluronate α(1→4) 1-thiophenyl-(6-O-acetyl-2-O-benzoyl-3-O-benzyl)-α-L-idopyranoside 25

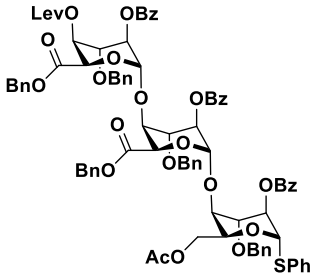

The synthetic procedure for the preparation of compound **6** was followed to obtain compound **25 (80%)** from compound **24** as syrup. $[\alpha]_D^{25}$-46.3 (*c* 1.0 $CHCl_3$); IR (cm^{-1}, $CHCl_3$): 1721, 1106, 1068. ^{1}H NMR (400 MHz, Chloroform-*d*) δ 8.04 – 7.99 (m, 6H), 7.61 – 7.56 (m, 3H), 7.52 – 7.41 (m, 8H), 7.39 – 7.33 (m, 5H), 7.32 – 7.24 (m, 13H), 7.21 – 7.13 (m, 10H), 5.56 (s, 1H), 5.45 – 5.44 (m, 1H), 5.36 (d, *J* = 5.7 Hz, 1H), 5.29 (d, *J* = 12.2 Hz, 1H), 5.17 (dd, *J* = 5.8, 3.7 Hz, 1H), 5.10 (ddd, *J* = 16.2, 12.9, 5.0 Hz, 5H), 5.00 (d, *J* = 2.1 Hz, 1H), 4.90 – 4.84 (m, 2H), 4.80 – 4.73 (m, 3H), 4.70 – 4.69 (m, 1H), 4.62(dd, *J* = 19.0, 11.6 Hz, 2H), 4.46 (d, *J* = 11.2 Hz, 1H), 4.32 (d, *J* = 3.1 Hz, 1H), 4.23 (dd, *J* = 11.4, 8.1 Hz, 1H), 4.04 (t, *J* = 4.9 Hz, 1H), 3.99 (dd, *J* = 11.5, 4.5 Hz, 1H), 3.94 (dd, *J* = 5.0, 3.7 Hz, 1H), 3.84 (dd, *J* = 6.8, 3.8 Hz, 2H), 2.38 (t, *J* = 6.4 Hz, 2H), 2.22 (dt, *J* = 17.3, 7.0 Hz, 1H), 2.11 – 2.05 (m, 1H), 2.03 (s, 3H), 1.92 (s, 3H). ^{13}C NMR (101 MHz, Chloroform-*d*) δ 205.77, 171.49, 170.28, 169.13, 167.48, 165.78, 165.27, 164.89, 137.93, 137.49, 137.13, 136.28, 135.24, 135.10, 133.74, 133.48, 133.38, 131.81, 130.13, 130.00, 129.98, 129.52, 129.27, 129.07, 128.91, 128.71, 128.68, 128.59, 128.55, 128.50, 128.46, 128.29, 128.17, 128.14, 127.81, 127.72, 127.44, 101.02, 100.38, 86.01, 76.49, 76.12, 73.57, 73.33, 72.82, 72.76, 72.47, 71.31, 71.27, 69.00, 67.97, 67.33, 67.03, 66.44, 66.27, 65.81, 63.29, 37.67, 29.68, 27.69, 20.81.HRMS m/z calculated for $C_{87}H_{82}O_{23}SNa$:1549.4865; found: 1549.4878.

Benzyl (2-O-benzoyl-3-O-benzyl-4-O-levulinoyl)-α-L-idopyranosyluronate-α(1→4) benzyl (2-O-benzoyl-3-O-benzyl)-α-L-idopyranosyluronate)-α(1→4) 1-thiophenyl-(2-O-benzoyl-3-O-benzyl)-α-L-idopyranoside 26

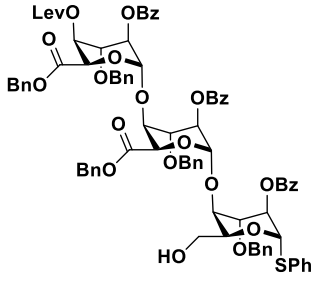

The synthetic procedure for the preparation of compound **21** was followed to obtain compound **26 (76%)** from compound **25** as syrup. $[\alpha]_D^{25}$ -37.9 (*c* 1.0 $CHCl_3$); IR (cm^{-1}, $CHCl_3$): 3104, 1720, 1214, 746.^{1}H NMR (400 MHz, Chloroform-*d*) δ 8.03 – 7.94 (m, 6H), 7.59 – 7.51 (m, 3H), 7.49 – 7.32 (m, 12H), 7.30 – 7.22 (m, 14H), 7.20 – 7.11 (m, 10H), 5.58 (s, 1H), 5.44 – 5.43 (m, 1H), 5.31 – 5.21 (m, 1H), 5.24 (d, *J* = 12.2 Hz, 1H), 5.15 – 5.05 (m, 6H), 5.00 (d, *J* = 2.2 Hz, 1H), 4.87 (d, *J* = 11.7 Hz, 1H), 4.79 (d, *J* = 11.5 Hz, 1H), 4.73 – 4.68 (m, 4H), 4.61 (t, *J* = 11.5 Hz, 2H), 4.44 (d, *J* = 11.2 Hz, 1H), 4.31 (dt, *J* = 3.3, 1.7 Hz, 1H), 4.05 (t, *J* = 4.6 Hz, 1H), 3.89 (dd, *J* = 4.7, 2.9 Hz, 1H), 3.85 – 3.83 (m, 2H), 3.69 (ddd, *J* = 11.0, 7.3, 3.2 Hz, 1H), 3.47 – 3.41 (m, 1H), 2.37 (t, *J* = 7.1 Hz, 2H), 2.20 (dt, *J* = 17.3, 7.0 Hz, 1H), 2.07 (dt, *J* = 15.6, 5.7 Hz, 1H), 2.01(s, 3H). ^{13}C NMR (101 MHz, Chloroform-*d*) δ 205.77, 171.48, 169.04, 167.46, 165.78, 165.43, 164.89, 137.99, 137.37, 137.02, 136.14, 135.13, 135.03, 133.74, 133.62, 133.30, 131.77, 130.09, 129.95, 129.86, 129.54, 129.20, 129.02, 128.97, 128.64, 128.56, 128.52, 128.43, 128.41, 128.31, 128.21, 128.14, 128.11, 127.77, 127.72, 127.42, 101.04, 100.67, 86.11, 76.56, 76.3, 73.61, 73.13, 72.73, 72.44, 71.32, 69.33, 68.00, 67.30, 67.04, 66.32, 66.30, 61.83, 37.63, 29.66, 27.66.HRMS m/z calculated for $C_{85}H_{80}O_{22}SNa$:1507.4760; found: 1507.4769.

Benzyl (2-O-benzoyl-3-O-benzyl-4-O-levulinoyl)-α-L-idopyranosyluronate)-α(1→4) benzyl (2-O-benzoyl-3-O-benzyl)-α-L-idopyranosyl uronate-α(1→4) benzyl (1-thiophenyl-2-O-benzoyl-3-O-benzyl)-α-L-idopyranoside uronate 27

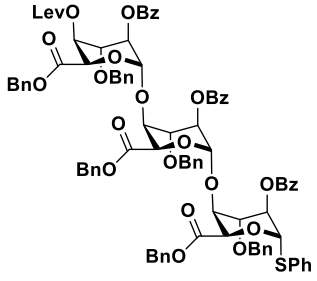

The synthetic procedure for the preparation of compound **7** was followed to obtain compound **27 (63%)** from compound **26** as syrup. $[\alpha]_D^{25}$-35.3 (*c* 1.0 $CHCl_3$); IR (cm^{-1}, $CHCl_3$): 1720, 1265, 1069. ^{1}H NMR (400 MHz, Chloroform-*d*) δ 8.00 – 7.96 (m, 6H), 7.5 – 7.52 (m, 3H), 7.45 – 7.33 (m, 9H), 7.32 – 7.27 (m, 8H), 7.25 – 7.19 (m, 12H), 7.18 – 7.10 (m, 12H), 5.70 (d, *J* = 2.9 Hz, 1H), 5.43 (d, *J* = 4.3 Hz, 1H), 5.39 (d, *J* = 2.4 Hz, 2H), 5.19 (t, *J* = 3.8 Hz, 1H), 5.13 – 5.04 (m, 4H), 5.04 – 4.96 (m, 3H), 4.88 (d, *J* = 2.1 Hz, 1H), 4.85 – 4.78 (m, 2H), 4.75 (d, *J* = 3.1 Hz, 1H), 4.73 (d, *J* = 3.8 Hz, 1H), 4.69 (d, *J* = 6.8

Hz, 1H), 4.67 – 4.60 (m, 3H), 4.43 (d, *J* = 11.0 Hz, 1H), 4.32 (d, *J* = 2.5 Hz, 1H), 4.30 (d, *J* = 2.7 Hz, 1H), 3.95 (t, *J* = 4.1 Hz, 1H), 3.89 – 3.87 (m, 1H), 3.77 (t, *J* = 2.6 Hz, 1H), 2.35 (t, *J* = 6.8 Hz, 2H), 2.20 – 2.02 (m, 2H), 2.00 (s, 3H). ^{13}C NMR (101 MHz, Chloroform-*d*) δ 205.77, 171.35, 168.75, 168.72, 167.56, 165.70, 165.11, 164.75, 137.66, 137.35, 137.23, 135.59, 135.36, 135.19, 134.98, 133.64, 133.43, 133.39, 131.63, 130.25, 130.19, 129.94, 129.29, 129.19, 129.15, 128.98, 128.64, 128.57, 128.56, 128.53, 128.50, 128.45, 128.40, 128.35, 128.33, 128.27, 128.24, 128.21, 128.10, 127.78, 127.50, 101.67, 100.87, 86.29, 76.61, 76.59, 76.27, 74.25, 73.00, 72.90, 72.23, 71.82, 70.11, 69.45, 68.99, 68.58, 68.30, 67.23, 67.04, 66.79, 66.42, 66.36, 37.66, 29.64, 27.69.HRMS m/z calculated for $C_{92}H_{84}O_{23}SNa$:1611.5022; found: 1611.5023.

Ethoxy-2-azidoethoxyl -O-(benzyl (2-O-benzoyl-3-O-benzyl-4-O-levulinoyl)-α-L-idopyranosyluronate-α(1→4) benzyl (2-O-benzoyl-3-O-benzyl)-α-L-idopyranosyluronate)-α(1→4) benzyl (2-O-benzoyl-3-O-benzyl))-α-L-idopyranoside uronate I-2

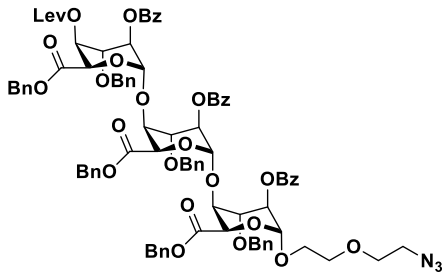

The synthetic procedure for the preparation of compound **9** was followed to obtain compound **I-2 (76%)** from compound **27** as syrup. $[\alpha]_D^{25}$-17.1 (*c* 1.0 $CHCl_3$); IR (cm^{-1}, $CHCl_3$): 1720, 1214, 667. ^{1}H NMR (400 MHz, Chloroform-*d*) δ 7.96 – 7.88 (m, 6H), 7.55 (t, *J* = 7.4 Hz, 1H), 7.41 – 7.34 (m, 8H), 7.31 – 7.27 (m, 6H), 7.26 – 7.22 (m, 6H), 7.21 – 7.14 (m, 13H), 7.11 – 7.04 (m, 6H), 5.29 (d, *J* = 2.7 Hz, 1H), 5.21 (p, *J* = 3.7, 3.2 Hz, 2H), 5.17 (d, *J* = 2.0 Hz, 1H), 5.08 (dd, *J* = 12.1, 7.9 Hz, 3H), 5.02 – 4.92 (m, 5H), 4.89 (t, *J* = 2.6 Hz, 1H), 4.79 – 4.69 (m, 6H), 4.59 (d, *J* = 11.4 Hz, 1H), 4.49 (t, *J* = 11.3 Hz, 2H), 4.26 (t, *J* = 3.2 Hz, 1H), 4.16 (t, *J* = 2.9 Hz, 1H), 3.97 – 3.88 (m, 3H), 3.75 (t, *J* = 2.9 Hz, 1H), 3.72 – 3.62 (m, 3H), 3.53 (dtt, *J* = 15.9, 10.6, 5.3 Hz, 2H), 3.12 (t, *J* = 5.1 Hz, 2H), 2.34 (t, *J* = 6.8 Hz, 2H), 2.18 – 2.03 (m, 2H), 2.00 (s, 2H). ^{13}C NMR (101 MHz, Chloroform-*d*) δ 205.65, 171.22 , 169.05, 168.40, 167.52, 165.57, 165.14, 164.63, 137.98, 137.30, 137.10, 135.20, 135.09, 134.85, 133.50, 133.33, 133.26, 130.10, 130.01, 129.85, 129.26, 129.02, 128.88, 128.57, 128.55, 128.47, 128.43, 128.42, 128.36, 128.33, 128.29, 128.24, 128.16, 127.97, 127.76, 127.68, 127.54, 101.68, 101.32, 98.83, 75.40, 75.14, 72.83, 72.57, 72.24, 72.07, 70.13, 70.11, 68.74, 68.41, 68.39, 68.36, 68.06,

67.99, 67.04, 67.01, 66.98, 66.55, 66.47, 50.66, 37.57, 29.54, 27.61.HRMS m/z calculated for $C_{90}H_{87}O_{24}N_3Na$:1632.5526; found: 1632.5525.

2.5.6 Synthesis of Iduronic Acid Tetrasaccharide Precursor

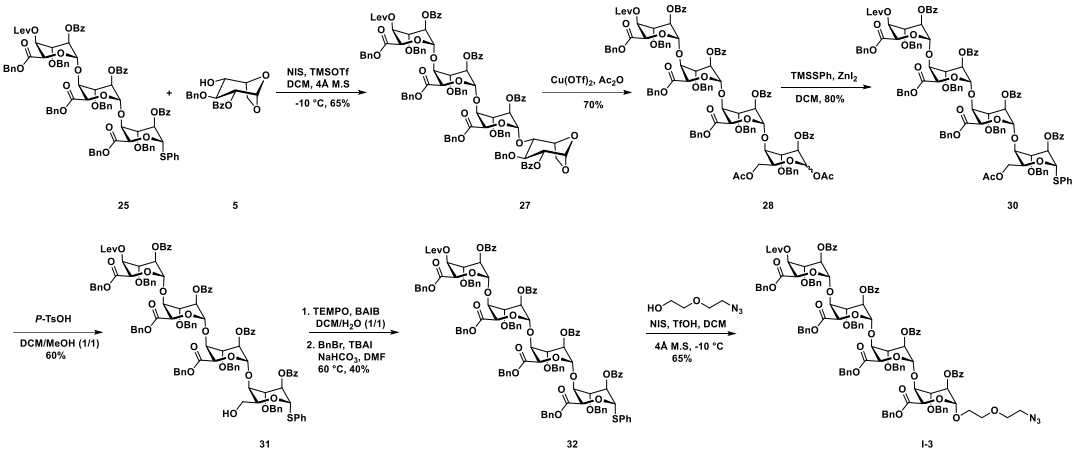

Scheme 10: Synthesis of Tetrasaccharide

Benzyl (2-O-benzoyl-3-O-benzyl-4-O-levulinoyl)-α-L-idopyranosyluronate-α(1→4) benzyl (2-O-benzoyl-3-O-benzyl)-α-L-idopyranosyl uronate-α(1→4) benzyl (2-O-benzoyl-3-O-benzyl)-α-L-idopyranosyluronate-α(1→4) (2-O-benzoyl-3-O-benzyl-1,6-anhydro)-β-L-idopyranose 28

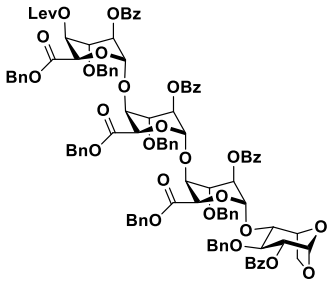

The synthetic procedure for the preparation of compound **18** was followed to obtain compound **28 (62%)** from compound **27** as syrup. $[\alpha]_D^{25}$+2.9 (*c* 1.0 $CHCl_3$); IR (cm^{-1}, $CHCl_3$): 1720, 1214, 1106. ^{1}H NMR (400 MHz, Chloroform-*d*) δ 7.98 – 7.89 (m, 8H), 7.58 – 7.53 (m, 2H), 7.45 – 7.38 (m, 9H), 7.33 – 7.27 (m, 8H), 7.25 – 7.21 (m, 9H), 7.19 – 7.13 (m, 11H), 7.12 – 7.09 (m, 4H), 7.02 – 6.98 (m, 4H), 5.49 (d, *J* = 1.8 Hz, 1H), 5.34 – 5.33 (m, 2H), 5.17 (t, *J* = 3.3 Hz, 2H), 5.10 (d, *J* = 12.0 Hz, 2H), 5.06 – 4.96 (m, 5H), 4.93 (s, 1H), 4.90 – 4.87 (m, 2H), 4.81 (d, *J* = 3.2 Hz, 1H), 4.79 (d, *J* = 2.5 Hz, 1H), 4.75 (t, *J* = 11.2, 2H), 4.68 (d, *J* = 10.9 Hz, 1H), 4.65 – 4.56 (m, 5H), 4.50 (d, *J* = 2.0 Hz, 1H), 4.47 (d, *J* = 2.4 Hz, 1H), 4.29 (t, *J* = 4.0 Hz, 1H), 4.24 (ddd, *J* = 8.5, 4.1, 1.1 Hz, 1H), 4.18 (t, *J* = 4.0 Hz, 1H), 4.07 (d, *J* = 7.8 Hz, 1H), 3.99 (t, *J* = 3.6 Hz, 1H), 3.93 (t, *J* = 3.5 Hz, 1H), 3.85 (t, *J* = 8.3 Hz, 1H), 376 (t, *J* = 2.8 Hz, 1H), 3.57 – 3.54 (m, 1H), 2.36 (t, *J* = 6.8 Hz, 2H), 2.20 – 2.06 (m, 2H), 2.01 (s, 3H).^{13}C NMR

(101 MHz, Chloroform-*d*) δ 205.78, 171.34, 168.82, 168.57, 167.62, 165.82, 165.67, 165.18, 164.76, 137.93, 137.78, 137.37, 137.24, 135.19, 135.14, 134.99, 133.63, 133.59, 133.46, 133.35, 130.22, 130.00, 129.96, 129.58, 129.36, 128.99, 128.97, 128.69, 128.59, 128.55, 128.50, 128.47, 128.36, 128.26, 128.16, 128.11, 127.90, 127.84, 127.46, 101.30, 100.91, 99.39, 96.34, 77.86, 75.87, 75.60 , 75.44, 75.35, 74.91, 73.39, 73.07, 72.33, 72.25, 72.17, 69.02, 68.90, 68.47, 68.32, 67.19, 67.13, 67.04, 66.69, 66.64, 65.45, 37.67, 29.67.HRMS m/z calculated for $C_{106}H_{98}O_{29}Na$:1857.6091; found: 1857.6085.

Benzyl (2-O-benzoyl-3-O-benzyl-4-O-levulinoyl)-α-L-idopyranosyluronate-α(1→4) benzyl (2-O-benzoyl-3-O-benzyl)-α-L-idopyranosyluronate-α(1→4) benzyl (2-O-benzoyl-3-O-benzyl)-α-L-idopyranosyl uronate-α(1→4) (1,6-O-diacetyl-2-O-benzoyl-3-O-benzyl)-α/β-L-idopyranoside 29

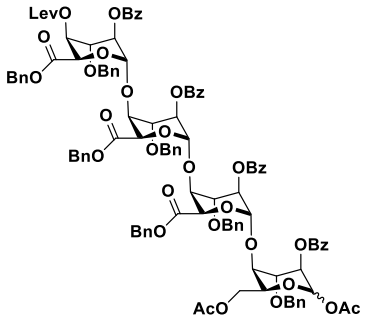

The synthetic procedure for the preparation of compound **19** was followed to obtain compound **29 (85%, α:β = 1:1)** from compound **23** as syrup. $[\alpha]_D^{25}$+6.7 (*c* 1.0 $CHCl_3$); IR (cm^{-1}, $CHCl_3$): 1721, 1215, 1095. ^{1}H NMR (400 MHz, Chloroform-*d*) δ 8.03 – 7.86 (m, 20H), 7.78 – 7.52 (m, 3H), 7.46 – 7.34 (m, 17H), 7.33 – 7.18 (m, 57H), 7.117 - 713 (m, 20H), 7.12 (s, 7H), 7.11 – 7.05 (m, 10H), 6.16 (s, 1H), 6.14 (d, *J* = 2.0 Hz, 1H), 5.28 (dd, *J* = 4.0, 2.0 Hz, 1H), 5.26 (d, *J* = 4.0 Hz, 2H), 5.19 – 5.09 (m, 12H), 5.04 (d, *J* = 19.4 Hz, 2H), 4.98 (dt, *J* = 9.2, 3.8 Hz, 5H), 4.93 (d, *J* = 1.6 Hz, 2H), 4.90 – 4.85 (m, 7H), 4.80 (d, *J* = 3.1 Hz, 2H), 4.76 (t, *J* = 2.3 Hz, 2H), 4.74 – 4.71 (m, 4H), 4.70 – 4.67 (m, 5H), 4.65 – 4.52 (m, 13H), 4.45 – 4.41 (m, 4H), 4.33 (t, *J* = 3.7 Hz, 1H), 4.30 – 4.21 (m, 5H), 4.14 – 4.10 (m, 2H), 4.05 (dq, *J* = 13.9, 3.9 Hz, 6H), 3.97 (t, *J* = 4.1 Hz, 1H), 3.91 (q, *J* = 3.5 Hz, 2H), 3.82 (q, *J* = 3.2 Hz, 2H), 3.74 (dt, *J* = 3.3, 1.8 Hz, 2H), 2.34 (td, *J* = 6.8, 1.5 Hz, 5H), 2.17 – 2.08 (m, 4H), 2.07 (s, 3H), 2.04 (dd, *J* = 3.8, 1.9 Hz, 1H), 2.02 (s, 3H), 2.00 (s, 6H), 1.95 (s, 3H), 1.93 (s, 3H). ^{13}C NMR (101 MHz, $CDCl_3$) δ 205.76, 171.32, 170.49, 170.47, 169.11, 169.02, 168.93, 168.75, 168.42, 168.37, 167.61, 166.04, 165.60, 165.41, 165.38, 165.22, 165.18, 164.77, 138.16, 137.75, 137.72, 137.70, 137.45, 137.44, 135.19, 135.12, 135.08, 134.99, 134.96, 133.64, 133.49, 133.46, 133.43, 133.33, 130.20, 130.13, 130.03, 129.99, 129.46, 129.38, 129.20, 129.15, 129.03, 128.96, 128.91, 128.70, 128.64, 128.59, 128.56, 128.49, 128.43, 128.41, 128.38, 128.37, 128.34, 128.31, 128.29, 128.21, 128.20, 128.14, 128.06, 127.92, 127.89, 127.85,

127.80, 127.73, 127.65, 127.55, 101.56, 101.40, 101.02, 101.00, 100.74, 100.54, 91.81, 90.72, 76.73, 76.63, 76.42, 76.23, 76.01, 75.78, 75.70, 75.41, 75.17, 73.69, 73.32, 73.18, 73.10, 73.07, 73.04, 72.53, 72.37, 72.30, 72.23, 72.14, 70.70, 70.55, 69.91, 69.76, 69.02, 68.90, 68.54, 68.52, 68.40, 67.30, 67.13, 67.11, 66.79, 66.78, 66.73, 66.51, 63.03, 62.57, 37.68, 29.69, 29.67, 27.71, 21.06, 20.86, 20.84.HRMS m/z calculated for $C_{110}H_{104}O_{32}Na$:1959.6408; found: 1959.6400.

Benzyl (2-O-benzoyl-3-O-benzyl-4-O-levulinoyl)-α-L-idopyranosyl uronate-α(1→4) benzyl (2-O-benzoyl-3-O-benzyl)-α-L-idopyranosyluronate-α(1→4) benzyl (2-O-benzoyl-3-O-benzyl)-α-L-idopyranosyluronate-α(1→4) 1-thiophenyl-(6-O-acetyl-2-O-benzoyl, 3-O-benzyl)-α-L-idopyranoside 30.

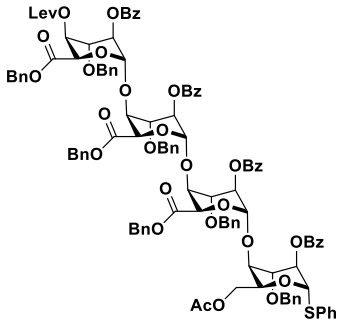

The synthetic procedure for the preparation of compound **6** was followed to obtain compound **30 (80%)** from compound **29** as syrup. $[\alpha]_D^{25}$-26.3 (*c* 1.0 $CHCl_3$); IR (cm^{-1}, $CHCl_3$): 1720, 1214, 742. ^1H NMR (400 MHz, Chloroform-*d*) δ 7.96 (ddd, *J* = 6.8, 6.0, 1.5 Hz, 6H), 7.86 (dd, *J* = 8.3, 1.1 Hz, 2H), 7.58 – 7.53 (m, 3H), 7.47 – 7.43 (m, 1H), 7.42 – 7.36 (m, 7H), 7.34 – 7.27 (m, 12H), 7.25 – 7.04 (m, 29H), 5.53 (s, 1H), 5.40 (dt, *J* = 2.4, 1.1 Hz, 1H), 5.29 (d, *J* = 5.2 Hz, 1H), 5.17 – 5.12 (m, 4H), 5.07 (dd, *J* = 16.1, 12.1 Hz, 2H), 4.98 – 4.97 (m, 1H), 4.96 – 4.90 (m, 2H), 4.87 – 4.84 (m, 4H), 4.79 – 4.67 (m, 6H), 4.59 (ddd, *J* = 15.8, 11.4, 4.1 Hz, 4H), 4.42 (d, *J* = 11.3 Hz, 1H), 4.26 – 4.21 (m, 2H), 4.06 – 4.02 (m, 4H), 3.93 (t, *J* = 3.2 Hz, 1H), 3.79 (t, *J* = 2.5 Hz, 1H), 3.74 (td, *J* = 3.3, 0.9 Hz, 1H), 2.34 (t, *J* = 6.8 Hz, 2H), 2.17 – 2.02 (m, 2H), 1.99 (s, 3H), 1.91 (s, 3H).^{13}C NMR (101 MHz, $CDCl_3$) δ 205.76, 171.33, 170.33, 168.96, 168.33, 167.63, 165.81, 165.36, 165.24, 164.77, 137.93, 137.74, 137.41, 137.26, 136.29, 135.18, 135.12, 134.97, 133.64, 133.52, 133.45, 133.35, 131.76, 130.20, 130.11, 130.02, 129.99, 129.45, 129.39, 129.19, 128.91, 128.88, 128.71, 128.63, 128.59, 128.56, 128.48, 128.44, 128.40, 128.34, 128.26, 128.17, 128.10, 127.96, 127.79, 127.75, 127.67, 127.41, 101.56, 101.29, 100.82, 86.10, 76.74, 76.30, 76.28, 75.58, 73.76, 73.18, 72.84, 72.36, 72.26, 70.89, 69.06, 68.70, 68.55, 68.11, 67.15, 67.11, 66.82, 66.76, 65.85, 63.18, 37.68, 29.67, 27.72, 20.83.HRMS m/z calculated for $C_{114}H_{106}O_{30}SNa$:2009.6387; found: 2009.6359.

Benzyl (2-O-benzoyl-3-O-benzyl-4-O-levulinoyl)-α-L-idopyranosyl uronate-α(1→4) benzyl (2-O-benzoyl-3-O-benzyl)-α-L-idopyranosyl uronate-α(1→4) benzyl (2-O-benzoyl-3-O-benzyl)-α-L-idopyranosyl uronate-α(1→4) 1-thiophenyl-(2-O-benzoyl-3-O-benzyl)-α-L-idopyranoside 31

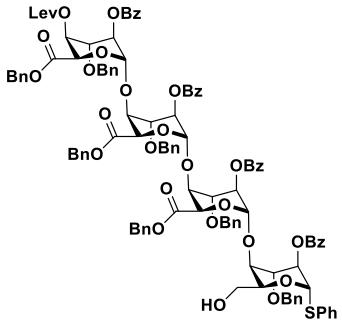

The synthetic procedure for the preparation of compound **27** was followed to obtain compound **31 (66%)** from compound **30** as syrup. $[\alpha]_D^{25}$-37.2 (*c* 1.0 $CHCl_3$); IR (cm^{-1}, $CHCl_3$): 1720, 1214, 742. ^{1}H NMR (400 MHz, Chloroform-*d*) δ 8.01 – 7.95 (m, 6H), 7.89 – 7.87 (m, 2H), 7.58 – 7.51 (m, 3H), 7.48 – 7.34 (m, 9H), 7.33 – 7.27 (m, 13H), 7.25 – 7.14 (m, 17H), 7.13 (s, 5H), 7.10 – 7.03 (m, 5H), 5.57 (s, 1H), 5.42 (dd, *J* = 2.6, 1.3 Hz, 1H), 5.29 – 5.27 (m, 1H), 5.20 (d, *J* = 2.9 Hz, 1H), 5.17 (t, *J* = 2.7 Hz, 2H), 5.14 (d, *J* = 2.0 Hz, 1H), 5.12 – 5.08 (m, 2H), 5.03 – 4.98 (m, 2H), 4.97 – 4.92 (m, 2H), 4.89 – 4.86 (m, 3H), 4.80 – 4.77 (m, 2H), 4.75 – 4.69 (m, 5H), 4.66 – 4.56 (m, 4H), 4.43 (d, *J* = 11.4 Hz, 1H), 4.27 – 4.26 (m, 1H), 4.09 – 4.03 (m, 3H), 3.96 (t, *J* = 3.4 Hz, 1H), 3.86 (s, 1H), 3.76 – 3.70 (m, 2H), 3.56 – 3.52 (m, 1H), 2.35 (t, *J* = 6.8 Hz, 2H), 2.17 – 2.03 (m, 2H), 2.00 (s, 3H).^{13}C NMR (101 MHz, $CDCl_3$) δ 205.77, 171.34, 168.90, 168.37, 167.63, 165.81, 165.61, 165.32, 164.78, 138.04, 137.69, 137.37, 137.24, 136.21, 135.18, 135.09, 134.94, 133.65, 133.62, 133.55, 133.29, 131.83, 130.21, 130.09, 129.98, 129.93, 129.53, 129.38, 129.13, 129.04, 128.87, 128.70, 128.61, 128.60, 128.57, 128.49, 128.42, 128.39, 128.31, 128.20, 128.12, 128.07, 128.00, 127.74, 127.70, 127.43, 101.35, 101.24, 101.04, 86.17, 76.62, 76.36, 76.33, 75.66, 73.87, 73.26, 72.97, 72.74, 72.38, 72.26, 71.16, 71.08, 69.46, 68.84, 68.51, 68.32, 68.09, 61.82, 53.56, 37.67, 29.66.HRMS m/z calculated for $C_{112}H_{104}O_{29}SNa$:1967.6282; found: 1967.6277.

Benzyl (2-O-benzoyl-3-O-benzyl-4-O-levulinoyl)-α-L-idopyranosyluronate-α(1→4) benzyl (2-O-benzoyl-3-O-benzyl)-α-L-idopyranosyluronate-α(1→4) benzyl (2-O-benzoyl-3-O-benzyl)-α-L-idopyranosyl uronate-α(1→4) benzyl (1-thiophenyl-2-O-benzoyl-3-O-benzyl)-α-L-idopyranoside uronate 32.

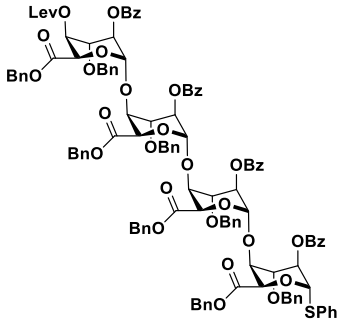

The preparation of the target compound **32 (58%)** was carried out from compound **31** according to the same procedure as for compound **7** as syrup. $[\alpha]_D^{25}$-21.3 (*c* 1.0 $CHCl_3$); IR (cm^{-1}, $CHCl_3$): 1720, 1453, 1096. ^1H NMR (400 MHz, Chloroform-*d*) δ 8.01 – 7.88 (m, 8H), 7.58 – 7.52 (m, 3H), 7.43 – 7.38 (m, 6H), 7.33 – 7.28 (m, 11H), 7.27 – 7.22 (m, 12H), 7.20 – 7.15 (m, 14H), 7.14 – 7.05 (m, 11H), 5.71 (d, *J* = 2.0 Hz, 1H), 5.39 (t, *J* = 2.6 Hz, 1H), 5.37 (d, *J* = 3.0 Hz, 2H), 5.20 (d, *J* = 3.1 Hz, 1H), 5.17 (t, *J* = 3.4 Hz, 1H), 5.12 (t, *J* = 3.3 Hz, 1H), 5.09 (dd, *J* = 7.0, 5.1 Hz, 2H), 5.04 – 4.96 (m, 3H), 4.93 (dd, *J*= 12.3, 10.7 Hz, 2H), 4.87 (s, 3H), 4.75 (q, *J* = 3.2 Hz, 4H), 4.71 (d, *J* = 3.0 Hz, 2H), 4.66 (dd, *J* = 13.9, 11.3 Hz, 2H), 4.56 (dd, *J* = 13.6, 11.4 Hz, 2H), 4.47 (dd, *J* = 30.7, 11.3 Hz, 2H), 4.29 (t, *J* = 3.1 Hz, 1H), 4.24 (t, *J* = 3.2 Hz, 1H), 4.06 (t, *J* = 3.6 Hz, 1H), 3.97 (t, *J* = 4.0 Hz, 1H), 3.95 (t, *J* = 3.6 Hz, 1H), 3.90 (t, *J* = 3.5 Hz, 1H), 3.74 (t, *J* = 3.2 Hz, 1H), 2.36 (t, *J* = 6.8 Hz, 2H), 2.19 – 2.02 (m, 2H), 2.01 (s, 3H).^{13}C NMR (101 MHz, Chloroform-*d*) δ 205.75, 171.30, 168.73, 168.58, 168.42, 167.58, 165.73, 165.21, 165.12, 164.74, 137.66, 137.63, 137.48, 137.23, 135.58, 135.41, 135.20, 135.07, 135.00, 133.61, 133.41, 133.39, 133.37, 131.59, 130.25, 130.20, 130.14, 129.96, 129.36 , 129.32, 129.11, 128.99, 128.67, 128.61, 128.57, 128.53, 128.51, 128.47, 128.45, 128.38, 128.32, 128.24, 128.16, 128.09, 127.87, 127.77, 127.74, 127.71, 127.48, 101.88, 101.20, 101.17, 86.18, 76.69, 76.41, 75.64, 75.34, 74.54, 73.04, 72.84, 72.26, 72.13, 69.58, 69.08, 69.00, 68.80, 68.52, 68.32, 67.08, 67.03, 66.90, 66.73, 66.68, 37.66, 29.65, 27.69. HRMS m/z calculated for $C_{119}H_{108}O_{30}SNa$:2071.6544; found: 2071.6555.

Ethoxy-2-azidoethoxyl-O-(benzyl (2-O-benzoyl-3-O-benzyl-4-O-levulinoyl)-α-L-idopyranosyl uronate-α(1→4) benzyl (2-O-benzoyl-3-O-benzyl)-α-L-idopyranosyluronate-α(1→4) benzyl (2-O-benzoyl-3-O-benzyl)-α-L-idopyranosyluronate-α(1→4) benzyl(2-O-benzoyl-3-O-benzyl))-α-L-idopyroside uronate I-3

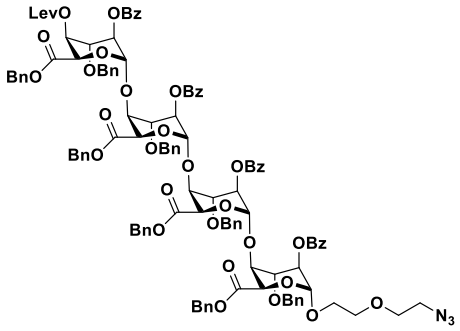

The synthetic procedure for the preparation of compound **9** was followed to obtain compound **I-3 (76%)** from compound **32** as syrup. $[\alpha]_D^{25}$-27.4 (*c* 1.0 $CHCl_3$); IR (cm^{-1}, $CHCl_3$): 1720, 1214, 1096, 749.^{1}H NMR (400 MHz, Chloroform-*d*) δ 7.95 (ddd, *J* = 8.3, 6.7, 1.5 Hz, 4H), 7.89 (ddd, *J* = 8.4, 4.6, 1.4 Hz, 3H), 7.58 – 7.54 (m, 1H), 7.38 (dt, *J* = 11.6, 7.9 Hz, 8H), 7.30 (tdd, *J* = 7.9, 6.2, 1.5 Hz, 9H), 7.24 – 7.15 (m, 22H), 7.14 – 7.07 (m, 10H), 6.98 (dd, *J* = 6.7, 2.9 Hz, 2H), 5.25 (d, *J* = 2.4 Hz, 1H), 5.22 – 5.14 (m, 5H), 5.11 – 5.05 (m, 4H), 5.03 – 5.00 (m, 2H), 4.97 (t, *J* = 2.7 Hz, 1H), 4.94 (d, *J* = 3.0 Hz, 1H), 4.86 (t, *J* = 2.9 Hz, 1H), 4.83 – 4.80 (m, 2H), 4.76 (d, *J* = 2.4 Hz, 1H), 4.73 – 4.68 (m, 5H), 4.67 – 4.57 (m, 3H), 4.47 (d, *J* = 11.0 Hz, 2H), 4.39 (d, *J* = 11.4 Hz, 1H), 4.24 (t, *J* = 3.4 Hz, 1H), 4.10 (d, *J* = 3.2 Hz, 2H), 3.98 – 3.96 (m, 1H), 3.94 (dt, *J* = 5.6, 2.5 Hz, 1H), 3.90 (t, *J* = 3.8 Hz, 1H), 3.86 (t, *J* = 3.6 Hz, 1H), 3.73 (t, *J* = 3.6 Hz, 1H), 3.70 – 3.61 (m, 3H), 3.58 – 3.45 (m, 2H), 3.12 (d, *J* = 5.4 Hz, 2H), 2.34 (t, *J* = 6.8 Hz, 2H), 2.17 – 2.03 (m, 2H), 2.00 (s, 3H).^{13}C NMR (101 MHz, Chloroform-*d*) δ 205.75, 171.30, 169.18, 168.52, 168.34, 167.56, 165.67, 165.31, 165.07, 164.74, 138.07, 137.69, 137.46, 137.24, 135.32, 135.20, 135.04, 135.00, 133.63, 133.40, 133.33, 130.21, 130.05, 129.97, 129.35, 129.19, 129.06, 129.04, 128.67, 128.62, 128.57, 128.53, 128.50, 128.48, 128.43, 128.40, 128.34, 128.31, 128.25, 128.23, 128.22, 128.10, 127.83, 127.77, 127.60 , 101.94 , 101.55, 101.09, 98.90, 76.67, 76.55, 75.66, 75.52, 74.91, 72.85, 72.78, 72.67, 72.18, 71.94, 70.22, 69.35, 68.66, 68.55, 68.50, 68.39, 67.78, 67.14, 67.08, 66.93, 66.64 , 66.58, 50.77, 37.67, 29.65, 27.70. HRMS m/z calculated for $C_{119}H_{108}O_{30}SNa$:2092.7048; found: 2092.7036.

2.6 References

1. Esko, J.D. & Selleck, S.B. Order out of chaos: assembly of ligand binding sites in heparan sulfate. *Ann. Rev. Biochem.***71**, 435-471 (2002).
2. Linhardt, R.J. 2003 Claude S. Hudson Award address in carbohydrate chemistry. Heparin: structure and activity. *J. Med. Chem.***46**, 2551-2564 (2003).
3. De Pasquale, V. & Pavone, L.M. Heparan sulfate proteoglycans: The sweet side of development turns sour in mucopolysaccharidoses. *Biochimica et Biophysica Acta (BBA)-Molecular Basis of Disease***1865**, 165539 (2019).
4. Whitelock, J.M. & Iozzo, R.V. Heparan sulfate: a complex polymer charged with biological activity. *Chem. Rev.***105**, 2745-2764 (2005).
5. Xu, D., Arnold, K. & Liu, J. Using structurally defined oligosaccharides to understand the interactions between proteins and heparan sulfate. *Curr. Opin. Struct. Biol.***50**, 155-161 (2018).
6. Zulueta, M.M.L., Chyan, C.-L. & Hung, S.-C. Structural analysis of synthetic heparan sulfate oligosaccharides with fibroblast growth factors and heparin-binding hemagglutinin. *Curr. Opin. Struct. Biol.***50**, 126-133 (2018).
7. Carlsson, P. & Kjellén, L. Heparin biosynthesis, in *Heparin-A Century of Progress* 23-41 (Springer, 2012).
8. Carlsson, P., Presto, J., Spillmann, D., Lindahl, U. & Kjellén, L. Heparin/heparan sulfate biosynthesis Processive formation of N-sulfated domains. *J. Biol. Chem.***283**, 20008-20014 (2008).
9. Capila, I. & Linhardt, R.J. Heparin–protein interactions. *Angew. Chem. Int. Ed.***41**, 390-412 (2002).
10. Esko, J.D., Kimata, K. & Lindahl, U. Proteoglycans and sulfated glycosaminoglycans, in *Essentials of Glycobiology. 2nd edition* (Cold Spring Harbor Laboratory Press, 2009).
11. Casu, B. *et al.* Controversial glycosaminoglycan conformations. *Nature***322**, 215-216 (1986).
12. Das, S.K. *et al.* Synthesis of conformationally locked carbohydrates: A skew-boat conformation of l-iduronic acid governs the antithrombotic activity of heparin. *Angew. Chem. Int. Ed.***40**, 1670-1673 (2001).

13. Ochsenbein, P., Bonin, M., Schenk-Joß, K. & El-Hajji, M. The 2SO Skew-Boat Conformation in L-Iduronic Acid. *Angew. Chem. Int. Ed.***123**, 11841-11843 (2011).
14. van Boeckel, C.A. & Petitou, M. The unique antithrombin III binding domain of heparin: a lead to new synthetic antithrombotics. *Angew. Chem. Int. Ed.* **32**, 1671-1690 (1993).
15. Petitou, M. & van Boeckel, C.A. A synthetic antithrombin III binding pentasaccharide is now a drug! What comes next? *Angew. Chem. Int. Ed.***43**, 3118-3133 (2004).
16. Wildt, W.d. *et al.* Extended Physicochemical Characterization of the Synthetic Anticoagulant Pentasaccharide Fondaparinux Sodium by Quantitative NMR and Single Crystal X-ray Analysis. *Molecules***22**, 1362 (2017).
17. Beecher, C.N., Young, R.P., Langeslay, D.J., Mueller, L.J. & Larive, C.K. Hydroxyl-proton hydrogen bonding in the heparin oligosaccharide Arixtra in aqueous solution. *J. Phys. Chem. B***118**, 482-491 (2014).
18. Muñoz-García, J.C., Corzana, F., de Paz, J.L., Angulo, J. & Nieto, P.M. Conformations of the iduronate ring in short heparin fragments described by time-averaged distance restrained molecular dynamics. *Glycobiology***23**, 1220-1229 (2013).
19. Muñoz-García, J.C. *et al.* Effect of the Substituents of the Neighboring Ring in the Conformational Equilibrium of Iduronate in Heparin-like Trisaccharides. *Chem. Eur. J.***18**, 16319-16331 (2012).
20. Hsieh, P.-H., Thieker, D.F., Guerrini, M., Woods, R.J. & Liu, J. Uncovering the relationship between sulphation patterns and conformation of iduronic acid in heparan sulphate. *Sci. Rep.* **6**, 29602 (2016).
21. Adibekian, A. *et al.* De novo synthesis of uronic acid building blocks for assembly of heparin oligosaccharides. *Chem. Eur. J.* **13**, 4510-4522 (2007).
22. Lohman, G.J., Hunt, D.K., Högermeier, J.A. & Seeberger, P.H. Synthesis of iduronic acid building blocks for the modular assembly of glycosaminoglycans. *J Org. Chem.***68**, 7559-7561 (2003).
23. Hansen, S.U. *et al.* Synthesis and scalable conversion of L-iduronamides to heparin-related di-and tetrasaccharides. *J Org. Chem***77**, 7823-7843 (2012).

24. Guedes, N. *et al.* Toward the solid-phase synthesis of heparan sulfate oligosaccharides: Evaluation of iduronic acid and idose building blocks. *J Org. Chem***78**, 6911-6934 (2013).
25. Arungundram, S. *et al.* Modular synthesis of heparan sulfate oligosaccharides for structure− activity relationship studies. *J. Am. Chem. Soc.***131**, 17394-17405 (2009).
26. Lee, J.C. *et al.* From D-Glucose to Biologically Potent L-Hexose Derivatives: Synthesis of α-L-Iduronidase Fluorogenic Detector and the Disaccharide Moieties of Bleomycin A2 and Heparan Sulfate. *Chem. Eur. J.***10**, 399-415 (2004).
27. Zong, C. *et al.* Heparan sulfate microarray reveals that heparan sulfate–protein binding exhibits different ligand requirements. *J. Am. Chem. Soc.* **139**, 9534-9543 (2017).
28. Dey, S. & Wong, C.-H. Programmable one-pot synthesis of heparin pentasaccharides enabling access to regiodefined sulfate derivatives. *Chem. Sci.***9**, 6685-6691 (2018).
29. Jayson, G.C. *et al.* Synthetic heparan sulfate dodecasaccharides reveal single sulfation site interconverts CXCL8 and CXCL12 chemokine biology. *Chem. Commun.***51**, 13846-13849 (2015).
30. Liu, J. & Linhardt, R.J. Chemoenzymatic synthesis of heparan sulfate and heparin. *Nat. Prod. Rep.***31**, 1676-1685 (2014).
31. Lu, L.-D. *et al.* Synthesis of 48 disaccharide building blocks for the assembly of a heparin and heparan sulfate oligosaccharide library. *Org. Lett.***8**, 5995-5998 (2006).
32. Shibata, I. & Isogai, A. Depolymerization of cellouronic acid during TEMPO-mediated oxidation. *Cellulose***10**, 151-158 (2003).
33. Isogai, A. & Kato, Y. Preparation of polyuronic acid from cellulose by TEMPO-mediated oxidation. *Cellulose***5**, 153-164 (1998).
34. Cumpstey, I. Chemical modification of polysaccharides. *International Scholarly Rresearch Notices***2013** (2013).
35. Isogai, A., Saito, T. & Fukuzumi, H. TEMPO-oxidized cellulose nanofibers. *Nanoscale***3**, 71-85 (2011).

2.7 Spectral Data

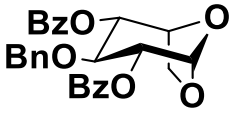

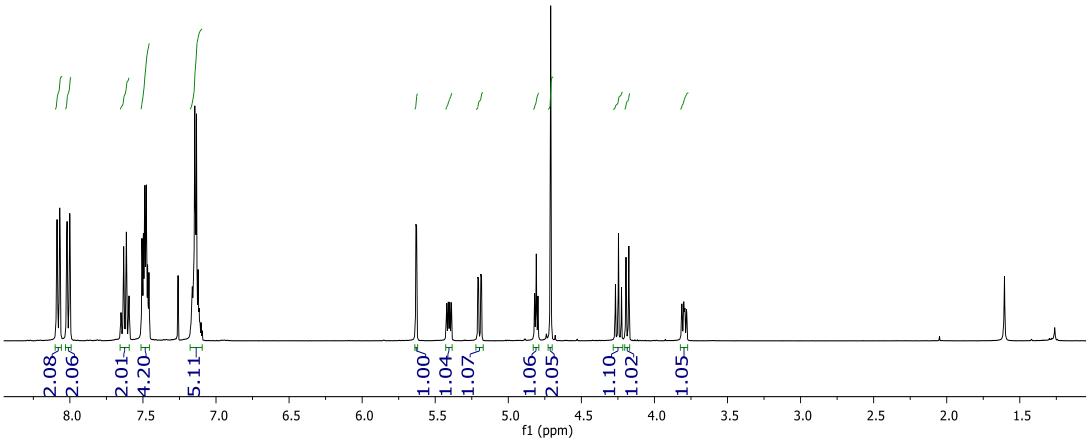

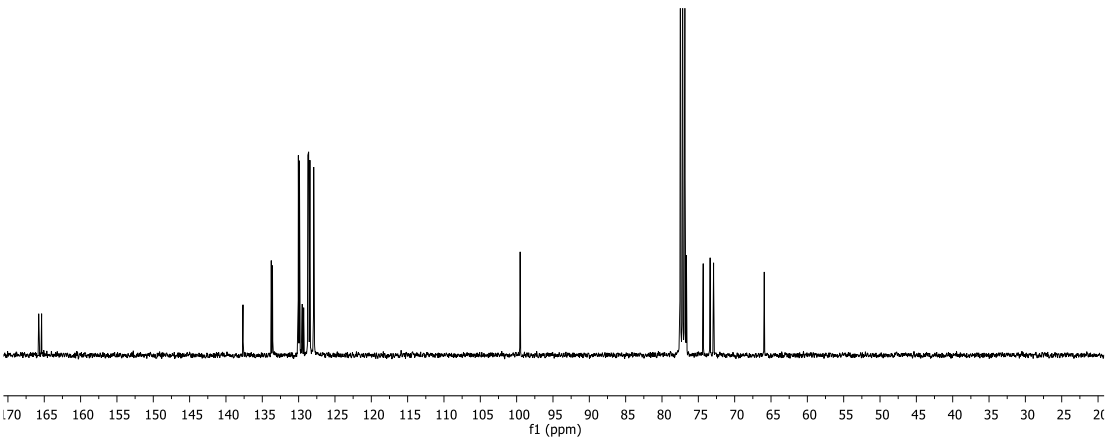

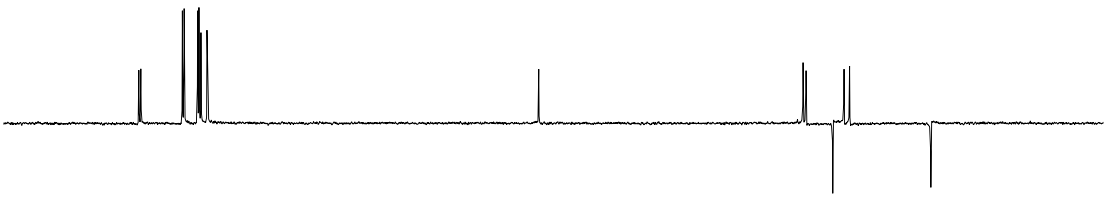

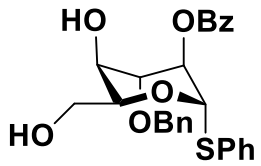
HO
OBz
O
OBn
HO
SPh

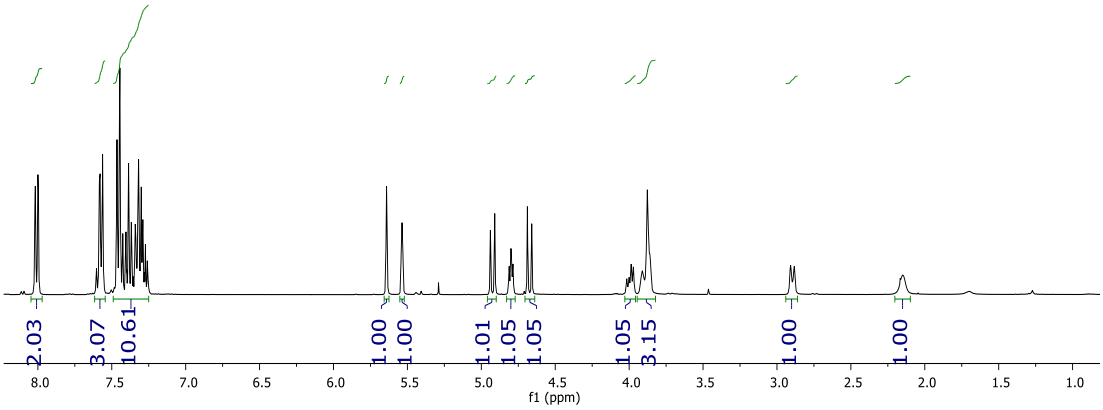
2.03
3.07
10.61
1.00
1.00
1.01
1.05
1.05
1.05
3.15
1.00
1.00
8.0
7.5
7.0
6.5
6.0
5.5
5.0
4.5
4.0
3.5
3.0
2.5
2.0
1.5
1.0
f1 (ppm)

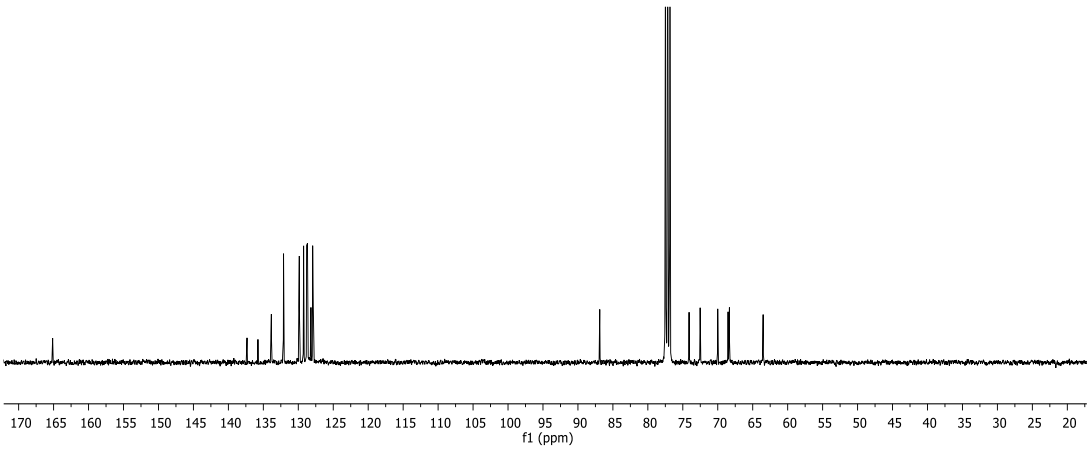
170 165 160 155 150 145 140 135 130 125 120 115 110 105 100 95 90 85 80 75 70 65 60 55 50 45 40 35 30 25 20
f1 (ppm)

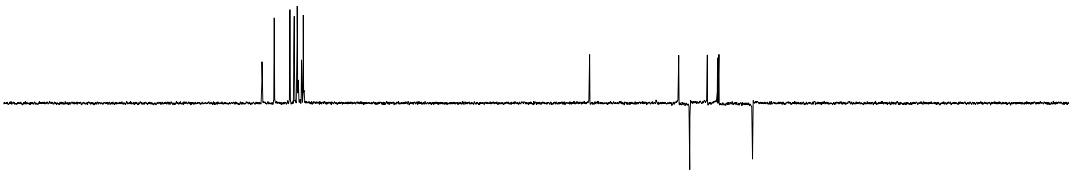

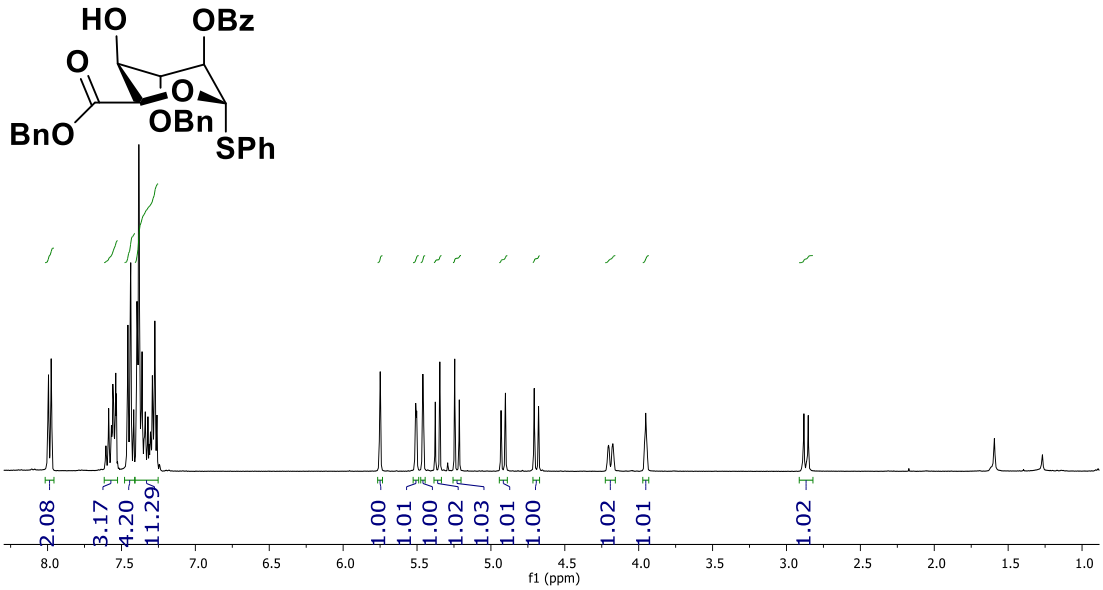
HO
OBz
O
O
BnO
OBn
SPh
2.08
3.17
4.20
11.29
1.00
1.01
1.00
1.02
1.03
1.01
1.00
1.02
1.01
1.02
f1 (ppm)

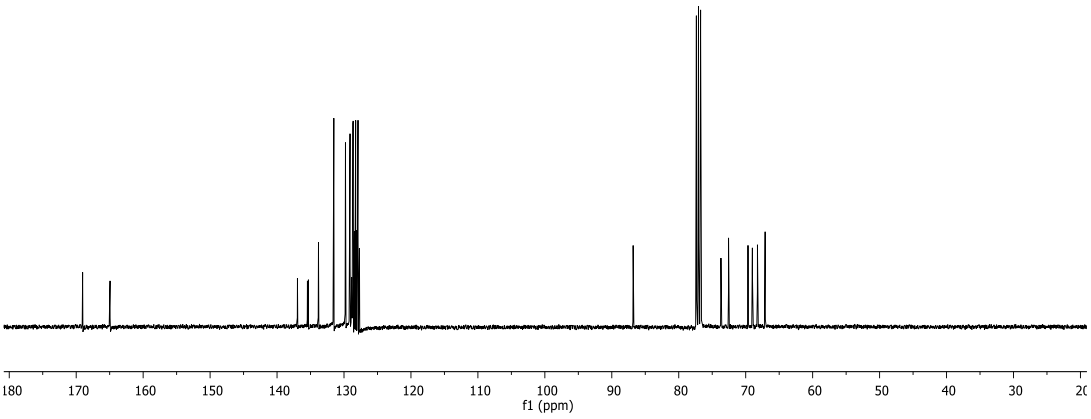
f1 (ppm)

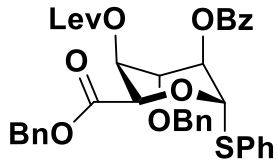
LevO
OBz
O
O
BnO
OBn
SPh

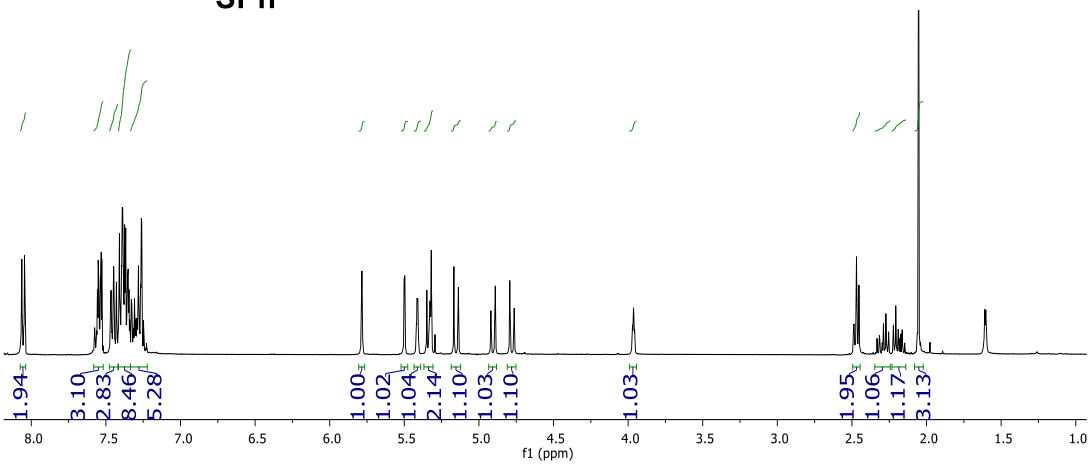
1.94
3.10
2.83
8.46
5.28
1.00
1.02
1.04
2.14
1.10
1.03
1.10
1.03
1.95
1.06
1.17
3.13
8.0
7.5
7.0
6.5
6.0
5.5
5.0
4.5
4.0
3.5
3.0
2.5
2.0
1.5
1.0
f1 (ppm)

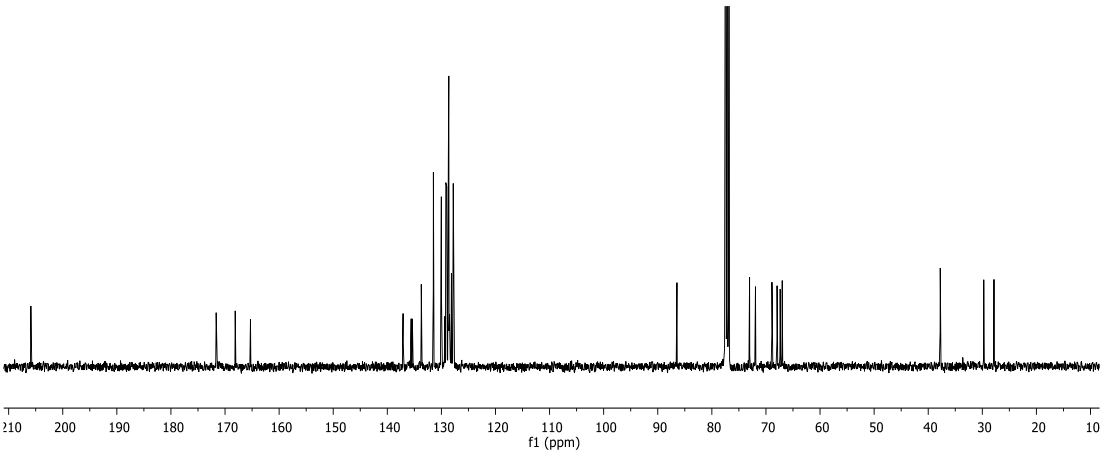
210
200
190
180
170
160
150
140
130
120
110
100
90
80
70
60
50
40
30
20
10
f1 (ppm)

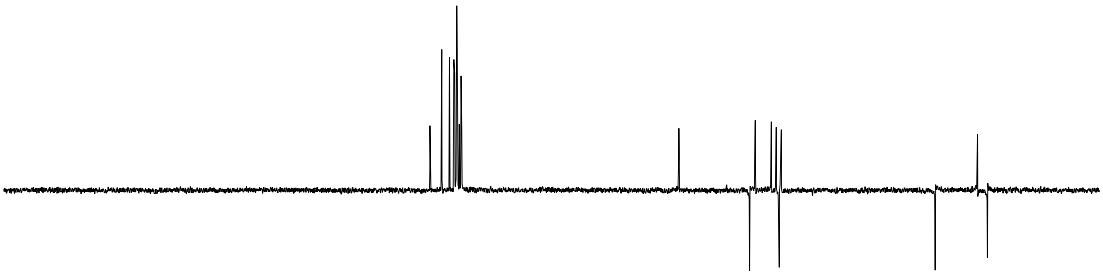

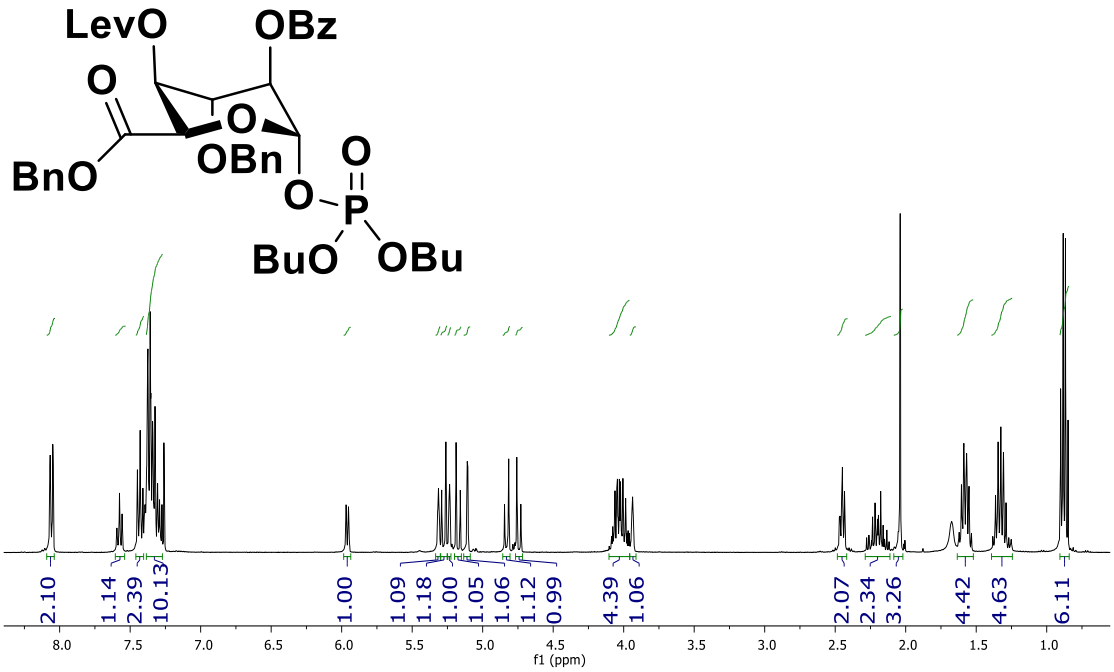
LevO
OBz
O
O
OBn
BnO
O
P
BuO
OBu
2.10
1.14
2.39
10.13
1.00
1.09
1.18
1.00
1.05
1.06
1.12
0.99
4.39
1.06
2.07
2.34
3.26
4.42
4.63
6.11
f1 (ppm)

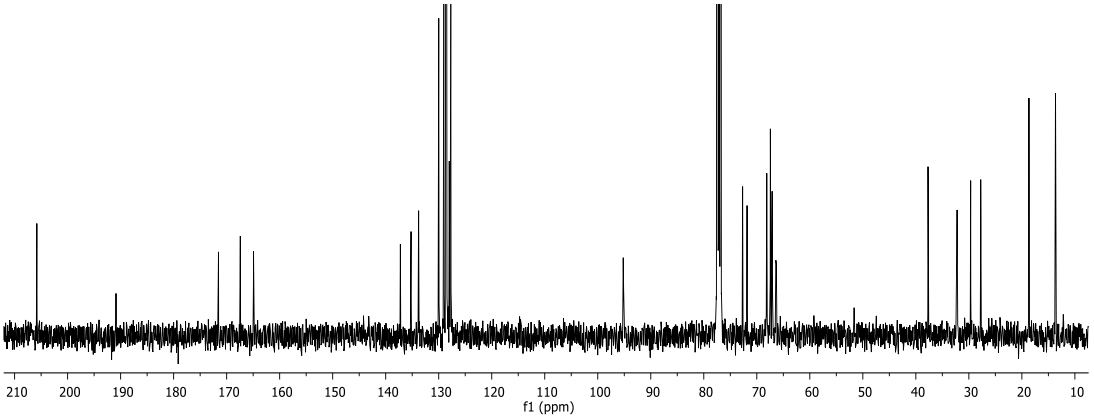
f1 (ppm)

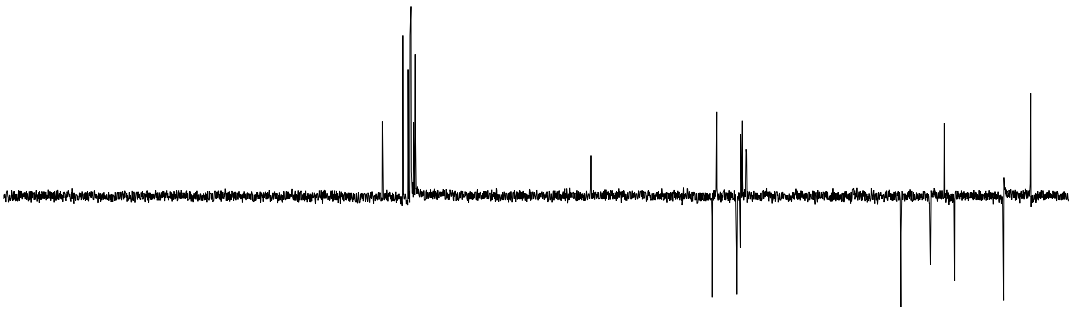

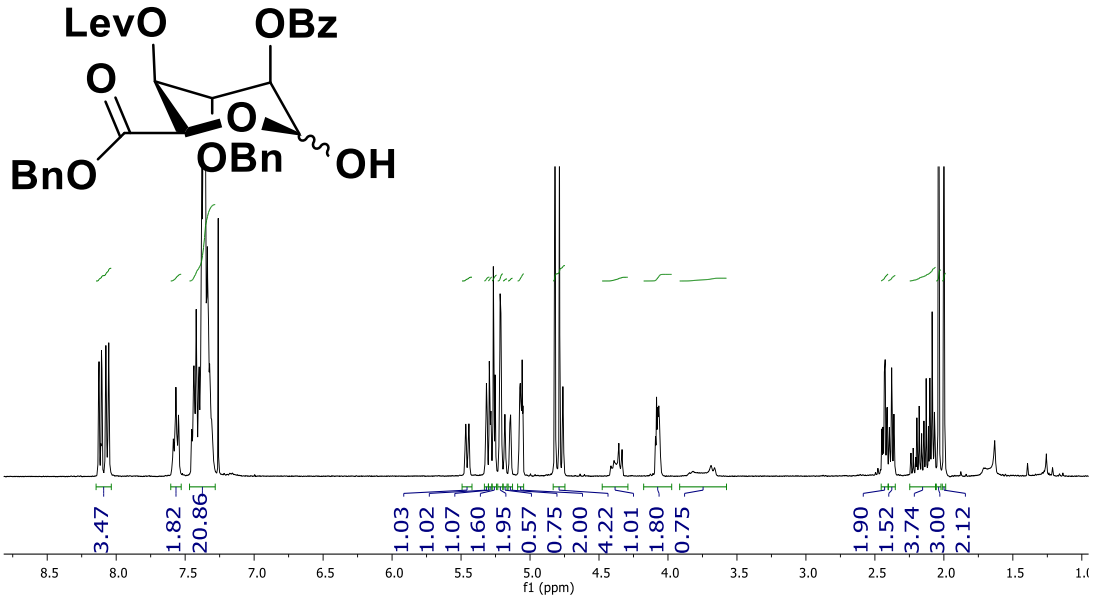
LevO
OBz
O
O
BnO
OBn
OH
3.47
1.82
20.86
1.03
1.02
1.07
1.60
1.95
0.57
0.75
2.00
4.22
1.01
1.80
0.75
1.90
1.52
3.74
3.00
2.12
f1 (ppm)

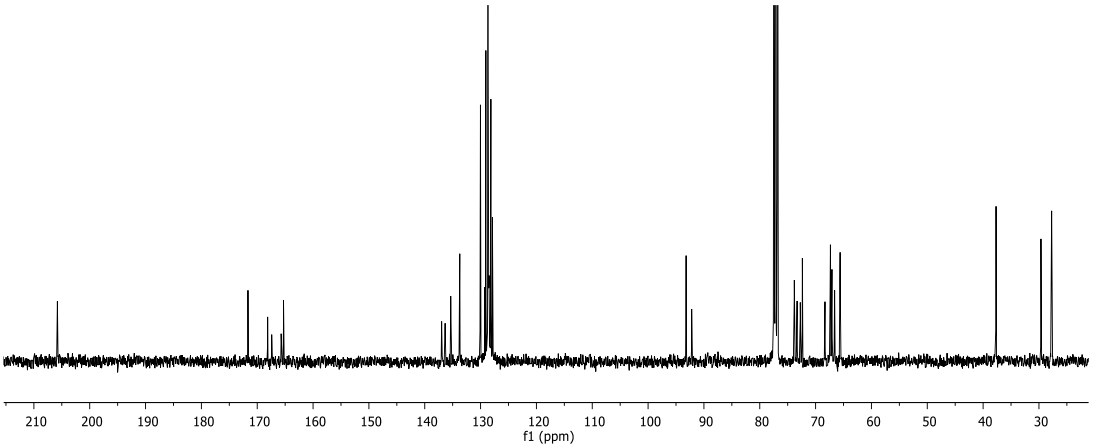
f1 (ppm)

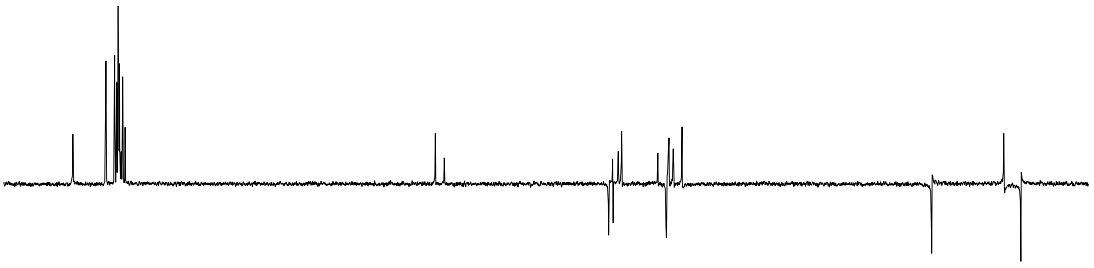

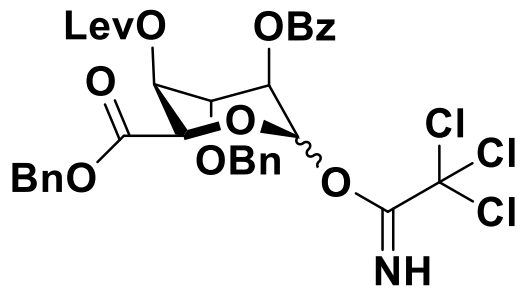
LevO
OBz
O
O
BnO
OBn
O
Cl
Cl
Cl
NH

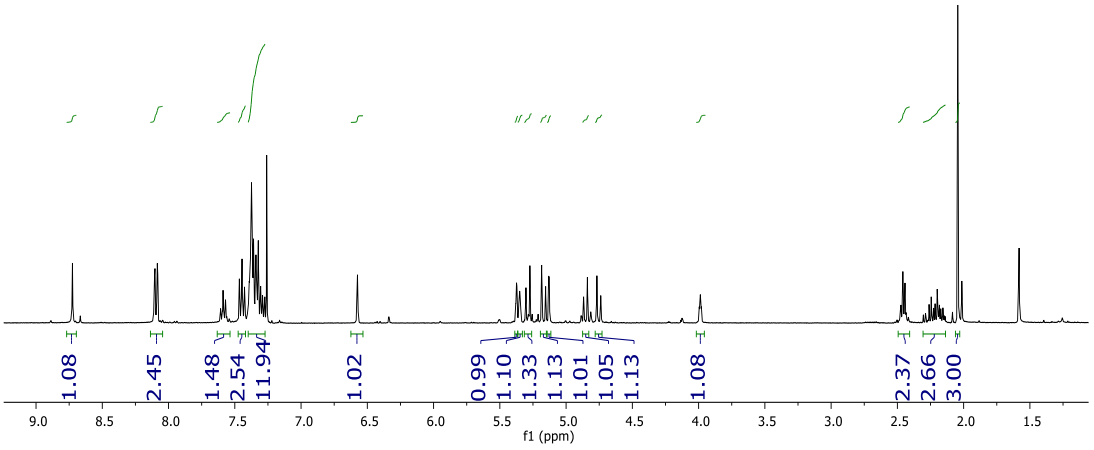
1.08
2.45
1.48
2.54
11.94
1.02
0.99
1.10
1.33
1.13
1.01
1.05
1.13
1.08
2.37
2.66
3.00
f1 (ppm)

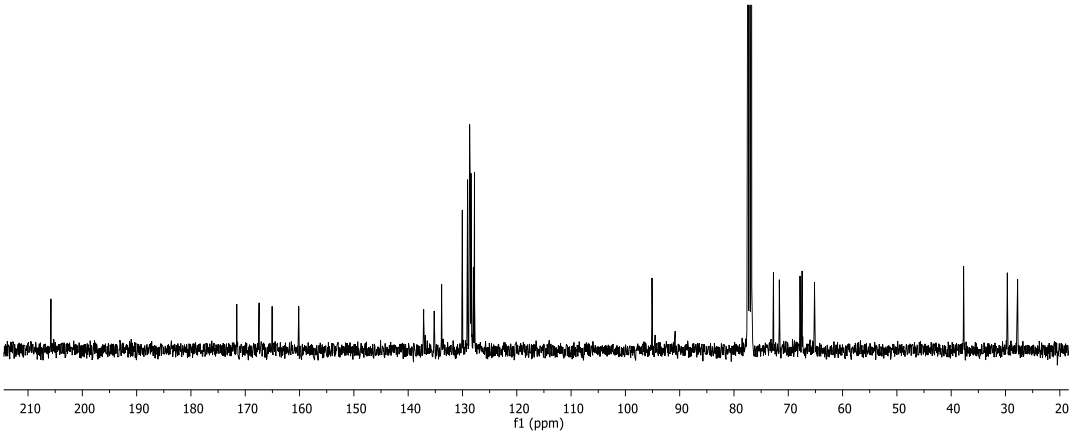
f1 (ppm)

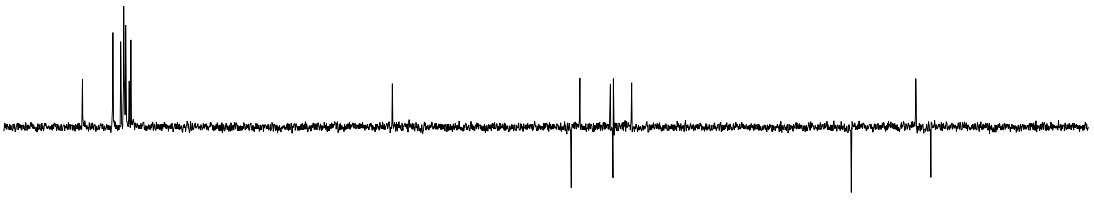

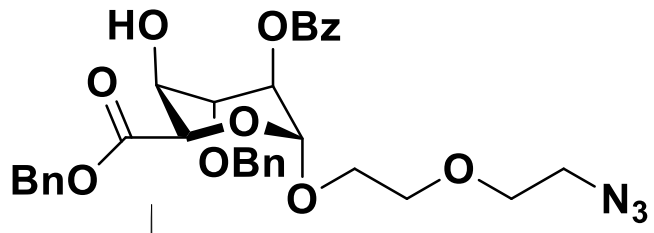
HO
OBz
O
O
OBn
BnO
O
O
N3

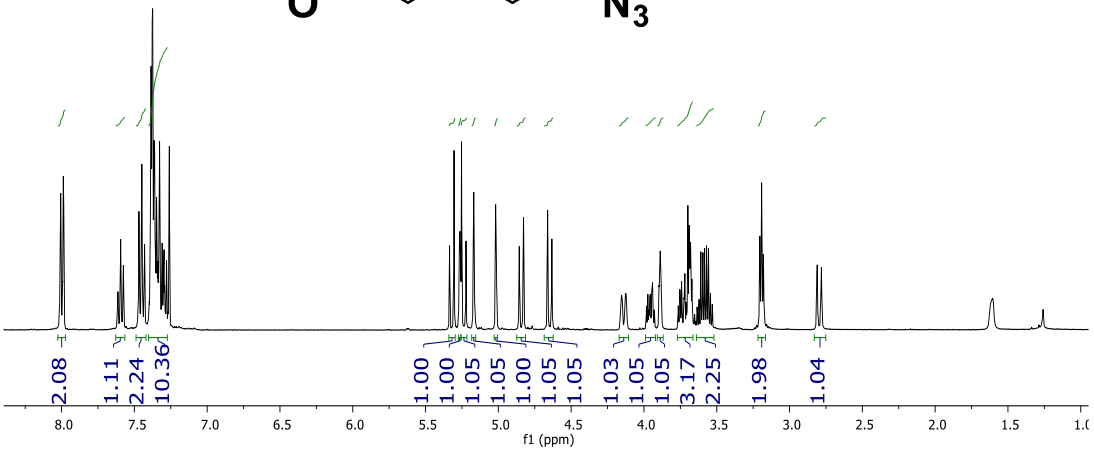
2.08
1.11
2.24
10.36
1.00
1.00
1.05
1.05
1.00
1.05
1.05
1.03
1.05
1.05
3.17
2.25
1.98
1.04
8.0
7.5
7.0
6.5
6.0
5.5
5.0
4.5
4.0
3.5
3.0
2.5
2.0
1.5
f1 (ppm)

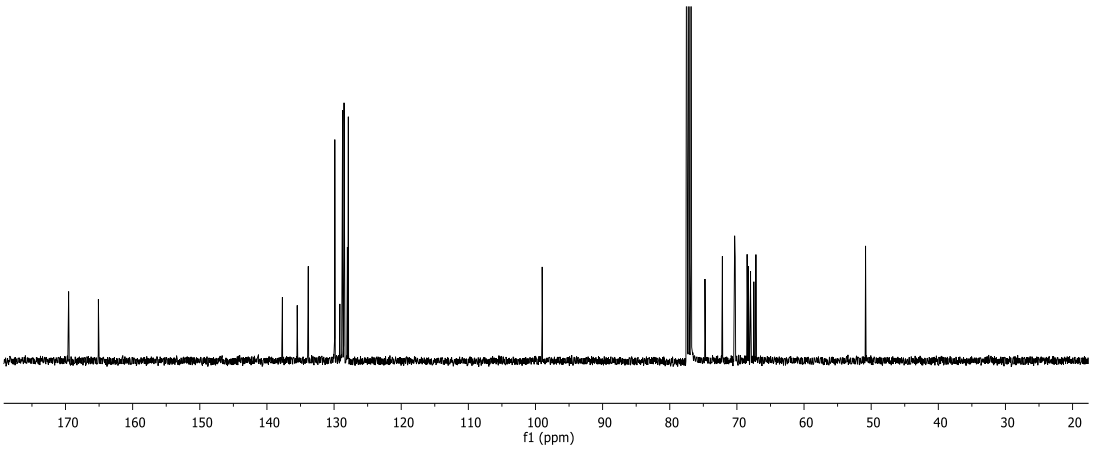
170
160
150
140
130
120
110
100
90
80
70
60
50
40
30
20
f1 (ppm)

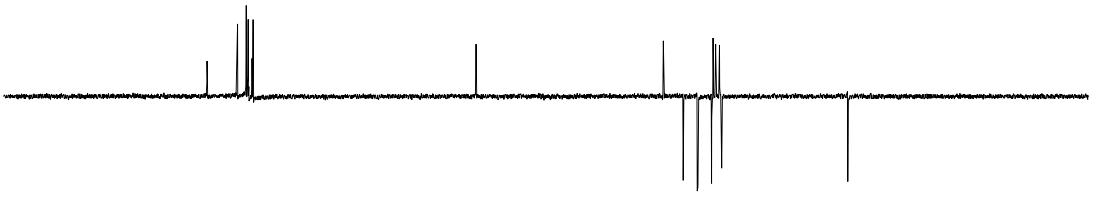

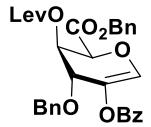
LevO
CO2Bn
O
BnO
OBz

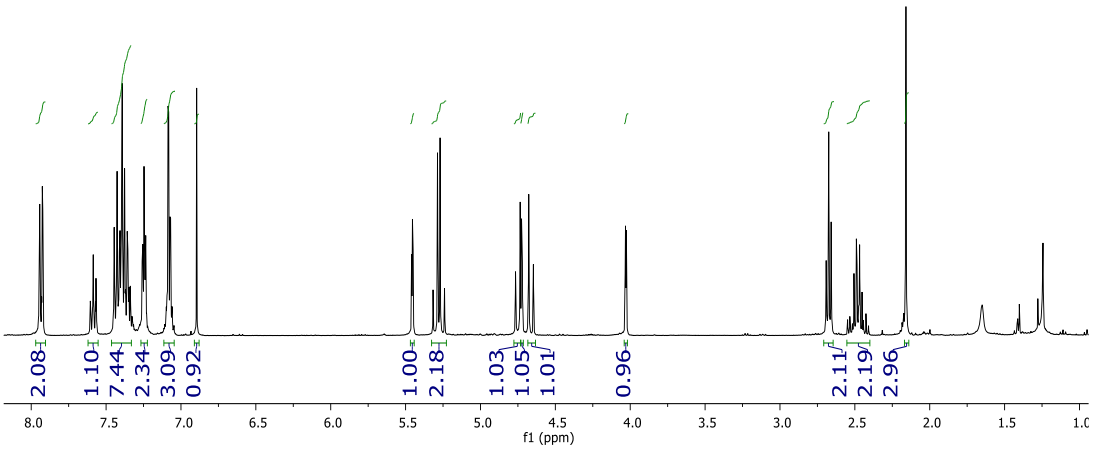
2.08
1.10
7.44
2.34
3.09
0.92
1.00
2.18
1.03
1.05
1.01
0.96
2.11
2.19
2.96
8.0
7.5
7.0
6.5
6.0
5.5
5.0
4.5
4.0
3.5
3.0
2.5
2.0
1.5
f1 (ppm)

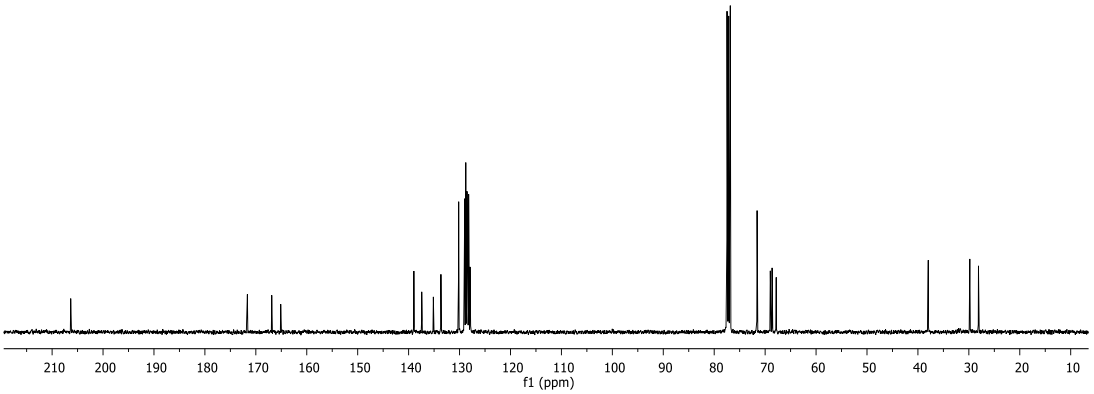
210
200
190
180
170
160
150
140
130
120
110
100
90
80
70
60
50
40
30
20
10
f1 (ppm)

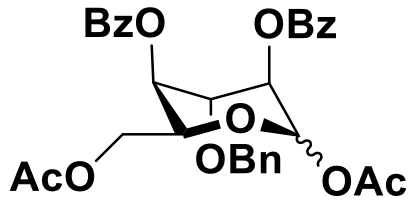
BzO
OBz
O
OBn
AcO
OAc

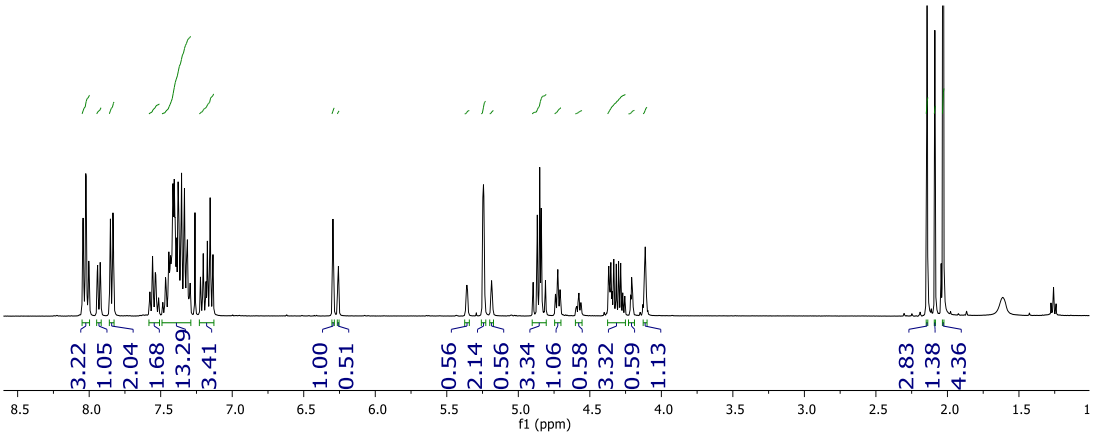
3.22
1.05
2.04
1.68
13.29
3.41
1.00
0.51
0.56
2.14
0.56
3.34
1.06
0.58
3.32
0.59
1.13
2.83
1.38
4.36
8.5
8.0
7.5
7.0
6.5
6.0
5.5
5.0
4.5
4.0
3.5
3.0
2.5
2.0
1.5
1
f1 (ppm)

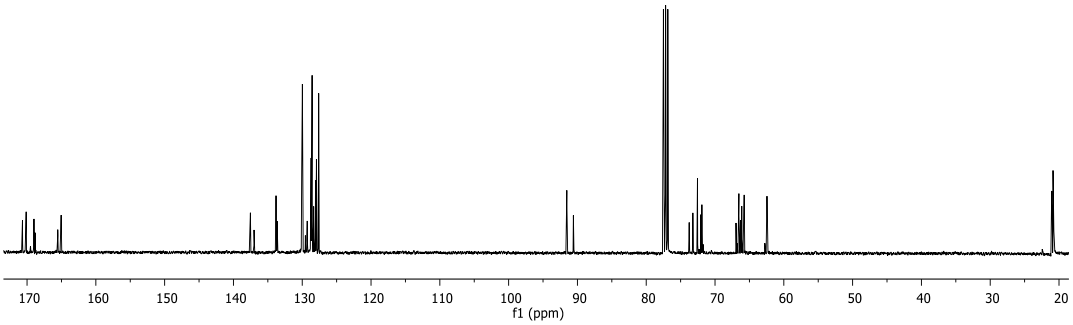
170
160
150
140
130
120
110
100
90
80
70
60
50
40
30
20
f1 (ppm)

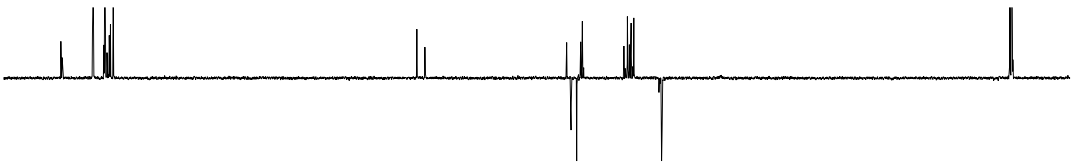

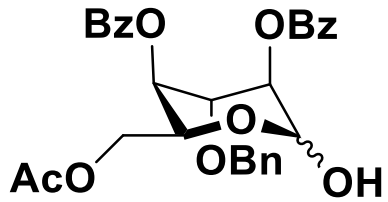
BzO
OBz
O
OBn
AcO
OH

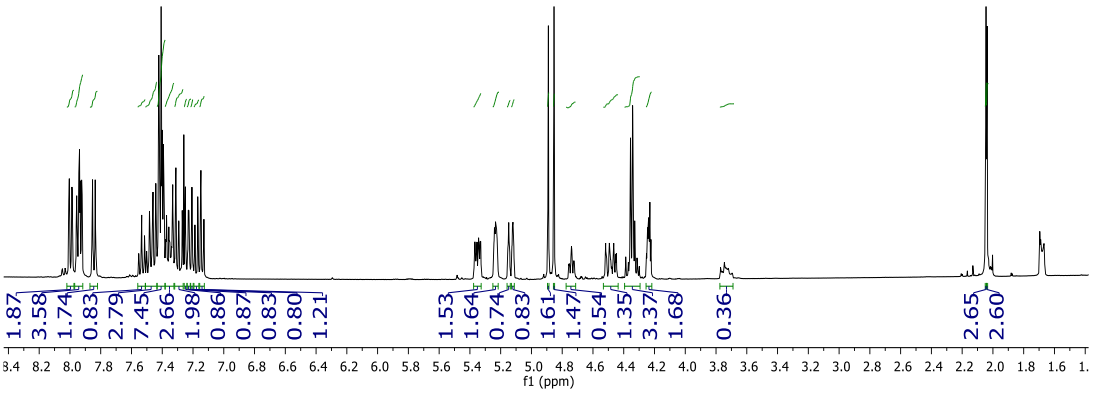
1.87
3.58
1.74
0.83
2.79
7.45
2.66
1.98
0.86
0.87
0.83
0.80
1.21
1.53
1.64
0.74
0.83
1.61
1.47
0.54
1.35
3.37
1.68
0.36
2.65
2.60
f1 (ppm)

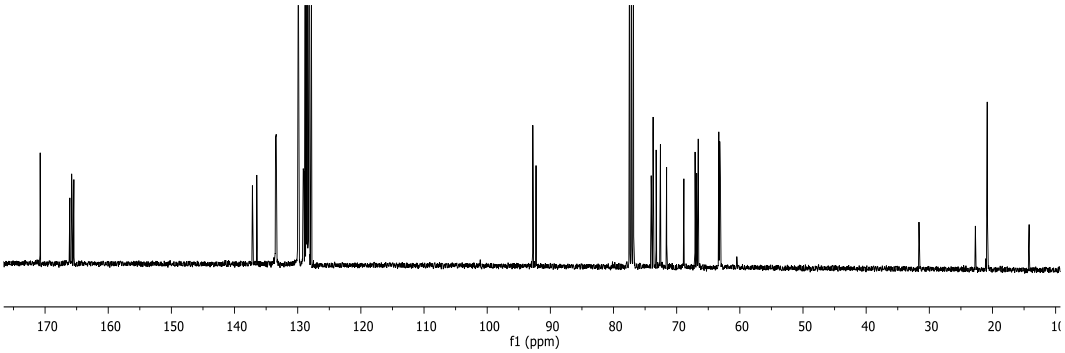
f1 (ppm)

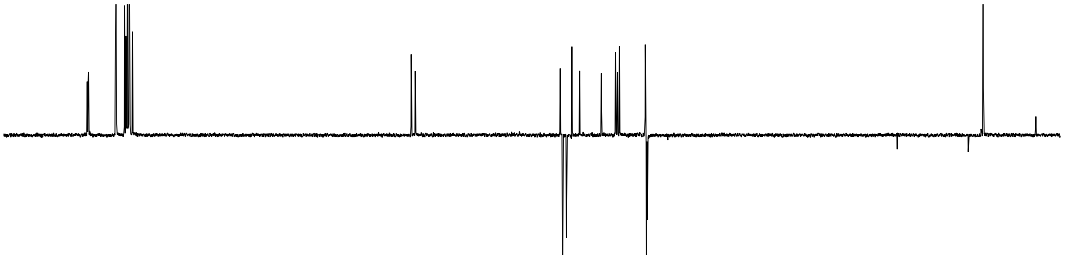

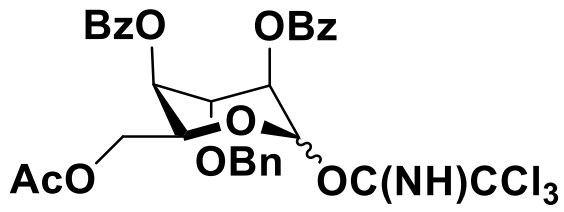
BzO
OBz
O
OBn
AcO
OC(NH)CCl3

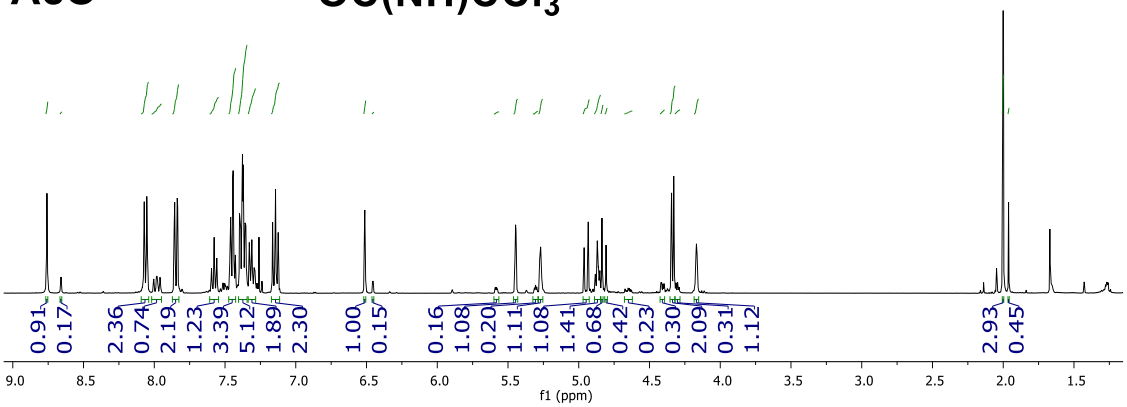
0.91
0.17
2.36
0.74
2.19
1.23
3.39
5.12
1.89
2.30
1.00
0.15
0.16
1.08
0.20
1.11
1.08
1.41
0.68
0.42
0.23
0.30
2.09
0.31
1.12
2.93
0.45
f1 (ppm)

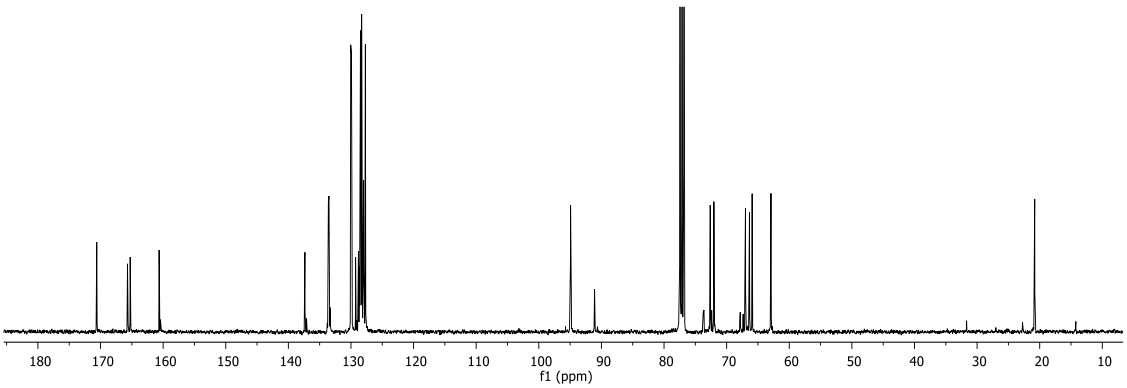
f1 (ppm)

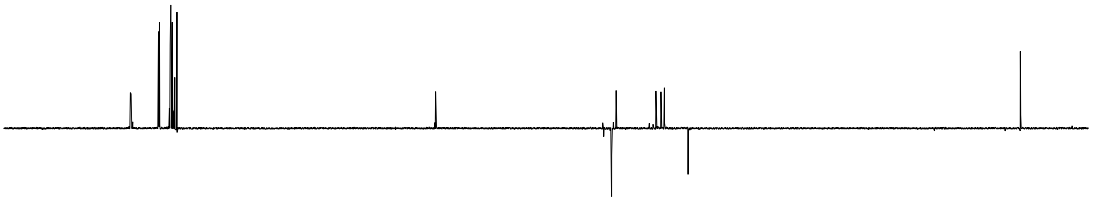

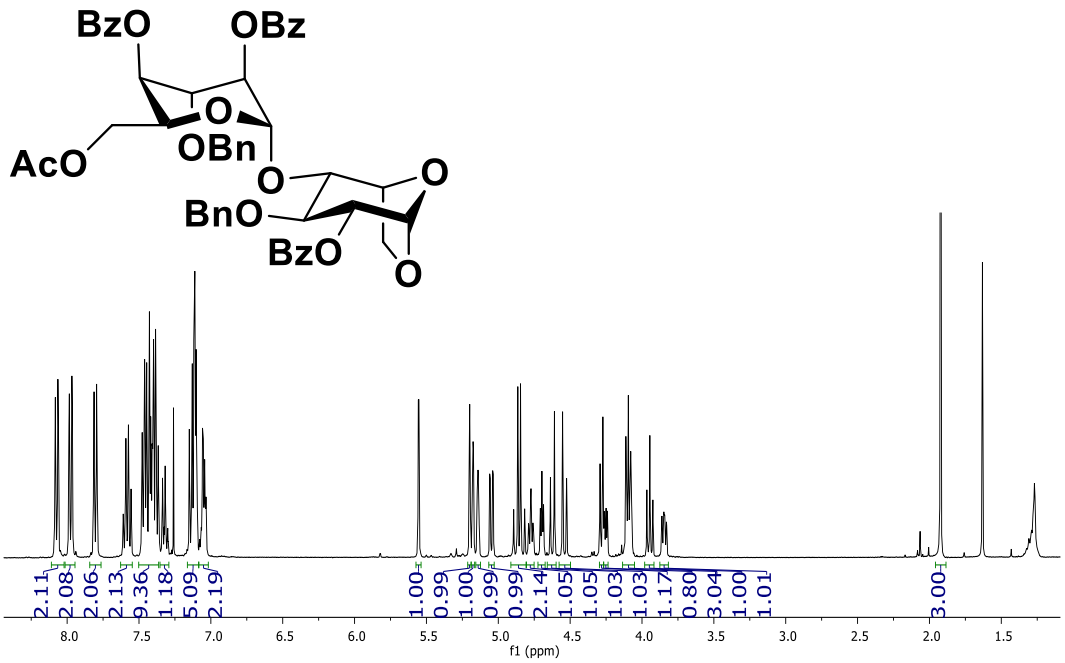
BzO
OBz
O
AcO
OBn
O
O
BnO
BzO
O
2.11
2.08
2.06
2.13
9.36
1.18
5.09
2.19
1.00
0.99
1.00
0.99
0.99
2.14
1.05
1.05
1.03
1.03
1.17
0.80
3.04
1.00
1.01
3.00
8.0
7.5
7.0
6.5
6.0
5.5
5.0
4.5
4.0
3.5
3.0
2.5
2.0
1.5
f1 (ppm)

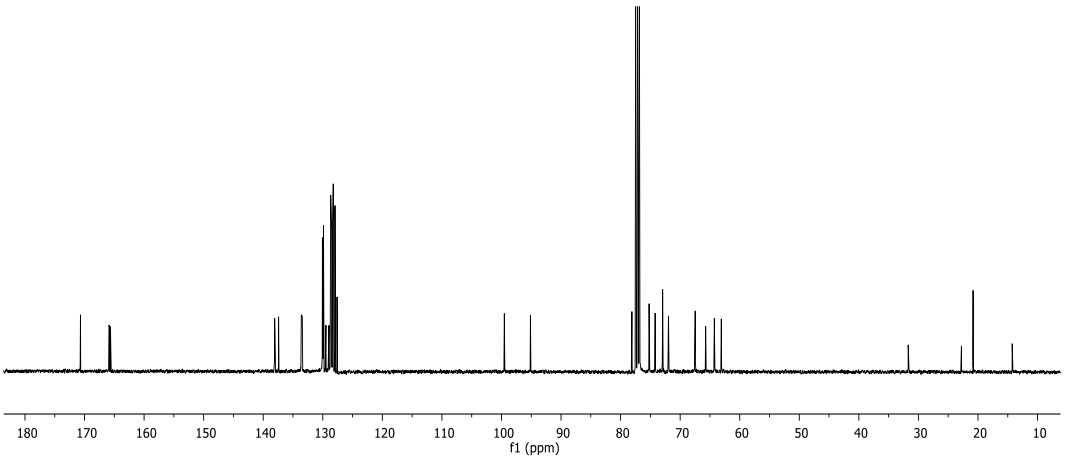
180
170
160
150
140
130
120
110
100
90
80
70
60
50
40
30
20
10
f1 (ppm)

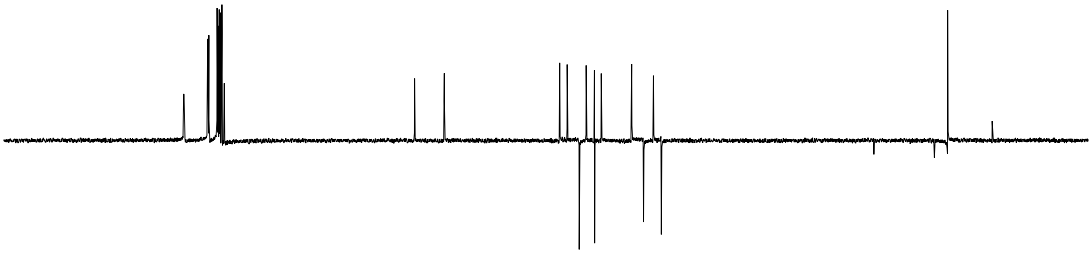

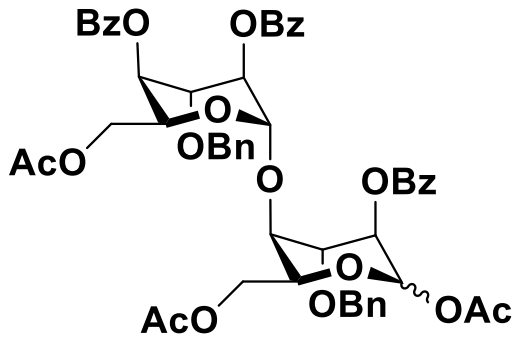
BzO
OBz
O
OBn
AcO
O
OBz
O
OBn
AcO
OAc

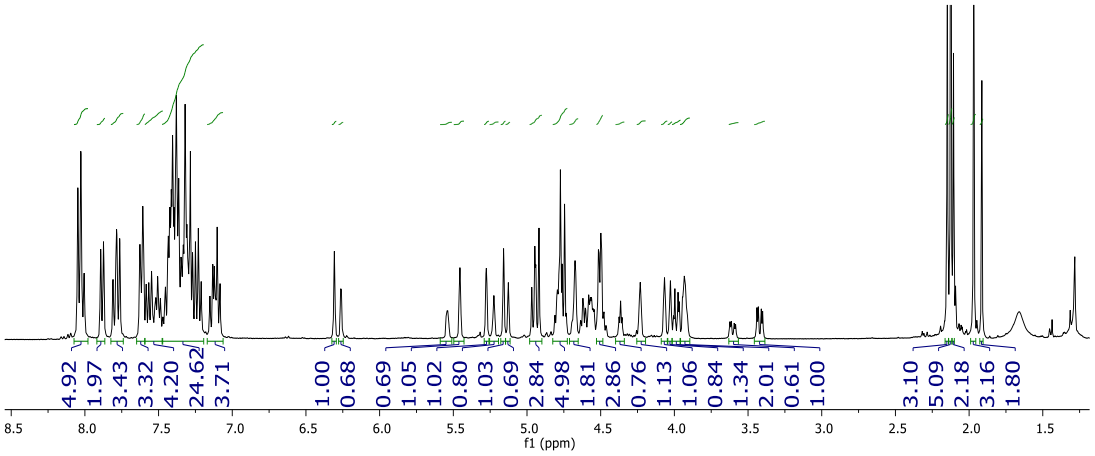
4.92
1.97
3.43
3.32
4.20
24.62
3.71
1.00
0.68
0.69
1.05
1.02
0.80
1.03
0.69
2.84
4.98
1.81
2.86
0.76
1.13
1.06
0.84
1.34
2.01
0.61
1.00
3.10
5.09
2.18
3.16
1.80
f1 (ppm)

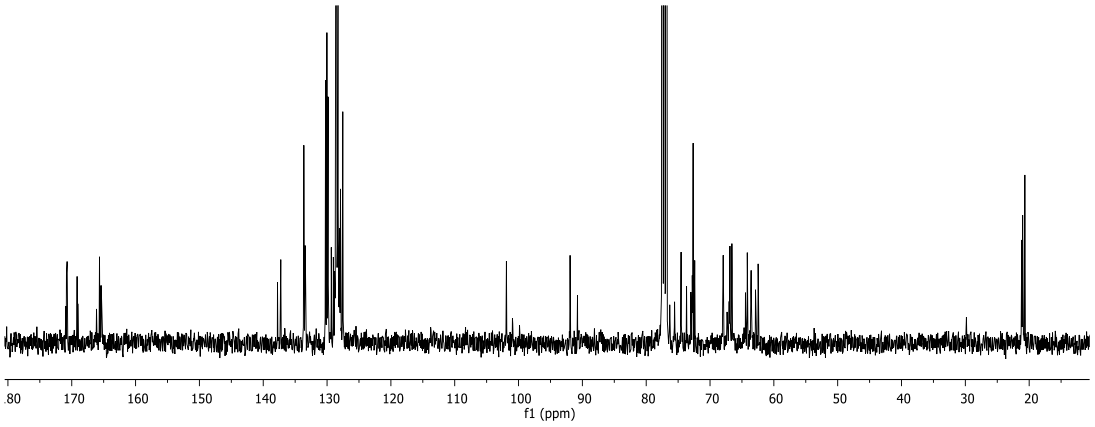
f1 (ppm)

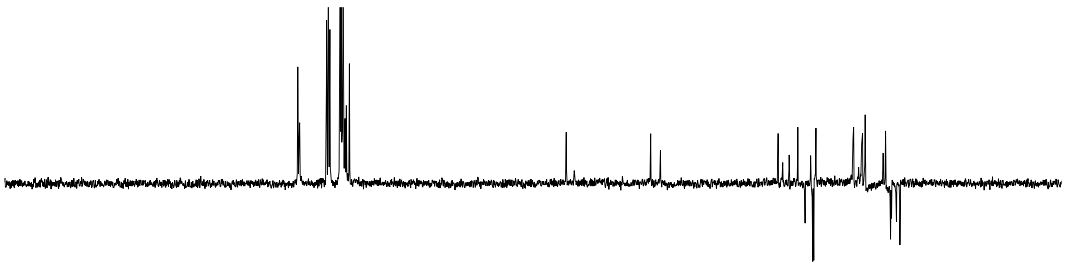

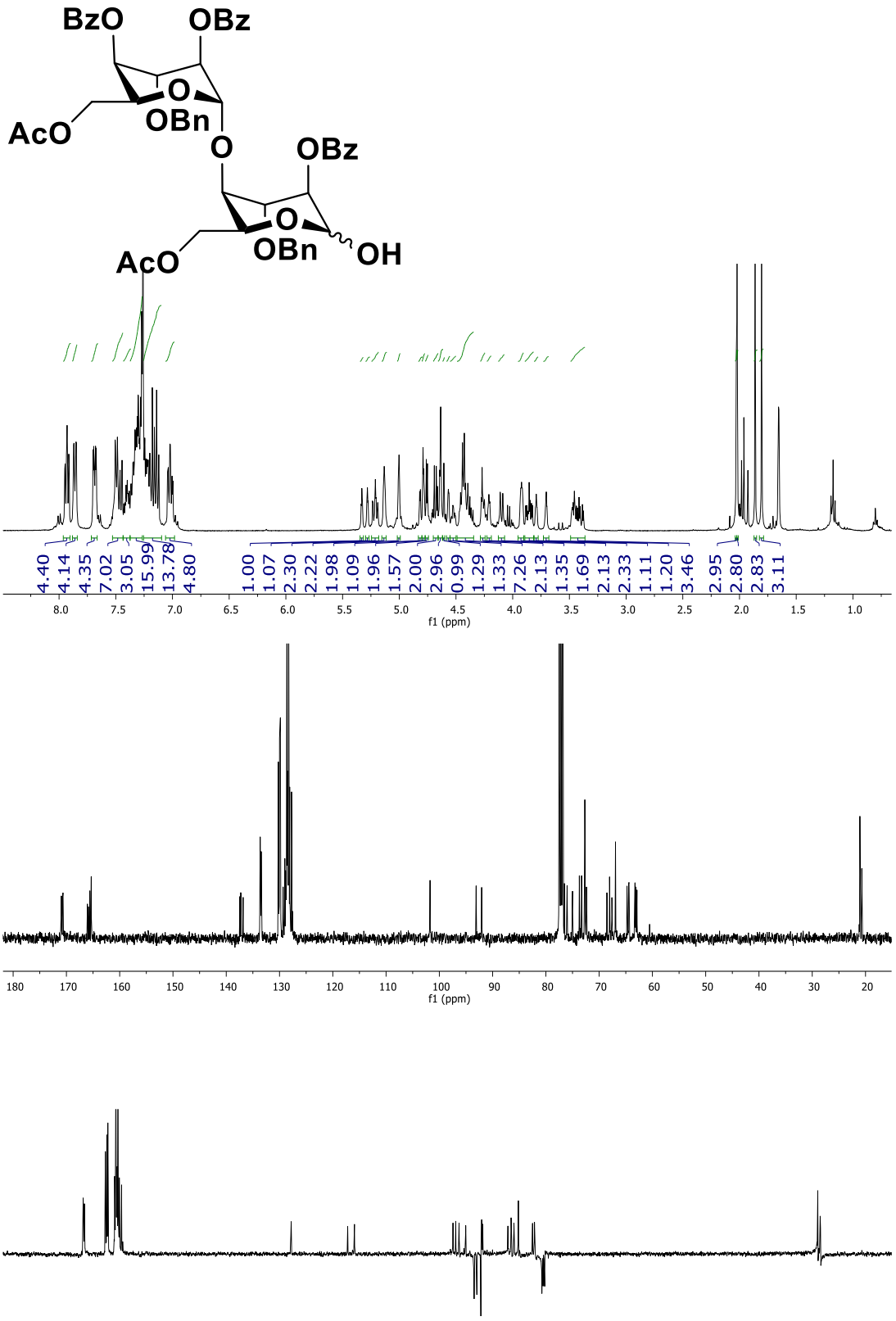
BzO
OBz
O
OBn
AcO
O
OBz
O
OBn
OH
AcO
4.40
4.14
4.35
7.02
3.05
15.99
13.78
4.80
1.00
1.07
2.30
2.22
1.98
1.09
1.96
1.57
2.00
2.96
0.99
1.29
1.33
7.26
2.13
1.35
1.69
2.13
2.33
1.11
1.20
3.46
2.95
2.80
2.83
3.11
f1 (ppm)
f1 (ppm)

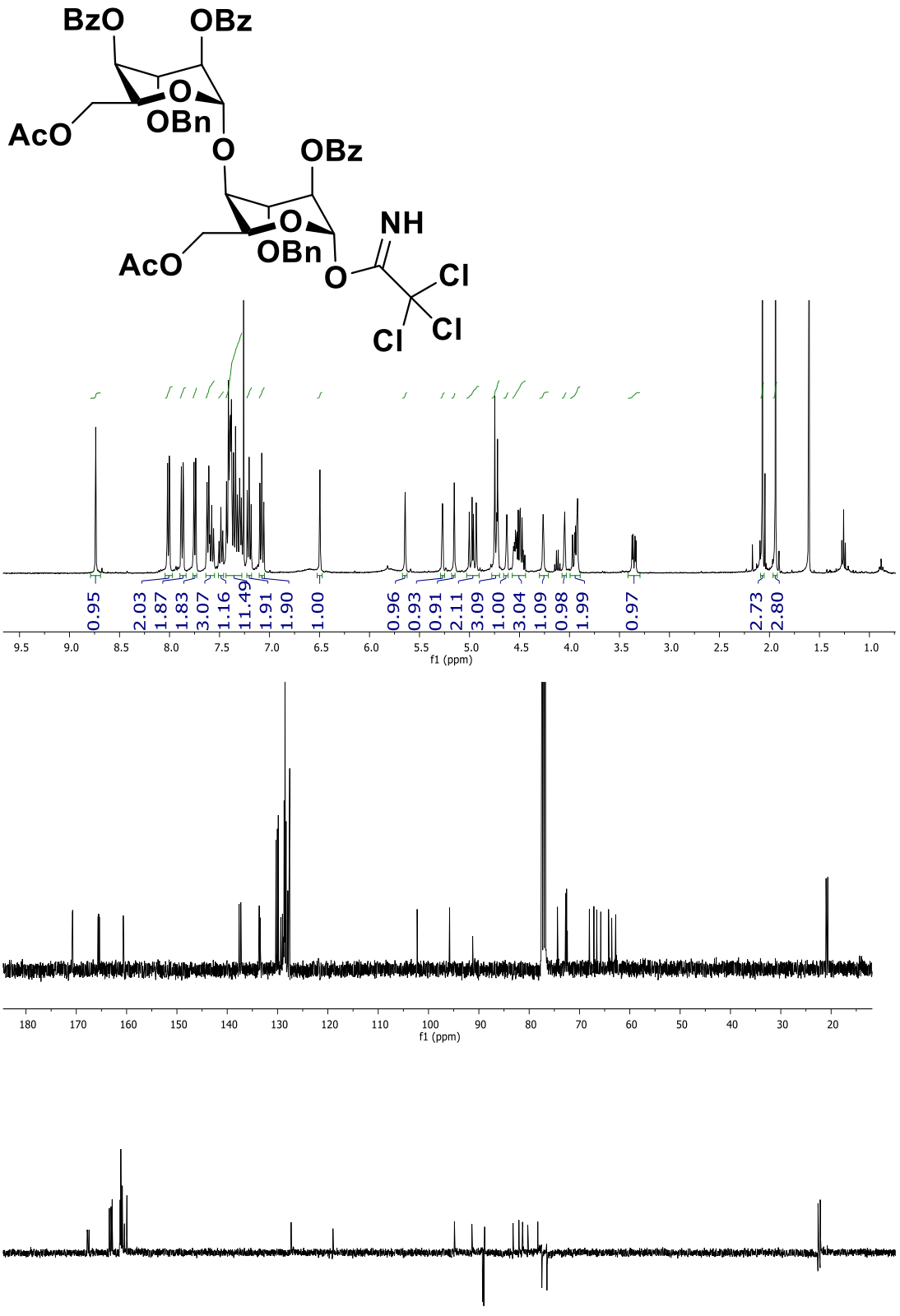
BzO
OBz
O
OBn
AcO
O
OBz
O
NH
AcO
OBn
O
Cl
Cl
Cl
0.95
2.03
1.87
1.83
3.07
1.16
11.49
1.91
1.90
1.00
0.96
0.93
0.91
2.11
3.09
1.00
3.04
1.09
0.98
1.99
0.97
2.73
2.80
f1 (ppm)
f1 (ppm)

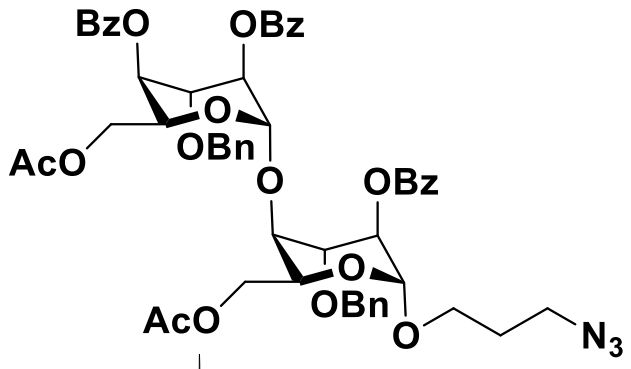
BzO
OBz
O
OBn
AcO
O
OBz
O
OBn
AcO
O
N3

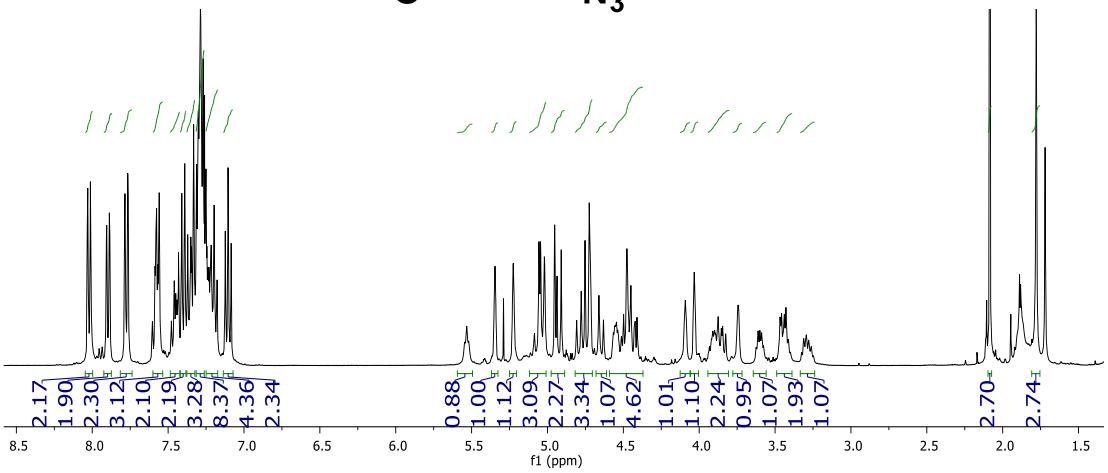
2.17
1.90
2.30
3.12
2.10
2.19
3.28
8.37
4.36
2.34
0.88
1.00
1.12
3.09
2.27
3.34
1.07
4.62
1.01
1.10
2.24
0.95
1.07
1.93
1.07
2.70
2.74
f1 (ppm)

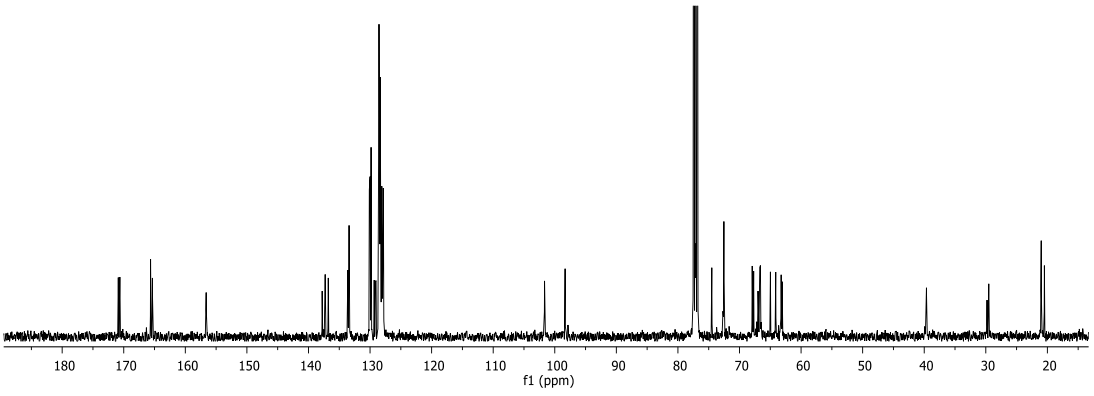
f1 (ppm)

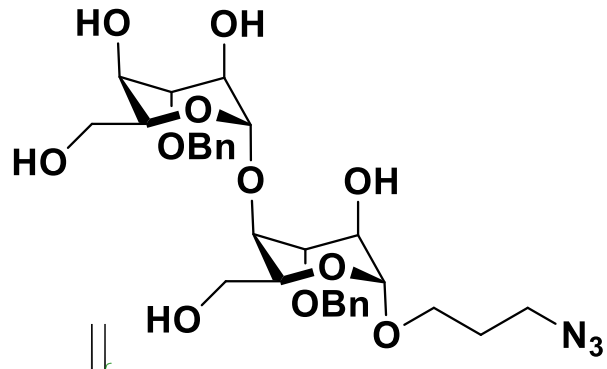
HO
OH
O
OBn
HO
O
OH
O
OBn
HO
O
N3

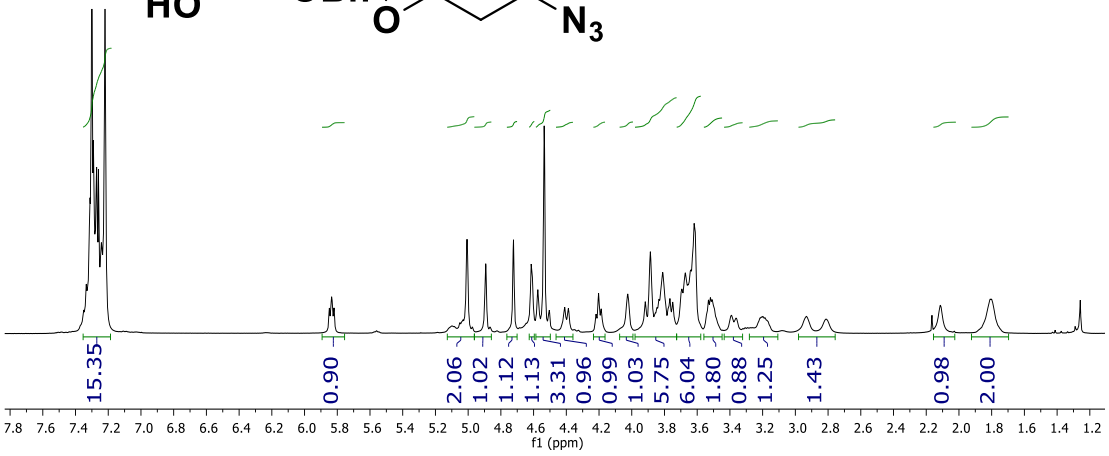
15.35
0.90
2.06
1.02
1.12
1.13
3.31
0.96
0.99
1.03
5.75
6.04
1.80
0.88
1.25
1.43
0.98
2.00
f1 (ppm)

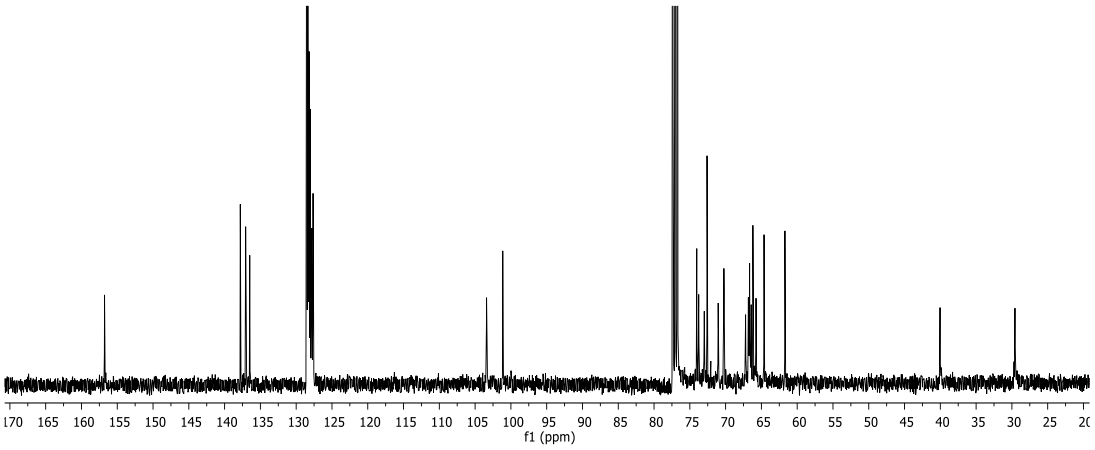
f1 (ppm)

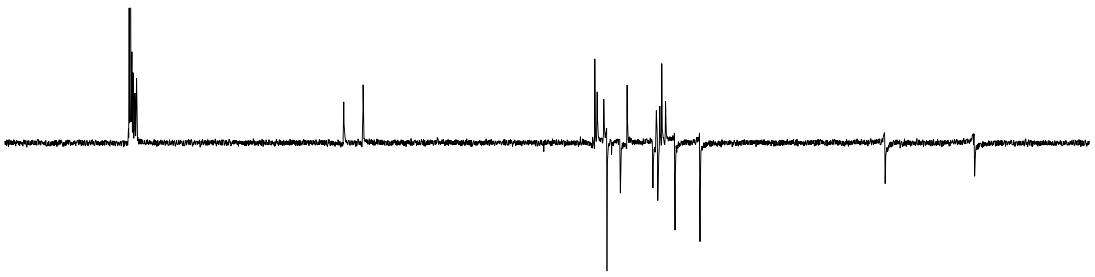

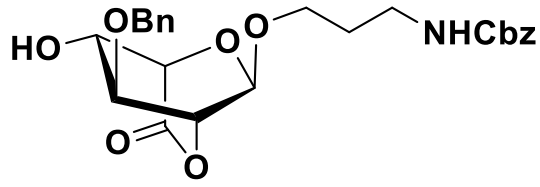
HO
OBn
O
O
NHCbz
O
O

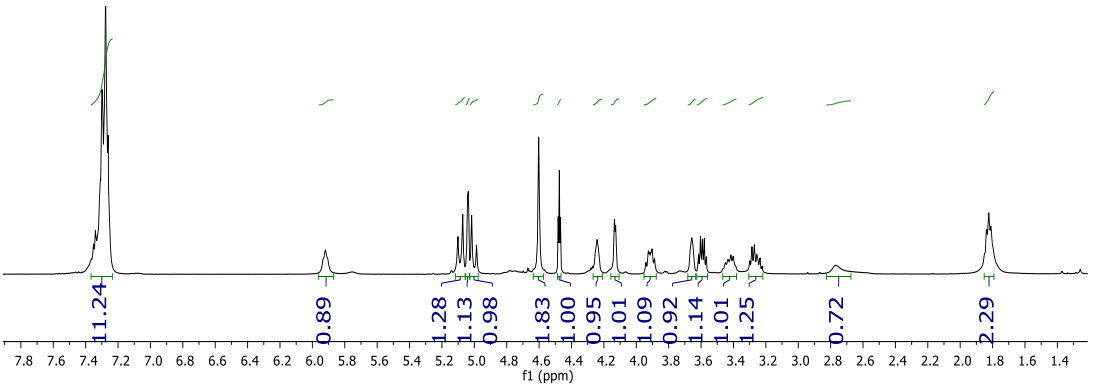
11.24
0.89
1.28
1.13
0.98
1.83
1.00
0.95
1.01
1.09
0.92
1.14
1.01
1.25
0.72
2.29
f1 (ppm)

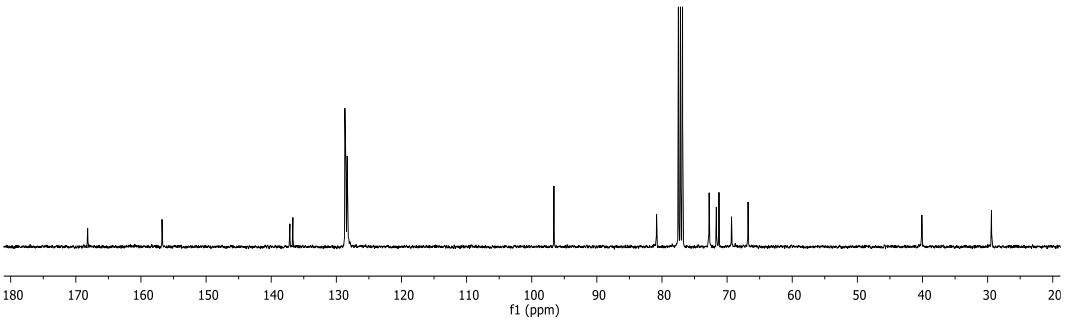
f1 (ppm)

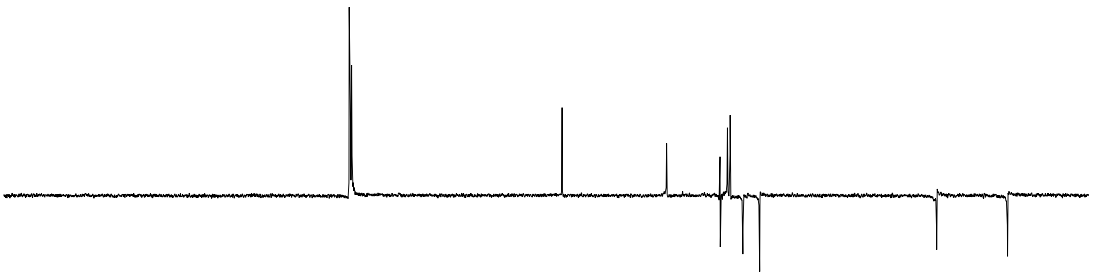

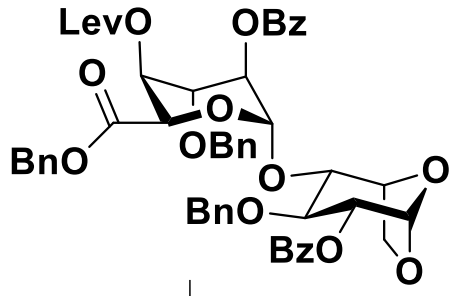
LevO
OBz
O
O
BnO
OBn
O
O
BnO
BzO
O

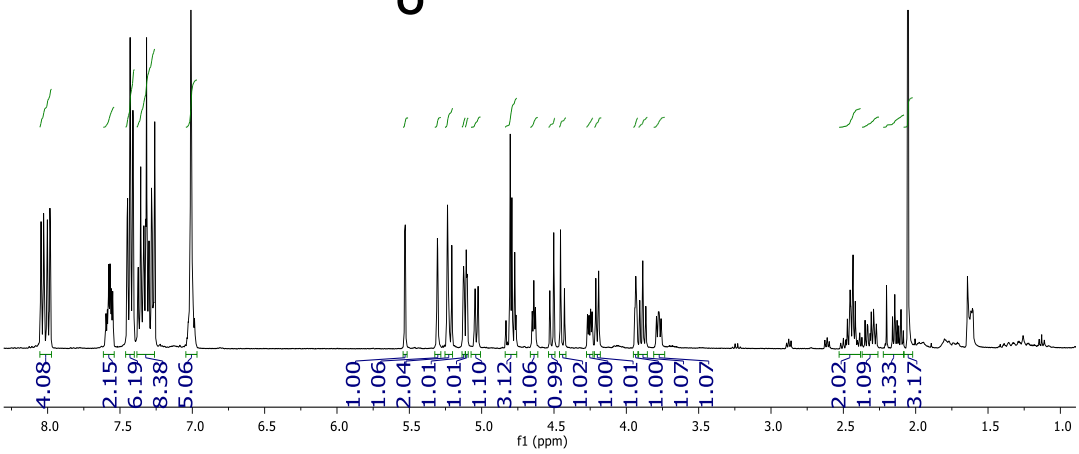
4.08
2.15
6.19
8.38
5.06
1.00
1.06
2.04
1.01
1.01
1.10
3.12
1.06
0.99
1.02
1.00
1.01
1.00
1.07
1.07
2.02
1.09
1.33
3.17
8.0
7.5
7.0
6.5
6.0
5.5
5.0
4.5
4.0
3.5
3.0
2.5
2.0
1.5
1.0
f1 (ppm)

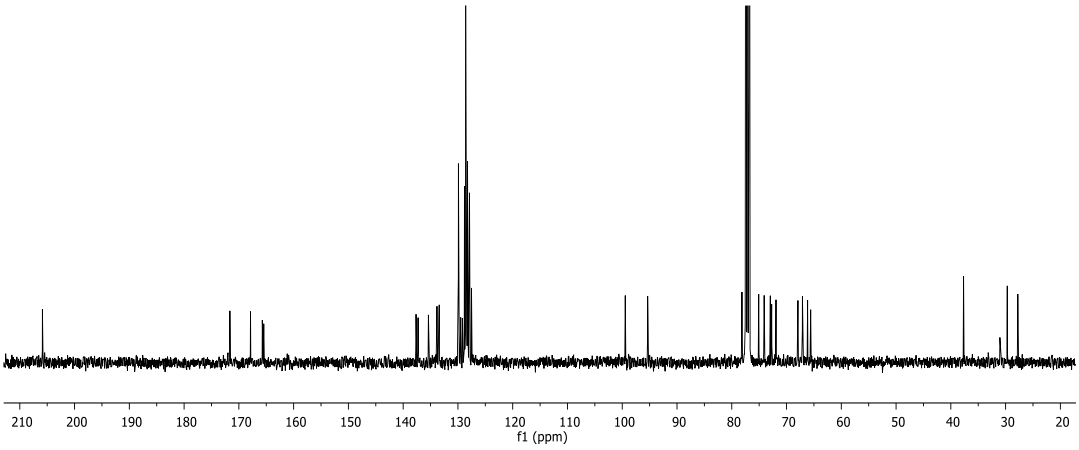
210
200
190
180
170
160
150
140
130
120
110
100
90
80
70
60
50
40
30
20
f1 (ppm)

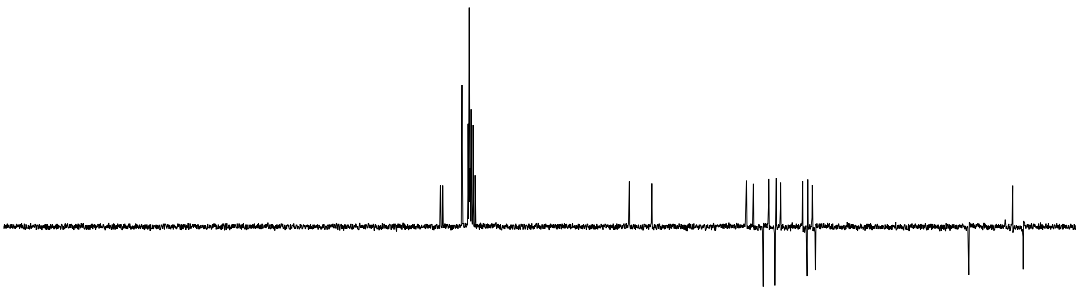

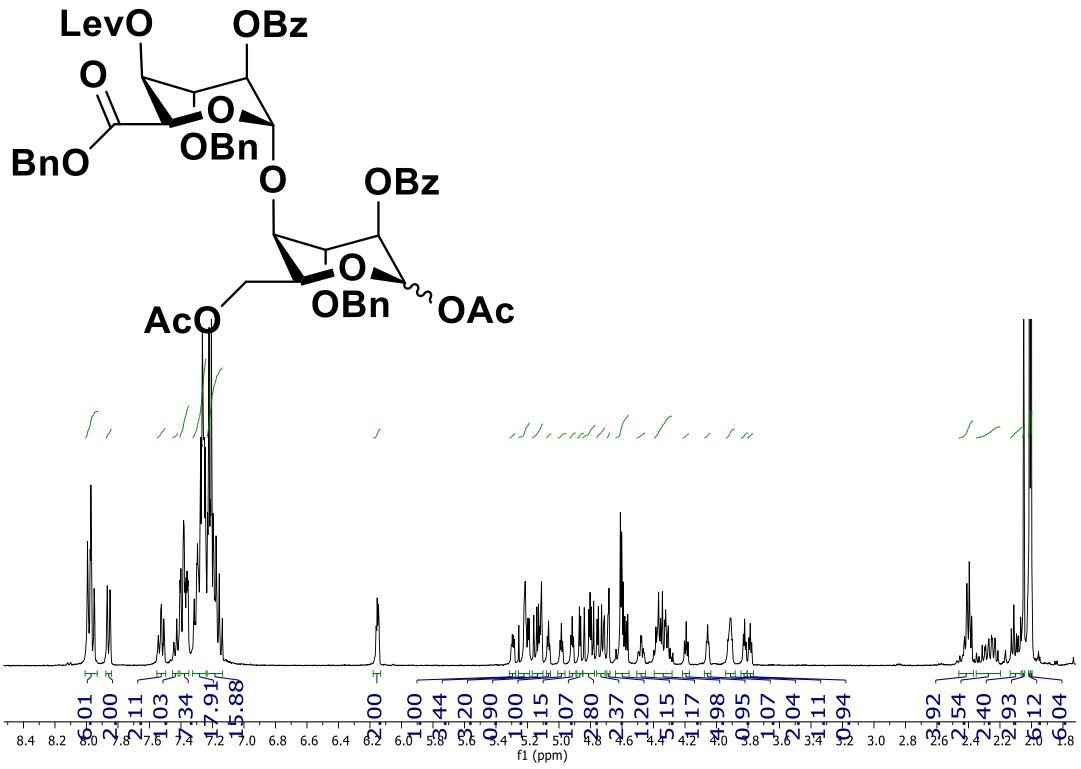
LevO
OBz
O
O
OBn
BnO
O
OBz
O
OBn
AcO
OAc
6.01
2.00
2.11
1.03
7.34
17.91
15.88
2.00
1.00
3.44
3.20
0.90
1.00
1.15
1.07
2.80
2.37
1.20
5.15
1.17
4.98
0.95
1.07
2.04
1.11
0.94
3.92
2.54
2.40
2.93
6.12
6.04
f1 (ppm)

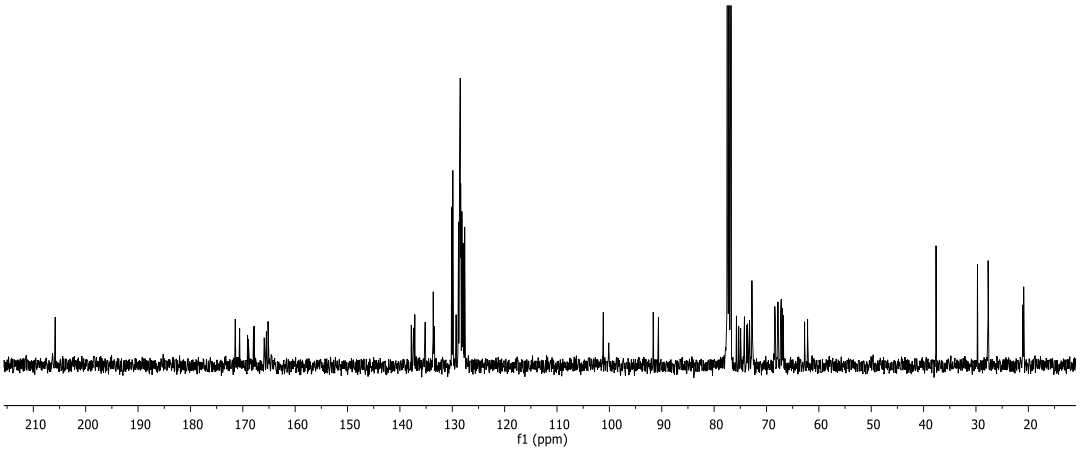
f1 (ppm)

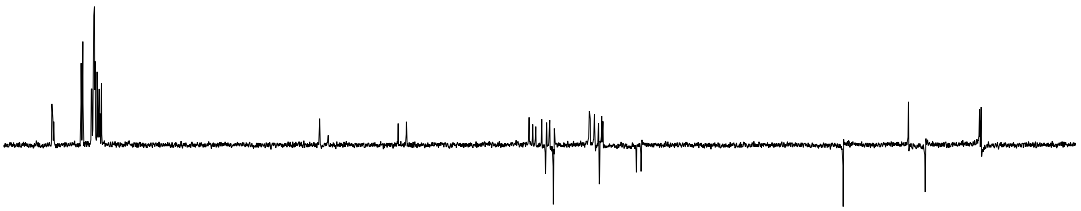

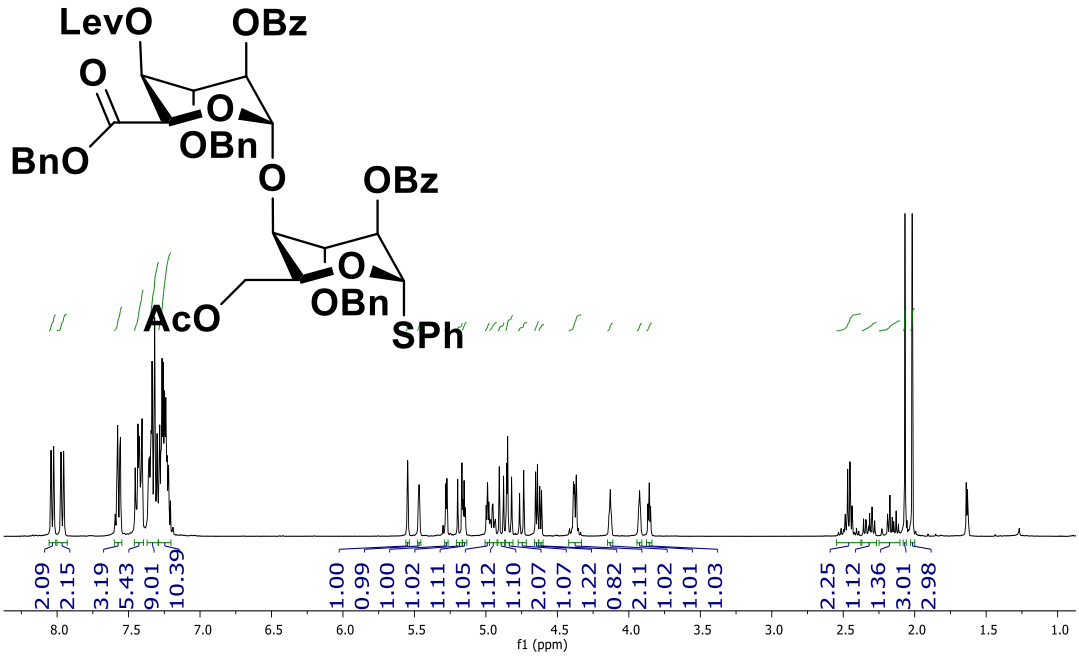
LevO
OBz
O
O
OBn
BnO
O
OBz
O
OBn
AcO
SPh
2.09
2.15
3.19
5.43
9.01
10.39
1.00
0.99
1.00
1.02
1.11
1.05
1.12
1.10
2.07
1.07
1.22
0.82
2.11
1.02
1.01
1.03
2.25
1.12
1.36
3.01
2.98
f1 (ppm)

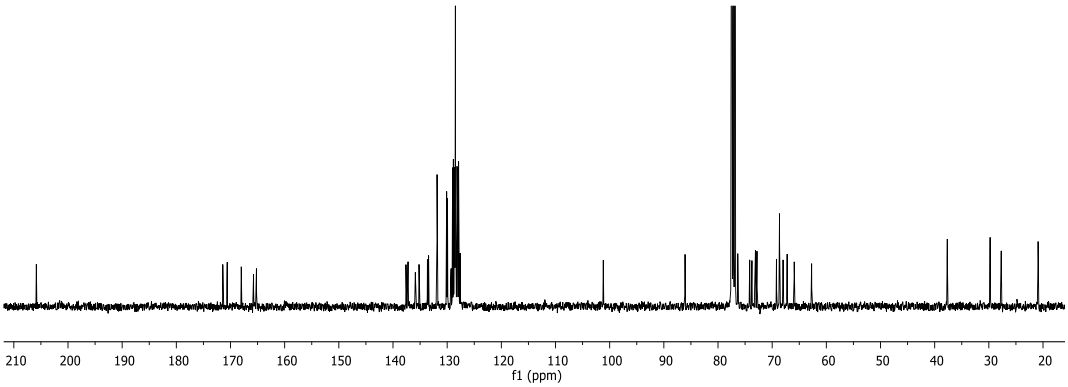
f1 (ppm)

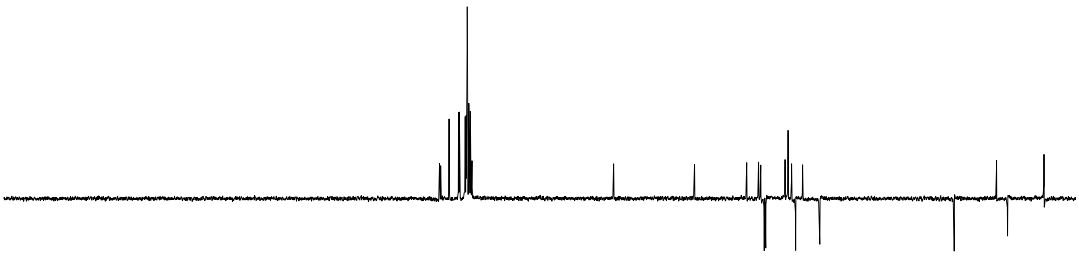

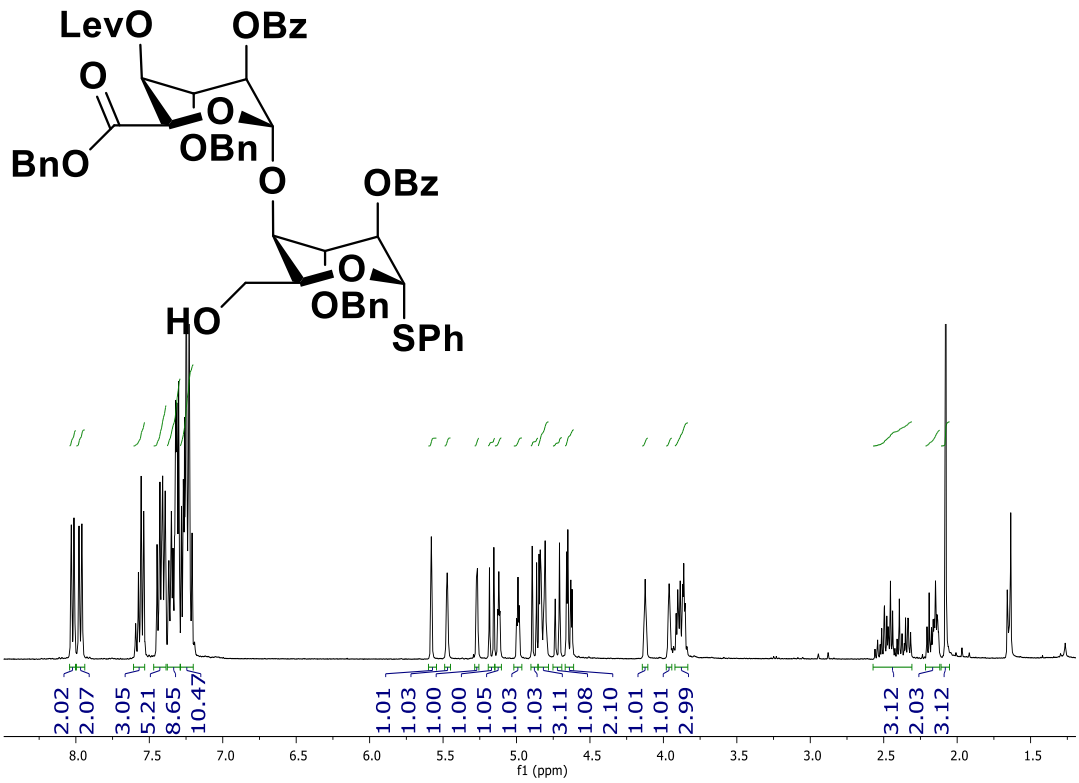
LevO
OBz
O
O
OBn
BnO
O
OBz
O
OBn
HO
SPh
2.02
2.07
3.05
5.21
8.65
10.47
1.01
1.03
1.00
1.00
1.05
1.03
1.03
3.11
1.08
2.10
1.01
1.01
2.99
3.12
2.03
3.12
f1 (ppm)

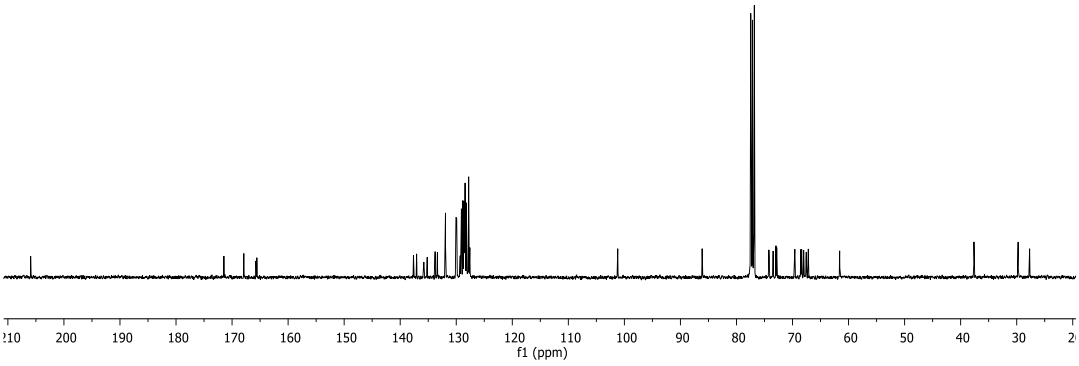
f1 (ppm)

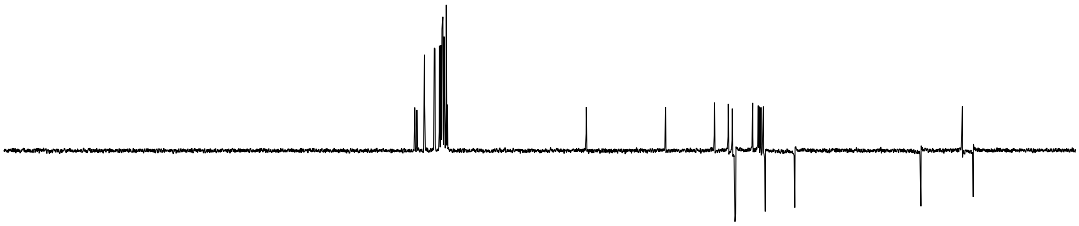

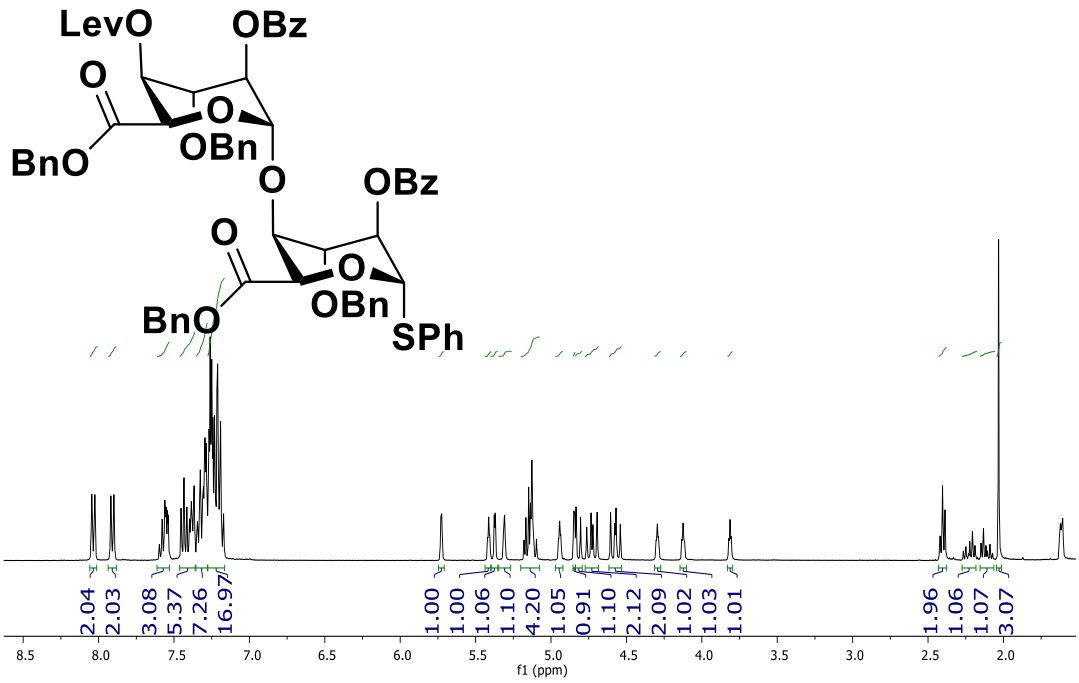
LevO
OBz
O
O
OBn
BnO
O
OBz
O
O
OBn
BnO
SPh
2.04
2.03
3.08
5.37
7.26
16.97
1.00
1.00
1.06
1.10
4.20
1.05
0.91
1.10
2.12
2.09
1.02
1.03
1.01
1.96
1.06
1.07
3.07
f1 (ppm)

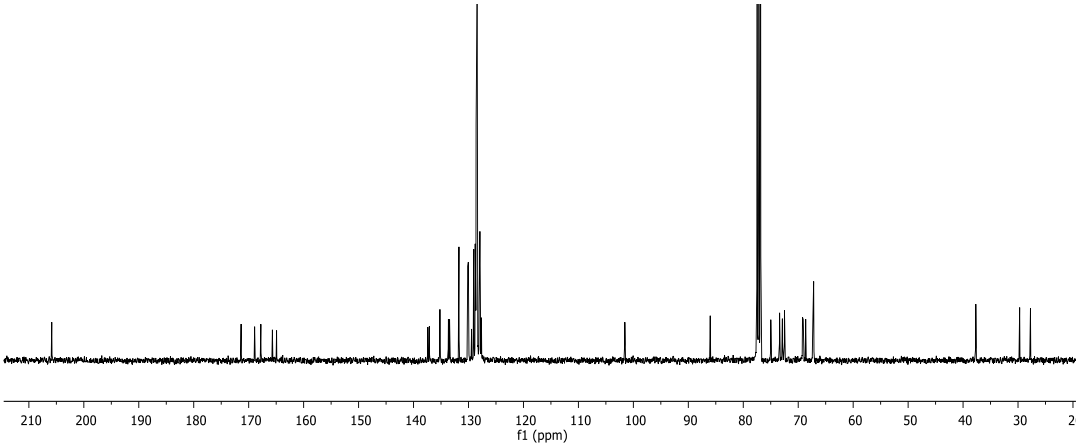
f1 (ppm)

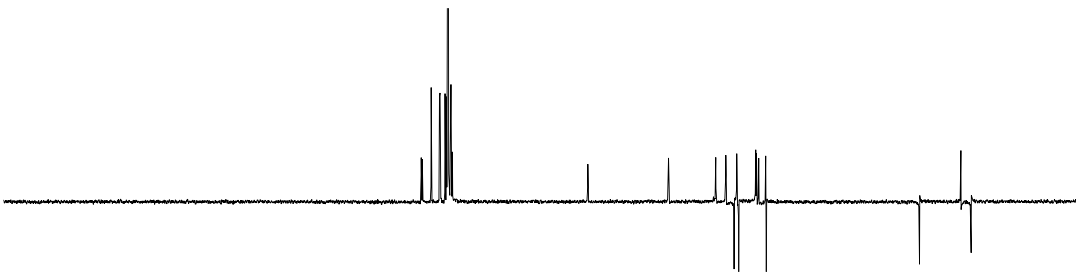

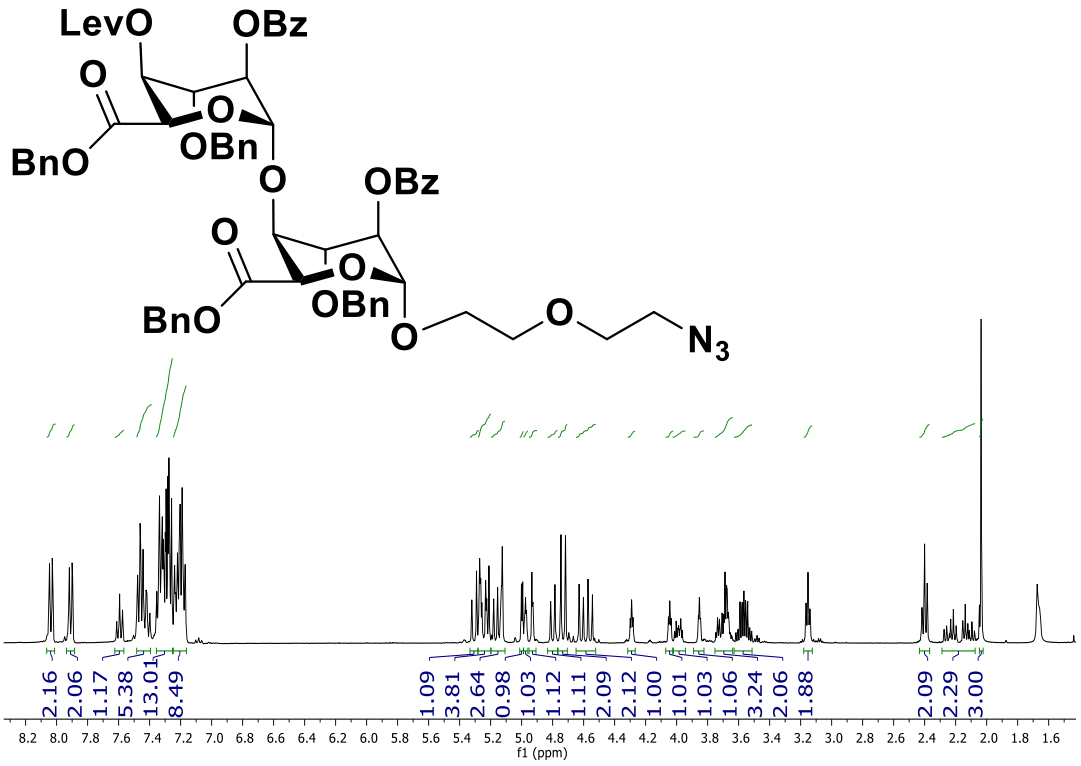
LevO
OBz
O
O
OBn
BnO
O
OBz
O
O
OBn
BnO
O
O
N3
2.16
2.06
1.17
5.38
13.01
8.49
1.09
3.81
2.64
0.98
1.03
1.12
1.11
2.09
2.12
1.00
1.01
1.03
1.06
3.24
2.06
1.88
2.09
2.29
3.00
f1 (ppm)

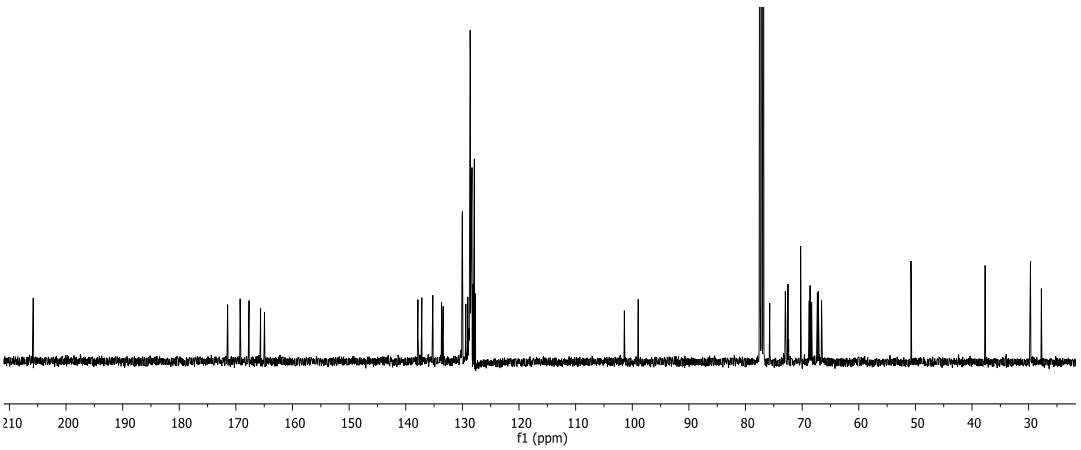
f1 (ppm)

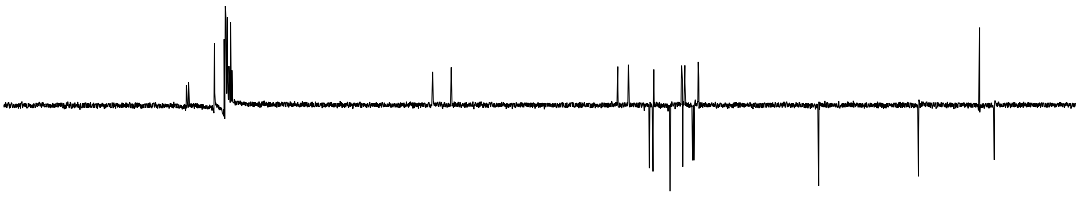

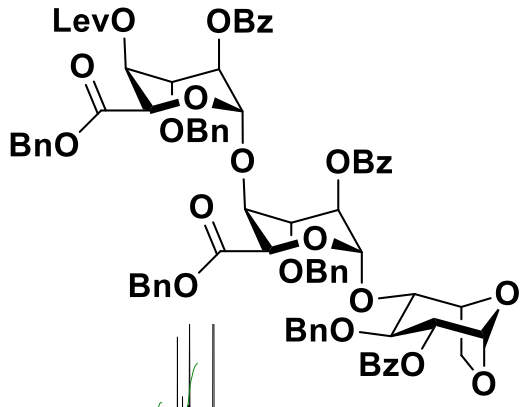
LevO
OBz
O
O
BnO
OBn
O
OBz
O
O
BnO
OBn
O
O
BnO
BzO
O

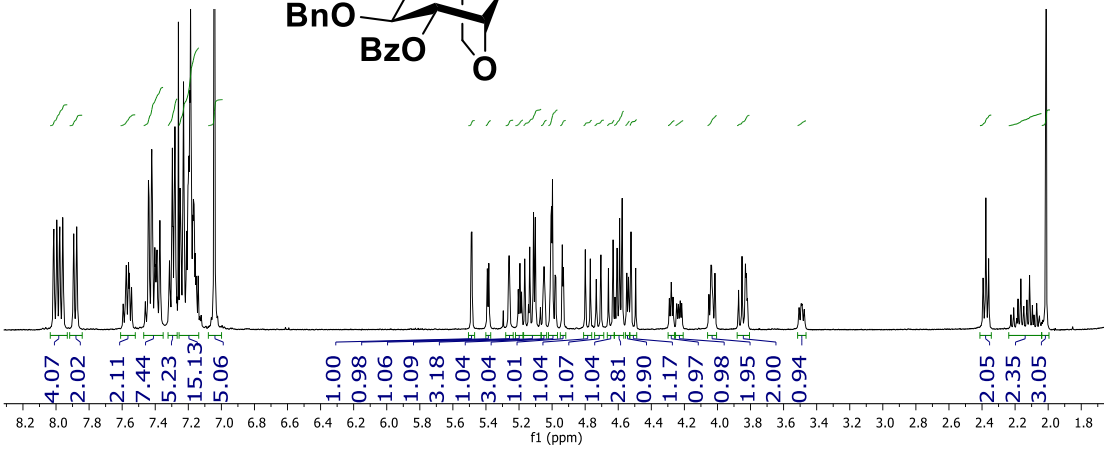
4.07
2.02
2.11
7.44
5.23
15.13
5.06
1.00
0.98
1.06
1.09
3.18
1.04
3.04
1.01
1.04
1.07
1.04
2.81
0.90
1.17
0.97
0.98
1.95
2.00
0.94
2.05
2.35
3.05
f1 (ppm)

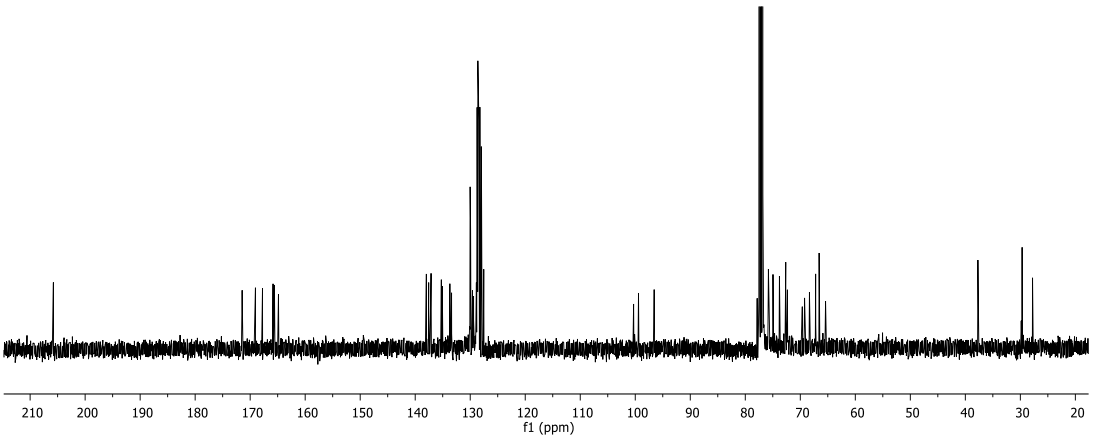
f1 (ppm)

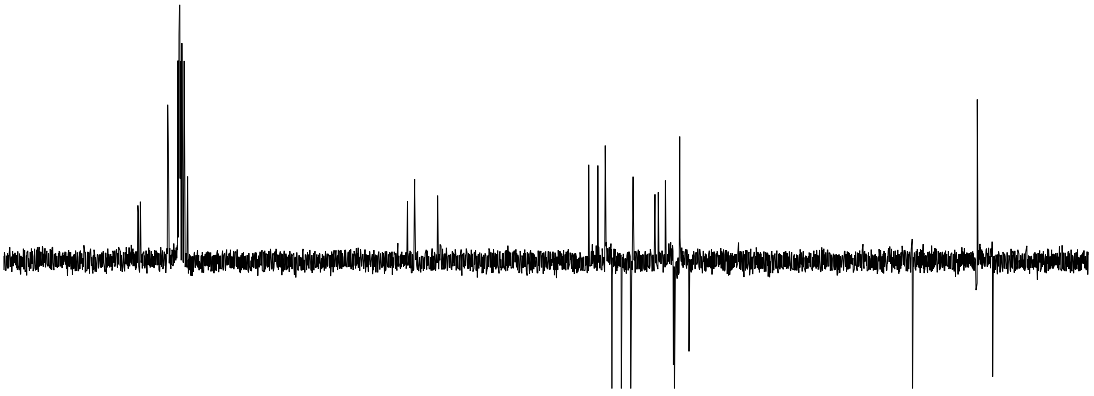

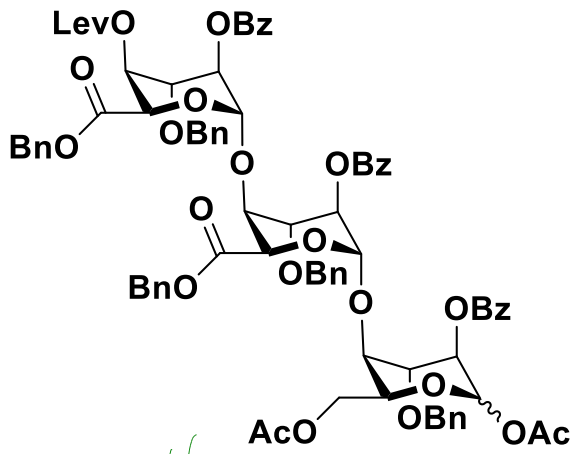
LevO
OBz
O
O
BnO
OBn
O
OBz
O
O
BnO
OBn
O
OBz
O
AcO
OBn
OAc

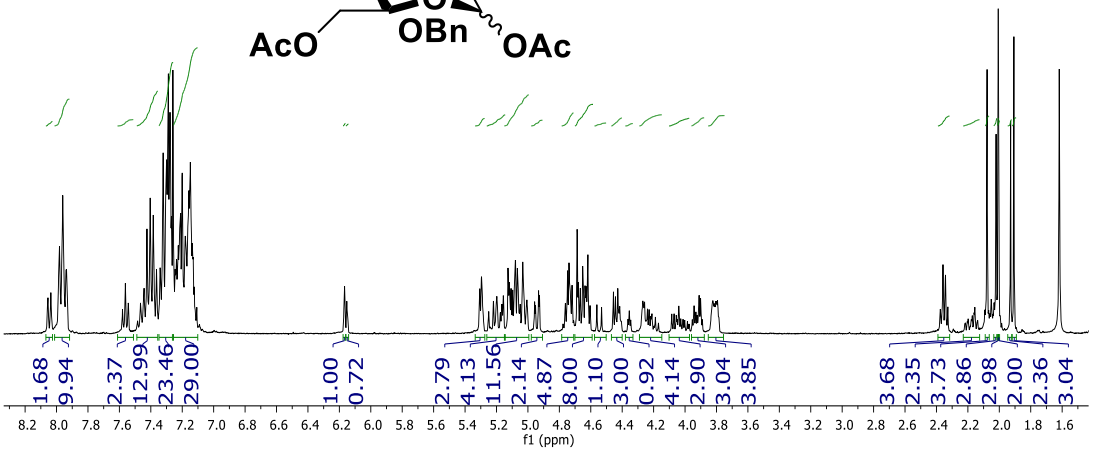
1.68
9.94
2.37
12.99
23.46
29.00
1.00
0.72
2.79
4.13
11.56
2.14
4.87
8.00
1.10
3.00
0.92
4.14
2.90
3.04
3.85
3.68
2.35
3.73
2.86
2.98
2.00
2.36
3.04
f1 (ppm)

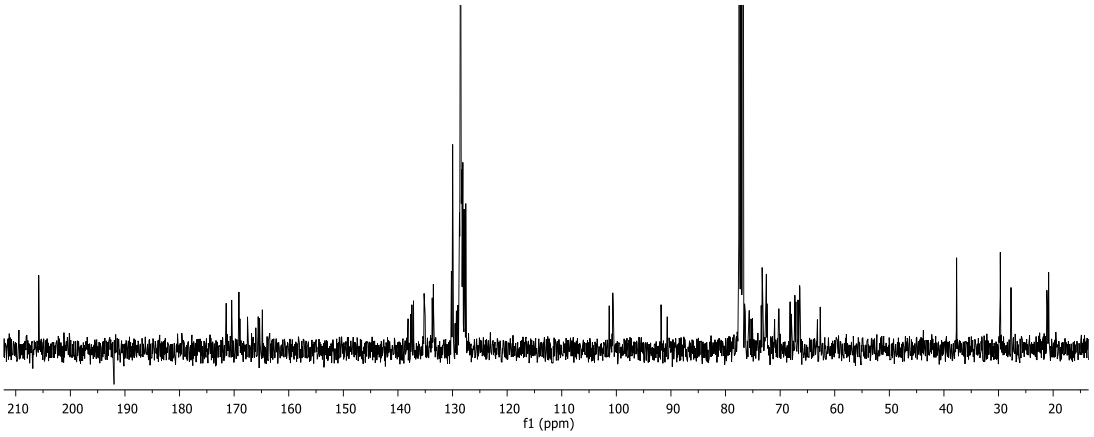
f1 (ppm)

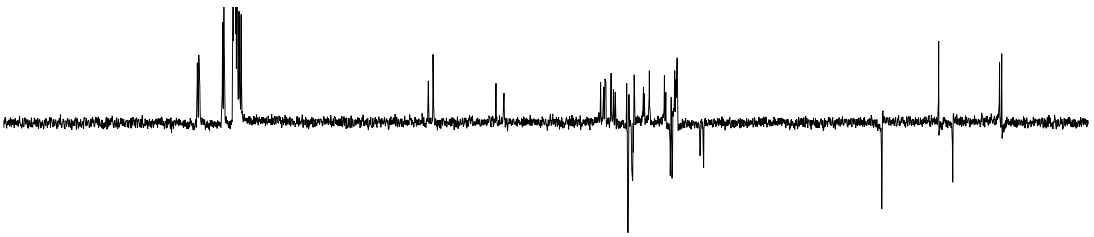

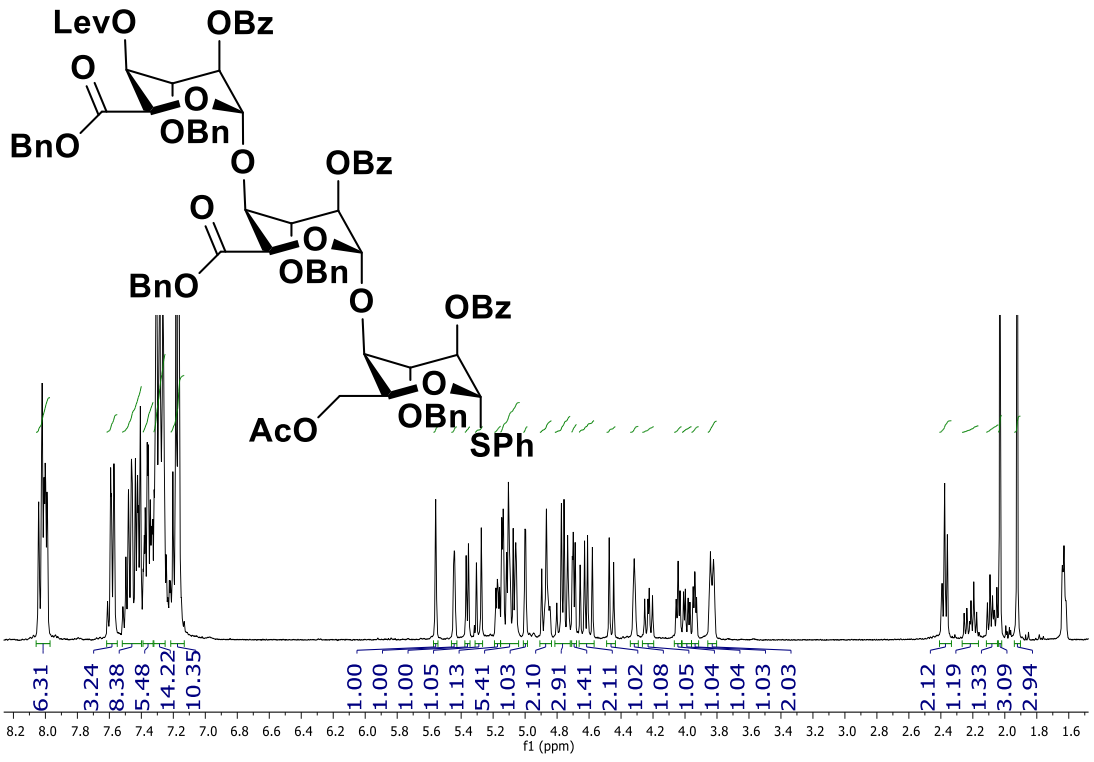
LevO
OBz
O
O
BnO
OBn
O
OBz
O
O
BnO
OBn
O
OBz
O
AcO
OBn
SPh
6.31
3.24
8.38
5.48
14.22
10.35
1.00
1.00
1.00
1.05
1.13
5.41
1.03
2.10
2.91
1.41
2.11
1.02
1.08
1.05
1.04
1.04
1.03
2.03
2.12
1.19
1.33
3.09
2.94
f1 (ppm)

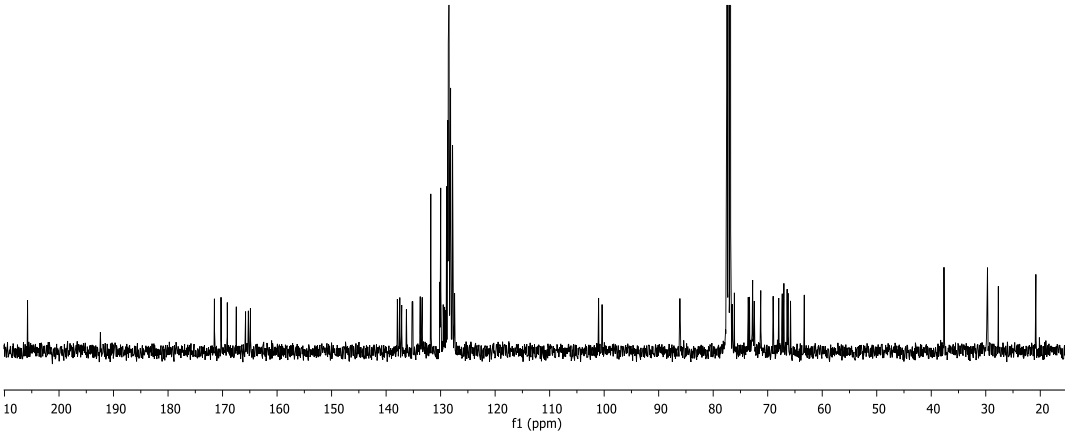
f1 (ppm)

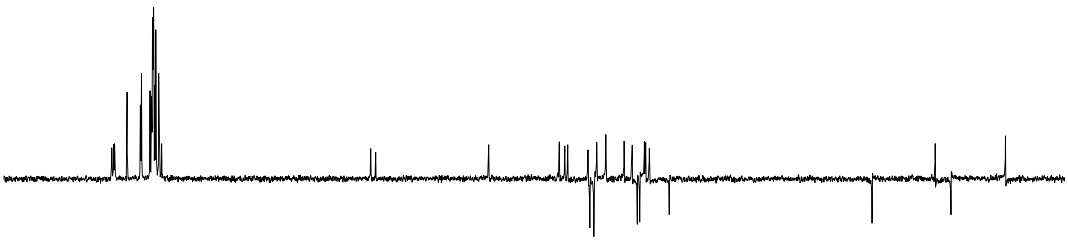

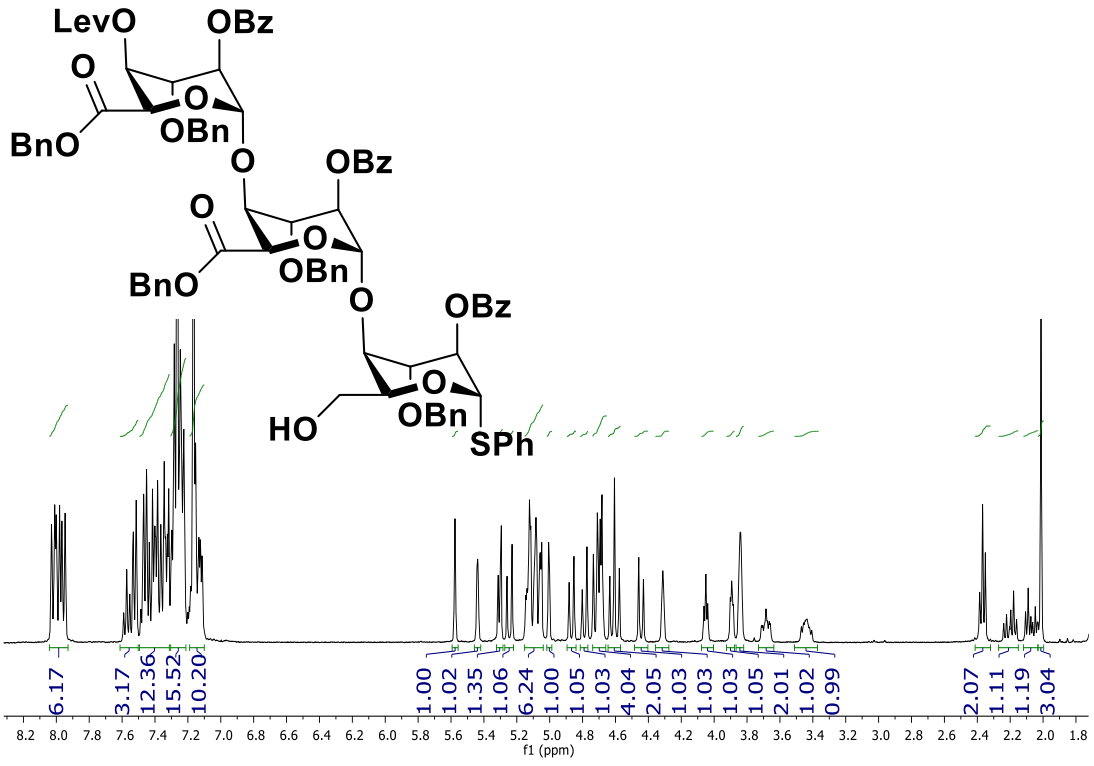
LevO
OBz
O
O
BnO
OBn
O
OBz
O
O
BnO
OBn
O
OBz
O
HO
OBn
SPh
6.17
3.17
12.36
15.52
10.20
1.00
1.02
1.35
1.06
6.24
1.00
1.05
1.03
4.04
2.05
1.03
1.03
1.03
1.05
2.01
1.02
0.99
2.07
1.11
1.19
3.04
f1 (ppm)

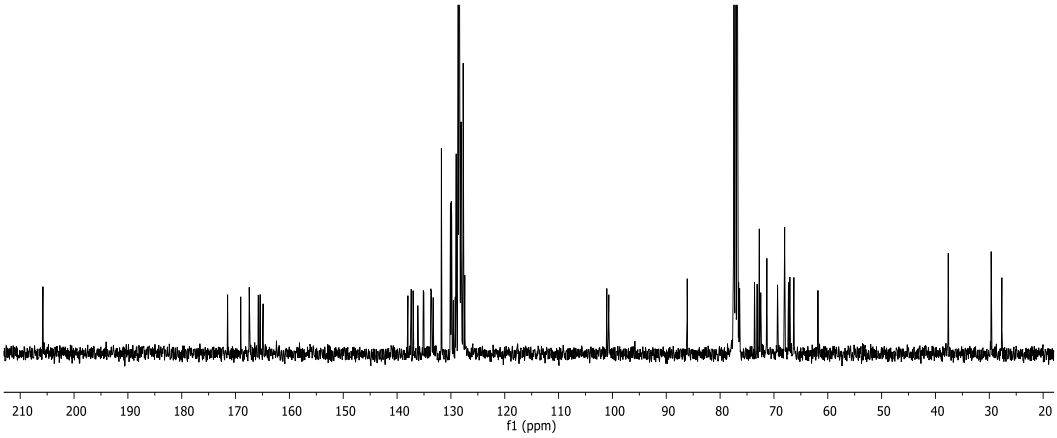
f1 (ppm)

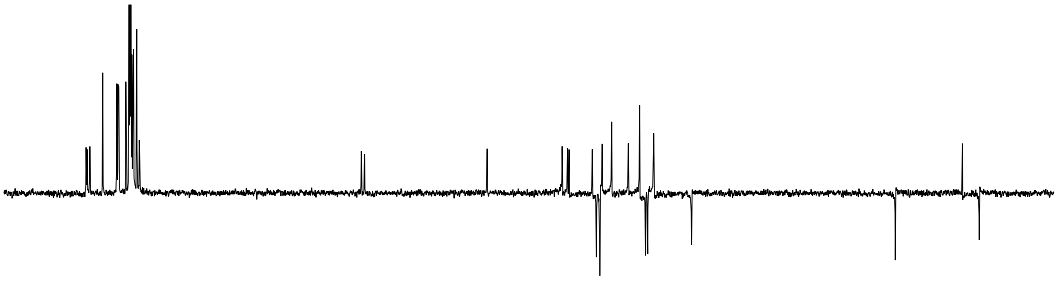

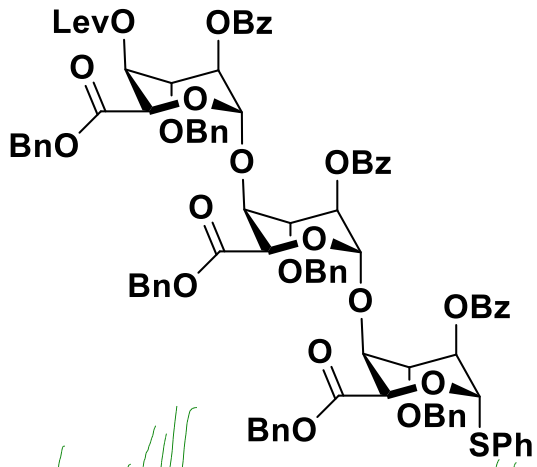
LevO
OBz
O
O
BnO
OBn
O
OBz
O
O
BnO
OBn
O
OBz
O
O
BnO
OBn
SPh

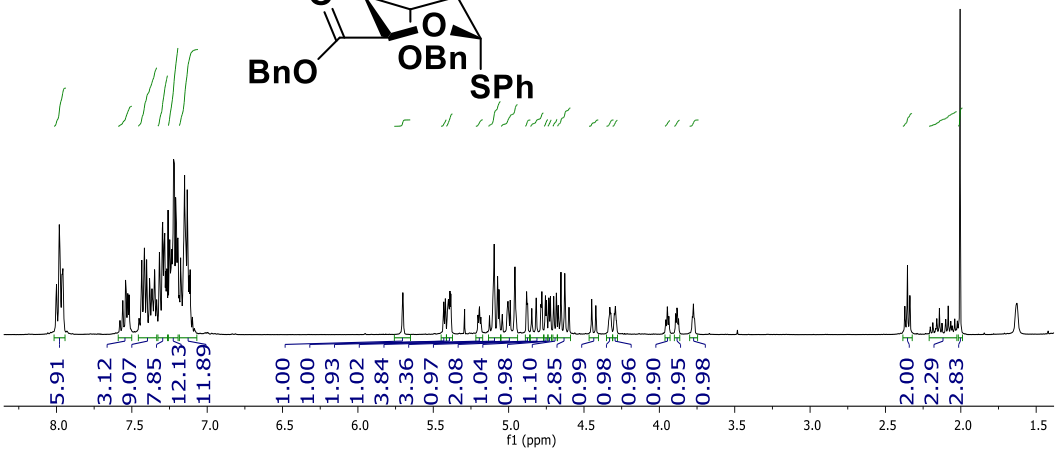
5.91
3.12
9.07
7.85
12.13
11.89
1.00
1.00
1.93
1.02
3.84
3.36
0.97
2.08
1.04
0.98
1.10
2.85
0.99
0.98
0.96
0.90
0.95
0.98
2.00
2.29
2.83
f1 (ppm)

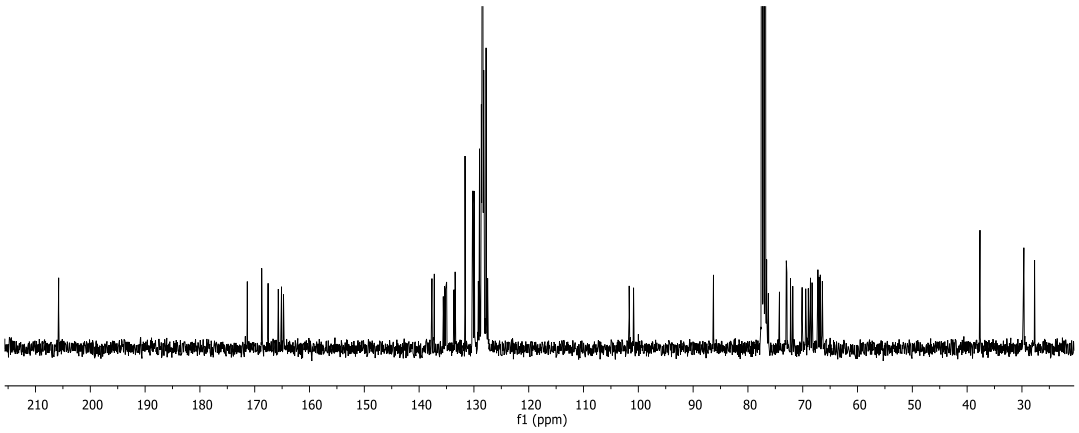
f1 (ppm)

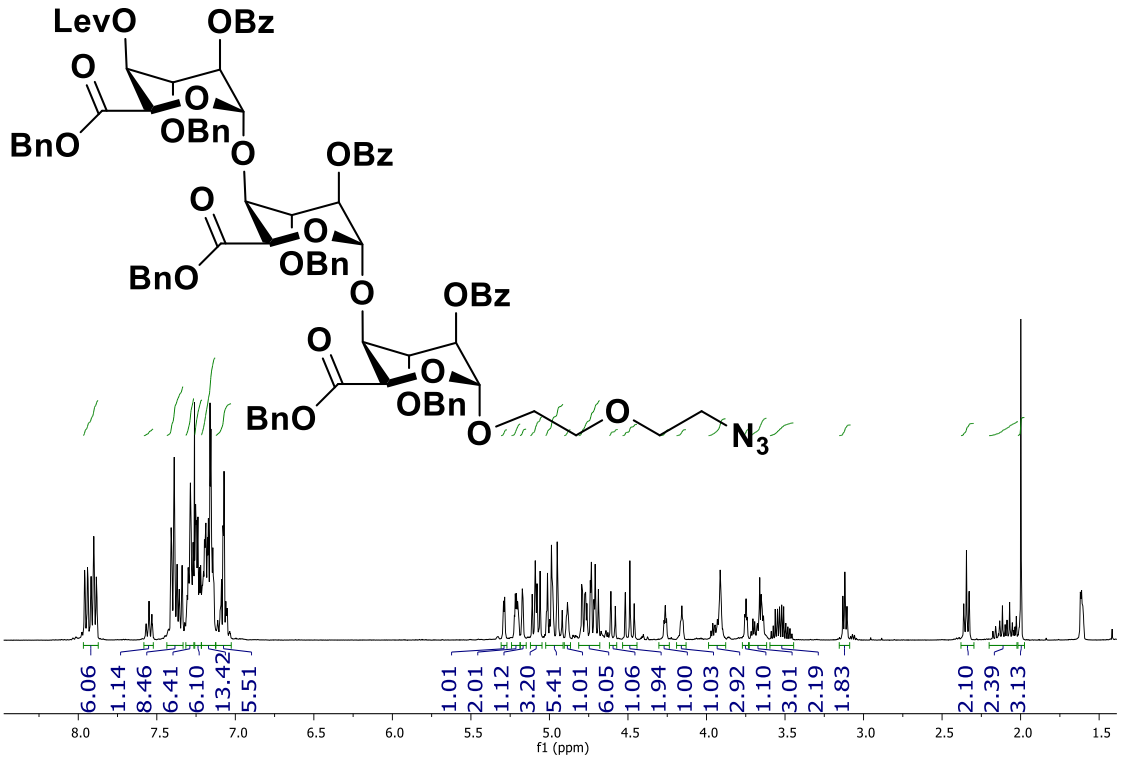
LevO
OBz
O
O
BnO
OBn
O
OBz
O
O
BnO
OBn
O
OBz
O
O
BnO
OBn
O
O
N3
6.06
1.14
8.46
6.41
6.10
13.42
5.51
1.01
2.01
1.12
3.20
5.41
1.01
6.05
1.06
1.94
1.00
1.03
2.92
1.10
3.01
2.19
1.83
2.10
2.39
3.13
8.0
7.5
7.0
6.5
6.0
5.5
5.0
4.5
4.0
3.5
3.0
2.5
2.0
1.5
f1 (ppm)

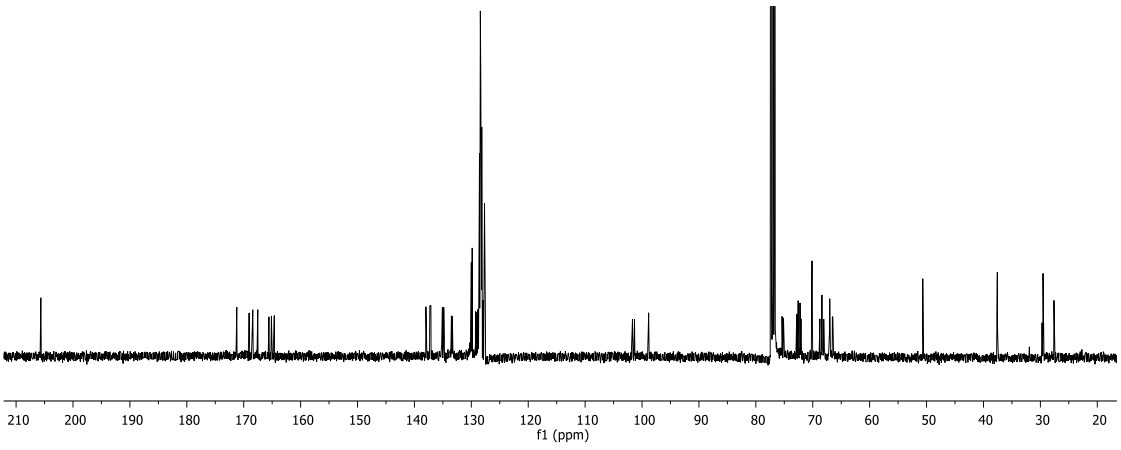
210
200
190
180
170
160
150
140
130
120
110
100
90
80
70
60
50
40
30
20
f1 (ppm)

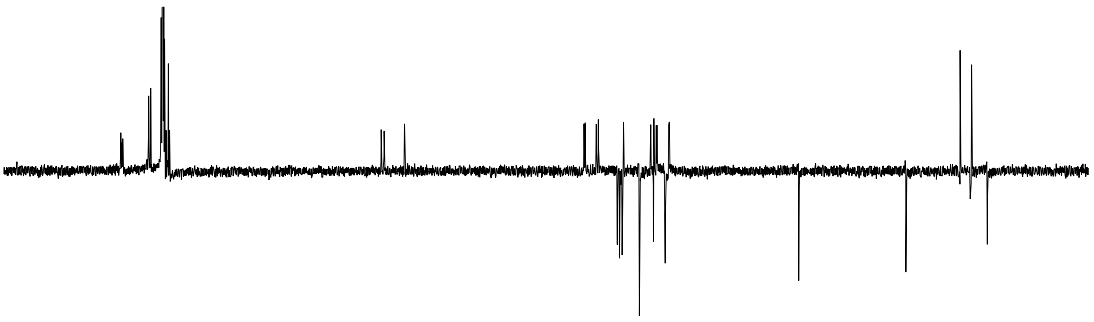

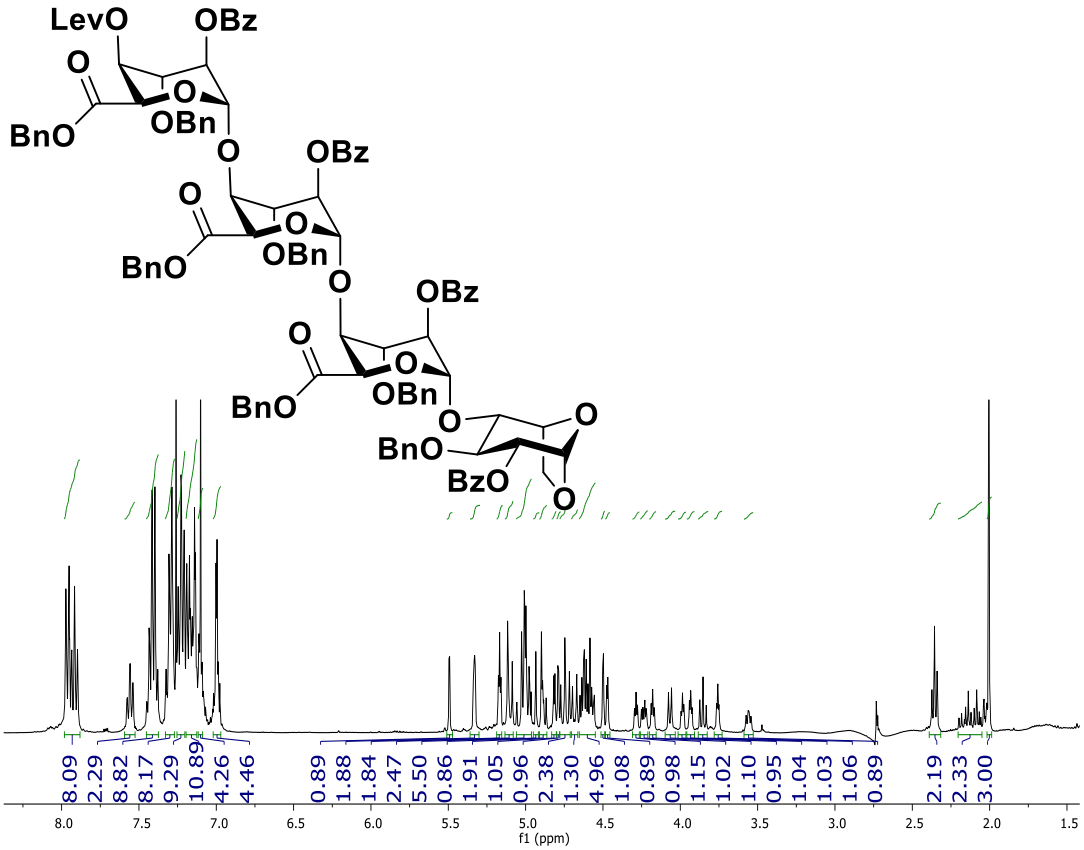
LevO
OBz
O
BnO
OBn
O
OBz
O
BnO
OBn
O
OBz
O
BnO
OBn
O
O
BnO
BzO
O
8.09
2.29
8.82
8.17
9.29
10.89
4.26
4.46
0.89
1.88
1.84
2.47
5.50
0.86
1.91
1.05
0.96
2.38
1.30
4.96
1.08
0.89
0.98
1.15
1.02
1.10
0.95
1.04
1.03
1.06
0.89
2.19
2.33
3.00
8.0
7.5
7.0
6.5
6.0
5.5
5.0
4.5
4.0
3.5
3.0
2.5
2.0
1.5
f1 (ppm)

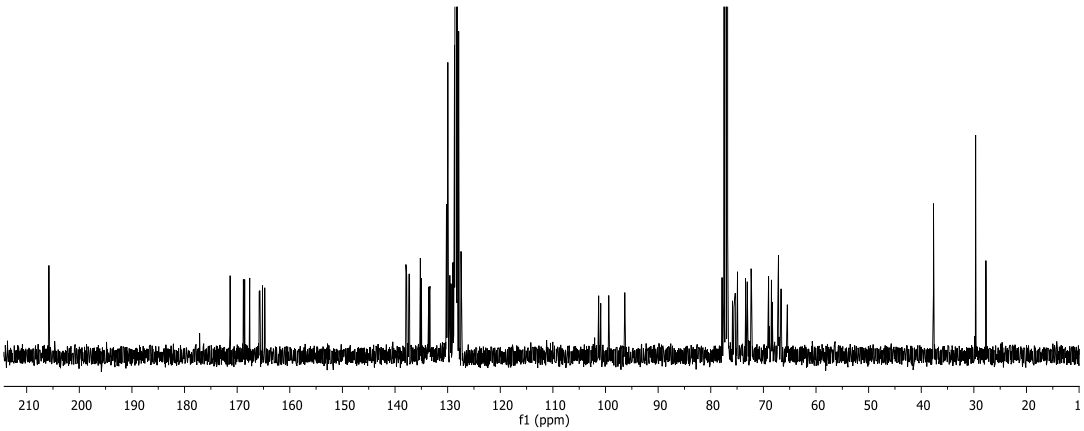
210
200
190
180
170
160
150
140
130
120
110
100
90
80
70
60
50
40
30
20
1
f1 (ppm)

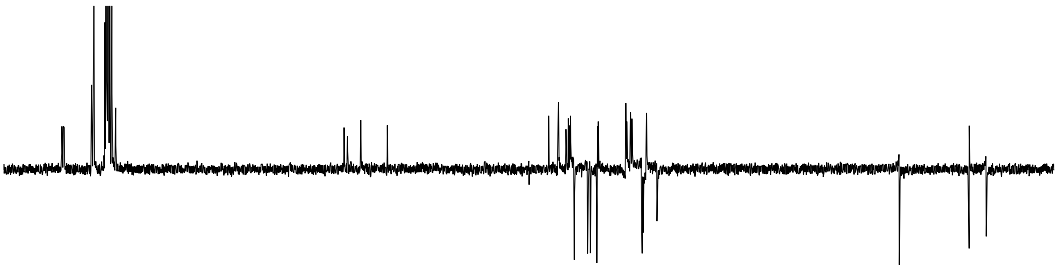

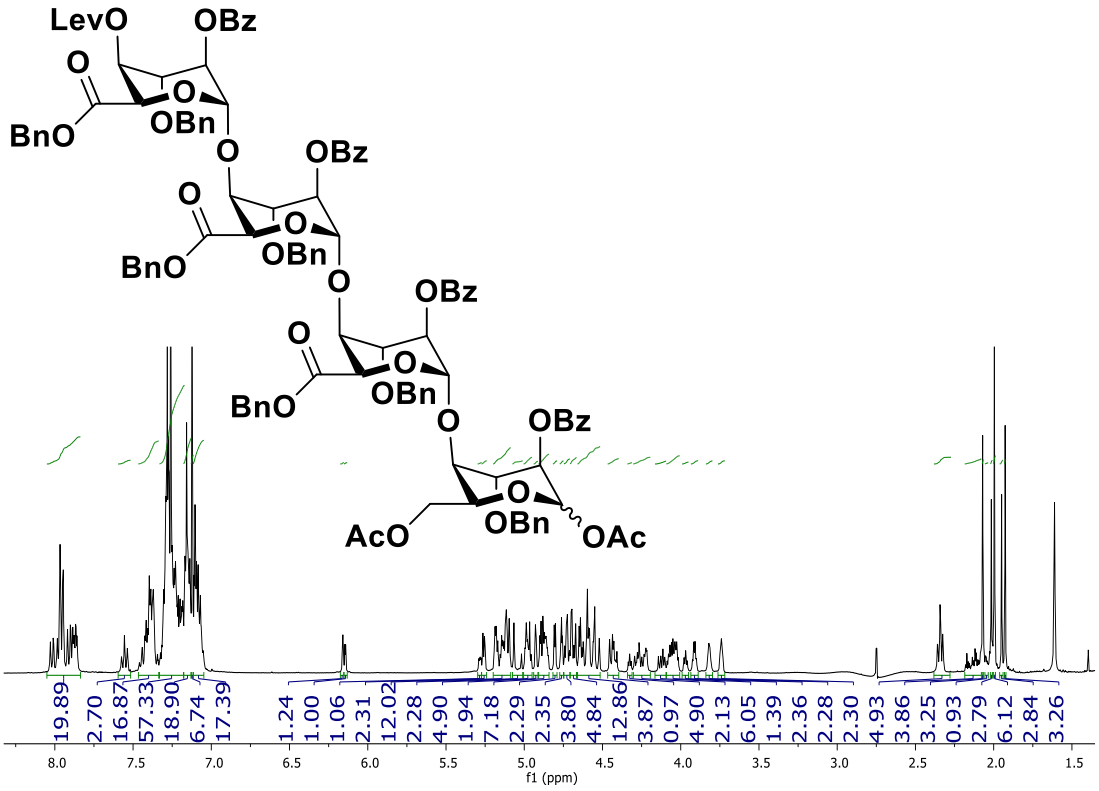
LevO
OBz
O
BnO
OBn
AcO
OAc
19.89
2.70
16.87
57.33
18.90
6.74
17.39
1.24
1.00
1.06
2.31
12.02
2.28
4.90
1.94
7.18
2.29
2.35
3.80
4.84
12.86
3.87
0.97
4.90
2.13
6.05
1.39
2.36
2.28
2.30
4.93
3.86
3.25
0.93
2.79
6.12
2.84
3.26
f1 (ppm)

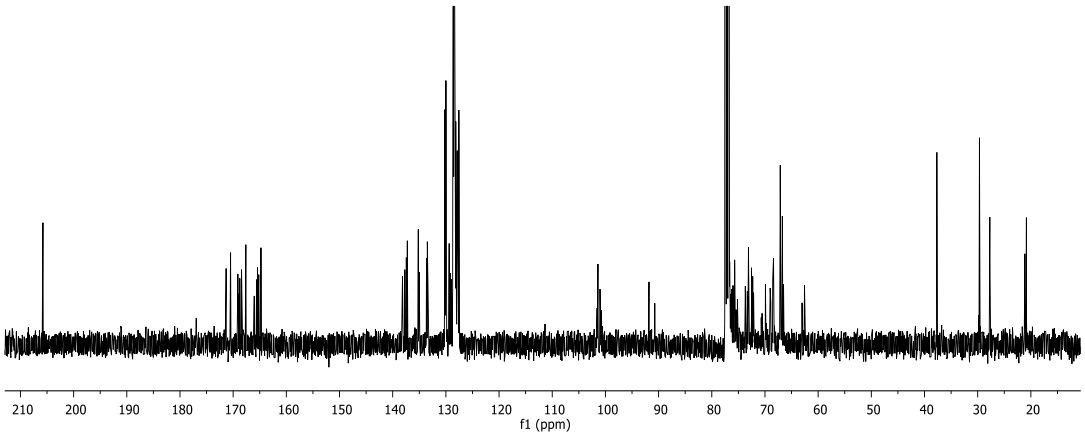
f1 (ppm)

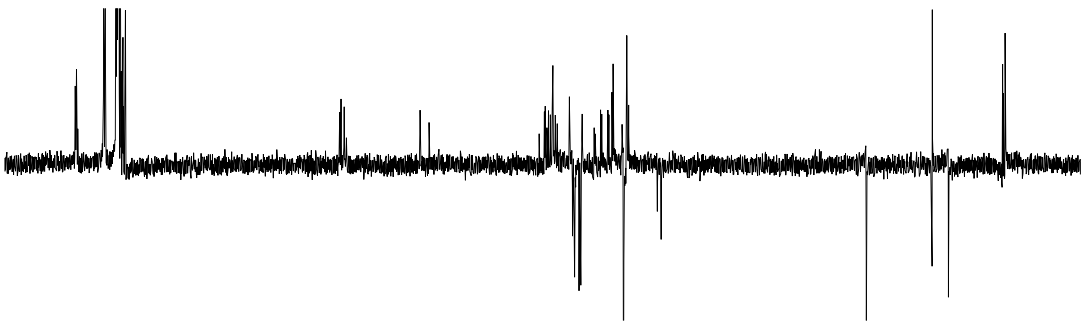

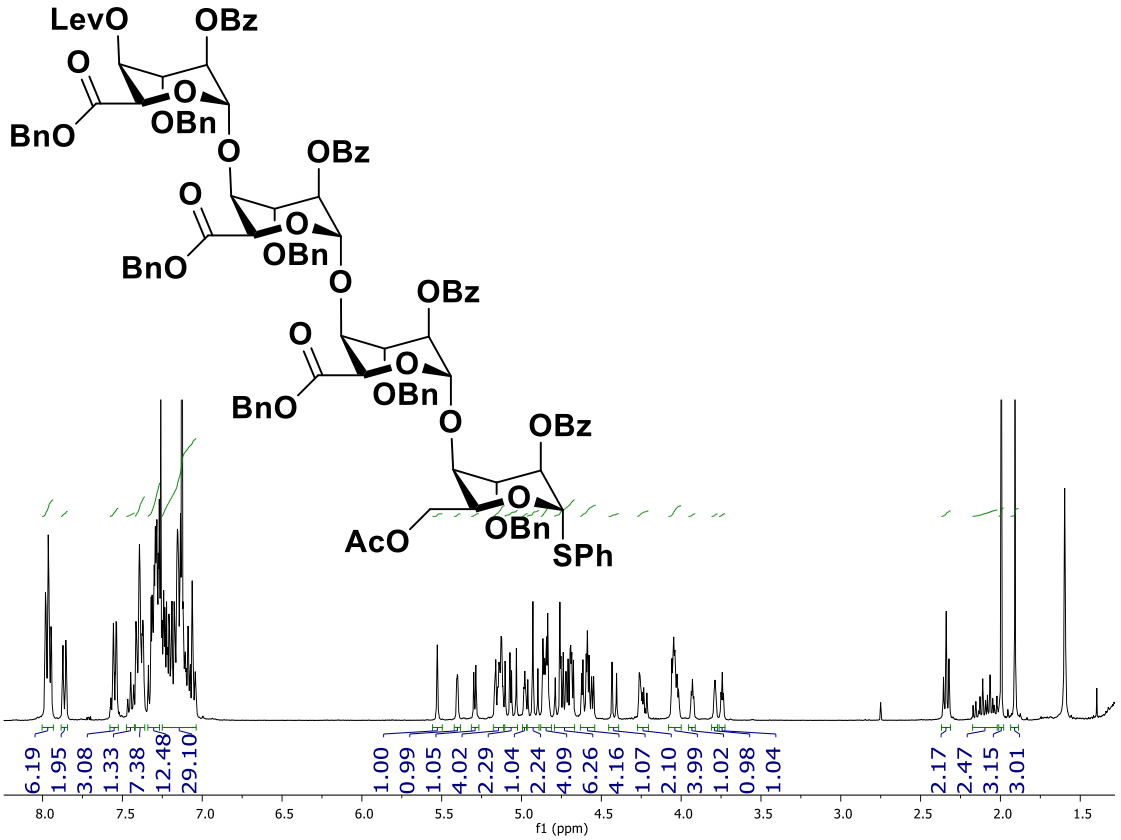
LevO
OBz
O
BnO
OBn
AcO
SPh
6.19
1.95
3.08
1.33
7.38
12.48
29.10
1.00
0.99
1.05
4.02
2.29
1.04
2.24
4.09
6.26
4.16
1.07
2.10
3.99
1.02
0.98
1.04
2.17
2.47
3.15
3.01
f1 (ppm)

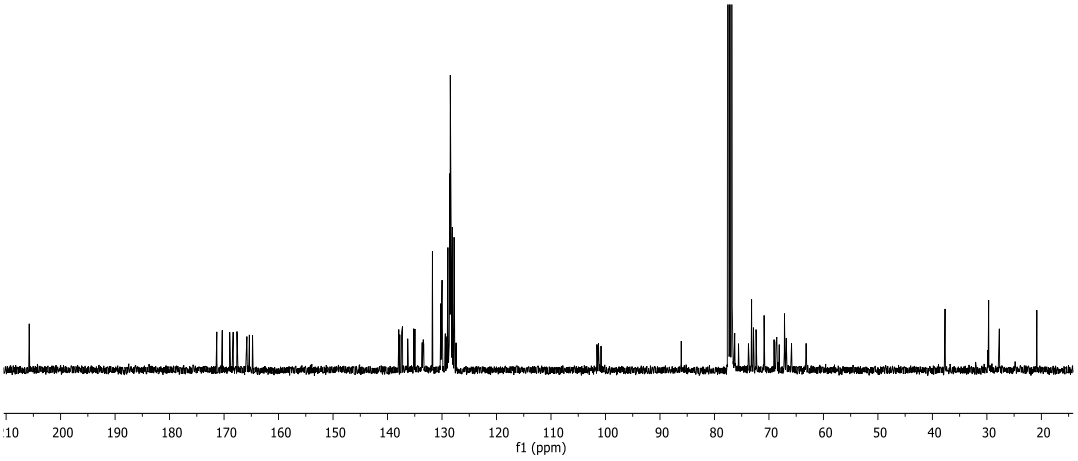
f1 (ppm)

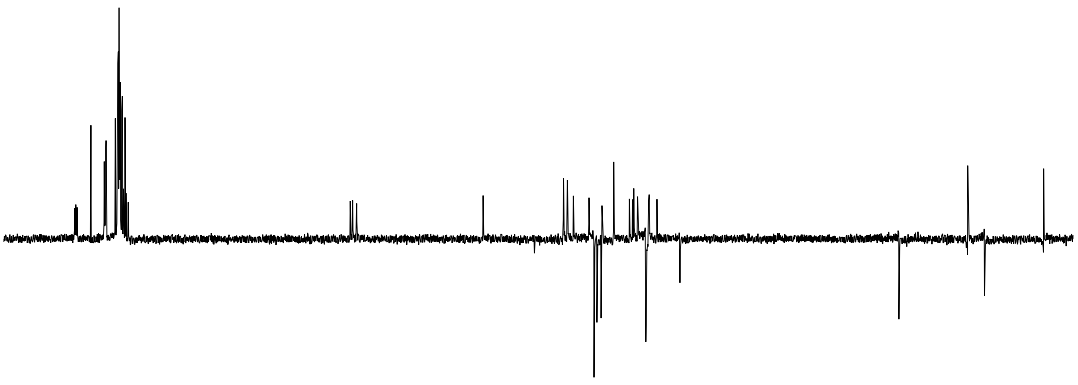

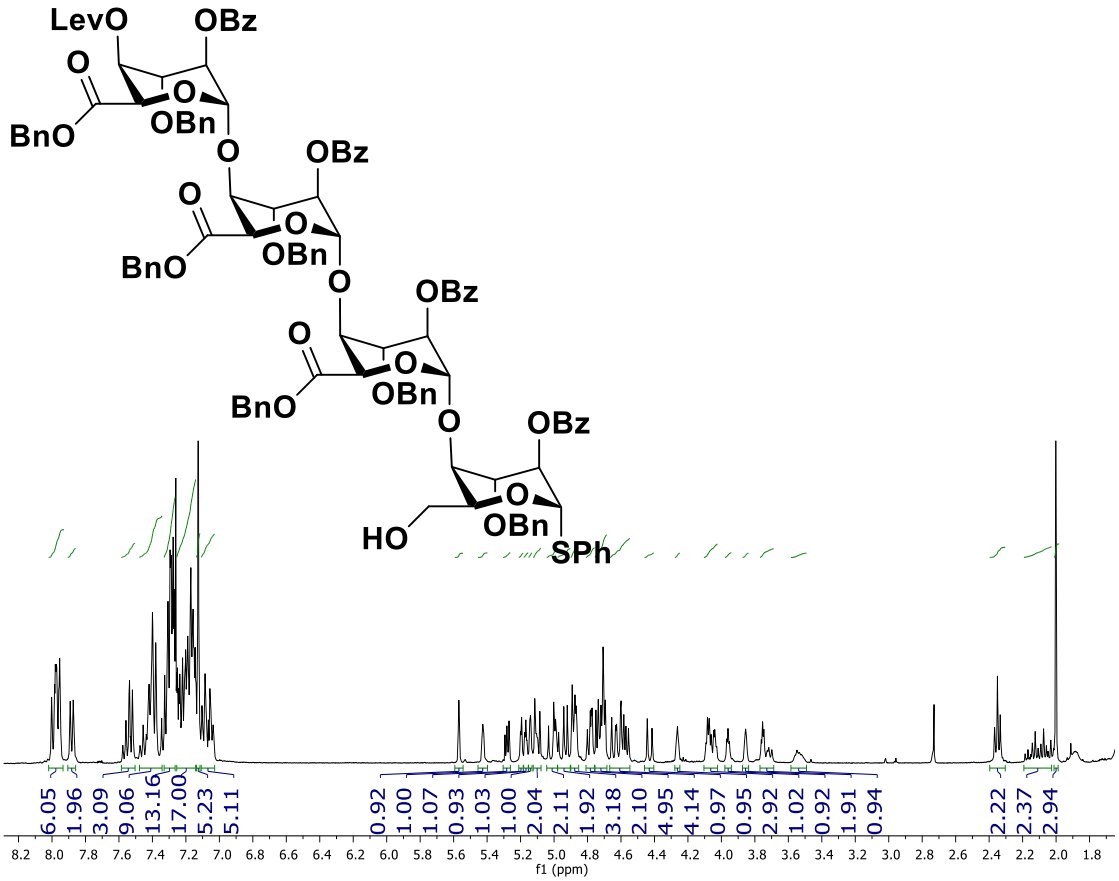
LevO
OBz
O
BnO
OBn
HO
SPh
6.05
1.96
3.09
9.06
13.16
17.00
5.23
5.11
0.92
1.00
1.07
0.93
1.03
1.00
2.04
2.11
1.92
3.18
2.10
4.95
4.14
0.97
0.95
2.92
1.02
0.92
1.91
0.94
2.22
2.37
2.94
f1 (ppm)

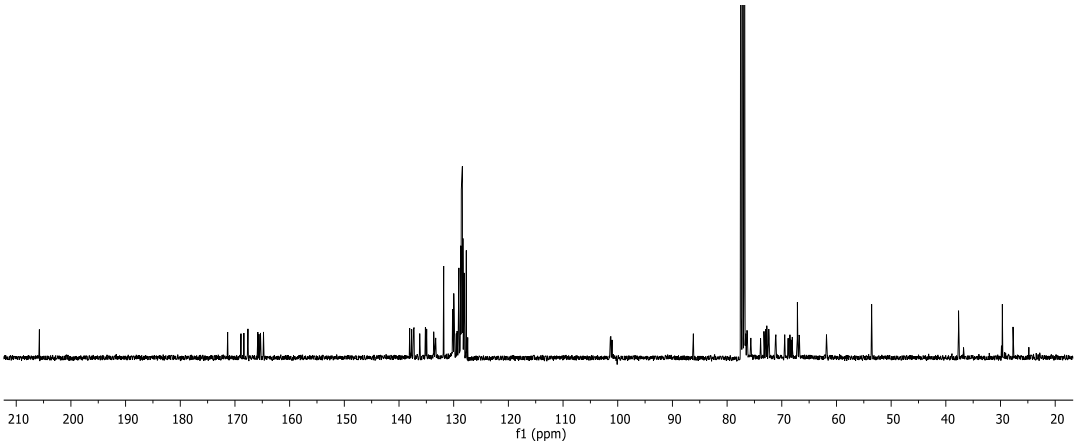
f1 (ppm)

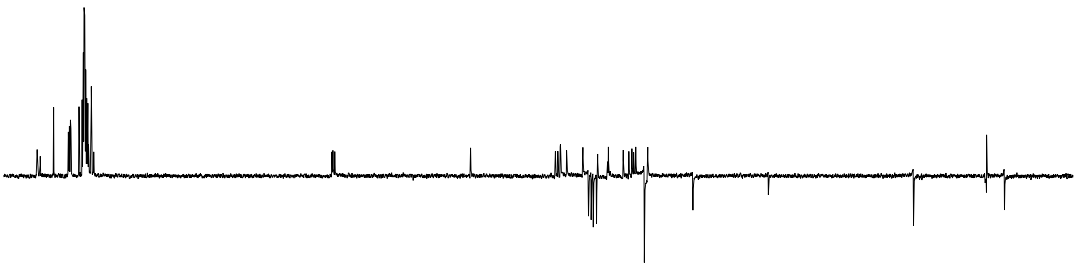

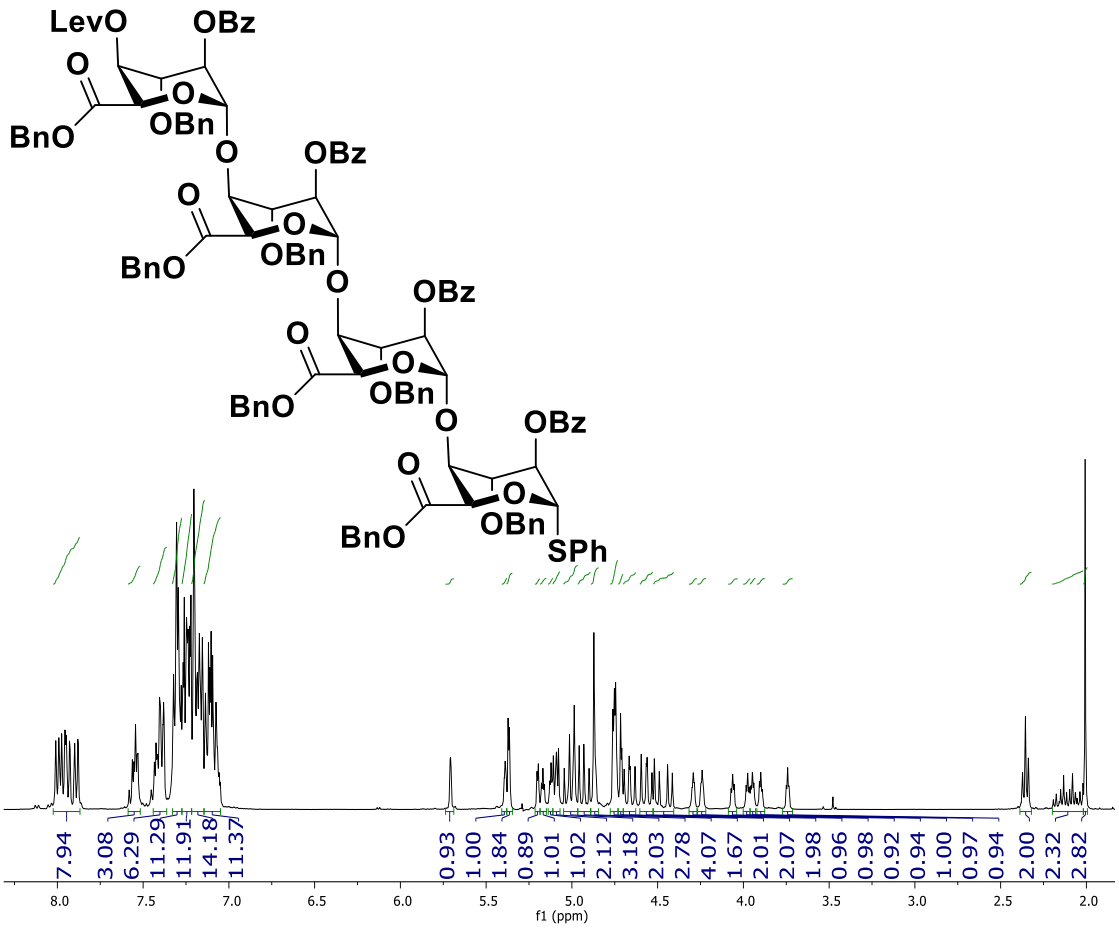
LevO
OBz
O
BnO
OBn
SPh
7.94
3.08
6.29
11.29
11.91
14.18
11.37
0.93
1.00
1.84
0.89
1.01
1.02
2.12
3.18
2.03
2.78
4.07
1.67
2.01
2.07
1.98
0.96
0.98
0.92
0.94
1.00
0.97
0.94
2.00
2.32
2.82
f1 (ppm)

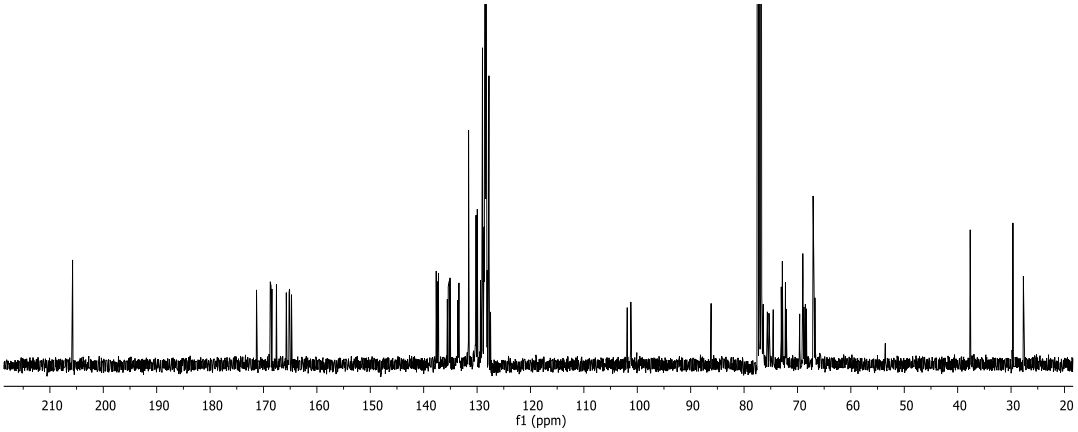
f1 (ppm)

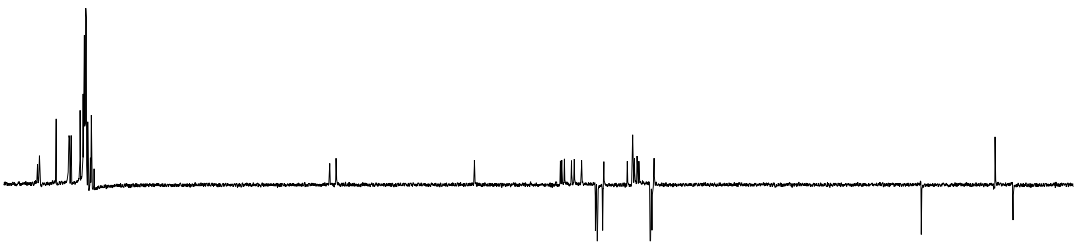

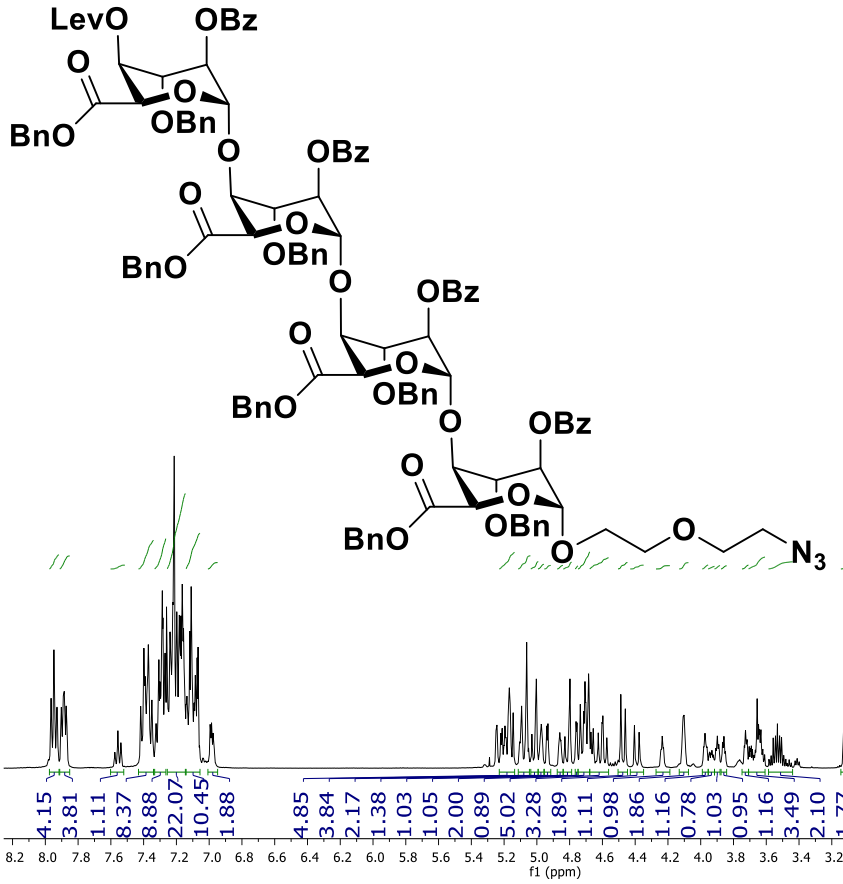
LevO
OBz
O
BnO
OBn
N3
4.15 3.81 1.11 8.37 8.88 22.07 10.45 1.88 4.85 3.84 2.17 1.38 1.03 1.05 2.00 0.89 5.02 3.28 1.89 1.11 0.98 1.86 1.16 0.78 1.03 0.95 1.16 3.49 2.10 1.77 2.00 2.19 3.05
f1 (ppm)

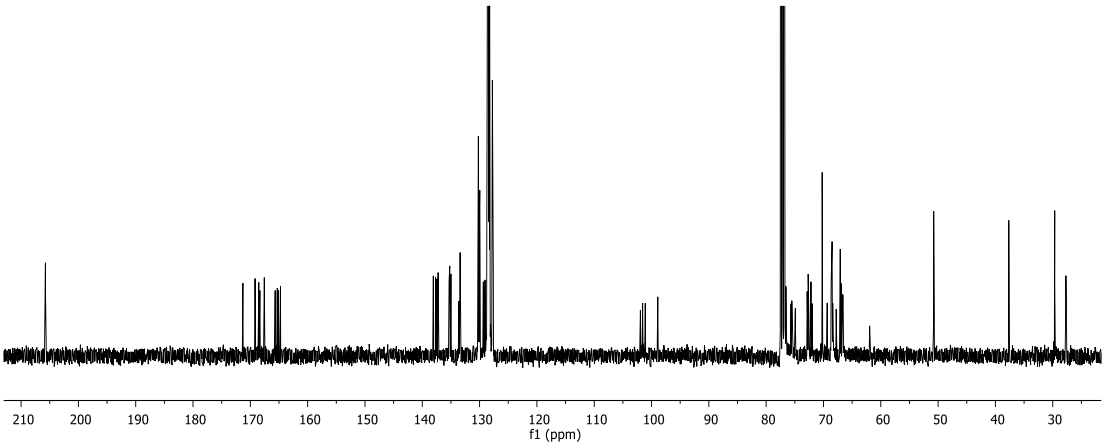
f1 (ppm)

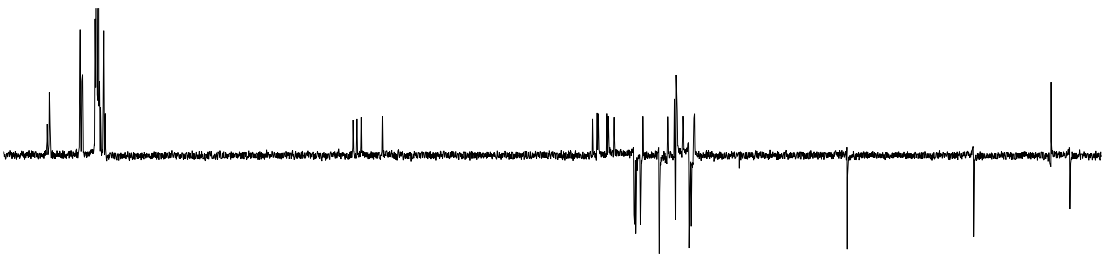

CHAPTER 3

Sulfation Patterns of the L-iduronic acid Homo-oligosaccharides Encode Conformation Plasticity and Molecular Recognition

Abstract

Recently, activity in heparan sulfate (HS) has led to the discovery of many drug molecules that have the potential to impact both medical science and human health. However, structural diversity and synthetic challenges impede the progress of HS research. Here we show that L-Iduronic acid (IdoA) based HS mimics can be engineered to produce many of the functions of native HS oligosaccharides. The NMR analysis of HS mimics, confirmed that 4-*O*-sulfation enhances the population of the $^{1}C_{4}$ geometry. Interestingly, the $^{1}C_{4}$ conformer becomes exclusive upon additional 2-*O*-sulfation. Microarray and SPR analysis with different growth factors established that oligosaccharide length, sulfation code and IdoA conformation synergistically affect the specificity and activity of growth factors. Particularly, 4-*O*-sulfated IdoA disaccharide (**I-21**) had a strong binding affinity to vascular endothelial growth factor ($VEGF_{165}$) and thereby, modulated endothelial cell proliferation, migration, and angiogenesis. Overall, these results encourage the consideration of HS mimics for therapeutic applications.

3.1 Introduction

The nearly 100 years of progress in Heparan sulfate/heparin (HS/HP) research has led to numerous advances in the development of anticoagulants and in cancer theranostics.[1-5] Nonetheless, complete utilization of HS/HP in clinical settings remains elusive due to the structural heterogeneity and the inability to synthesize all possible HS oligosaccharides.[6-8] For example, despite the emergence of efficient chemical and enzymatic methods to synthesize HS oligosaccharides, only a small number of synthetic HS analogueshave been reported.[9-13] These challenges are further exacerbated by the limited ability to structural characterization and track their biological functions.[14]

Heparan sulfate recognizes the myriad of protein surfaces[15,16] with its four key inherent components, (a) sulfation patterns (*O*- and *N*-sulfation),[17-20] (b) uronic acid composition (L-iduronic acid (IdoA) and D-glucuronic acid)[20-21] (c) oligosaccharide chain length[15,16,22] and (d) conformation plasticity of IdoA.[25-28] It has been found that the precise combination of these components dictate the ability of specific HS domain to bind proteins, an attribute that challenges the discovery of specific HS structural domain to modulate individual heparan sulfate binding protein (HSBP) activity.

This challenge has spurred the development of biomimetic analogues of HS, which incorporate essential structural features of HS on simplified structures and study its effect in molecular recognition processes. Several HS mimics have been reported in the literature.[29,31] These HS mimics, however, do not provide the structural variation needed to produce multiple functions like the native HS does. Here, we report the synthesis of a novel, IdoA-based library of HS mimics, which enables the use of multiple parameters including sulfation pattern, conformation plasticity and oligosaccharide chain length to establish a structure-function relationship with growth factors and to modulate biological functions. As a prototype, we describe the synthesis of a library of four non-sulfated (**I-10, I-20, I-30,** and **I-40**), four 4-*O*-sulfated (**I-11, I-21, I-31,** and **I-41**), and four highly sulfated (**I-12, I-23, I-34,** and **I-45**) IdoA ligands that mimic the essential structural features of native HS. Extensive NMR studies, glycan microarrays, and surface plasmon resonance binding assays established the relationship between the binding activity of several growth factors, the conformation of IdoA, and sulfation codes. Candidates with high affinities and specificities to vascular endothelial growth factor ($VEGF_{165}$) were cross linked with star shape dendrimers, and

systematic anti-angiogenic properties were investigated. The results uncovered a novel avenue for developing HS mimics to target HSBPs and influence drug discovery.

3.2 Results and Discussion

3.2.1 Synthesis of Mono-and Di-iduronic Acid Analogues

The synthesis of iduronic acid homo-oligosaccharides is not straightforward, as L-iduronic acid is not commercially available and controlling the α-glycosidic linkages between the successive IdoA residues is difficult. Synthesis of mono-IdoA derivatives (**I-10**, **I-11** and **I-12**) were carried out using iduronic acid-thiophenol donor **1**. Compound **1** synthesized with an overall yield of 0.31% from 1,2:5,6-di-*O*-isopropylideneα-D-glucofuranose by nine-step reactions.[32] The stereoselective linker glycosylation of **1**, followed by global or selective deprotection and sulfation by using $SO_3.Et_3N$ complex yielded mono-IdoA derivatives. The di-IdoA derivatives (**I-20**, **I-21**&**I-23**) were synthesized by stereoselective 1,4-cis glycosidic linkages between iduronic acid-thiophenol 1 and 1,6-anhydro-*β*-L-idopyranosyl 4-alcohol **2** building blocks respectively. It is followed by subsequent modification of reducing end Idose residue by the previously described protocol with slight modification to previous procedure to improve the overall yield (**Scheme 1**).[32] Briefly, the anhydro-ring of **9** was acetalized in the presence of copper (II) trifluoromethanesulfonate [$Cu(OTf)_2$] and acetic anhydride, followed by regioselective thioglycosylated by using trimethyl(phenylthio)silane in the presence of ZnI_2. Then, we performed linker glycosylation before selective deprotction of acetate and oxidation and benzyl esterification in one-pot in the presence TEMPO and benzyl bromide to yield fully protect di-IdoA precursor **14**. This synthetic route improved the overall yield and also avoided poisoning thiophenol donor by TEMPO oxidation.[32] Finally, global or selective deprotection, sulfation and hydrogenolysis yielded desired di-IdoA analogues **(Scheme 1).**

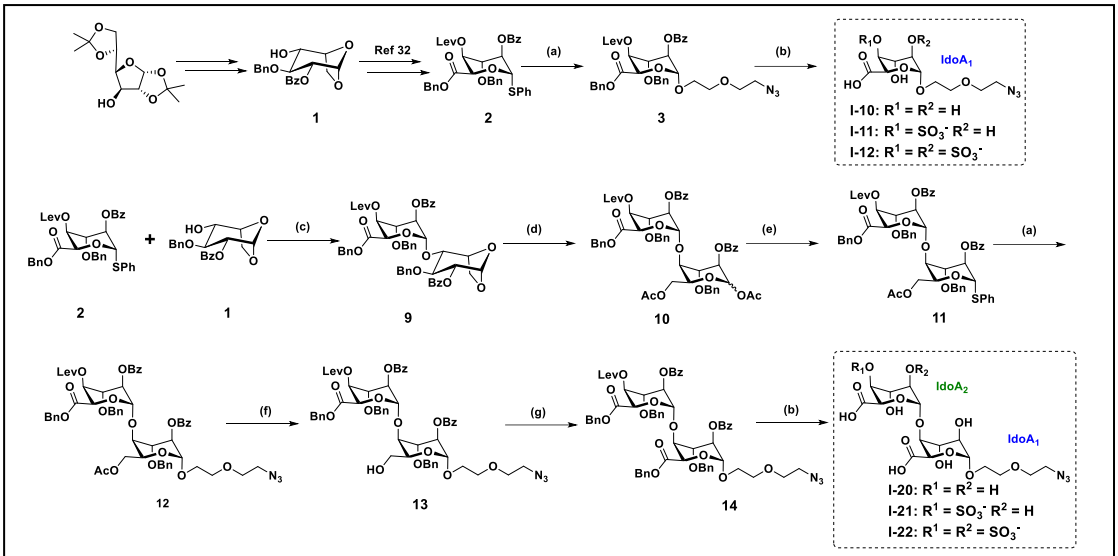

Scheme 1. Synthesis of mono and di-IdoA analogues: (a) azidoethoxyethanol, NIS, TfOH, 4 Å M.S, –10 °C; (b) for **I-10** & **I-20**: LiOH, THF/MeOH/H_2O (4:2:1); $Pd(OH)_2$, MeOH; for **I-11** & **I-21**: NH_2-NH_2.H_2O, AcOH, DCM/MeOH; SO_3.Et_3N, DMF 60 ºC; LiOH, THF/MeOH/H_2O (4:2:1); $Pd(OH)_2$, MeOH; for **I-12** & **I-23**: THF/MeOH/H_2O (4:2:1); SO_3.Et_3N, DMF 60 ºC; $Pd(OH)_2$, MeOH; (c)NIS, TMSOTf, CH_2Cl_2, 4 Å M.S, –10 °C; (d) $Cu(OTf)_2$, Ac_2O, 0 °C; (e) TMSSPh, ZnI_2, CH_2Cl_2, RT; (f) *P*-TsOH, CH_2Cl_2/MeOH(1:1); (g) TEMPO, BAIB, CH_2Cl_2/H_2O (1:1); BnBr, TBAI, $NaHCO_3$, DMF, 60 °C.

3.2.2 Synthesis of Tri- and Tetra-iduronic Acid Analogues

Tri-IdoA derivatives (**I-30**, **I-31**&**I-34**) were synthesized by glycosylating donor **11** and acceptor **1** followed by selective deacetylation of **20** under mild acidic condition, followed by oxidation and esterification. Finally, the IdoA residue at the reducing end of **22** was subjected series of five linear reactions as mentioned above to yield tri-IdoA precursor **27**, which was selectively or globally deprotected and sulfated to obtain desired tri-IdoA derivatives, Similar successive reaction with tri-IdoA donor **24** and acceptor **2** yielded desired tetra-IdoA analogues (**I-40**, **I-41**&**I-45**). All sulfated-IdoA derivatives were purified by ion-exchange resin chromatography, eluted through a C-18 column, and their structures were confirmed by standard NMR and mass spectrometry techniques **(Scheme 2).**

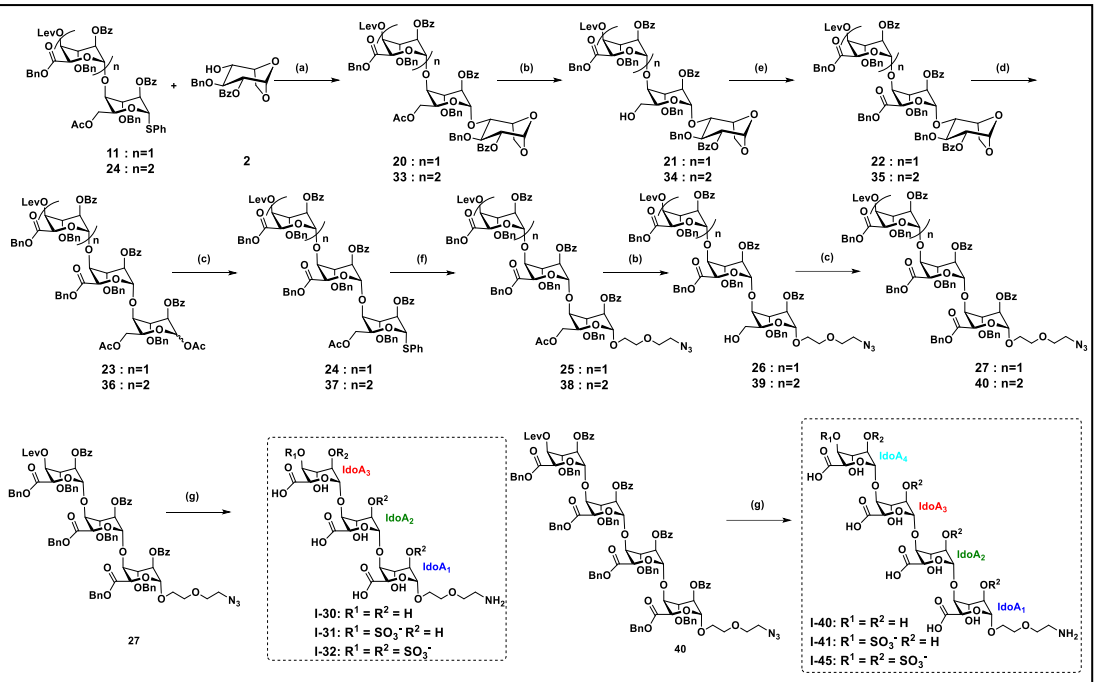

Scheme 2. Synthesis of tri and tetra-IdoA analogues: (a) NIS, TMSOTf, CH_2Cl_2, 4 Å M.S, –10 °C; (b) *P*-TsOH, CH_2Cl_2/MeOH(1:1); (c) TEMPO, BAIB, CH_2Cl_2/H_2O (1:1); BnBr, TBAI, $NaHCO_3$, DMF, 60 °C; (d) $Cu(OTf)_2$, Ac_2O, 0 °C; (e) TMSSPh, ZnI_2, CH_2Cl_2, RT; (f) azidoethoxyethanol, NIS, TfOH, 4 Å M.S, –10 °C; (g) for **I-30** & **1-40**: LiOH, THF/MeOH/H_2O; $Pd(OH)_2$, MeOH; for **I-31** & **I-41**: NH_2-NH_2.H_2O, AcOH, DCM/MeOH; SO_3.Et_3N, DMF 60 ºC; LiOH, THF/MeOH/H_2O (4:2:1); $Pd(OH)_2$, MeOH; for **I-34** & **I-45**: THF/MeOH/H_2O (4:2:1); SO_3.Et_3N, DMF 60 ºC; $Pd(OH)_2$, MeOH

3.2.3 Conformation Analysis of Iduronic Acid Using NMR

To decipher the conformational plasticity of the IdoA ring in these molecules and the effect of the sulfation pattern on their three-dimensional shapes, the conformational features of the monosaccharide series were first analysed. From the NMR perspective, the typical approach involves derivation of model geometries for each of the three basic geometries, calculation of their key NMR expected parameters (usually NOE and J data) and then fitting them to the experimental resulting parameters. The populations combination that provides the best fit is assumed to be the actual conformational distribution in solution. However, it is evident that this approach suffers from some intrinsic caveats; although the calculated molecular geometries can now be very well approximated, especially for the $^2S_0$ conformer, the intrinsic mobility of this form makes it very difficult to estimate the exact J and NOE data.[33] Nevertheless, NOE-derived distances between H2 and H5 within the IdoA ring have been traditionally used

as an estimation of the relative population of the $^{2}S_{0}$-form.[34] In fact, the existence of short distance between H2 and H5 protons, ca. 2.5Å, is a unique feature of the $^{2}S_{0}$ geometry. Therefore, the corresponding NOE is exclusive for the presence of this conformer, since the intra-ring H2-H5 distance is longer for the $^{1}C_{4}$ and $^{4}C_{1}$ chairs (4.1 and 4.0 Å, respectively) (**Fig. 1a**). However, slight variations around the basic skew-boat geometry modify all the intra-ring proton-proton distances, including the H2-H5 ones, and thus, strongly hamper the quantitative analysis of the NOEs. On the other hand, the $^{1}C_{4}$ chair is basically invisible to NOEs since only the existence of a very strong H1-H2 NOE could be considered as indicative of the presence of this conformer in the equilibrium.

Finally, although the H1-H3 and H2-H4 NOEs are expected to be much stronger in the $^{4}C_{1}$ chair, the corresponding distances are also smaller than 3 Å in the $^{2}S_{0}$ alternative. Moreover, the existence of motional anisotropy can also hamper the extraction of accurate proton-proton distances.[35] Therefore, the NOE-based quantitative analysis of the conformational distribution of IdoA rings is far from trivial. In addition, the derivation of the expected $^{3}J_{HH}$ couplings for the basic geometries also suffer from diverse drawbacks. The direct derivation of *J*-couplings for complex molecules such as those of the IdoA rings, including sulfate groups is elusive. The application of the "best" Karplus-type equations to the basic conformers also provides errors due to the intrinsic approximations of the equations, due to the possible distortions that take place upon sulfation, and to the existing fluctuations of the molecules, especially around the skew boat form, which may modify the torsion angles and heavily affect the computed couplings.[33] Therefore, both approaches suffer from different caveats. Herein, we have compared the data extracted from the independent analysis of NOEs and Js to provide an integrated answer. Once the conclusions were reached for the monosaccharide series, the protocol was transferred to the oligosaccharide molecules. In particular, the ^{1}H NMR signals of the 12 analogues were assigned using standard 1D and 2D-NMR experiments (**Fig. 4-7** in experimental section**)** while the key proton-proton distance information that encodes the distribution of the different conformers was extracted from the 2D-NOESY experiments using the procedure described in the experimental section (**Fig. 8-19)**. In brief, besides the skew boat H2-H5 exclusive one, other key NOEs, including H1-H2 (shorter distance in $^{1}C_{4}$), H1-H3 and H2-H4 (shorter distances in $^{4}C_{1}$) and H4-H5 (always fairly short, between 2.3-2.4 Å) were also considered and employed to estimate a relative population of conformers for each molecule by least square

analysis. A somehow different estimation of the population of conformers was also derived from the analysis of the vicinal $^{3}J_{HH}$ coupling constants following the procedure described in the experimental section. Finally, the conclusions of the NOE-analysis were compared to those from the J-based approach to propose the conformational equilibria for the 12 analogues. The complete analysis is gathered in the experimental section **(Table 2 - 21).**

The analysis of the NOE and J data for monosaccharides **I-10**, **I-11**, and **I-12** showed a clear correlation between the sulfation pattern and the population of the $^{1}C_4$ conformer. According to both the J and NOE-based analysis, for the non-sulfated IdoA, **I-10,** the $^{4}C_1$ conformer was predominant (ca. 60-65%), with minor contributions (10-30% each) of the $^{2}S_0$ and $^{1}C_4$ conformations. Interestingly, in **I-11**, sulfation at *O*-4 produced a population shift (50%) towards the $^{1}C_4$ form, decreasing the $^{4}C_1$ chair (20-30%), thus indicating that 4-*O*-sulfation contributes to drive the conformational equilibrium towards the $^{1}C_4$-form. The population of the $^{2}S_0$ skew boat remained between 15-30%. Strikingly, the analysis of the NMR data for **I-12** showed that the introduction of 2-*O*-sulfate group brought about a dramatic decrease in the populations of the $^{2}S_0$ and $^{4}C_1$ forms (less than 10%) in favour of the $^{1}C_4$ conformer, which is now populated in more than 90%. Both NOE data and coupling constants are in agreement with this population distribution **(Table 1)** see experimental section, **(Table 2 - 21).**

Table 1. Conformation plasticity of IdoA in monosaccharides I-10, I-11 and I-12. Key NOEs and $^{3}J_{HH}$ constants employed to determine $^{1}C_4$, $^{4}C_1$ and $^{2}S_0$ contribution were also indicated.

	Measured $^{3}J_{HH}$ (Hz)				**Measured NOE[a]**				**Population[b]**		
	$^{3}J_{H1-H2}$	**$^{3}J_{H2-H3}$**	**$^{3}J_{H3-H4}$**	**$^{3}J_{H4-H5}$**	**H1-H2**	**H1-H3**	**H2-H4**	**H2-H5**	**$^{1}C_4$**	**$^{4}C_1$**	**$^{2}S_0$**
I-10	5.4	7.3	7.2	4.3	0.385	0.422	0.495	0.239	19±4/ 8±5 **13±8**	67±7 /60±4 **63±5**	15±10/33±5 **24±13**
I-11	3.6	5.3	4.9	3.1	0.549	0.211	0.265	0.29	50±4/50±4 **50±4**	29±7/18±5 **23±8**	21±10/33±5 **27±8**
I-12	1.2	2.6	2.9	2	1	0.06	0.05	0.204	90±5/90±5 **90±5**	5±5/5±5 **5±5**	5±5/5±5 **5±5**

[a]NOE ratio using H4-H5 signal as reference. [b]Derived conformer population from J analysis/NOE analysis and average (in bold) was indicated for each compound.

It is not straightforward to deduce the molecular basis of these shifts in the conformational distribution. For **I-10**, it can be speculated that stabilizing hydrogen-bonding and/or ionic interactions between OH3 and OH4 are in favour of the $^{2}S_{0}$ and $^{4}C_{1}$ conformers.[27] The 4-*O*-sulfate group slightly prefers to be accommodated in the $^{1}C_{4}$ form, although according to the population distribution, the free energy difference with the other $^{4}C_{1}$ and $^{2}S_{0}$ conformers remains minimal (**Fig. 1b**). The new interaction between OH2 and 4-*O*-SO_3 in the $^{1}C_{4}$ geometry may account for this slight shift, almost insignificant from the free energy perspective. However, the presence of the double sulfation at *O*-2 and *O*-4 completely shifts the equilibrium towards the $^{1}C_{4}$ conformer. The dipole moment of this geometry for **I-12** is the highest of all possible geometries and would be highly favoured in aqueous environment. Thus, the observed equilibrium shift could be driven by this factor. Taken together, these results point out, that at the monosaccharide level, 4-*O*-sulfation slightly favours the $^{1}C_{4}$-IdoA geometry where double sulfation at *O*-2 and *O*-4 drives the $^{1}C_{4}$ chair conformation to be the most favourable one (**Fig. 1b**).

A similar approach was employed to analyse the ring pucker in the di-, tri- and tetra IdoA-ligands **(Table 5 - 21).** For the non-substituted disaccharide, **I-20** or for **I-21**, the latter sulfated at the terminal *O*-4, the existence of major conformational plasticity was deduced, with the presence of the three geometries. The $^{1}C_{4}$ is slightly predominant and becomes even more populated at IdoA2 of **I-21** upon sulfation at *O*-4 (>70%). Nevertheless, there are always notorious participations of the $^{2}S_{0}$ and $^{4}C_{1}$ forms. The NOE-derived populations are smaller for the $^{4}C_{1}$ conformer (below 9%) versus the skew boat (above 27%), while the J-based analysis displays the opposite tendency: the $^{4}C_{1}$ conformer between 13 and 39% and the skew boat, between 7 and 24%. Thus, for these disaccharides, the conformational plasticity present in the **I-10** and **I-11** monosaccharides is kept. Sulfation at *O*-2 (**I-23**) increases the populations of the $^{1}C_{4}$ chair at both rings (ca. 90%). A similar trend was observed for the trisaccharide and tetrasaccharides. Although the associated energy differences are rather small, it may be inferred that the double *O*-2 and *O*-4 substitution for the internal IdoA2 ring in **I-30** provides a larger population (above 70% for both J- and NOE-based analysis) of the $^{1}C_{4}$ chair. Sulfation at *O*-4 of the terminal ring again increases the population of the $^{1}C_{4}$ (>70%) at the corresponding residues. Nevertheless, the plasticity observed for the disaccharides is kept in the tri- and tetra-saccharide series and small to medium

contributions of $^{4}C_1$ and $^{2}S_0$ forms were also detected. In contrast, the $^{1}C_4$ contribution is highly increased at all rings of **I-34** and **I-45** when sulfation at *O*-2 takes place.

Moreover, the glycosidic linkages provide additional torsional degrees of freedom in these molecules. For heparin and heparan sulfate oligosaccharides, it has been described that the IdoA-containing glycosidic linkages mainly populate one conformational family on the Φ/Ψ map in the exo-anomeric/synregion.[35,36] Therefore, disaccharide models of the nine possible combinations of the $^{2}S_0$, $^{4}C_1$ and $^{1}C_4$ geometries were built for **I-20**, as basic scaffold of all the oligosaccharides (**Fig. 21**), submitted to energy minimisation and the global minima for each combination was carefully analysed. Fittingly, besides the intra-ring H2-H5 distance, the $H5_{i+1}/H3_i$ inter-residue contact also contains conformational information on the shapes of the pyranose rings at the glycosidic linkage. In particular, very close contacts (2.3-2.4 Å) between these two protons are expected only for certain combinations ($^{1}C_4$ - $^{1}C_4$ and $^{1}C_4$ – $^{2}S_0$) of the pyranose rings and moderate contacts (2.9-3.0 Å) for the $^{2}S_0$ – $^{2}S_0$ and $^{2}S_0$ –$^{1}C_4$ shapes' pairs around the glycosidic linkages. The estimated distances for the other five combinations are longer than 4.5 and mostly beyond 5 Å. Regarding other inter-residue NOEs, the $H1_{i+1}/H4_i$ distance does not significantly depend on the shape of the flanking residues (2.2-2.5 Å), except for the $^{4}C_1$–$^{2}S_0$ combination (3.1 Å). However, in this particular case, the $H1_{i+1}/H3_i$ distance would be fairly short (2.3 Å), as in the $^{4}C_1$ –$^{1}C_4$ arrangement.

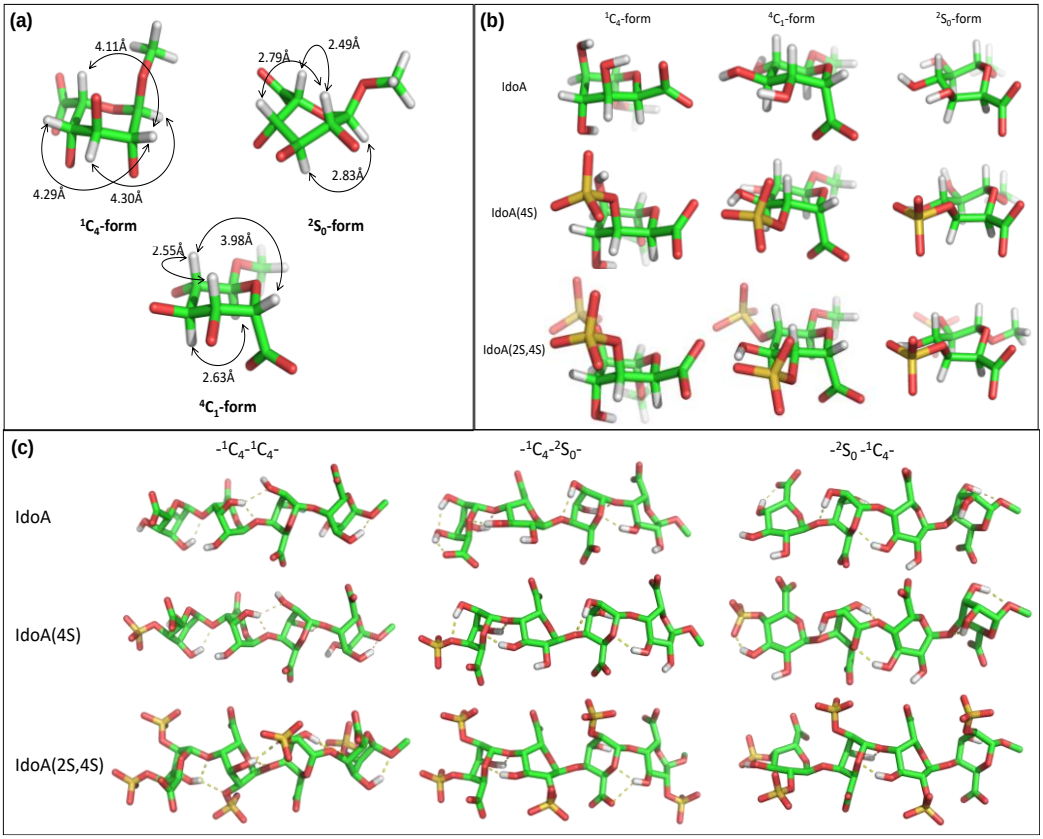

Figure 1. (a) Structures of $^1C_4$, $^4C_1$ and $^2S_0$ conformers of IdoA. Distinguishing proton-proton distances for each conformer are indicated by arrows; (b) DFT optimized geometries of $^1C_4$, $^4C_1$, and $^2S_0$ conformers for non-sulfated, 4-sulfated and 2,4-sulfated IdoA monosaccharides; (c) Modelled geometries for **I-40**, **I-41** and **I-45**. $^1C_4$-$^1C_4$, $^1C_4$-$^2S_0$ and $^2S_0$-$^1C_4$ pairs were considered on the basis of NOE data. Intra and inter-residue hydrogen contacts were indicated.

Indeed, regarding the conformation around the glycosidic linkages, very strong NOEs were observed for the H1 IdoA$_{i+1}$-H4 Ido$_i$ proton pairs, corresponding to very short distances (2.0-2.4 Å), which strongly suggested the existence of the typical exo-anomeric/syn conformation around the glycosidic linkages together with a negligible contribution of the $^4C_1$ –$^2S_0$ combination. Although very rarely (**I-20**, **I-30**), very weak H1 IdoA$_{i+1}$-H3 Ido$_i$ NOEs were detected, which also allowed discarding a significant contribution of the $^4C_1$ –$^1C_4$ arrangement. In contrast, for most of the glycosidic linkages in most of the analogues, as exemplified in **I-45**, significant H5$_{i+1}$/H3$_i$ inter-residue NOEs were measured, corresponding to short distances (2.0-2.7 Å) between the corresponding protons pairs (Experimental section: 2.3-2.7 Å for **I-41**, 2.5-2.6 Å for **I-40**, 2.0-2.2 Å for **I-34**, 2.4-2.5 Å for **I-31**, 2.4 Å for **I-30**, 2.1 Å for **I-23**, 2.4 Å for **I-21**). Therefore, this feature supported the presence of major contributions of $^1C_4$– $^1C_4$,

$^1C_4$ – $^2S_0$, or $^2S_0$ –$^1C_4$ pyranose chairs at both sides of the glycosidic linkages, as also deduced from the analysis at the monosaccharide level.

Then, NOE-derived NMR distances were employed as restraints to build representative 3D structures of IdoA homo-oligomers and thus, to account for the observed conformational preferences and the distinctive role of the 4-*O*and 2-*O*-SO_3 groups. In particular, tetrasaccharides differing in the sulfation pattern and displaying $^1C_4$–$^1C_4$, $^1C_4$– $^2S_0$, and $^2S_0$– $^1C_4$ pairs, are depicted in figure **3c**. All non-, mono- and penta-sulfated tetrasaccharide **I-40**, **I-41** and **I-45** structures displayed inter-residue hydrogen bonds, either between 3-O(i) and 3-OH(i+1), which may stabilize the $^1C_4$ conformers, or between 3-OH(i) and O5(i+1), in the case of molecules containing $^2S_0$-skew boat conformers (**Fig 3c**). These observations made difficult to disentangle the origin of little energy differences between the possible pyranose forms and as it was discussed at the monosaccharide level, other factors such as those related with polarity effects would contribute to tilt the conformer equilibrium. This effect was completely noticeable when overall sulfation takes place and the $^1C_4$ form became predominant. This conformer allows maintaining the inter-residue hydrogen bonds without generating strong electronic repulsion as in the case of molecules containing $^2S_0$ form. The $^1C_4$–$^2S_0$, and $^2S_0$– $^1C_4$ pairs would locate the 2-*O*-SO_3 and COOH groups of two adjacent units very close, thus increasing the energy of the corresponding geometry.

3.3 Microarray Analysis

With the ability to access either to pure $^1C_4$-shape or to mixed geometries of mono- and oligo-IdoA ligands, we embarked on a systematic investigation ofthe role of sulfation patterns and the conformation of IdoA on their recognition by different growth factors (**Fig. 23**), alongside with a positive control (natural heparin) and negative control glycans (sialic acid containing glycans; Sia-glycans). First, the binding preference of

Sulfation	Oligomerization	ID	FGF2	HB-EGF	Amph.	BMP2	$VEGF_{165}$
None	Mono-saccharide	I-10	35	22	52	41	23
	Di-saccharide	I-20	35	25	47	35	13
	Tri-saccharide	I-30	26	22	65	45	8
	Tetra-saccharide	I-40	27	28	59	47	24
Mono-4-O-sulfate	Mono-saccharide	I-11	40	55	60	83	89
	Di-saccharide	I-21	54	47	66	91	99
	Tri-saccharide	I-31	57	45	72	73	59
	Tetra-saccharide	I-41	49	20	67	47	5
2,4-O-sulfate	Mono-saccharide	I-12	50	79	66	71	72
	Di-saccharide	I-23	63	63	57	74	76
	Tri-saccharide	I-34	97	97	93	73	76
	Tetra-saccharide	I-45	41	48	51	66	70
Positive control	Natural Heparin	Hep	39	58	57	24	84
Negative control	None	9OAc-Acα3Core1α	1	4	10	0	0
		9OAc-Gcα3Core1α	1	1	6	0	0
		Acα6LacNAcβ	1	2	14	2	2
		Gcα6LacNAcβ	3	1	15	1	2

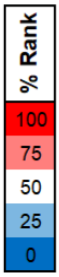

Figure 2. Growth factors glycan microarray binding assay: Binding was tested at 3 serial dilutions, then detected with the relevant biotinylated secondary antibody (1 µg/ml) followed by Cy3-Strepavidin (1.5 µg/ml) (***Table 24***). Arrays were scanned, relative fluorescent units (RFU) obtained, then rank binding of growth factors (each at three dilutions) to glycans printed at four replicates each was calculated: for each binding assay per printed block, the maximum RFU was determined and set as 100% binding. Then, binding to all the other glycans in the same block was ranked in comparison to the maximal binding, and the average rank binding (and SEM) for each glycan across the three examined concentrations of each growth factor was calculated. This analysis allowed to compare the glycan binding profiles of the different growth factors and dissect their binding preferences. The mean rank is shown as a heatmap of all the examined binding assays together (red highest, blue lowest and white 50th percentile of ranking).

human basic-fibroblast growth factor (FGF2) was examined against 12 different HS analogues by nano-printed glycan microarrays. To facilitate comparison of these high-throughput binding profiles, ranking of binding was computed for each FGF2 dilution. As shown in Fig. 2, non-sulfated glycans (**I-10** to **I-40** ranked 35%, 35%, 26% and 37% respectively) exhibited weak binding whereas the mono-4-*O*-sulfated glycans (**I-11** to **I-41** ranked 40%, 54%, 57%, and 49%, respectively) displayed moderate binding. On the other hand, highly sulfated IdoA ligands (**I-12** to **I-34** ranked 50%, 63%, and 97%, respectively) showed moderate to stronger binding with increasing oligosaccharide length. Interestingly, **I-45** displayed a dramatically reduced binding efficiency (ranked 45%). Similar results were observed for the heparin binding-epidermal growth factor (HB-EGF) and amphiregulin (**Fig. 2**), which are both classified as ligands that bind

EGF receptors (EGFRs).[37,38] Of note, FGF2 showed low binding to all the fournegative control Sia-glycans.

In contrast, bone morphogenic protein-2 (BMP2) and vascular endothelial growth factor ($VEGF_{165}$), a key synergistic mediator in angiogenesis and osteogenesis[39,40] exhibited unexpected strong binding affinities to **I-11** and **I-21** (ranked 83% and 91% with BMP2 and 88% and 99% with $VEGF_{165}$) whereas **1-31** and **I-41** displayed moderate to poor binding (ranked 73% and 47% with BMP2 and 58% and 5% with $VEGF_{165}$). Of note, the binding to intermediate sulfated analogues was higher than the binding to natural heparin, and binding to Sia-glycans negative control was low. Based on these findings, **I-11** and **I-21** were identified as simple and highly efficient unnatural carbohydrate ligands to target BMP2 and $VEGF_{165}$.

3.3.1 SPR Analysis

Additional SPR binding experiment to further support the microarray data were performed by immobilizing **I-21** on CM5 gold chips and determining real-time binding affinities with $VEGF_{165}$ and BMP2. The K_D value of **I-21** with $VEGF_{165}$ and BMP-2 was 10.27 µM and 3.15 µM respectively (**Fig.3a & 3b**).

3.3.2 Computational Modelling

Regarding a putative structure-function relationship, the binding analysis witha series of growth factors (FGF2, HB-EGF and amphiregulin) showed that the optimum length of the tested ligands is in the trisaccharide range with a high sulfation content, being **I-34** the best candidate. This molecule displays an almost exclusive $^1C_4$ shape for the different rings. Interestingly, a HSGAG tetrasaccharide displaying a trisaccharide kink with a $^1C_4$ IdoA has been suggested to be the minimal binding motif for FGF2.[41] A 3D model of the possible complex between FGF2 and **I-34** is shown in the Supporting information (**Fig. 22a**). Alternatively, other growth factors ($VEGF_{165}$ and BMP-2) prefer the small mono and disaccharide entities, with intermediate sulfate content. In these cases, both molecules display a wide conformational equilibrium in the IdoA rings with participation of the three conformers (**Fig. 22b**). These data confirm the importance of conformational plasticity to modulate the interactions of HS and its analogues with their receptors.

3.3.3 Synthesis of Multivalent Probes

The biological significance of HS mimics was further evaluated by constructing the HS mimic glycodendrimer **D-I21**, as the multivalent display of HS ligands significantly enhances HSBPs activity.[42-45] The glycodendrimer was synthesized by the reaction of **I-21** amine linker with the active carboxylic acid ester of the star dendrimer. The desired glycodendrimer was purified by centrifugation with a 3 kDa cutoff filter. The conjugation of the HS mimic was determined by ^{1}H and ^{13}C-NMR, which display the stoichiometric 1:4 loading of **I-21** on each dendrimer unit. Similarly, the negative control dendrimer, **D-L (Fig. 3c)**, was also synthesized and characterized.

3.3.4 Cell Proliferation and Western Blot Analysis

Using these two dendrimers, thedegree to which the proliferation of endothelial cells was inhibited in the presence of $VEGF_{165}$was measured. **D-I21** displays a stronger inhibition of cell proliferation in a dose dependent manner compared to **D-L (Fig. 3d)**. To determine the mechanism that inhibits cell-proliferation, western blot analysis of phosphorylated (Tyr951) vascular endothelial growth factor receptor-2 (VEGFR-2) in the presence of different concentrations of **D-I21** (10 to 80 µg/ml) and $VEGF_{165}$ (20 ng/ml) was performed (**Fig. 3e**). It was hypothesized that the strong binding between $VEGF_{165}$ and **D-121** will inhibit $VEGF_{165}$-dependent VEGFR-2 phosphorylation.[46]A concentration between 40-80 µg/ml of **D-121** caused a significant reduction in the phosphorylation of VEGFR-2, indicating that **I-21** is directly involved in the VEGF mediated biological activity.

3.3.5 Cell Migration and Endothelial Tube Formation Assay

To further verify VEGF/**I-21** cellular activity, cell migration and a capillary tube formation assay were performed. As expected, the addition of **D-I21** (50 µg/ml) to $VEGF_{165}$-treated HUVEC cells significantly reduced cell migration in the wound healing assay (**Fig 3f**). Furthermore, the formation of a capillary-like structure was substantially inhibited in the presence of **D-I21 (Fig. 3g)**, demonstrating the anti-angiogenic nature of the HS mimic glycodendrimer. Collectively, these results establish that **I-21** dendrimers may provide opportunities in regenerative medicine and tissue repair and in discovering a novel therapeutic agent for cancer.

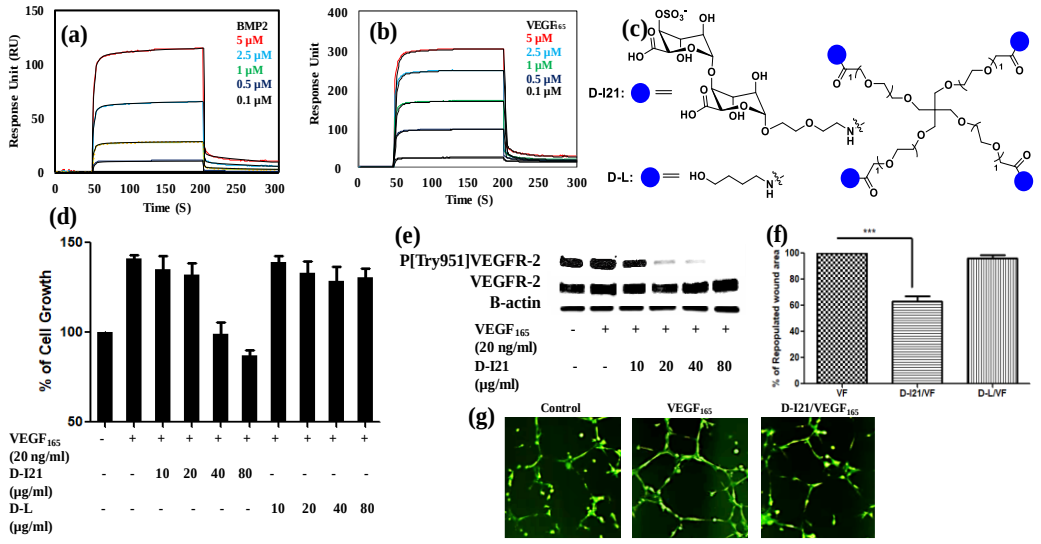

Figure 3. (a) SPR binding analysis of the interaction between BMP-2 and I-21 (Conc of BMP-2 was 0.1-5 µM; dissociation constant (KD) is 10.27 ± 0.3 µM, k_{on} of $3.37 \pm 0.2 \times 10^4\ M^{-1}\ s^{-1}$, and k_{off} of $3.46 \pm 0.12 \times 10^{-1}\ s^{-1}$; (b) Dissociation constant (K_D) of $VEGF_{165}$ and **I-21** is 3.15 ± 0.7 µM, k_{on} of $5.78 \pm 0.2 \times 10^4\ M^{-1}\ s^{-1}$, and k_{off} of $1.83 \pm 0.5 \times 10^{-1}\ s^{-1}$; (c) Structure of star shaped dendrimer **D-I21** and **D-L**; (d) Effect of HS mimics glycodendrimer on HUVECs cells proliferation in presence of $VEGF_{165}$ growth factors. Cell proliferation was evaluated using SRB assay. Cells growth without growth factor is considered as control (100%), Results are represented as the mean SD (n=3); (e) Effect of **D-I21** on VEGFR-2 phosphorylation; (f) Effect of **D-I21** and **D-L** on HUVEC cells migration assay in the presence of $VEGF_{165}$. Conc of dendrimer is 50 µg/ml and Conc of $VEGF_{165}$ is 20 ng/ml (n=3); (g) Confocal images of tube formation in the presence and absence of dendrimers and $VEGF_{165}$ after 12 h. Conc of dendrimer is 50 µg/ml and Conc of $VEGF_{165}$ is 20 ng/ml, Cells were stained with Calcein AM and imaged scale bar 30 µm.

3.4 Conclusions

In conclusion, the synthesis of a new set of HS mimics by utilizing IdoA scaffolds and sulfation patterns is described herein. Extensive NMR studies confirmed that the sulfation code modulates the shape of the IdoA ring and provides a rational approach to enhance the population of the $^1C_4$ conformations. Microarray- and SPR-based binding assays with various growth factors have revealed that the sulfation code and the optimal homo-oligosaccharide length synergistically modulate the binding specificity. Previous $VEGF_{165}$-HS interactions have shownthat HS hexasaccharides with unique sulfation patterns are the minimum necessary sequence for binding to $VEGF_{165}$.[47] However, our results reveal that simple disaccharide entities (**I-21**) with unusual conformation plasticity and sulfation pattern can selectively interact with $VEGF_{165}$ and thereby modulate angiogenesis activity. These results open a new avenue

for generating structurally well-defined HS mimics using IdoA scaffolds with similar functions of native heparin/heparan sulfate.

3.5 EXPERIMENTAL SECTION

3.5.1 General Instructions

All chemicals were reagent grade and used as supplied except where noted. Analytical thin layer chromatography (TLC) was performed on Merck silica gel 60 F254 plates (0.25 mmol). Compounds were visualized by UV irradiation or dipping the plate in CAM/ninhydrin solution followed by heating. Column chromatography was carried out using force flow of the indicated solvent on Flukab Kieselgel 60 (230–400 mesh). ^{1}H and ^{13}C NMR spectra were recorded on Jeol 400 MHz, with cryo probe using residual solvents signals as an internal reference ($CDCl_3 \delta_H$, 7.26 ppm, δ_C 77.3 ppm and CD_3OD δ_H 3.31 ppm, δ_C 49.0 ppm). The chemical shifts (δ) are reported in ppm and coupling constants (*J*) in Hz.

3.5.2 Synthetic Procedure

General Procedure for Lev Deprotection: Compound was dissolved in a mixture of dry DCM/MeOH (4/1) and 5 eq of hydrazinehydrate ($H_2NNH_2 \cdot H_2O$), acetic acid (for 1 g, 1mL) was added, under nitrogen atmosphere. Allow the reaction flask stirred for another 4 h. After completion of reaction, quench with 10 mL of acetone, solvent was evaporated under reduced pressure. The residue was purified by flash column chromatography (EtOAc/Hexane = 1/1) to afford Lev deprotected compound.

General Procedure for Esters Deprotection: Compound was dissolved in THF/MeOH/$H_2$0 water mixture (4/2/1). 50 eq. of $LiOH \cdot H_2O$ was added. Allowed the reaction flask stirred for 2-3 days. After completion of reaction quench with amberlite IR120 acidic resin (If the compound is sulfated quench with Dowex 50WX8 H^+ resin) filtered reaction mixture and evaporate under reduced pressure, purified using silica column chromatography using DCM and MeOH as eluent to deprotected compounds.

General Procedure for *O*-Sulfation: Compound was dissolved in dry, DMF (6 mL). $SO_3 \cdot Et_3N$ (OH 5 eq per OH group) was added. Allowed the reaction flask stirred for 3 days at 60°C. After completion of reaction cool to room temperature add the aqueous solution of $NaHCO_3$ (10 eq per OH group) and kept it for another 16 h. Filtered the

reaction mixture using what's man filter and wash with DCM/ MeOH (1/1, 10 mL), solvents were evaporated under reduced pressure and the resulting residue was purified using silica column chromatography (DCM/MeOH = 1/9 for mono sulfated compound). For heavily sulfated compound were purified by using Sephadex LH-20 resin and elute with 50% of DCM, MeOH, and pass-through sodium (Na^+) resin column using water as eluent. The product fraction was lyophilized to afford sulfated compounds as a white powder.

General Procedure for Hydrogenolysis: Compound was dissolved in dry methanol, 20% $Pd(OH)_2$ on carbon (0.025 g per one benzyl group) and purged with a hydrogen gas. The reaction mixture was stirred at room temperature for 2-3 days. The mixture was filtered through celite, and the filtrate was evaporated under reduced pressure. The residue was purified through bond elute C-18 column eluted with water. Sulfated compound pass through sodium (Na^+) resin. The product fraction was lyophilized to afford sulfated compounds as a white powder.

General Procedure for Multivalent Dendrimer Conjugation: Deprotected compound (**I-21**) or 3-Amino-1-propanol (5 mmol) were dissolved in PBS (pH= 7.4) along with 4arm-PEG5K-Succinimidyl Carboxymethyl Ester (1 mmol, average Mn= 5000) and stirred overnight at room temperature. Next day, both I-21 and linker conjugated dendrimers were passed through centrifuge filter (MWCO: 3kDa) and washed twice with DI water. Finally, compounds were lyophilized to obtain multivalent probes as a white solid powder.

3.5.2.1 Synthesis of Iduronic Acid Monosaccharide and its Sulfated Analogues

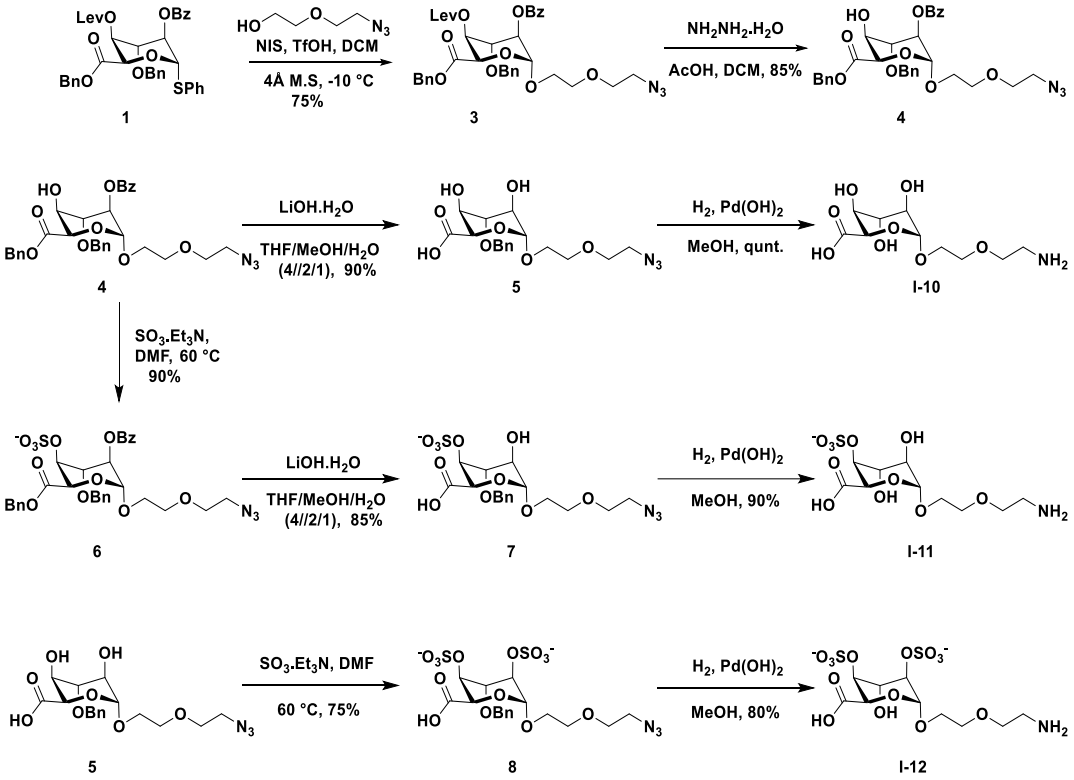

Scheme 1. Synthesis of Monosaccharides Building Block and Sulfated Compounds.

Ethoxy-2-azidoethoxyl-O-(benzyl(2-O-benzoyl-3-O-benzyl-4-O-levulinoyl))-α-L-idopyranosideuronate 3

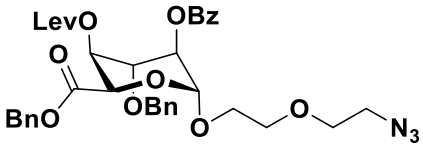

Compound **1** (1.2 g, 1.79 mmol), 2-(2-azidoethoxy)ethan-1-ol (0.28 g, 2.16 mmol) and freshly dried 4 Å molecular sieves were dissolved in dry DCM (20 mL) and stirred at RT for 1 h. Then *N*-iodosuccinimide (0.61 g, 2.69 mmol), TfOH (0.032 mL, 0.36 mmol) were added at -10°C and stirred for 30 min. After the completion of reaction, the reaction mixture was quenched with triethylamine and filtered through celite. The organic layer was washed with $Na_2S_2O_3$ followed by $NaHCO_3$, brine solution and dried over Na_2SO_4, then filtered and concentrated under reduced pressure. The residue was purified by column chromatography (EtOAc/Hexane = 1/4) to afford **3 (0.94 g, 75%)** as syrup. ^{1}H NMR (400 MHz, Chloroform-*d*) δ 8.07 – 8.04 (m, 2H), 7.59 – 7.54 (m, 1H), 7.44 – 7.27 (m, 12H), 5.30 – 5.27 (m, 2H), 5.19 (d, *J* = 1.2 Hz, 2H), 5.16 (d, *J* = 11.9 Hz, 1H), 5.05 (d,

J = 2.2 Hz, 1H), 4.83 (d, *J* = 11.6 Hz, 1H), 4.72 (d, *J* = 11.6 Hz, 1H), 3.98 – 3.92 (m, 1H), 3.88 (dt, *J* = 3.2, 1.7 Hz, 1H), 3.76 – 3.6 (m, 3H), 3.62 – 3.52 (m, 2H), 3.17 (t, *J* = 5.0 Hz, 2H), 2.48 (td, *J* = 6.7, 2.6 Hz, 2H), 2.31 (ddd, *J* = 17.1, 7.5, 6.4 Hz, 1H), 2.20 (dt, *J* = 17.2, 6.5 Hz, 1H), 2.06 (s, 3H). ^{13}C NMR (101 MHz, CHLOROFORM-*D*) δ 205.98, 171.66, 168.51, 165.32, 137.65, 135.42, 133.67, 129.97, 129.48, 129.07, 128.70, 128.62, 128.55, 128.45, 127.94, 127.80, 98.61, 72.71, 72.46, 70.34, 70.22, 68.40, 68.08, 67.34, 66.93, 66.09, 50.82, 37.80, 29.73, 27.90. HRMS m/z calculated for $C_{36}H_{39}O_{11}N_3Na$: 712.2482; found: 712.2481.

Ethoxy-2-azidoethoxyl-O-(benzyl(2-O-benzoyl-3-O-benzyl-4-hydroxyl))-α-L-idopyranosideuronate 4

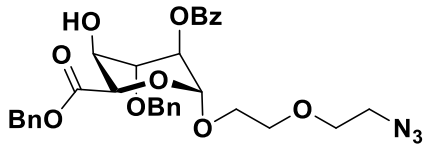

Compound **3** (0.9 g, 1.29 mmol) was dissolved in a mixture of dry DCM/MeOH (4/1, 10 mL) and hydrazinehydrate (0.32 mL, 6.45 mmol), acetic acid (1.12 mL, 19.59 mmol) was added, under nitrogen atmosphere. Allow the reaction flask stirred for another 4 h. After completion of reaction, quench with 5 mL of acetone, solvents were evaporated under reduced pressure. The residue was purified by flash column chromatography (EtOAc/Hexane = 1/1) to afford compound **4 (1.9 g, 80%)** as syrup. ^{1}H NMR (400 MHz, Chloroform-*d*) δ 8.00 (dd, *J* = 8.3, 1.4 Hz, 2H), 7.62 – 7.57 (m, 1H), 7.48 – 7.43 (m, 2H), 7.40 – 7.28 (m, 10H), 5.32 (d, *J* = 12.3 Hz, 1H), 5.27 – 5.26 (m, 1H), 5.24 (d, *J* = 12.3 Hz, 1H), 5.17 (s, 1H), 5.02 (d, *J* = 1.7 Hz, 1H), 4.84 (d, *J* = 11.6 Hz, 1H), 4.65 (d, *J* = 11.6 Hz, 1H), 4.16 – 4.12 (m, 1H), 3.98 – 3.93 (m, 1H), 3.89 (td, *J* = 3.0, 1.3 Hz, 1H), 3.76 – 3.67 (m, 3H), 3.63 – 3.53 (m, 2H), 3.19 (t, *J* = 5.0 Hz, 2H), 2.80 (d, *J* = 11.6 Hz, 1H). ^{13}C NMR (101 MHz, Chloroform-*d*) δ 169.54, 165.11, 137.70, 135.49, 133.84, 129.89, 129.14, 128.77, 128.73, 128.55, 128.52, 128.44, 128.02, 127.88, 99.00, 74.75, 72.16, 70.33, 70.25, 68.48, 68.29, 67.96, 67.47, 67.17, 50.83. HRMS m/z calculated for $C_{31}H_{33}N_3O_9Na$: 614.2114 found: 614.2109.

Ethoxy-2-azidoethoxyl-O-(3-O-benzyl)-α-L-idopyranoside uronic acid 5

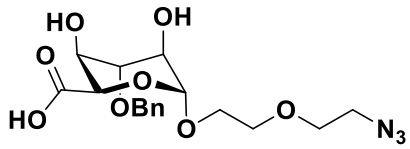

Esters deprotection: Followed general procedure for deprotection of esters which yielded compound **5 (90%).** ^{1}H NMR (400 MHz, Methanol-d_4) δ 7.41 – 7.25 (m, 5H), 4.75 – 4.71 (m, 2H), 4.65 – 4.60 (m, 1H), 4.08 (s, 1H), 3.93 – 3.87 (m, 1H), 3.81 – 3.80 (m, 1H), 3.71 – 3.66 (m, 5H), 3.64 – 3.56 (m, 1H), 3.23 (t, *J* = 4.9 Hz, 2H). ^{13}C NMR (101 MHz, Methanol-d_4) δ 173.88, 139.69, 129.32, 128.86, 128.67, 102.77, 78.04, 72.92, 71.28, 71.21, 69.92, 69.67, 69.24, 68.10, 51.75. HRMS m/z calculated for $C_{17}H_{23}N_3O_8Na$: 420.1383 found: 420.1378.

Ethoxy-2-azidoethoxyl-O-(benzyl (2-O-benzoyl-3-O-benzyl-4-Osulfonato))-α-L-idopyranosideuronate 6

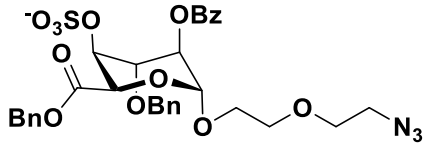

***O*-Sulfation:** Followedgeneral procedure for sulfation yielded compound **6 (90%).** ^{1}H NMR (400 MHz, Methanol-d_4) δ 8.17 (dd, *J* = 8.4, 1.3 Hz, 2H), 7.61 – 7.57 (m, 1H), 7.47 (ddd, *J* = 8.6, 4.4, 2.8 Hz, 4H), 7.40– 7.32 (m, 5H), 7.30 – 7.22 (m, 3H), 5.37 (d, *J* = 12.0 Hz, 1H), 5.15 – 5.10 (m, 2H), 5.09 (d, *J* = 2.3 Hz, 1H), 5.07(s, 1H), 4.81 – 4.76 (m, 2H), 4.65 (d, *J* = 60.6 Hz, 1H), 4.39 (ddd, *J* = 3.5, 2.7, 1.1 Hz, 1H), 3.88 – 3.83 (m, 1H), 3.70 – 3.62 (m, 3H), 3.59 – 3.46 (m, 2H), 3.09 (t, *J* = 5.1 Hz, 2H). ^{13}C NMR (101 MHz, Methanol-d_4) δ 170.70, 167.13, 139.36, 136.96, 134.34, 131.33, 130.94, 129.77, 129.49, 129.46, 129.28, 128.99, 128.70, 99.71, 74.93, 73.48, 73.08, 71.27, 71.11, 69.43, 68.97, 68.51, 68.46, 51.70. HRMS m/z calculated for $C_{31}H_{33}N_3O_{12}S^-$: 670.1712 found (M-H): 669.1715.

Ethoxy-2-azidoethoxyl-O-(-3-O-benzyl-4-O-sulfonato)-α-L-idopyranoside uronic acid7

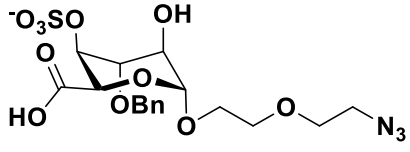

Esters deprotection: Followed general procedure for deprotection of esters yielded compound **7 (85%)**.^{1}H NMR (400 MHz, Deuterium Oxide) δ 7.52 – 7.41 (m, 5H), 4.92 (dd, *J* = 2.0, 0.9 Hz, 1H), 4.83 (d, *J* = 11.7 Hz, 1H), 4.70 (d, *J* = 11.6 Hz, 1H), 4.61 (d, *J* = 2.3 Hz, 1H), 4.20 (td, *J* = 3.3, 1.0 Hz, 1H), 3.93 – 3.87 (m, 1H), 3.76 – 3.68 (m, 6H), 3.44 – 3.42 (m, 2H). ^{13}C NMR (101 MHz, Deuterium Oxide)

δ 174.75, 137.21, 128.63, 128.62, 128.32, 100.31, 74.72, 73.42, 72.37, 69.48, 69.30, 67.75, 67.47, 67.38, 50.13. HRMS m/z calculated for $C_{17}H_{22}N_3O_{11}S^-$: 476.0981 found (M-H): 475.0980.

Ethaoxy-2-aminoethoxyl-O-α-L-idopyranoside uronic acid I-1

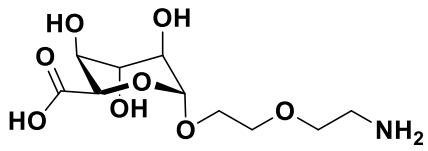

Hydrogenalysis: Followed general procedure for hydrogenalysis yielded compound **I-10 (90%).** ^{1}H NMR (400 MHz, Deuterium Oxide) δ 4.86 (d, J = 4.2 Hz, 1H), 4.62 (d, J = 3.6 Hz, 1H), 3.91 – 3.86 (m, 2H), 3.74 (dd, J = 6.9, 5.1 Hz, 2H), 3.71 – 3.68 (m, 4H), 3.51 (dd, J = 6.4, 4.2 Hz, 1H), 3.14 (t, J = 5.1 Hz, 2H). 13C NMR (101 MHz, Deuterium Oxide) δ 173.78, 101.00, 71.07, 70.15, 69.96, 69.85, 69.67, 67.92, 66.34, 39.08. HRMS m/z calculated for $C_{10}H_{19}NO_8Na$: 304.1008 found: 304.1001.

Ethoxy-2-aminoethoxyl-O-(4-O-sulfonato)-α-L-idopyranoside uronic acid I-11

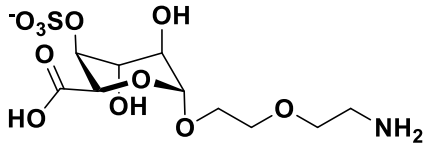

Hydrogenalysis: Followed general procedure for hydrogenalysis yielded compound **I-11 (90%).** ^{1}H NMR (400 MHz, Deuterium Oxide) δ 4.78 (d, *J* = 3.5 Hz, 1H), 4.46 (d, *J* = 3.1 Hz, 1H), 4.41 – 4.39 (m, 1H), 4.11 (t, *J* = 5.0 Hz, 1H), 3.80 – 3.75 (m, 1H), 3.67 (dt, *J* = 11.8, 4.2 Hz, 1H), 3.62 – 3.59 (m, 4H), 3.47 – 3.45 (m, 1H), 3.07 – 3.04 (m, 2H). ^{13}C NMR (101 MHz, Deuterium Oxide) δ 174.64, 100.66, 76.67, 69.84, 69.66, 69.00, 68.92, 67.79, 66.29, 39.10. HRMS m/z calculated for $C_{10}H_{18}NO_{11}S^-$: 360.0606 found: 360.0611.

Ethoxy-2-azidoethoxyl-O-(2,4-O-disulfonato-3-O-benzyl)-α-L-idopyranosideuronic acid 8

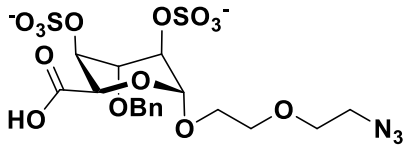

***O*-Sulfation:** Followedgeneral procedure for sulfation yielded compound **8 (75%).** ^{1}H NMR (400 MHz, Deuterium Oxide) δ 7.49 – 7.36 (m, 5H), 5.10 (s, 1H), 4.76 – 4.71 (m, 3H), 4.64 (d, *J* = 1.7 Hz, 1H), 4.34 (dd, *J* = 2.3, 1.1 Hz, 1H), 4.33 – 4.32 (m, 1H), 3.89 – 3.83 (m, 1H), 3.76 – 3.70 (m, 3H), 3.68 – 3.62 (m, 2H),

3.38 – 3.36 (m, 2H). ^{13}C NMR (101 MHz, Deuterium Oxide) δ 174.22, 136.95, 128.69, 128.63, 128.41, 98.50z, 72.98, 72.31, 71.92, 71.17, 69.49, 69.42, 67.57, 66.33, 50.18. HRMS m/z calculated for $C_{17}H_{21}N_3O_{14}S_2^{2-}$: 277.5238 found: 277.5233.

Ethoxy-2-aminoethoxyl-O-(2,4-O-disulfonato)-α-L-idopyranoside uronic acid I-12.

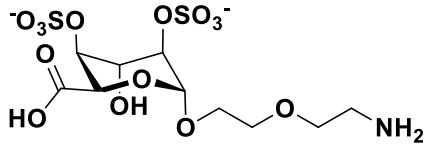

Hydrogenalysis: Followed general procedure for hydrogenalysis yielded compound **I-12 (90%).** ^{1}H NMR (400 MHz, Deuterium Oxide) δ 5.14 (s, 1H), 4.59 (d, *J* = 2.0 Hz, 1H), 4.57 (d, *J* = 2.8 Hz, 1H), 4.48 (dt, *J* = 2.8, 1.4 Hz, 1H), 4.21 (dt, *J* = 2.5, 1.2 Hz, 1H), 3.84 (ddd, *J* = 13.9, 8.6, 4.4 Hz, 2H), 3.73 (q, *J* = 4.7, 4.2 Hz, 4H), 3.20 – 3.18 (m, 2H). ^{13}C NMR (101 MHz, Deuterium Oxide) δ 174.88, 98.67, 74.60, 73.28, 69.86, 67.51, 66.46, 66.37, 66.26, 39.18. HRMS m/z calculated for $C_{10}H_{27}NO_{14}S_2^{2-}$: 219.5051 found: 219.5048.

3.5.2.2 Synthesis of Iduronic Acid Disaccharide Precursor

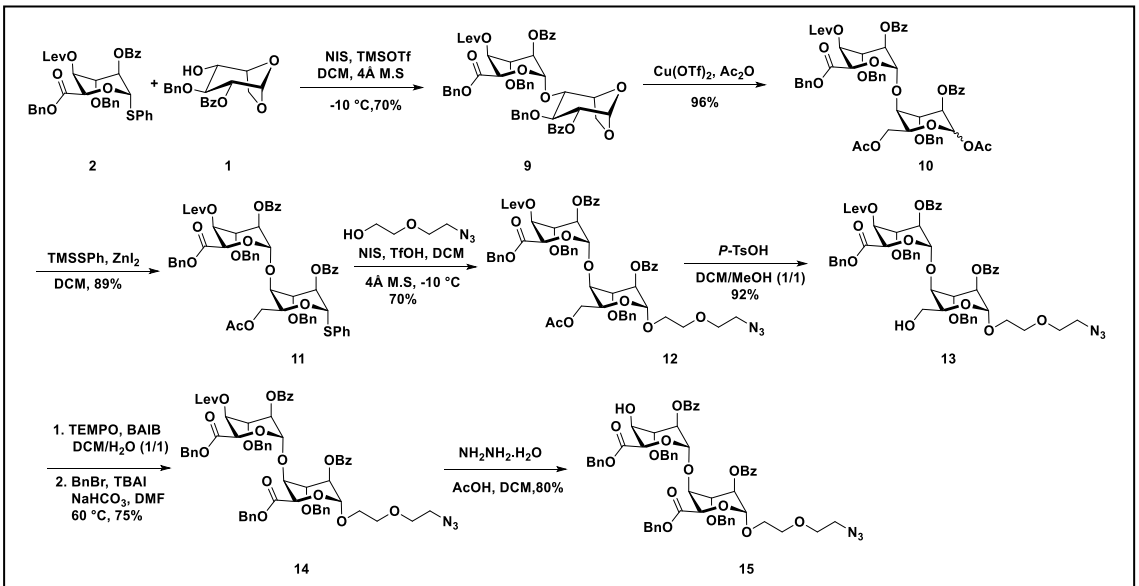

Scheme 2. Synthesis of Disaccharides Building Block.

Benzyl (2-O-benzoyl-3-O-benzyl-4-O-levulinoyl)-α-L-idopyranosyluronate)-α(1→4) 2-O-benzoyl-3-O-benzyl-1,6-anhydro-β-L-idopyranose 9

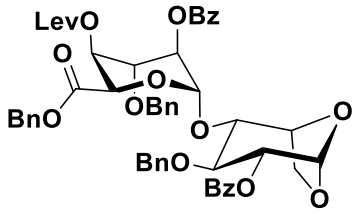

Compound **2** (6.2 g, 9.28 mmol), Compound **1** (3.63 g, 10.21 mmol) and freshly dried 4 Å molecular sieves were dissolved in dry DCM (70 mL) and stirring at RT for 1 h. Then the reaction mixture was cooled to -10 °C and *N*-Iodosuccinimide (3.13 g, 13.92 mmol), TMSOTf (0.35 mL, 1.85 mmol) were added and monitored the reaction by using TLC. After the completion of reaction, quenched with triethylamine and diluted with DCM. The molecular sieves were filtered using celite and organic layer was washed with $Na_2S_2O_3$, followed by $NaHCO_3$, brine solution and dried over Na_2SO_4, then filtered and concentrated under reduced pressure. The residue was purified by column chromatography (EtOAc/Hexane = 1/4) to afford **9 (5.9 g, 70%)** as syrup. ^{1}H NMR (400 MHz, Chloroform-*d*) δ 8.05 – 7.98 (m, 4H), 7.60 – 7.55 (m, 2H), 7.45 – 7.41 (m, 6H), 7.38 – 7.26 (m, 8H), 7.04 – 6.98 (m, 5H), 5.53 (d, *J* = 1.8 Hz, 1H), 5.31 (s, 1H), 5.22 (d, *J* = 11.9 Hz, 2H), 5.12 (dt, *J* = 2.5, 1.1 Hz, 1H), 5.10 (d, *J* = 2.3 Hz, 1H), 5.04 (dd, *J* = 8.3, 1.8 Hz, 1H), 4.83 – 4.76 (m, 3H), 4.64 (t, *J* = 4.5 Hz, 1H), 4.52 (d, *J* = 10.9 Hz, 1H), 4.44 (d, *J* = 10.9 Hz, 1H), 4.25 (dd, *J* = 8.5, 4.0 Hz, 1H), 4.20 (d, *J* = 7.8 Hz, 1H), 3.94 – 3.93 (m, 1H), 3.89 (t, *J* = 8.4 Hz, 1H), 3.78 (dd, *J* = 7.4, 5.4 Hz, 1H), 2.52 – 2.39 (m, 2H), 2.35 – 2.27 (m, 1H), 2.21 – 2.09 (m, 1H), 2.05 (s, 3H). ^{13}C NMR (101 MHz, Chloroform-*d*) δ 205.87, 171.64, 167.88, 165.72, 165.45, 137.66, 137.28, 135.39, 133.83, 133.42, 129.90, 129.48, 129.16, 128.80, 128.59, 128.50, 128.43, 128.25, 128.20, 127.89, 127.52, 99.45, 95.35, 78.14, 75.08, 74.09, 72.96, 72.71, 71.92, 67.92, 67.10, 66.98, 66.15, 65.59, 37.68, 29.69, 27.77. HRMS m/z calculated for $C_{52}H_{50}O_{15}Na$:937.3047; found: 937.3042.

Benzyl (2-O-benzoyl-3-O-benzyl-4-O-levulinoyl))-α-L-idopyranosyluronate-α(1→4) 1,6-O-diacetyl-2-O-benzoyl-3-O-benzyl-α/β-L-idopyranoside 10

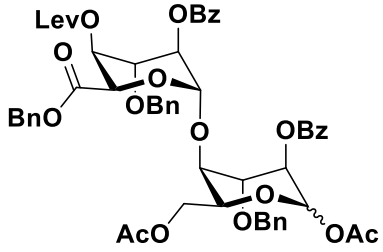

Compound **9** (5.6 g, 6.12 mmol) and copper trifluromethanesulfonate (0.02 g, 0.61 mmol) were dissolved in acetic anhydride (56 mL) at 0 °C. The temperature of the reaction mixture was slowly increased to RT and stirred for another 16 h. Then,

EtOAc (50 mL) was added and organic layer was washed with $NaHCO_3$ and brine solution, dried over Na_2SO_4 and concentrated under reduced pressure. The residue was purified by flash column chromatography (EtOAc/Hexane = 1/4) to afford anomeric mixture **10** (**5.9 g, 96%, α:β = 1:1)** as syrup. ^{1}H NMR (400 MHz, Chloroform-*d*) δ 7.97 (ddd, *J* = 9.7, 7.7, 1.3 Hz, 6H), 7.86 (dd, *J* = 8.2, 1.1 Hz, 2H), 7.55 – 7.50 (m, 2H), 7.45 – 7.43 (m, 1H), 7.41 – 7.36 (m, 7H), 7.32 – 7.24 (m, 18H), 7.23 – 7.14 (m, 16H), 6.16 – 6.15 (m, 2H), 5.29 (dd, *J* = 4.5, 2.2 Hz, 1H), 5.26 – 5.19 (m, 3H), 5.16 – 5.11 (m, 3H), 5.07 (t, *J* = 2.9 Hz, 1H), 4.98 (t, *J* = 3.3 Hz, 1H), 4.92 (t, *J* = 3.2 Hz, 1H), 4.87 (d, *J* = 3.1 Hz, 1H), 4.84 – 4.78 (m, 3H), 4.76 – 4.71 (m, 2H), 4.69 (d, *J* = 2.0 Hz, 1H), 4.64 – 4.56 (m, 5H), 4.48 (td, *J* = 6.7, 2.2 Hz, 1H), 4.40 – 4.28 (m, 5H), 4.19 (t, *J* = 4.4 Hz, 1H), 4.06 (t, *J* = 2.7 Hz, 1H), 3.91 (q, *J* = 4.3, 3.3 Hz, 2H), 3.82 (t, *J* = 3.2 Hz, 1H), 3.79 (t, *J* = 3.4 Hz, 1H), 2.45 – 2.38 (m, 4H), 2.35 – 2.21 (m, 2H), 2.13 – 2.07 (m, 2H), 2.05 (s, 3H), 2.01 (s, 6H), 2.00 (s, 6H). ^{13}C NMR (101 MHz, CHLOROFORM-*D*) δ 205.82, 205.78, 171.44, 171.40, 170.67, 170.60, 169.08, 168.95, 167.96, 167.85, 165.91, 165.49, 165.18, 165.16, 137.82, 137.39, 137.19, 137.15, 135.19, 135.16, 133.64, 133.52, 133.41, 130.09, 129.89, 129.30, 129.26, 128.86, 128.80, 128.64, 128.61, 128.56, 128.53, 128.48, 128.42, 128.40, 128.17, 128.12, 127.99, 127.95, 127.91, 127.80, 127.63, 101.16, 100.12, 91.63, 90.63, 75.74, 75.31, 74.94, 74.21, 73.75, 73.62, 73.24, 72.78, 72.70, 68.41, 68.32, 67.81, 67.75, 67.32, 67.21, 67.18, 66.93, 66.78, 62.72, 62.15, 37.63, 29.71, 27.68, 21.08, 21.02, 20.88, 20.87.HRMS m/z calculated for $C_{56}H_{56}O_{18}Na$:1039.3364; found: 1039.3359.

Benzyl (2-O-benzoyl-3-O-benzyl-4-O-levulinoyl)-α-L-idopyranosyluronate-α(1→4) 1-thiophenyl-(6-O-acetyl-2-O-benzoyl-3-O-benzyl)-α-L-idopyranoside 11

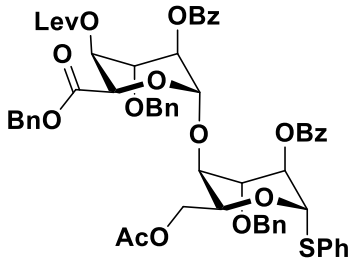

Compound **10** (5.7 g, 5.61 mmol), ZnI_2 (3.76 g, 11.78 mmol) and trimethyl(phenylthio)-silane (3.29 mL, 17.39mmol) were dissolved in dry DCM (80 mL) under the nitrogen atmosphere and stirred at room temperature for 16 h. The reaction mixture was filtered through celite and diluted with 4N HCl, Dioxane, and water [1/1/1 (v/v/v), 40mL] mixture and stirred for 20 min. The organic layer was separated, washed with saturated $NaHCO_3$ and brine solution, dried over Na_2SO_4 and concentrated under reduced pressure. The residue was purified by flash column chromatography (EtOAc/Hexane = 1/1) to afford **11 (5.3 g, 89%)** as solid. ^{1}H NMR (400 MHz,

Chloroform-*d*) δ 8.03 (d, *J* = 7.4 Hz, 2H), 7.96 (d, *J* = 7.3 Hz, 2H), 7.59 – 7.56 (m, 3H), 7.45 – 7.41 (m, 5H), 7.36 – 7.30 (m, 9H), 7.29 – 7.21 (m, 9H), 5.55 (s, 1H), 5.47 (s, 1H), 5.28 (d, *J* = 3.3 Hz, 1H), 5.18 (d, *J* = 12.0 Hz, 1H), 5.15 (t, *J* = 3.4 Hz, 1H), 4.99 (t, *J* = 3.7 Hz, 1H), 4.95 (td, *J* = 6.6, 1.9 Hz, 1H), 4.89 (d, *J* = 12.0 Hz, 1H), 4.86 – 4.82 (m, 2H), 4.75 (d, *J* = 11.5 Hz, 1H), 4.65 (d, *J* = 5.2 Hz, 1H), 4.62 (d, *J* = 5.2 Hz, 1H), 4.42 – 4.34 (m, 2H), 4.13 (t, *J* = 2.4 Hz, 1H), 3.92 (s, 1H), 3.86 (t, *J* = 3.7 Hz, 1H), 2.53 – 2.39 (m, 2H), 2.36 – 2.28 (m, 1H), 2.23 – 2.21 (m, 1H), 2.07 (s, 3H), 2.02 (s, 3H). ^{13}C NMR (101 MHz, Chloroform-*d*) δ 205.84, 171.43, 170.61, 168.01, 165.74, 165.21, 137.61, 137.23, 135.88, 135.20, 133.64, 133.43, 131.86, 130.09, 129.94, 129.34, 129.28, 129.00, 128.85, 128.69, 128.59, 128.48, 128.18, 128.04, 127.89, 127.59, 101.17, 86.08, 76.35, 74.15, 73.74, 73.09, 72.81, 69.20, 68.65, 67.99, 67.23, 65.93, 62.72, 37.67, 29.76, 27.72, 20.91. HRMS m/z calculated for $C_{60}H_{58}O_{16}SNa$:1089.3343; found: 1089.3338.

Ethoxy-2-azidoethoxyl-O-(benzyl (2-O-benzoyl-3-O-benzyl-4-O-levulinoyl)-α-L-idopyranosyluronate-α(1→4) (6-O-acetyl-2-O-benzoyl-3-O-benzyl))-α-L-idopyranoside 12

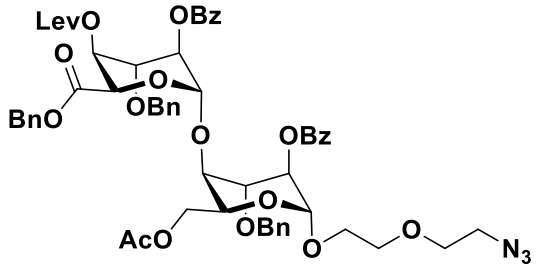

Compound **11** (5.1 g, 4.78 mmol), 2-(2-azidoethoxy)ethan-1-ol (0.75 g, 5.74 mmol) and freshly dried 4 Å molecular sieves were dissolved in dry DCM (50 mL) and stirred at RT for 1 h. Then *N*-iodosuccinimide (1.61 g, 7.17 mmol), TfOH (0.085 mL, 0.956 mmol) were added at -10°C and stirred for 30 min. After the completion of reaction, the reaction mixture was quenched with triethylamine and filtered through celite. The organic layer was washed with $Na_2S_2O_3$ followed by $NaHCO_3$, brine solution and dried over Na_2SO_4, then filtered and concentrated under reduced pressure. The residue was purified by column chromatography (EtOAc/Hexane = 1/4) to afford **12 (3.7 g, 70%)** as syrup. ^{1}H NMR (400 MHz, Chloroform-*d*) δ 8.04 – 8.04 (m, 2H), 7.97 – 7.94 (m, 2H), 7.61 – 7.57 (m, 1H), 7.47 – 7.42 (m, 5H), 7.35 – 7.28 (m, 9H), 7.37 – 7.22 (m, 6H), 5.29 (q, *J* = 3.1, 2.2 Hz, 2H), 5.21 – 5.17 (m, 2H), 5.03 (t, *J* = 3.3 Hz, 1H), 5.00 – 4.99 (m, 1H), 4.92 (d, *J* = 2.9 Hz, 1H), 4.83 (d, *J* = 11.7 Hz, 2H), 4.76 (d, *J* = 11.4 Hz, 1H), 4.69 (d, *J* = 11.4 Hz, 1H), 4.60 (d, *J* = 11.3 Hz, 1H), 4.50 (td, *J* = 6.5, 2.4 Hz, 1H), 4.44 – 4.35 (m, 2H), 4.06 (t, *J* = 3.1 Hz, 1H), 3.96 – 3.90

(m, 3H), 3.74 – 3.64 (m, 4H), 3.59 (ddd, *J* = 10.4, 5.9, 4.1 Hz, 1H), 3.25 – 3.15 (m, 2H), 2.54 – 2.40 (m, 2H), 2.34 (ddd, *J* = 17.2, 7.6, 6.2 Hz, 1H), 2.16 (dt, *J* = 17.2, 6.5 Hz, 1H), 2.07 (s, 3H), 2.07 (s, 3H). ^{13}C NMR (101 MHz, CHLOROFORM-*D*) δ 205.82, 171.47, 170.67, 167.89, 165.66, 165.21, 138.01, 137.24, 135.20, 133.62, 133.34, 130.00, 129.90, 129.34, 129.24, 128.77, 128.59, 128.54, 128.48, 128.37, 128.28, 128.21, 128.03, 127.84, 127.67, 100.91, 98.41, 76.21, 75.01, 73.28, 72.79, 72.74, 70.38, 70.23, 68.38, 68.21, 67.86, 67.27, 67.13, 65.15, 62.63, 50.80, 37.64, 29.71, 27.71, 20.91. HRMS m/z calculated for $C_{56}H_{61}O_{18}N_3Na$:1111.3848; found: 1111.3845.

Ethoxy-2-azidoethoxyl-O-(benzyl (2-O-benzoyl-3-O-benzyl-4-O-levulinoyl)-α-L-idopyranosyl uronate-α(1→4)(2-O-benzoyl-3-O-benzyl-))-α-L-idopyroside 13

Compound **12** (3.5 g, 3.21 mmol) and *p*-toluenesulfonicacid (1.66 g, 9.65 mmol) was dissolved in equal ratio of mixture of dry DCM (25 mL) and methanol (25 mL) and stirred at RT for 3 days. The reaction mixture was quenched with triethylamine. Solvents were evaporated under reduced pressure, extracted with EtOAc and $NaHCO_3$ and water respectively. The combined organic layer washed with brine solution, dried over Na_2SO_4 and concentrated under reduced pressure. The residue was purified by column chromatography (EtOAc/Hexane = 1/3) to afford **13 (3.2 g, 92%)** as syrup. ^{1}H NMR (400 MHz, Chloroform-*d*) δ 8.01 (dd, *J* = 8.2, 1.3 Hz, 2H), 7.92 (dd, *J* = 8.3, 1.1 Hz, 2H), 7.56 (tt, *J* = 7.0, 1.3 Hz, 1H), 7.43 – 7.38 (m, 5H), 7.32 – 7.24 (m, 8H), 7.23 – 7.18 (m, 7H), 5.26 – 5.25 (m, 2H), 5.15 – 5.12 (m, 2H), 5.01 (t, *J* = 3.0 Hz, 1H), 4.99 – 4.98 (m, 2H), 4.89 (d, *J* = 2.6 Hz, 1H), 4.79 (d, *J* = 5.0 Hz, 1H), 4.76 (d, *J* = 4.4 Hz, 1H), 4.72 – 4.65 (m, 2H), 4.58 (d, *J* = 11.3 Hz, 1H), 4.37 (td, *J* = 6.3, 2.4 Hz, 1H), 4.02 (t, *J* = 3.2 Hz, 1H), 3.98 – 3.97 (m, 1H), 3.89 (ddd, *J* = 12.7, 5.9, 3.7 Hz, 4H), 3.70 – 3.64 (m, 3H), 3.63 – 3.54 (m, 2H), 3.23 – 3.13 (m, 2H), 2.53 – 2.30 (m, 4H), 2.18 – 2.09 (m, 1H), 2.05 (s, 3H). ^{13}C NMR (101 MHz, CHLOROFORM-*D*) δ 205.96, 171.58, 167.88, 165.70, 165.67, 138.12, 137.15, 135.26, 133.81, 133.35, 130.03, 129.97, 129.34, 129.24, 128.82, 128.63, 128.57, 128.52, 128.40, 128.33, 128.29, 128.18, 127.79, 127.63, 100.85, 98.63, 75.37, 73.11, 72.86, 72.70, 70.48, 70.35, 68.83, 68.18, 67.91, 67.83, 67.43, 67.16, 67.01, 61.76, 50.86, 37.68, 29.78, 27.76. HRMS m/z calculated for $C_{56}H_{59}O_{17}N_3Na$:1068.3742; found: 1068.3739.

Ethoxy-2-azidoethoxyl-O-(benzyl (2-O-benzoyl-3-O-benzyl-4-O-levulinoyl)-α-L-idopyranosyluronate-α(1→4) benzyl (2-O-benzoyl-3-O-benzyl))-α-L-idopyranosideuronate 14

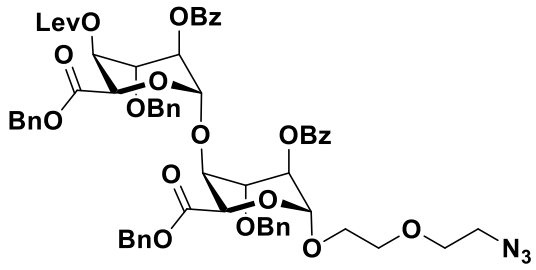

Compound **13** (3.4 g, 3.25 mmol) and [Bis(acetoxy)iodo]benzene (BAIB, 2.62 g, 8.12 mmol) were dissolved in mixture of water and DCM [1/1 (v/v), 60mL]. After 15 mins, 2,2,6,6-tetramethyl-1-piperidinyloxyl free radical (TEMPO, 0.10 g, 0.65 mmol) was added at room temperature and stirred at RT for 6 h. The organic layer was washed with saturated $NH_4Cl_{(aq)}$, dried over Na_2SO_4, filtered, and concentrated under reduced pressure. The dried crude compound (3.18 g, 3.01 mmol) was dissolved in dry DMF (15 mL), benzyl bromide (0.89 mL, 7.50 mmol), tetrabutylammonium iodide (TBAI, 2.22 g, 6.03 mmol), $NaHCO_3$(0.38 g, 4.50 mmol) were added. The reaction mixture was heated at 60°C for 4 h. Then organic layer was washed with brine solution (3x10mL), dried over Na_2SO_4, filtered, and concentrated under reduced pressure. The residue was purified by flash column chromatography (EtOAc/Hexane = 1/4) to afford **14 (2.8 g, 75%)** as syrup. ^{1}H NMR (400 MHz, Chloroform-*d*) δ 8.00 (dd, *J* = 8.2, 1.3 Hz, 2H), 7.87 (dd, *J* = 8.3, 1.1 Hz, 2H), 7.58 – 7.54 (m, 1H), 7.45 – 7.36 (m, 5H), 7.32 – 7.22 (m, 12H), 7.21 – 7.13 (m, 8H), 5.29 – 5.26 (m, 1H), 5.24 – 5.23 (m, 2H), 5.20 (d, *J* = 2.7 Hz, 1H), 5.17 (d, *J* = 12.2 Hz, 1H), 5.11 (d, *J* = 12.0 Hz, 2H), 4.97 (d, *J* = 3.2 Hz, 1H), 4.94 (t, *J* = 2.4 Hz, 1H), 4.90 (d, *J* = 2.3 Hz, 1H), 4.77 (d, *J* = 11.1 Hz, 1H), 4.71 (d, *J* = 2.8 Hz, 1H), 4.68 (d, *J* = 3.7 Hz, 1H), 4.58 (d, *J* = 11.1 Hz, 1H), 4.52 (d, *J* = 11.3 Hz, 1H), 4.26 (t, *J* = 3.6 Hz, 1H), 4.01 (t, *J* = 3.4 Hz, 1H), 3.98 – 3.93 (m, 1H), 3.82 (t, *J* = 2.5 Hz, 1H), 3.71 – 3.63 (m, 3H), 3.58 – 3.48 (m, 2H), 3.11 (td, *J* = 5.0, 4.5, 1.2 Hz, 2H), 2.37 (t, *J* = 6.8 Hz, 2H), 2.24 – 2.16 (m, 1H), 2.08 (dt, *J* = 17.1, 6.5 Hz, 1H), 2.00 (s, 3H). ^{13}C NMR (101 MHz, CHLOROFORM-*D*) δ 205.80, 171.43, 169.24, 167.65, 165.61, 164.92, 137.81, 137.13, 135.20, 135.17, 133.66, 133.39, 130.02, 129.97, 129.34, 128.99, 128.71, 128.61, 128.57, 128.55, 128.50, 128.46, 128.42, 128.34, 128.28, 128.08, 127.86, 127.69, 101.38, 98.91, 75.67, 72.93, 72.45, 72.31, 70.25, 70.20, 68.70, 68.57, 68.54, 68.28, 67.28, 67.11, 66.50, 66.41, 50.74, 37.65, 29.67, 27.71. HRMS m/z calculated for $C_{63}H_{63}O_{18}N_3Na$:1172.4004; found: 1172.3998.

Ethoxy-2-azidoethoxyl-O-(benzyl (2-O-benzoyl-3-O-benzyl)-α-L-idopyranosyluronate-α(1→4)benzyl(2-O-benzoyl-3-O-benzyl))-α-L-idopyranosideuronate 15

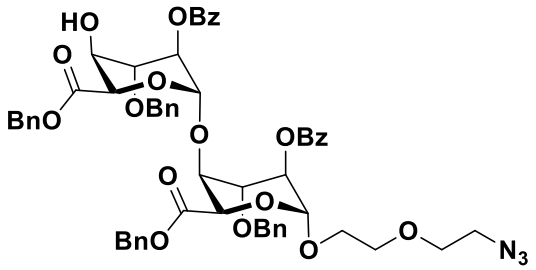

Compound **14** (2.5 g, 2.36 mmol) was dissolved in a mixture of dry DCM/MeOH (4/1, 30 mL) and hydrazinehydrate (0.57 mL, 11.80 mmol), acetic acid (2.70 mL, 47.21 mmol) was added, under nitrogen atmosphere. Allow the reaction flask stirred for another 4 h. After completion of reaction, quench with 5 mL of acetone, solvents were evaporated under reduced pressure. The residue was purified by flash column chromatography (EtOAc/Hexane = 1/1) to afford compound **15 (1.9 g, 80%)** as syrup. ^{1}H NMR (400 MHz, Chloroform-*d*) δ 8.03 (ddd, *J* = 11.1, 8.3, 1.4 Hz, 4H), 7.71 – 7.66 (m, 1H), 7.55 – 7.48 (m, 5H), 7.42 – 7.33 (m, 12H), 7.32 – 7.26 (m, 6H), 7.24 – 7.71 (m, 2H), 5.40 (d, *J* = 12.2 Hz, 1H), 5.33 (t, *J* = 2.8 Hz, 1H), 5.29 – 5.25 (m, 4H), 5.23 (d, *J* = 12.3 Hz, 1H), 5.06 (d, *J* = 3.1 Hz, 1H), 4.96 (d, *J* = 1.7 Hz, 1H), 4.89 (dd, *J* = 11.8, 6.9 Hz, 2H), 4.78 (d, *J* = 11.3 Hz, 1H), 4.62 (dd, *J* = 24.6, 11.3 Hz, 2H), 4.32 (t, *J* = 3.5 Hz, 1H), 4.09 – 4.03 (m, 2H), 3.94 – 3.88 (m, 2H), 3.82 – 3.73 (m, 3H), 3.69 – 3.59 (m, 2H), 3.23 (td, *J* = 5.0, 4.3, 1.3 Hz, 2H), 2.71 (d, *J* = 10.3 Hz, 1H). ^{13}C NMR (101 MHz, Chloroform-*d*) δ 169.24, 168.86, 165.72, 164.80, 137.82, 137.23, 135.27, 135.22, 133.84, 133.37, 130.17, 129.96, 129.12, 129.08, 128.80, 128.73, 128.67, 128.64, 128.62, 128.55, 128.52, 128.42, 128.35, 128.33, 128.20, 127.91, 127.77, 101.77, 98.97, 75.64, 74.39, 72.87, 72.20, 70.29, 70.25, 68.65, 68.59, 68.50, 68.43, 67.38, 67.05, 50.80. HRMS m/z calculated for $C_{58}H_{57}O_{16}N_3Na$:1074.3637; found: 1074.3629.

3.5.2.3 Synthesis of Sulfated Disaccharide Analogues (I-20, I-21 and I-23)

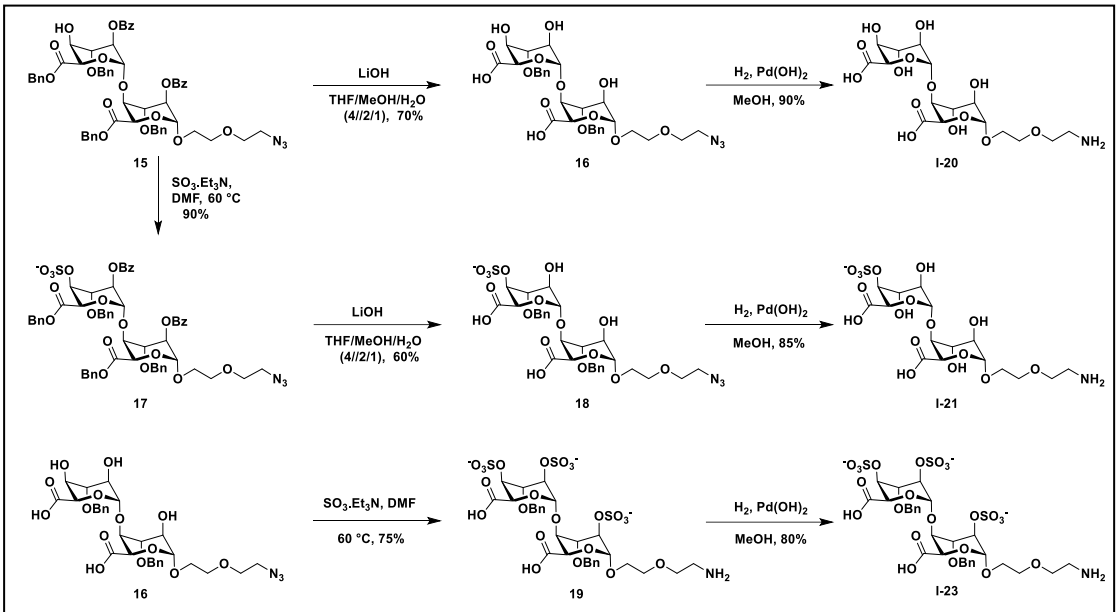

Scheme 3. Synthesis of Disaccharide Sulfated Compounds.

Ethoxy-2-azidoethoxyl-O-((3-O-benzyl)-L-idopyranosyl uronic acid-α(1→4)(3-O-benzyl))-α-L-idopyranoside uronic acid 16

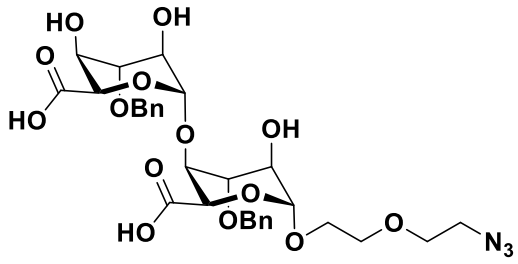

Esters deprotection: Followed general procedure for deprotection of esters which yielded compound **16 (70%).** ^{1}H NMR (400 MHz, Methanol-d_4) δ 7.47 – 7.24 (m, 10H), 5.05 (d, J = 1.9 Hz, 1H), 4.94 – 4.93 (m, 1H), 4.86 (d, J = 2.2 Hz, 1H), 4.83 (d, J = 1.7 Hz, 1H), 4.66 – 4.58 (m, 4H), 4.29 – 4.28 (m, 1H), 4. (p, J = 1.8 Hz, 2H), 3.94 – 3.88 (m, 1H), 3.77 (t, J = 3.4 Hz, 1H), 3.73 (dt, J = 2.7, 1.3 Hz, 1H), 3.71 – 3.56 (m, 7H), 3.25 (t, J = 4.9 Hz, 2H). ^{13}C NMR (101 MHz, Methanol-d_4) δ 173.17, 173.01, 139.35, 138.89, 129.53, 129.51, 129.39, 129.02, 128.75, 104.09, 102.87, 76.69, 76.58, 76.10, 73.26, 73.17, 71.28, 71.24, 69.62, 69.37, 69.15, 68.59, 68.57, 67.19, 51.80. HRMS m/z calculated for $C_{30}H_{37}N_3O_{14}Na$: 686.2173 found: 686.2189.

Ethoxy-2-azidoethoxyl-O-(benzyl (2-O-benzoyl-3-O-benzyl-4-O-sulfonato)-L-idopyranosyluronate-α(1→4)benzyl (2-O-benzoyl-3-O-benzyl))-α-L-idopyranosideuronate 17

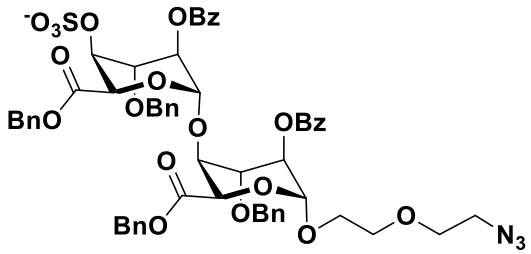

***O*-Sulfation:** Followed general procedure for sulfation yielded compound **17 (90%)**. ^{1}H NMR (400 MHz, Methanol-d_4) δ 8.14 (dd, *J* = 8.4, 1.3 Hz, 2H), 7.88 (dd, *J* = 8.4, 1.2 Hz, 2H), 7.62 – 7.57 (m, 1H), 7.49 – 7.45 (m, 2H), 7.42 – 7.33 (m, 5H), 7.27 – 7.15 (m, 18H), 5.24 (d, *J* = 12.1 Hz, 1H), 5.19 (d, *J* = 1.8 Hz, 2H), 5.17 (d, *J* = 2.9 Hz, 1H), 5.11 – 5.06 (m, 3H), 5.00 (d, *J* = 3.3 Hz, 1H), 4.95 (d, *J* = 12.2 Hz, 1H), 4.90 (d, *J* = 2.8 Hz, 1H), 4.74 (d, *J* = 11.0 Hz, 1H), 4.66 (t, d, *J* = 3.3 Hz, 1H), 4.64 (d, *J* = 11.1 Hz, 1H), 4.58 (s, 2H), 4.56 – 4.47 (m, 2H), 4.38 (dt, *J* = 3.9, 2.0 Hz, 1H), 4.19 (t, *J* = 3.6 Hz, 1H), 3.99 (t, *J* = 3.6 Hz, 1H), 3.89 (ddd, *J* = 10.4, 5.5, 3.2 Hz, 1H), 3.70 – 3.64 (m, 1H), 3.63 – 3.60 (m, 2H), 3.57 – 3.46 (m, 2H), 3.11 (t, *J* = 5.0 Hz, 2H). ^{13}C NMR (101 MHz, Methanol-d_4) δ 170.85, 169.99, 166.98, 166.97, 139.02, 138.92, 136.80, 136.69, 134.37, 134.35, 131.41, 130.99, 130.95, 130.27, 129.76, 129.68, 129.60, 129.51, 129.46, 129.43, 129.30, 129.25, 129.12, 129.08, 128.81, 128.72, 102.17, 99.96, 77.50, 76.81, 75.13, 74.07, 73.67, 73.58, 71.19, 71.12, 70.35, 69.88, 69.57, 69.54, 69.02, 68.38, 51.70. HRMS m/z calculated for $C_{58}H_{56}N_3O_{19}S^-$: 1130.3234 found (M-H): 1129.3237.

Ethoxy-2-azidoethoxyl-O-((3-O-benzyl-4-O-sulfonato)-L-idopyranosyl uronic acid-α(1→4)(3-O-benzyl))-α-L-idopyranoside uronic acid 18

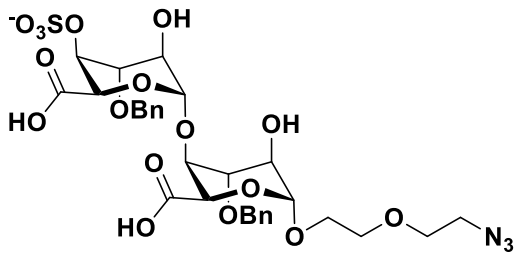

Esters deprotection: Followed general procedure for deprotection of esters yielded compound **18 (60%).** ^{1}H NMR (400 MHz, Methanol-d_4) δ 7.46 – 7.22 (m, 10H), 5.07 (s, 1H), 4.90 (s, 1H), 4.76 (d, *J* = 12.2 Hz, 2H), 4.63 (t, *J* = 13.9 Hz, 4H), 4.44 (s, 1H), 4.17 (s, 1H), 3.90 – 3.87 (m, 1H), 3.77 (s, 1H), 3.711 – 3.55 (m, 7H), 3.17 (t, *J* = 4.2 Hz, 2H). ^{13}C NMR (101 MHz, Methanol-d_4) δ 176.72, 170.27, 139.66, 138.82, 129.66, 129.45, 129.27, 128.96, 128.86, 128.54, 103.28, 102.98, 77.31, 76.36, 75.05, 73.28, 72.89, 72.85, 71.32, 71.23, 69.60, 69.14, 68.74, 68.07, 67.32, 51.72. HRMS m/z calculated for $C_{30}H_{36}N_3O_{17}S^-$: 742.1771 found: 742.1767.

Ethoxy-2-aminoethoxyl-O-(α-L-idopyranosyl uronicacid-α(1→4))-α-L-idopyranosyl uronicacid I-20

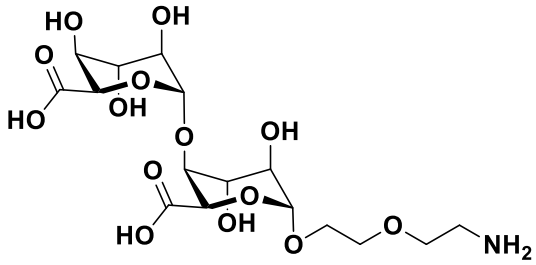

Hydrogenolysis: Followed general procedure for hydrogenolysis yielded compound **I-20 (90%)**. ^{1}H NMR (400 MHz, Deuterium Oxide) δ 4.95 (d, J = 3.0 Hz, 1H), 4.89 (d, J = 3.4 Hz, 1H), 4.57 (d, J = 3.2 Hz, 1H), 4.55 (d, J = 2.7 Hz, 1H), 4.10 – 4.09 (m, 1H), 3.96 – 3.90 (m, 3H), 3.83 – 3.75 (m, 6H), 3.63 – 3.60 (m, 2H), 3.23 – 3.20 (m, 2H). ^{13}C NMR (101 MHz, Deuterium Oxide) δ 176.14, 175.60, 102.36, 101.09, 78.52, 70.55, 70.40, 70.04, 69.86, 69.80, 69.29, 69.13, 68.82, 67.50, 66.29, 39.08. HRMS m/z calculated for $C_{16}H_{27}NO_{14}Na$: 480.1329 found: 480.1327.

Ethoxy-2-aminoethoxyl-O-((4-O-sulfonato)-α-L-idopyranosyl uronic acid-α(1→4))-α-L-idopyranoside uronic acid I-21

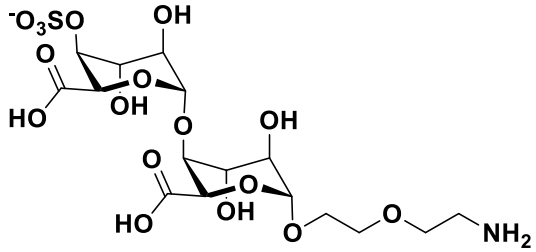

Hydrogenolysis: Followed general procedure for hydrogenolysis yielded compound **I-21 (90%).** ^{1}H NMR (400 MHz, Deuterium Oxide) δ 4.87 (dd, *J* = 4.4, 2.7 Hz, 2H), 4.66 (d, *J* = 2.4 Hz, 1H), 4.52 (t, *J* = 3.1 Hz, 1H), 4.47 (d, *J* = 2.7 Hz, 1H), 4.20 (t, *J* = 3.8 Hz, 1H), 4.01 (dd, *J* = 4.2, 2.8 Hz, 1H), 3.87 – 3.81 (m, 2H), 3.74 – 3.66 (m, 6H), 3.59 (ddd, *J* = 4.2, 2.3, 1.0 Hz, 1H), 3.53 (dd, *J* = 5.3, 3.0 Hz, 1H), 3.14 – 3.12 (m, 1H). ^{13}C NMR (101 MHz, D_2O) δ 175.54, 174.70, 102.20, 101.13, 78.41, 76.12, 69.80, 69.12, 68.88, 68.30, 68.06, 67.92, 67.49, 66.30, 39.09. HRMS m/z calculated for $C_{16}H_{26}NO_{17}S^-$: 536.0927 found (M-H): 535.0917.

Ethoxy-2-azidoethoxy-O-((2,4-O-disulfonato-3-O-benzyl)-α-L-idopyranosyl uronic acid-α(1→4)(2-O-sulfonato-3-O-benzyl))-α-L-idopyranoside uronic acid 19

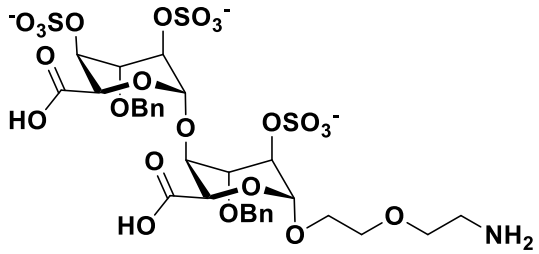

***O*-Sulfation:** Followed general procedure for sulfation yielded compound **19 (75%).** ^{1}H NMR (400 MHz, Deuterium Oxide) δ 7.41 – 7.27 (m, 10H), 5.06 (s, 1H), 5.03 (s, 1H), 4.73 (d, *J* = 13.0 Hz, 2H), 4.68 (d, *J* = 7.5 Hz, 1H), 4.61 (dd, *J* = 12.0, 7.2 Hz, 2H), 4.42 (d, *J* = 1.9 Hz, 1H), 4.26 – 4.25 (m, 1H), 4.23 – 4.18 (m, 3H), 3.83 (d, *J* = 2.6 Hz, 1H), 3.76 (ddd, *J* = 7.4, 5.3, 3.1 Hz, 1H), 3.66 – 3.51 (m, 6H), 3.27 – 3.25 (m, 2H). ^{13}C NMR (101 MHz, Deuterium Oxide) δ 175.18, 174.24, 137.15, 137.05, 128.68, 128.64, 128.56, 128.55, 128.30, 128.07, 100.61, 98.74, 75.90, 73.96, 72.88, 71.73, 71.56, 71.33, 71.27, 71.13, 69.41, 67.50, 67.25, 66.94, 50.15. HRMS m/z calculated for $C_{30}H_{34}N_3O_{23}S_3^{3-}$: 300.0254 found :300.0245.

Ethoxy-2-aminoethoxyl-O-((2,4-O-disulfonato)-α-L-idopyranosyl uronic acid-α(1→4)(2-sulfonato))-α-L-idopyroside uronic acid I-23

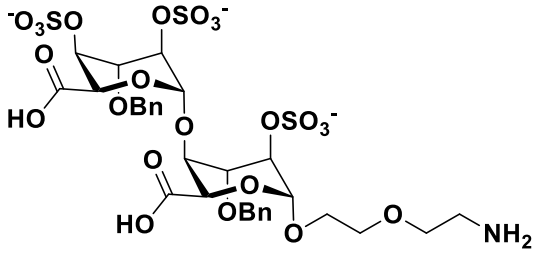

Hydrogenolysis: Followed general procedure for hydrogenolysis yielded compound **I-23 (80%).** ^{1}H NMR (600 MHz, Deuterium Oxide) δ 5.05 (s, 2H), 4.76 (s, 1H), 4.54 (s, 1H), 4.47 (s, 1H), 4.40 (s, 1H), 4.13 (s, 1H), 4.09 (s, 1H), 3.96 (d, *J* = 8.8 Hz, 2H), 3.78 – 3.70 (m, 3H), 3.65 – 3.62 (m, 3H), 3.09 (t, *J* = 5.1 Hz, 2H). ^{13}C NMR (151 MHz, D_2O) δ 174.96, 174.07, 100.74, 98.94, 77.93, 74.24, 74.03, 71.88, 69.80, 68.04, 67.61, 67.39, 66.21, 65.53, 39.07. HRMS m/z calculated for $C_{16}H_{24}NO_{24}S_3^{3-}$: 231.3306 found : 231.3313.

3.5.2.4 Synthesis of Iduronic Acid Trisaccharide Precursor

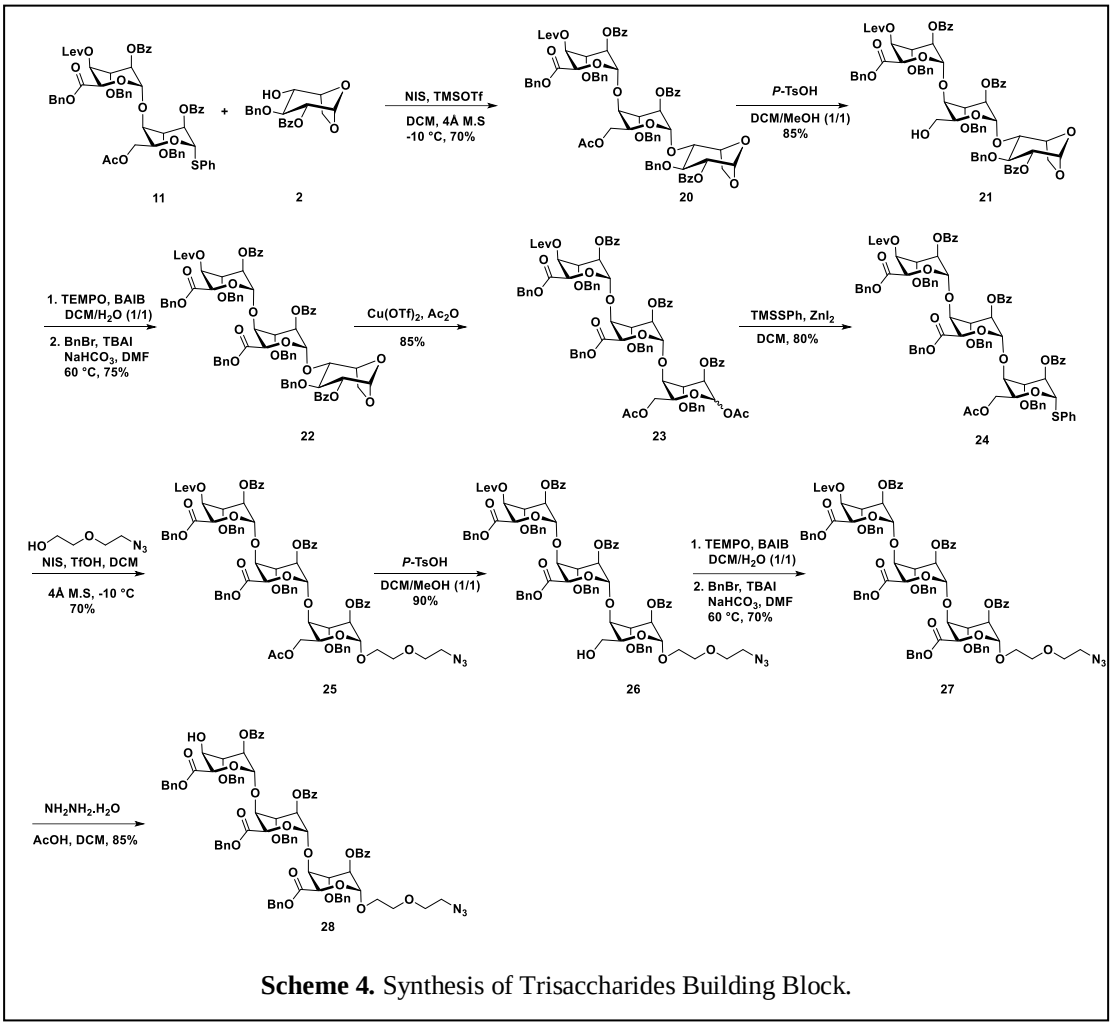

Scheme 4. Synthesis of Trisaccharides Building Block.

Benzyl (2-O-benzoyl-3-O-benzyl-4-O-levulinoyl)-α-L-idopyranosyl uronate-α(1→4)-(6-O-acetyl-2-O-benzoyl-3-O-benzyl)-α-L-idopyranosyl-α(1→4)(2-O-benzoyl-3-O-benzyl-1,6-anhydro)-β-L-idopyranose 20

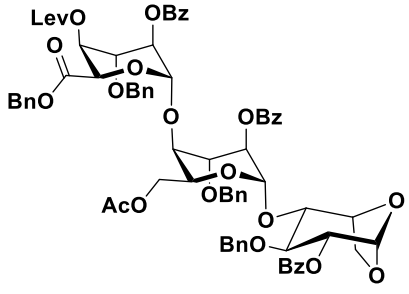

The synthetic procedure for the preparation of compound **9** was followed to obtain compound **20 (70%)** from compound **11** and **1** as syrup. ^{1}H NMR (400 MHz, Chloroform-*d*) δ 8.07 (dd, *J* = 8.4, 1.4 Hz, 2H), 7.96 (ddd, *J* = 8.5, 3.3, 1.4 Hz, 4H), 7.59 (dtt, *J* = 8.3, 6.9, 1.3 Hz, 2H), 7.50 – 7.41 (m, 8H), 7.34 – 7.30 (m, 7H), 7.29 – 7.24 (m, 7H), 7.12 – 7.05 (m, 5H), 5.53 (d, *J* = 1.8 Hz, 1H), 5.29 (d, *J* = 2.7 Hz, 1H), 5.23 – 5.18 (m, 3H), 5.10 (dd, *J* = 4.9, 2.5 Hz, 2H), 5.03 (dd, *J* = 8.3, 1.8 Hz, 1H), 4.97 (d, *J* = 2.9 Hz, 1H), 4.89 (d, *J* = 12.0 Hz, 1H), 4.83 (d, *J* = 11.4

Hz, 1H), 4.75 – 4.72 (m, 2H), 4.69 – 4.63 (m, 3H), 4.59 (td, *J* = 7.2, 6.5, 2.6 Hz, 1H), 4.53 (d, *J* = 11.4 Hz, 1H), 4.35 – 4.26 (m, 2H), 4.21 (ddd, *J* = 8.4, 4.1, 1.1 Hz, 1H), 4.16 (d, *J* = 7.7 Hz, 1H), 4.06 (t, *J* = 3.8 Hz, 1H), 3.98 (t, *J* = 3.3 Hz, 1H), 3.93 – 3.91 (m, 1H), 3.89 (d, *J* = 8.3 Hz, 1H), 3.68 (ddd, *J* = 7.9, 5.1, 1.1 Hz, 1H), 2.56 – 2.42 (m, 2H), 2.39 – 2.32 (m, 1H), 2.23 – 2.16 (m, 1H), 2.08 (s, 3H), 1.99 (s, 3H). ^{13}C NMR (101 MHz, $CDCl_3$) δ 205.79, 171.47, 170.68, 167.90, 165.84, 165.73, 165.20, 138.13, 137.61, 137.15, 135.18, 133.66, 133.55, 133.31, 129.92, 129.89, 129.50, 129.27, 128.99, 128.75, 128.60, 128.56, 128.51, 128.49, 128.47, 128.41, 128.39, 128.20, 128.08, 127.92, 127.90, 127.39, 100.44, 99.39, 95.56, 77.80, 76.67, 75.64, 75.17, 75.00, 74.84, 73.36, 73.33, 72.86, 72.02, 68.89, 68.33, 67.93, 67.33, 67.17, 65.89, 65.49, 62.14, 37.63, 29.69, 27.71, 20.88. HRMS m/z calculated for $C_{74}H_{72}O_{22}Na$:1335.4413; found: 1335.4413.

Benzyl (2-O-benzoyl-3-O-benzyl-4-O-levulinoyl)-α-L-idopyranosyl uronate-α(1→4) benzyl (2-O-benzoyl-3-O-benzyl)-α-L-idopyranosyl-α(1→4)(2-O-benzoyl-3-O-benzyl-1,6-anhydro)-β-L-idopyranose 21

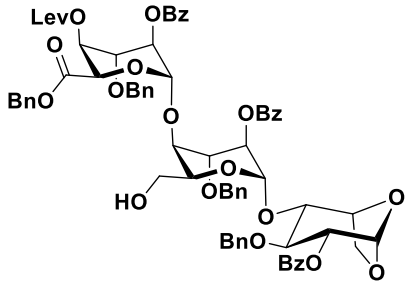

The synthetic procedure for the preparation of compound **13** was followed to obtain compound **21 (85%)** from compound **20** as syrup. ^{1}H NMR (400 MHz, Chloroform-*d*) δ 8.05 (ddd, *J* = 8.5, 5.8, 1.4 Hz, 4H), 7.95 (d,*J* = 7.4 Hz, 2H), 7.62 – 7.57 (m, 2H), 7.48 – 7.40 (m, 9H), 7.37 – 7.29 (m, 7H), 7.28 – 7.23 (m, 6H), 7.19 – 7.16 i(m, 3H), 7.10 (dd, *J* = 6.7, 3.0 Hz, 2H), 5.56 (d, *J* = 1.7 Hz, 1H), 5.27 (d, *J* = 2.4 Hz, 1H), 5.23 (t, *J* = 2.3 Hz, 1H), 5.19 (d, *J* = 12.1 Hz, 1H), 5.16 (t, *J* = 2.6 Hz, 1H), 5.08 (td, *J* = 7.7, 7.2, 2.5 Hz, 3H), 4.94 (d, *J* = 2.7 Hz, 1H), 4.88 (d, *J* = 12.0 Hz, 1H), 4.79 (dd, *J* = 13.6, 11.3 Hz, 2H), 4.71 (d, *J* = 1.7 Hz, 1H), 4.68 (d, *J* = 1.3 Hz, 1H), 4.62 (t, *J* = 4.6 Hz, 1H), 4.58 (d, *J* = 1.9 Hz, 2H), 4.36 (td, *J* = 6.4, 2.2 Hz, 1H), 4.24 (t, *J* = 4.2 Hz, 1H), 4.22 (s, 1H), 4.07 (t, *J* = 3.3 Hz, 1H), 3.94 (t, *J* = 8.4 Hz, 1H), 3.90 (t, *J* = 3.1 Hz, 2H), 3.78 – 3.75 (m, 1H), 3.65 (dt, *J* = 11.3, 5.5 Hz, 1H), 3.53 (dt, *J* = 11.9, 6.5 Hz, 1H), 2.55 – 2.41 (m, 2H), 2.37 – 2.29 (m, 1H), 2.24 – 2.12 (m, 1H), 2.08 (s, 3H). ^{13}C NMR (101 MHz, $CDCl_3$) δ 205.85, 171.46, 167.91, 165.88, 165.79, 165.34, 137.95, 137.91, 137.14, 135.22, 133.70, 133.52, 133.44, 129.97, 129.93, 129.92, 129.52, 129.31, 129.01, 128.74, 128.61, 128.56, 128.53, 128.51, 128.49, 128.47, 128.44, 128.35, 128.29, 128.24, 128.16, 128.11, 127.94, 127.85,

100.97, 99.43, 96.06, 78.43, 77.01, 76.16, 75.32, 75.18, 74.14, 73.16, 73.01, 72.84, 72.19, 68.64, 68.39, 67.82, 67.16, 67.12, 65.67, 61.40, 37.66, 29.71, 27.74. HRMS m/z calculated for $C_{72}H_{71}O_{21}Na$:1293.4307; found: 1293.4298.

Benzyl (2-O-benzoyl-3-O-benzyl-4-O-levulinoyl)-α-L-idopyranosyl uronate-α(1→4) benzyl (2-O-benzoyl-3-O-benzyl)-α-L-idopyranosyl uronate-α(1→4)(2-O-benzoyl-3-O-benzyl-1,6-anhydro)-β-L-idopyranose 22

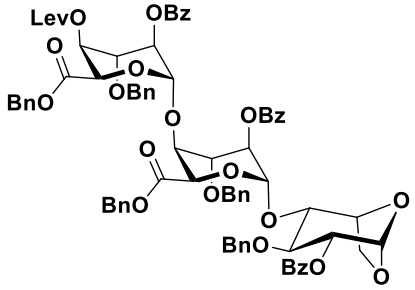

The synthetic procedure for the preparation of compound **14** was followed to obtain compound **22 (75%)** from compound **21** as solid. ^{1}H NMR (400 MHz, Chloroform-*d*) δ 8.02 (ddd, *J* = 15.0, 8.4, 1.5 Hz, 4H), 7.92 (dd, *J* = 7.5, 2.3 Hz, 2H), 7.63 – 7.57 (m, 2H), 7.49 – 7.41 (m, 7H), 7.35 – 7.31 (m, 5H), 7.28 – 7.17 (m, 15H), 7.08 (s, 5H), 5.52 (d, *J* = 1.7 Hz, 1H), 5.43 (d, *J* = 3.5 Hz, 1H), 5.31 – 5.30 (m, 1H), 5.23 (t, *J* = 4.0 Hz, 1H), 5.20 – 5.14 (m, 3H), 5.11 – 5.02 (m, 4H), 4.98 (d, *J* = 4.0 Hz, 1H), 4.82 (dd, *J* = 12.2, 1.4 Hz, 1H), 4.76 (d, *J* = 11.1 Hz, 1H), 4.70 – 4.62 (m, 4H), 4.59 – 4.53 (m, 2H), 4.32 (t, *J* = 4.5 Hz, 1H), 4.27 (dd, *J* = 8.4, 4.1 Hz, 1H), 4.10 – 4.65 (m, 2H), 3.92 – 3.86 (m, 2H), 3.53 (dd, *J* = 7.8, 5.2 Hz, 1H), 2.41 (t, *J* = 6.7 Hz, 2H), 2.27 – 2.09 (m, 2H), 2.04 (s, 3H). ^{13}C NMR (101 MHz, CHLOROFORM-*D*) δ 205.78, 171.41, 168.99, 167.72, 165.79, 165.54, 164.79, 137.87, 137.46, 137.04, 135.17, 134.98, 133.67, 133.62, 133.37, 129.95, 129.93, 129.87, 129.48, 129.29, 128.76, 128.71, 128.61, 128.56, 128.50, 128.46, 128.38, 128.34, 128.21, 128.18, 128.12, 127.92, 127.85, 127.51, 100.24, 99.34, 96.46, 77.74, 76.62, 75.71, 75.65, 74.92, 73.73, 72.55, 72.26, 69.46, 69.09, 68.24, 67.28, 67.16, 66.46, 66.40, 65.35, 37.64, 29.64, 27.70. HRMS m/z calculated for $C_{79}H_{74}O_{22}Na$:1397.4569; found: 1397.4564.

Benzyl (2-O-benzoyl-3-O-benzyl-4-O-levulinoyl)-α-L-idopyranosyl uronate-α(1→4) benzyl (2-O-benzoyl-3-O-benzyl)-α-L-idopyranosyl uronate-α(1→4)(1,6-O-diacetyl-2-O-benzoyl-3-O-benzyl)-α/β-L-idopyranoside 23

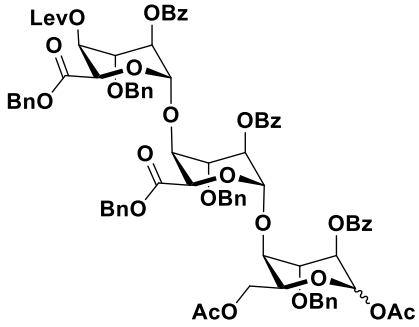

The synthetic procedure for the preparation of compound **10** was followed to obtain compound **23 (85%, α:β = 1:1)** from compound **22** as solid. ^{1}H NMR (400 MHz, Chloroform-*d*) δ 8.05 – 8.03 (m, 2H), 7.98 – 7.93 (m, 10H), 7.56 (t, *J* = 7.4 Hz, 2H), 7.42 (tt, *J* = 16.4, 8.0 Hz, 13H), 7.34 – 7.27 (m, 23H), 7.26 – 711 (m, 29H), 6.17 (s, 1H), 6.15 (d, *J* = 1.8 Hz, 1H), 5.30 (t, *J* = –4.3 Hz, 3H), 5.25 – 5.16 (m, 4H), 5.13 – 5.01 (m, 12H), 4.94 (dd, *J* = 10.0, 2.2 Hz, 2H), 4.78 – 4.72 (m, 5H), 4.69 – 4.60 (m, 6H), 4.55 (d, *J* = 12.0 Hz, 1H), 4.46– 4.41 (m, 3H), 4.35 (t, *J* = 3.6 Hz, 1H), 4.22 (ddd, *J* = 23.8, 14.2, 6.0 Hz, 4H), 4.03 (dtd, *J* = 21.3, 11.4, 5.1 Hz, 3H), 3.92 (dq, *J* = 13.2, 4.6 Hz, 3H), 3.82 – 3.79 (m, 4H), 2.35 (q, *J* = 6.4, 5.9 Hz, 4H), 2.22 – 2.14 (m, 2H), 2.08 (s, 4H), 2.02 (s, 3H), 2.01 (s, 3H), 2.00 (s, 2H), 1.93 (s, 2H), 1.91 (s, 3H). ^{13}C NMR (101 MHz, Chloroform-*d*) δ 205.80, 205.75, 171.46, 170.45, 169.13, 169.03, 168.95, 167.55, 167.49, 166.81, 166.03, 165.60, 165.34, 165.30,164.88, 164.83, 138.15, 137.70, 137.48, 137.45, 137.19, 137.15, 135.21, 135.08, 135.02, 133.72, 133.51, 133.49, 133.37, 130.21, 130.16, 129.98, 128.71, 128.66, 128.60, 128.53, 128.48, 128.42, 128.38, 128.31, 128.28, 128.21, 128.15, 128.11, 127.97, 127.87, 127.78, 127.58, 101.31, 100.65, 100.58, 91.81, 90.68, 76.51 , 76.38 , 75.66 , 75.33 , 75.07 , 73.46 , 73.29 , 73.20 , 73.15 , 72.75 , 72.62 , 72.53 , 72.41 , 71.12 , 71.01, 70.29, 70.19, 68.1, 67.97, 67.35, 67.30, 67.22, 67.11, 67.03, 66.73, 66.58, 66.50, 66.43, 66.38, 63.17, 62.66, 37.67, 29.83, 29.68, 27.71, 21.14, 21.06, 20.82. HRMS m/z calculated for $C_{83}H_{80}O_{25}Na$:1499.4886; found: 1499.4883.

Benzyl (2-O-benzoyl-3-O-benzyl-4-O-levulinoyl)-α-L-idopyranosyl uronate-α(1→4) benzyl (2-O-benzoyl-3-O-benzyl)-α-L-idopyranosyl uronate-α(1→4)1-thiophenyl (6-O-acetyl-2-O-benzoyl-3-O-benzyl)-α-L-idopyranoside 24

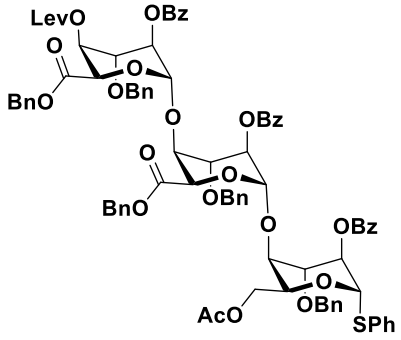

The synthetic procedure for the preparation of compound **11** was followed to obtain compound **24 (80%)** from compound **23** as solid. ^{1}H NMR (400 MHz, Chloroform-*d*) δ 8.04 – 7.99 (m, 6H), 7.61 – 7.56 (m, 3H), 7.52 – 7.41 (m, 8H), 7.39 – 7.33 (m, 5H), 7.32 – 7.24 (m, 13H), 7.21 – 7.13 (m, 10H), 5.56 (s, 1H), 5.45 – 5.44 (m, 1H), 5.36 (d, *J* = 5.7 Hz, 1H), 5.29 (d, *J* = 12.2 Hz, 1H), 5.17 (dd, *J* = 5.8, 3.7 Hz, 1H), 5.10 (ddd, *J* = 16.2, 12.9, 5.0 Hz, 5H), 5.00 (d, *J* = 2.1 Hz, 1H), 4.90 – 4.84 (m, 2H), 4.80 – 4.73 (m, 3H), 4.70 – 4.69 (m, 1H), 4.62(dd, *J* = 19.0, 11.6 Hz, 2H), 4.46 (d, *J* = 11.2 Hz, 1H), 4.32 (d, *J* = 3.1 Hz, 1H), 4.23 (dd, *J* = 11.4, 8.1 Hz, 1H), 4.04 (t, *J* = 4.9 Hz, 1H), 3.99 (dd, *J* = 11.5, 4.5 Hz, 1H), 3.94 (dd, *J* = 5.0, 3.7 Hz, 1H), 3.84 (dd, *J* = 6.8, 3.8 Hz, 2H), 2.38 (t, *J* = 6.4 Hz, 2H), 2.22 (dt, *J* = 17.3, 7.0 Hz, 1H), 2.11 – 2.05 (m, 1H), 2.03 (s, 3H), 1.92 (s, 3H). ^{13}C NMR (101 MHz, Chloroform-*d*) δ 205.77, 171.49, 170.28, 169.13, 167.48, 165.78, 165.27, 164.89, 137.93, 137.49, 137.13, 136.28, 135.24, 135.10, 133.74, 133.48, 133.38, 131.81, 130.13, 130.00, 129.98, 129.52, 129.27, 129.07, 128.91, 128.71, 128.68, 128.59, 128.55, 128.50, 128.46, 128.29, 128.17, 128.14, 127.81, 127.72, 127.44, 101.02, 100.38, 86.01, 76.49, 76.12, 73.57, 73.33, 72.82, 72.76, 72.47, 71.31, 71.27, 69.00, 67.97, 67.33, 67.03, 66.44, 66.27, 65.81, 63.29, 37.67, 29.68, 27.69, 20.81. HRMS m/z calculated for $C_{87}H_{82}O_{23}SNa$:1549.4865; found: 1549.4862.

Ethoxy-2-azidoethoxyl-O-(benzyl (2-O-benzoyl-3-O-benzyl-4-O-levulinoyl)-α-L-idopyranosyl uronate-α(1→4) benzyl (2-O-benzoyl-3-O-benzyl)-α-L-idopyranosyl uronate-α(1→4)(6-O-acetyl-2-O-benzoyl-3-O-benzyl))-α-L-idopyroside25

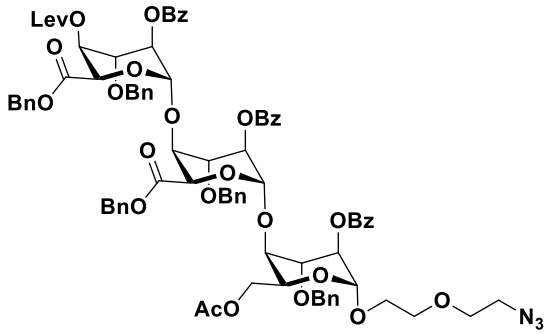

The synthetic procedure for the preparation of compound **12** was followed to obtain compound **25 (70%)** from compound **24** as syrup. ^{1}H NMR (400 MHz, Chloroform-*d*) δ 7.99 (ddd, *J* = 10.4, 8.2, 1.4 Hz, 6H), 7.61 – 7.57 (m, 1H), 7.49 – 7.40 (m, 6H), 7.37 – 7.13 (m, 27H), 5.36 (d, *J* = 4.7 Hz, 1H), 5.25 – 5.22 (m, 2H), 5.19 – 5.08 (m, 4H), 5.05 (dt, *J* = 4.9, 2.3 Hz, 2H), 4.97 (t, *J* = 2.2 Hz, 2H), 4.78 (dd, *J* = 11.5, 7.8 Hz, 2H), 4.72 – 4.67 (m, 4H), 4.63 (d, *J* = 11.5 Hz, 1H), 4.50 (d, *J* = 11.1 Hz, 1H), 4.41 (ddd, *J* = 7.4, 5.2, 1.9 Hz, 1H), 4.27 (dd, *J* = 11.3, 7.5 Hz, 1H), 4.22 (t, *J* = 3.0 Hz, 1H), 4.11 (dd, *J* = 11.3, 5.2 Hz, 1H), 4.03 (t, *J* = 4.5 Hz, 1H), 3.97 – 3.90 (m, 2H), 3.84 (dt, *J* = 8.6, 2.8 Hz, 2H), 3.72 (td, *J* = 5.7, 2.9 Hz, 2H), 3.69 – 3.57 (m, 3H), 3.26 – 3.15 (m, 2H), 2.39 (t, *J* = 6.8 Hz, 2H), 2.21 (dt, *J* = 17.2, 7.0 Hz, 1H), 2.13 – 2.07 (m, 1H), 2.03 (s, 3H), 1.95 (s, 3H). ^{13}C NMR (101 MHz, $CDCl_3$) δ 205.73, 171.40, 170.42, 168.93, 167.53, 165.73, 165.35, 164.79, 138.29, 137.48, 137.09, 135.19, 135.01, 133.66, 133.41, 133.31, 130.07, 129.97, 129.93, 129.43, 129.28, 129.03, 128.66, 128.58, 128.56, 128.51, 128.48, 128.46, 128.41, 128.34, 128.28, 128.20, 128.07, 127.78, 127.73, 127.63, 101.09, 100.56, 98.33, 76.54, 76.37, 76.13, 74.39, 73.31, 72.58, 72.46, 72.34, 70.36, 70.32, 70.25, 70.21, 68.14, 67.77, 67.59, 67.22, 67.05, 66.45, 66.38, 64.95, 63.05, 50.81, 37.64, 29.63, 27.68, 20.79. HRMS m/z calculated for $C_{85}H_{85}O_{25}N_3Na$:1570.5357; found: 1570.5352.

Ethoxy-2-azidoethoxyl-O-(benzyl (2-O-benzoyl-3-O-benzyl-4-O-levulinoyl)-α-L-idopyranosyl uronate-α(1→4) benzyl (2-O-benzoyl-3-O-benzyl)-α-L-idopyranosyl uronate-α(1→4)(2-O-benzoyl-3-O-benzyl))-α-L-idopyroside 26

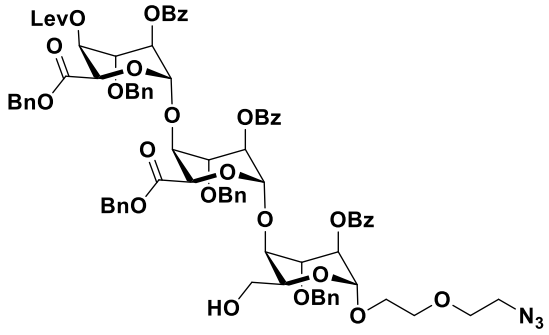

The synthetic procedure for the preparation of compound **13** was followed to obtain compound **26 (90%)** from compound **25** as syrup. ^{1}H NMR (400 MHz, Chloroform-*d*) δ 8.03– 7.99 (m, 4H), 7.98 – 7.95 (m, 2H), 7.61 – 7.57 (m, 1H), 7.49 – 7.39 (m, 6H), 7.36 (dd, *J* = 8.1, 1.6 Hz, 2H), 7.32 – 7.19 (m, 20H), 7.18 – 7.13 (m, 5H), 5.33 (d, *J* = 4.6 Hz, 1H), 5.25 (t, *J* = 2.1 Hz, 1H), 5.20 – 5.18 (m, 1H), 5.15 – 5.06 (m, 6H), 5.01 – 5.00 (m, 2H), 4.79 (d, *J* = 11.5 Hz, 2H), 4.73 (d, *J* = 4.1 Hz, 1H), 4.71 – 4.64 (m, 4H), 4.51 (d, *J* = 11.1 Hz, 1H), 4.32 (ddd, *J* = 7.4, 5.3, 2.0 Hz, 1H), 4.24 – 4.22 (m, 1H), 4.06 (t, *J* = 4.3 Hz, 1H), 3.96 – 3.89 (m, 3H), 3.86 – 3.84 (m, 1H), 3.79 (dd, *J* = 11.3, 7.3 Hz, 1H), 3.73 – 3.71 (m, 2H), 3.70 – 3.55 (m, 4H), 3.22 (ddd, *J* = 6.2, 4.2, 2.0 Hz, 2H), 2.39 (t, *J* = 6.8 Hz, 2H), 2.21 (dt, *J* = 17.3, 6.8 Hz, 1H), 2.14 – 2.09 (m, 1H), 2.03 (s, 3H). ^{13}C NMR (101 MHz, $CDCl_3$) δ 205.77, 171.45, 168.91, 167.57, 165.78, 165.64, 164.85, 138.42, 137.43, 137.05, 135.17, 135.03, 133.70, 133.58, 133.27, 130.08, 129.96, 129.92, 129.53, 129.28, 128.97, 128.65, 128.59, 128.57, 128.55, 128.51, 128.45, 128.42, 128.40, 128.36, 128.30, 128.27, 128.23, 128.14, 127.83, 127.72, 127.58, 101.04, 100.89, 98.48, 76.67, 76.52, 76.48, 74.59, 73.20, 72.63, 72.38, 70.54, 70.41, 70.30, 68.19, 68.02, 67.76, 67.24, 67.22, 67.09, 66.45, 61.91, 50.84, 37.66, 29.65, 27.71. HRMS m/z calculated for $C_{83}H_{83}O_{24}N_3Na$:1528.5264; found: 1528.5259.

Ethoxy-2-azidoethoxyl-O-(benzyl (2-O-benzoyl-3-O-benzyl-4-O-levulinoyl)-α-L-idopyranosyl uronate-α(1→4) benzyl (2-O-benzoyl-3-O-benzyl)-α-L-idopyranosyl uronate-α(1→4) benzyl (2-O-benzoyl-3-O-benzyl))-α-L-idopyranoside uronate 27

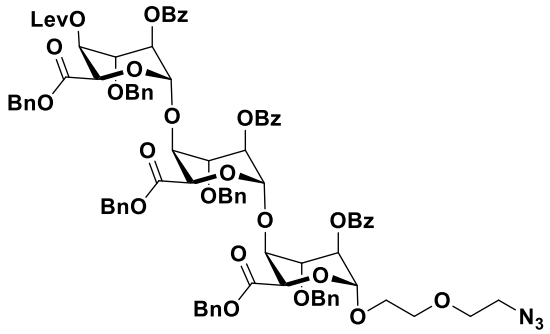

The synthetic procedure for the preparation of compound **14** was followed to obtain compound **27 (70%)** from compound **26** as syrup. ^{1}H NMR (400 MHz, Chloroform-*d*) δ 7.96 – 7.88 (m, 6H), 7.55 (t, *J* = 7.4 Hz, 1H), 7.41 – 7.34 (m, 8H), 7.31 – 7.27 (m, 6H), 7.26 – 7.22 (m, 6H), 7.21 – 7.14 (m, 13H), 7.11 – 7.04 (m, 6H), 5.29 (d, *J* = 2.7 Hz, 1H), 5.21 (p, *J* = 3.7, 3.2 Hz, 2H), 5.17 (d, *J* = 2.0 Hz, 1H), 5.08 (dd, *J* = 12.1, 7.9 Hz, 3H), 5.02 – 4.92 (m, 5H), 4.89 (t, *J* = 2.6 Hz, 1H), 4.79 – 4.69 (m, 6H), 4.59 (d, *J* = 11.4 Hz, 1H), 4.49 (t, *J* = 11.3 Hz, 2H), 4.26 (t, *J* = 3.2 Hz, 1H), 4.16 (t, *J* = 2.9 Hz, 1H), 3.97 – 3.88 (m, 3H), 3.75 (t, *J* = 2.9 Hz, 1H), 3.72 – 3.62 (m, 3H), 3.53 (dtt, *J* = 15.9, 10.6, 5.3 Hz, 2H), 3.12 (t, *J* = 5.1 Hz, 2H), 2.34 (t, *J* = 6.8 Hz, 2H), 2.18 – 2.03 (m, 2H), 2.00 (s, 2H). ^{13}C NMR (101 MHz, Chloroform-*d*) δ 205.65, 171.22 , 169.05, 168.40, 167.52, 165.57, 165.14, 164.63, 137.98, 137.30, 137.10, 135.20, 135.09, 134.85, 133.50, 133.33, 133.26, 130.10, 130.01, 129.85, 129.26, 129.02, 128.88, 128.57, 128.55, 128.47, 128.43, 128.42, 128.36, 128.33, 128.29, 128.24, 128.16, 127.97, 127.76, 127.68, 127.54, 101.68, 101.32, 98.83, 75.40, 75.14, 72.83, 72.57, 72.24, 72.07, 70.13, 70.11, 68.74, 68.41, 68.39, 68.36, 68.06, 67.99, 67.04, 67.01, 66.98, 66.55, 66.47, 50.66, 37.57, 29.54, 27.61. HRMS m/z calculated for $C_{90}H_{87}O_{25}N_3Na$:1632.5526; found: 1632.5522.

Ethoxy-2-azidoethoxyl-O-(benzyl (2-O-benzoyl-3-O-benzyl)-α-L-idopyranosyl uronate-α(1→4) benzyl (2-O-benzoyl-3-O-benzyl)-L-idopyranosyl uronate-α(1→4) benzyl (2-O-benzoyl-3-O-benzyl))-α-L-idopyranoside uronate 28

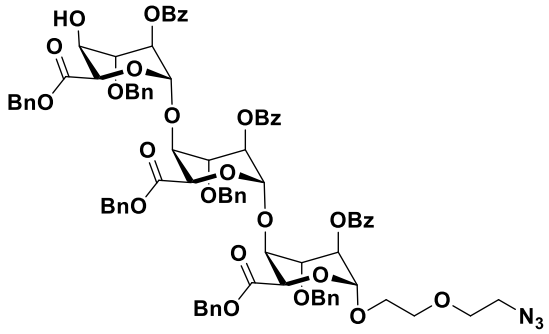

The synthetic procedure for the preparation of compound **15** was followed to obtain compound **28 (85%)** from compound **27** as syrup. ^{1}H NMR (400 MHz, Chloroform-*d*) δ 7.97 – 7.88 (m, 6H), 7.59 – 7.55 (m, 1H), 7.44 – 7.37 (m, 6H), 7.35 – 7.27 (m, 9H), 7.26 – 7.16 (m, 14H), 7.16 – 7.06 (m, 9H), 5.31 (d, *J* = 3.1 Hz, 1H), 5.21 (t, *J* = 2.6 Hz, 2H), 5.17 (d, *J* = 2.3 Hz, 1H), 5.12 (d, *J* = 12.3 Hz, 1H), 5.07 – 4.97 (m, 6H), 4.95 (d, *J* = 2.9 Hz, 1H), 4.81 (d, *J* = 6.1 Hz, 1H), 4.79 – 4.76 (m, 3H), 4.71 (dd, *J* = 11.2, 5.5 Hz, 2H), 4.55 (dd, *J* = 15.3, 11.5 Hz, 2H), 4.44 (d, *J* = 10.8 Hz, 1H), 4.28 (t, *J* = 3.3 Hz, 1H), 4.17 (t, *J* = 3.2 Hz, 1H), 3.97 – 3.88 (m, 3H), 3.77 – 3.63 (m, 5H), 3.59 – 3.46 (m, 2H), 3.12 (t, *J* = 4.9 Hz, 2H), 2.53 (d, *J* = 10.4 Hz, 1H). ^{13}C NMR (101 MHz, Chloroform-*d*) δ 169.19, 168.78, 168.55, 16.70, 165.30, 164.61, 138.13, 137.37, 137.29, 135.35, 135.22, 134.99, 133.76, 133.41, 133.36, 130.33, 130.13, 129.91, 129.17, 129.11, 129.06, 128.74, 128.67, 128.65, 128.63, 128.56, 128.44, 128.42, 128.39, 128.34, 128.29, 128.28, 128.19, 128.15, 127.92, 127.80, 127.66, 101.77, 101.71, 98.97, 75.60, 75.22, 73.99, 72.88, 72.69, 72.00, 70.26, 70.24, 69.03, 68.74, 68.63, 68.53, 68.46, 68.43, 68.29, 68.13, 67.23, 67.08, 67.03, 67.00, 50.79. HRMS m/z calculated for $C_{85}H_{81}O_{23}N_3Na$:1534.5159; found: 1534.5157.

3.5.2.5 Synthesis of Sulfated Trisaccharide Analogues (I-20, I-31 and I-34)

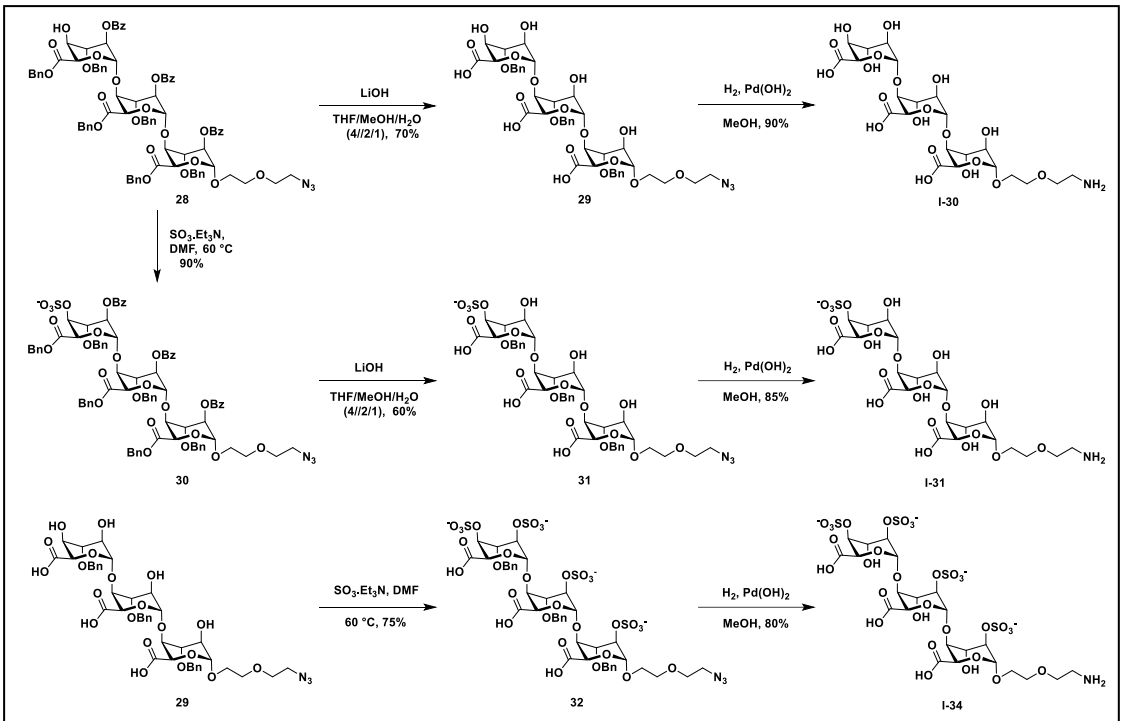

Scheme 5. Synthesis of Trisaccharide Sulfated Compounds.

Ethoxy-2-azidoethoxyl-O-((3-O-benzyl)-α-L-idopyranosyl uronic acid-α(1→4)(3-O-benzyl)-α-L-idopyranosyl uronic acid-α(1→4)(3-O-benzyl))-α-L-idopyranoside uronic acid29

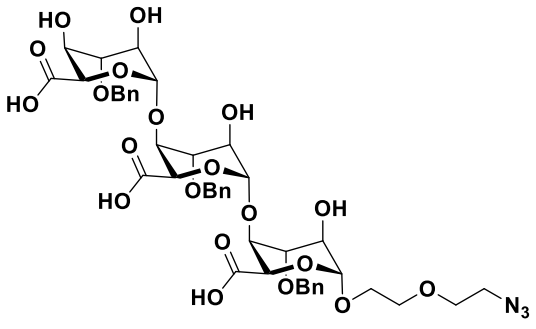

Esters deprotection: Followed general procedure for deprotection of esters yielded compound **29 (75%).** ^{1}H NMR (400 MHz, Methanol-d_4) δ 7.40 – 7.27 (m, 15H), 5.00 (d, J = 4.0 Hz, 2H), 4.96 (d, J = 2.2 Hz, 1H), 4.86 (d, J = 2.4 Hz, 1H), 4.73 (d, J = 1.8 Hz, 1H), 4.69 – 4.63 (m, 2H), 4.59 (d, J = 7.5 Hz, 4H), 4.29 (t, J = 3.1 Hz, 1H), 4.23 (d, J = 3.7 Hz, 1H), 4.01 (d, J = 2.9 Hz, 1H), 3.94 – 3.89 (m, 1H), 3.80 (t, J = 3.8 Hz, 1H), 3.73 – 3.57 (m, 9H), 3.49 (s, 1H), 3.25 (t, J = 5.0 Hz, 2H). ^{13}C NMR (101 MHz, Methanol-d_4) δ 173.11, 172.79, 172.36, 139.41, 138.69, 138.46, 129.84, 129.64, 129.60, 129.55, 129.39, 129.20, 129.13, 129.00,

128.75, 104.44, 104.18, 102.87, 76.83, 76.58, 76.22, 75.78, 74.89, 73.52, 73.33, 73.29, 71.27, 71.24, 69.58, 69.39, 68.94, 68.65, 68.63, 68.47, 67.63, 67.15, 51.80. HRMS m/z calculated for $C_{43}H_{51}N_3O_{20}Na$: 952.2964 found: 952.2954.

Ethoxy-2-azidoethoxyl-O-(benzyl (2-O-benzoyl-3-O-benzyl-4-O-sulfonato)-α-L-idopyranosyl uronate-α(1→4) benzyl (2-O-benzoyl-3-O-benzyl)-L-idopyranosyl uronate-α(1→4) benzyl (2-O-benzoyl-3-O-benzyl))-α-L-idopyroside uronate 30

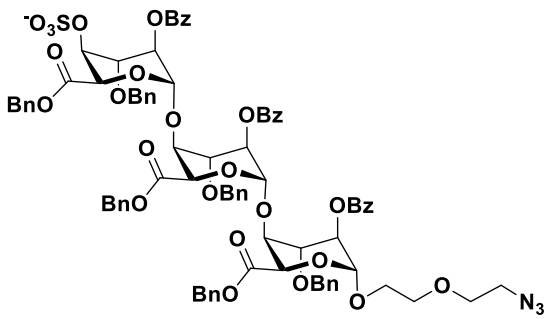

***O*-Sulfation:** Followedgeneral procedure for sulfation yielded compound **30 (90%).** ^{1}H NMR (400 MHz, Methanol-d_4) δ 8.06 (dd, *J* = 8.3, 1.1 Hz, 2H), 7.92 – 7.86 (m, 4H), 7.56 – 7.52 (m, 1H), 7.42 – 7.34 (m, 6H), 7.28 – 7.05 (m, 33H), 5.25 (d, *J* = 3.8 Hz, 1H), 5.11 – 5.05 (m, 6H), 5.05 – 4.96 (m, 3H), 4.92 – 4.87 (m, 3H), 4.81 (d, *J* = 2.7 Hz, 1H), 4.72 – 4.59 (m, 5H), 4.52 – 4.45 (m, 2H), 4.39 (d, *J* = 11.0 Hz, 1H), 4.31 (t, *J* = 3.2 Hz, 1H), 4.19 – 4.18 (m, 1H), 4.13 (t, *J* = 2.8 Hz, 1H), 3.86 (ddt, *J* = 12.2, 7.5, 4.4 Hz, 3H), 3.67 – 3.58 (m, 3H), 3.55 – 3.43 (m, 2H), 3.07 (t, *J* = 5.0 Hz, 2H). ^{13}C NMR (101 MHz, Methanol-d_4) δ 170.72, 170.14, 169.82, 166.93, 166.87, 166.68, 139.30, 139.01, 138.73, 136.95, 136.63, 136.59, 134.52, 134.46, 134.31, 131.40, 131.18, 131.03, 130.96, 130.49, 130.39, 129.73 , 129.58, 129.56, 129.55, 129.50, 129.44, 129.42, 129.35, 129.33, 129.30, 129.27, 129.07, 129.02, 128.85, 128.77, 128.72, 102.59, 101.75, 100.00, 77.77, 77.14, 77.06, 76.28, 75.12, 74.19, 73.83, 73.66, 73.61, 71.22, 71.13, 70.64, 70.48, 69.91, 69.59, 69.56, 69.48, 69.07, 68.27, 68.22, 68.12, 51.73. HRMS m/z calculated for $C_{85}H_{80}N_3O_{26}S^-$: 1590.4756 found (M-H): 1589.4755.

Ethoxy-2-azidoethoxyl-O-((3-O-benzyl-4-O-sulfonato)-α-L-idopyranosyl uronic acid-α(1→4)(3-O-benzyl)-L-idopyranosyl uronic acid-α(1→4)(3-O-benzyl))-α-L-idopyranoside uronic acid 31

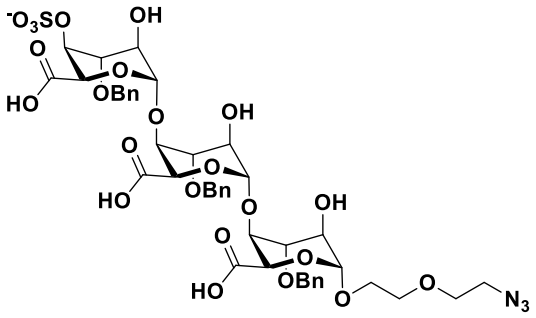

Esters deprotection: Followed general procedure for deprotection of esters yielded compound **31 (60%)**. ^{1}H NMR (400 MHz, Methanol-d_4) δ 7.44 – 7.24 (m, 15H), 5.15 (d, *J* = 3.6 Hz, 2H), 4.86 (d, *J* = 2.9 Hz, 1H), 4.72 – 4.52 (m, 11H), 4.25 (t, *J* = 2.5 Hz, 1H), 3.93 – 3.90 (m, 1H), 3.82 (d, *J* = 3.5 Hz, 1H), 3.73 (t, *J* = 3.1 Hz, 1H), 3.69 – 3.56 (m, 8H), 3.18 (ddd, *J* = 5.6, 4.2, 1.0 Hz, 2H). ^{13}C NMR (101 MHz, MeOD) δ 176.72, 176.14, 175.28, 139.79, 139.22, 138.76, 129.82, 129.60, 129.45, 129.30, 129.24, 128.91, 128.70, 128.49, 103.80, 103.07, 102.74, 76.96, 75.80, 75.51, 74.75, 74.32, 73.68, 72.96, 72.90, 72.72, 71.30, 71.28, 69.92, 69.33, 69.02, 68.82, 68.41, 68.20, 67.87, 51.74. HRMS m/z calculated for $C_{43}H_{50}N_3O_{23}S^-$: 1008.2561 found: 1008.2558.

Ethoxy-2-aminoethoxyl-O-(α-L-idopyranosyl uronic acid-α(1→4)-α-L-idopyranosyl uronic acid-α(1→4))-α-L-idopyranoside uronic acid 1-30

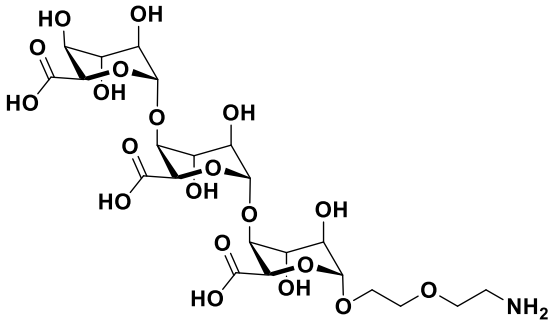

Hydrogenolysis: Followed general procedure for hydrogenolysis yielded compound **I-30 (90%).** ^{1}H NMR (400 MHz, Deuterium Oxide) δ 4.95 (d, *J* = 2.4 Hz, 2H), 4.90 (d, *J* = 3.1 Hz, 1H), 4.67 (d, *J* = 2.1 Hz, 1H), 4.57 (d, *J* = 2.8 Hz, 1H), 4.55 (d, *J* = 2.4 Hz, 1H), 4.11 (dt, *J* = 11.6, 3.1 Hz, 2H), 3.94 (ddd, *J* = 15.7, 8.6, 4.2 Hz, 4H), 3.82 (q, *J* = 4.3 Hz, 2H), 3.78 – 3.74 (m, 4H), 3.63 (dd, *J* = 8.0, 4.8 Hz, 3H), 3.21 (t, *J* = 5.1 Hz, 2H). ^{13}C NMR (101 MHz, D_2O) δ 176.11, 175.61, 175.55, 102.50, 102.41, 101.09, 77.97, 77.87, 70.23, 70.18, 70.15, 69.82, 69.50, 68.88, 68.52, 68.35, 68.13, 67.47, 66.27, 39.08. HRMS m/z calculated for $C_{22}H_{35}NO_{20}Na$: 656.1650 found: 656.1659.

Ethoxy-2-aminoethoxyl-O-((4-O-sulfonato)-α-L-idopyranosyl uronic acid-α(1→4)-L-idopyranosyl uronic acid-α(1→4))-α-L-idopyranoside uronic acid I-31

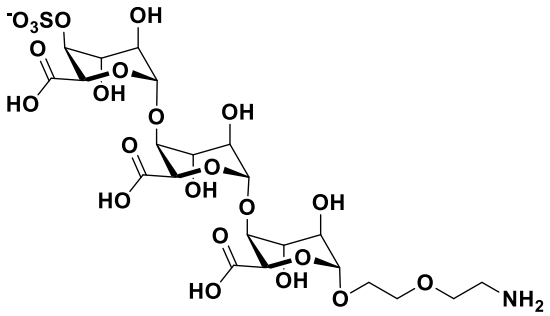

Hydrogenolysis: Followed general procedure for hydrogenolysis yielded compound **I-31 (85%).** ^{1}H NMR (400 MHz, Deuterium Oxide) δ 4.87 (dd, *J* = 5.6, 2.3 Hz, 3H), 4.67 (d, *J* = 2.4 Hz, 1H), 4.59 (d, *J* = 2.3 Hz, 1H), 4.51 (t, *J* = 3.0 Hz, 1H), 4.47 (d, *J* = 2.4 Hz, 1H), 4.19 (td, *J* = 3.8, 1.0 Hz, 1H), 4.02 (dt, *J* = 10.4, 3.2 Hz, 2H), 3.82 (q, *J* = 5.0 Hz, 2H), 3.74 – 3.65 (m, 5H), 3.58 (ddd, *J* = 3.9, 2.2, 1.0 Hz, 1H), 3.55 – 3.51 (m, 2H), 3.15 – 3.09 (m, 1H). ^{13}C NMR (101 MHz, D_2O) δ 175.51, 175.38, 174.38, 102.56, 102.29, 101.10, 78.00, 77.89, 75.84, 69.81, 69.53, 68.88, 68.53, 68.45, 68.18, 68.04, 67.82, 67.65, 67.48, 66.28, 39.08. HRMS m/z calculated for $C_{22}H_{34}NO_{23}S^{-}$: 712.1248 found: 712.1239.

Ethoxy-2-aminoethoxyl-O-((2,4-O-disulfonato-3-O-benzyl)-α-L-idopyranosyl uronic acid-α(1→4)(2-O-sulfonato-3-O-benzyl)-α-L-idopyranosyl uronic acid-α(1→4)(2-O-sulfonato-3-O-benzyl))-α-L-idopyranoside uronic acid 32

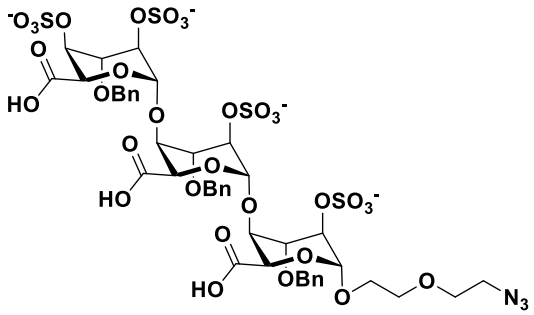

***O*-Sulfation:** Followedgeneral procedure for sulfation yielded compound **32 (75%).** ^{1}H NMR (400 MHz, Deuterium Oxide) δ 7.42 – 7.26 (m, 15H), 5.10 (d, *J* = 9.3 Hz, 2H), 5.03 (s, 1H), 4.75 (d, *J* = 2.9 Hz, 1H), 4.73 – 4.61 (m, 3H), 4.68 – 4.59 (m, 5H), 4.42 (d, *J* = 1.9 Hz, 1H), 4.31 (s, 1H), 4.23 (d, *J* = 10.6 Hz, 8H), 3.87 (s, 2H), 3.77 (dt, *J* = 10.6, 3.6 Hz, 1H), 3.68 – 3.52 (m, 5H), 3.30 – 3.28 (m, 2H). ^{13}C NMR (101 MHz, Deuterium Oxide) δ 175.24, 174.71, 174.11, 137.24, 137.21, 137.17, 128.73, 128.71, 128.69, 128.61, 128.57, 128.30, 128.09, 100.82, 100.34, 98.88, 76.11, 74.54, 74.09, 72.85, 72.69, 72.12, 71.91, 71.71, 71.28, 71.24, 70.90, 70.89, 69.46, 69.43, 67.54, 67.33, 67.07, 50.19. HRMS m/z calculated for $C_{43}H_{47}N_3O_{32}S_4^{4-}$: 311.2762 found: 311.2769.

Ethoxy-2-aminoethoxyl-O-((2,4-O-disulfonato)-α-L-idopyranosyl uronic acid-α(1→4)(2-O-sulfonato)-α-L-idopyranosyl uronic acid -α(1→4)(2-O-sulfonato)-α-L-idopyranoside uronic acid I-34

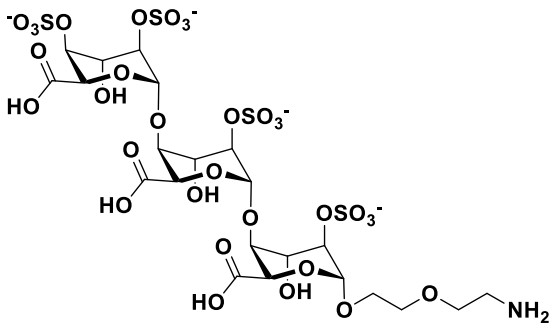

Hydrogenolysis: Followed general procedure for hydrogenolysis yielded compound **I-34 (80%).** ^{1}H NMR (600 MHz, Deuterium Oxide) δ 5.19 (s, 1H), 5.17 – 5.16 (m, 2H), 4.68 (t, *J* = 2.3 Hz, 2H), 4.57 (d, *J* = 2.1 Hz, 1H), 4.52 (td, *J* = 2.6, 1.2 Hz, 1H), 4.27 (dt, *J* = 2.4, 1.2 Hz, 1H), 4.25 (dd, *J* = 2.6, 1.3 Hz, 1H), 4.21 (t, *J* = 2.9 Hz, 1H), 4.17 (t, *J* = 2.4 Hz, 1H), 4.09 – 4.07 (m, 3H), 3.90 – 3.82 (m, 1H), 3.80 – 3.72 (m, 5H), 3.22 – 3.21 (m, 2H). ^{13}C NMR (151 MHz, D_2O) δ 175.13, 174.92, 174.36, 100.79, 99.00, 77.75, 77.01, 74.33, 72.22, 71.67, 69.89, 68.14, 67.71, 67.47, 67.31, 67.14, 66.53, 66.29, 65.56, 39.16. HRMS m/z calculated for $C_{22}H_{31}NO_{32}S_4^{4-}$: 237.2433 found: 237.2439.

3.5.2.6 Synthesis of Iduronic Acid Tetrasaccharide Precursor

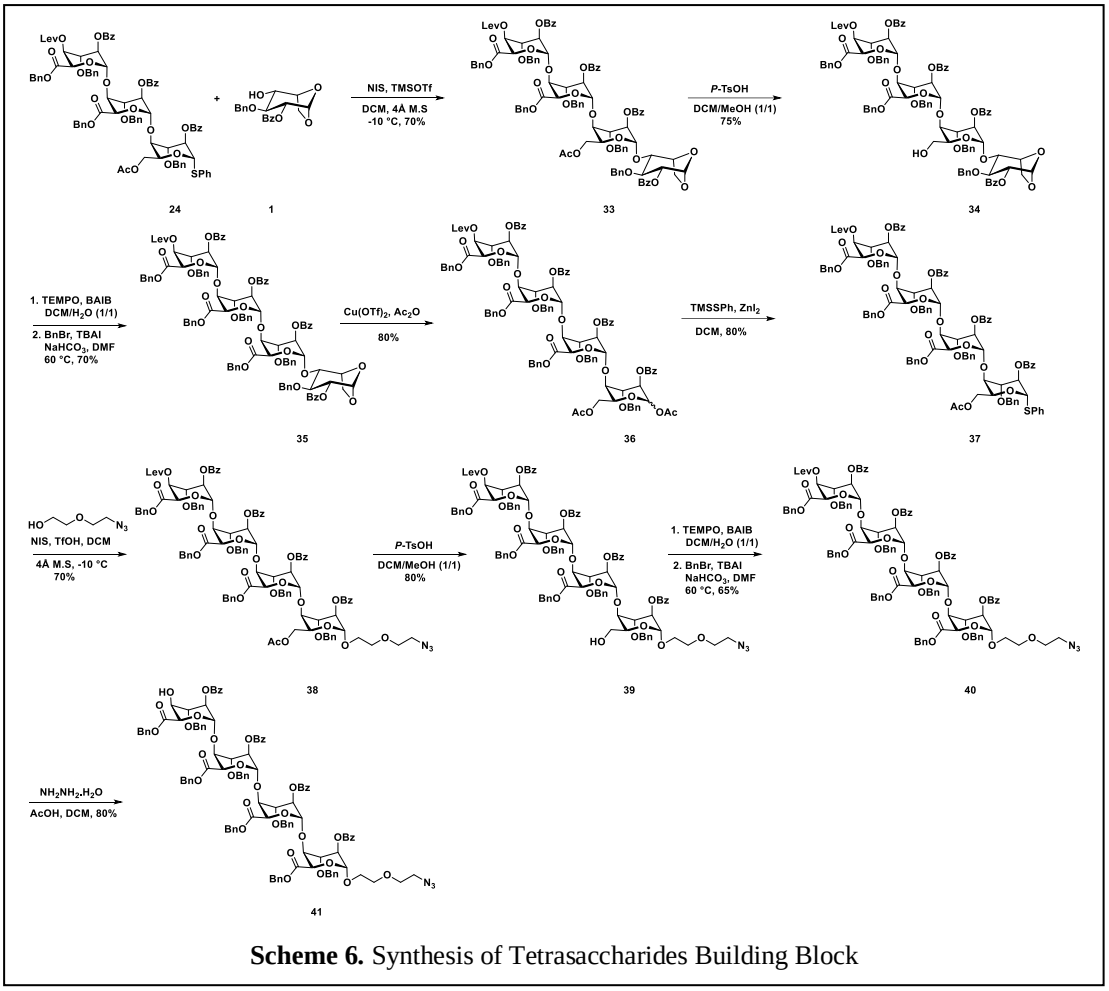

Scheme 6. Synthesis of Tetrasaccharides Building Block

Benzyl (2-O-benzoyl-3-O-benzyl-4-O-levulinoyl)-α-L-idopyranosyl uronate-α(1→4) benzyl (2-O-benzoyl-3-O-benzyl)-α-L-idopyranosyl uronate-α(1→4)(6-O-acetyl-2-O-benzoyl-3-O-benzyl)-α-L-idopyranosyl-α(1→4)(2-O-benzoyl-3-O-benzyl-1,6-anhydro)-β-L-idopyranose 33

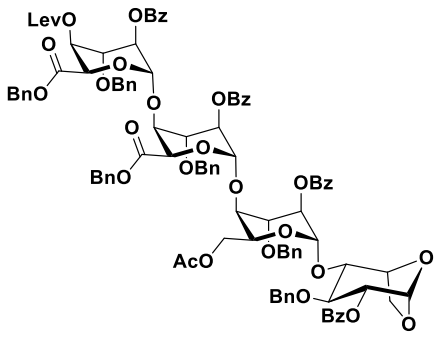

The synthetic procedure for the preparation of compound **9** was followed to obtain compound **33 (70%)** from compound **24** and **2** as solid. ^{1}H NMR (400 MHz, Chloroform-*d*) δ 7.99– 7.96 (m, 5H), 7.95 – 7.90 (m, 3H), 7.59 – 7.53 (m, 2H), 7.48 – 7.38 (m, 8H), 7.34 – 7.27 (m, 11H), 7.24 – 7.11 (m, 16H), 7.06 – 6.99 (m, 5H), 5.50 (s, 1H), 5.34 (d, *J* = 4.6 Hz, 1H), 5.21 – 5.16 (m, 3H), 5.11 (dd, *J* = 12.1, 3.8 Hz, 3H), 5.07 – 5.03 (m, 3H), 4.99 – 4.95 (m, 2H), 4.76 – 4.72 (m, 3H), 4.69 – 4.62 (m, 6H), 4.49 (d, *J* = 11.4

Hz, 3H), 4.20 – 4.13 (m, 4H), 4.07 – 4.02 (m, 2H), 3.95 (t, *J* = 3.9 Hz, 1H), 3.88 – 3.81 (m, 3H), 3.71 – 3.68 (m, 1H), 2.37 (t, *J* = 6.8 Hz, 2H), 2.23 – 2.15 (m, 1H), 2.10 – 2.04 (m, 1H), 2.02 (s, 3H), 1.88 (s, 3H). ^{13}C NMR (101 MHz, CHLOROFORM-*D*) δ 205.80, 171.43, 170.51, 168.96, 167.56, 165.88, 165.85, 165.37, 164.81, 138.23, 137.87, 137.42, 137.06, 135.17, 134.99, 133.71, 133.55, 133.51, 133.30, 130.04, 129.95, 129.50, 129.25, 129.15, 128.94, 128.70, 128.60, 128.58, 128.54, 128.51, 128.46, 128.42, 128.38, 128.32, 128.24, 128.20, 128.15, 128.08, 127.91, 127.81, 127.36, 100.82, 100.53, 99.39, 95.34, 77.74, 76.63, 76.50, 76.30, 75.82, 74.97, 74.62, 73.41, 73.10, 72.58, 72.25, 71.96, 70.24, 68.21, 68.13, 67.28, 67.10, 66.42, 66.40, 65.77, 65.54, 62.70, 37.65, 29.67, 27.68, 20.82. HRMS m/z calculated for $C_{101}H_{96}O_{29}Na$:1795.5935; found: 1795.5930.

Benzyl (2-O-benzoyl-3-O-benzyl-4-O-levulinoyl)-α-L-idopyranosyl uronatel-α(1→4) benzyl (2-O-benzoyl-3-O-benzyl)-α-L-idopyranosyl uronate-α(1→4)(2-O-benzoyl-3-O-benzyl)-α-L-idopyranosyl-α(1→4)(2-O-benzoyl-3-O-benzyl-1,6-anhydro)-β-L-idopyranose 34

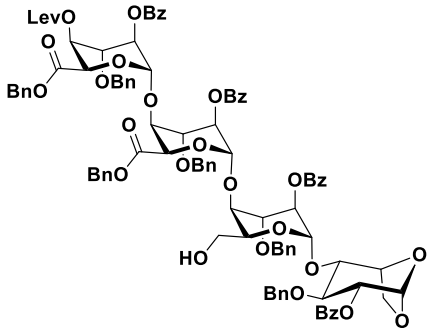

The synthetic procedure for the preparation of compound **13** was followed to obtain compound **34 (85%)** from compound **33** as syrup. ^{1}H NMR (400 MHz, Chloroform-*d*) δ 799 – 7.93 (m, 8H), 7.55 (t, *J* = 7.4 Hz, 2H), 7.46 – 7.37 (m, 10H), 7.34 – 7.26 (m, 8H), 7.24 – 7.10 (m, 17H), 7.08 – 7.01 (m, 5H), 5.51 (d, *J* = 1.7 Hz, 1H), 5.32 (d, *J* = 4.7 Hz, 1H), 5.18 – 5.14 (m, 3H), 5.10 – 5.06 (m, 3H), 5.04 – 5.01 (m, 3H), 5.00 – 4.99 (m, 1H), 4.93 (d, *J* = 2.1 Hz, 1H), 4.79 – 4.70 (m, 4H), 4.68 (s, 1H), 4.63 (d, *J* = 12.5 Hz, 2H), 4.59 (t, *J* = 4.5 Hz, 1H), 4.53 (s, 2H), 4.47 (d, *J* = 11.2 Hz, 1H), 4.27 (t, *J* = 6.8 Hz, 1H), 4.22 – 4.19 (m, 2H), 4.19 – 4.16 (m, 1H), 4.05 (t, *J* = 4.3 Hz, 1H), 3.91 – 3.87 (m, 2H), 3.81 (s, 1H), 3.76 (dt, *J* = 14.0, 3.8 Hz, 2H), 3.47 (dd, *J* = 11.3, 6.9 Hz, 1H), 3.26 (dd, *J* = 11.3, 6.1 Hz, 1H), 2.35 (t, *J* = 6.8 Hz, 2H), 2.17 (dt, *J* = 17.2, 7.0 Hz, 1H), 2.09 – 2.01 (m, 1H), 2.00 (s, 3H). ^{13}C NMR (101 MHz, CHLOROFORM-*D*) δ 205.80, 171.40, 168.96, 167.54, 165.98, 165.79, 165.46, 164.81, 138.20, 137.93, 137.41, 137.06, 135.15, 135.02, 133.71, 133.55, 133.47, 133.42, 130.06, 129.94, 129.50, 129.23, 129.21, 128.99, 128.67, 128.58, 128.50, 128.44, 128.39, 128.31, 128.23, 128.21, 128.07, 127.91, 127.82, 127.76, 101.03, 100.82, 99.40, 95.79, 78.37, 77.36, 76.95,

76.70, 76.58, 75.80, 75.13, 74.68, 73.97, 73.18, 72.77, 72.39, 72.15, 71.92, 70.49, 70.43, 67.23, 67.09, 66.98, 66.38, 66.35, 65.68, 61.49, 37.64, 29.66, 27.67. HRMS m/z calculated for $C_{99}H_{94}O_{28}Na$:1753.5829; found: 1753.5825.

Benzyl (2-O-benzoyl-3-O-benzyl-4-O-levulinoyl)-α-L-idopyranosyl uronate-α(1→4) benzyl (2-O-benzoyl-3-O-benzyl)-α-L-idopyranosyl uronate-α(1→4)benzyl (2-O-benzoyl-3-O-benzyl)-α-L-idopyranosyl uronate-α(1→4)(2-O-benzoyl-3-O-benzyl-1,6-anhydro)-β-L-idopyranose 35

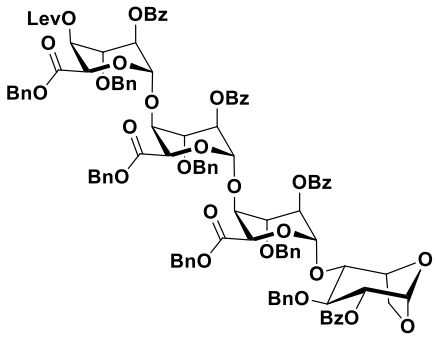

The synthetic procedure for the preparation of compound **14** was followed to obtain compound **35 (70%)** from compound **34** as solid. ^{1}H NMR (400 MHz, Chloroform-*d*) δ 7.97 – 7.88 (m, 8H), 7.55 (td, *J* = 7.3, 1.4 Hz, 2H), 7.44 – 7.37 (m, 8H), 7.32 – 7.28 (m, 7H), 7.25 – 7.07 (m, 25H), 7.02 – 6.96 (m, 5H), 5.49 (d, *J* = 1.6 Hz, 1H), 5.32 (t, *J* = 2.6 Hz, 2H), 5.17 – 5.16 (m, 2H), 5.11 – 5.08 (m, 2H), 5.04 (d, *J* = 12.3 Hz, 1H), 5.00 (d, *J* = 2.7 Hz, 3H), 4.97 – 4.96 (m, 1H), 4.94 – 4.856 (m, 3H), 4.81 (d, *J* = 3.1 Hz, 1H), 4.76 – 474 (m, 3H), 4.70 (d, *J* = 5.6 Hz, 1H), 4.65 (d, *J* = 9.0 Hz, 1H), 4.62 (d, *J* = 4.4 Hz, 1H), 4.60 – 4.55 (m, 3H), 4.49 (s, 1H), 4.46 (d, *J* = 1.7 Hz, 1H), 4.28 (t, *J* = 3.8 Hz, 1H), 4.23 (dd, *J* = 8.4, 4.1 Hz, 1H), 4.17 (t, *J* = 3.9 Hz, 1H), 4.06 (d, *J* = 7.7 Hz, 1H), 3.97 (t, *J* = 3.4 Hz, 1H), 3.92 (t, *J* = 3.2 Hz, 1H), 3.85 (t, *J* = 8.4 Hz, 1H), 3.75 (d, *J* = 2.9 Hz, 1H), 3.57 – 3.54 (m, 1H), 2.35 (t, *J* = 6.7 Hz, 2H), 2.19 – 2.02 (m, 2H), 2.00 (s, 3H). ^{13}C NMR (101 MHz, $CDCl_3$) δ 205.74, 171.32, 168.80, 168.56, 167.60, 165.81, 165.66, 165.17, 164.75, 137.92, 137.77, 137.36, 137.23, 135.18, 135.13, 134.98, 133.62, 133.58, 133.46, 133.34, 130.21, 129.99, 129.96, 129.57, 129.35, 128.98, 128.97, 128.69, 128.58, 128.54, 128.49, 128.46, 128.35, 128.25, 128.16, 128.10, 127.90, 127.83, 127.46, 101.30, 100.91, 99.38, 96.33, 77.85, 76.78, 76.72, 75.87, 75.59, 75.43, 75.34, 74.91, 73.39, 73.06, 72.33, 72.24, 72.17, 69.00, 68.89, 68.46, 68.31, 67.19, 67.13, 67.03, 66.68, 66.64, 65.44, 37.66, 29.65, 27.70. HRMS m/z calculated for $C_{106}H_{98}O_{29}Na$:1834.6194; found: 1834.6189.

Benzyl (2-O-benzoyl-3-O-benzyl-4-O-levulinoyl)-α-L-idopyranosyl uronate-α(1→4) benzyl (2-O-benzoyl-3-O-benzyl)-α-L-idopyranosyl uronate-α(1→4) benzyl (2-O-benzoyl-3-O-benzyl)-α-L-idopyranosyl uronate-α(1→4)(1,6-O-diacetyl-2-O-benzoyl-3-O-benzyl)-α/β-L-idopyranoside 36

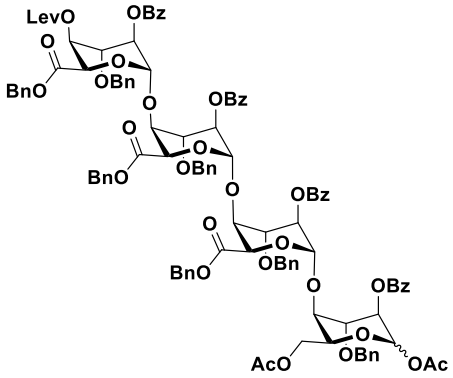

The synthetic procedure for the preparation of compound **10** was followed to obtain compound **36 (80%, α:β = 1:1)** from compound **35** as solid. ^{1}H NMR (400 MHz, Chloroform-*d*) δ 8.03 – 7.86 (m, 20H), 7.78 – 7.52 (m, 3H), 7.46 – 7.34 (m, 17H), 7.33 – 7.18 (m, 57H), 7.117 - 713 (m, 20H), 7.12 (s, 7H), 7.11 – 7.05 (m, 10H), 6.16 (s, 1H), 6.14 (d, *J* = 2.0 Hz, 1H), 5.28 (dd, *J* = 4.0, 2.0 Hz, 1H), 5.26 (d, *J* = 4.0 Hz, 2H), 5.19 – 5.09 (m, 12H), 5.04 (d, *J* = 19.4 Hz, 2H), 4.98 (dt, *J* = 9.2, 3.8 Hz, 5H), 4.93 (d, *J* = 1.6 Hz, 2H), 4.90 – 4.85 (m, 7H), 4.80 (d, *J* = 3.1 Hz, 2H), 4.76 (t, *J* = 2.3 Hz, 2H), 4.74 – 4.71 (m, 4H), 4.70 – 4.67 (m, 5H), 4.65 – 4.52 (m, 13H), 4.45 – 4.41 (m, 4H), 4.33 (t, *J* = 3.7 Hz, 1H), 4.30 – 4.21 (m, 5H), 4.14 – 4.10 (m, 2H), 4.05 (dq, *J* = 13.9, 3.9 Hz, 6H), 3.97 (t, *J* = 4.1 Hz, 1H), 3.91 (q, *J* = 3.5 Hz, 2H), 3.82 (q, *J* = 3.2 Hz, 2H), 3.74 (dt, *J* = 3.3, 1.8 Hz, 2H), 2.34 (td, *J* = 6.8, 1.5 Hz, 5H), 2.17 – 2.08 (m, 4H), 2.07 (s, 3H), 2.04 (dd, *J* = 3.8, 1.9 Hz, 1H), 2.02 (s, 3H), 2.00 (s, 6H), 1.95 (s, 3H), 1.93 (s, 3H). ^{13}C NMR (101 MHz, $CDCl_3$) δ 205.76, 171.32, 170.49, 170.47, 169.11, 169.02, 168.93, 168.75, 168.42, 168.37, 167.61, 166.04, 165.60, 165.41, 165.38, 165.22, 165.18, 164.77, 138.16, 137.75, 137.72, 137.70, 137.45, 137.44, 135.19, 135.12, 135.08, 134.99, 134.96, 133.64, 133.49, 133.46, 133.43, 133.33, 130.20, 130.13, 130.03, 129.99, 129.46, 129.38, 129.20, 129.15, 129.03, 128.96, 128.91, 128.70, 128.64, 128.59, 128.56, 128.49, 128.43, 128.41, 128.38, 128.37, 128.34, 128.31, 128.29, 128.21, 128.20, 128.14, 128.06, 127.92, 127.89, 127.85, 127.80, 127.73, 127.65, 127.55, 101.56, 101.40, 101.02, 101.00, 100.74, 100.54, 91.81, 90.72, 76.73, 76.63, 76.42, 76.23, 76.01, 75.78, 75.70, 75.41, 75.17, 73.69, 73.32, 73.18, 73.10, 73.07, 73.04, 72.53, 72.37, 72.30, 72.23, 72.14, 70.70, 70.55, 69.91, 69.76, 69.02, 68.90, 68.54, 68.52, 68.40, 67.30, 67.13, 67.11, 66.79, 66.78, 66.73, 66.51, 63.03, 62.57, 37.68, 29.69, 29.67, 27.71, 21.06, 20.86, 20.84. HRMS m/z calculated for $C_{110}H_{104}O_{32}Na$:1959.6408; found: 1959.6398.

Benzyl (2-O-benzoyl-3-O-benzyl-4-O-levulinoyl)-α-L-idopyranosyl uronate-α(1→4) benzyl (2-O-benzoyl-3-O-benzyl)-α-L-idopyranosyl uronate-α(1→4) benzyl (2-O-benzoyl-3-O-benzyl)-α-L-idopyranosyl uronate-α(1→4) 1-thiophenyl (6-O-acetyl-2-O-benzoyl, 3-O-benzyl)-α-L-idopyranoside 37

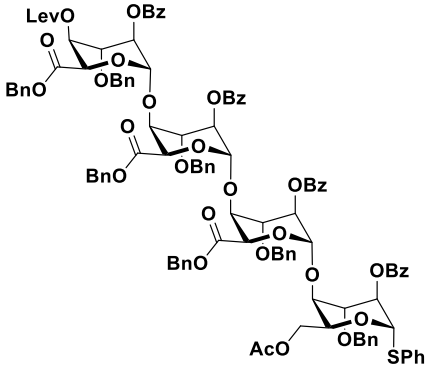

The synthetic procedure for the preparation of compound **11** was followed to obtain compound **37 (80%)** from compound **36** as syrup. ^{1}H NMR (400 MHz, Chloroform-*d*) δ 7.96 (ddd, *J* = 6.8, 6.0, 1.5 Hz, 6H), 7.86 (dd, *J* = 8.3, 1.1 Hz, 2H), 7.58 – 7.53 (m, 3H), 7.47 – 7.43 (m, 1H), 7.42 – 7.36 (m, 7H), 7.34 – 7.27 (m, 12H), 7.25 – 7.04 (m, 29H), 5.53 (s, 1H), 5.40 (dt, *J* = 2.4, 1.1 Hz, 1H), 5.29 (d, *J* = 5.2 Hz, 1H), 5.17 – 5.12 (m, 4H), 5.07 (dd, *J* = 16.1, 12.1 Hz, 2H), 4.98 – 4.97 (m, 1H), 4.96 – 4.90 (m, 2H), 4.87 – 4.84 (m, 4H), 4.79 – 4.67 (m, 6H), 4.59 (ddd, *J* = 15.8, 11.4, 4.1 Hz, 4H), 4.42 (d, *J* = 11.3 Hz, 1H), 4.26 – 4.21 (m, 2H), 4.06 – 4.02 (m, 4H), 3.93 (t, *J* = 3.2 Hz, 1H), 3.79 (t, *J* = 2.5 Hz, 1H), 3.74 (td, *J* = 3.3, 0.9 Hz, 1H), 2.34 (t, *J* = 6.8 Hz, 2H), 2.17 – 2.02 (m, 2H), 1.99 (s, 3H), 1.91 (s, 3H).^{13}C NMR (101 MHz, $CDCl_3$) δ 205.76, 171.33, 170.33, 168.96, 168.33, 167.63, 165.81, 165.36, 165.24, 164.77, 137.93, 137.74, 137.41, 137.26, 136.29, 135.18, 135.12, 134.97, 133.64, 133.52, 133.45, 133.35, 131.76, 130.20, 130.11, 130.02, 129.99, 129.45, 129.39, 129.19, 128.91, 128.88, 128.71, 128.63, 128.59, 128.56, 128.48, 128.44, 128.40, 128.34, 128.26, 128.17, 128.10, 127.96, 127.79, 127.75, 127.67, 127.41, 101.56, 101.29, 100.82, 86.10, 76.74, 76.30, 76.28, 75.58, 73.76, 73.18, 72.84, 72.36, 72.26, 70.89, 69.06, 68.70, 68.55, 68.11, 67.15, 67.11, 66.82, 66.76, 65.85, 63.18, 37.68, 29.67, 27.72, 20.83. HRMS m/z calculated for $C_{114}H_{106}O_{30}SNa$:2009.6387; found: 2009.6379.

Ethoxy-2-azidoethoxyl-O-(benzyl (2-O-benzoyl-3-O-benzyl-4-O-levulinoyl))-α-L-idopyranosyl uronate-α(1→4) benzyl (2-O-benzoyl-3-O-benzyl)-α-L-idopyranosyl uronate-α(1→4) benzyl (2-O-benzoyl-3-O-benzyl)-α-L-idopyranosyl uronate-α(1→4)(6-acetyl-2-O-benzoyl-3-O-benzyl)-α-L-idopyranoside 38

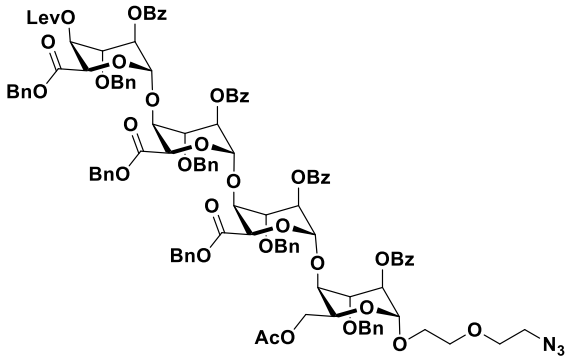

The synthetic procedure for the preparation of compound **12** was followed to obtain compound **38 (70%)** from compound **37** as syrup. ^{1}H NMR (400 MHz, Chloroform-*d*) δ 7.97 – 7.93 (m, 6H), 7.89 – 7.86 (m, 2H), 7.58 – 7.53 (m, 1H), 7.45 – 7.37 (m, 6H), 7.34 – 7.06 (m, 40H), 5.28 (d, *J* = 4.8 Hz, 1H), 5.20 – 5.16 (m, 3H), 5.14 – 5.07 (m, 3H), 5.00 – 4.97 (m, 2H), 4.91 (dd, *J* = 15.6, 3.6 Hz, 3H), 4.86 (t, *J* = 2.7 Hz, 1H), 4.82 (d, *J* = 3.1 Hz, 1H), 4.76 (d, *J* = 2.4 Hz, 1H), 4.73 (d, *J* = 1.8 Hz, 1H), 4.71 (t, *J* = 2.7 Hz, 2H), 4.68 (d, *J* = 2.5 Hz, 1H), 4.66 (d, *J* = 2.8 Hz, 1H), 4.59 – 4.46 (m, 4H), 4.40 – 4.37 (m, 1H), 4.28 (dd, *J* = 11.2, 7.4 Hz, 1H), 4.16 – 4.13 (m, 1H), 4.10 (dd, *J* = 9.0, 4.9 Hz, 1H), 4.04 – 4.01 (m, 1H), 3.92 – 3.87 (m, 2H), 3.81 (s, 1H), 3.77 – 3.73 (m, 2H), 3.71 – 3.67 (m, 3H), 3.65 – 3.61 (m, 3H), 3.56 (ddd, *J* = 10.3, 6.1, 4.0 Hz, 1H), 3.42 – 3.40 (m, 1H), 3.22 – 3.11 (m, 2H), 2.34 (t, *J* = 6.8 Hz, 1H), 2.14 (dt, *J* = 17.2, 6.9 Hz, 1H), 2.89 – 2.04 (m, 1H), 2.00 (s, 3H), 1.94 (s, 3H).^{13}C NMR (101 MHz, CHLOROFORM-*D*) δ 205.74, 171.28, 170.49, 168.76, 168.39, 167.58, 165.74, 165.41, 165.14, 164.73, 138.28, 137.74, 137.37, 137.21, 135.14, 135.05, 134.95, 133.60, 133.44, 133.38, 133.28, 130.16, 130.03, 130.01, 129.95, 129.33, 129.16, 128.90, 128.66, 128.59, 128.53, 128.46, 128.38, 128.32, 128.24, 128.15, 128.07, 127.86, 127.77, 127.67, 127.59, 101.41, 101.32, 100.95, 98.33, 76.25, 76.23, 76.01, 75.57, 74.57, 73.11, 73.00, 72.48, 72.25, 72.09, 70.37, 70.21, 69.85, 68.89, 68.50, 68.23, 67.78, 67.70, 67.09, 67.02, 66.73, 66.66, 64.99, 62.97, 61.91, 50.81, 37.63, 29.63, 27.67, 20.82. HRMS m/z calculated for $C_{112}H_{109}O_{32}N_3Na$:2030.6892; found: 2030.6890.

Ethoxy-2-azidoethoxyl-O-(benzyl (2-O-benzoyl-3-O-benzyl-4-O-levulinoyl)-α-L-idopyranosyl uronate-α(1→4) benzyl (2-O-benzoyl-3-O-benzyl)-α-L-idopyranosyl uronate-α(1→4) benzyl (2-O-benzoyl-3-O-benzyl)-α-L-idopyranosyl uronate-α(1→4)(2-O-benzoyl-3-O-benzyl))-α-L-idopyranoside 39

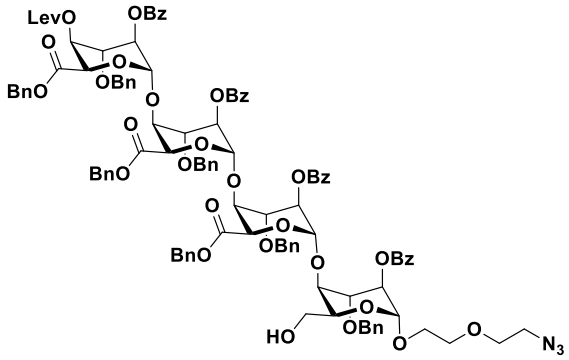

The synthetic procedure for the preparation of compound **13** was followed to obtain compound **39 (80%)** from compound **38** as syrup. ^{1}H NMR (400 MHz, Chloroform-*d*) δ 7.96 – 7.94 (m, 6H), 7.88 (dd, *J* = 8.3, 1.2 Hz, 2H), 7.58 – 7.53 (m, 1H), 7.45 – 7.38 (m, 7H), 7.32 – 7.26 (m, 13H), 7.25 – 7.14 (m, 18H), 7.11 – 7.04 (m, 8H), 5.27 (d, *J* = 4.1 Hz, 1H), 5.21 (d, *J* = 2.8 Hz, 2H), 5.15 – 5.12 (m, 3H), 5.09 (d, *J* = 12.0 Hz, 1H), 4.99 – 4.94 (m, 4H), 4.91 – 4.85 (m, 3H), 4.77 (d, *J* = 2.6 Hz, 1H), 4.71 (ddd, *J* = 9.4, 7.4, 3.7 Hz, 4H), 4.67 – 4.64 (m, 2H), 4.60 – 4.52 (m, 3H), 4.47 (d, *J* = 11.4 Hz, 1H), 4.31 – 4.28 (m, 1H), 4.15 (t, *J* = 2.7 Hz, 1H), 4.09 – 4.05 (m, 3H), 3.94 – 3.88 (m, 3H), 3.81 – 3.73 (m, 2H), 3.69 (dd, *J* = 5.6, 3.7 Hz, 1H), 3.67 – 3.55 (m, 4H), 3.24 – 3.14 (m, 2H), 2.34 (t, *J* = 6.8 Hz, 2H), 2.18 – 2.12 (m, 1H), 2.10 – 2.04 (m, 1H), 2.00 (s, 3H). ^{13}C NMR (101 MHz, $CDCl_3$) δ 205.65, 171.21, 168.64, 168.34, 167.49, 165.66, 165.13, 164.66, 138.32, 137.59, 137.24, 137.12, 135.06, 134.95, 134.84, 133.53, 133.45, 133.39, 133.12, 130.09, 129.94, 129.86, 129.35, 129.25, 128.99, 128.81, 128.47, 128.45, 128.42, 128.38, 128.37, 128.31, 128.27, 128.26, 128.24, 128.22, 128.12, 128.09, 128.06, 128.00, 127.81, 127.66, 127.58, 127.42, 101.19, 101.09, 98.39, 76.59, 76.40, 76.19, 76.13, 75.55, 74.71, 73.01, 72.88, 72.27, 72.20, 72.03, 70.30, 70.21, 70.14, 70.00, 68.93, 68.38, 68.32, 68.03, 67.67, 67.14, 67.02, 66.94, 66.66, 66.62, 61.78, 50.75, 37.55, 29.71, 29.54, 27.59. HRMS m/z calculated for $C_{110}H_{107}O_{31}N_3Na$:1988.6786; found: 1988.6783.

Ethoxy-2-azidoethoxyl-O-(benzyl (2-O-benzoyl-3-O-benzyl-4-O-levulinoyl)-α-L-idopyranosyl uronate-α(1→4) benzyl (2-O-benzoyl-3-O-benzyl)-α-L-idopyranosyl uronate-α(1→4) benzyl (2-O-benzoyl-3-O-benzyl)-α-L-idopyranosyl uronate-α(1→4) benzyl (2-O-benzoyl-3-O-benzyl))-α-L-idopyranoside uronate 40

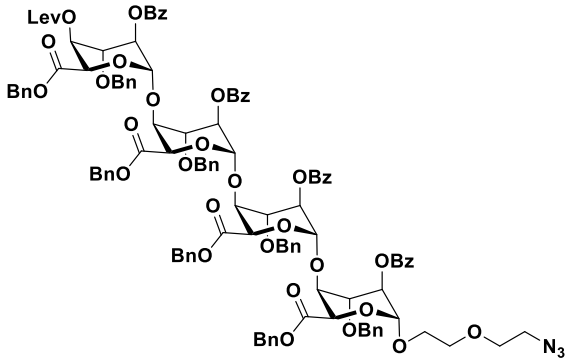

The synthetic procedure for the preparation of compound **14** was followed to obtain compound **40 (65%)** from compound **39** as solid. ^{1}H NMR (400 MHz, Chloroform-*d*) δ 7.94 (tt, *J* = 7.2, 1.3 Hz, 4H), 7.88 (ddd, *J* = 8.4, 4.7, 1.4 Hz, 4H), 7.57 – 7.53 (m, 1H), 7.41 – 7.34 (m, 8H), 7.32 – 7.26 (m, 8H), 7.25 – 7.12 (m, 24H), 7.11 – 7.05 (m, 9H), 6.99 – 6.96 (m, 2H), 5.24 (d, *J* = 2.4 Hz, 1H), 5.21 (d, *J* = 3.5 Hz, 1H), 5.18 (d, *J* = 2.6 Hz, 1H), 5.17 – 5.14 (m, 3H), 5.10 – 5.02 (m, 4H), 4.99 (d, *J* = 1.7 Hz, 2H), 4.97 – 4.96 (m, 1H), 4.92 (d, *J* = 3.1 Hz, 1H), 4.85 (t, *J* = 2.9 Hz, 1H), 4.82 – 4.79 (m, 2H), 4.75 (d, *J* = 2.4 Hz, 1H), 4.72 – 4.65 (m, 6H), 4.59 (dd, *J* = 11.5, 9.1 Hz, 2H), 4.46 (d, *J* = 11.0 Hz, 2H), 4.38 (d, *J* = 11.4 Hz, 1H), 4.22 (t, *J* = 3.4 Hz, 1H), 4.09 (q, *J* = 2.9 Hz, 2H), 3.97 – 3.91 (m, 2H), 3.89 (t, *J* = 3.8 Hz, 1H), 3.85 (t, *J* = 3.7 Hz, 1H), 3.72 (td, *J* = 3.2, 0.9 Hz, 1H), 3.70 – 3.62 (m, 3H), 3.57 – 3.49 (m, 2H), 3.11 (ddd, *J* = 5.8, 4.3, 1.1 Hz, 2H), 2.34 (t, *J* = 6.8 Hz, 2H), 2.18 – 2.02 (m, 2H), 1.99 (s, 3H). ^{13}C NMR (101 MHz, $CDCl_3$) δ 205.77, 171.32, 169.20, 168.54, 168.35, 167.58, 165.69, 165.32, 165.09, 164.76, 138.09, 137.71, 137.48, 137.26, 135.34, 135.22, 135.06, 135.02, 133.64, 133.42, 133.35, 130.24, 130.07, 129.99, 129.37, 129.21, 129.08, 129.06, 128.69, 128.64, 128.59, 128.55, 128.52, 128.50, 128.45, 128.42, 128.36, 128.35, 128.33, 128.27, 128.25, 128.24, 128.12, 127.85, 127.79, 127.62, 101.96, 101.58, 101.11, 98.92, 77.36, 76.69, 76.57, 75.68, 75.54, 74.93, 72.87, 72.80, 72.69, 72.20, 71.95, 70.25, 70.24, 69.37, 68.68, 68.66, 68.57, 68.52, 68.40, 67.79, 67.16, 67.10, 66.95, 66.66, 66.59, 50.79, 37.69, 29.84, 29.67, 27.72. HRMS m/z calculated for $C_{117}H_{111}O_{32}N_3Na$: 2092.7048; found: 2092.7043.

Ethoxy-2-azidoethoxyl-O-(benzyl (2-O-benzoyl-3-O-benzyl))-α-L-idopyranosyl uronate-α(1→4) benzyl (2-O-benzoyl-3-O-benzyl)-α-L-idopyranosyl uronate-α(1→4) benzyl (2-O-benzoyl-3-O-benzyl)-α-L-idopyranosyl uronate-α(1→4) benzyl (2-O-benzoyl-3-O-benzyl)-α-L-idopyranoside uronate 41

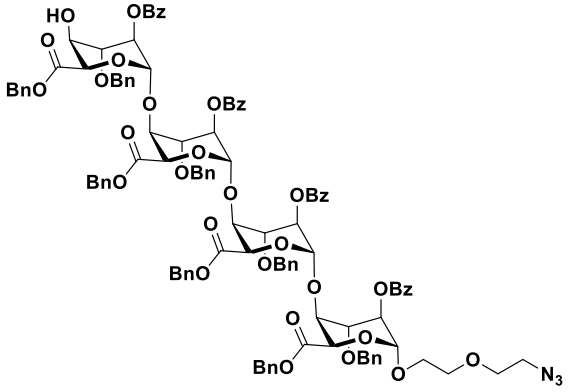

The synthetic procedure for the preparation of compound **15** was followed to obtain compound **41 (80%)** from compound **40** as syrup. ^{1}H NMR (400 MHz, Chloroform-*d*) δ 7.95 – 7.91 (m, 4H), 7.86 (ddd, *J* = 13.4, 8.2, 1.0 Hz, 4H), 7.59 – 7.54 (m, 1H), 7.42 – 7.33 (m, 8H), 7.32 – 7.22 (m, 15H), 7.20 – 7.13 (m, 15H), 7.12 – 7.03 (m, 11H), 6.96 (dd, *J* = 6.6, 3.0 Hz, 2H), 5.22 (dd, *J* = 5.3, 2.9 Hz, 2H), 5.18 – 5.14 (m, 4H), 5.11 – 5.00 (m, 6H), 4.92 (d, *J* = 3.0 Hz, 1H), 4.81 – 4.71 (m, 6H), 4.67 (d, *J* = 3.5 Hz, 1H), 4.65 – 4.56 (m, 3H), 4.51 (dd, *J* = 17.0, 11.5 Hz, 2H), 4.41 (d, *J* = 11.1 Hz, 1H), 4.33 (d, *J* = 11.4 Hz, 1H), 4.21 (t, *J* = 3.2 Hz, 1H), 4.13 (t, *J* = 2.9 Hz, 1H), 4.06 (t, *J* = 2.9 Hz, 1H), 3.98 (t, *J* = 2.9 Hz, 1H), 3.96 – 3.91 (m, 1H), 3.89 (t, *J* = 3.7 Hz, 1H), 3.82 – 3.81 (m, 1H), 3.71 – 3.62 (m, 5H), 3.57 – 3.46 (m, 2H), 3.11 – 3.08 (m, 2H), 2.49 (d, *J* = 10.3 Hz, 1H). ^{13}C NMR (101 MHz, $CDCl_3$) δ 169.19, 168.69, 168.58, 168.31, 165.66, 165.33, 165.12, 164.64, 138.07, 137.74, 137.41, 137.33, 135.33, 135.22, 135.07, 135.04, 133.79, 133.37, 133.33, 130.34, 130.22, 130.03, 129.91, 129.24, 129.18, 129.02, 128.99, 128.92, 128.66, 128.60, 128.57, 128.56, 128.49, 128.47, 128.39, 128.36, 128.32, 128.29, 128.23, 128.21, 128.10, 127.88, 127.79, 127.77, 127.61, 102.05, 101.53, 101.41, 98.91, 76.49, 75.93, 75.59, 74.79, 73.46, 72.77, 72.67, 71.71, 70.24, 69.73, 68.99, 68.70, 68.58, 68.56, 68.39, 68.35, 67.63, 67.18, 66.93, 66.91, 50.78. HRMS m/z calculated for $C_{112}H_{105}O_{30}N_3Na$:1994.6681; found: 1994.6679.

3.5.2.7 Synthesis of Sulfated Tetrasaccharide Analogues (I-40, I-41 and I-45)

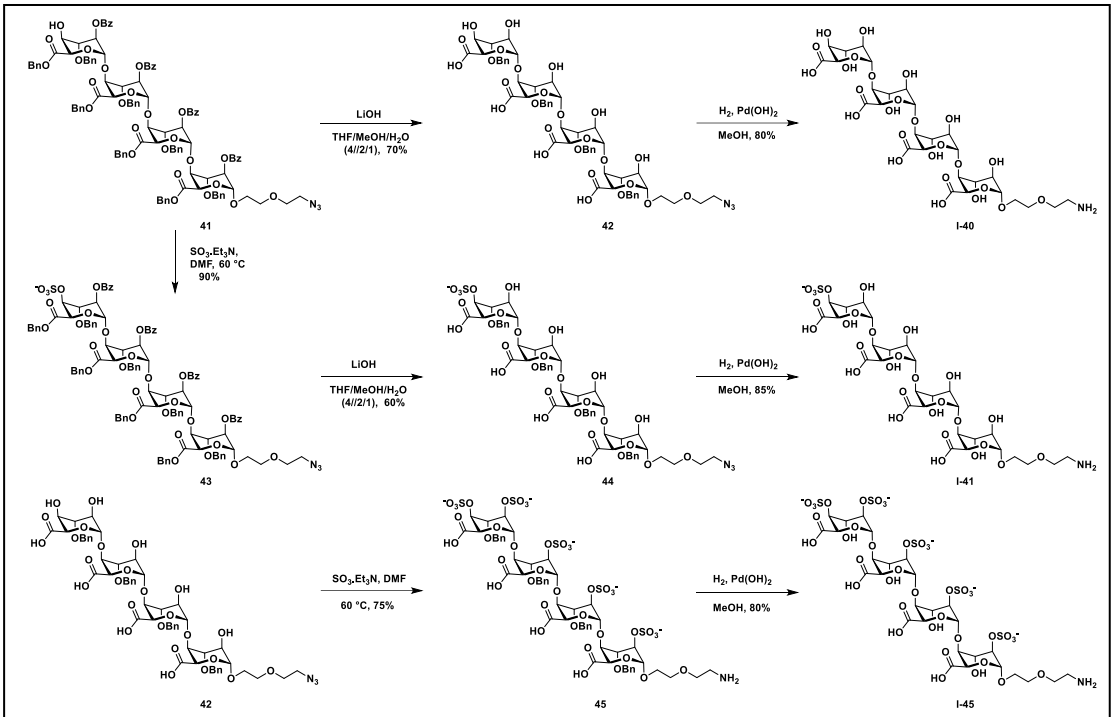

Scheme 7. Synthesis of Tetrsaccharide Sulfated Compounds.

Ethoxy-2-azidoethoxyl-O-((3-O-benzyl)-α-L-idopyranosyl uronic acid-α(1→4)(3-O-benzyl)-α-L-idopyranosyl uronic acid-α(1→4)(3-O-benzyl)-α-L-idopyranosyl uronic acid-α(1→4) (3-O-benzyl))-α-L-idopyranoside uronic acid 42

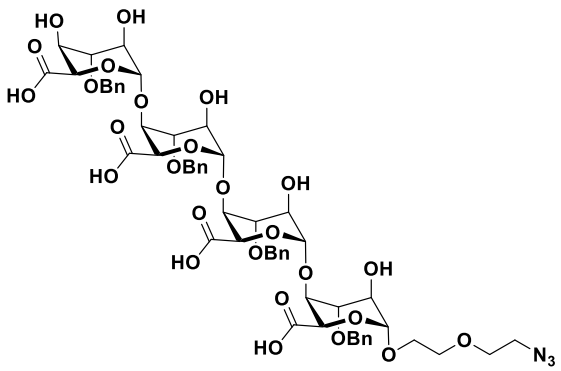

Ester deprotection: Followed general procedure for deprotection of ester yielded compound **42 (70%).** ^{1}H NMR (400 MHz, Methanol-d_4) δ 7.42 – 7.27 (m, 20H), 5.03 (s, 1H), 4.99 (s, 1H), 4.96 (d, J = 2.1 Hz, 1H), 4.94 (s, 1H), 4.79 (d, J = 1.7 Hz, 1H), 4.70 – 4.69 (m, 1H), 4.66 – 4.61 (m, 4H), 4.58 – 4.53 (m, 4H), 4.31 (t, J = 3.2 Hz, 1H), 4.24 – 4.21 (m, 2H), 4.01 (dt, J = 3.4, 1.7 Hz, 1H), 3.95 – 3.89 (m, 1H), 3.80 (t, J = 3.7 Hz, 1H), 3.74 (t, J = 3.4 Hz, 1H), 3.71 – 3.62 (m, 10H), 3.61 – 3.55 (m, 3H), 3.53 (dt, J = 2.7, 1.2 Hz, 1H), 3.40 (dt, J = 2.6, 1.2 Hz, 1H), 3.25 (t, J = 5.0 Hz, 2H). ^{13}C NMR (101 MHz, MeOD) δ 173.43, 173.09, 172.66, 172.52, 139.62, 138.90, 138.78, 138.50, 130.13, 130.04, 129.89, 129.85, 129.81, 129.76, 129.60, 129.50, 129.40, 129.34, 129.22, 128.96,

104.74, 104.62, 104.44, 103.09, 77.02, 76.81, 76.41, 76.19, 76.03, 75.36, 74.83, 73.85, 73.73, 73.52, 71.49, 71.46, 69.82, 69.60, 69.14, 68.84, 68.71, 67.91, 67.37, 62.47, 52.02. HRMS m/z calculated for $C_{56}H_{65}N_3O_{26}Na$: 1218.3754. found: 1218.3750.

Ethoxy-2-azidoethoxyl-O-(benzyl (2-O-benzoyl-3-O-benzyl-4-O-Sulfonato)-α-L-idopyranosyl uronate-α(1→4) benzyl (2-O-benzoyl-3-O-benzyl)-α-L-idopyranosyl uronate-α(1→4) benzyl (2-O-benzoyl-3-O-benzyl)-α-L-idopyranosyl uronate-α(1→4) benzyl (2-O-benzoyl-3-O-benzyl))-α-L-idopyranoside uronate 43

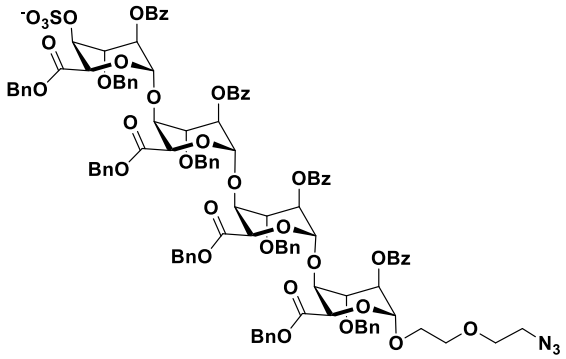

***O*-Sulfation:** Followed general procedure for sulfation yielded compound **43 (90%).** ^{1}H NMR (400 MHz, Methanol-d_4) δ 8.09 (d, *J* = 7.7 Hz, 2H), 7.96 (d, *J* = 7.8 Hz, 2H), 7.88 (dd, *J* = 10.3, 7.9 Hz, 4H), 7.57 (t, *J* = 7.4 Hz, 1H), 7.42 (dd, J = 17.4, 7.6 Hz, 6H), 7.29 – 7.13 (m, 37H), 7.09 (dd, *J* = 4.9, 2.5 Hz, 6H), 7.00 – 6.98 (m, 2H), 5.22 (t, *J* = 3.3 Hz, 2H), 5.09 (ddd, *J* = 15.2, 9.5, 3.5 Hz, 9H), 4.99 – 4.90 (m, 4H), 4.75 – 4.65 (m, 7H), 4.58 (t, *J* = 11.6 Hz, 2H), 4.49 – 4.38 (m, 4H), 4.33 (t, *J* = 3.3 Hz, 1H), 4.20 (t, J = 3.3 Hz, 1H), 4.11 (d, *J* = 3.2 Hz, 2H), 3.97 (t, *J* = 3.6 Hz, 1H), 3.89 (dt, *J* = 19.3, 4.3 Hz, 3H), 3.67 – 3.58 (m, 3H), 3.55 – 3.44 (m, 2H), 3.08 (q, *J* = 4.8 Hz, 2H). ^{13}C NMR (101 MHz, MeOD) δ 170.79, 170.14, 169.87, 169.84, 166.88, 166.85, 166.67, 166.58, 139.26, 139.01, 138.94, 138.71, 136.92, 136.65, 136.60, 136.41, 134.65, 134.49, 134.48, 134.32, 131.41, 131.17, 131.16, 131.00, 130.92, 130.54, 130.37, 130.31, 129.85, 129.59, 129.57, 129.52, 129.50, 129.45, 129.42, 129.40, 129.38, 129.36, 129.32, 129.30, 129.26, 129.23, 129.14, 129.06, 128.99, 128.90, 128.81, 128.68, 102.74, 102.16, 101.63, 99.96, 77.95, 77.30, 77.20, 77.06, 76.60, 76.40, 74.76, 74.18, 73.89, 73.86, 73.53, 73.50, 71.20, 71.11, 70.96, 70.77, 70.23, 70.10, 69.95, 69.78, 69.49, 69.43, 68.80, 68.25, 68.23, 68.18, 67.96, 51.70. HRMS m/z calculated for $C_{112}H_{104}N_3O_{33}S^-$: 2050.6278 found (M-H): 2049.6274.

Ethoxy-2-azidoethoxyl-O-((3-O-benzyl-4-O-sulfonato)-α-L-idopyranosyl uronic acid-α(1→4) (3-O-benzyl)-α-L-idopyranosyl uronic acid-α(1→4) (3-O-benzyl)-α-L-idopyranosyl uronic acid-α(1→4)(3-O-benzyl))-α-L-idopyranoside uronic acid44

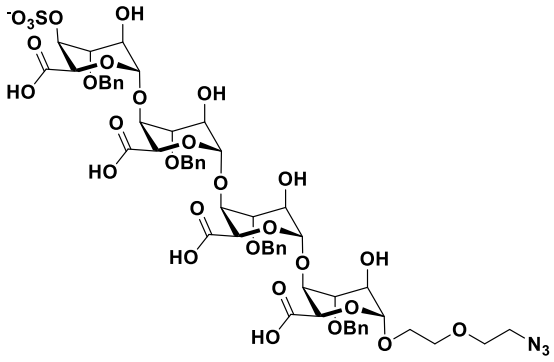

Esters deprotection: Followed general procedure for deprotection of esters yielded compound **44 (60%)**. ^{1}H NMR (600 MHz, Methanol-d_4) δ 7.44 – 7.23 (m, 20H), 5.13 (d, *J* = 3.4 Hz, 2H), 5.10 (s, 1H), 4.88 (s, 2H), 4.84 (d, *J* = 5.2 Hz, 1H), 4.69 – 4.60 (m, 10H), 4.58 – 4.50 (m, 8H), 4.23 (t, *J* = 3.0 Hz, 1H), 3.90 (ddd, *J* = 10.5, 4.9, 3.2 Hz, 1H), 3.82 (d, *J* = 6.1 Hz, 1H), 3.73 (d, *J* = 6.2 Hz, 1H), 3.67 – 3.65 (m, 3H), 3.65 – 3.60 (m, 4H), 3.58 (dd, *J* = 6.1, 4.1 Hz, 1H), 3.57 – 3.56 (m, 1H), 3.51 – 3.50 (m, 1H), 3.19 – 3.13 (m, 2H). ^{13}C NMR (151 MHz, MeOD) δ 176.76, 176.08, 175.94, 175.20, 139.79, 139.21, 138.79, 138.65, 129.92, 129.83, 129.65, 129.60, 129.49, 129.31, 129.26, 128.98, 128.93, 128.89, 128.71, 128.50, 103.95, 103.62, 103.02, 102.79, 76.86, 75.83, 75.41, 75.20, 74.57, 74.54, 74.13, 73.64, 72.98, 72.85, 72.81, 72.72, 71.35, 71.27, 69.81, 69.32, 69.22, 69.01, 68.71, 68.37, 68.29, 68.19, 67.86, 51.71. HRMS m/z calculated for $C_{56}H_{64}N_3O_{29}S^-$: 1274.3352 found: 1274.3342.

Ethoxy-2-aminoethoxyl-O-(α-L-idopyranosyl uronic acid-α(1→4)-α-L-idopyranosyl uronic acid -α(1→4)-α-L-idopyranosyl uronic acid-α(1→4))-α-L-idopyranoside uronic acid I-40

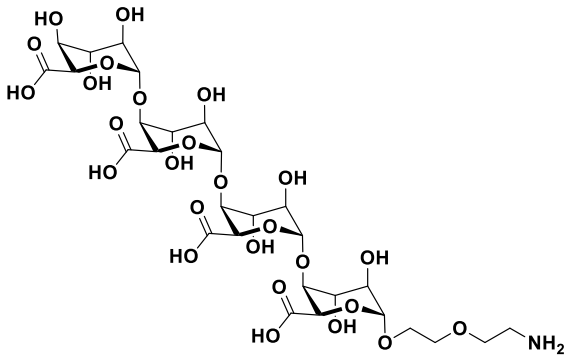

Hydrogenolysis: Followed general procedure for hydrogenolysis yielded compound **I-40 (80%).** ^{1}H NMR (600 MHz, Deuterium Oxide) δ 4.99 – 4.91 (m, 6H), 4.14 (d, *J* = 12.9 Hz, 3H), 4.03 (t, *J* = 3.8 Hz, 1H), 3.92 (dt, *J* = 9.8, 4.5 Hz, 3H), 3.84 (t, *J* = 5.2 Hz, 1H), 3.80 – 3.73 (m, 5H), 3.65 – 3.58 (m, 5H), 3.20 (t, *J* = 5.0 Hz, 2H). ^{13}C NMR (151 MHz, D_2O) δ 173.00, 172.78, 172.72, 102.78, 102.74, 102.64, 101.12, 77.61, 77.58, 77.50, 70.02, 69.83, 69.62, 69.47, 69.25, 69.03, 68.96, 68.84, 68.56, 68.40, 68.05, 67.94, 67.70, 39.01. HRMS m/z calculated for $C_{28}H_{43}NO_{26}Na$: 832.1971 found: 832.1968.

Ethoxy-2-aminoethoxyl-O-((4-O-sulfonato)-α-L-idopyranosyl uronic acid-α(1→4)-α-L- idopyranosyl uronic acid-α(1→4)-α-L-idopyranosyl uronic acid-α(1→4)-α-L-idopyranoside uronic acid I-41

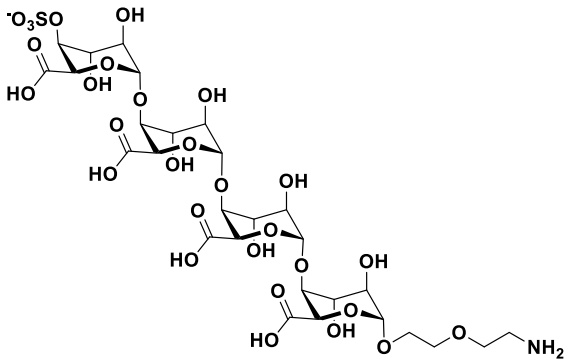

Hydrogenolysis: Followed general procedure for hydrogenolysis yielded compound **I-41 (85%).** ^{1}H NMR (600 MHz, Deuterium Oxide) δ 4.90 (s, 1H), 4.87 – 4.54 (m, 3H), 4.65 (d, *J* = 8.2 Hz, 2H), 4.53 – 4.51 (m, 2H), 4.16 (t, *J* = 3.7 Hz, 1H), 4.03 (d, *J* = 14.3 Hz, 3H), 3.82 (p, *J* = 4.4 Hz, 4H), 3.72 – 3.63 (m, 5H), 3.58 (d, *J* = 4.1 Hz, 1H), 3.52 (dq, *J* = 5.2, 2.5 Hz, 3H), 3.11 (t, *J* = 5.0 Hz, 2H). ^{13}C NMR (151 MHz, D_2O) δ 174.83, 174.64, 174.44, 173.09, 102.68, 102.42, 102.18, 101.00, 77.87, 77.76, 77.37, 75.18, 69.66, 69.34, 68.84, 68.64, 68.42, 68.31, 68.20, 68.07, 68.00, 67.82, 67.52, 67.43, 67.22, 66.18, 38.94. HRMS m/z calculated for $C_{28}H_{42}NO_{29}S^-$: 888.1569 found (M-H): 887.1559.

Ethoxy-2-azidoethoxyl-O-((2-4-O-disulfonato-3-O-benzyl)-α-L-idopyranosyl uronic acid-α(1→4) (2-O-sulfonato-3-O-benzyl)-α-L-idopyranosyl uronic acid-α(1→4) (2-O-sulfonato-3-O-benzyl)-α-L-idopyranosyl uronic acid-α(1→4)(2-O-sulfonato-3-O-benzyl))-α-L-idopyranoside uronic acid 45

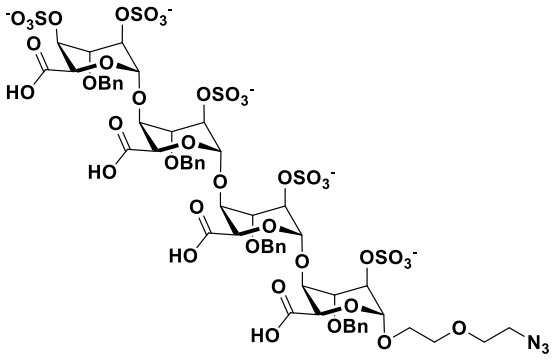

***O*-Sulfation:** Followedgeneral procedure for sulfation yielded compound **45 (75%).** ^{1}H NMR (600 MHz, Deuterium Oxide) δ 753 - 738 (m, 20H), 5.24 (s, 2H), 5.17 (d, *J* = 33.8 Hz, 2H), 4.87 – 478 (m, 6H), 4.74 (d, *J* = 13.8 Hz, 5H), 4.67 (d, *J* = 12.3 Hz, 2H), 4.52 (s, 1H), 4.42 (s, 1H), 4.38 – 4.34(m, 6H), 3.97 (d, *J* = 19.6 Hz, 3H), 3.89 – 3.87 (m, 1H), 3.78 – 3.67 (m, 5H), 3.41 – 3.39 (m, 2H). ^{13}C NMR (151 MHz, D_2O) δ 175.20, 174.75, 174.57, 173.99, 137.19, 137.13, 128.72, 128.65, 128.57, 128.52, 128.24, 128.03, 100.75, 100.44, 100.00, 98.84, 76.14, 74.60, 74.07, 73.93, 72.82, 72.55, 72.39, 72.19, 71.84, 71.71, 71.65, 71.28, 71.17, 70.81, 70.72, 69.42, 69.38, 67.53, 67.49, 67.39, 67.31, 67.06, 50.14. HRMS m/z calculated for $C_{56}H_{60}N_3O_{41}S_5^{5-}$: 318.0267 found: 318.0266.

Ethoxy-2-aminoethoxyl-O-((2-4-O-disulfonato)-α-L-idopyranosyl uronic acid-α(1→4)(2-O-sulfonato)-α-L-idopyranosyl uronic acid-α(1→4) (2-O-sulfonato)-α-L-idopyranosyl uronic acid-α(1→4)(2-O-sulfonato))-α-L-idopyranoside uronic acid I-43

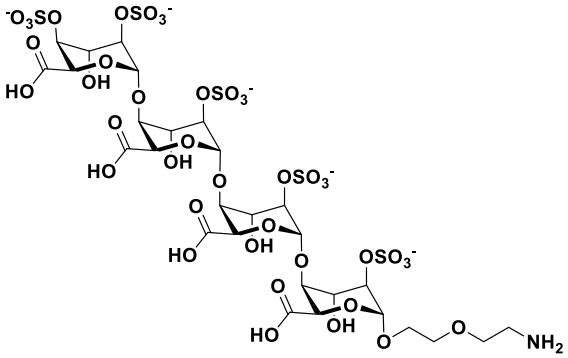

Hydrogenolysis: Followed general procedure for hydrogenolysis yielded compound **I-45 (80%).** ^{1}H NMR (600 MHz, Deuterium Oxide) δ 5.17 – 5.11 (m, 4H), 5.06 (t, *J* = 6.1 Hz, 3H), 4.78 (s, 1H), 4.57 (s, 1H), 4.35 (s, 1H), 4.13 – 4.03 (m, 10H), 3.81 (dt, *J* = 12.1, 4.0 Hz, 1H), 3.74 (dt, *J* = 12.1, 3.8 Hz, 1H), 3.67 (q, *J* = 7.3, 6.1 Hz, 4H), 3.12 (t, *J* = 4.9 Hz, 2H). ^{13}C NMR (151 MHz, D_2O) δ 172.79, 172.36, 171.79, 102.17, 102.03, 101.97, 98.80, 78.81, 78.63, 78.53, 73.31, 73.15, 72.26, 69.63, 67.65, 67.03, 66.76, 66.61, 66.34, 65.57, 39.09. HRMS m/z calculated for $C_{28}H_{38}NO_{41}S_5^{5-}$: 240.7910 found: 240.7909.

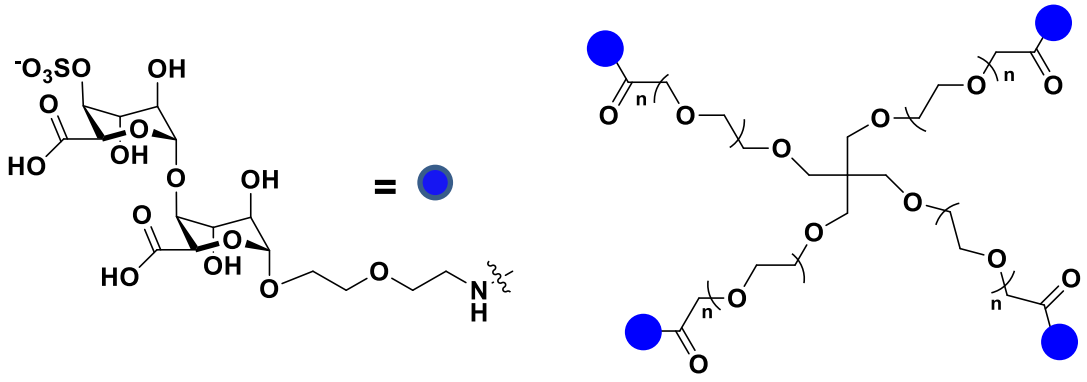

Multivalent Dendrimer (D-I21): ^{1}H NMR (400 MHz, Deuterium Oxide) δ 4.89 – 4.87 (m, 1H), 4.83 (d, *J* = 2.8 Hz, 1H), 4.52 – 4.50 (m, 1H), 4.46 (d, *J* = 2.5 Hz, 1H), 4.19 – 4.17 (m, 1H), 4.01 (s, 2H), 3.89 (s, 2H), 3.81– 3.79 (m, 2H), 3.67- 3.57 (s, 177H), 3.45 – 3.36 (m, 6H). ^{13}C NMR (151 MHz, D_2O) δ 172.59, 102.16, 101.05, 79.97, 78.42, 70.52, 70.23, 69.81, 69.54, 68.68, 67.89, 62.41, 45.01, 38.43.

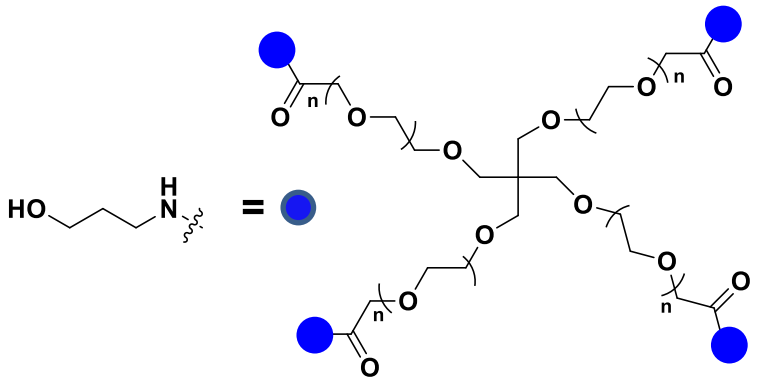

Multivalent Dendrimer (D-L): ^{1}H NMR (400 MHz, Deuterium Oxide) δ 3.99 (s, 2H), 3.80 (dd, J = 5.4, 3.5 Hz, 1H), 3.67- 3.54 (m, 140H), 3.45 – 3.42 (m, 3H), 3.25 (t, J = 6.9 Hz, 2H), 1.70 (p, J = 6.7 Hz, 2H).

3.6 NMR Experiments

3.6.1 General Remarks

All NMR experiments were performed at 10- 35°C on a Bruker AVANCE 2 600 MHz spectrometer equipped with standard triple-channel probe. 500uL samples with typical concentrations of 1-5 mM were prepared by dissolving the purified compounds in D_2O. 1H-NMR resonances of monosaccharides I-10, I-11 and I-12, disaccharides I-20, I-21 and I-23, trisaccharides I-30, I-31 and I-34, and tetrasaccharides I-40, I-41 and I-45 were assigned through standard TOCSY (60 and 90 ms mixing times), NOESY (50-500 ms mixing times), ROESY and HSQC experiments. ^{1}H-NMR assignment was indicated in **figures 4-7.**

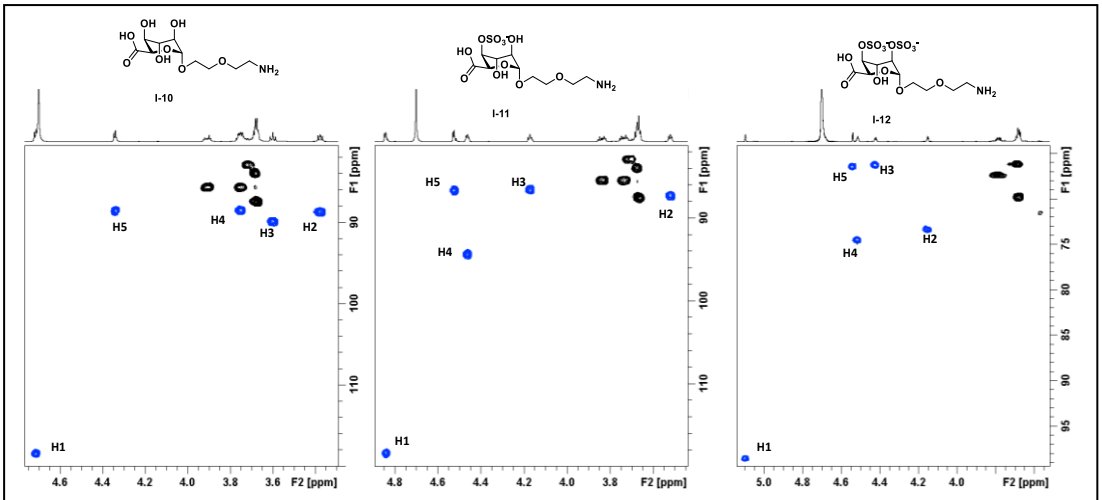

Figure 4. ^{1}H-^{13}C HSQC spectrum of compound **I-10, I-11** ***and*** **I-12** displaying the ^{1}H-NMR assignment.

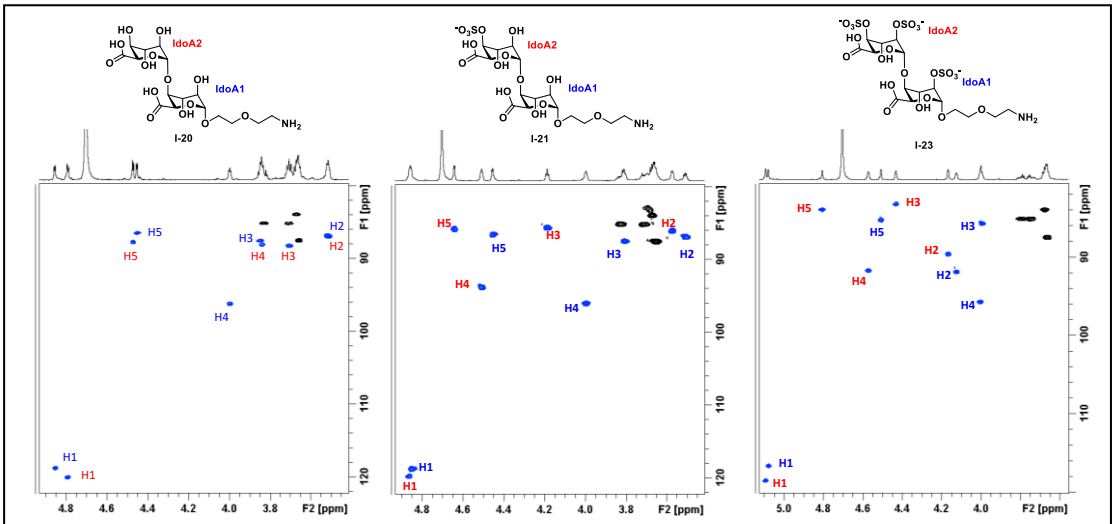

Figure 5. ^{1}H-^{13}C HSQC spectra of compounds **I-20**, **I-21** and **I-23** displaying the ^{1}H-NMR

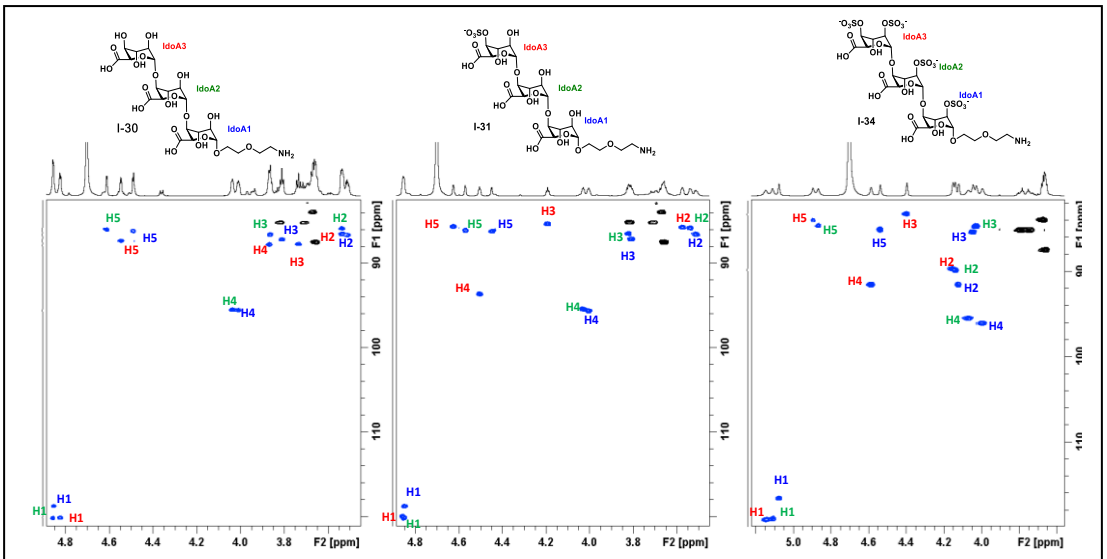

Figure 6. ^{1}H-^{13}C HSQC spectra of compounds **I-30**, **I-31 and I-34** displaying the ^{1}H-NMR assignment.

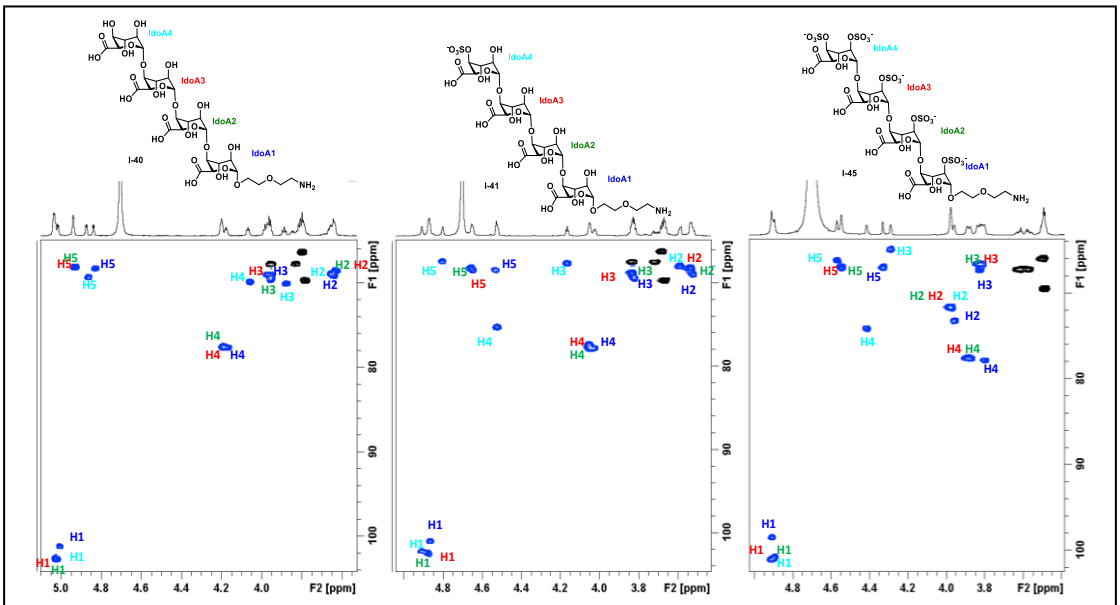

Figure 7. ^{1}H-^{13}C HSQC spectra of compounds **I-40**, **I-41** and **I-45** displaying the ^{1}H-NMR

3.6.2 Conformational Analysis

2D-NOESY experiments of mono-, di-, tri- and tetramers of IdoA were acquired at 600MHz (mixing time varying between 250ms and 600ms). NOE-derived distances for proton-proton pairs were calculated following the isolated spin pair approximation and compared with the theoretical distance of the pure conformers. Intra-residue NOE

cross-peaks between H4 and H5 were used as reference. $^{1}C_{4}$, $^{4}C_{1}$ and $^{2}S_{0}$ conformer distribution was estimated by least sum of square difference analysis of the calculated and experimental NOE intensity and $^{3}J_{HH}$. The theoretical distances and thus, NOE intensities were calculated for DFT optimized geometries of non-, mono-and di-sulfated IdoA monosaccharides, whereas reported theoretical $^{3}J_{HH}$ values for IdoA(2S)[27] were employed for the analysis based on coupling constants. The residual sum of squares (RSS) was used to determine how well the calculated population ratios fit the experimental data. Moreover, the estimated population was indicated as an average of the 10 conformer distributions with lowest RSS. The standard deviation was used to estimate the error in the determined values. Finally, conformer distribution was indicated as an average of the populations derived from analysis of NOE and $^{3}J_{HH}$ data.

Monosaccharide I-10:

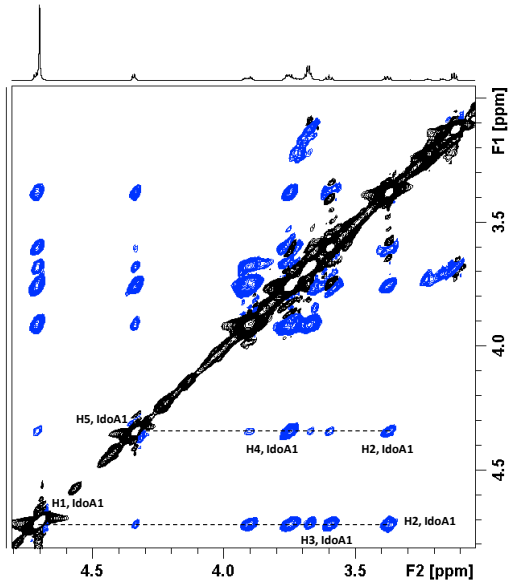

Figure 8. 2D-NOESY spectrum of **I-10** acquired at 25 °C using a mixing time of 600ms. The compound displayed positive NOEs.

Table 2. Conformation plasticity of **I-10**. Key NOEs and $^{3}J_{HH}$ constants employed to determine $^{1}C_4$, $^{4}C_1$ and $^{2}S_0$ contribution were also indicated.

I-10	Measured $^{3}J_{H-H}$ (Hz)				Measured NOE				Conformer Distribution		
	J_{H1-H2}	J_{H2-H3}	J_{H3-H4}	J_{H4-H5}	H1-H2	H1-H3	H2-H4	H2-H5	$^{1}C_4$	$^{4}C_1$	$^{2}S_0$
$^{3}J_{HH}$	5.4	7.3	7.2	4.3					19±4	67±7	15±10
NOE					0.3852	0.4223	0.4956	0.2397	8±5	60±4	33±5
Average									13±8	63±5	24±13

Monosaccharide I-11:

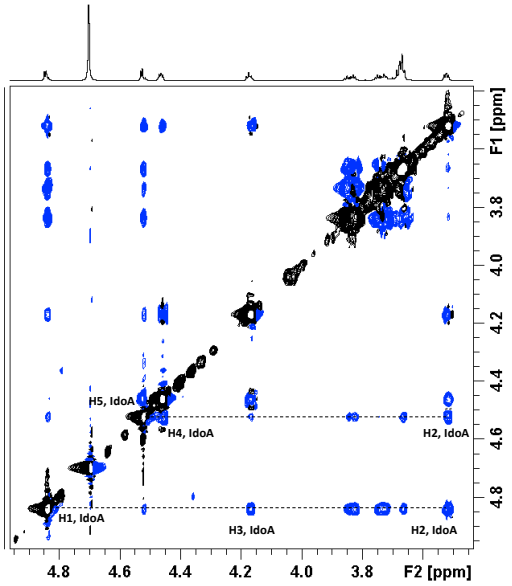

Figure 9. 2D-NOESY spectrum of **I-11** acquired at 25 °C using a mixing time of 600ms. The compound displayed positive NOEs.

Table 3. Conformation plasticity of **I-11**. Key NOEs and $^{3}J_{HH}$ constants employed to determine $^{1}C_4$, $^{4}C_1$ and $^{2}S_0$ contribution were also indicated.

I-11	Measured $^{3}J_{H-H}$ (Hz)				Measured NOE				Conformer Distribution		
	J_{H1-H2}	J_{H2-H3}	J_{H3-H4}	J_{H4-H5}	H1-H2	H1-H3	H2-H4	H2-H5	$^{1}C_4$	$^{4}C_1$	$^{2}S_0$
$^{3}J_{HH}$	3.6	5.3	4.9	3.1					50±4	29±7	21±10
NOE					0.5491	0.2111	0.2656	0.2909	50±4	18±5	33±5
Average									50±4	23±8	27±8

Monosaccharide I-12:

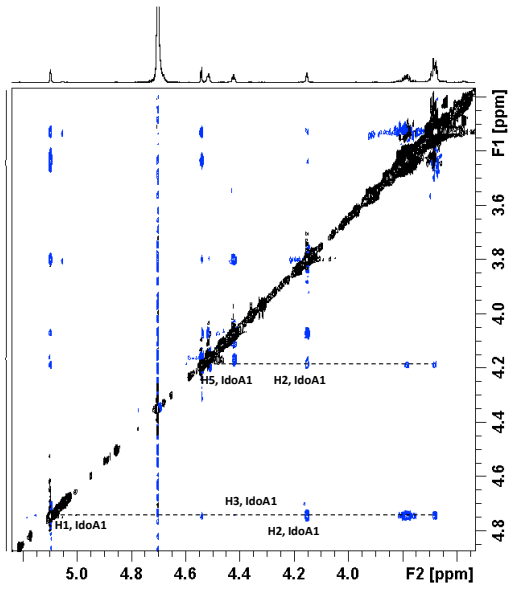

Figure 10. 2D-NOESY spectrum of **I-12** acquired at 25 °C using a mixing time of 600ms. The compound displayed positive NOEs.

Table 4. Conformation plasticity of **I-12**. Key NOEs and $^{3}J_{HH}$ constants employed to determine $^{1}C_4$, $^{4}C_1$ and $^{2}S_0$ contribution were also indicated.

I-12	Measured $^{3}J_{H-H}$ (Hz)				Measured NOE				Conformer Distribution		
	J_{H1-H2}	J_{H2-H3}	J_{H3-H4}	J_{H4-H5}	H1-H2	H1-H3	H2-H4	H2-H5	$^{1}C_4$	$^{4}C_1$	$^{2}S_0$
$^{3}J_{HH}$	1.2	2.6	2.9	2.0					90±5	5±5	5±5
NOE					1.00[a]	0.0603	0.05	0.2042	90±5	5±5	5±5
Average									90±5	5±5	5±5
[a]NOE between H1-H2 was used as reference.											

Disaccharide I-20:

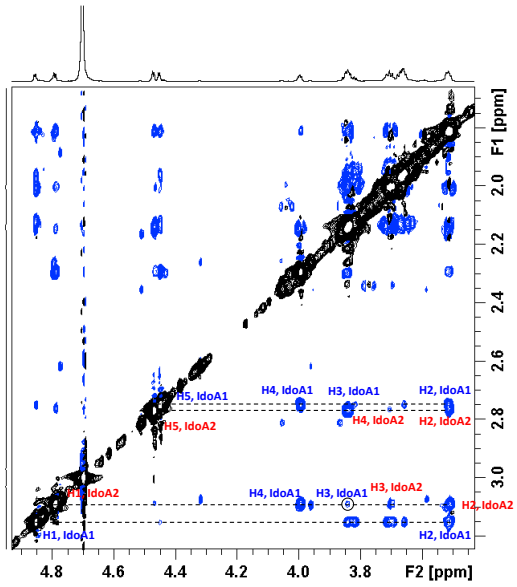

Figure 11. 2D-NOESY spectrum of **I-20** acquired at 25 °C using a mixing time of 600ms. The compound displayed positive NOEs.

Table 5. Conformation plasticity of **I-20**. Key NOEs and $^{3}J_{HH}$ constants employed to determine $^{1}C_4$, $^{4}C_1$ and $^{2}S_0$ contribution were indicated.

I-20	**Measured $^{3}J_{H-H}$ (Hz)**				**Measured NOE**				**Conformer Distribution**		
IdoA2	**J_{H1-H2}**	**J_{H2-H3}**	**J_{H3-H4}**	**J_{H4-H5}**	**H1-H2**	**H1-H3**	**H2-H4**	**H2-H5**	**$^{1}C_4$**	**$^{4}C_1$**	**$^{2}S_0$**
$^{3}J_{HH}$	3.6	5.5	5.5	3.2					49±3	39±7	12±9
NOE					0.4798	0.1274	-	0.1909	64±5	9±5	27±5
Average									56±11	24±22	20±11
IdoA1	**J_{H1-H2}**	**J_{H2-H3}**	**J_{H3-H4}**	**J_{H4-H5}**	**H1-H2**	**H1-H3**	**H2-H4**	**H2-H5**	**$^{1}C_4$**	**$^{4}C_1$**	**$^{2}S_0$**
$^{3}J_{HH}$	3.0	nd	3.5	2.7					67±7	13±8	20±14
NOE					0.7032	-	0.2517	0.4826	53±8	2±3	46±8
Average									59±10	8±8	33±18

Table 6. NOE-derived proton-proton inter-residue distances for compound **I-20**.

Proton	**Proton**	**Volume cross-peak**	**NOE-derived distance(Å)**
H1, IdoA2	H3, IdoA1	0.1274	3.37
	H4, IdoA1	0.9401	2.39
H5, IdoA2	H4, IdoA2	1.000[a]	2.37 (ref)
	H3, IdoA1	-[a]	-
[a]Overlapped with H5, IdoA2-H3, IdoA1 NOE cross-peak.			

NOEs between H1, IdoA2-H3, IdoA1, H1, IdoA2-H4, IdoA1 and H5, IdoA2-H3, IdoA1 proton pairs defined the exo-*syn*-Φ/*syn(*-)-Ψconformation around the linkage IdoAα1-4IdoA.

Disaccharide I-21:

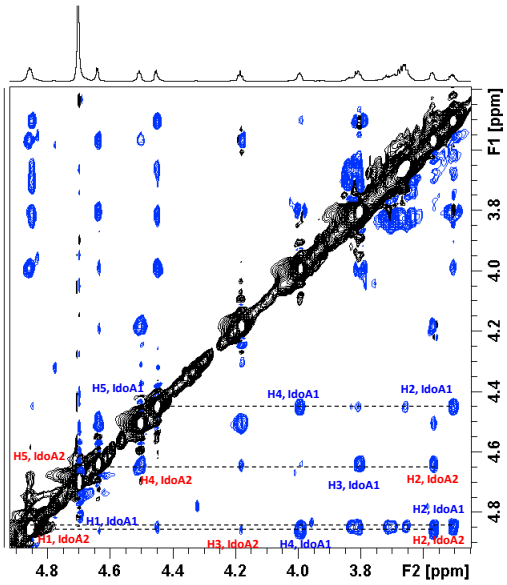

Figure 12. 2D-NOESY spectrum of **I-21** acquired at 25 °C using a mixing time of 600ms. The compound displayed positive NOEs.

Table 7. Conformation plasticity of **I-21**. Key NOEs and $^{3}J_{HH}$ constants employed to determine $^{1}C_4$, $^{4}C_1$ and $^{2}S_0$ contribution were indicated.

I-21	**Measured $^{3}J_{H-H}$ (Hz)**				**Measured NOE**				**Conformer Distribution**		
IdoA2	**J_{H1-H2}**	**J_{H2-H3}**	**J_{H3-H4}**	**J_{H4-H5}**	**H1-H2**	**H1-H3**	**H2-H4**	**H2-H5**	**$^{1}C_4$**	**$^{4}C_1$**	**$^{2}S_0$**
$^{3}J_{HH}$	3.2	3.4	4.0	2.6					72±5	21±5	7±6
NOE					0.9110	0.0589	0.2488	0.4696	71±8	2±3	27±8
Average									71±8	12±14	17±15
IdoA1	**J_{H1-H2}**	**J_{H2-H3}**	**J_{H3-H4}**	**J_{H4-H5}**	**H1-H2**	**H1-H3**	**H2-H4**	**H2-H5**	**$^{1}C_4$**	**$^{4}C_1$**	**$^{2}S_0$**
$^{3}J_{HH}$	3.1	5.2	4.6	2.8					54±4	22±7	24±10
NOE					0.9131	-	0.1688	0.7553	47±11	1±2	52±11
Average									50±5	11±15	39±20

Table 8. NOE-derived proton-proton inter-residue distances for compound **I-21.**

Proton	Proton	Volume cross-peak	NOE-derived distance(Å)
H1, IdoA2	H4, IdoA1	1.7472	2.16
H5, IdoA2	H4, IdoA2	1.000	2.37 (ref)
	H3, IdoA1	0.8957	2.41

NOEs between H1, IdoA2-H4, IdoA1 and H5, IdoA2-H3, IdoA1 proton pairs defined the exo-*syn*-*Φ*/*syn*(-)-*Ψ*conformation around the linkage IdoAα1-4IdoA.

Disaccharide I-23:

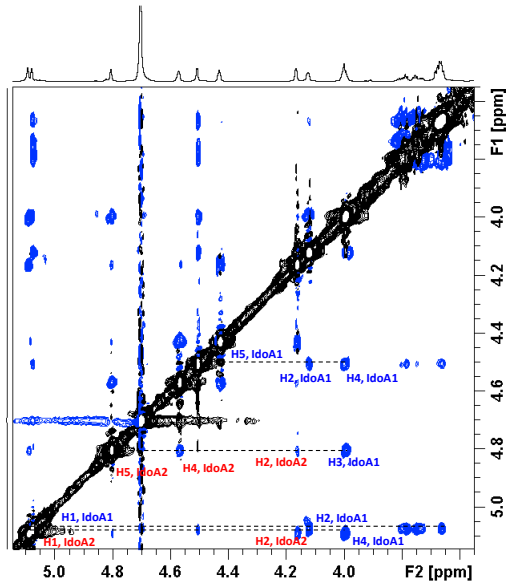

Figure 13. 2D-NOESY spectrum of **I-23** acquired at 25 °C using a mixing time of 600ms. The compound displayed positive NOEs.

Table 9. Conformation plasticity of **I-23**. Key NOEs and $^{3}J_{HH}$ constants employed to determine $^{1}C_4$, $^{4}C_1$ and $^{2}S_0$ contribution were indicated.

I-23	**Measured $^{3}J_{H-H}$ (Hz)**				**Measured NOE**				**Conformer Distribution**		
IdoA2	**J_{H1-H2}**	**J_{H2-H3}**	**J_{H3-H4}**	**J_{H4-H5}**	**H1-H2**	**H1-H3**	**H2-H4**	**H2-H5**	**$^{1}C_4$**	**$^{4}C_1$**	**$^{2}S_0$**
$^{3}J_{HH}$	<2.6	2.5	2.5	1.8					90±5	5±5	5±5
NOE					1.3756	0.0185	0.1655	0.1840	89±7	3±3	8±7
Average									89±1	4±1	7±2
IdoA1	**J_{H1-H2}**	**J_{H2-H3}**	**J_{H3-H4}**	**J_{H4-H5}**	**H1-H2**	**H1-H3**	**H2-H4**	**H2-H5**	**$^{1}C_4$**	**$^{4}C_1$**	**$^{2}S_0$**
$^{3}J_{HH}$	1.5	-	-	2.0					89±6	4±4	7±7
NOE					0.8396	0.2806	-	0.5012	88±8	2±3	10±8
Average									88±1	3±1	9±2

Table 10. NOE-derived proton-proton inter-residue distances for compound **I-23**.

Proton	**Proton**	**Volume cross-peak**	**NOE-derived distance(Å)**
H1, IdoA2	H4, IdoA1	1.9363	2.12
	H3, IdoA1	-[a]	-
H5, IdoA2	H4, IdoA2	1.000	2.37 (ref.)
	H3, IdoA1	1.4691	2.22
[a] Overlapped signal.			

NOEs between H1, IdoA2-H4, IdoA1 and H5, IdoA2-H3, IdoA1 proton pairs defined the exo-*syn*-Φ/*syn(-)*-Ψ conformation around the linkage IdoAα1-4IdoA.

Trisaccharide I-30:

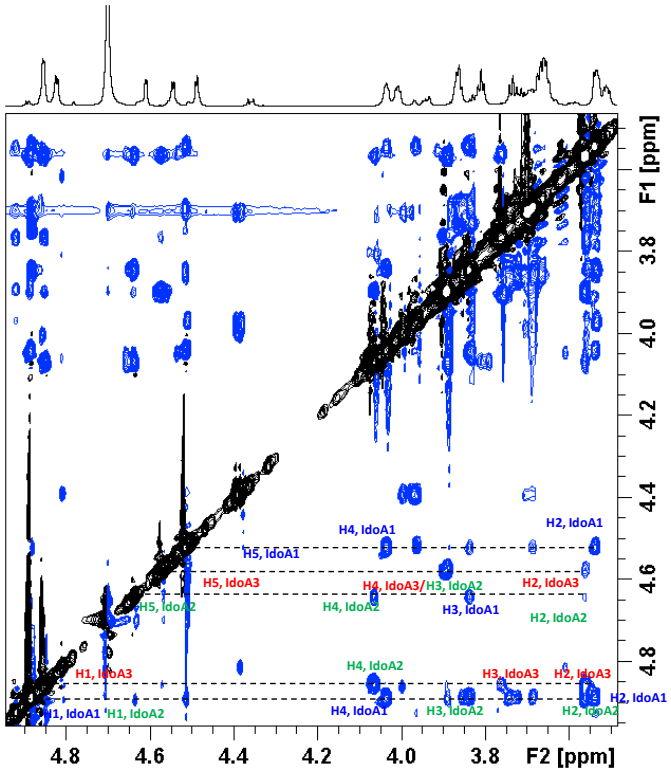

Figure 14. 2D-ROESY spectrum of **I-30** acquired at 25 °C using a mixing time of 500ms.

Table 11. Conformation plasticity of **I-30**. Key NOEs and $^{3}J_{HH}$ constants employed to determine $^{1}C_4$, $^{4}C_1$ and $^{2}S_0$ contribution were indicated.

I-30	**Measured $^{3}J_{H-H}$ (Hz)**				**Measured NOE**				**Conformer Distribution**		
IdoA3	**J_{H1-H2}**	**J_{H2-H3}**	**J_{H3-H4}**	**J_{H4-H5}**	**H1-H2**	**H1-H3**	**H2-H4**	**H2-H5**	**$^{1}C_4$**	**$^{4}C_1$**	**$^{2}S_0$**
$^{3}J_{HH}$	3.1	5.6	5.6	3.0					51±4	33±7	16±10
NOE					0.4803	0.1738	-	0.1865	56±5	17±6	27±5
Average									54±4	25±12	21±8
IdoA2	**J_{H1-H2}**	**J_{H2-H3}**	**J_{H3-H4}**	**J_{H4-H5}**	**H1-H2**	**H1-H3**	**H2-H4**	**H2-H5**	**$^{1}C_4$**	**$^{4}C_1$**	**$^{2}S_0$**
$^{3}J_{HH}$	2.6	-	3.7	2.3					73±5	16±5	11±8
NOE					1.0337	0.2512	0.1780	0.2949	76±6	4±4	20±6
Average									75±2	10±9	15±6
IdoA1	**J_{H1-H2}**	**J_{H2-H3}**	**J_{H3-H4}**	**J_{H4-H5}**	**H1-H2**	**H1-H3**	**H2-H4**	**H2-H5**	**$^{1}C_4$**	**$^{4}C_1$**	**$^{2}S_0$**
$^{3}J_{HH}$	2.9	4.9	4.4	2.6					57±3	15±7	28±9
NOE					0.6320	-	0.2656	0.4199	51±6	4±4	45±6
Average									54±4	10±8	36±12

Table 12. NOE-derived proton-proton inter-residue distances and conformer distribution obtained by least sum of square difference analysis for compound **I-30**.

Proton	Proton	Volume cross-peak	NOE-derived distance(Å)
H1, IdoA3	H4, IdoA2	1.0920	2.33
	H3, IdoA2	0.0590	3.78
H5, IdoA3	H4, IdoA3	1.000[a]	2.37 (ref)
	H3, IdoA2	-[a]	
H1, IdoA2 **H5, IdoA2**	H4, IdoA1	1.7226	2.16
	H4, IdoA2	1.000	2.37 (ref)
	H3, IdoA1	0.8520	2.43
[a] Overlapped signals.			

NOEs between H1, IdoA3-H4, IdoA2, H1, IdoA3-H3, IdoA2, H5, IdoA3-H3, IdoA2, H1, IdoA2-H4, IdoA1 and H5, IdoA2-H3, IdoA1proton pairs defined the exo-*syn*-Φ/*syn*(-)-Ψ conformation around the linkages IdoAα1-4IdoA.

Trisaccharide I-31:

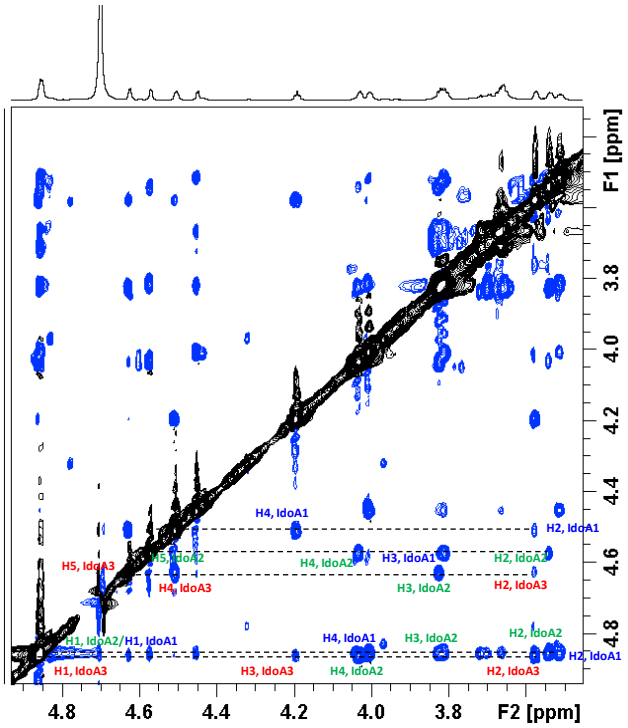

Figure 15. 2D-ROESY spectrum of **I-31** acquired at 25 °C using a mixing time of 500ms.

Table 13. Conformation plasticity of **I-31**. Key NOEs and $^{3}J_{HH}$ constants employed to determine $^{1}C_4$, $^{4}C_1$ and $^{2}S_0$ contribution were indicated.

I-31	**Measured $^{3}J_{H-H}$ (Hz)**				**Measured NOE**				**Conformer Distribution**		
IdoA3	**J_{H1-H2}**	**J_{H2-H3}**	**J_{H3-H4}**	**J_{H4-H5}**	**H1-H2**	**H1-H3**	**H2-H4**	**H2-H5**	**$^{1}C_4$**	**$^{4}C_1$**	**$^{2}S_0$**
$^{3}J_{HH}$	2.5	3.7	3.4	2.5					74±4	12±7	15±9
NOE					1.1538	0.1129	0.1568	0.3300	75±8	2±3	23±8
Average									75±1	7±7	19±6
IdoA2	**J_{H1-H2}**	**J_{H2-H3}**	**J_{H3-H4}**	**J_{H4-H5}**	**H1-H2**	**H1-H3**	**H2-H4**	**H2-H5**	**$^{1}C_4$**	**$^{4}C_1$**	**$^{2}S_0$**
$^{3}J_{HH}$	2.0	4.2	3.8	2.2					71±4	9±7	20±10
NOE					0.800	0.3264	0.0925	0.2516	60±4	12±5	28±5
Average									66±8	10±3	24±5
IdoA1	**J_{H1-H2}**	**J_{H2-H3}**	**J_{H3-H4}**	**J_{H4-H5}**	**H1-H2**	**H1-H3**	**H2-H4**	**H2-H5**	**$^{1}C_4$**	**$^{4}C_1$**	**$^{2}S_0$**
$^{3}J_{HH}$	2.8	4.7	4.1	2.5					60±4	12±5	28±8
NOE					0.7000	0.3316	0.1591	0.2960	60±4	12±5	28±8
Average									60±4	12±5	28±8

Table 14. NOE-derived proton-proton inter-residue distances for compound **I-31**.

Proton	Proton	Volume cross-peak	NOE-derived distance(Å)
H1, IdoA3 H5, IdoA3	H4, IdoA2	2.7917	2.00
	H4, IdoA3	1.000	2.37 (ref)
	H3, IdoA2	1.2857	2.27
H1, IdoA2 H5, IdoA2	H4, IdoA1	1.5352	2.20
	H4, IdoA2	1.000	2.37 (ref)
	H3, IdoA1	0.7932	2.46

NOEs between H1, IdoA3-H4, IdoA2, H5, IdoA3-H3, IdoA2, H1, IdoA2-H4, IdoA1 and H5, IdoA2-H3, IdoA1 proton pairs defined the exo-*syn*-Φ/*syn*(-)-Ψ conformation around the linkages IdoAα1-4IdoA.

Trisaccharide I-34:

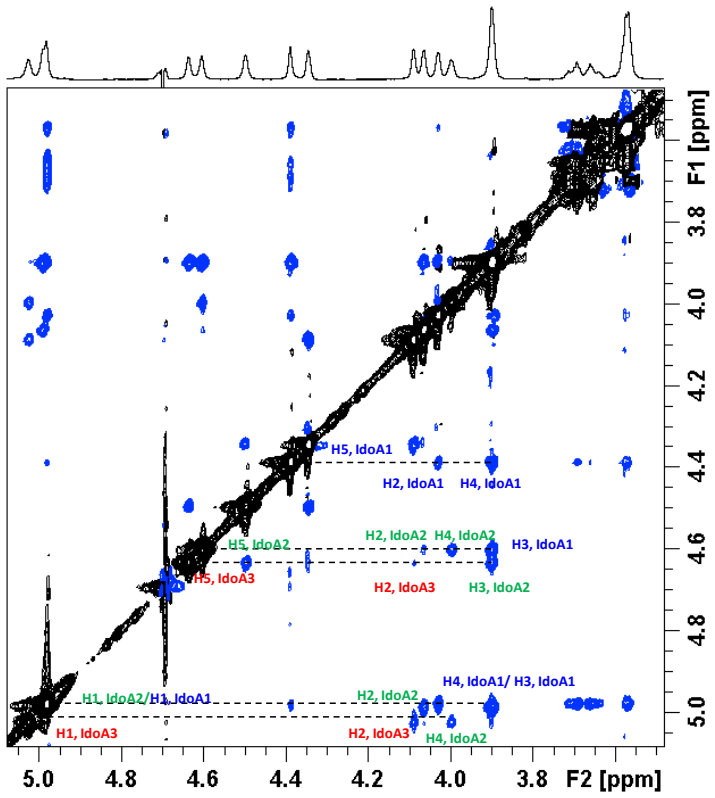

Figure 16. 2D-ROESY spectrum of **I-34** acquired at 17 °C using a mixing time of 250 ms.

Table 15. Conformation plasticity of **I-34**. Key NOEs and $^{3}J_{HH}$ constants employed to determine $^{1}C_4$, $^{4}C_1$ and $^{2}S_0$ contribution were indicated.

I-34	**Measured $^{3}J_{H-H}$ (Hz)**				**Measured NOE**				**Conformer Distribution**		
IdoA3	**J_{H1-H2}**	**J_{H2-H3}**	**J_{H3-H4}**	**J_{H4-H5}**	**H1-H2**	**H1-H3**	**H2-H4**	**H2-H5**	**$^{1}C_4$**	**$^{4}C_1$**	**$^{2}S_0$**
$^{3}J_{HH}$	-	1.7	2.6	-					90±5	5±5	5±5
NOE					0.6308	0.03	0.03	0.0726	90±5	5±5	5±5
Average									90±5	5±5	5±5
IdoA2	**J_{H1-H2}**	**J_{H2-H3}**	**J_{H3-H4}**	**J_{H4-H5}**	**H1-H2**	**H1-H3**	**H2-H4**	**H2-H5**	**$^{1}C_4$**	**$^{4}C_1$**	**$^{2}S_0$**
$^{3}J_{HH}$	-	1.9	-	-					90±5	5±5	5±5
NOE					1.1992	-	0.03	0.1986	90±5	5±5	5±5
Average									90±5	5±5	5±5
IdoA1	**J_{H1-H2}**	**J_{H2-H3}**	**J_{H3-H4}**	**J_{H4-H5}**	**H1-H2**	**H1-H3**	**H2-H4**	**H2-H5**	**$^{1}C_4$**	**$^{4}C_1$**	**$^{2}S_0$**
$^{3}J_{HH}$	1.6	3.2	3.1	-					84±4	8±5	8±7
NOE					0.71	-	0.03	0.1648	86±8	2±3	12±8
Average									85±1	5±4	10±3

Table 16. NOE-derived proton-proton inter-residue distances s for compound **I-34**.

Proton	**Proton**	**Volume cross-peak**	**NOE-derived distance(Å)**
H1, IdoA3 H5, IdoA3	H4, IdoA2	0.6356	2.55
	H4, IdoA3	1.000	2.37 (ref)
	H3, IdoA2	1.5336	2.21
H1, IdoA2 H5, IdoA2	H4, IdoA1	[a]	-
	H4, IdoA2	1.000	2.37 (ref)
	H3, IdoA1	2.6322	2.01

NOEs between H1, IdoA3-H4, IdoA2, H5, IdoA3-H3, IdoA2, H1, IdoA2-H4, IdoA1 and H5, IdoA2-H3, IdoA1 proton pairs defined the exo-*syn*-Φ/*syn(*-)-Ψ conformation around the linkages IdoAα1-4IdoA.

Tetrasaccharide I-40:

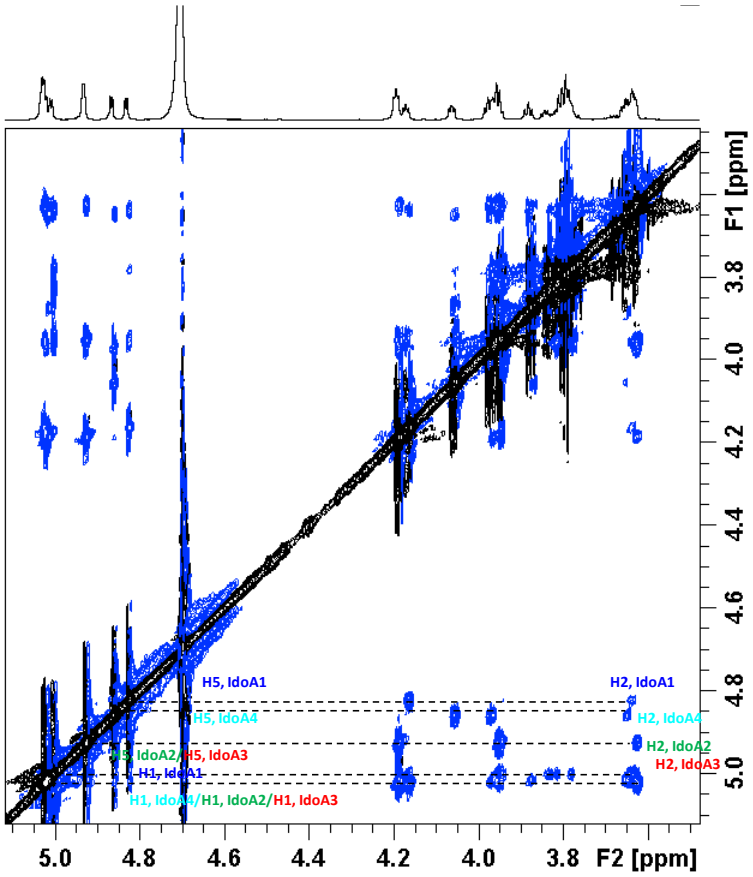

Figure 17. 2D-ROESY spectrum of **I-40** acquired at 35 °C using a mixing time of 300 ms.

Table 17. Conformation plasticity of **I-40**. Key NOEs and $^{3}J_{HH}$ constants employed to determine $^{1}C_4$, $^{4}C_1$ and $^{2}S_0$ contribution were indicated.

I-40	**Measured $^{3}J_{H-H}$ (Hz)**				**Measured NOE**				**Conformer Distribution**		
IdoA4	**J_{H1-H2}**	**J_{H2-H3}**	**J_{H3-H4}**	**J_{H4-H5}**	**H1-H2**	**H1-H3**	**H2-H4**	**H2-H5**	**$^{1}C_4$**	**$^{4}C_1$**	**$^{2}S_0$**
$^{3}J_{HH}$	2.6	5.1	4.7	3					58±3	22±7	20±9
NOE					0.5009	0.2006	0.0517	0.2594	62±6	4±4	35±6
Average									60±2	13±13	27±10
IdoA3/2	**J_{H1-H2}**	**J_{H2-H3}**	**J_{H3-H4}**	**J_{H4-H5}**	**H1-H2**	**H1-H3**	**H2-H4**	**H2-H5**	**$^{1}C_4$**	**$^{4}C_1$**	**$^{2}S_0$**
$^{3}J_{HH}$	3.5	-	4.5	2.4					61±6	25±6	14±11
NOE					0.3587	0.2128	0.1289	0.2031	50±4	12±5	38±5
Average									55±7	19±9	26±17
IdoA1	**J_{H1-H2}**	**J_{H2-H3}**	**J_{H3-H4}**	**J_{H4-H5}**	**H1-H2**	**H1-H3**	**H2-H4**	**H2-H5**	**$^{1}C_4$**	**$^{4}C_1$**	**$^{2}S_0$**
$^{3}J_{HH}$	3.2	-	4.6	3.1					61±5	28±5	11±8
NOE					0.3494	-	0.1552	0.1865	49±5	17±5	34±5
Average									55±9	23±8	22±17

Table 18. NOE-derived proton-proton inter-residue distances for compound **I-40**.

Proton	Proton	Volume cross-peak	NOE-derived distance(Å)
H1, IdoA4	H4, IdoA3	-a	
H5, IdoA4	H4, IdoA4	1.000	2.37 (ref)
	H3, IdoA3	0.6302	2.55
H1, IdoA3/2	H4, IdoA1	a	-
H5, IdoA3/2	H4, IdoA2	1.000	2.37 (ref)
	H3, IdoA1	0.6075	2.56
[a] **Overlapped signals**			

NOEs between H1, IdoA4-H4, IdoA3, H5, IdoA4-H3, IdoA3, H1, IdoA3-H4, IdoA2 (H1, IdoA2-H4, IdoA1) and H5, IdoA3-H3, IdoA2 (H5, IdoA2-H3, IdoA1) proton pairs defined the exo-*syn*-Φ/*syn*(-)-Ψ conformation around the linkages IdoAα1-4IdoA.

Tetrasaccharide I-41:

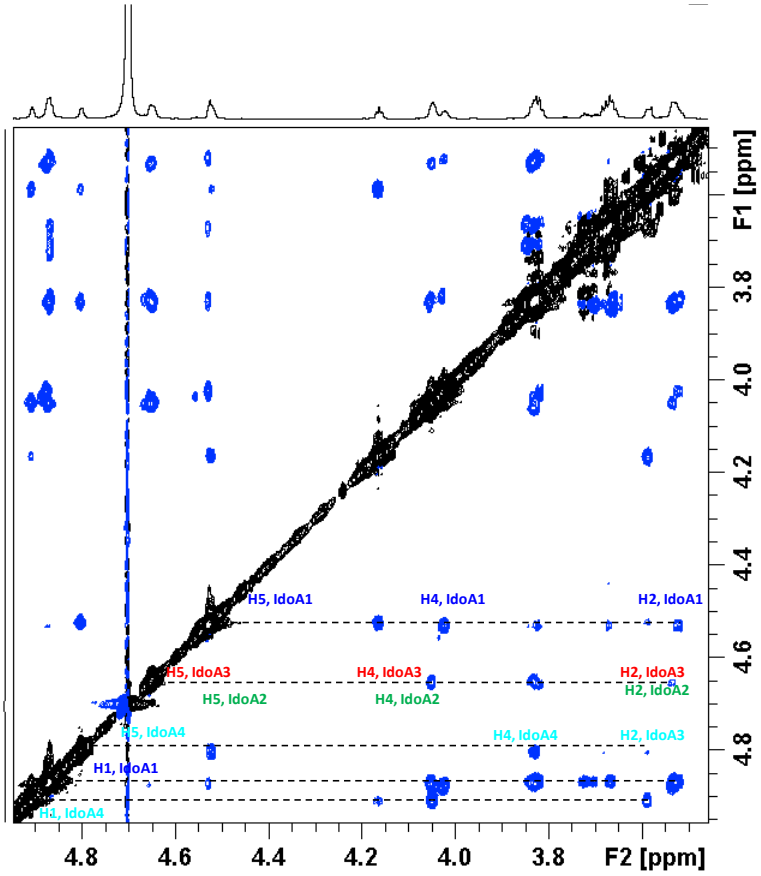

Figure 18. 2D-ROESY spectrum of **I-41** acquired at 25 °C using a mixing time of 250 ms.

Table 19. Conformation plasticity of **I-41**. Key NOEs and $^{3}J_{HH}$ constants employed to determine $^{1}C_4$, $^{4}C_1$ and $^{2}S_0$ contribution were indicated.

I-41	**Measured $^{3}J_{H-H}$ (Hz)**				**Measured NOE**				**Conformer Distribution**		
IdoA4	**J_{H1-H2}**	**J_{H2-H3}**	**J_{H3-H4}**	**J_{H4-H5}**	**H1-H2**	**H1-H3**	**H2-H4**	**H2-H5**	**$^{1}C_4$**	**$^{4}C_1$**	**$^{2}S_0$**
$^{3}J_{HH}$	1.9	3.6	4.1	2.0					80±6	17±7	3±4
NOE					0.7166	0.2712	0.2184	0.2348	66±4	16±6	18±6
Average									73±9	16±1	11±11
IdoA3/2	**J_{H1-H2}**	**J_{H2-H3}**	**J_{H3-H4}**	**J_{H4-H5}**	**H1-H2**	**H1-H3**	**H2-H4**	**H2-H5**	**$^{1}C_4$**	**$^{4}C_1$**	**$^{2}S_0$**
$^{3}J_{HH}$	2.2	4.1	-	2.2					82±6	14±6	4±4
NOE					0.6530	-	0.1621	0.3016	69±7	3±3	28±7
Average									75±9	9±8	16±17
IdoA1	**J_{H1-H2}**	**J_{H2-H3}**	**J_{H3-H4}**	**J_{H4-H5}**	**H1-H2**	**H1-H3**	**H2-H4**	**H2-H5**	**$^{1}C_4$**	**$^{4}C_1$**	**$^{2}S_0$**
$^{3}J_{HH}$	2.9	5.0	4.2	2.6					64±7	33±7	3±3
NOE					0.6333	-	0.2613	0.2941	60±4	7±5	33±5
Average									62±3	20±18	18±21

Table 20. NOE-derived proton-proton inter-residue distances for compound **I-41**.

Proton	**Proton**	**Volume cross-peak**	**NOE-derived distance(Å)**
H1, IdoA4 **H5, IdoA4**	H4, IdoA3	1.7516	2.15
	H4, IdoA4	1.000	2.37 (ref)
	H3, IdoA3	0.7622	2.47
H1, IdoA3/2 **H5, IdoA3/2**	H4, IdoA2	4.9128	1.81[b]
	H4, IdoA3	1.000	2.37 (ref)
	H3, IdoA2	1.1778	2.30

NOEs between H1, IdoA4-H4, IdoA3, H5, IdoA4-H3, IdoA3, H1, IdoA3-H4, IdoA2, H5, IdoA3-H2, IdoA2, H1, IdoA2-H4, IdoA1 and H5, IdoA2-H3, IdoA1 proton pairs defined the exo-*syn*-Φ/*syn*(-)-Ψ conformation around the linkages IdoAα1-4IdoA.

Tetrasaccharide I-45:

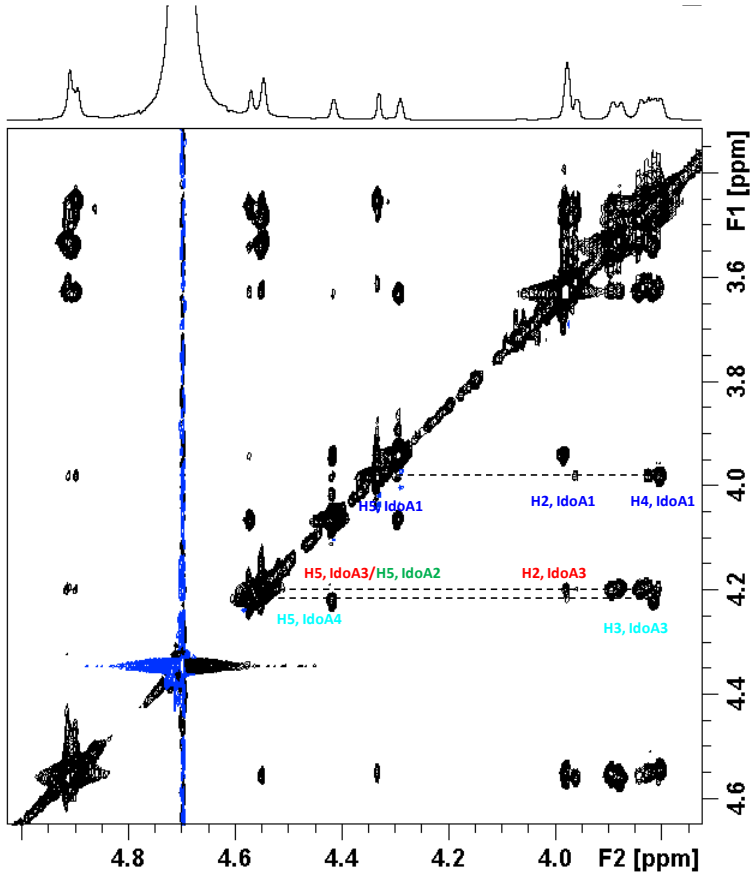

Figure 19. 2D-NOESY spectrum of **I-45** acquired at 10 °C using a mixing time of 300 ms.

Table 21. Conformation plasticity of **I-45**. Key NOEs and $^{3}J_{HH}$ constants employed to determine $^{1}C_4$, $^{4}C_1$ and $^{2}S_0$ contribution were indicated.

I-45	**Measured $^{3}J_{H-H}$ (Hz)**				**Measured NOE**				**Conformer Distribution**		
IdoA4	**J_{H1-H2}**	**J_{H2-H3}**	**J_{H3-H4}**	**J_{H4-H5}**	**H1-H2**	**H1-H3**	**H2-H4**	**H2-H5**	**$^{1}C_4$**	**$^{4}C_1$**	**$^{2}S_0$**
$^{3}J_{HH}$	<2.0	2.6	2.6	1.1					90±5	5±5	5±5
NOE					0.5249	0.003	0.0934	0.1545	80±6	4±4	16±6
$^{3}J_{HH}$	<2.0	2.6	2.6	1.1					90±5	5±5	5±5
IdoA3/2	**J_{H1-H2}**	**J_{H2-H3}**	**J_{H3-H4}**	**J_{H4-H5}**	**H1-H2**	**H1-H3**	**H2-H4**	**H2-H5**	**$^{1}C_4$**	**$^{4}C_1$**	**$^{2}S_0$**
$^{3}J_{HH}$	<2.0	-	<2.0	<2.0					90±5	5±5	5±5
NOE					0.5686	0.1064	0.003	0.0721	84±5	11±7	5±4
Average									87±4	8±4	5±0
IdoA1	**J_{H1-H2}**	**J_{H2-H3}**	**J_{H3-H4}**	**J_{H4-H5}**	**H1-H2**	**H1-H3**	**H2-H4**	**H2-H5**	**$^{1}C_4$**	**$^{4}C_1$**	**$^{2}S_0$**
$^{3}J_{HH}$	1.5	3.1	-	2.0					90±5	5±5	5±5
NOE						0.4048	0.1475	0.0527	72±5	19±5	9±5
Average									81±13	12±10	7±3

Table 22. NOE-derived proton-proton inter-residue distances for compound **I-45**.

Proton	Proton	Volume cross-peak	NOE-derived distance(Å)
H1, IdoA4 H5, IdoA4	H4, IdoA3	1.3931	2.24
	H4, IdoA4	1.000	2.36(ref.)
	H3, IdoA3	1.0686	2.33
H1, IdoA3 H5, IdoA3	H4, IdoA2	1.8013	2.14
	H4, IdoA3	1.000	2.37 (ref)
	H3, IdoA2	1.0804	2.33
H1, IdoA2 H5, IdoA2	H4, IdoA2	2.2975	2.05
	H4, IdoA2	1.000	2.37 (ref)
	H3, IdoA1	0.9094	2.40

NOEs between H1, IdoA4-H4, IdoA3, H5, IdoA4-H3, IdoA3, H1, IdoA3-H4, IdoA2, H5, IdoA3-H3, IdoA2, H1, IdoA2-H4, IdoA1 and H5, IdoA2-H3, IdoA1 proton pairs defined the exo-*syn*-Φ/*syn(*-)-Ψ conformation around the linkages IdoAα1-4IdoA.

3.6.3 Molecular Modelling of IdoA Monosaccharides

Initial model geometries of $^{1}C_{4}$, $^{4}C_{1}$ and $^{2}S_{0}$ conformers for compounds I-10, I-11 and I-12 were generated using the carbohydrate builder module available in the GLYCAM web portal (Glycam Biomolecule Builder), www.glycam.org. Then, the structures were submitted to energy minimization with Gaussian09. DFT calculations were performed at the B3LYP level, with 6-31+d(d,p) basis set, and charge -1, -2 and -3 for no-sulfated, 2-sulfated and 2,4-sulfated IdoA monosaccharides. Proton-proton distances for all optimized structures were also determined and used as theoretical values. **(Fig.1a)**

Table 23. Calculated proton-proton distances of DFT optimized geometries.

Non-sulfated IdoA			
H-H Distances (Å)	**$^1C_4$**	**$^4C_1$**	**$^2S_0$**
H1-H2	2.56	3.06	3.02
H2-H3	2.55	3.06	3.06
H3-H4	2.53	3.05	3.02
H4-H5	2.42	2.37	2.29
H1-H3	4.30	2.63	2.83
H2-H4	4.29	2.55	2.79
H2-H5	4.11	3.98	2.49
H3-H5	3.83	3.85	3.66
4-*O*-sulfated IdoA			
H-H Distances (Å)	**$^1C_4$**	**$^4C_1$**	**$^2S_0$**
H1-H2	2.56	3.06	3.02
H2-H3	2.55	3.06	3.06
H3-H4	2.55	3.05	3.01
H4-H5	2.42	2.36	2.32
H1-H3	4.30	2.66	2.86
H2-H4	4.30	2.65	2.93
H2-H5	4.03	3.97	2.46
H3-H5	3.78	3.86	3.67
2,4-sulfated IdoA			
H-H Distances (Å)	**$^1C_4$**	**$^4C_1$**	**$^2S_0$**
H1-H2	2.58	3.07	3.02
H2-H3	2.56	3.05	3.06
H3-H4	2.56	3.05	3.01
H4-H5	2.38	2.35	2.32
H1-H3	4.29	2.71	2.90
H2-H4	4.26	2.72	2.97
H2-H5	3.98	4.06	2.55
H3-H5	3.81	3.88	3.66

3.6.4 Molecular Modelling of IdoA Disaccharides

Initial geometries of **I-20** were built in MAESTRO suite of programs using the optimized coordinates of the corresponding monosaccharides. The oligosaccharide structures were submitted to an energy minimization with a low gradient convergence threshold (0.05) in 2500 steps employing the AMBER force field. NOE-derived distances were used to check the goodness of the structures modeled. This procedure was performed for I-20 displaying $^1C_4$, $^4C_1$ and $^2S_0$ ring puckering.

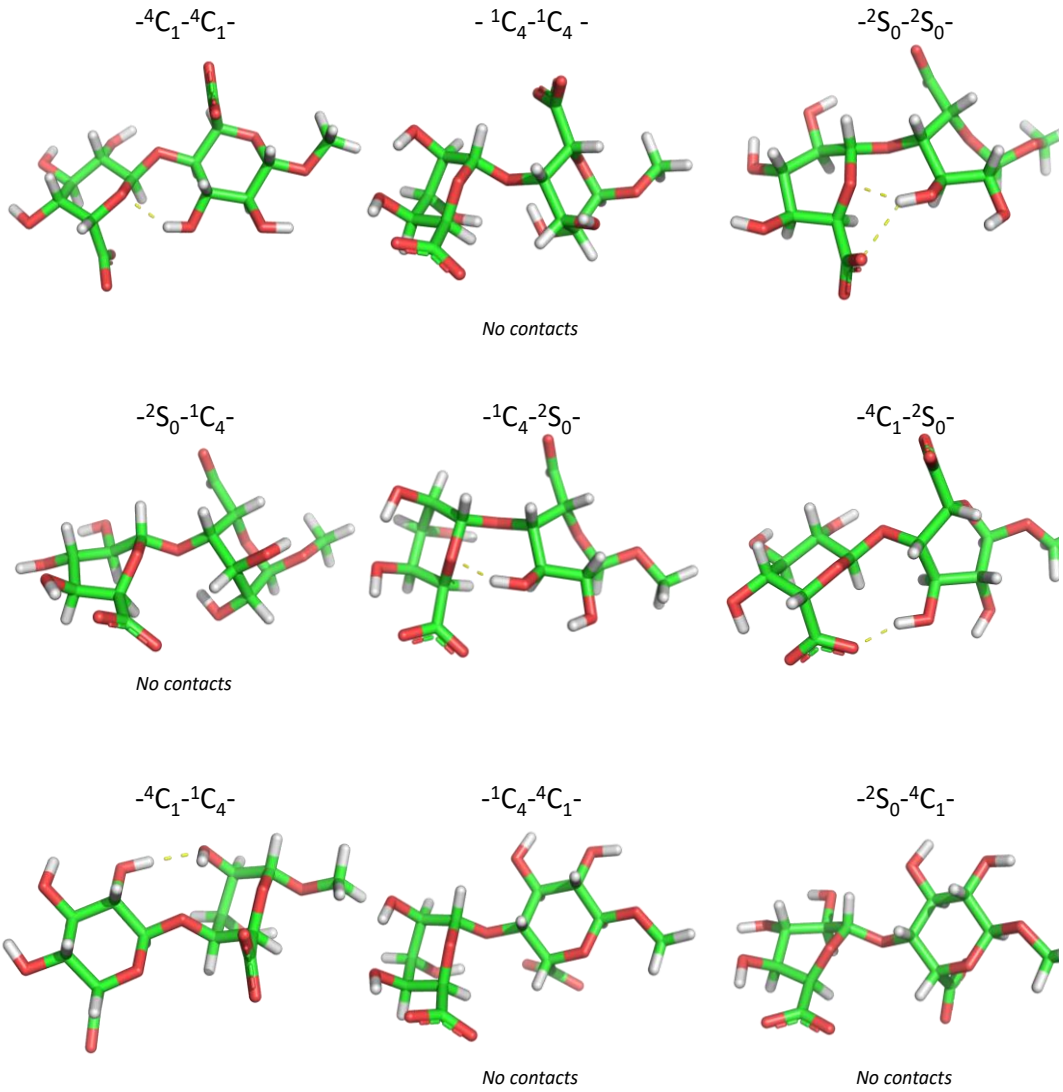

Figure 20. Modeled disaccharide epitopes displaying $^{1}C_{4,}$ $^{4}C_{1}$ and $^{2}S_{0}$ conformations. Inter-residue hydrogen-bond contacts were indicated.

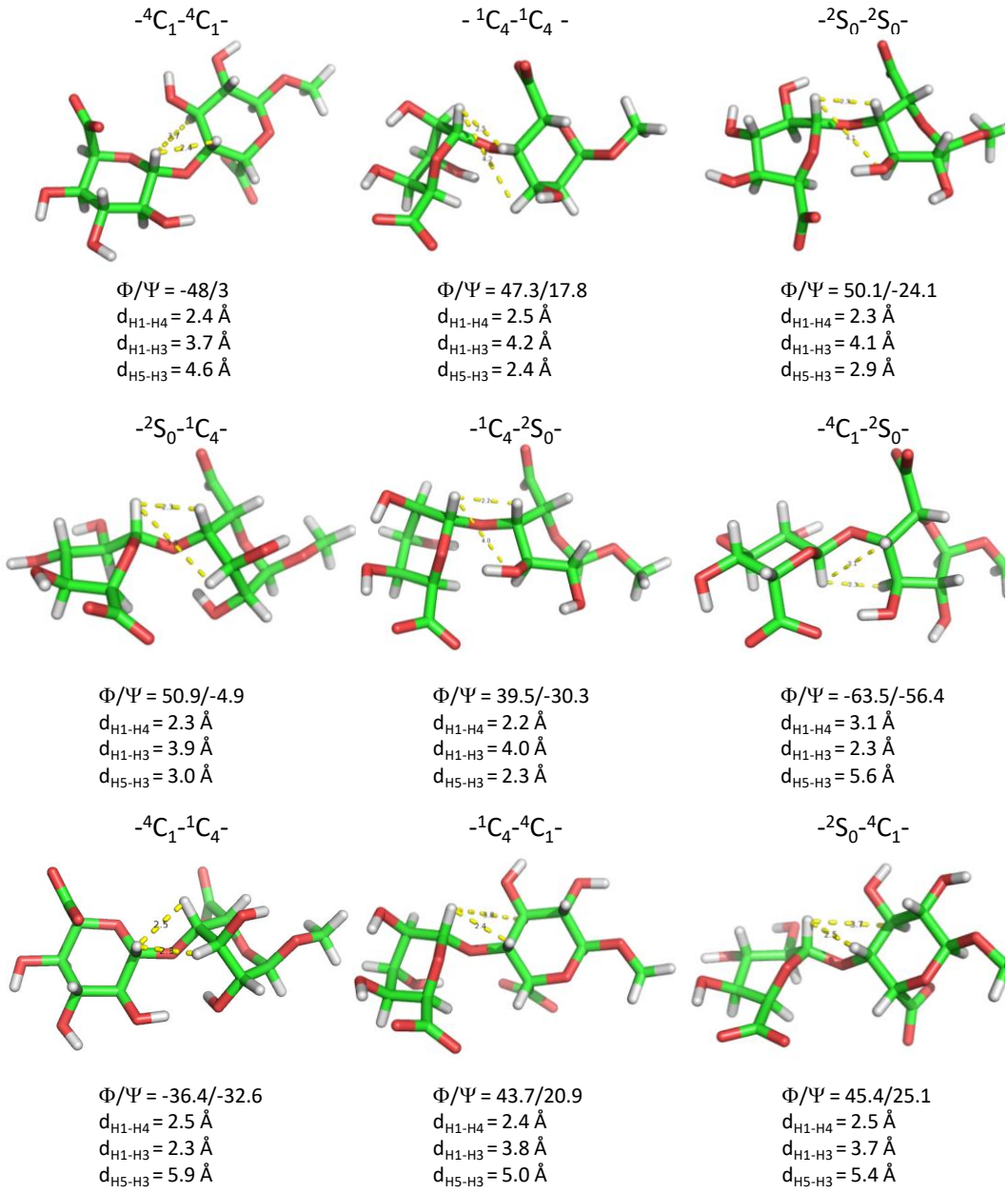

Figure 21. Modeled disaccharide epitopes displaying $^{1}C_{4,}$ $^{4}C_{1}$ and $^{2}S_{0}$ conformations. Key inter-residue proton-proton distances were indicated. The exo-*syn*-*Φ*/*syn*(+)-*Ψ* conformers of disaccharides displaying $^{4}C_{1}$-$^{2}S_{0}$, $^{4}C_{1}$-$^{1}C_{4}$ ring puckering were those displaying short and long inter-residue H1-H4 and H1-H3 distances, respectively; however, minimization procedure of these structures yielded exo-*syn*-*Φ*/*syn*(-)-*Ψ* conformers.

3.6.5 Molecular Modelling of IdoA Tetrasaccharides

Initial geometries of I-40, I-41 and I-45 displaying the $^{1}C_{4}$-$^{1}C_{4}$, $^{1}C_{4}$-$^{2}S_{0}$, and $^{2}S_{0}$-$^{1}C_{4}$ conformational pairswere built in MAESTRO suite of programs using the optimized coordinates of the corresponding IdoA forms. The oligosaccharide structures were submitted to an energy minimization with a low gradient convergence threshold (0.05) in 2500 steps employing the AMBER force field. NOE-derived distances were used to check the goodness of the structures modelled **(Fig. 1c).**

3.6.6 Docking Study of FGF2/I-34 and VEGF165/I-2 Complex

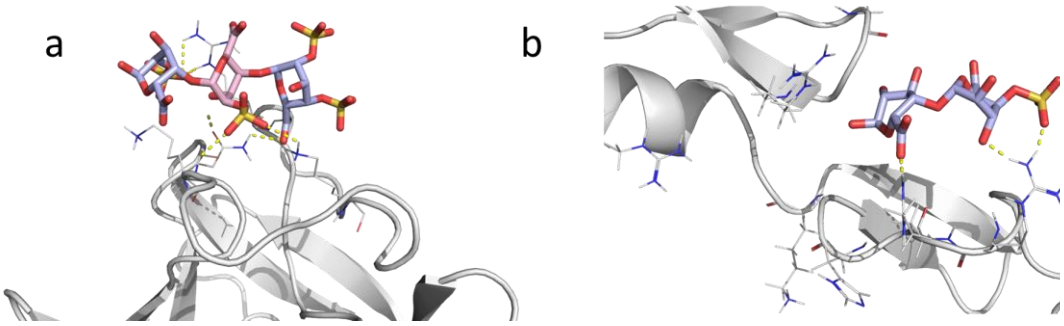

Figure 22. (a) A possible model for the FGF2/**I-34** complex. The structure **of I-34** was manually superimposed in the FGF2 binding site, employing the X-ray structure of the FGF2 complexed with a HSGAG hexasaccharide (pdb file 1bfc) as submitted to energy optimization using MACROMODEL. The three residues display the $^{1}C_{4}$ chair conformation. Two sulfate groups and one carboxylate moiety display stabilizing interactions with positively charged amino acid residues (Lys, Arg) at the protein. (b) A possible model for the $VEGF_{165}$ (pdb code 2VGH) with a docked **I-21** structure. A modelled complex between $VEGF_{165}$ and heparin heptasaccharide was used as a template. A possible model for the FGF2/**I-21** complex. The structure **of I-21** was manually superimposed in the possible $VEGF_{165}$ binding site, as described in literature.[2]The two residues display the $^{1}C_{4}$ chair and $^{2}S_{0}$ conformations. One sulfate group and one carboxylate moiety display stabilizing interactions with positively charged amino acid residues (Lys, Arg) at the protein

3.7 Glycan Microarray

3.7.1 General Information

Human $VEGF_{165}$ (AF-100-20), human HB-EGF (100-47), human Amphiregulin (100-55B), human BMP2 (AF-120-02), biotinylated-rabbit-anti-human $VEGF_{165}$ (500-P10BT), biotinylated-rabbit-anti-human HB-EGF (500-P329BT), biotinylated-rabbit-anti-humanamphiregulin (500-P322BT), anti-human BMP2 (500-P195BT), were all from Peprotech. Human FGF2 basic recombinant (RP-8626) and polyclonal biotinylated-anti-human-FGF2 antibody (PA1-25521) were purchased from Thermo

Fischer. Cy3-sterptavidin was purchased from Jackson ImmunoResearch. All growth factors were rehydrated according to manufacturer instructions, diluted with blocking buffer (PBS pH 7.4, 1% ovalbumin) to the highest concentration tested (20, 5 or 2 ng/µl according to manufacturer recommendations, (see **Table 24**), serially diluted 1:1 twice and immediately applied to the microarray blocks. Biotinylated detections of each growth factor were all diluted in PBS to 1 ng/µl. Secondary streptavidin detection was diluted in PBS.

3.7.2 Heparin-saccharide Glycan Microarray Fabrication

Arrays were fabricated with NanoPrint LM-60 Microarray Printer (Arrayit) on epoxide-derivatized slides (PolyAn 2D) with four 946MP3 pins (5 µm tip, 0.25 µl sample channel, ~100 µm spot diameter; Arrayit). Primary-amine containing glycoconjugates were distributed into 384-well source plates using 7 µl per well. Each glycoconjugate was printed at 50 µM and 100 µM in an optimized printing buffer (300 mM phosphate buffer, pH 8.4), four replicate spots per glycan. Control glycans were printed as well, namely, natural heparin as positive control at 50 µM and 100 µM, and four additional sialylated Siaα2–3/6-glycans as negative controls at 100 µM,[48] Neu5,9Ac_2α3Galβ3GalNAcα$ProNH_2$(9OAc-Acα3Core1α), Neu5Gc9Acα3Galβ3GalNAcα$ProNH_2$(9OAc-Gcα3Core1α), Neu5Acα6Galβ4GlcNAcβ$ProNH_2$(Acα6LacNAcβ), Neu5Gcα6Galβ4GlcNAcβ$ProNH_2$ (Gcα6LacNAcβ). Each slide contained 16 identical blocks, each nano-printed with all the listed glycans (array VrHI.01). To monitor printing, AlexaFlour-555-hydraside was also printed per block (Invitrogen A20501MP, at 1 ng/µl in 178 mM phosphate buffer, pH 5.5). The humidity level in the arraying chamber was maintained at ~70% during printing. Printed slides were left on arrayer deck over-night, allowing humidity to drop to ambient levels (40-45%). Next, slides were packed, vacuum-sealed and stored at room temperature (RT) until used.

3.7.3 Heparin-saccharide Glycan Microarray Binding Assay

Slides were developed and analyzed as previously described[48] with some modifications. Slides were rehydrated with dH_2O and incubated for 30 min in a staining dish with 50 °C pre-warmed ethanolamine (0.05 M) in Tris-HCl (0.1 M, pH 9.0) to block the remaining reactive epoxy groups on the slide surface, then washed with 50 °C pre-

warmed dH_2O. Slides were centrifuged at 200×*g* for three min then fitted with ProPlate™ Multi-Array 16-well slide module (Grace Bio-lab) to divide into the sub-arrays (blocks). Slides were washed with PBST (PBS pH 7.3 + 0.1% Tween 20), aspirated and blocked with 200 µl/sub-array of blocking buffer (PBS pH 7.3 + 1% w/v Ovalbumin grade V, Sigma) for 1 hour at RT with gentle shaking. Next, the blocking solution was aspirated and 100 µl/block of growth factor proteins (for each detection, 3 serially decreasing concentrations were used, see Table S21) diluted in blocking buffer, were incubated with gentle shaking for 2 hours at RT. Slides were washed 4 times with PBST, then with PBS for 2 min. Bound antibodies were detected by incubating with biotinylated secondary detections (1 ng/µl, see Table S21) diluted in PBS, at 200 µl/block at RT for 1 hour. Slides were washed 4 times with PBST, then with PBS for 2 min and biotinylated antibodies detected with Cy3-sterptavidin (1.2µg/ml). Slides were washed 4 times with PBST, then with PBS for 10 min followed by removal from ProPlate™ Multi-Array slide module and immediately dipping in a staining dish with dH_2O for 10 min with shaking. Slide then were centrifuged at 200×*g* for 3 min. and the dry slides immediately scanned.

Table 24. Primary and secondary antibodies and detection concentrations used on the array.

Primary growth factor detection	Concentrations examined on glycan microarray (ng/µl)	Secondary detection
Human FGF2 (basic recombinant)	20, 10, 5	Polyclonal biotinylated-anti-human-FGF2
Human VEGF-165	5, 2.5, 1.25	Biotinylated-rabbit-anti-human VEGF-165
Human HB-EGF	20, 10, 5	Biotinylated-rabbit-anti-human HB-EGF
Human Amphiregulin	20, 10, 5	Biotinylated-rabbit-anti-human Amphiregulin
Human BMP2	2, 1, 0.5	anti-human BMP-2

3.7.4 Array slide processing

Processed slides were scanned and analyzed as described at 10 µm resolution with a Genepix 4000B microarray scanner (Molecular Devices) using 350 gain. Image analysis was carried out with Genepix Pro 4.0 analysis software (Molecular Devices).

Spots were defined as circular features with a variable radius as determined by the Genepix scanning software. Local background subtraction was performed. RFU from each spot was calculated and ranking was used to compare the data between detections; each detection was tested at 3 dilutions. For each detection protein and at each dilution, the binding RFU's of the glycans were listed, maximum RFU was determined and set as 100% binding while all the others were calculated in comparison to the max. Next, the rank for each glycan was averaged between the three dilutions and SEM calculated.

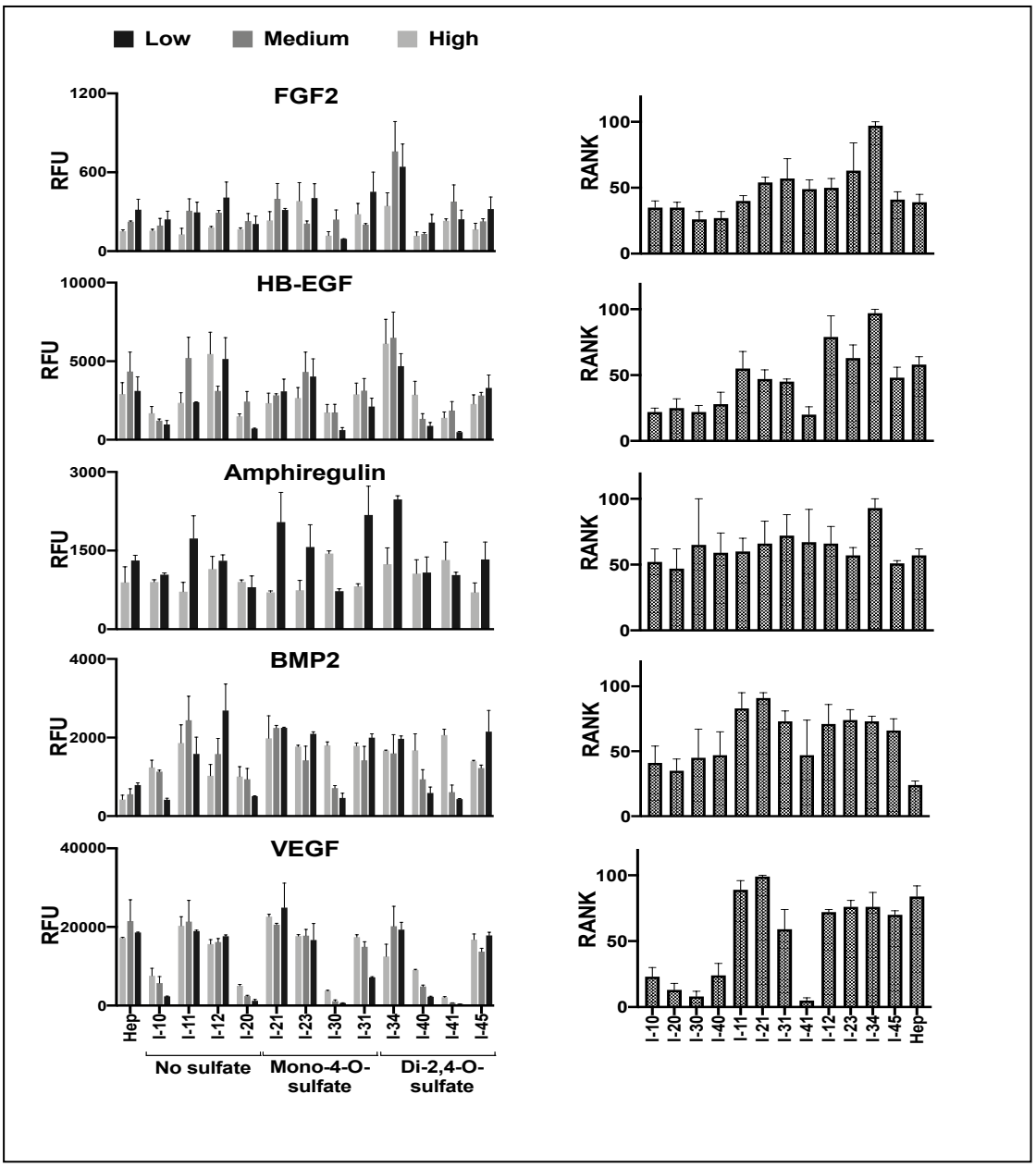

Figure 23. Growth factors glycan microarray binding assay: (a). Binding was tested at 3 serial dilutions, then detected with the relevant biotinylated secondary antibody (1 μg/ml) followed by Cy3-Strepavidin (1.5 μg/ml). Arrays were scanned and relative fluorescent units (RFU) calculated. (a) RFU binding of

growth factors to 100 µM glycans printed at four replicates. (b) Rank binding of growth factors (each at three dilutions) to glycans printed at four replicates each. For each binding assay per printed block, the maximum RFU was determined and set as 100% binding. Then binding to all the other glycans in the same block was ranked in comparison to the maximal binding, and average rank binding (and SEM) for each glycan across the three examined concentrations of each growth factor was calculated. This analysis allowed to compare the glycan binding profiles of the different growth factors and dissect their binding preferences.

3.7.5 Surface Plasmon Resonance Binding Kinetics

I-21 and propanol amine linker (control cell) (1 mM) was covalently immobilized on CM5 sensor surface using a coupling and active ester and amine coupling reaction. For K_D experiments, immobilized **I-21** and control linker was treated with different growth factors at a flow rate of 50 µL/min and 25 °C. HBS-EP buffer without growth factor was then flowed over the sensor surface for 3 min to enable dissociation. Kinetic analysis was performed using the BIAevaluation software for T100. Association and dissociation phase data were globally fitted to a simple 1:1 interaction model.

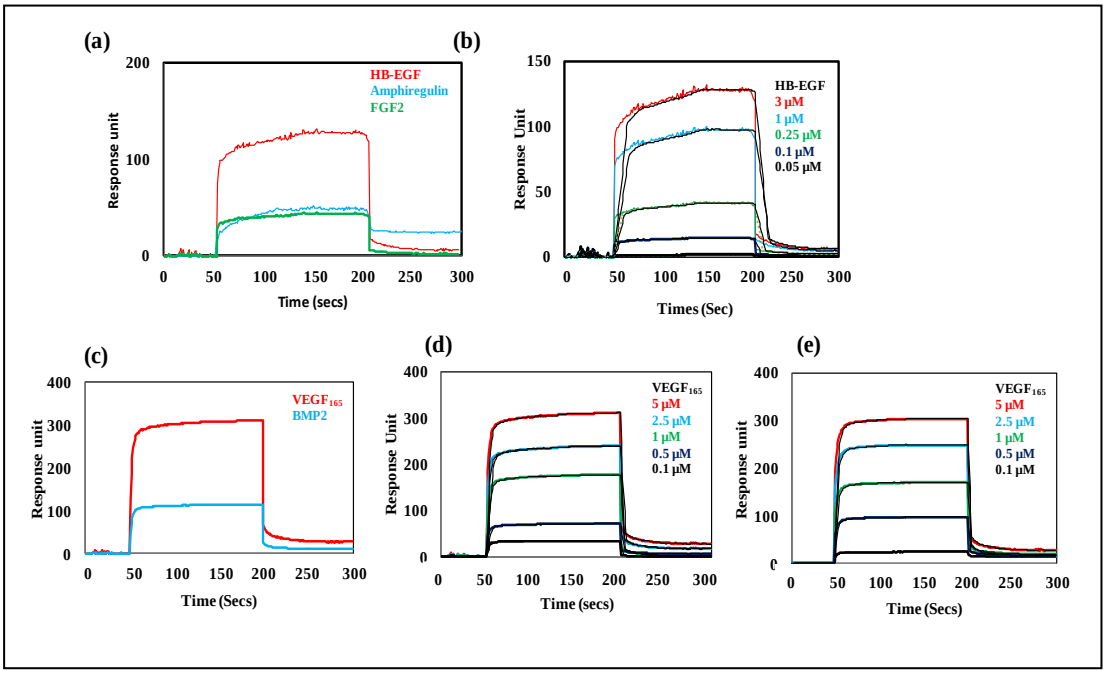

Figure 24. SPR analysis of growth factors binding profile on sensor chip having 1-34, I-11 and I-21 ligands: (a) binding profiles of growth factors (HB-EGF, FGF2 and amphiregulin with I-34 ligand. I-34 wasw immobilized on CM5 sensor chip. The protein samples were flowed for 150 secs at 3 µ M in HBS-EP buffer. At the end of the sample injection. The dissociation was performed by using same buffer for another 100 secs.; (b)SPR binding analysis of the interaction between HB-EGF and **I-34**, concentrations of HB-EGF were 0.05–3 µM. A global fit according to a 1:1 binding model was applied (black curves), resulting in a dissociation constant (K_D) of 4.98 ± 0.6 µM, k_{on} of $3.4 \pm 0.3 \times 10^4\ M^{-1}\ s^{-1}$, and k_{off} of

$1.7 \pm 0.38 \times 10^{-1}\ s^{-1}$: (c) SPR binding profiles of $VEGF_{165}$ and BMP2 on **I-11**; (d) SPR binding analysis of the interaction between $VEGF_{165}$ and I-11, concentrations of $VEGF_{165}$ were 0.1–5 μM. dissociation constant (K_D) of 3.27 ± 0.22 μM, k_{on} of $5.76 \pm 0.2 \times 10^4\ M^{-1}\ s^{-1}$, and k_{off} of $1.9 \pm 0.16 \times 10^{-1}\ s^{-1}$; (e) SPR binding analysis of the interaction between $VEGF_{165}$ and I-21, concentrations of $VEGF_{165}$ were 0.1–5 μM. dissociation constant (K_D) of 3.15 ± 0.7 μM, k_{on} of $5.78 \pm 0.2 \times 10^4\ M^{-1}\ s^{-1}$, and k_{off} of $1.83 \pm 0.5 \times 10^{-1}\ s^{-1}$.Additional SPR binding experiment to further support the microarray data were performed by immobilizing **I-11** and **I-21** on CM5 gold chips and determining real-time binding affinities with $VEGF_{165}$ and BMP2. The SPR results confirmed that $VEGF_{165}$ bound best to **I-11**, followed by BMP-2 (**Fig 5c**). The K_D values of **I-11** and **I-21** with $VEGF_{165}$ were 3.27 and 3.15 μM, respectively (**Fig 5d & 5e**).

3.7.6 Cell Proliferation Assay

HUVECs were placed on 24 well plates in a EBM-2 medium in 1% FBS without growth supplements. Cells were incubated for 4 hr before the experiments. Dendrimers (**D-I21** and **D-L**) at different concentration (10 to 80 μg/ml) were preincubated with $VEGF_{165}$ (20 ng/ml). and added to the cells. After 48 h of incubation, cells were washed and fixed with paraformaldehyde. Cell were stained with 4% sulforhodamine B in 1% acetic acid for 30 min and washed with 1% acetic acid solution. Cells were dissolved in 200 ml of 10 mM Tris pH 8.8 and transferred to 96-well plate for reading on a microplate reader at 540 nm.

3.7.7 Western Blotting

HUVECs were cultured in EBM-2 having 20 ng/ml of $VEGF_{165}$ and different concentrations of **D-I21** (10-80 μg/ml) for 1 h at 37 °C. The cells were then lysed. The cell extracts were subjected to SDS–PAGE and later transferred to polyvinylidene difluoride (PVDF) membranes. The membranes were incubated with a primary antibody (against β-actin, VEGF receptor-2 or pVEGF receptor-2 [Tyr 951]) for 24 h at 4 °C. Then, they were incubated for 1 h at room temperature with HRP-conjugated respective secondary antibody. Finally developed by using chemiluminescent substrate.

3.7.8 Wound Healing Assay

HUVEC cells were cultured on 24-well plates EBM-2 media. After monolayer formation, a wound was created by using 1000 μl pipette tip. Cells were then treated with D-I21 (50 μg/ml) and $VEGF_{165}$ or $VEGF_{165}$ alone (20 ng/ml). After 12 h, $VEGF_{165}$ treated monolayer showed complete wound healing, which was considered as 100%

wound healing, and at that point, the percentage of cell migrated in other wells were quantified

3.7.9 Tube Formation Assay

Matrigel with a reduced amount of growth factor was spread evenly over an 8-well imaging chamber well for 1 h at 37 °C. Approximately 10^4 cells well of HUVEC cells were coated on matrigel in DMEM media with 1% FBS supplemented. To this, $VEGF_{165}$ (20 ng/ml) growth factor with or without **D-I21** ligand (20 µg/ml) were added. After 12 h of incubation, cells were fixed and stained with Calcein AM and imaged in confocal microscopy.

3.8 References

1. Wardrop, D. & Keeling D. The story of the discovery of heparin and warfarin. *Br. J. Haematol.* **141**, 757-763 (2008).
2. Lever, R., Mulloy, B. & Page, C. P. Heparin-A century of progress. *Handbook of Experimental Pharmacology*. Springer, Berlin, Germany. 281-305 (2012).
3. Bishop, J. R., Schuksz, M. & Esko, J. D. Heparan sulfate proteoglucans fine-tune mammalian physiology. *Nature*, **446**, 1030-1037 (2007).
4. Whitelock J. M. & Iozzo, R. V. Heparan sulfate: A complex polymer charged with bilogical activity. *Chem. Rev.***105**, 2745-2764 (2005).
5. Lindahl, U., Couchman, J., Kimmata K. & Esko, J. D. *Essentials of Glycobiology, 3rd edition* (Eds: Varki, A. et al.), Cold spring Harbor Laboratory press, Chapter **17** (2015-2017).
6. Lever, R. & Page, C. P. Novel drug development opportunities for heparin. *Nat. Rev. Drug. Discov*. **2**, 140-148 (2002).
7. Esko, J. D. & Lindahl, U. Molecular diversity of heparan sulfate. *J. Clin. Invest*. **108**, 169-173 (2001).
8. Shriyer, Z., Capilla, I., Venkataraman, G. & Sasisekharan, R. Heparin and heparan sulfate: Analyzing structure and microheterogeneity. *Handb. Exp. Pharmacol*. **207**, 159-176 (2012).

9. Mende, M. et al. Chemical synthesis of glycosaminoglycans. *Chem. Rev.***116**, 8193-8255 (2016).
10. Pwar, N. J. et al. Expedient synthesis of core disaccharide building blocks from natural polysaccharides for heparan sulfate oligosaccharide assembly. *Angew. Chem. Int. Ed.* **58**, 18577-18583 (2019).
11. Tsai, C. T., Zulueta, M. M. L. & Hung, S. C. Synthetic heparin and heparan sulfate: probes in defining biological functions. *Curr. Opin. Chem. Bio.* **40**, 152-159 (2017).
12. Xu. D., Arnoid, K. & Liu. J. Using structurally defined oligosaccharides to understand the interaction between proteins and heparan sulfate. *Curr. Opin. Struct. Biol*. **50**, 155-161 (2018).
13. Liu, J. & Lindhardt, R. J. Chemoenzymatic synthesis of heparan sulfate and heparin. *Nat. Prod. Resp*. **31**, 1676-1685 (2014).
14. Heiss, C. & Azadi, P. Structural analysis of glycosaminoglycans-An indispensible toold for the diagnosis, treatment and prevention of human disease. *Glycobiology and Human diseases*(Edit by Wiederschain, G) CRC press 1st edition. 26-64 (2016).
15. Capila, I. &Linhardt, R. J. Heparin-protein interactions. *Angew. Chem. Int. Ed.***41**, 390-412 (2002).
16. Xu, D. &Esko, J. D. Demystifying heparan sulfate-protein interactions. *Annu. Rev. Biochem.***83,** 129-157 (2014).
17. Yamada, M. & Hamaguchi, T. The sulfation code for propagation of neurodegenration. *J. Bio. Chem*. **293**, 10841-10842 (2018).
18. de Costa, D. S., Reis, R. L. & Pashkuleva, I. Sulfation of glycosaminoglycans and its implications in human health and disorders. *Annu. Rev. Biomed. Eng*. **19**, 1-26 (2017).
19. Hu, Y. -P. et al. Divergent synthesis of 48 heparan sulfate-based disaccharides and probing the specific sugar-fibroblast growth factors-1 interaction. *J. Am. Chem. Soc.***134**, 20722-20727 (2012).
20. Zulueta, M. M. L., Chyan C.-L. & Hung, S.-C. Structural analysis of synthetic heparan sulfate oligosaccharides with fibroblast growth factors and heparin-binding hemagglutinin. *Curr. Opin. Struc. Biol.***50**, 126-133 (2018).

21. Subramani, B. et al. Demystifying a hexauronic acid ligand that recognizes toxoplasma gondii and block its invasion into host cells. *Org. Biomol. Chem*. **17**, 4535-4542 (2019).

22. de Paz, J. L., Noti, C.& Seeberger, P. H. Microarray of synthetic heparin oligosaccharides. *J. Am. Chem. Soc.***128,** 2766-2767 (2006).

23. Das, S. K. et al. Synthesis of conformationally locked L-iduronic acid derivatives: direct evidence for a critical role of the skew-boat $^{2}S_{0}$ conformer in the activation of antithrombin by heparin. *Chem. Eur. J*.**7**, 4821-3834 (2001).

24. Nieto, L. et al. Heparin modulates the mitogenic activity of fibroblast growth factors by inducing dimerization of its receptors. A 3D view by using NMR. *ChemBioChem*.**14**, 1732-1744 (2013).

25. Muńoz-Garcìa, J. C., Corzana, F., de Paz, J. L., Angulo, J.& Nieto, P. M. Conformations of the iduronate ring in short heparin fragments described by time-averaged distance restrained molecular dynamics. *Glycobiology*.**23**, 1220-1229 (2013).

26. Muńoz-Garcìa, J. C. et al. Effect of the substituents of the neighboring ring in the conformational equilibrium of iduronate in heparin-like trisaccharides. *Chem. Eur. J*.**18,** 16319-16331 (2013).

27. Hsieh, P. H., Thieker, D. F., Guerrini, M., Woods, R. J.& Liu, J. Uncovering the relationship between sulphation patterns and conformation of iduronic acid in heparan sulfate. *Sci. Rep*.**6,** 29602 (2016).

28. Canales, A. et al. Conformational flexibility of a synthetic glycosaminoglycan bound to a fibroblast growth factor. FGF-1 recognized both the $^{1}C_{4}$ and $^{2}S_{0}$-conformations of a bioactive heparin-like hexasaccharide. *J. Am. Chem. Soc*.**127**, 16, 5778-5779 (2005).

29. Casu, B., Naggi, A. & Torri, G. Heparin-derived heparan sulfate mimics to modulate heparan sulfate-protein interaction in inflammation and cancer. *Matrix. Bio.* **29**, 442-452 (2010).

30. Bendensky, V., Yang, Y. & Brennen, T. V. Immunomodulatory activities of the heparan sulfate mimics PG545. *Adv. Exp. Med. Biol*. **1221**, 461-470 (2020).

31. Chhabra, M. & Ferro, V. PI-88 and related heparan sulfate mimics. *Adv. Exp. Med. Bio.* **1221**, 473-491 (2020).

32. Shanthamurthy, C. D., & Kikkeri, R. Linear synthesis of de novo oligo-iduronic acid. *Eur. J. Org. Chem*. 2950-2953 (2019).

33. Haasnoot, C. A., de Gelder, R., Kooijman, H.& Kellenbach, E. R. The conformation of the idopyranose ring revisited: How subtle O-substituent induce changes can be deduced from vicinal ^{1}H-NMR coupling constants. *Carbohydr. Res*. 108052 (2020).

34. Hricovíni, M., Guerrini, M. & Torri, G. NMR of sulfated oligo- and polysaccharides, in Jimenez-Barbero, J.; Peter, T. (eds). *NMR spectroscopy of glycoconjugates*. Wiley-VCH. Weinheim, Germany 189-229 (2002).

35. Angulo, J. et al. Dynamic properties of biologically active synthetic heparin-like hexasaccharides. *Glycbiology*. **15**, 1008-1015 (2005).

36. Mulloy, B.& Forster, M. J. Conformation and dynamics of heparin and heparan sulfate. *Glycobiology.***10**, 1147-1156 (2000).

37. Tebbutt, N., Pedersen, M. W. &Johns, T. G. Targeting the ERBB family in cancer: couples therapy. *Nat. Rev. Cancer.***13**, 663-673 (2013).

38. Sigismund, S.; Avanzato, D. & Lanzetti, L. Emerging functions of the EGFR in cancer. *Mol. Oncol*. **12**, 3–20 (2018).

39. Wang, L., Huang, Y., Pan, K., Jiang, X.& Liu, C. Osteogenic responses to different concentration/ratios of BMP-2 and bFGF in bone formation. *Ann. Biomed. Eng.***38**, 77-87 (2010),

40. Wang, Z. et al. Experimental study of the synergistic effect and network regulation mechanisms of an applied combination of BMP-2, VEGF and TGF-β1 on steogenic differentiation.*J. Cell.Biochem.***121**, 2394-2405 (2020).

41. Guglier, S. et al. Minimum FGF2 binding structural requirements for heparin and heparan sulfate oligosaccharides as determined by NMR spectroscopy. *Biochemistry.***47**, 13862−13869 (2008).

42. de Paz, J. L., Noti, C.., Bδhm, F., Werner, S. & Seeberger, P. H. Potentiation of fibroblast growth factor activity by synthetic heparin oligosaccharide glycodendrimers. *Chem. Bio.***14**, 879-887 (2007).

43. Rodrigo, A. C., Barnard, A., Cooper, J. & Smith, D. K. Self-assembling ligands for multivalent nanoscale heparin binding. *Angew. Chem. Int. Ed.* **50**, 4675-4679 (2011).

44. Tyler, P. C., Guimond, S. E., Turnbull, J. E. & Zubkova, O. V. Single-entity heparan sulfate glycomimetic clusters for therapeutic applications. *Angew. Chem. Int .Ed.***54**, 2718-2723 (2015).

45. Koide, H. et al. A polymer nanoparticle with eneigneered affinity for vascular endothelial growth factor ($VEGF_{165}$). *Nat. Chem*. **9**, 715-722 (2017).

46. Graells, J. et al. Overproduction of $VEGF_{165}$ concomitantly expressed with its recetors promotes growth and surfavail of metanoma cells through MAPK and PI3K signling. *J. Invest. Dermatol.***124**, 1151-1161 (2004).

47. Wenjing, Z., McCallum, S. A., Xiao, Z., Zhang, F.& Linhardt, R. J. Binding affinities of vaclular endothelial growth factor (VEGF) for heparin-derived oligosaccharides. *BioSci. Rep*. **32**, 71-81 (2012).

48. Ben-Areye, S. L., Schneider, C., Yu, H., Bashir, S., Chen, X., von Gunten, S. & Padler-Karavani, V. Presentation mode of glycans affect recognition of human serum anti-Neu5Gc IgG antibodies. *BioConjug. Chem*. **30**, 15650-15674 (2019).

3.9 Spectral Data

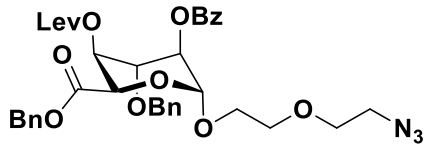

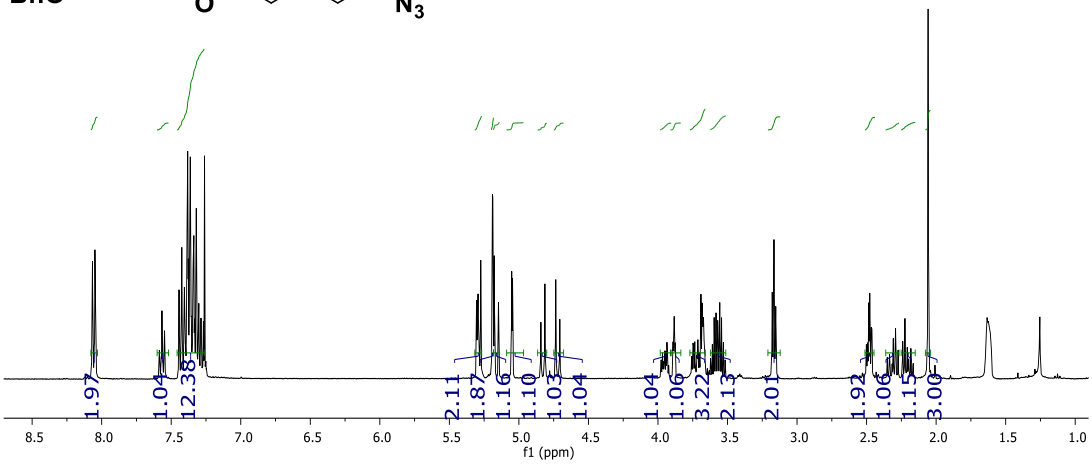

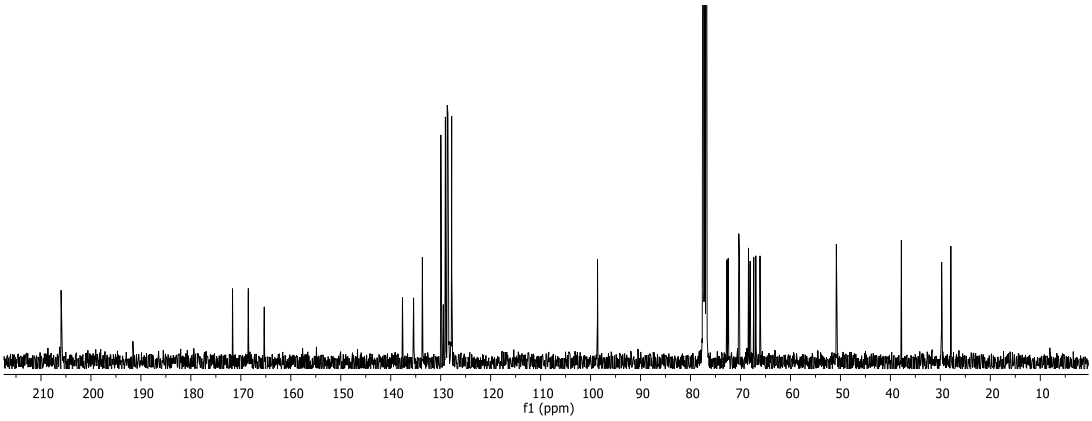

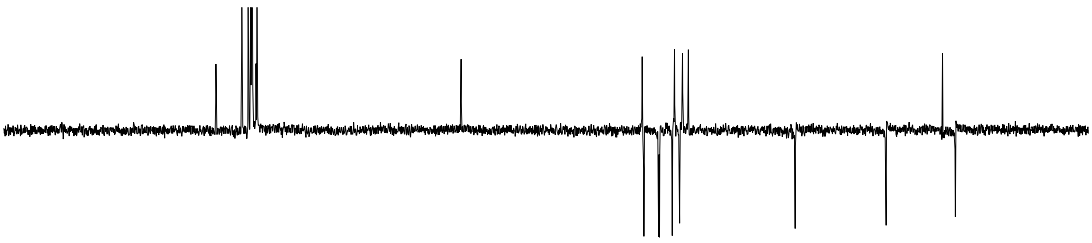

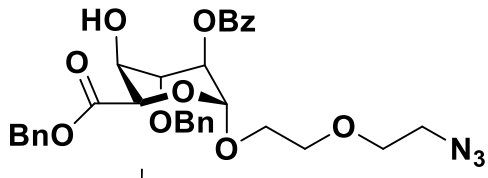
HO
OBz
O
O
BnO
OBn
O
O
N3

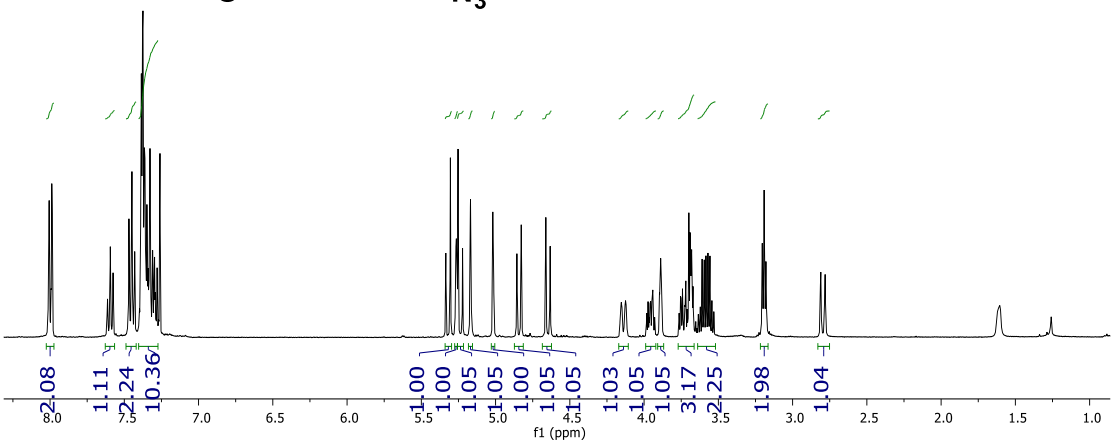
2.08
1.11
2.24
10.36
1.00
1.00
1.05
1.05
1.00
1.05
1.05
1.03
1.05
1.05
3.17
2.25
1.98
1.04
8.0
7.5
7.0
6.5
6.0
5.5
5.0
4.5
4.0
3.5
3.0
2.5
2.0
1.5
1.0
f1 (ppm)

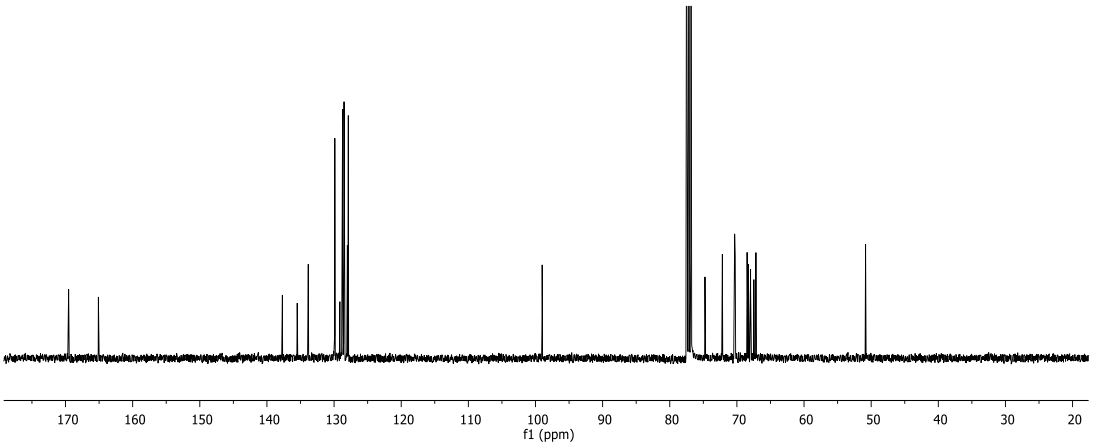
170
160
150
140
130
120
110
100
90
80
70
60
50
40
30
20
f1 (ppm)

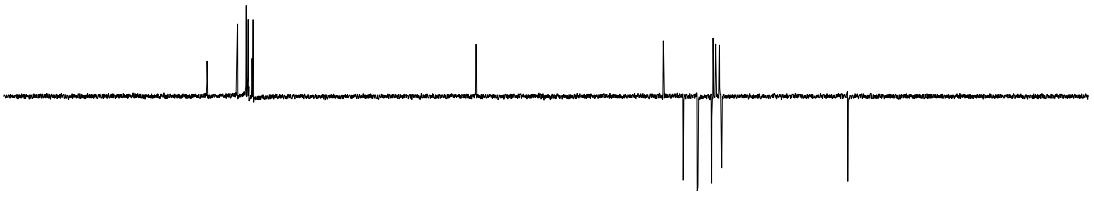

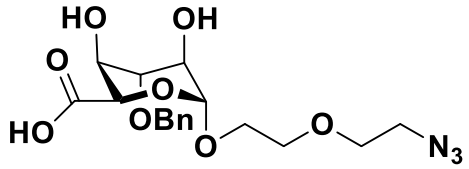
HO
OH
O
O
HO
OBn
O
O
N3

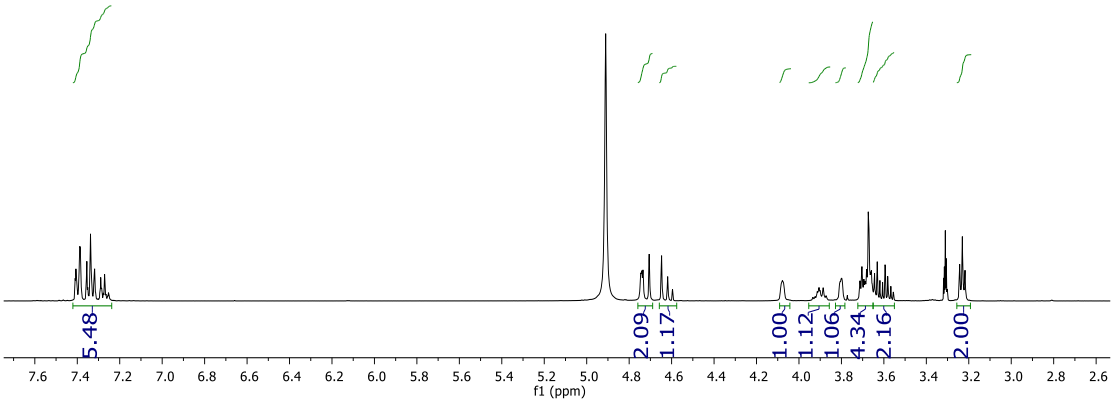
5.48
2.09
1.17
1.00
1.12
1.06
4.34
2.16
2.00
f1 (ppm)

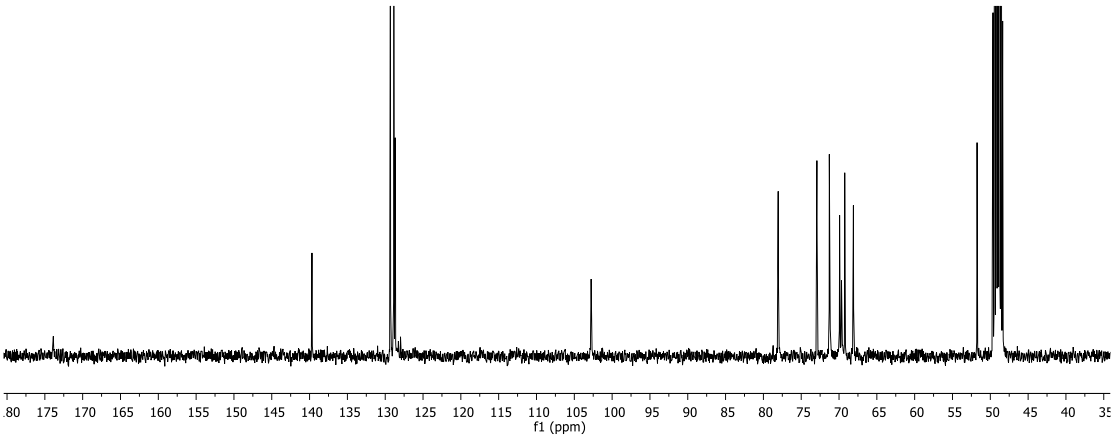
f1 (ppm)

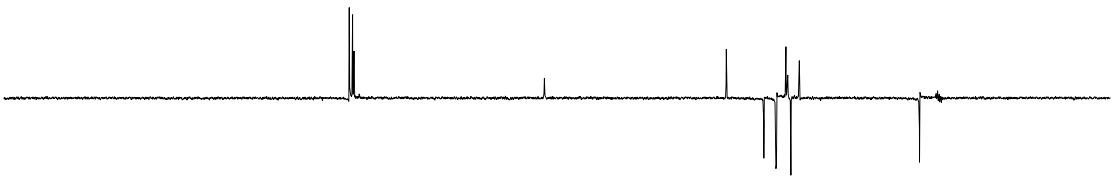

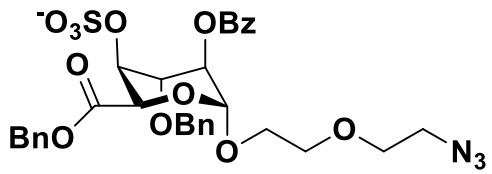
-O3SO
OBz
O
O
BnO
OBn
O
O
N3

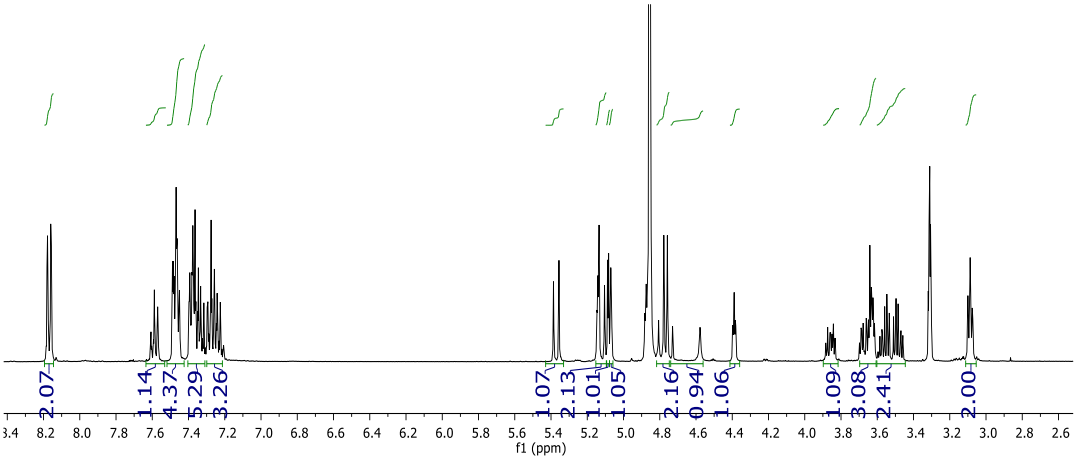
2.07
1.14
4.37
5.29
3.26
1.07
2.13
1.01
1.05
2.16
0.94
1.06
1.09
3.08
2.41
2.00
f1 (ppm)

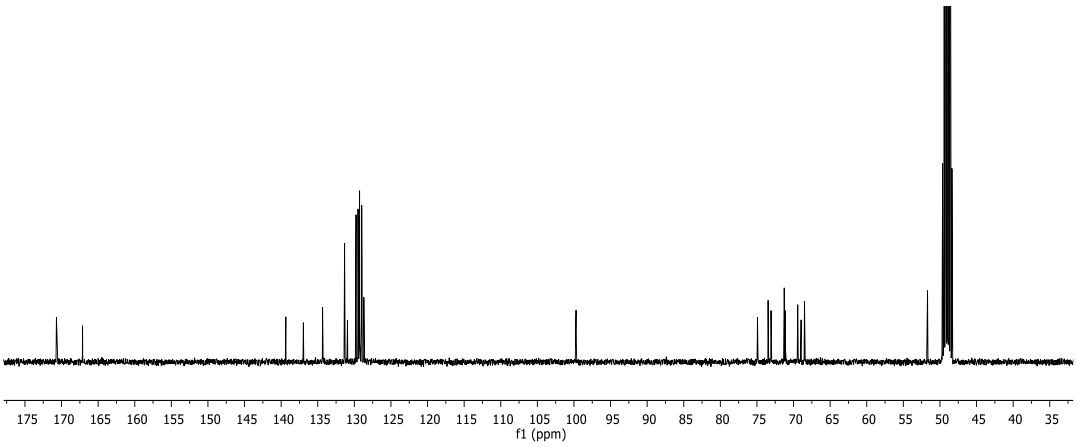
f1 (ppm)

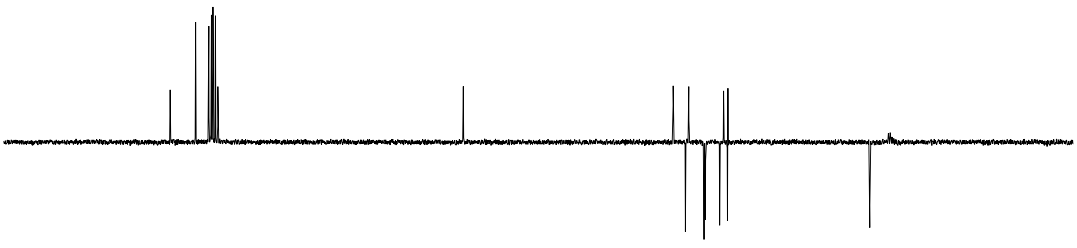

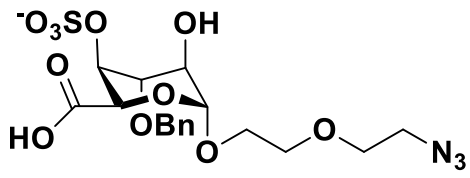
$^{-}O_3SO$
OH
O
O
HO
OBn
O
O
N_3

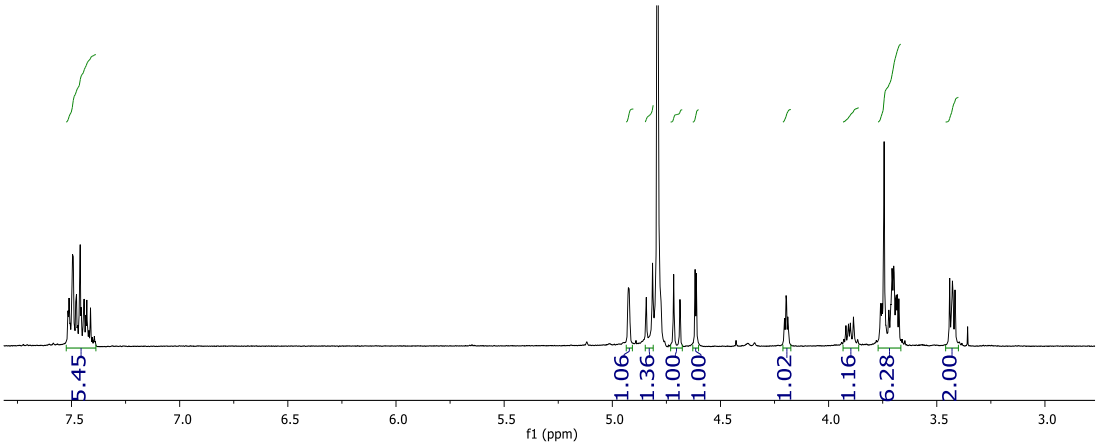
5.45
1.06
1.36
1.00
1.00
1.02
1.16
6.28
2.00
7.5
7.0
6.5
6.0
5.5
5.0
4.5
4.0
3.5
3.0
f1 (ppm)

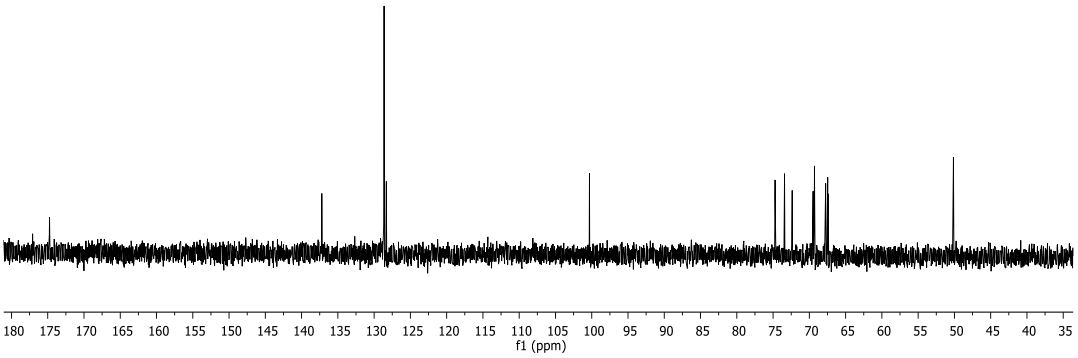
180 175 170 165 160 155 150 145 140 135 130 125 120 115 110 105 100 95 90 85 80 75 70 65 60 55 50 45 40 35
f1 (ppm)

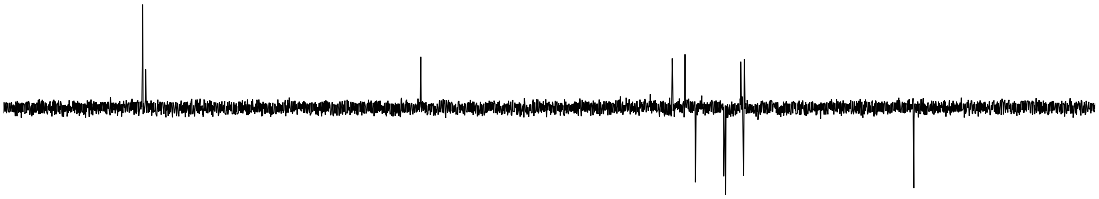

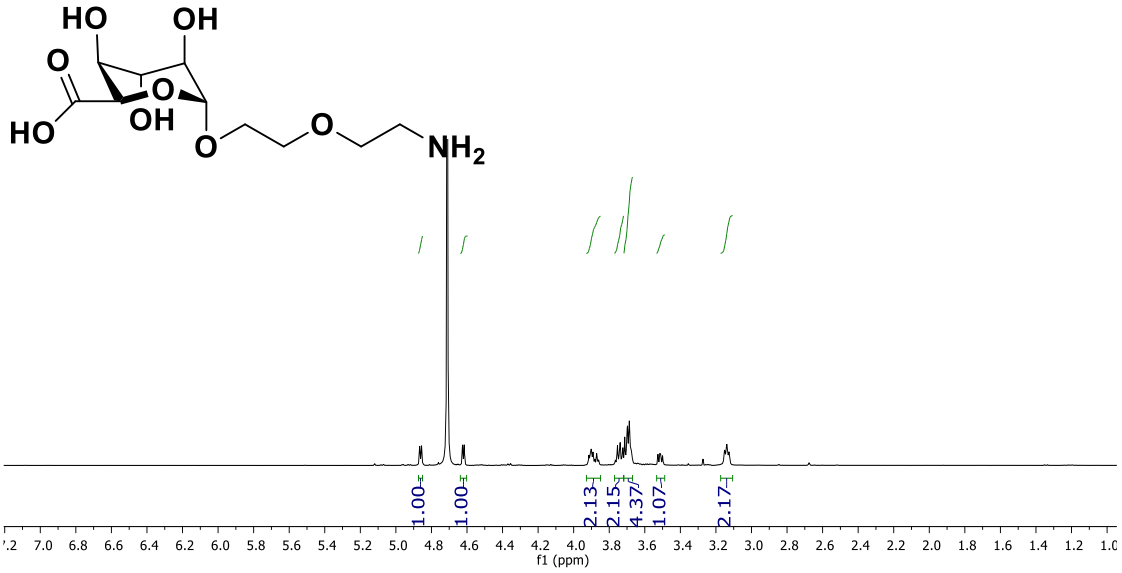
HO
OH
O
O
HO
OH
O
O
NH2
1.00
1.00
2.13
2.15
4.37
1.07
2.17
f1 (ppm)

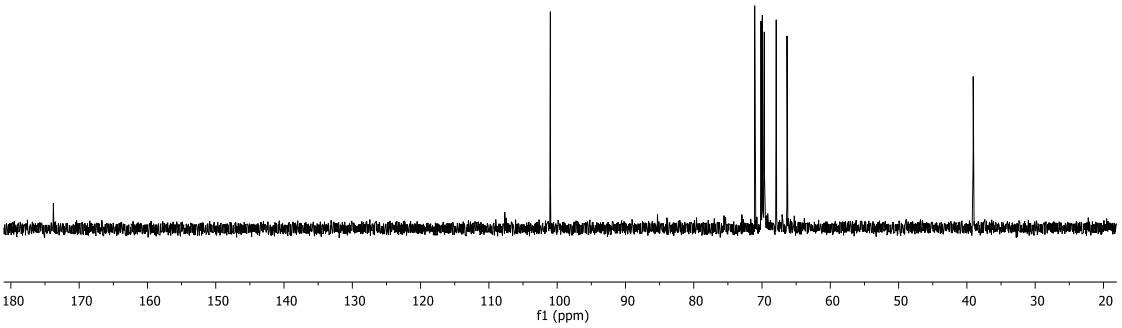
f1 (ppm)

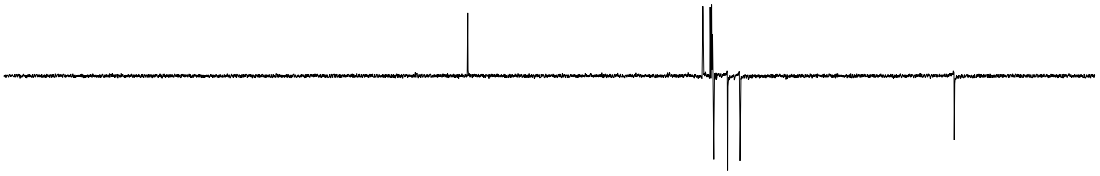

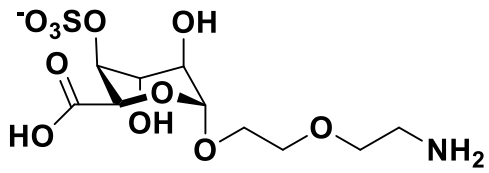
-O3SO
OH
O
O
HO
OH
O
O
NH2

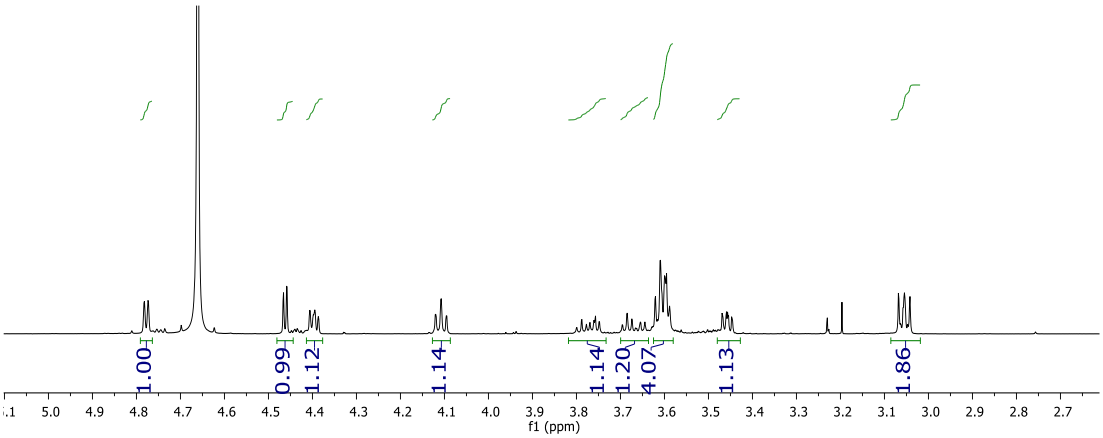
1.00
0.99
1.12
1.14
1.14
1.20
4.07
1.13
1.86
f1 (ppm)

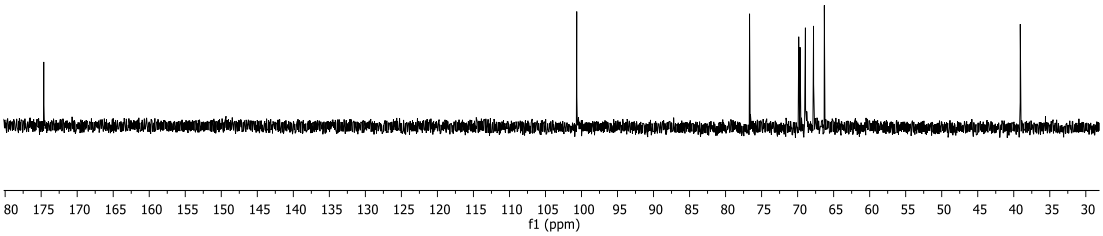
f1 (ppm)

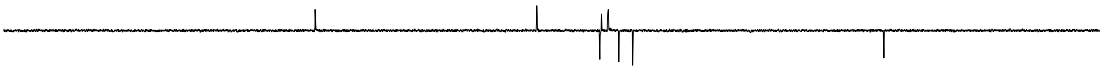

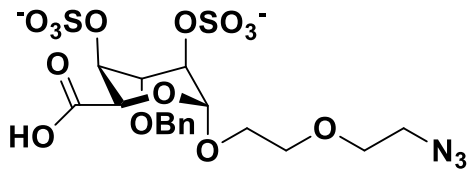
-O3SO
OSO3-
O
HO
O
OBn
O
O
N3

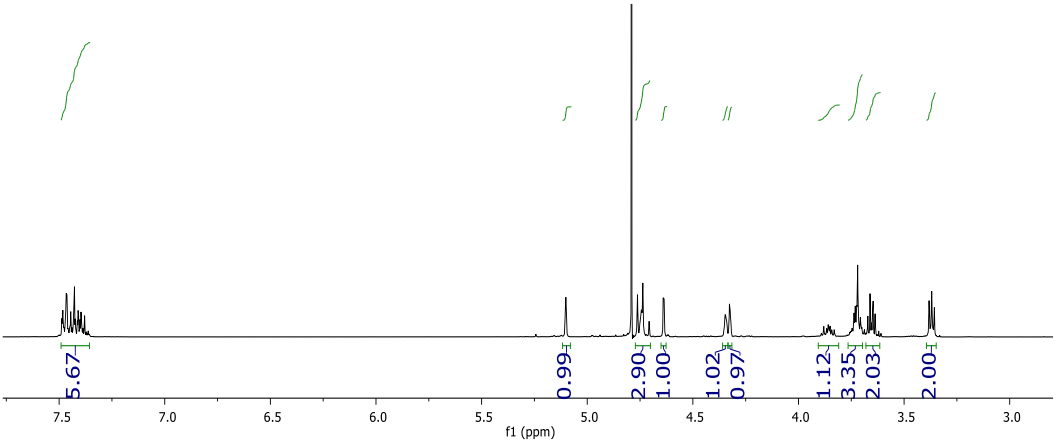
5.67
0.99
2.90
1.00
1.02
0.97
1.12
3.35
2.03
2.00
7.5
7.0
6.5
6.0
5.5
5.0
4.5
4.0
3.5
3.0
f1 (ppm)

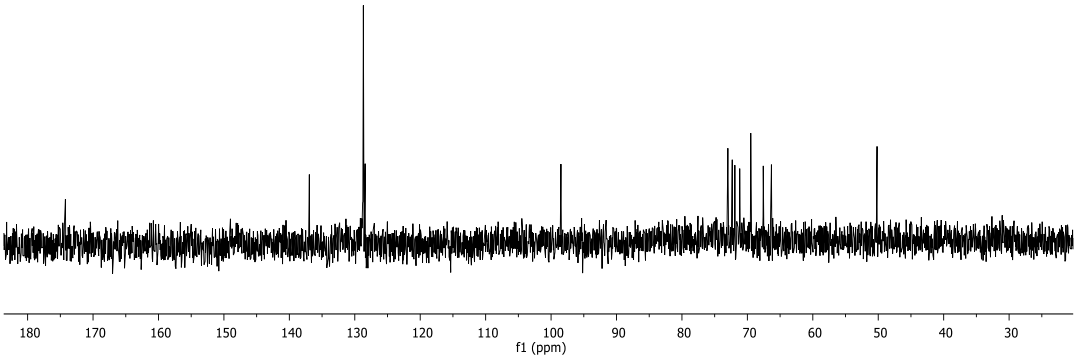
180
170
160
150
140
130
120
110
100
90
80
70
60
50
40
30
f1 (ppm)

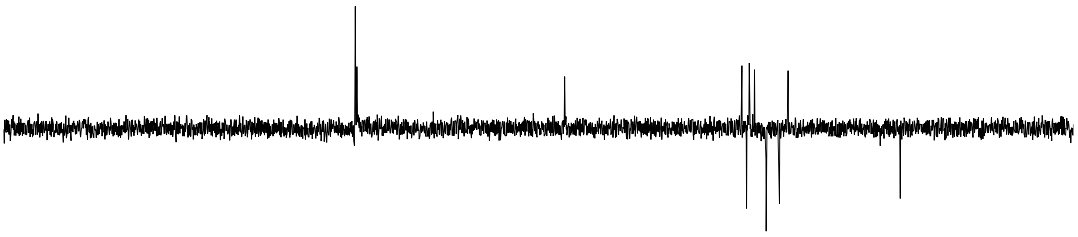

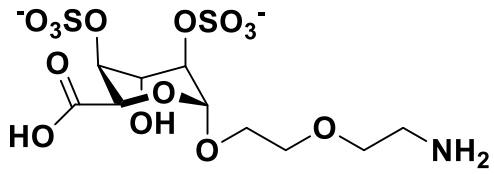
-O3SO
OSO3-
O
O
HO
OH
O
O
NH2

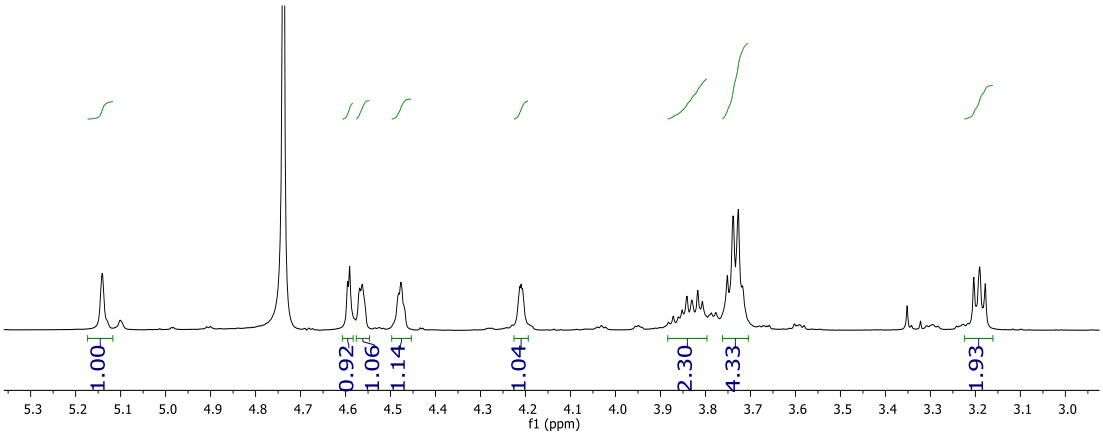
1.00
0.92
1.06
1.14
1.04
2.30
4.33
1.93
5.3 5.2 5.1 5.0 4.9 4.8 4.7 4.6 4.5 4.4 4.3 4.2 4.1 4.0 3.9 3.8 3.7 3.6 3.5 3.4 3.3 3.2 3.1 3.0
f1 (ppm)

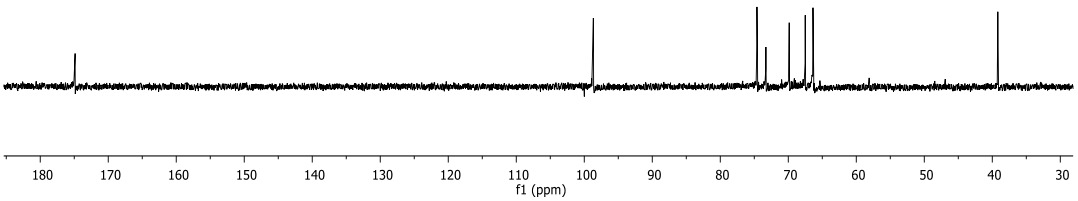
180 170 160 150 140 130 120 110 100 90 80 70 60 50 40 30
f1 (ppm)

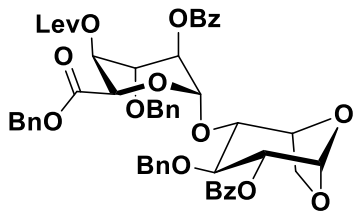
LevO
OBz
O
O
BnO
OBn
O
O
BnO
BzO
O

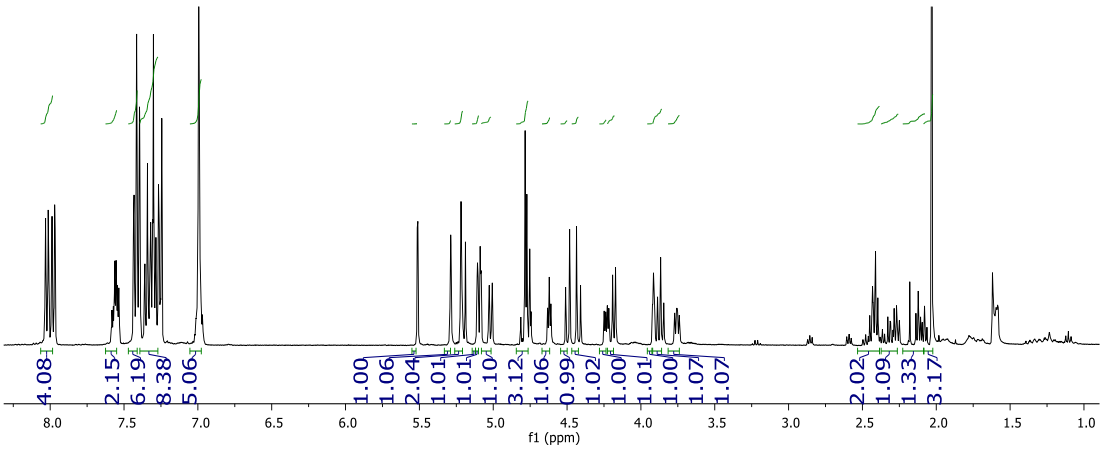
4.08
2.15
6.19
8.38
5.06
1.00
1.06
2.04
1.01
1.01
1.10
3.12
1.06
0.99
1.02
1.00
1.01
1.00
1.07
1.07
2.02
1.09
1.33
3.17
8.0
7.5
7.0
6.5
6.0
5.5
5.0
4.5
4.0
3.5
3.0
2.5
2.0
1.5
1.0
f1 (ppm)

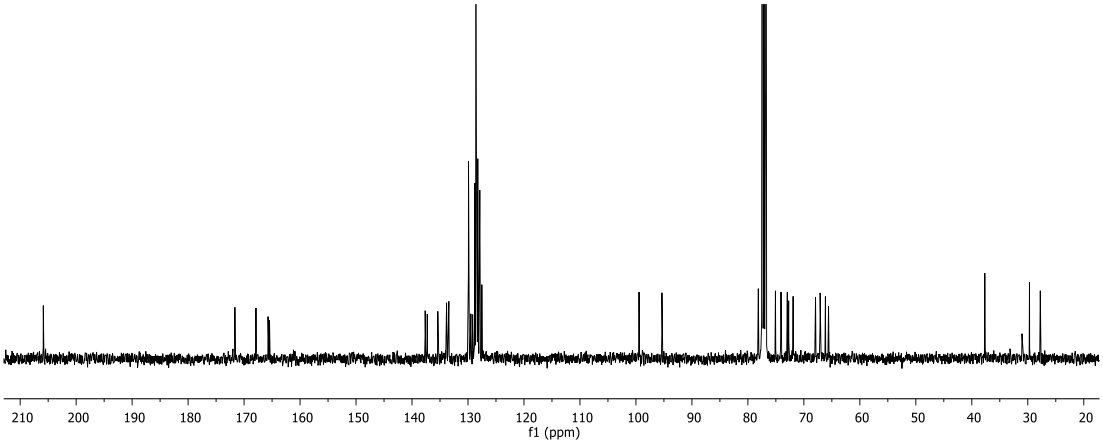
210
200
190
180
170
160
150
140
130
120
110
100
90
80
70
60
50
40
30
20
f1 (ppm)

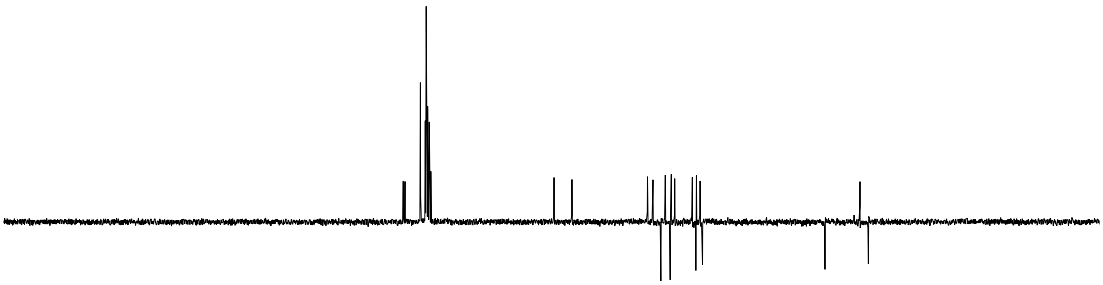

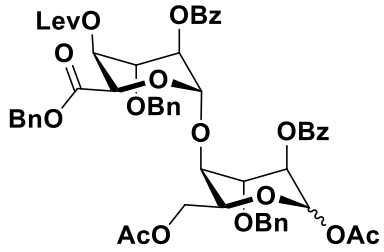
LevO
OBz
O
O
OBn
BnO
O
OBz
O
OBn
AcO
OAc

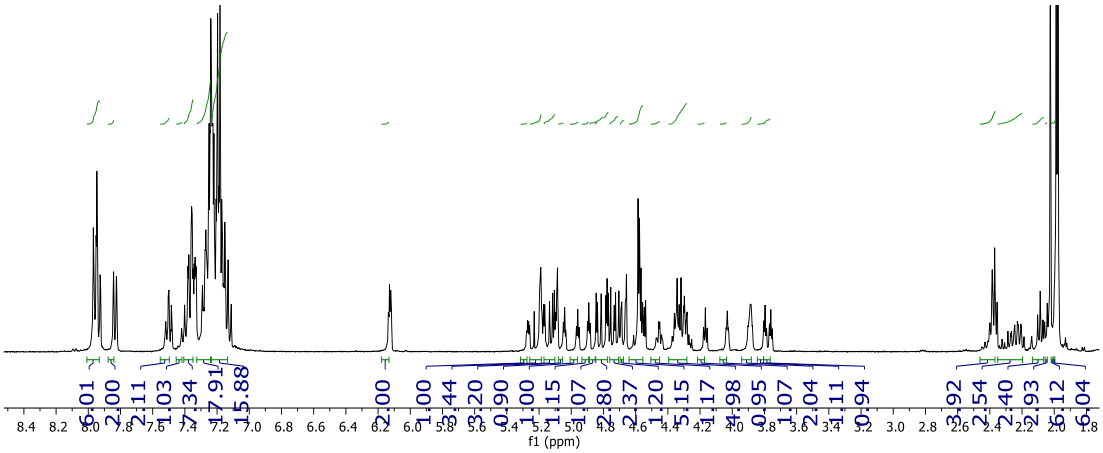
6.01 2.00 2.11 1.03 7.34 17.91 15.88 2.00 1.00 3.44 3.20 0.90 1.00 1.15 1.07 2.80 2.37 1.20 5.15 1.17 4.98 0.95 1.07 2.04 1.11 0.94 3.92 2.54 2.40 2.93 6.12 6.04
f1 (ppm)

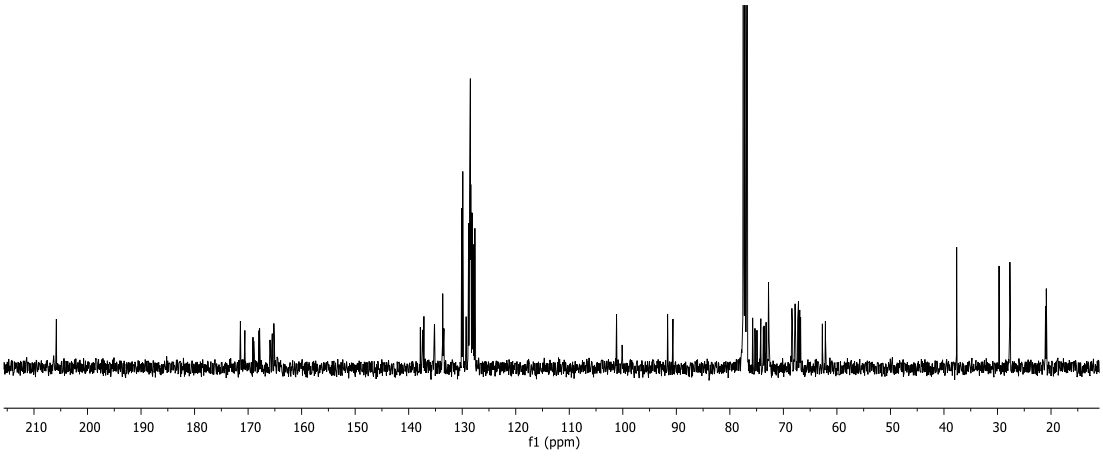
f1 (ppm)

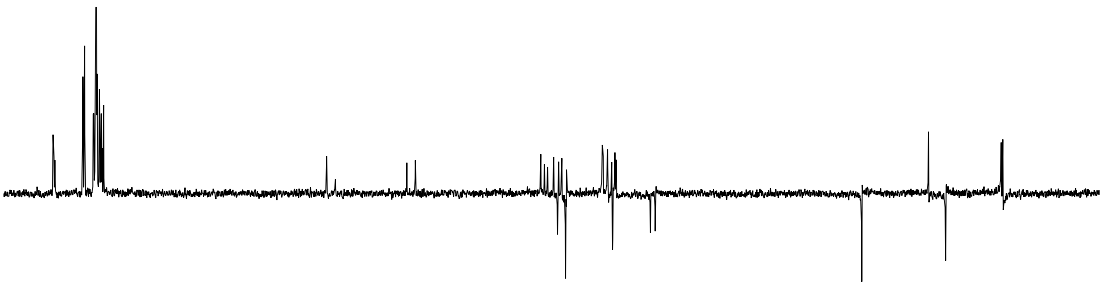

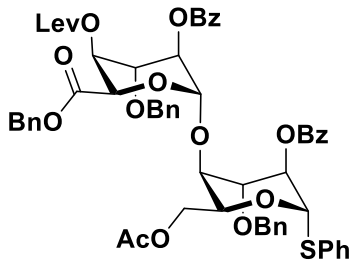
LevO
OBz
O
O
BnO
OBn
O
OBz
O
OBn
AcO
SPh

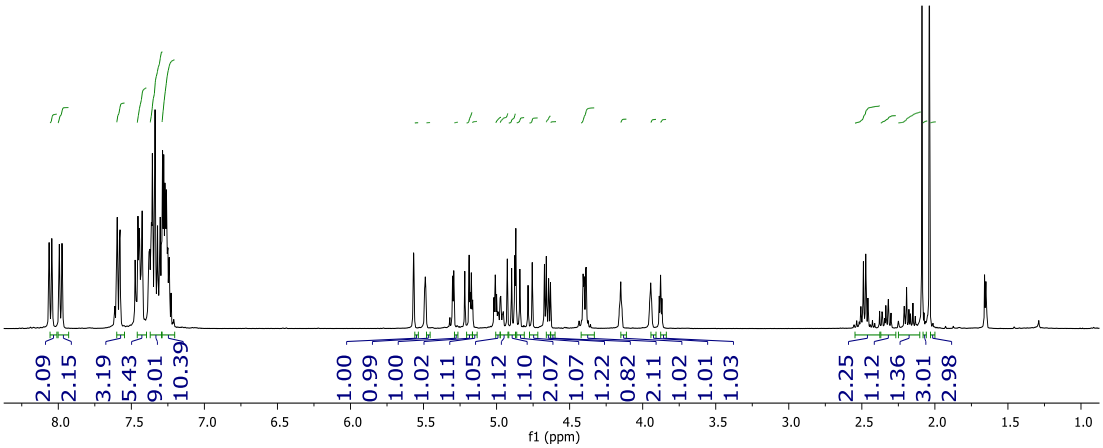
2.09
2.15
3.19
5.43
9.01
10.39
1.00
0.99
1.00
1.02
1.11
1.05
1.12
1.10
2.07
1.07
1.22
0.82
2.11
1.02
1.01
1.03
2.25
1.12
1.36
3.01
2.98
f1 (ppm)

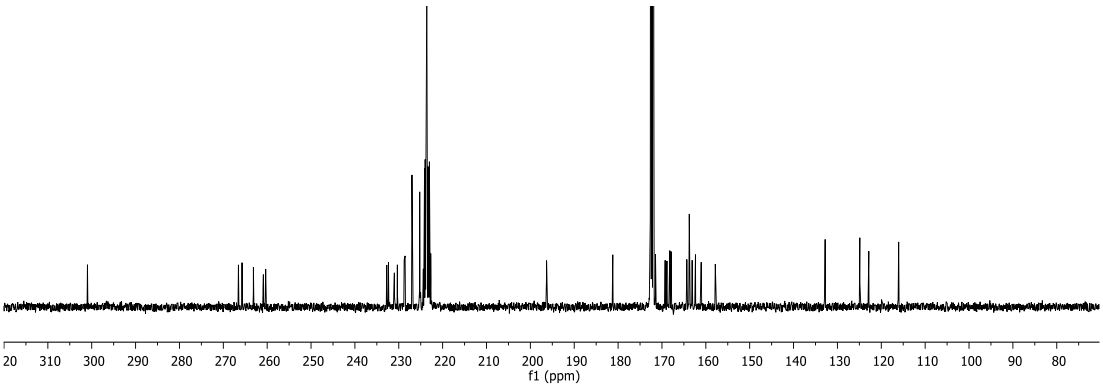
f1 (ppm)

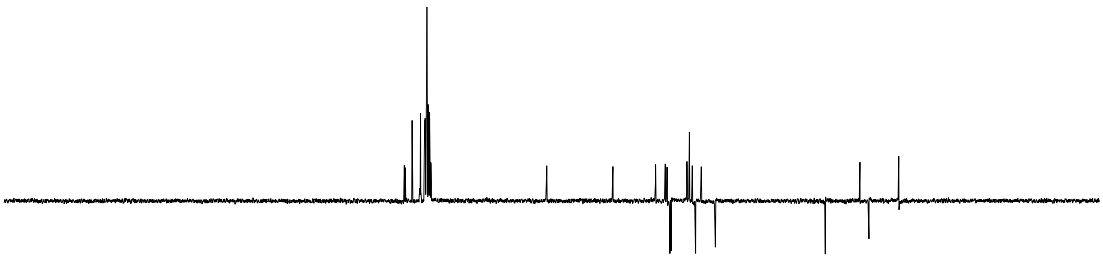

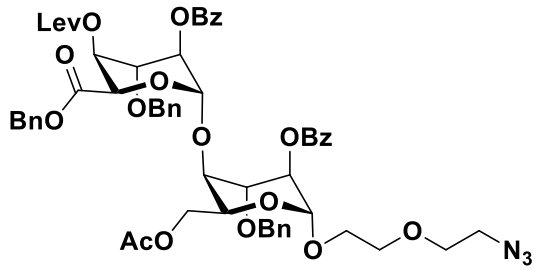
LevO
OBz
O
O
OBn
BnO
O
OBz
O
OBn
AcO
O
O
N3

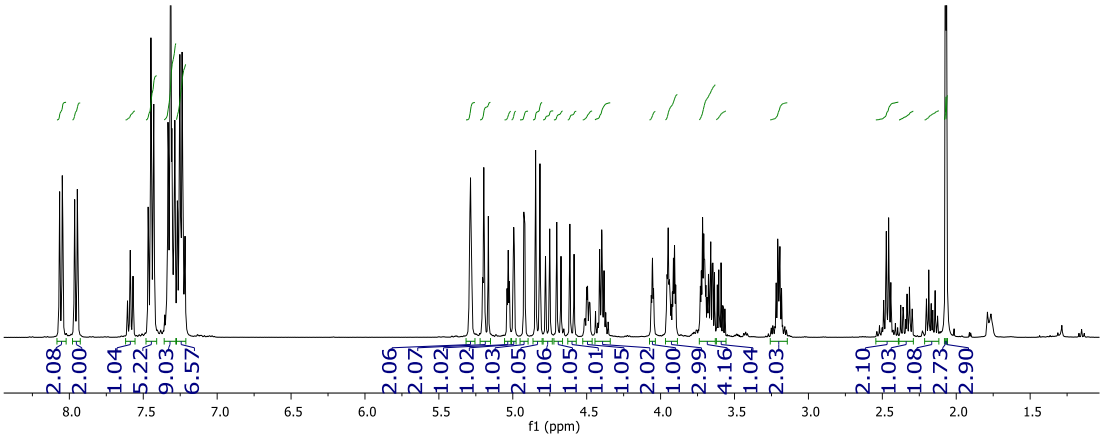
2.08
2.00
1.04
5.22
9.03
6.57
2.06
2.07
1.02
1.02
1.03
2.05
1.06
1.05
1.01
1.05
2.02
1.00
2.99
4.16
1.04
2.03
2.10
1.03
1.08
2.73
2.90
8.0
7.5
7.0
6.5
6.0
5.5
5.0
4.5
4.0
3.5
3.0
2.5
2.0
1.5
f1 (ppm)

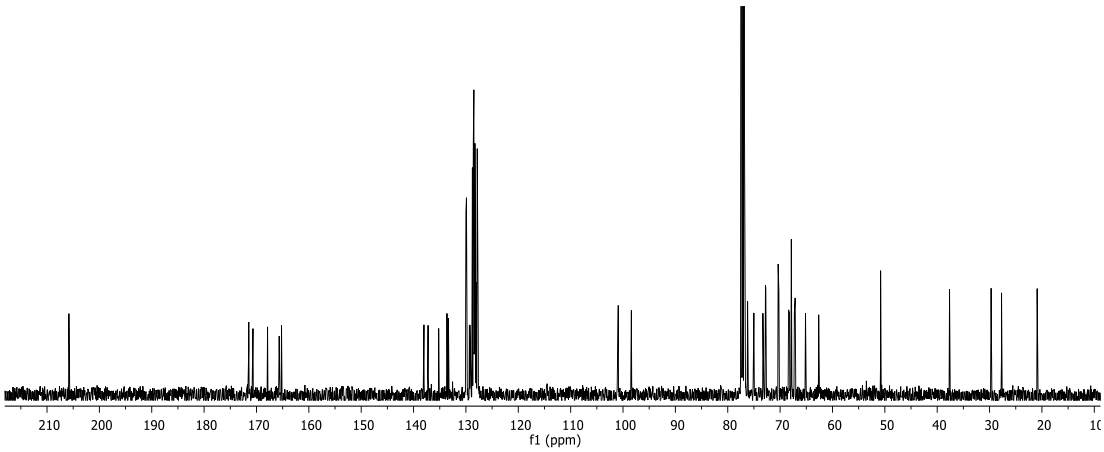
210
200
190
180
170
160
150
140
130
120
110
100
90
80
70
60
50
40
30
20
f1 (ppm)

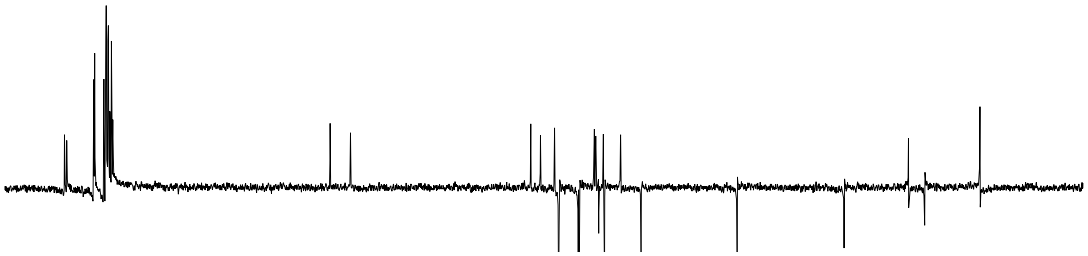

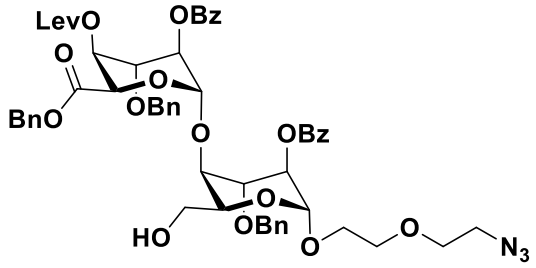
LevO
OBz
O
O
BnO
OBn
O
OBz
O
HO
OBn
O
O
N3

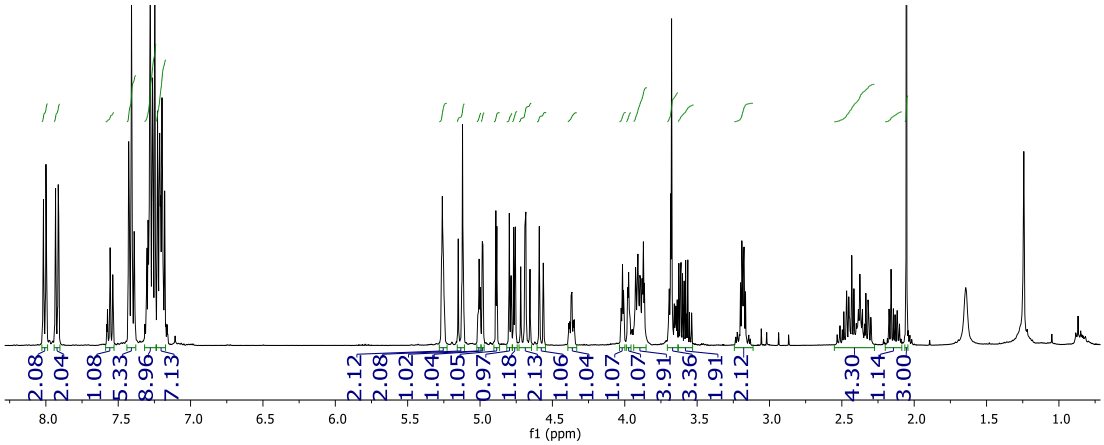
2.08
2.04
1.08
5.33
8.96
7.13
2.12
2.08
1.02
1.04
1.05
0.97
1.18
2.13
1.06
1.04
1.07
1.07
3.91
3.36
1.91
2.12
4.30
1.14
3.00
8.0
7.5
7.0
6.5
6.0
5.5
5.0
4.5
4.0
3.5
3.0
2.5
2.0
1.5
1.0
f1 (ppm)

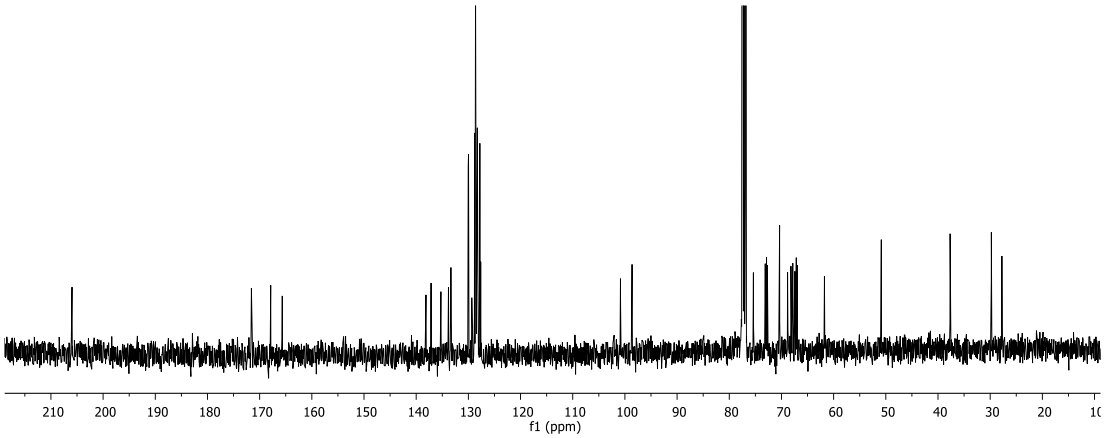
210
200
190
180
170
160
150
140
130
120
110
100
90
80
70
60
50
40
30
20
f1 (ppm)

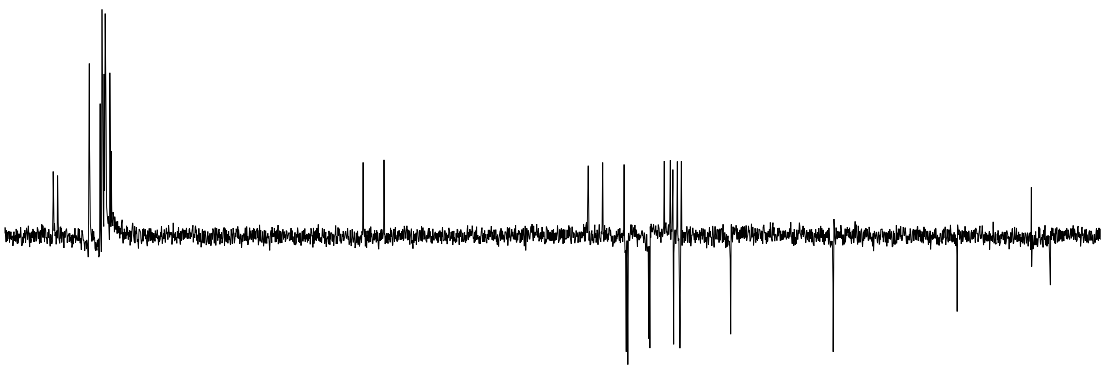

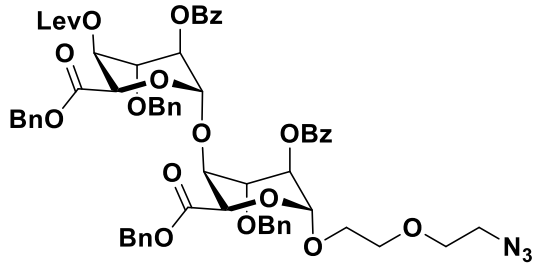
LevO
OBz
O
O
OBn
BnO
O
OBz
O
O
OBn
BnO
O
O
N3

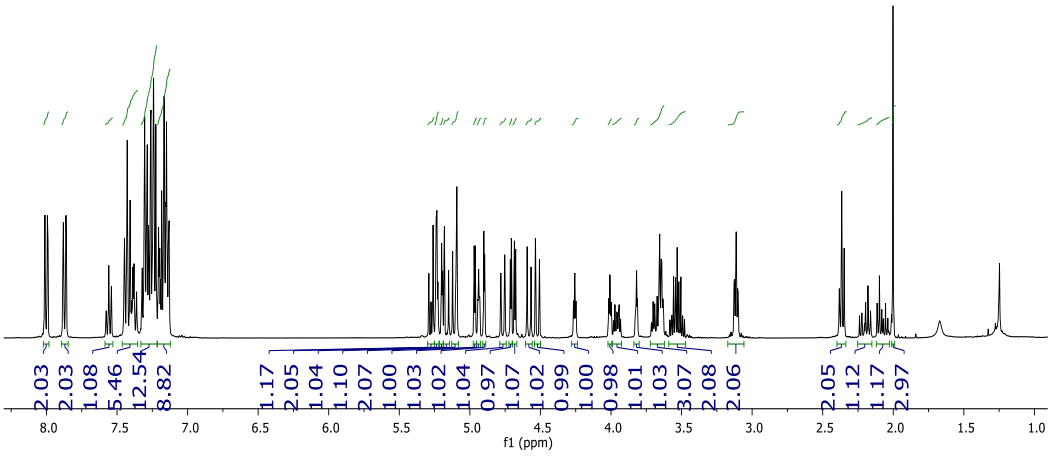
2.03 2.03 1.08 5.46 12.54 8.82 1.17 2.05 1.04 1.10 2.07 1.00 1.03 1.02 1.04 0.97 1.07 1.02 0.99 1.00 0.98 1.01 1.03 3.07 2.08 2.06 2.05 1.12 1.17 2.97
8.0 7.5 7.0 6.5 6.0 5.5 5.0 4.5 4.0 3.5 3.0 2.5 2.0 1.5 1.0
f1 (ppm)

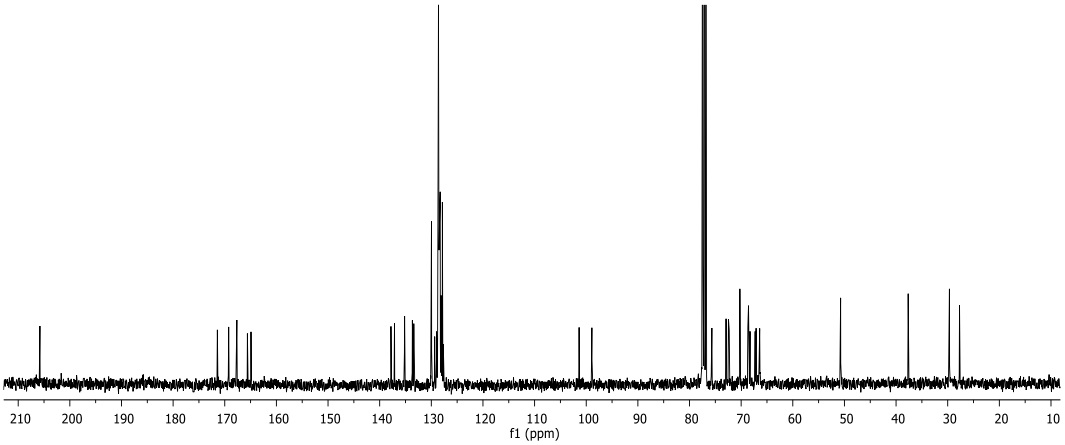
210 200 190 180 170 160 150 140 130 120 110 100 90 80 70 60 50 40 30 20 10
f1 (ppm)

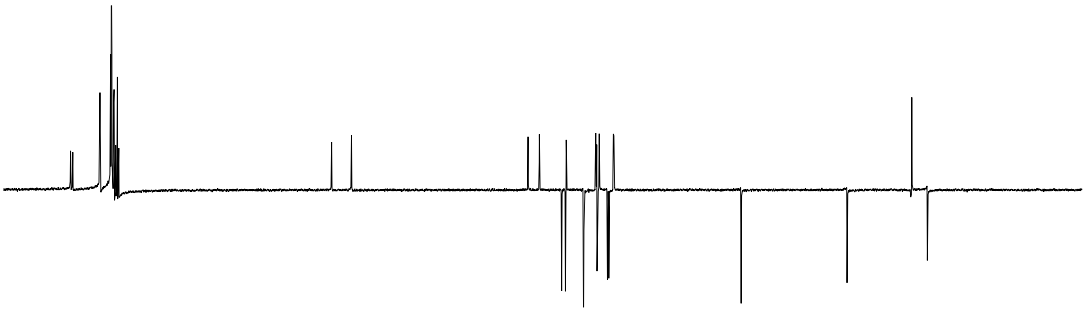

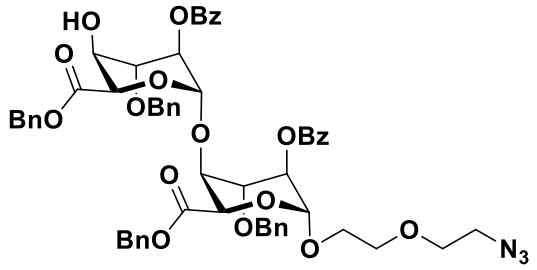
HO
OBz
O
O
BnO
OBn
O
OBz
O
O
BnO
OBn
O
O
N3

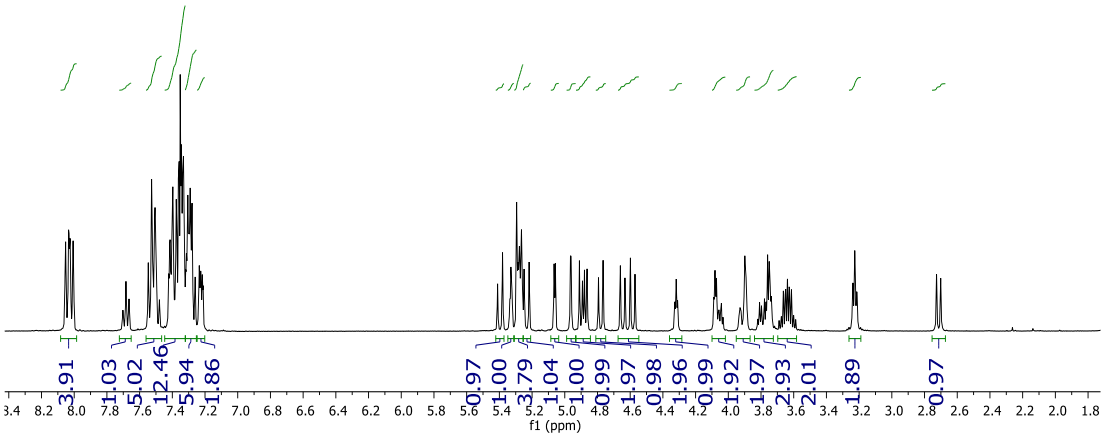
3.91
1.03
5.02
12.46
5.94
1.86
0.97
1.00
3.79
1.04
1.00
0.99
1.97
0.98
1.96
0.99
1.92
1.97
2.93
2.01
1.89
0.97
f1 (ppm)

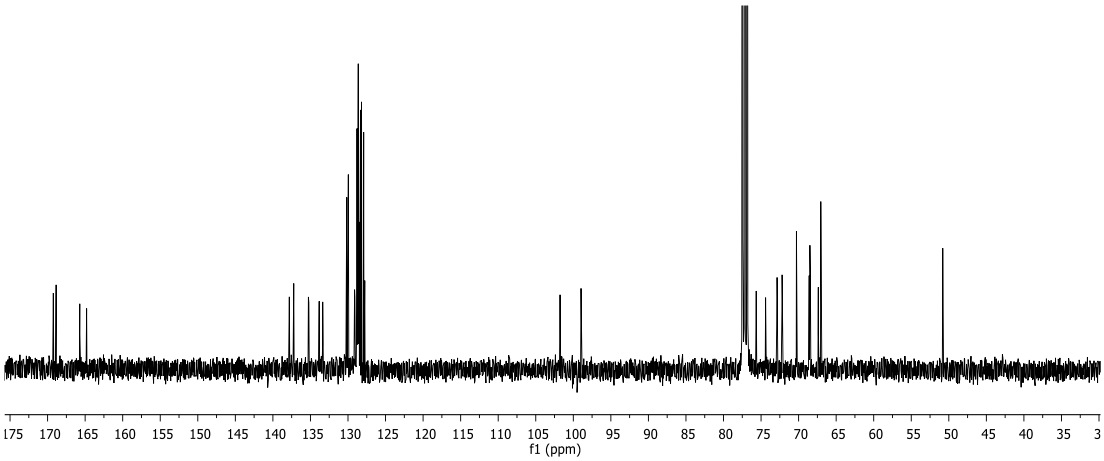
f1 (ppm)

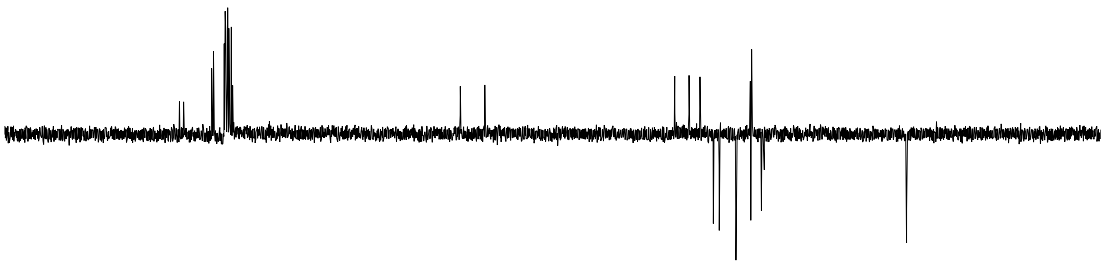

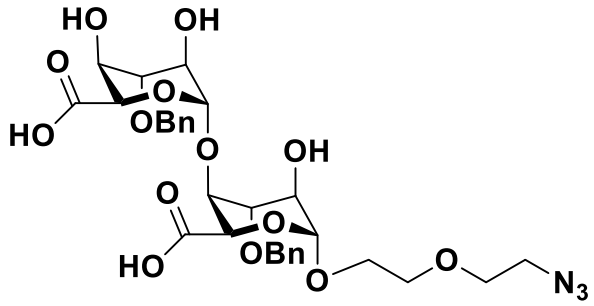
HO
OH
O
O
HO
OBn
O
OH
O
O
HO
OBn
O
O
N3

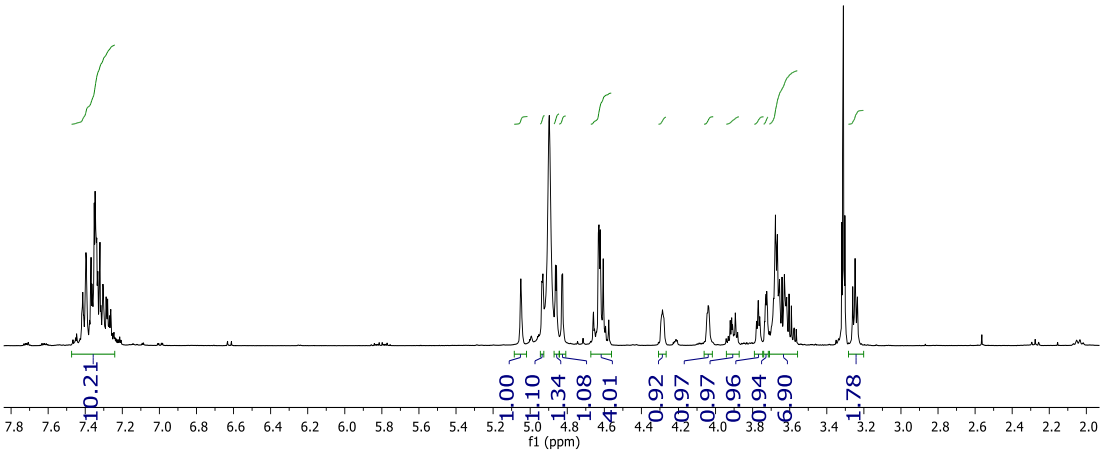
10.21
1.00
1.10
1.34
1.08
4.01
0.92
0.97
0.97
0.96
0.94
6.90
1.78
7.8 7.6 7.4 7.2 7.0 6.8 6.6 6.4 6.2 6.0 5.8 5.6 5.4 5.2 5.0 4.8 4.6 4.4 4.2 4.0 3.8 3.6 3.4 3.2 3.0 2.8 2.6 2.4 2.2 2.0
f1 (ppm)

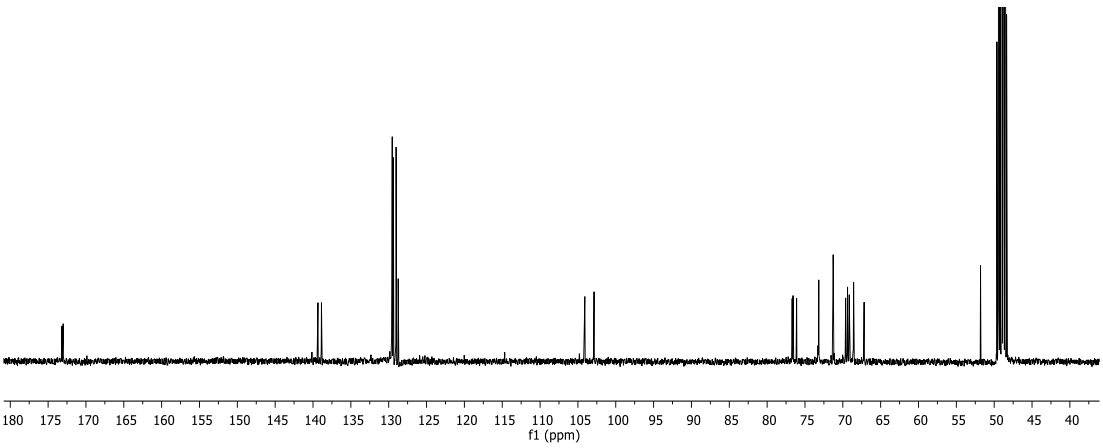
180 175 170 165 160 155 150 145 140 135 130 125 120 115 110 105 100 95 90 85 80 75 70 65 60 55 50 45 40
f1 (ppm)

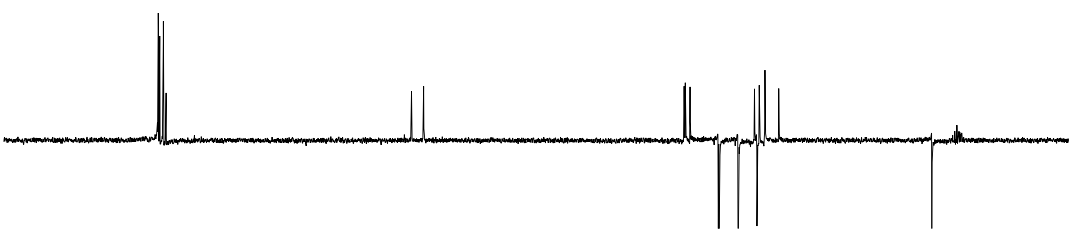

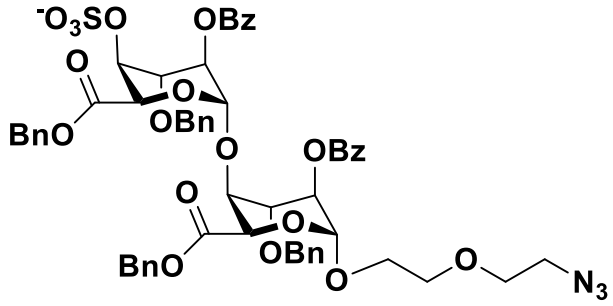
-O3SO
OBz
O
O
BnO
OBn
O
OBz
O
O
BnO
OBn
O
O
N3

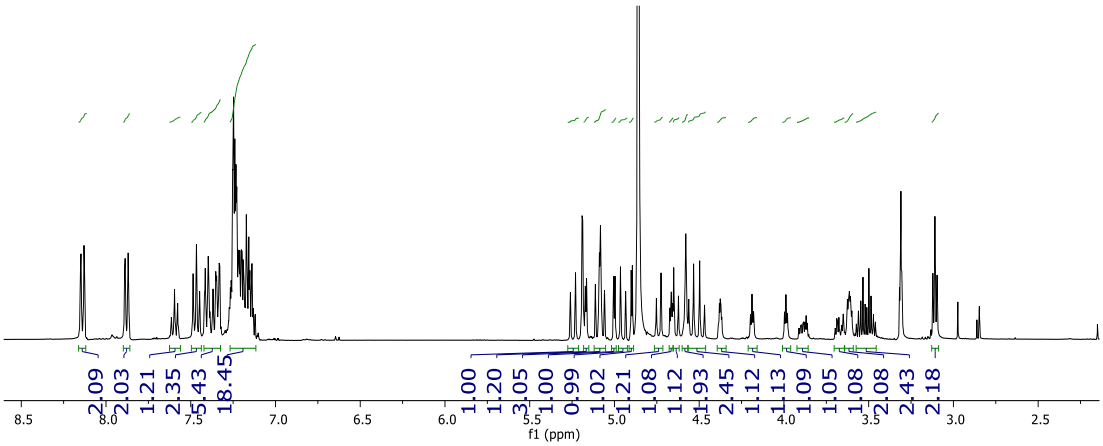
2.09
2.03
1.21
2.35
5.43
18.45
1.00
1.20
3.05
1.00
0.99
1.02
1.21
1.08
1.12
1.93
2.45
1.12
1.13
1.09
1.05
1.08
2.08
2.43
2.18
8.5
8.0
7.5
7.0
6.5
6.0
5.5
5.0
4.5
4.0
3.5
3.0
2.5
f1 (ppm)

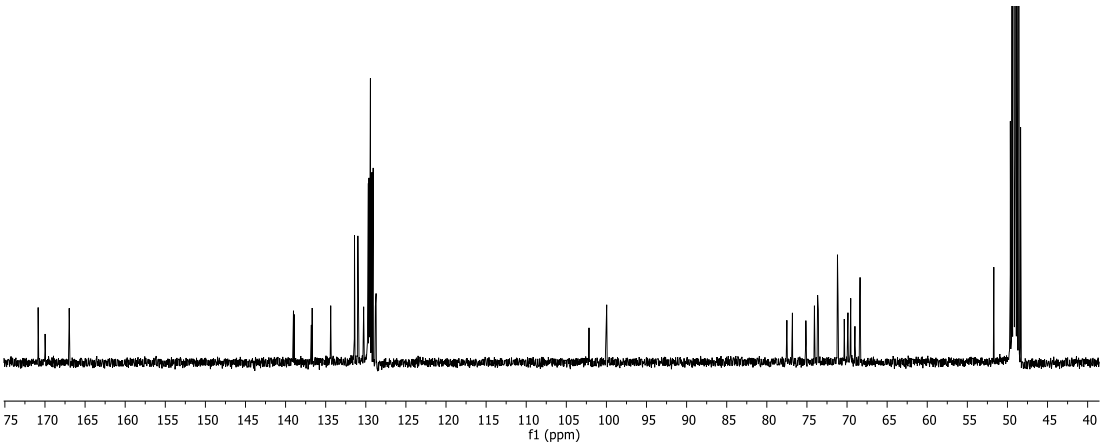
75
170
165
160
155
150
145
140
135
130
125
120
115
110
105
100
95
90
85
80
75
70
65
60
55
50
45
40
f1 (ppm)

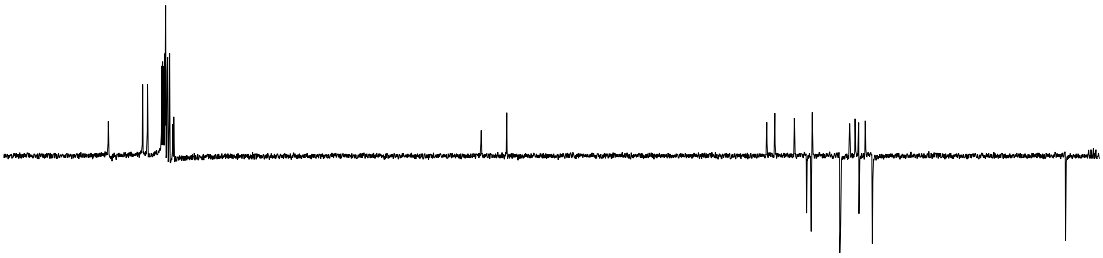

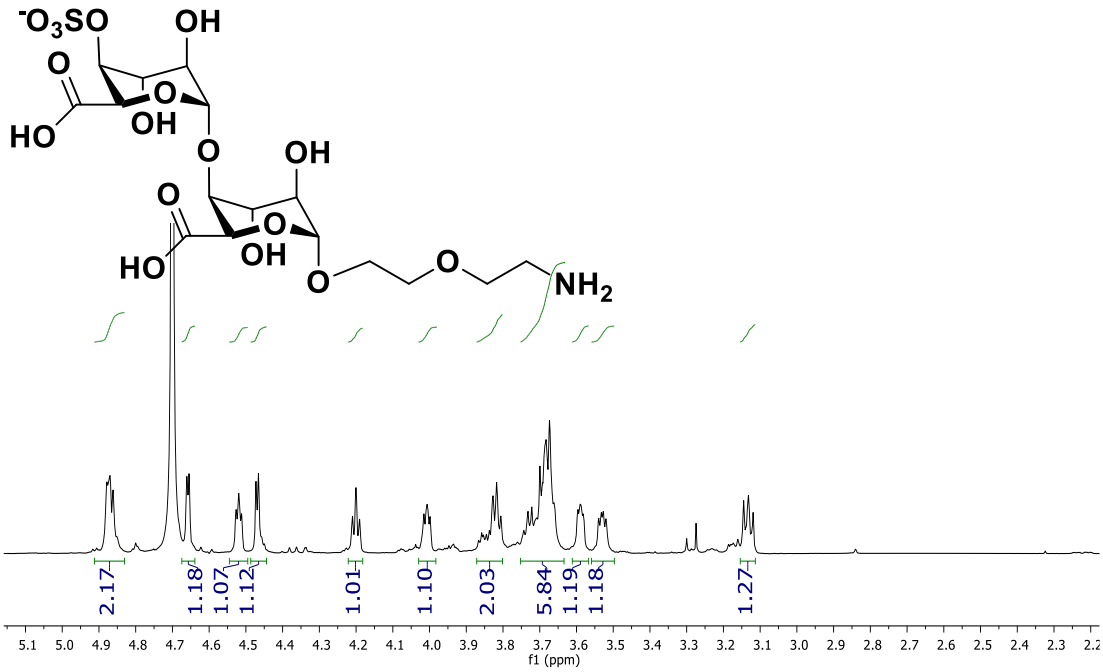
-O3SO
OH
O
O
HO
OH
O
OH
O
O
HO
OH
O
O
NH2
2.17
1.18
1.07
1.12
1.01
1.10
2.03
5.84
1.19
1.18
1.27
f1 (ppm)

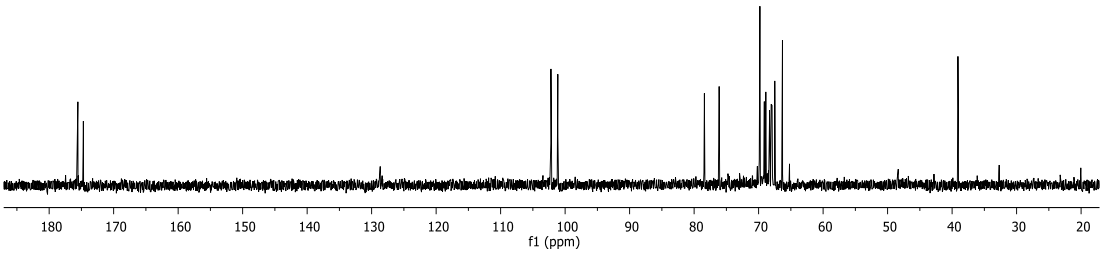
f1 (ppm)

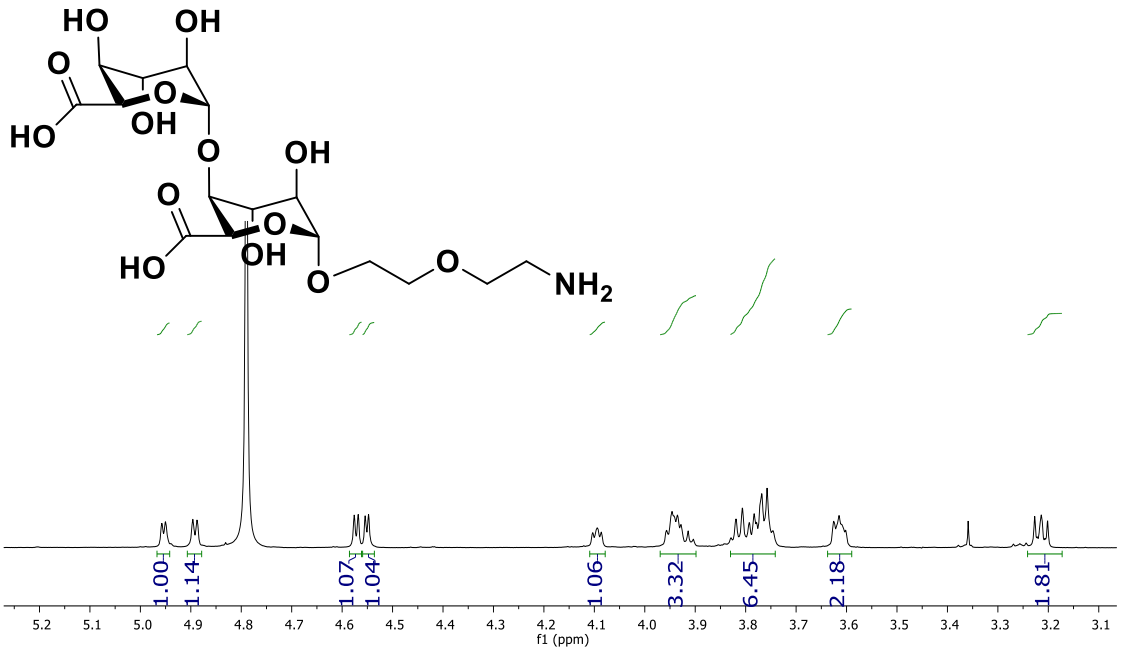
HO
OH
O
O
HO
OH
O
OH
O
O
HO
OH
O
O
NH2
1.00
1.14
1.07
1.04
1.06
3.32
6.45
2.18
1.81
5.2 5.1 5.0 4.9 4.8 4.7 4.6 4.5 4.4 4.3 4.2 4.1 4.0 3.9 3.8 3.7 3.6 3.5 3.4 3.3 3.2 3.1
f1 (ppm)

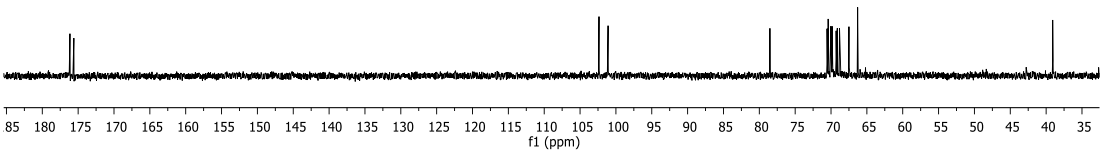
85 180 175 170 165 160 155 150 145 140 135 130 125 120 115 110 105 100 95 90 85 80 75 70 65 60 55 50 45 40 35
f1 (ppm)

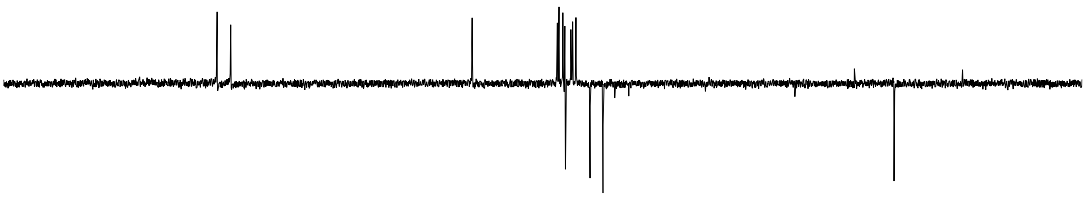

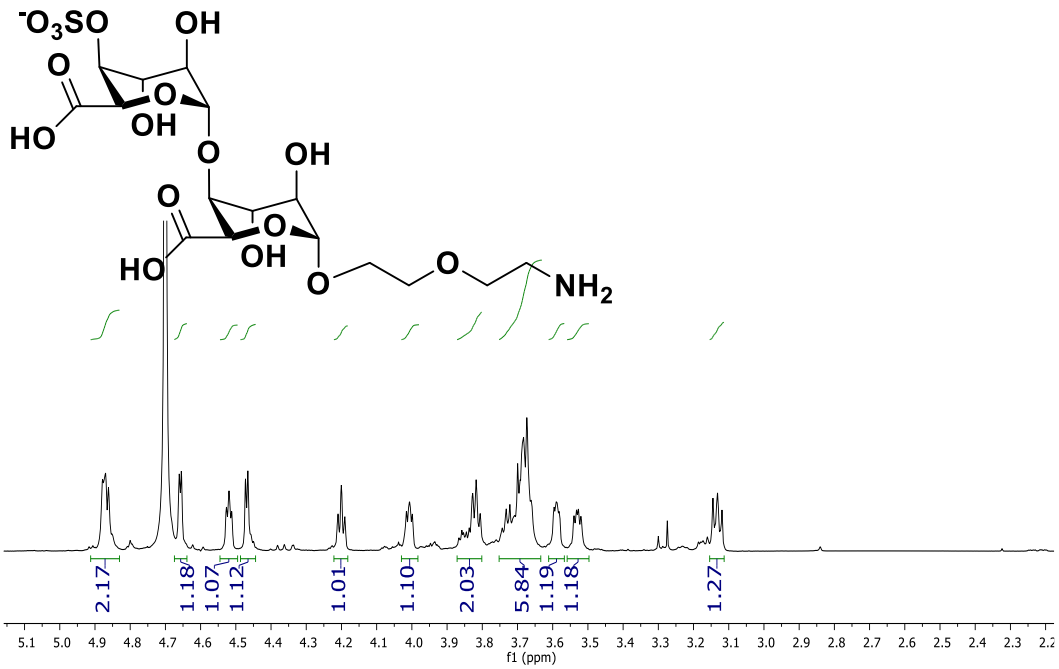
$^{-}O_3SO$
OH
O
O
HO
OH
O
OH
O
O
OH
HO
O
NH2
2.17
1.18
1.07
1.12
1.01
1.10
2.03
5.84
1.19
1.18
1.27
f1 (ppm)

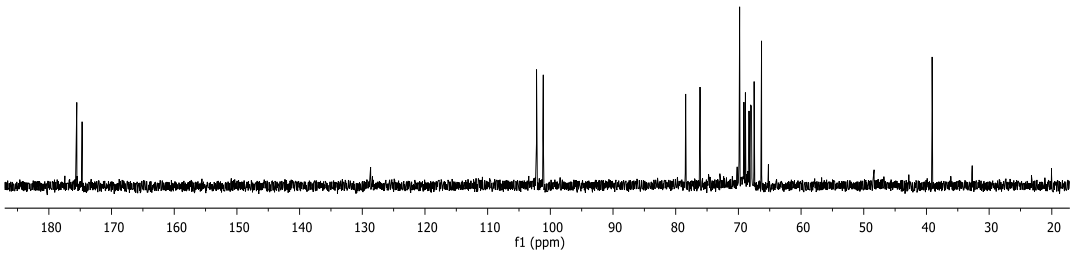
f1 (ppm)

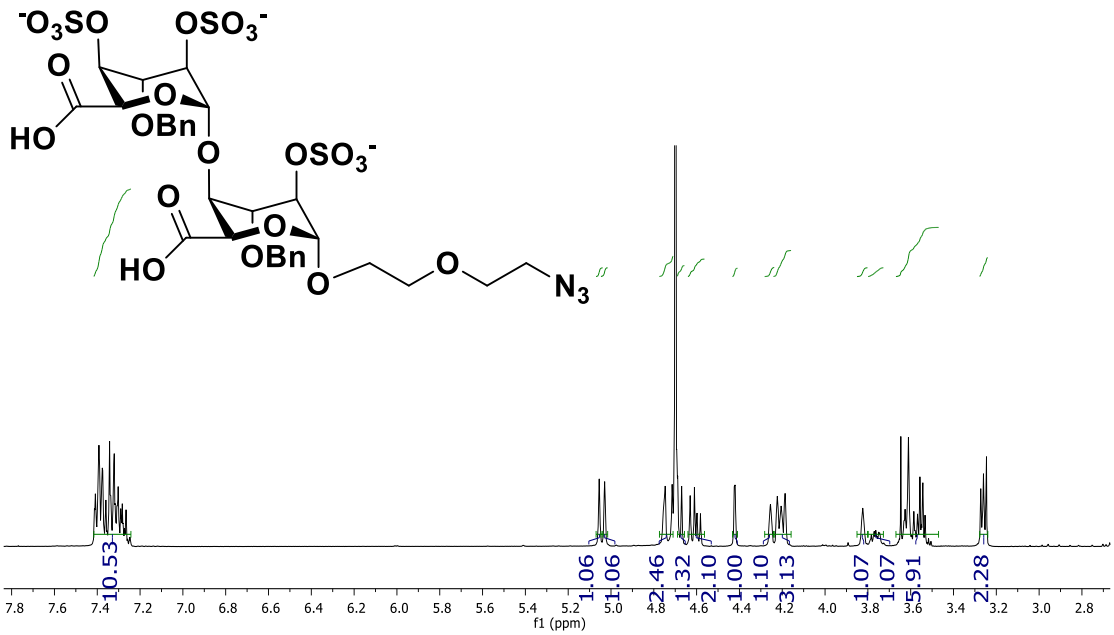
-O3SO
OSO3-
O
HO
O
OBn
O
OSO3-
O
HO
O
OBn
O
O
N3
10.53
1.06
1.06
2.46
1.32
2.10
1.00
1.10
3.13
1.07
1.07
5.91
2.28
f1 (ppm)

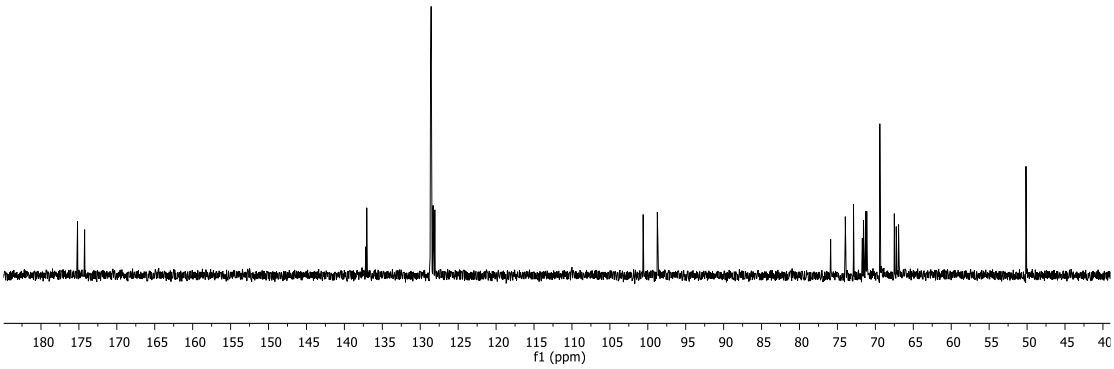
f1 (ppm)

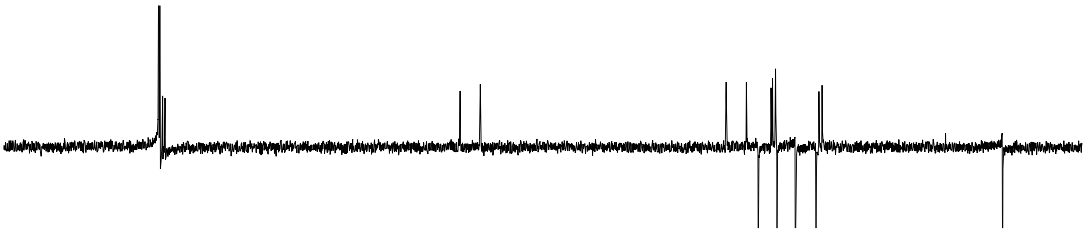

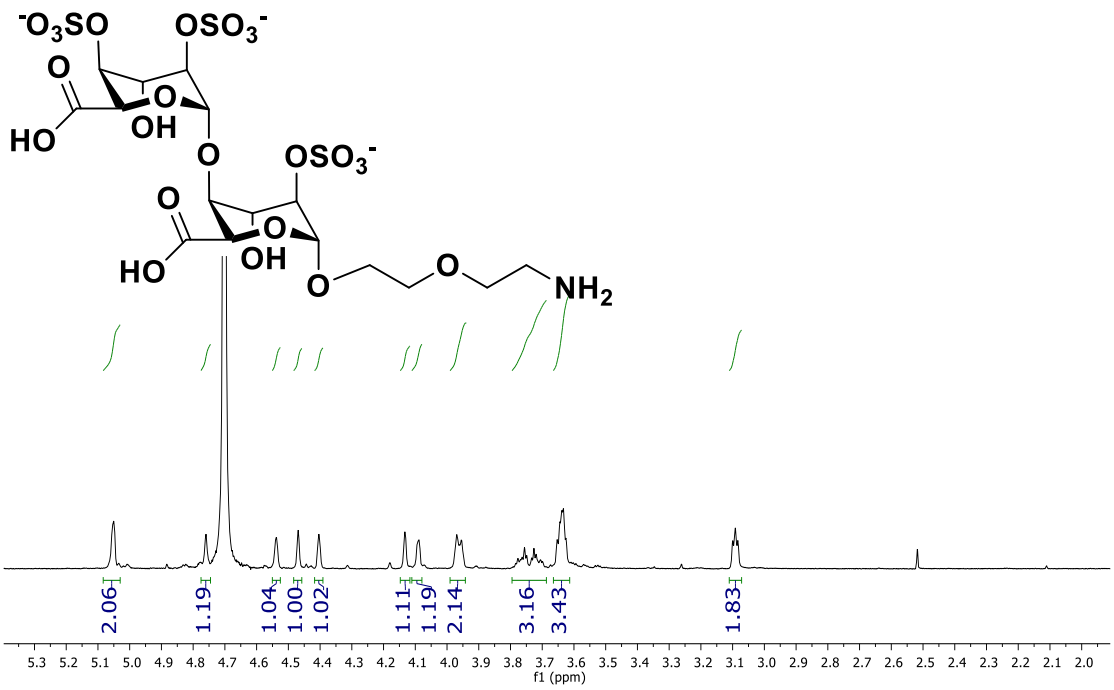
-O3SO
OSO3-
O
HO
O
OH
O
OSO3-
O
HO
O
OH
O
O
NH2
2.06
1.19
1.04
1.00
1.02
1.11
1.19
2.14
3.16
3.43
1.83
5.3 5.2 5.1 5.0 4.9 4.8 4.7 4.6 4.5 4.4 4.3 4.2 4.1 4.0 3.9 3.8 3.7 3.6 3.5 3.4 3.3 3.2 3.1 3.0 2.9 2.8 2.7 2.6 2.5 2.4 2.3 2.2 2.1 2.0
f1 (ppm)

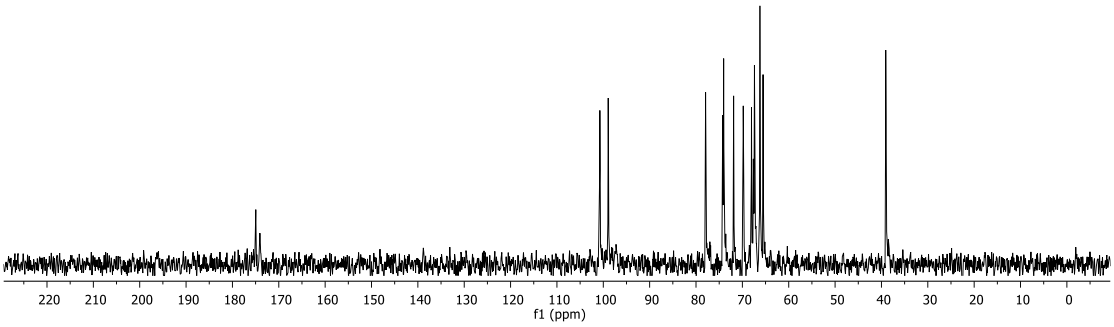
220 210 200 190 180 170 160 150 140 130 120 110 100 90 80 70 60 50 40 30 20 10 0
f1 (ppm)

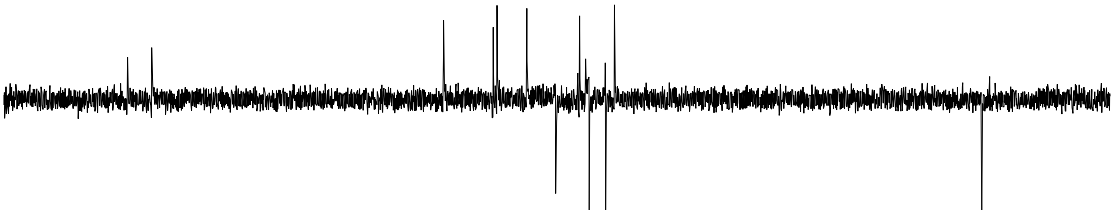

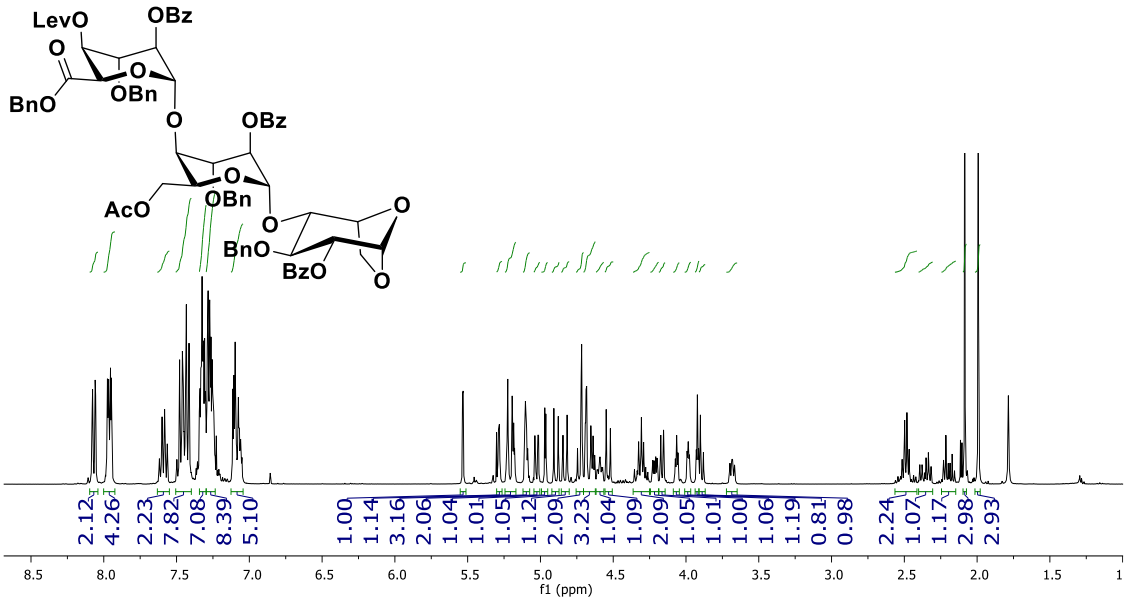
LevO
OBz
O
O
OBn
BnO
O
OBz
O
AcO
OBn
O
BnO
BzO
O
2.12
4.26
2.23
7.82
7.08
8.39
5.10
1.00
1.14
3.16
2.06
1.04
1.01
1.05
1.12
2.09
3.23
1.04
1.09
2.09
1.05
1.01
1.00
1.06
1.19
0.81
0.98
2.24
1.07
1.17
2.98
2.93
f1 (ppm)

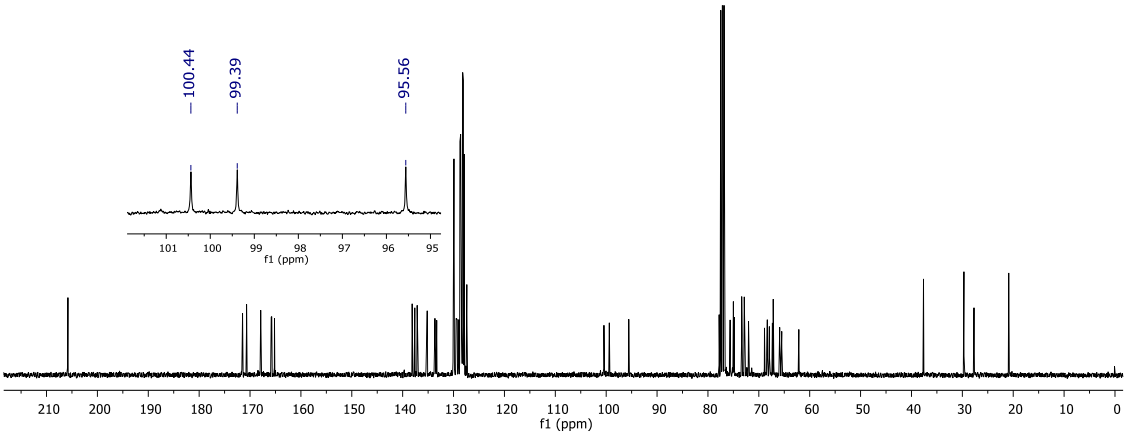
100.44
99.39
95.56
f1 (ppm)
f1 (ppm)

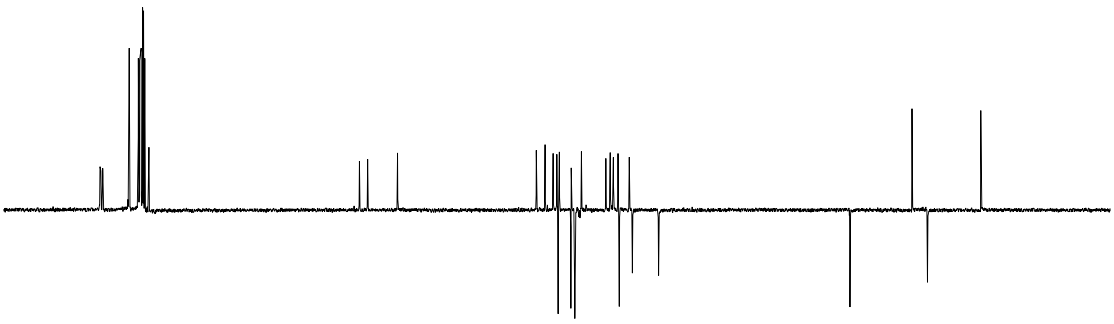

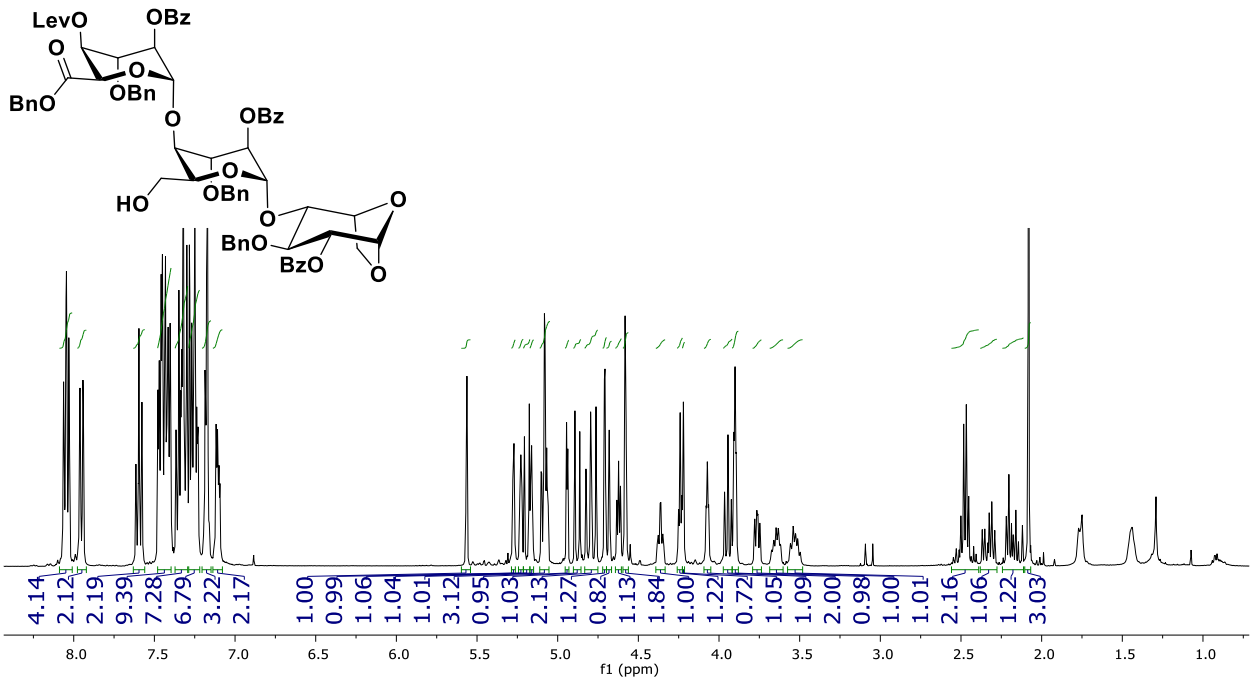
LevO
OBz
O
BnO
O
OBn
O
OBz
HO
O
OBn
O
BnO
BzO
O
O
4.14
2.12
2.19
9.39
7.28
6.79
3.22
2.17
1.00
0.99
1.06
1.04
1.01
3.12
0.95
1.03
2.13
1.27
0.82
1.13
1.84
1.00
1.22
0.72
1.05
1.09
2.00
0.98
1.00
1.01
2.16
1.06
1.22
3.03
8.0
7.5
7.0
6.5
6.0
5.5
5.0
4.5
4.0
3.5
3.0
2.5
2.0
1.5
1.0
f1 (ppm)

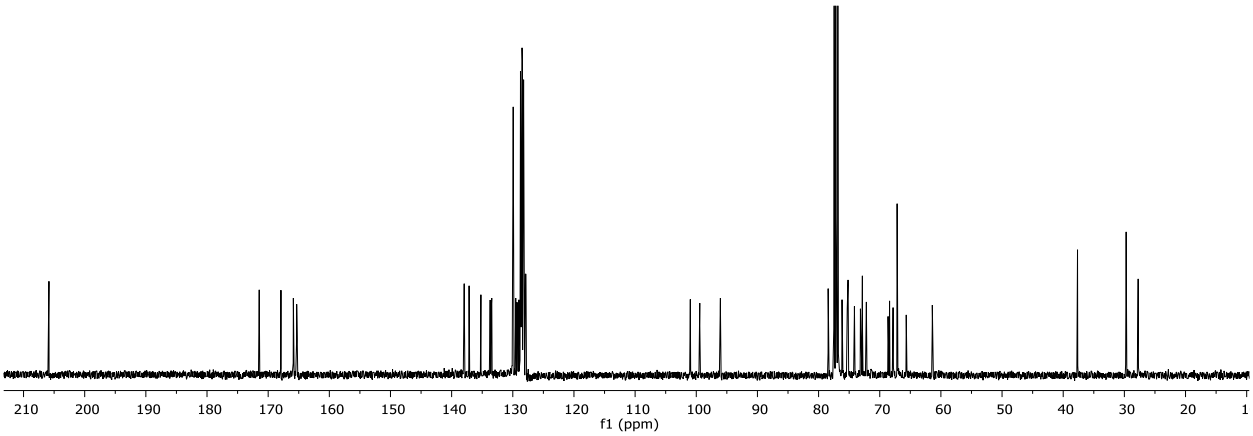
210
200
190
180
170
160
150
140
130
120
110
100
90
80
70
60
50
40
30
20
1
f1 (ppm)

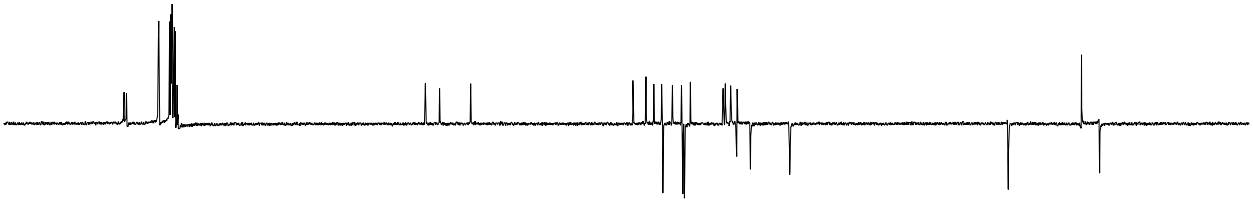

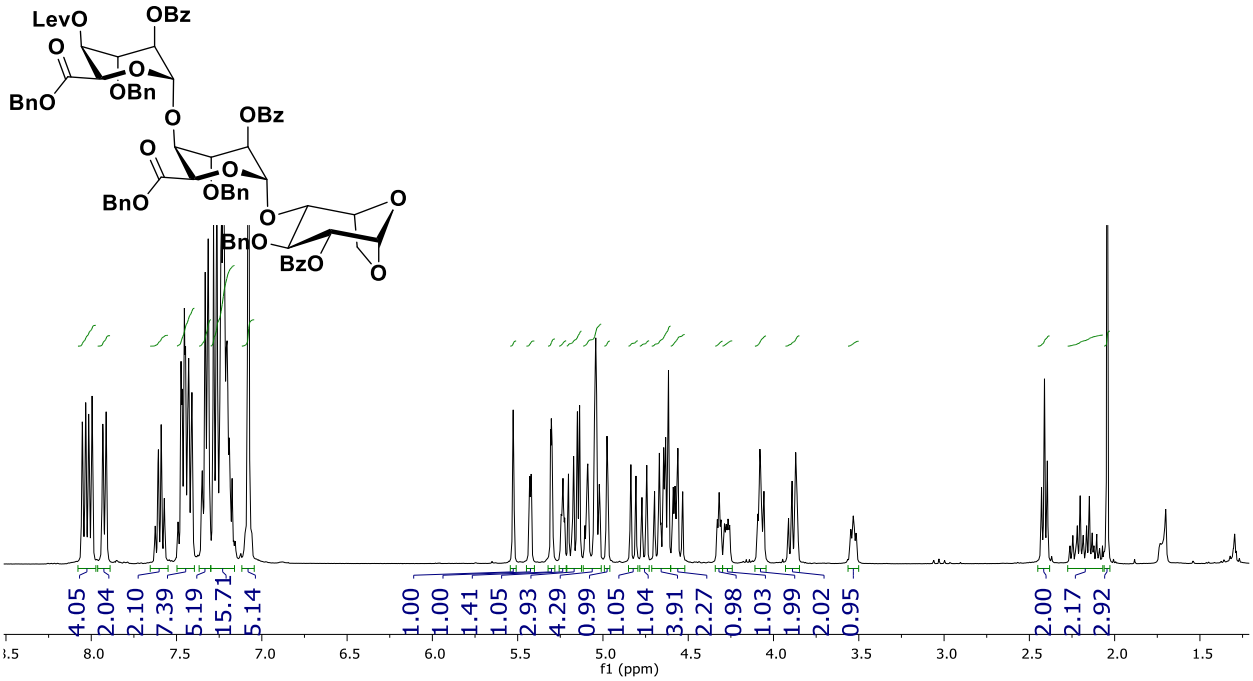
LevO
OBz
O
O
OBn
BnO
O
OBz
O
O
OBn
BnO
O
BnO
BzO
O
O
4.05
2.04
2.10
7.39
5.19
15.71
5.14
1.00
1.00
1.41
1.05
2.93
4.29
0.99
1.05
1.04
3.91
2.27
0.98
1.03
1.99
2.02
0.95
2.00
2.17
2.92
f1 (ppm)

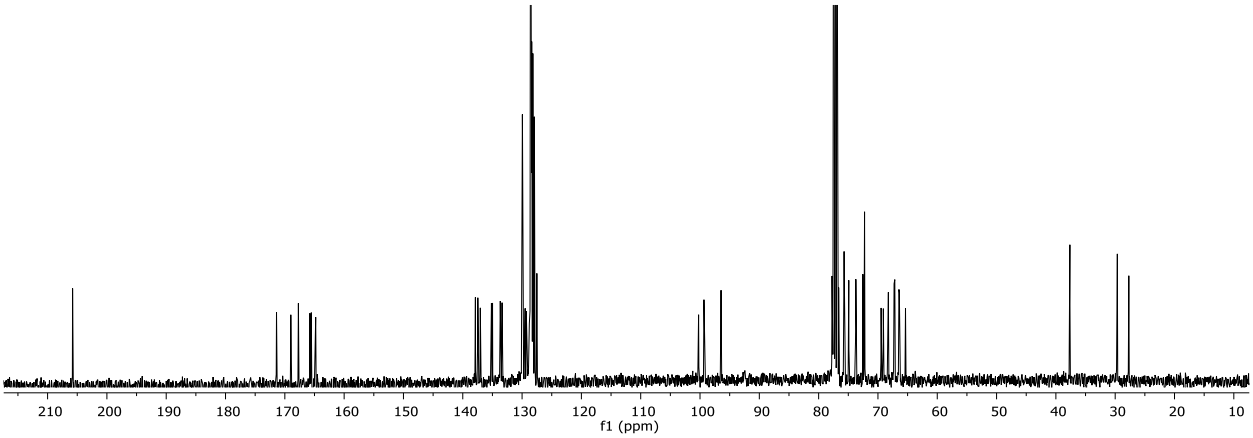
f1 (ppm)

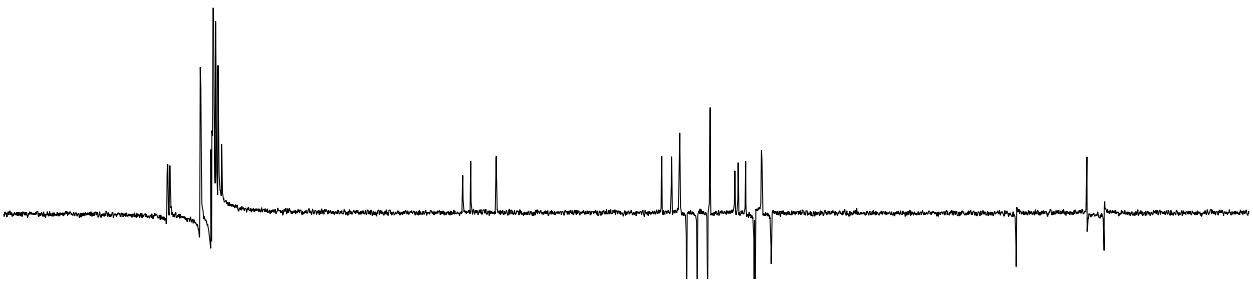

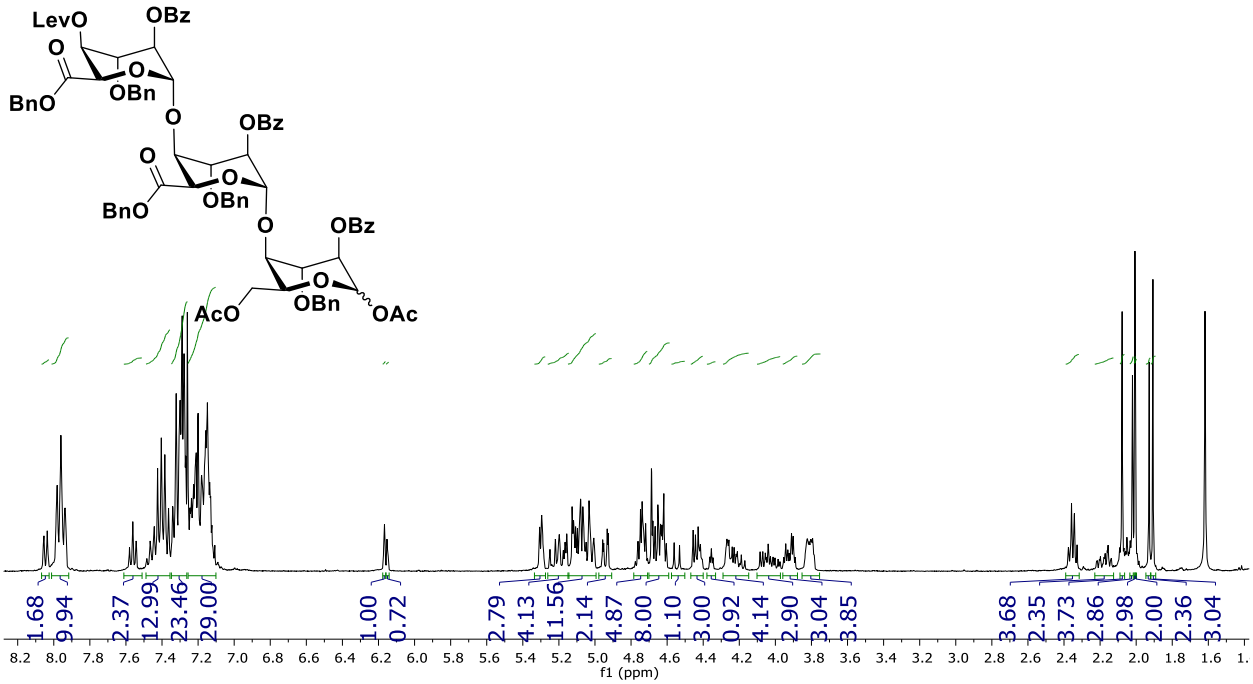
LevO
OBz
O
O
OBn
BnO
O
OBz
O
O
OBn
BnO
O
OBz
O
OBn
AcO
OAc
1.68
9.94
2.37
12.99
23.46
29.00
1.00
0.72
2.79
4.13
11.56
2.14
4.87
8.00
1.10
3.00
0.92
4.14
2.90
3.04
3.85
3.68
2.35
3.73
2.86
2.98
2.00
2.36
3.04
f1 (ppm)

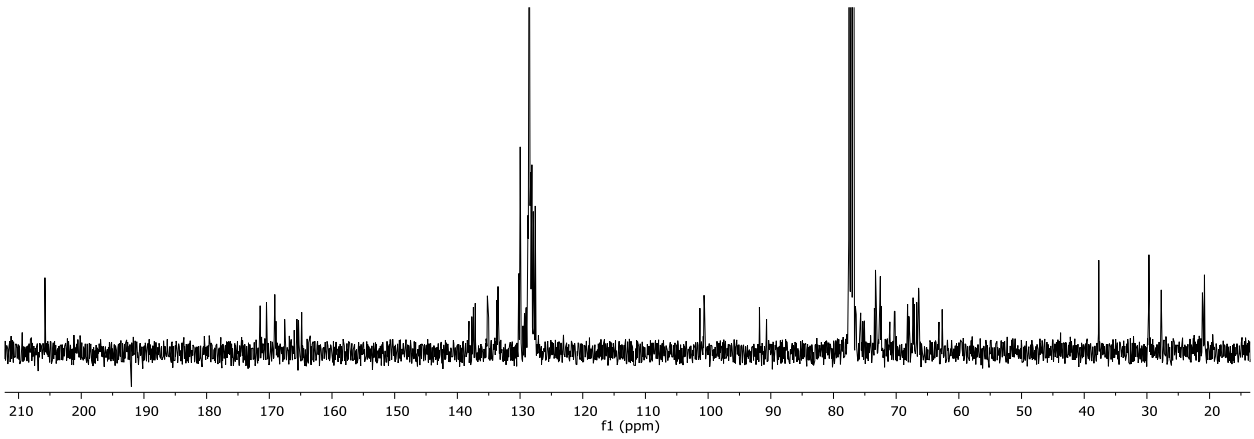
f1 (ppm)

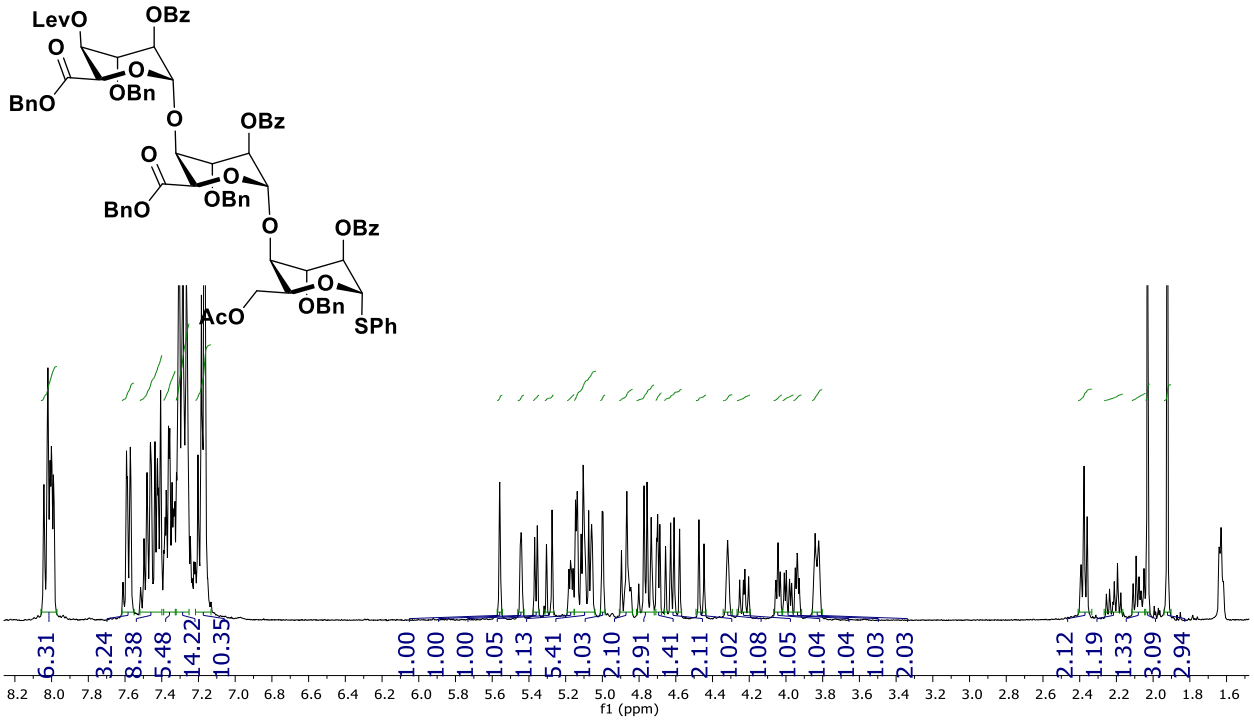
LevO
OBz
O
O
OBn
BnO
O
OBz
O
O
OBn
BnO
O
OBz
O
OBn
AcO
SPh
6.31
3.24
8.38
5.48
14.22
10.35
1.00
1.00
1.00
1.05
1.13
5.41
1.03
2.10
2.91
1.41
2.11
1.02
1.08
1.05
1.04
1.04
1.03
2.03
2.12
1.19
1.33
3.09
2.94
f1 (ppm)

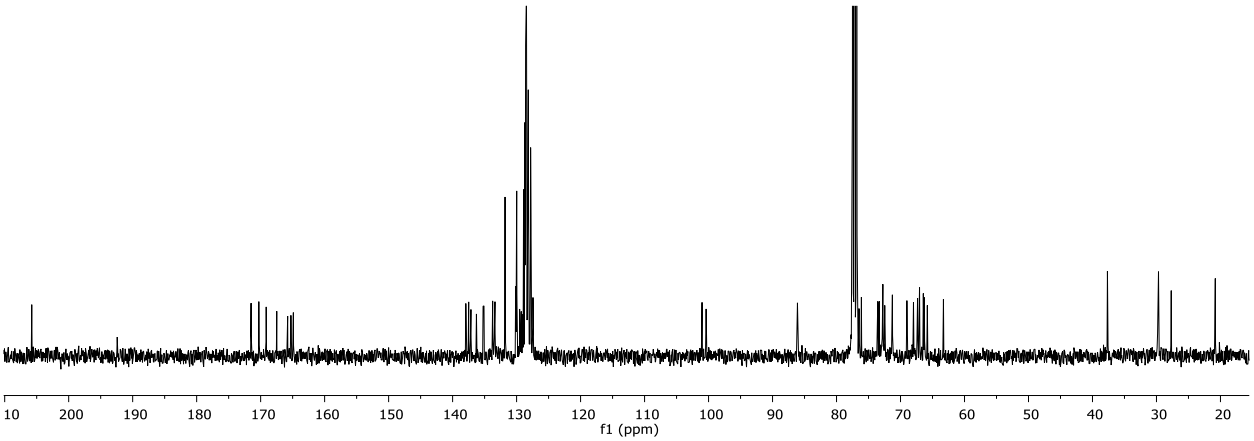
f1 (ppm)

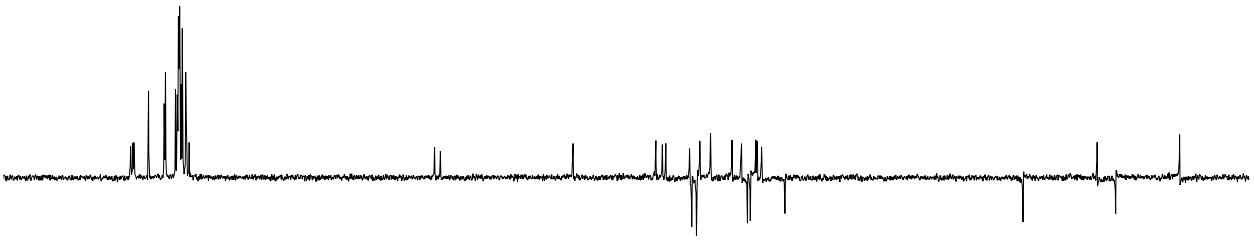

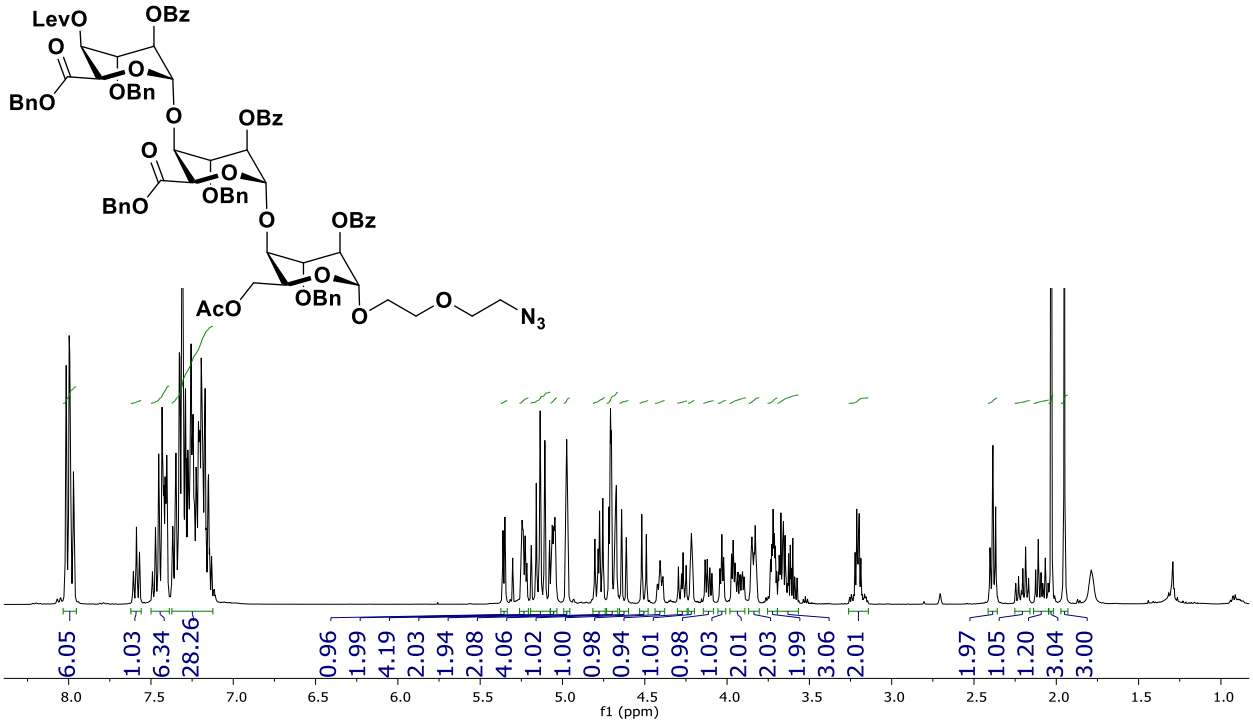
LevO
OBz
O
O
OBn
BnO
O
OBz
O
O
OBn
BnO
O
OBz
O
OBn
AcO
O
O
N3
6.05
1.03
6.34
28.26
0.96
1.99
4.19
2.03
1.94
2.08
4.06
1.02
1.00
0.98
0.94
1.01
0.98
1.03
2.01
2.03
1.99
3.06
2.01
1.97
1.05
1.20
3.04
3.00
8.0
7.5
7.0
6.5
6.0
5.5
5.0
4.5
4.0
3.5
3.0
2.5
2.0
1.5
1.0
f1 (ppm)

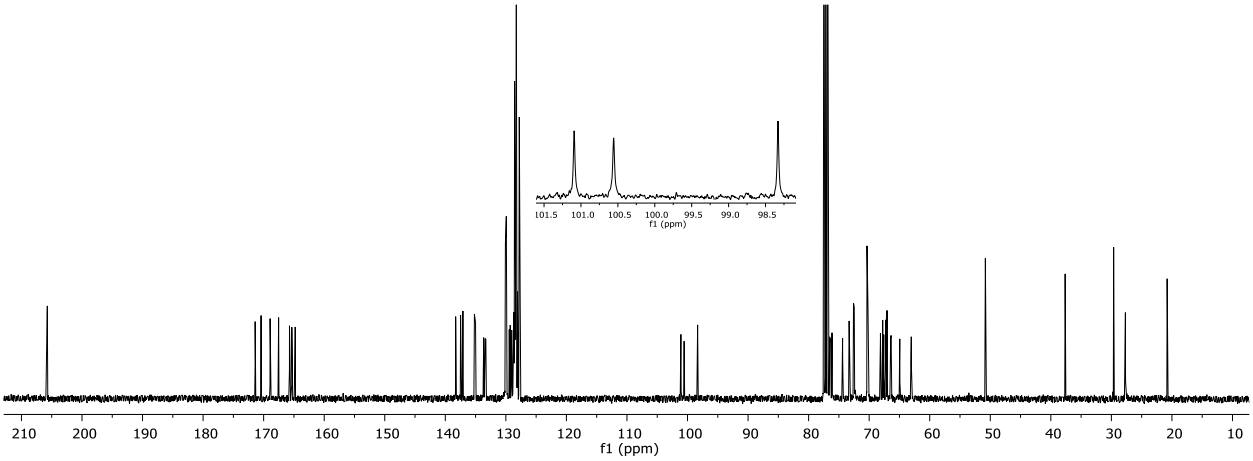
101.5
101.0
100.5
100.0
99.5
99.0
98.5
f1 (ppm)
210
200
190
180
170
160
150
140
130
120
110
100
90
80
70
60
50
40
30
20
10
f1 (ppm)

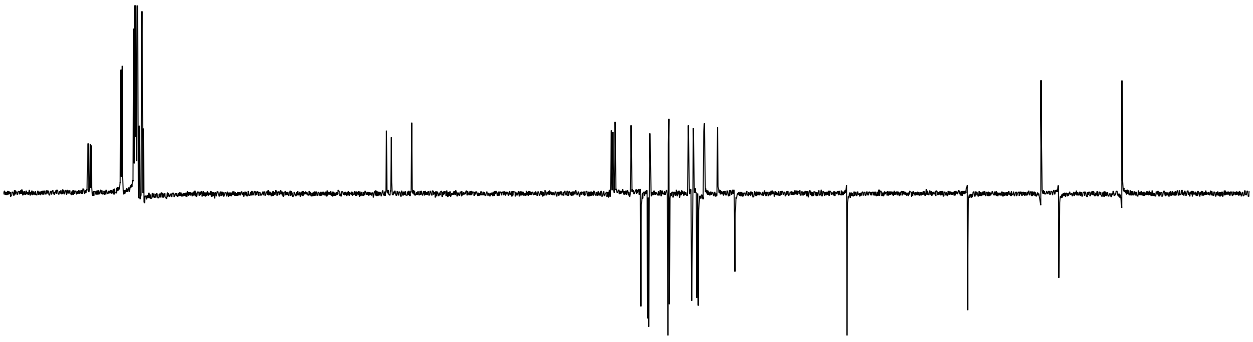

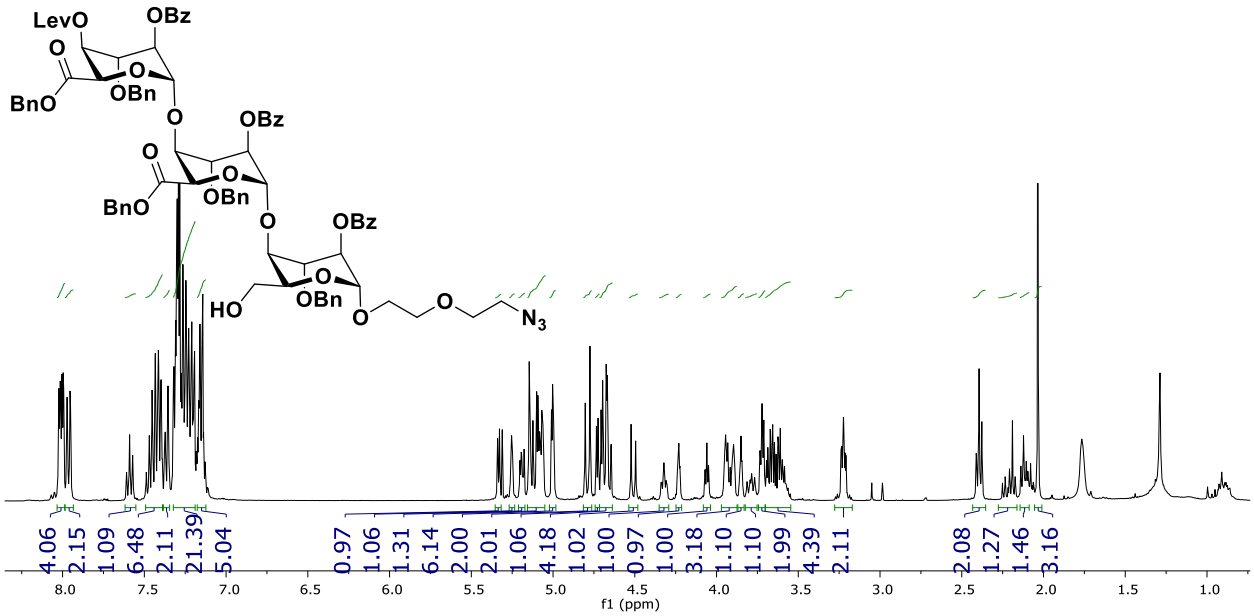
LevO
OBz
O
BnO
OBn
O
OBz
O
BnO
OBn
O
OBz
HO
O
OBn
O
O
N3
4.06
2.15
1.09
6.48
2.11
21.39
5.04
0.97
1.06
1.31
6.14
2.00
2.01
1.06
4.18
1.02
1.00
0.97
1.00
3.18
1.10
1.10
1.99
4.39
2.11
2.08
1.27
1.46
3.16
f1 (ppm)

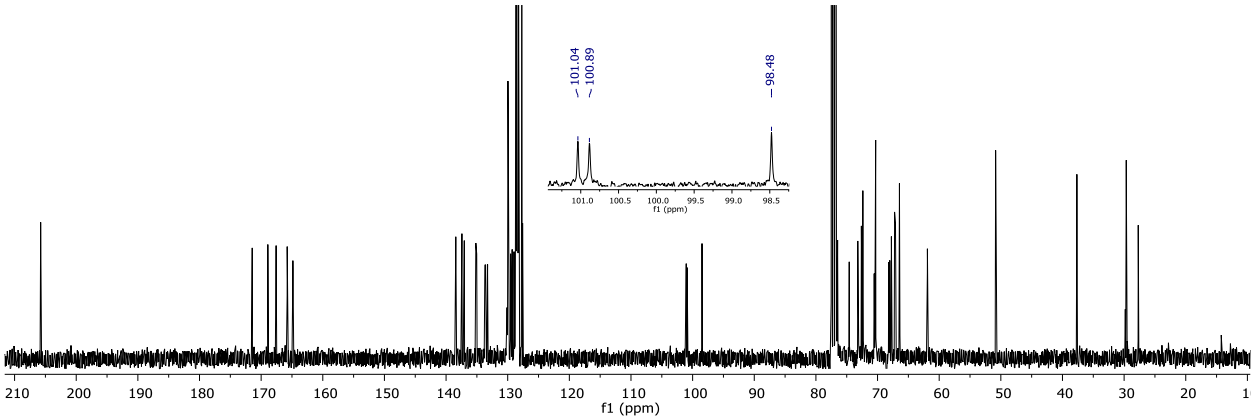
101.04
100.89
98.48
f1 (ppm)

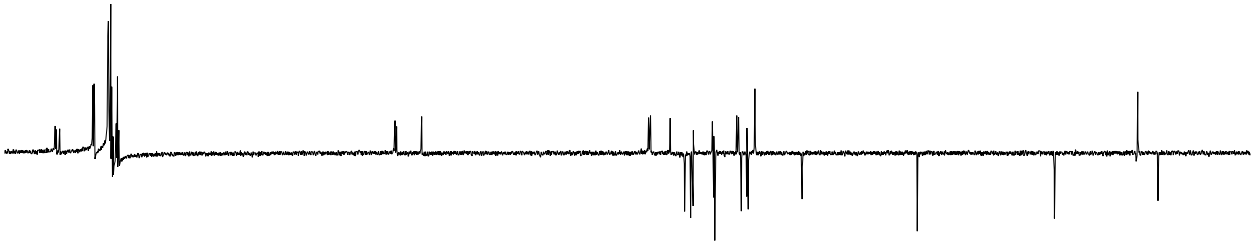

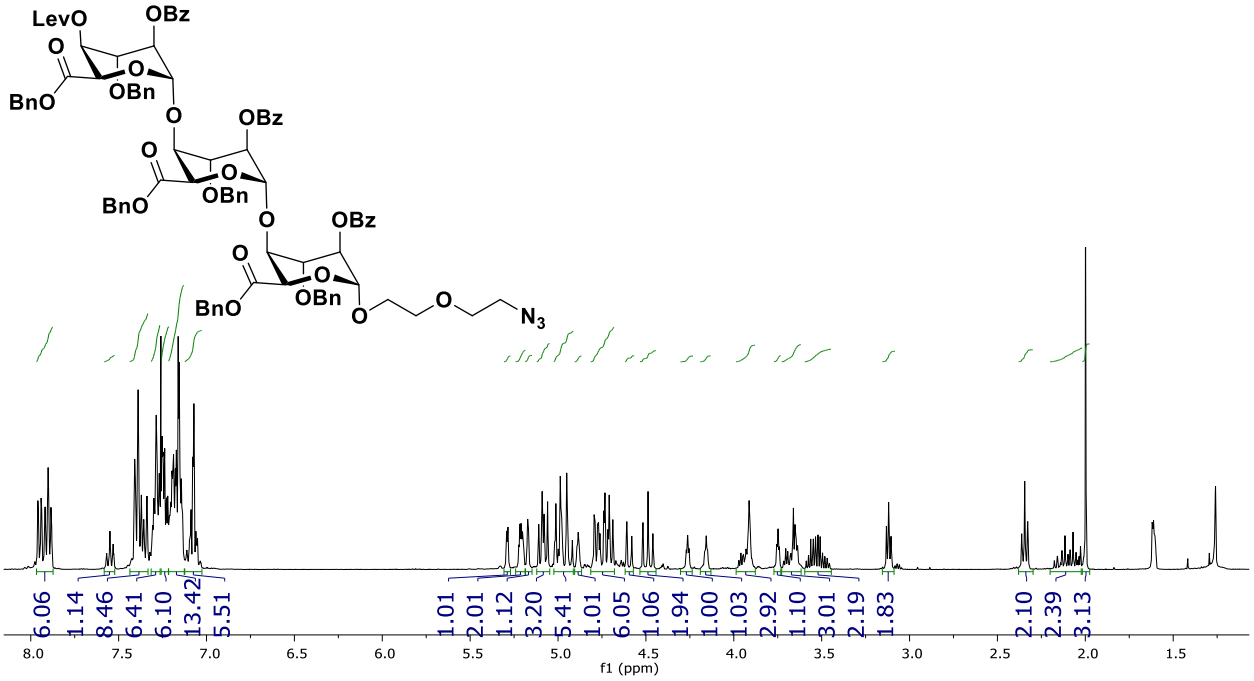
LevO
OBz
O
O
OBn
BnO
O
OBz
O
O
OBn
BnO
O
OBz
O
O
OBn
BnO
O
O
N3
6.06 1.14 8.46 6.41 6.10 13.42 5.51
1.01 2.01 1.12 3.20 5.41 1.01 6.05 1.06 1.94 1.00 1.03 2.92 1.10 3.01 2.19 1.83
2.10 2.39 3.13
f1 (ppm)

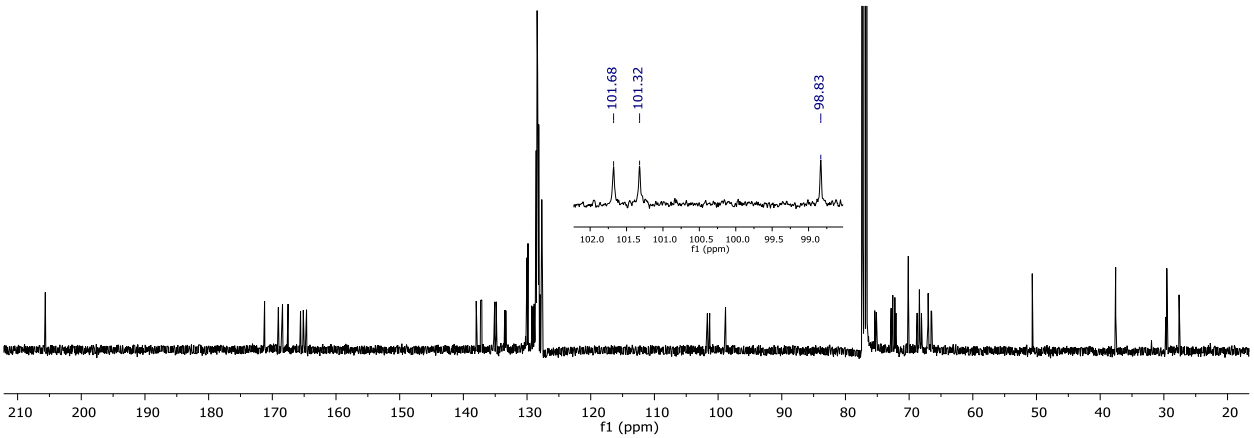
101.68
101.32
98.83
f1 (ppm)

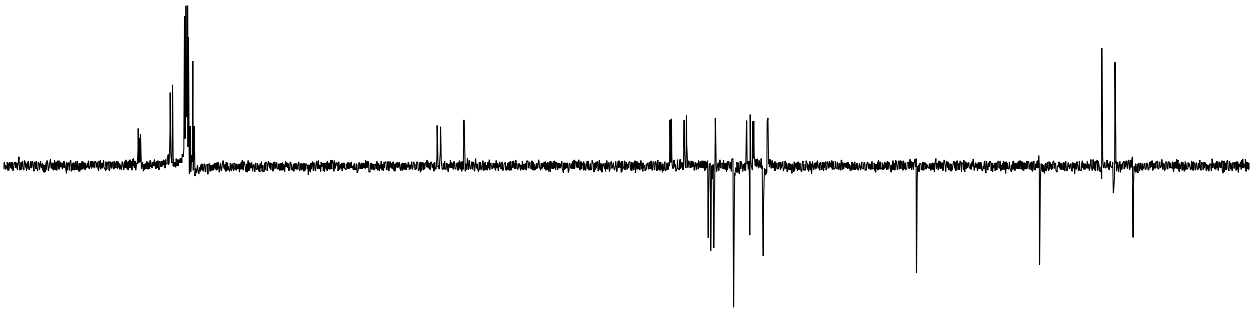

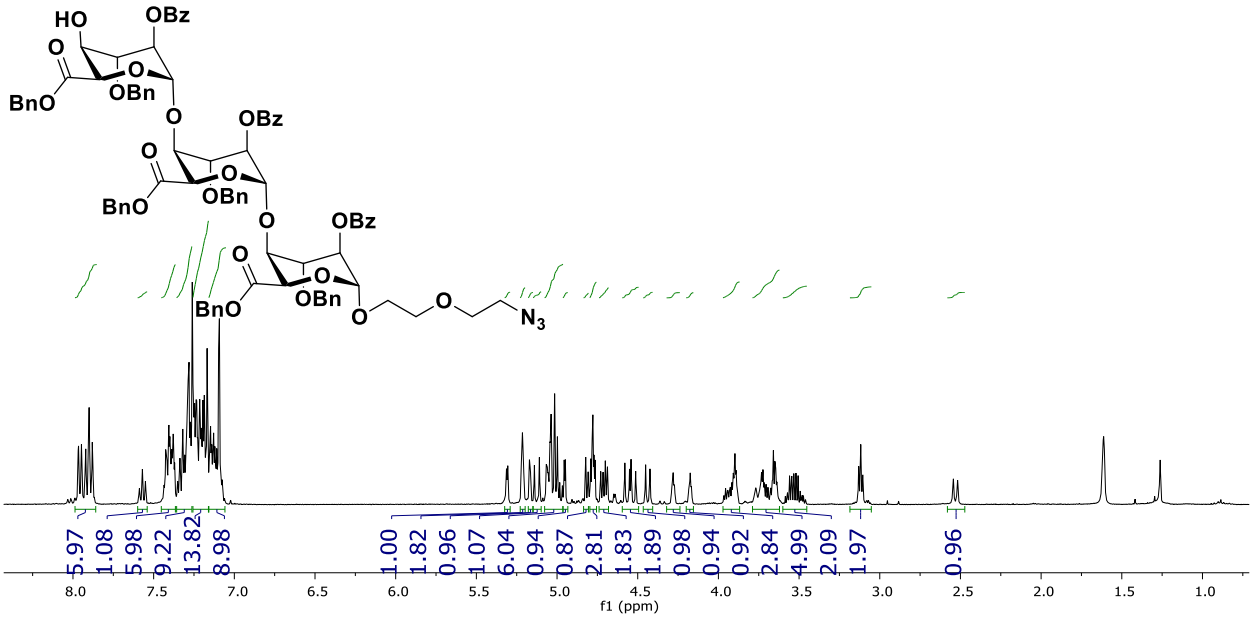
HO
OBz
O
O
OBn
BnO
O
OBz
O
O
OBn
BnO
O
OBz
O
O
OBn
BnO
O
N3
5.97
1.08
5.98
9.22
13.82
8.98
1.00
1.82
0.96
1.07
6.04
0.94
0.87
2.81
1.83
1.89
0.98
0.94
0.92
2.84
4.99
2.09
1.97
0.96
f1 (ppm)

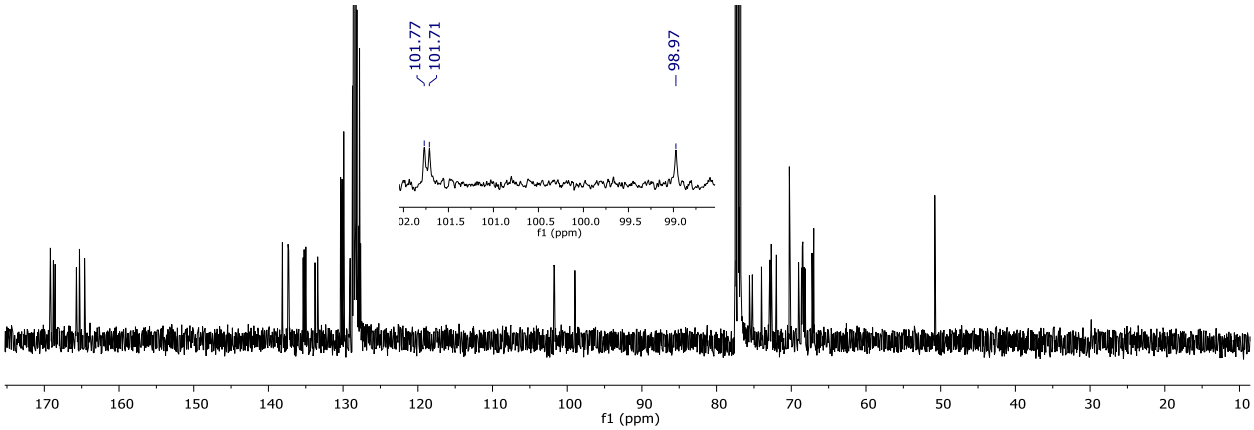
101.77
101.71
98.97
f1 (ppm)

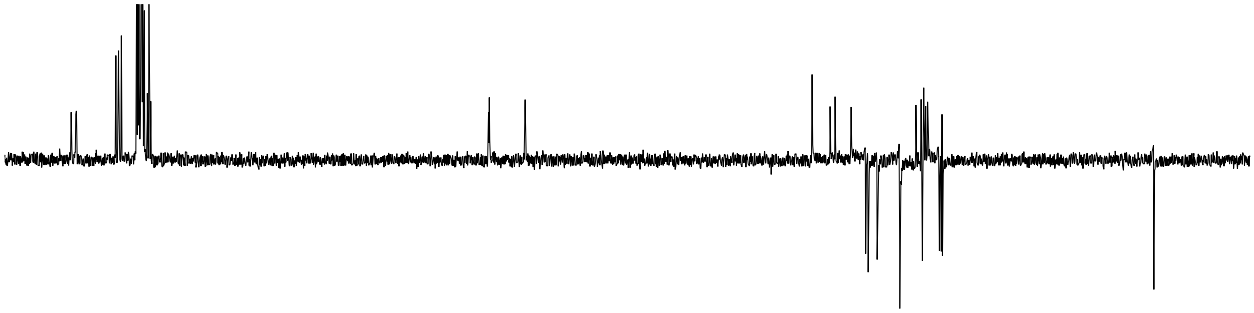

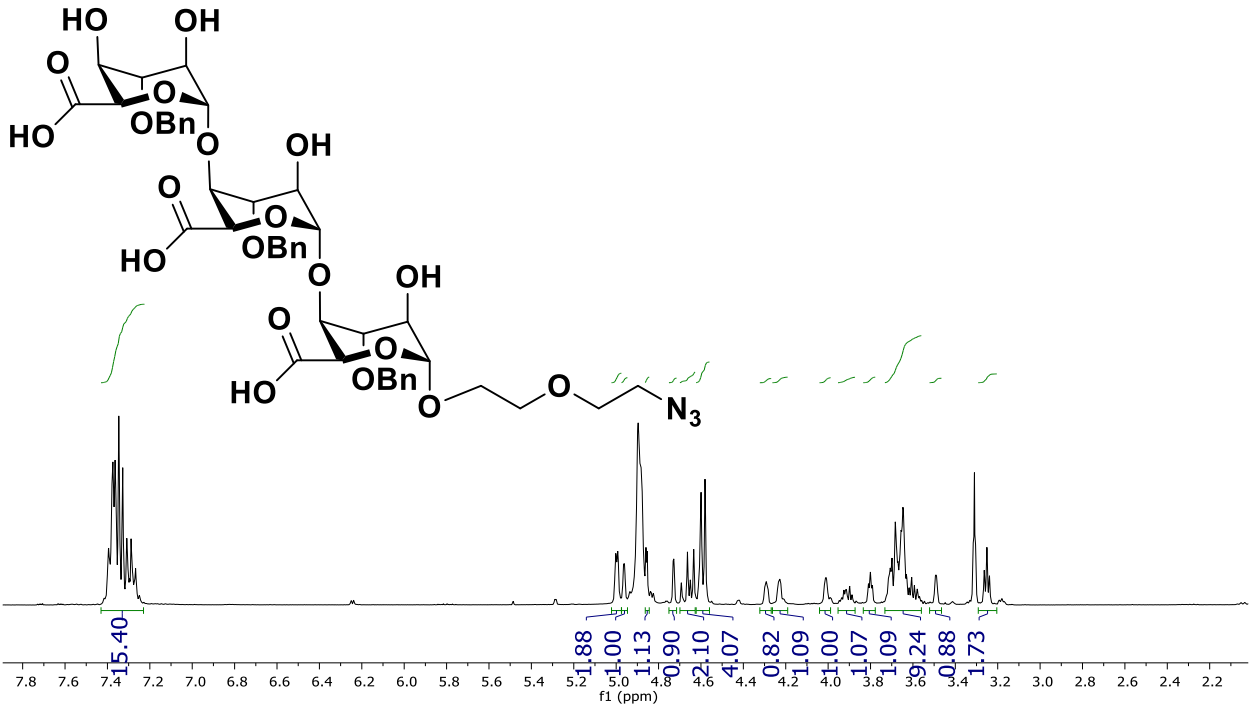
HO
OH
O
HO
OBn
O
OH
O
HO
OBn
O
OH
O
HO
OBn
O
O
N3
15.40
1.88
1.00
1.13
0.90
2.10
4.07
0.82
1.09
1.00
1.07
1.09
9.24
0.88
1.73
f1 (ppm)

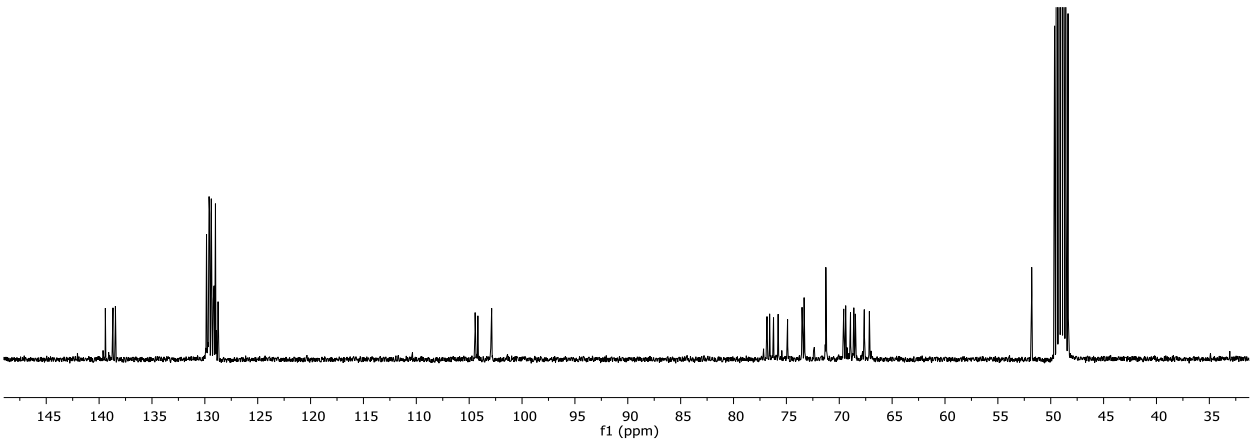
f1 (ppm)

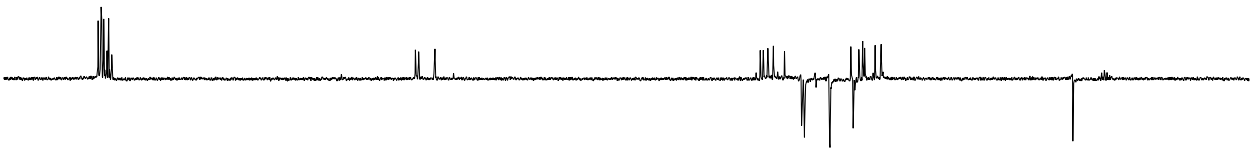

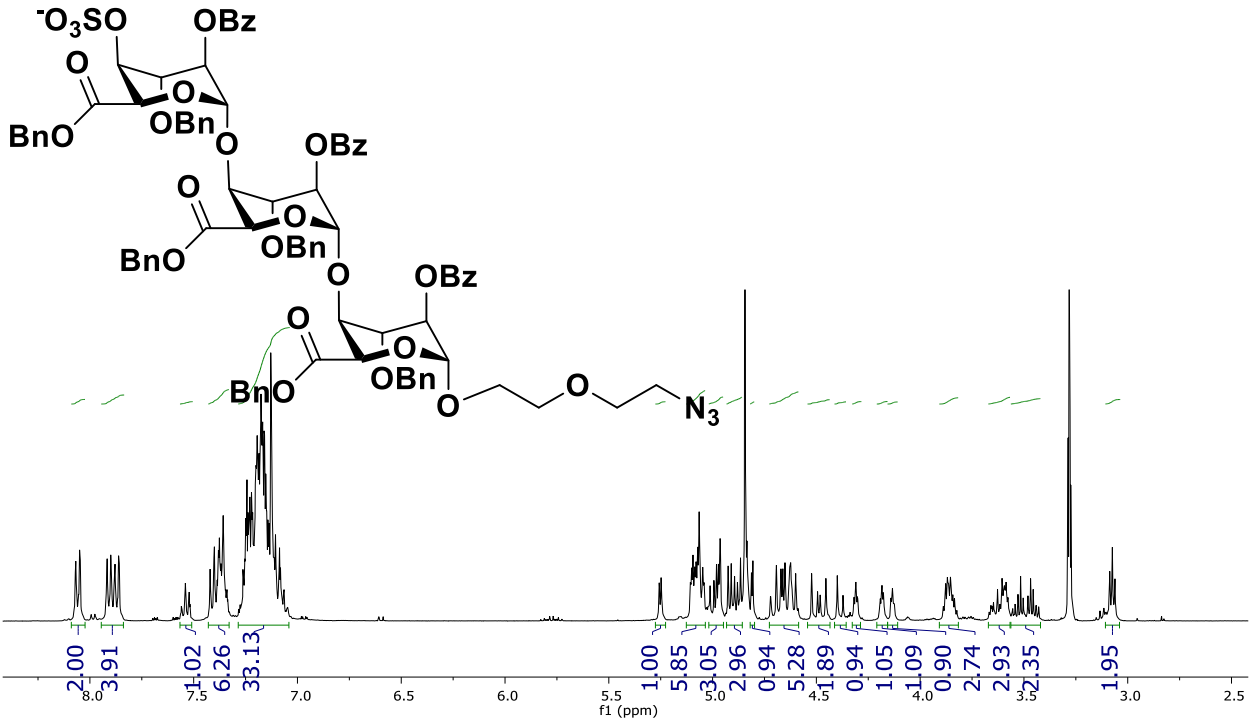
-O3SO
OBz
O
BnO
OBn
O
OBz
O
BnO
OBn
O
OBz
O
BnO
OBn
O
O
N3
2.00
3.91
1.02
6.26
33.13
1.00
5.85
3.05
2.96
0.94
5.28
1.89
0.94
1.05
1.09
0.90
2.74
2.93
2.35
1.95
8.0
7.5
7.0
6.5
6.0
5.5
5.0
4.5
4.0
3.5
3.0
2.5
f1 (ppm)

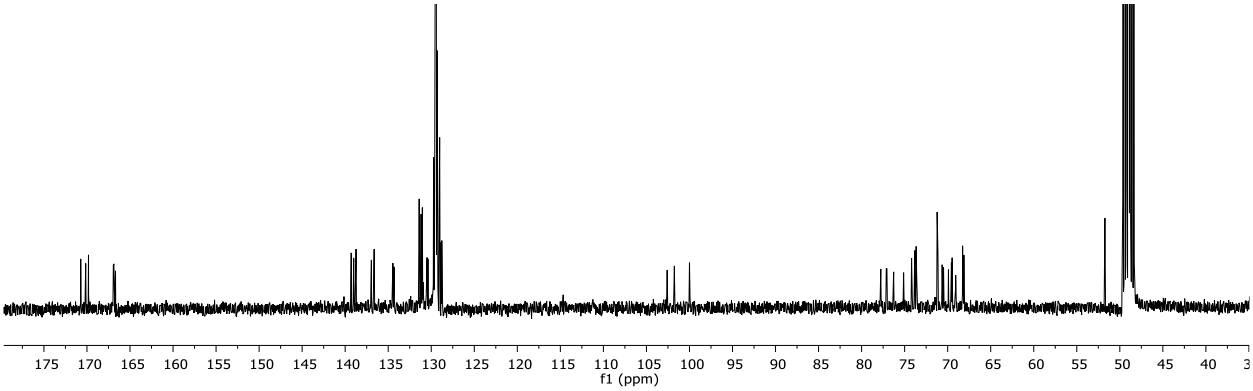
175 170 165 160 155 150 145 140 135 130 125 120 115 110 105 100 95 90 85 80 75 70 65 60 55 50 45 40
f1 (ppm)

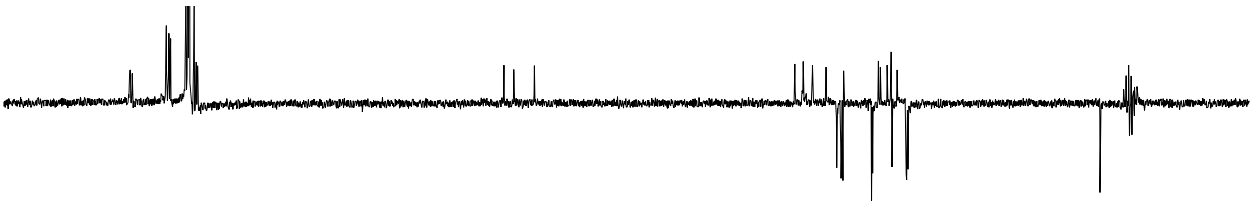

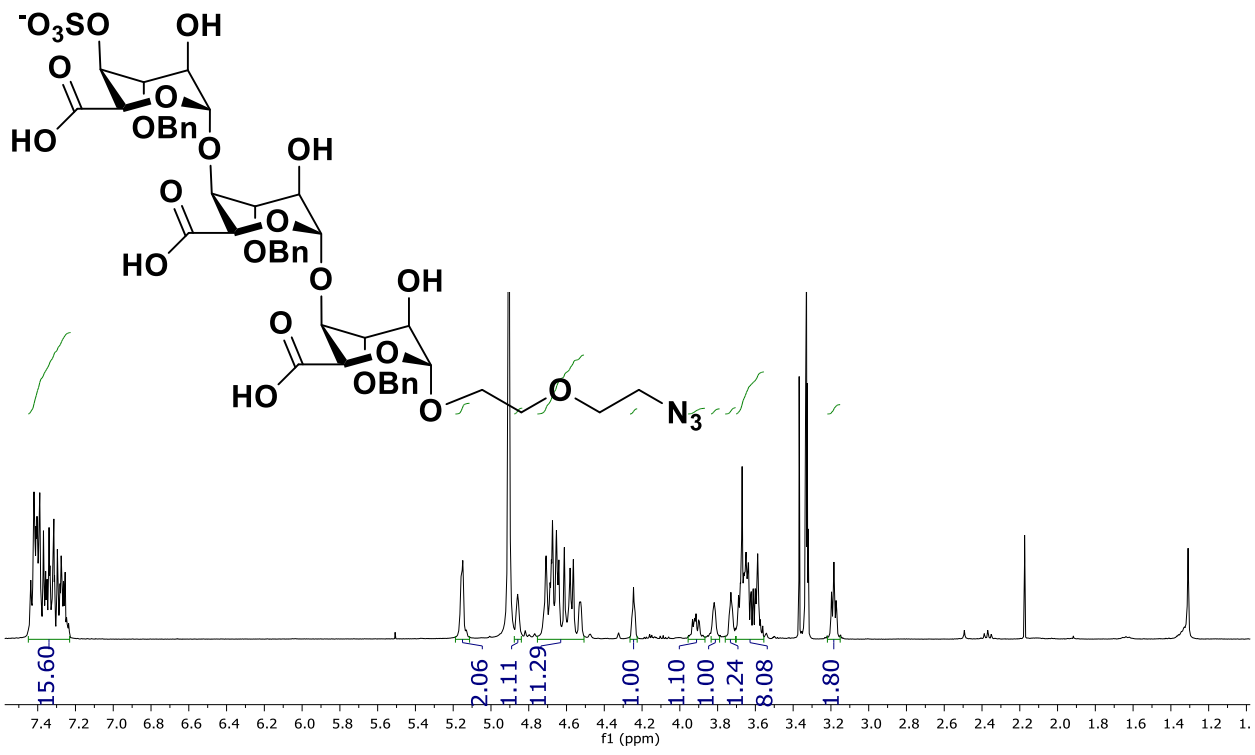
-O3SO
OH
O
HO
O
OBn
O
OH
O
HO
O
OBn
O
OH
O
HO
O
OBn
O
O
N3
15.60
2.06
1.11
11.29
1.00
1.10
1.00
1.24
8.08
1.80
f1 (ppm)

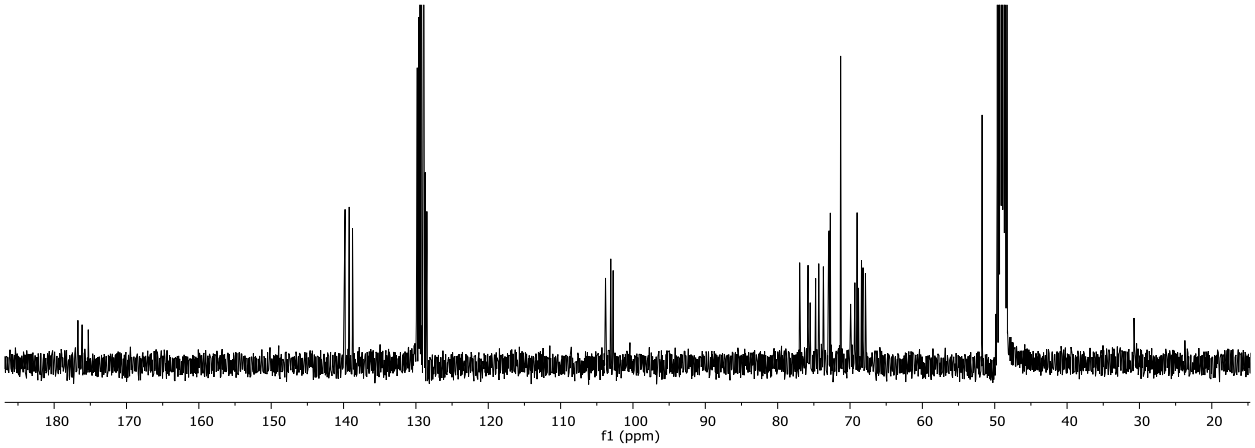
f1 (ppm)

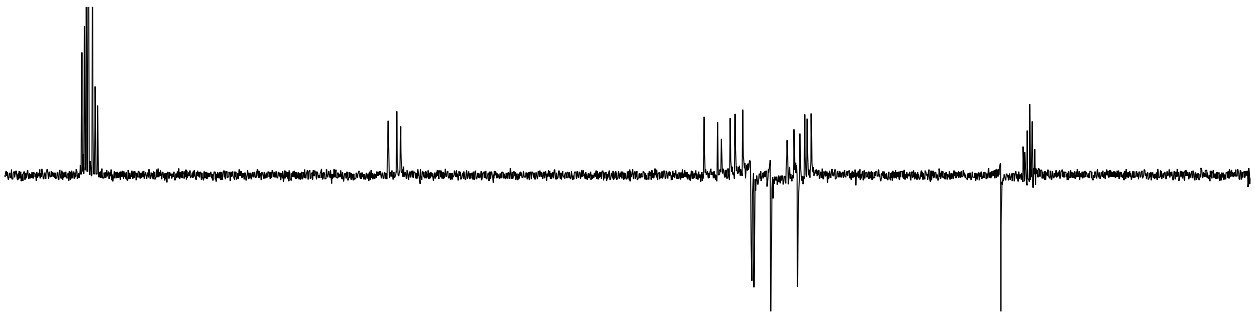

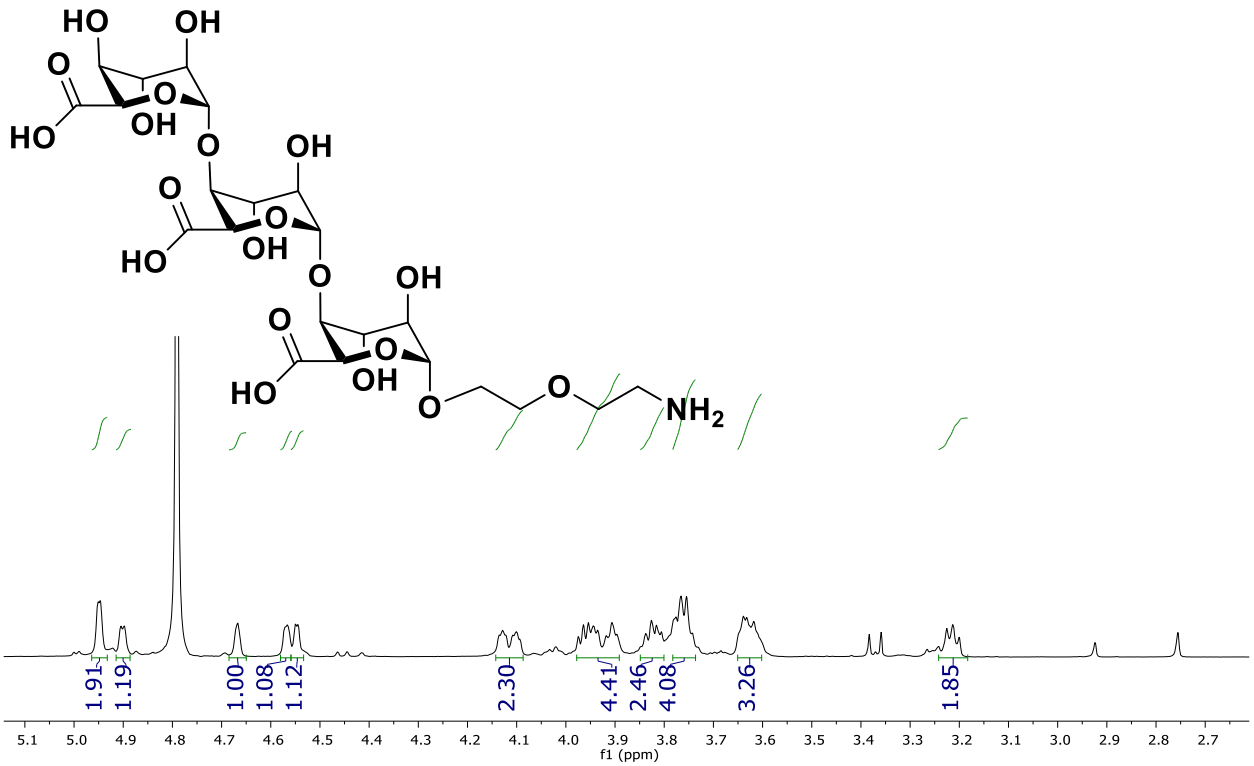
HO
OH
O
HO
OH
O
OH
O
HO
OH
O
OH
O
HO
OH
O
O
NH2
1.91
1.19
1.00
1.08
1.12
2.30
4.41
2.46
4.08
3.26
1.85
5.1 5.0 4.9 4.8 4.7 4.6 4.5 4.4 4.3 4.2 4.1 4.0 3.9 3.8 3.7 3.6 3.5 3.4 3.3 3.2 3.1 3.0 2.9 2.8 2.7
f1 (ppm)

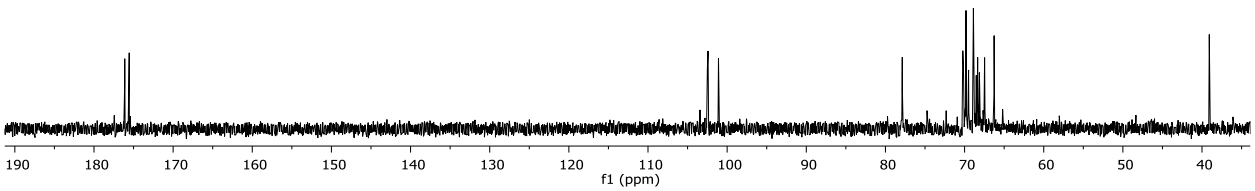
190 180 170 160 150 140 130 120 110 100 90 80 70 60 50 40
f1 (ppm)

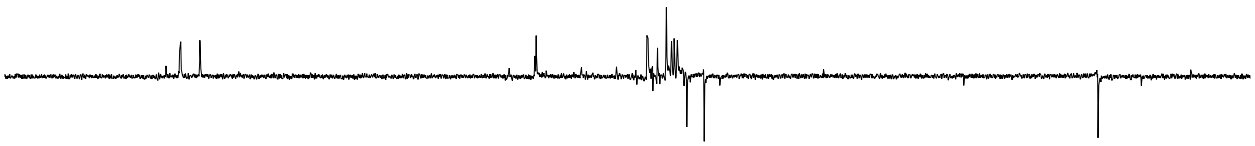

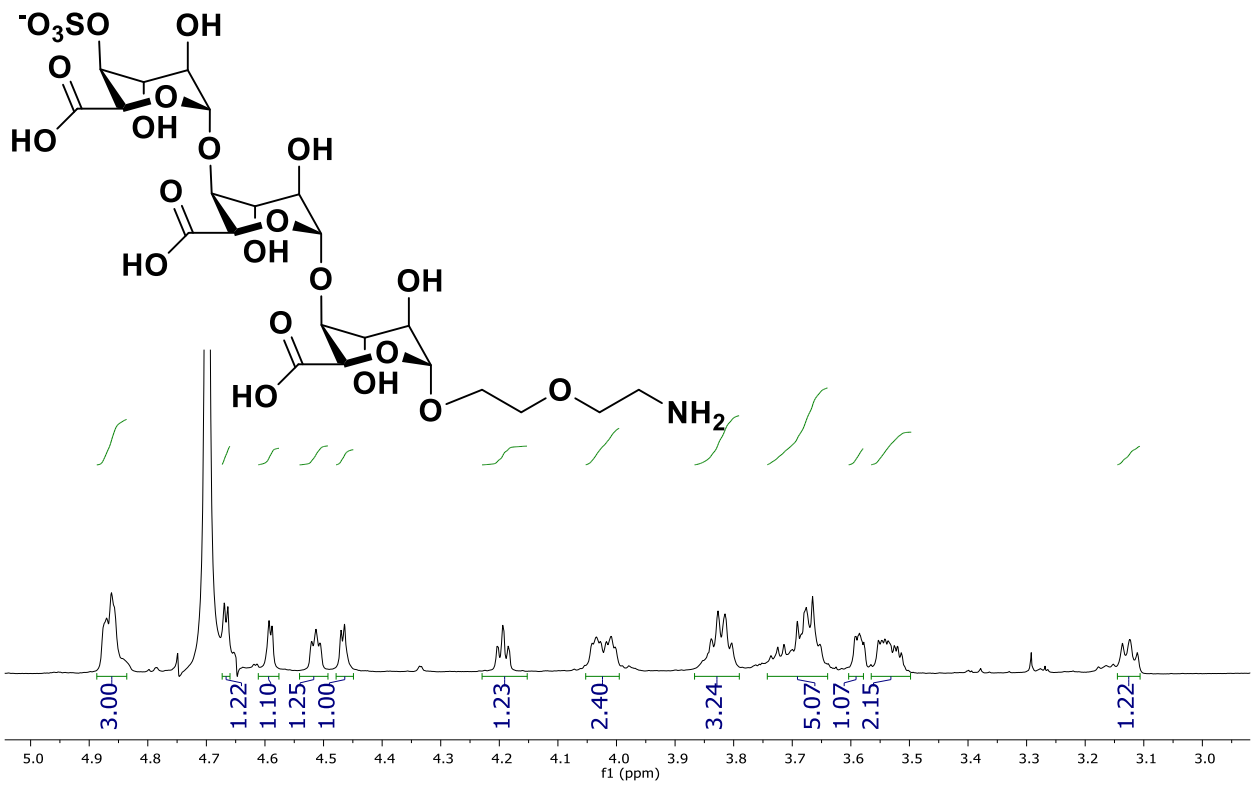
$^{-}O_3SO$
OH
O
HO
O
OH
O
OH
O
HO
O
OH
O
OH
O
HO
O
OH
O
O
NH_2
3.00
1.22
1.10
1.25
1.00
1.23
2.40
3.24
5.07
1.07
2.15
1.22
5.0 4.9 4.8 4.7 4.6 4.5 4.4 4.3 4.2 4.1 4.0 3.9 3.8 3.7 3.6 3.5 3.4 3.3 3.2 3.1 3.0
f1 (ppm)

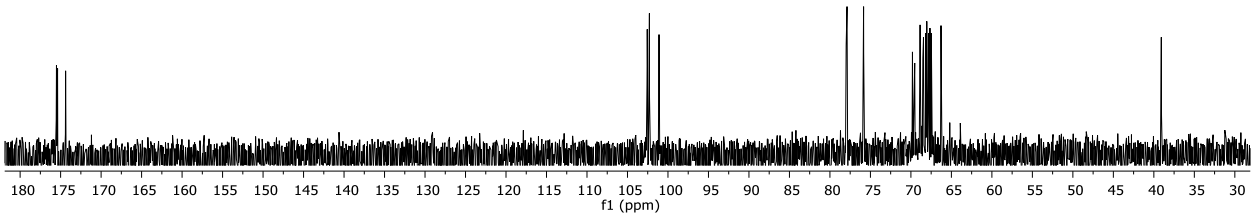
180 175 170 165 160 155 150 145 140 135 130 125 120 115 110 105 100 95 90 85 80 75 70 65 60 55 50 45 40 35 30
f1 (ppm)

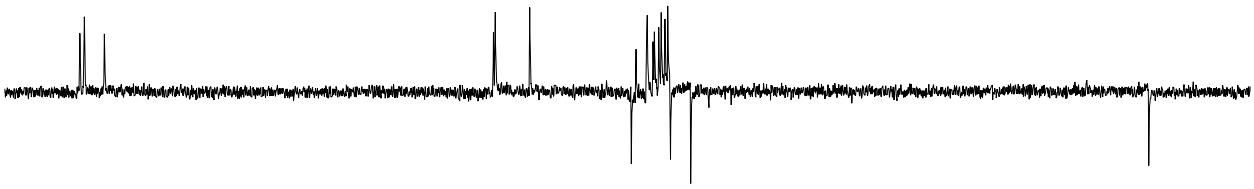

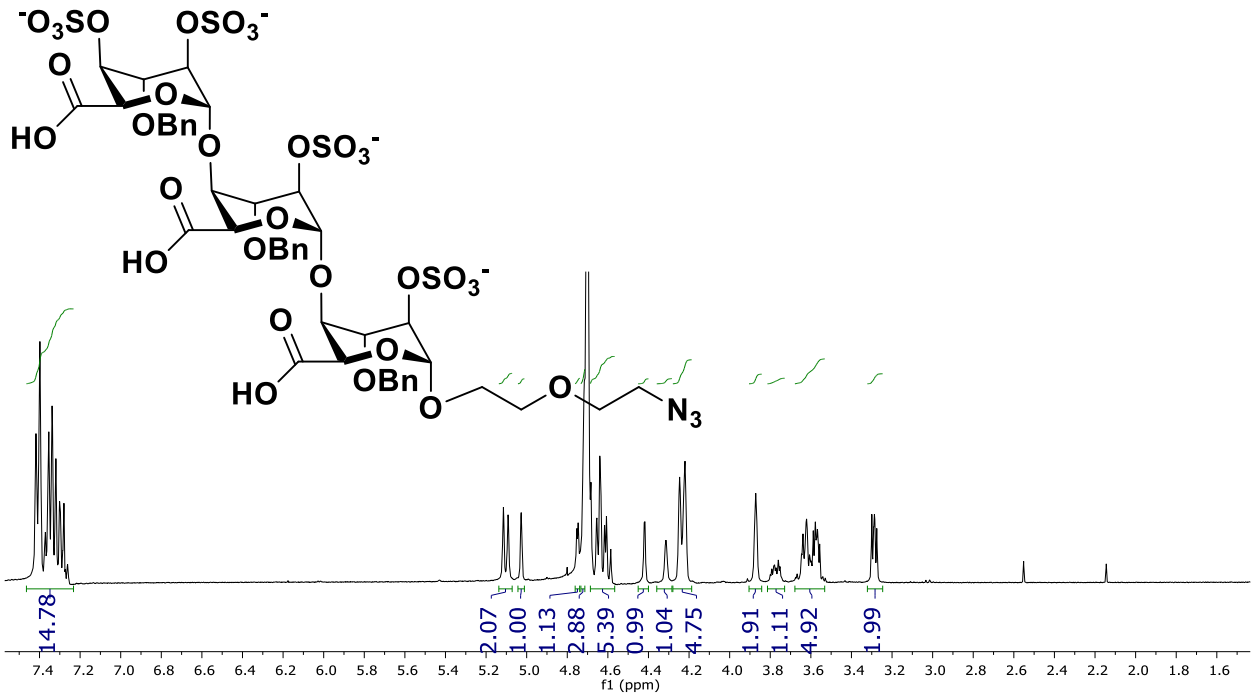
-O3SO
OSO3-
O
HO
O
OBn
O
OSO3-
O
HO
O
OBn
O
OSO3-
O
HO
O
OBn
O
O
N3
14.78
2.07
1.00
1.13
2.88
5.39
0.99
1.04
4.75
1.91
1.11
4.92
1.99
f1 (ppm)

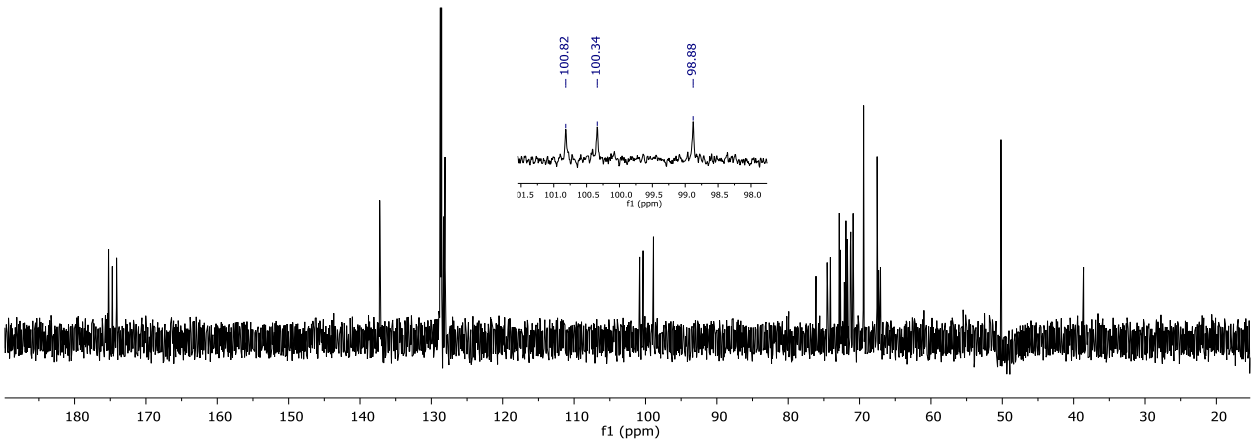
100.82
100.34
98.88
f1 (ppm)

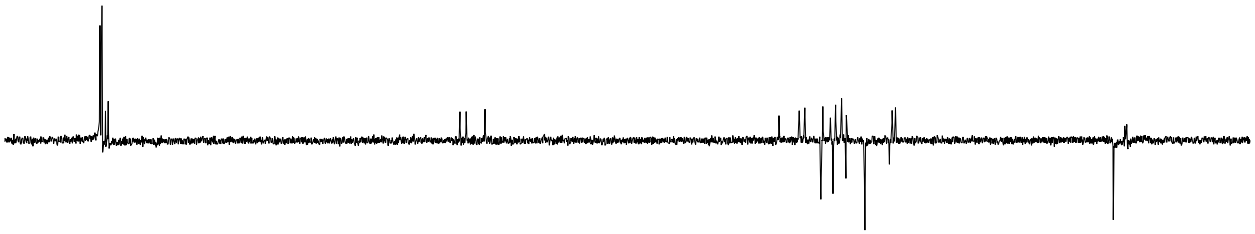

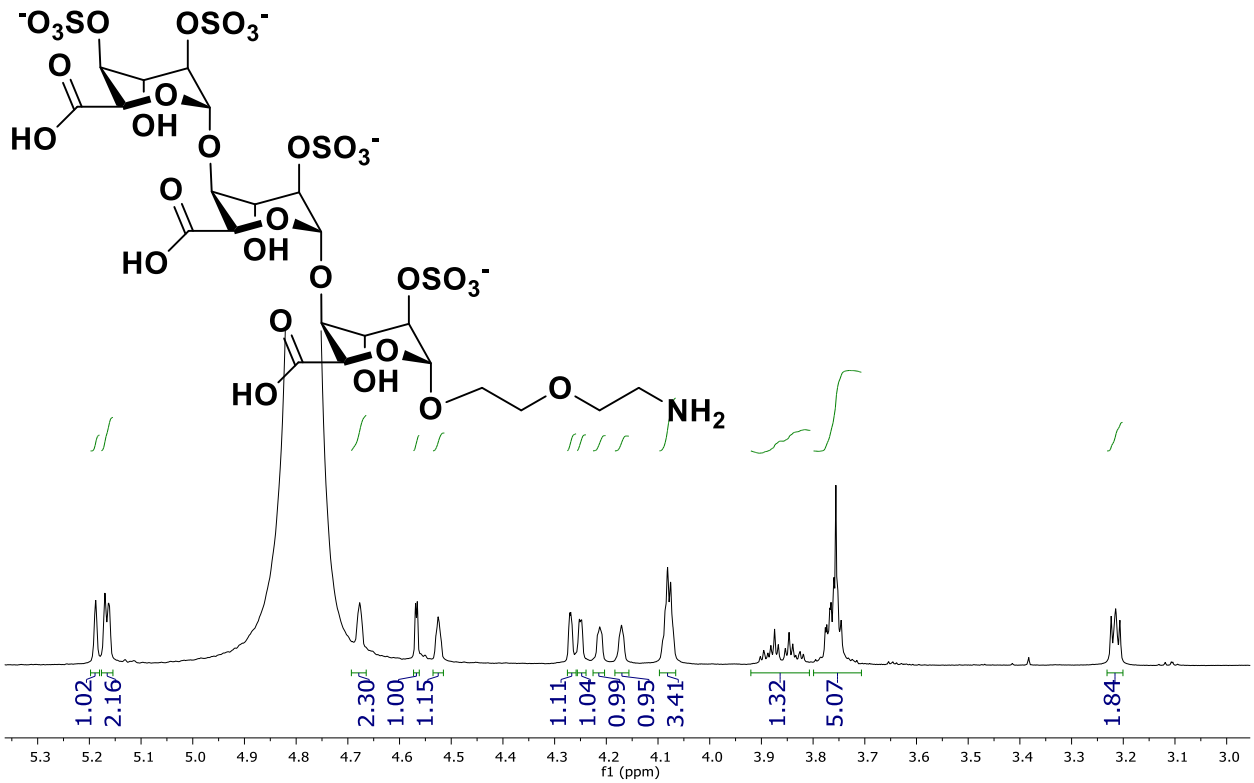
-O3SO
OSO3-
HO
OH
O
OSO3-
HO
OH
O
OSO3-
HO
OH
O
NH2
1.02
2.16
2.30
1.00
1.15
1.11
1.04
0.99
0.95
3.41
1.32
5.07
1.84
f1 (ppm)

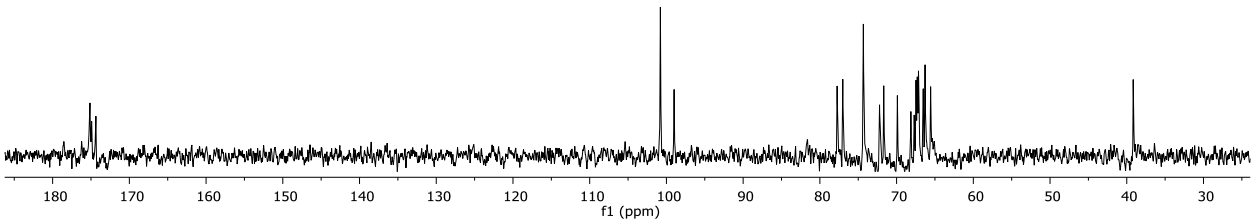
f1 (ppm)

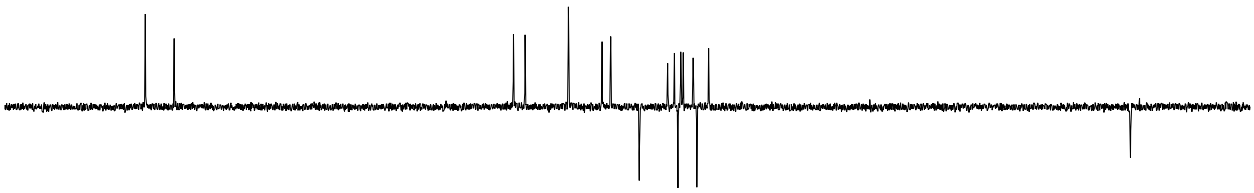

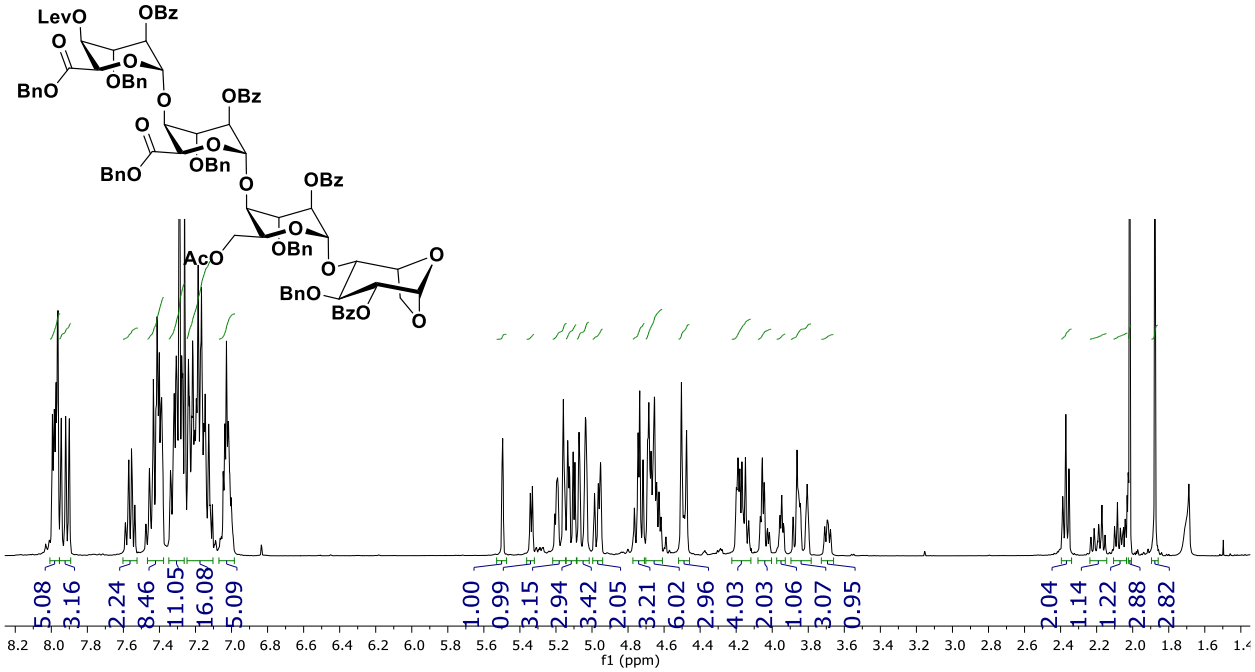
LevO
OBz
BnO
OBn
AcO
BzO
5.08
3.16
2.24
8.46
11.05
16.08
5.09
1.00
0.99
3.15
2.94
3.42
2.05
3.21
6.02
2.96
4.03
2.03
1.06
3.07
0.95
2.04
1.14
1.22
2.88
2.82
f1 (ppm)

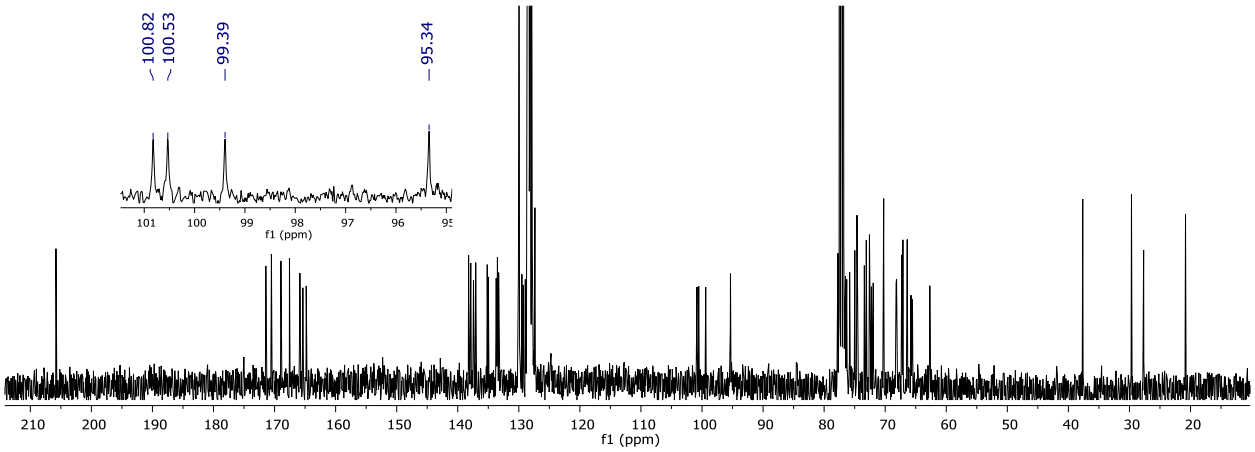
100.82
100.53
99.39
95.34
f1 (ppm)

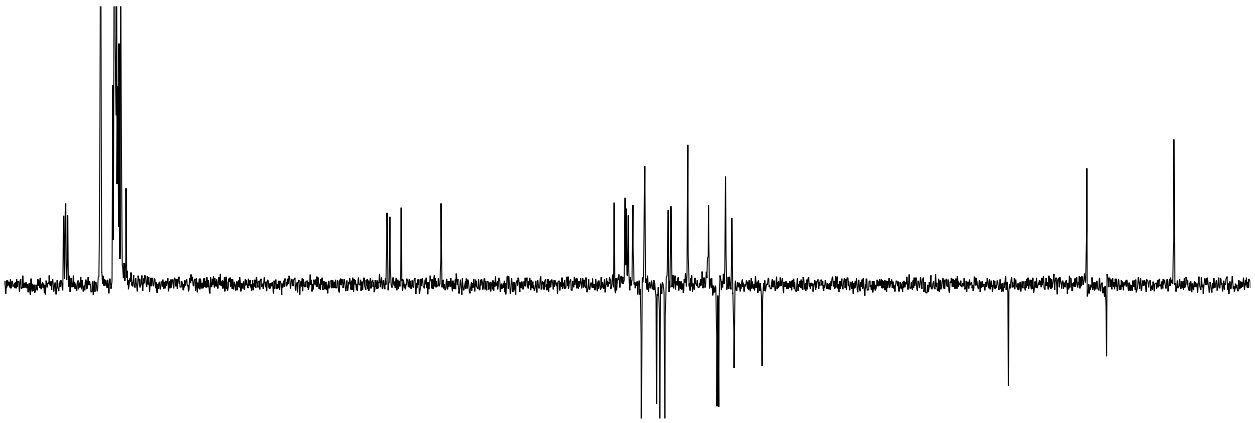

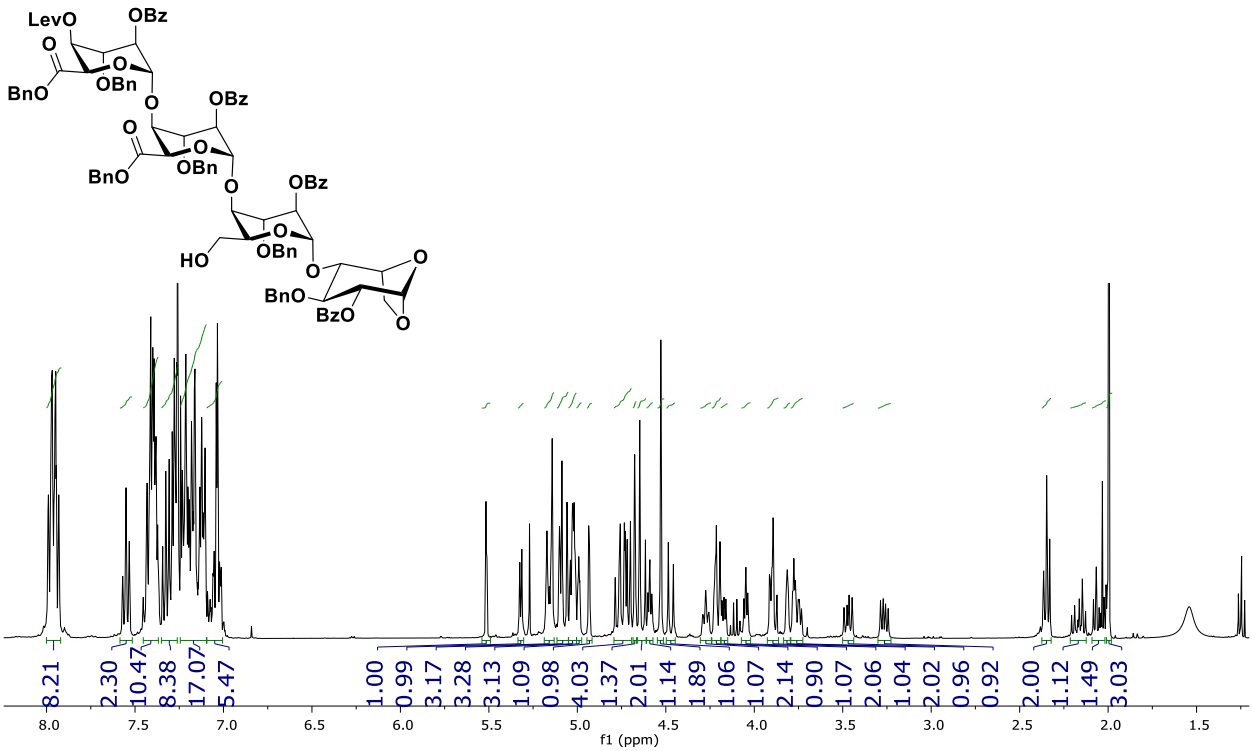
LevO
OBz
O
BnO
OBn
HO
BzO
8.21
2.30
10.47
8.38
17.07
5.47
1.00
0.99
3.17
3.28
3.13
1.09
0.98
4.03
1.37
2.01
1.14
1.89
1.06
1.07
2.14
0.90
1.07
2.06
1.04
2.02
0.96
0.92
2.00
1.12
1.49
3.03
f1 (ppm)

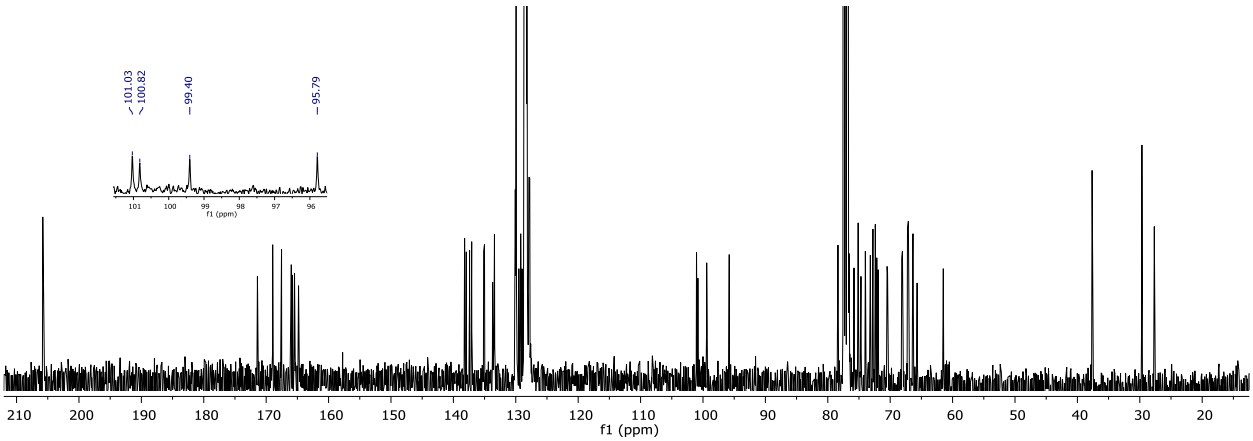
101.03
100.82
99.40
95.79
f1 (ppm)

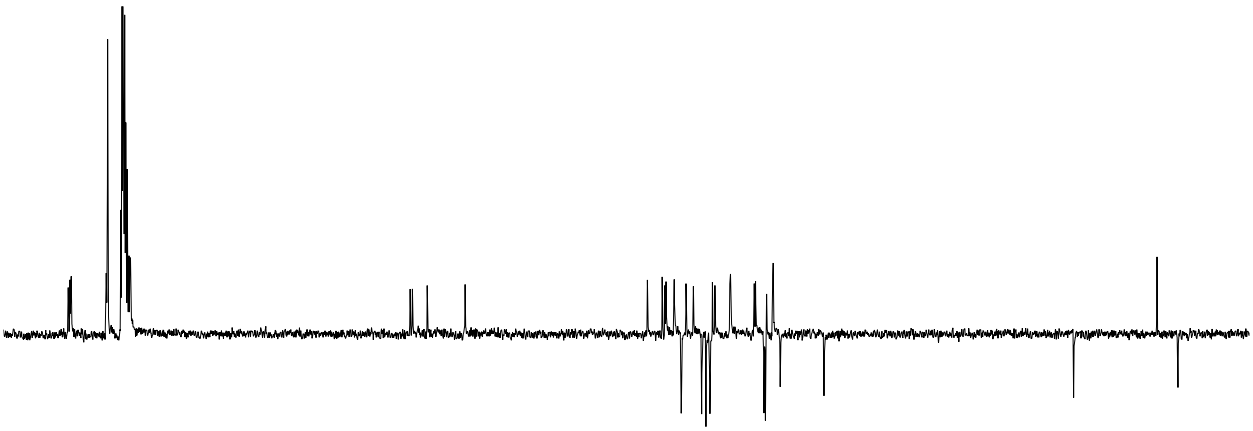

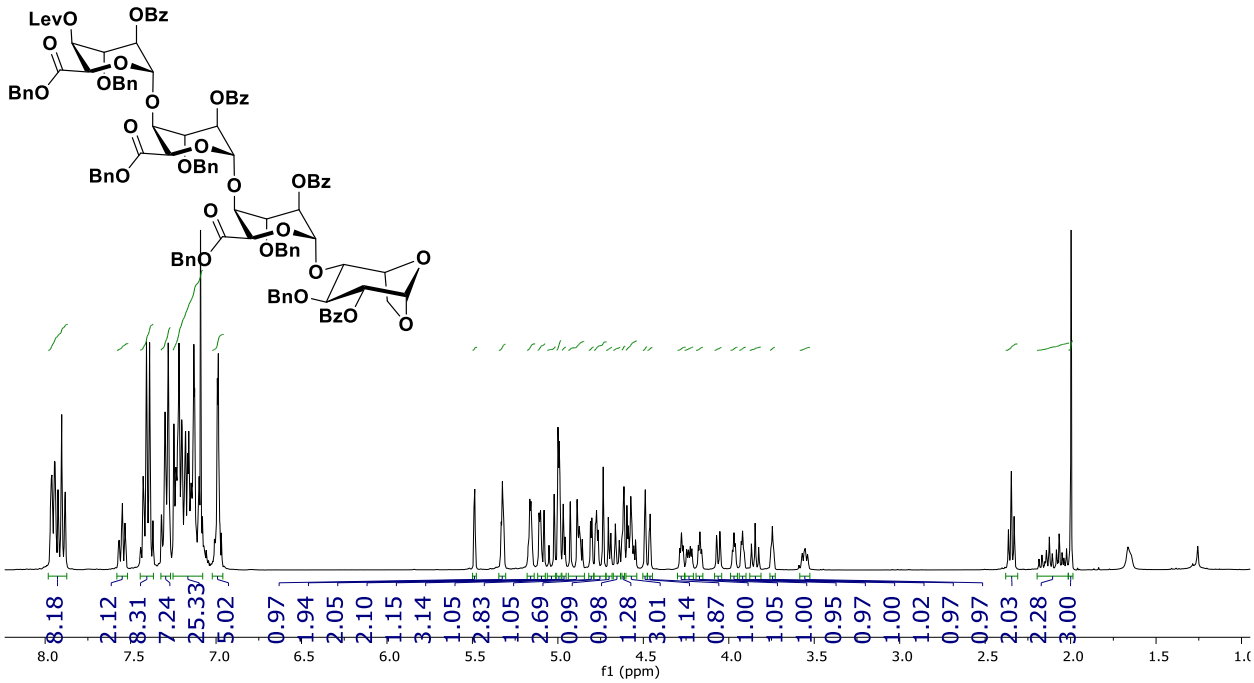
LevO
OBz
BnO
OBn
BzO
8.18
2.12
8.31
7.24
25.33
5.02
0.97
1.94
2.05
2.10
1.15
3.14
1.05
2.83
1.05
2.69
0.99
0.98
1.28
3.01
1.14
0.87
1.00
1.05
1.00
0.95
0.97
1.00
1.02
0.97
0.97
2.03
2.28
3.00
f1 (ppm)

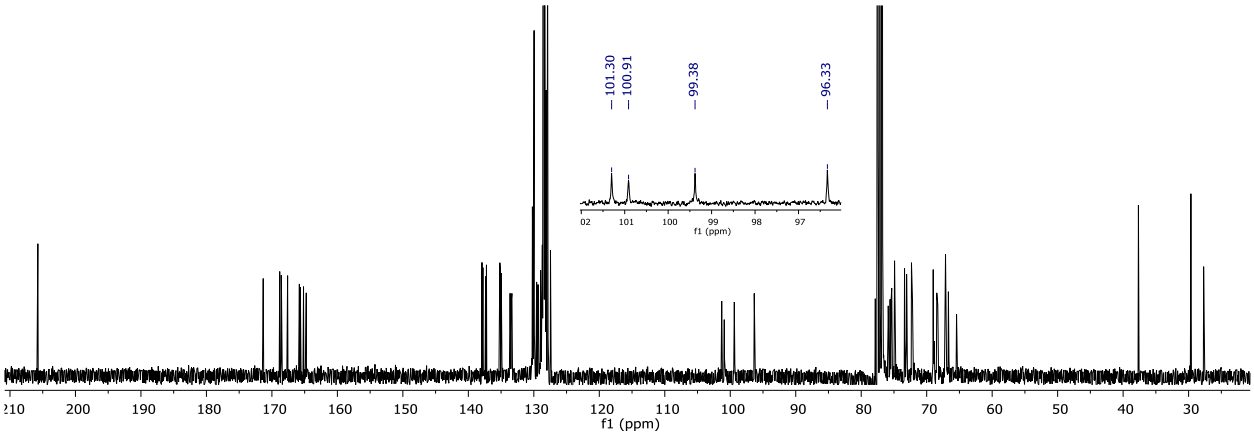
101.30
100.91
99.38
96.33
f1 (ppm)

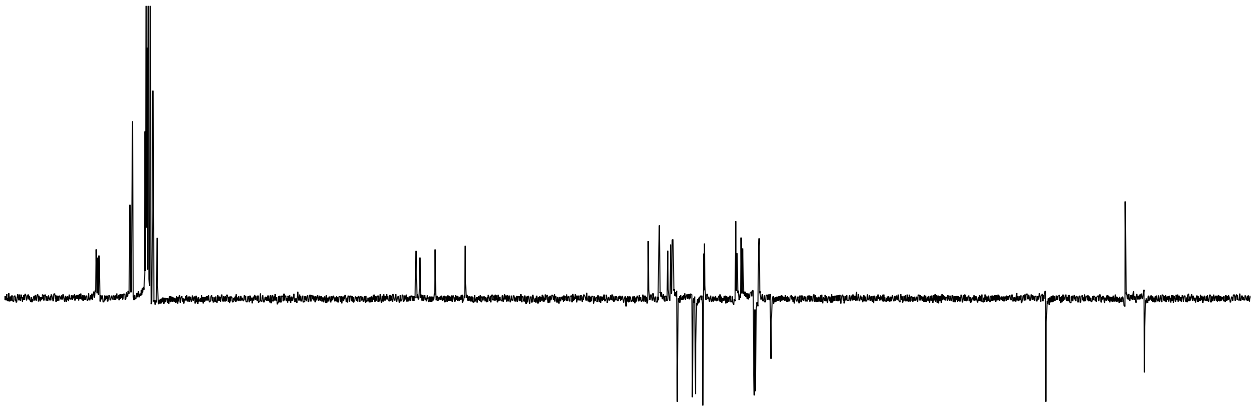

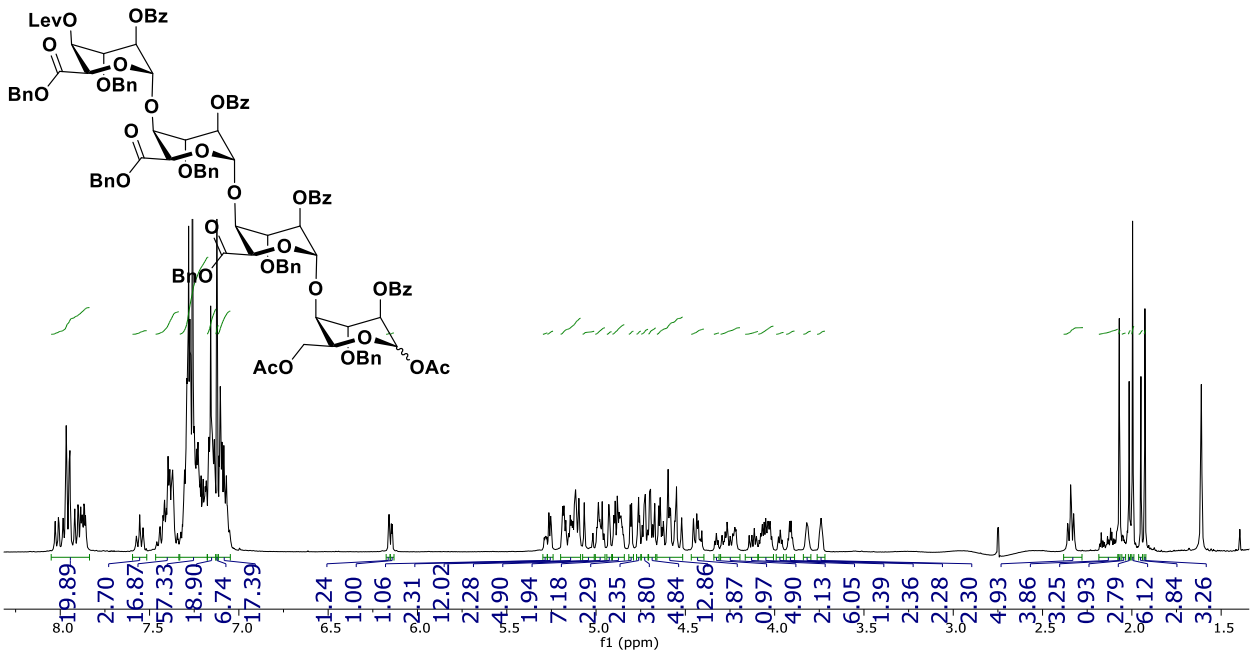
LevO
OBz
BnO
OBn
O
AcO
OAc
19.89
2.70
16.87
57.33
18.90
6.74
17.39
1.24
1.00
1.06
2.31
12.02
2.28
4.90
1.94
7.18
2.29
2.35
3.80
4.84
12.86
3.87
0.97
4.90
2.13
6.05
1.39
2.36
2.28
2.30
4.93
3.86
3.25
0.93
2.79
6.12
2.84
3.26
f1 (ppm)

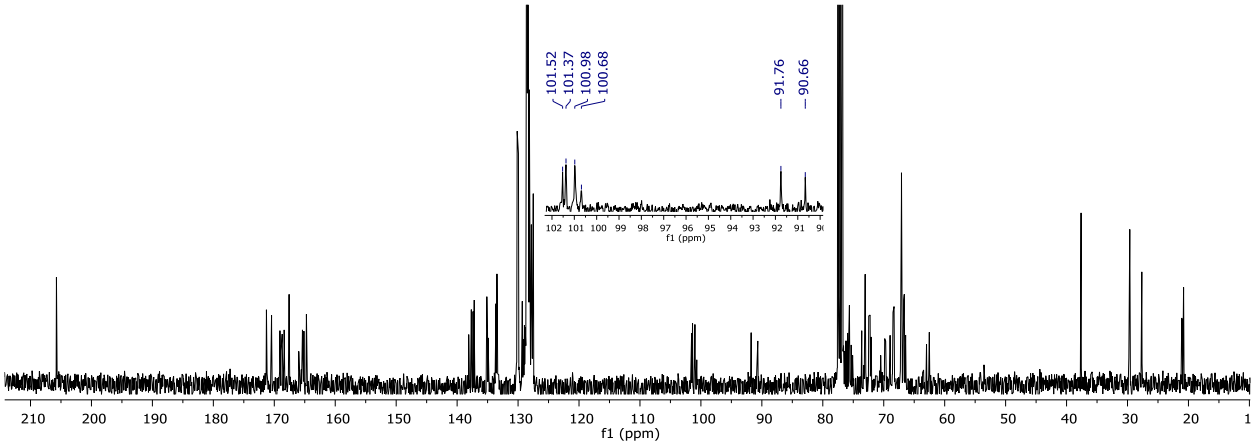
101.52
101.37
100.98
100.68
91.76
90.66
f1 (ppm)

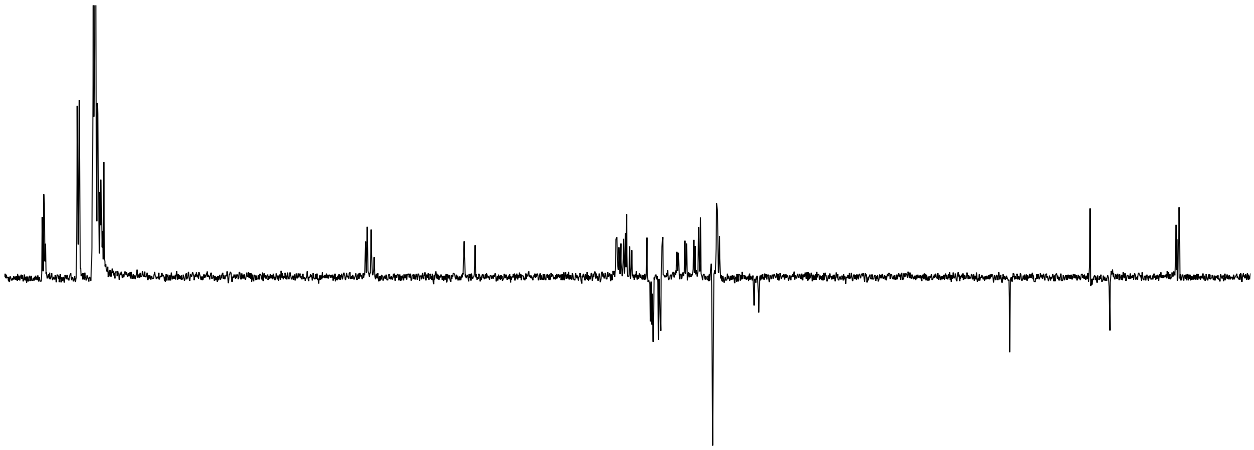

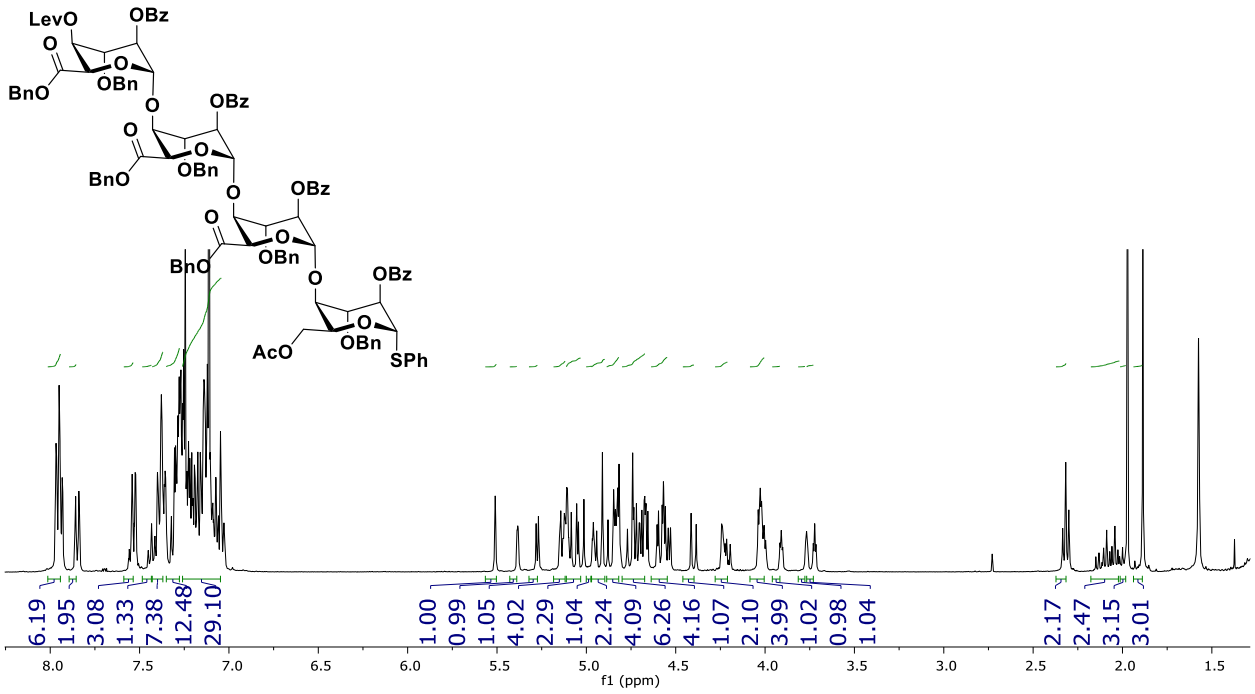
LevO
OBz
BnO
OBn
AcO
SPh
6.19
1.95
3.08
1.33
7.38
12.48
29.10
1.00
0.99
1.05
4.02
2.29
1.04
2.24
4.09
6.26
4.16
1.07
2.10
3.99
1.02
0.98
1.04
2.17
2.47
3.15
3.01
f1 (ppm)

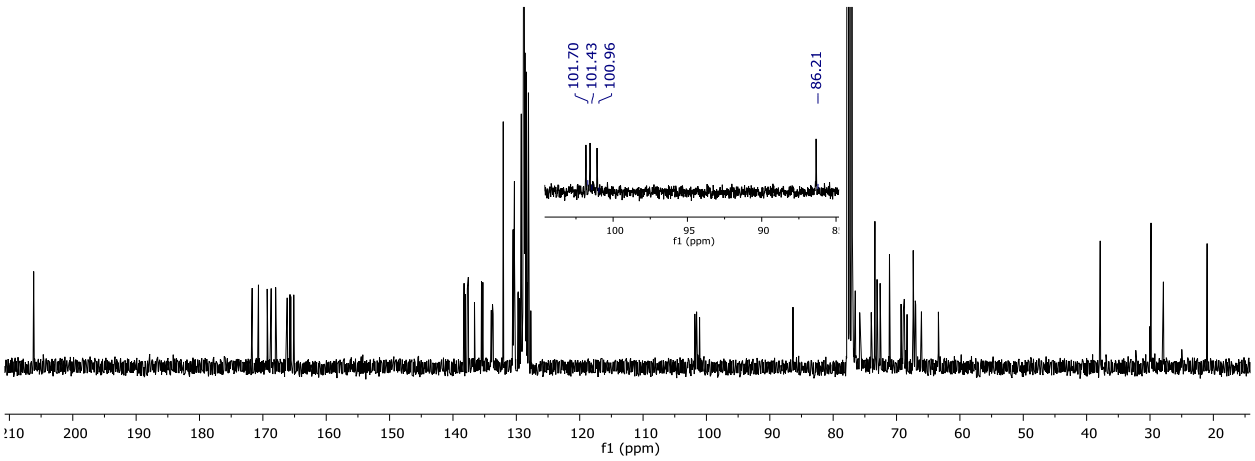
101.70
101.43
100.96
86.21
f1 (ppm)

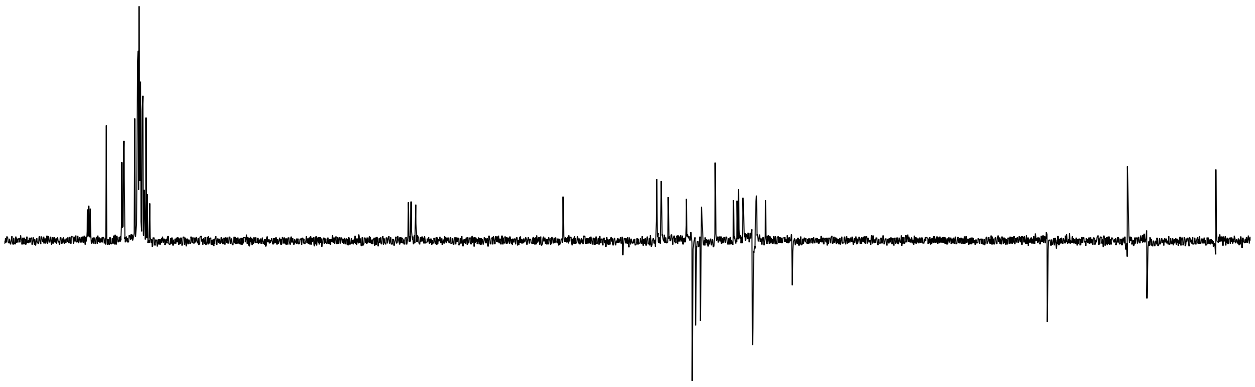

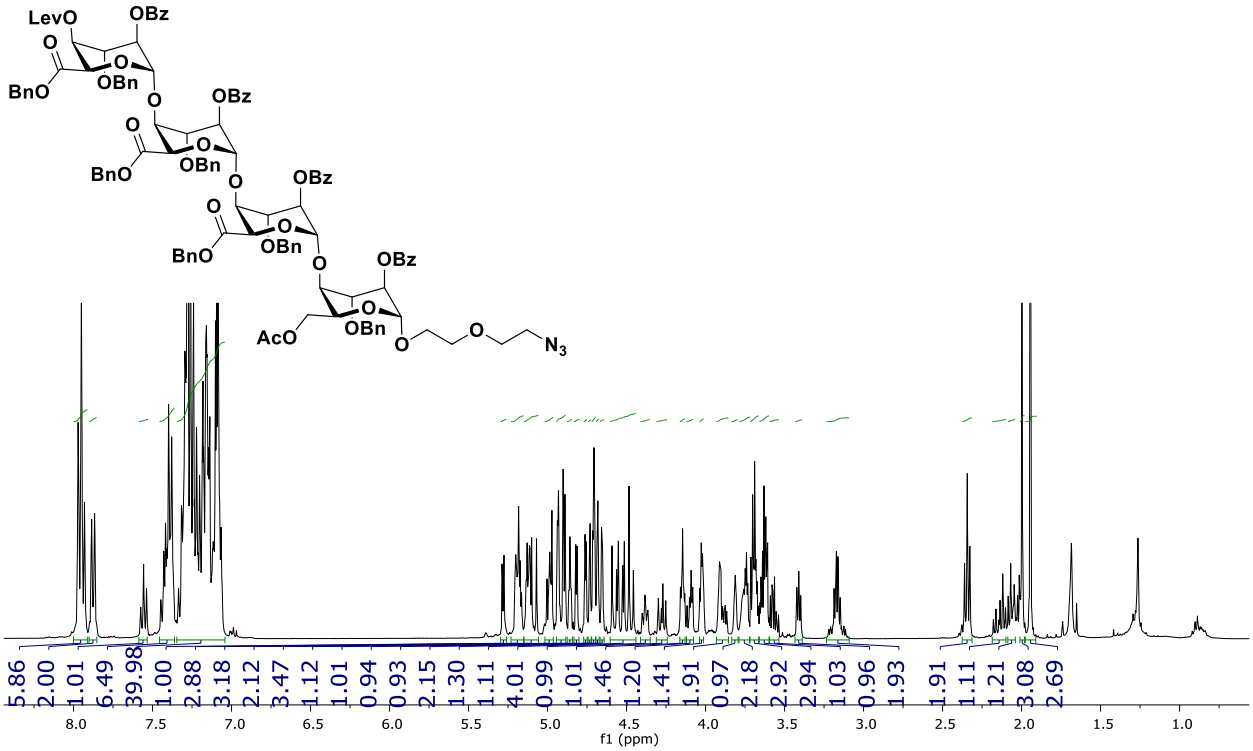
LevO
OBz
BnO
OBn
AcO
N3
5.86 2.00 1.01 6.49 39.98 1.00 2.88 3.18 2.12 3.47 1.12 1.01 0.94 0.93 2.15 1.30 1.11 4.01 0.99 1.01 1.46 1.20 1.41 1.91 0.97 2.18 2.92 2.94 1.03 0.96 1.93 1.91 1.11 1.21 3.08 2.69
f1 (ppm)

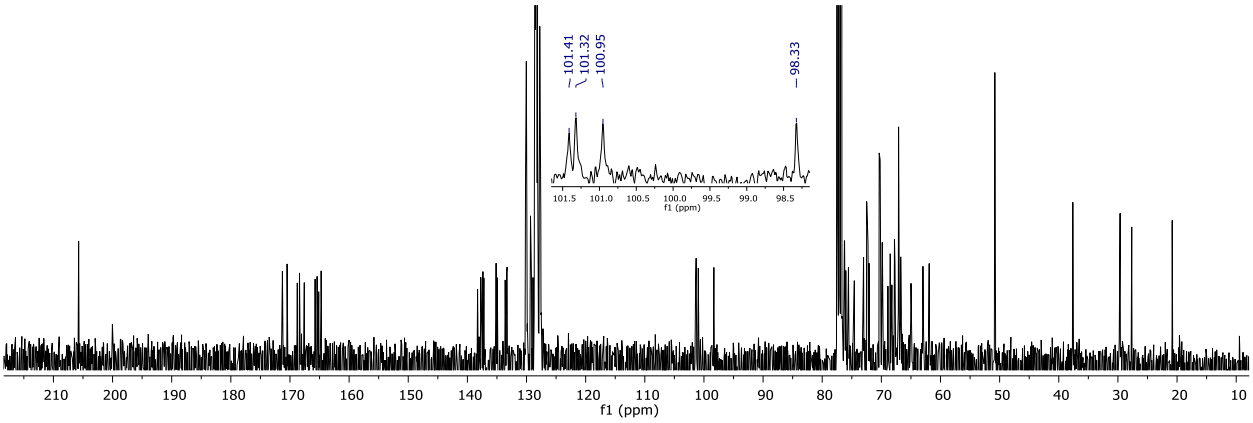
101.41
101.32
100.95
98.33
f1 (ppm)

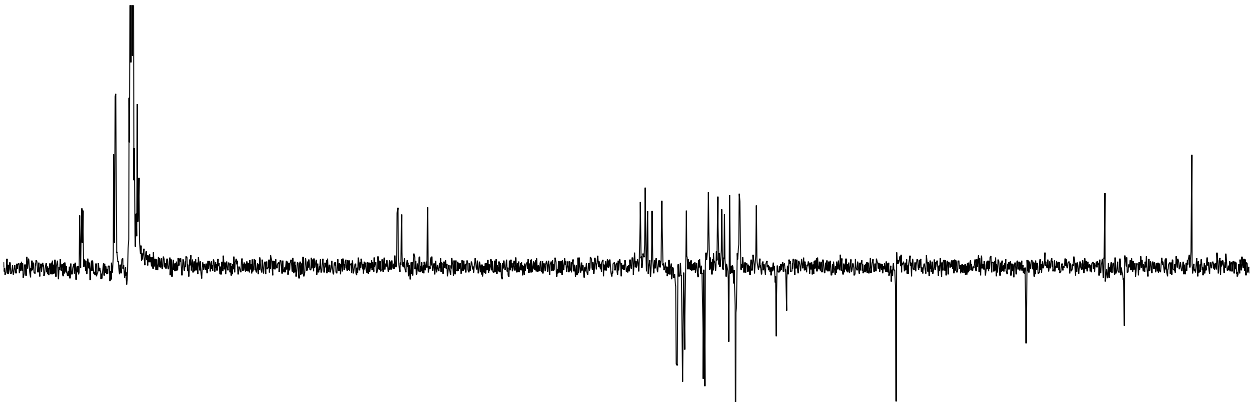

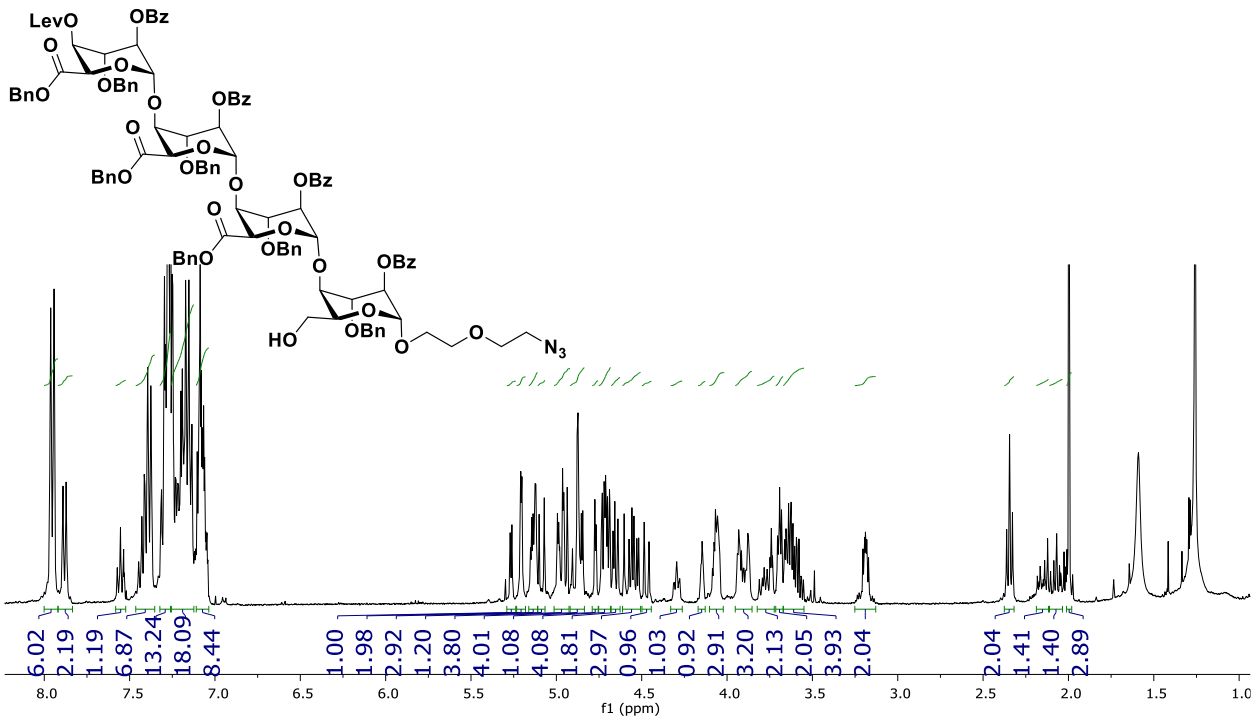
LevO
OBz
BnO
OBn
HO
N3
6.02 2.19 1.19 6.87 13.24 18.09 8.44 1.00 1.98 2.92 1.20 3.80 4.01 1.08 4.08 1.81 2.97 0.96 1.03 0.92 2.91 3.20 2.13 2.05 3.93 2.04 2.04 1.41 1.40 2.89
f1 (ppm)

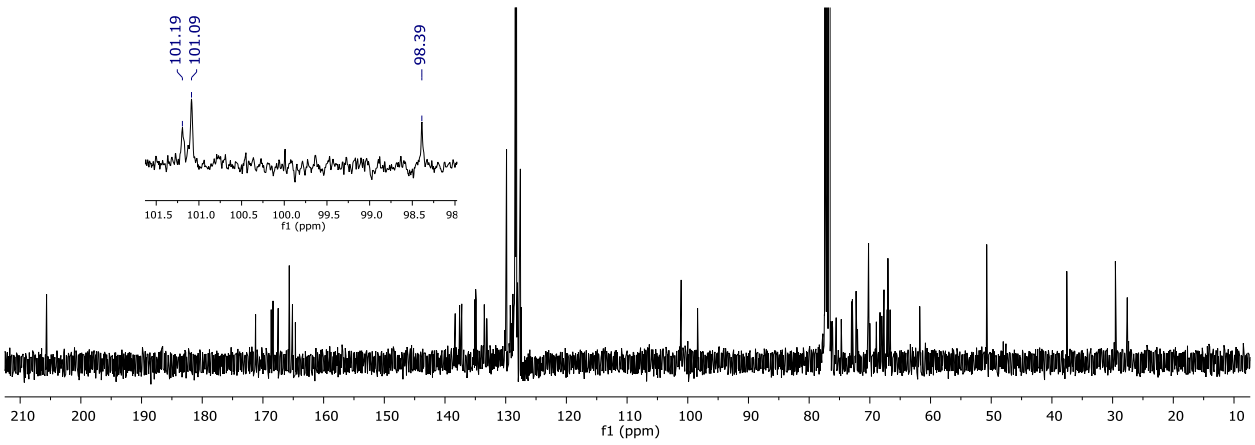
101.19
101.09
98.39
f1 (ppm)

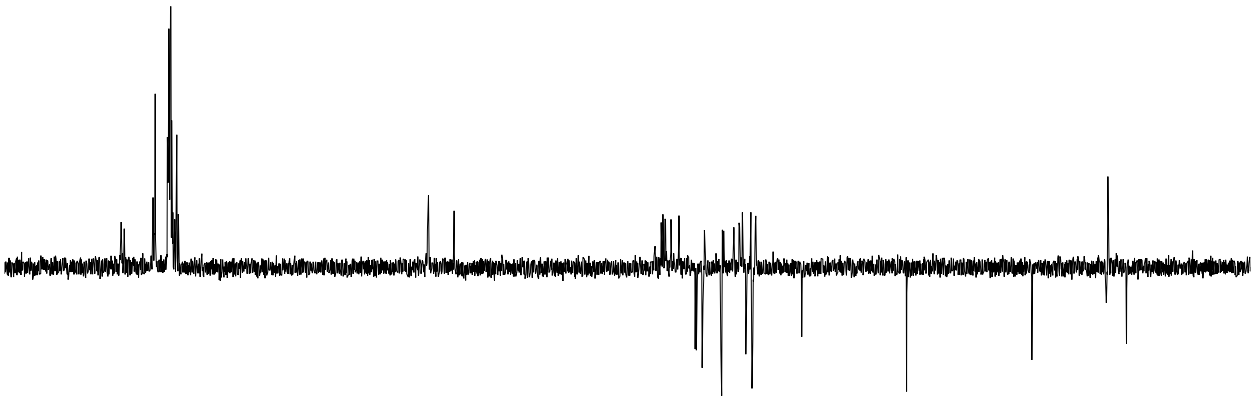

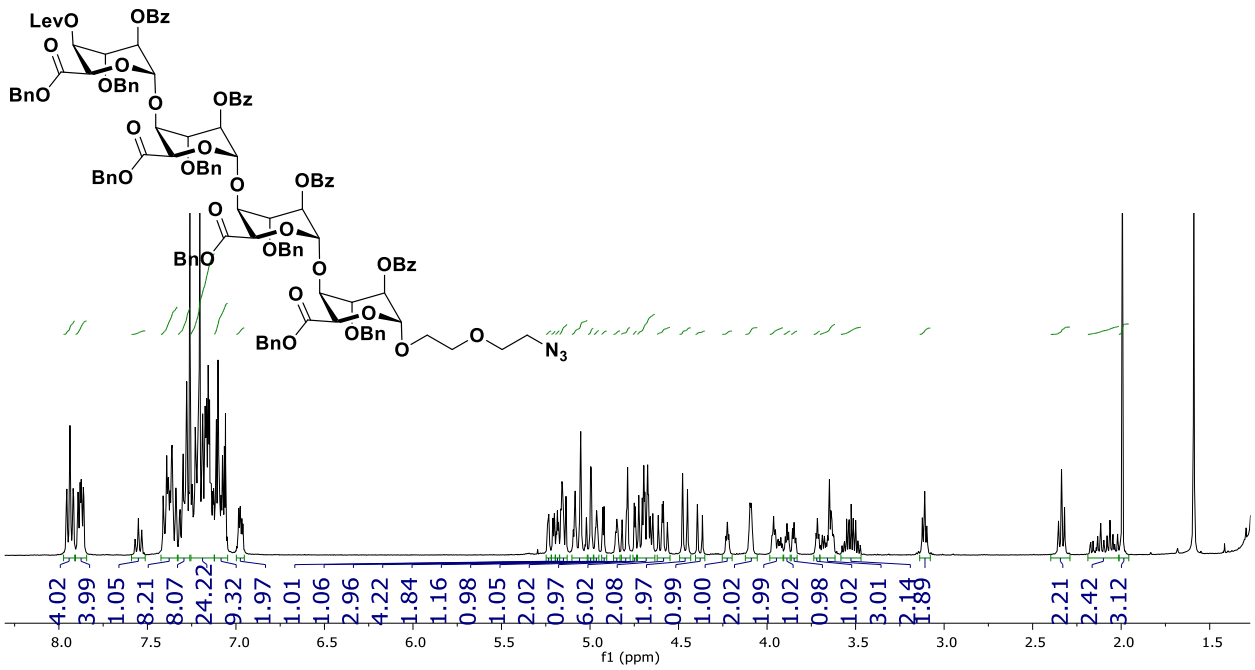
LevO
OBz
BnO
OBn
O
N3
4.02 3.99 1.05 8.21 8.07 24.22 9.32 1.97 1.01 1.06 2.96 4.22 1.84 1.16 0.98 1.05 2.02 0.97 6.02 2.08 1.97 0.99 1.00 2.02 1.99 1.02 0.98 1.02 3.01 2.14 1.89 2.21 2.42 3.12
8.0 7.5 7.0 6.5 6.0 5.5 5.0 4.5 4.0 3.5 3.0 2.5 2.0 1.5
f1 (ppm)

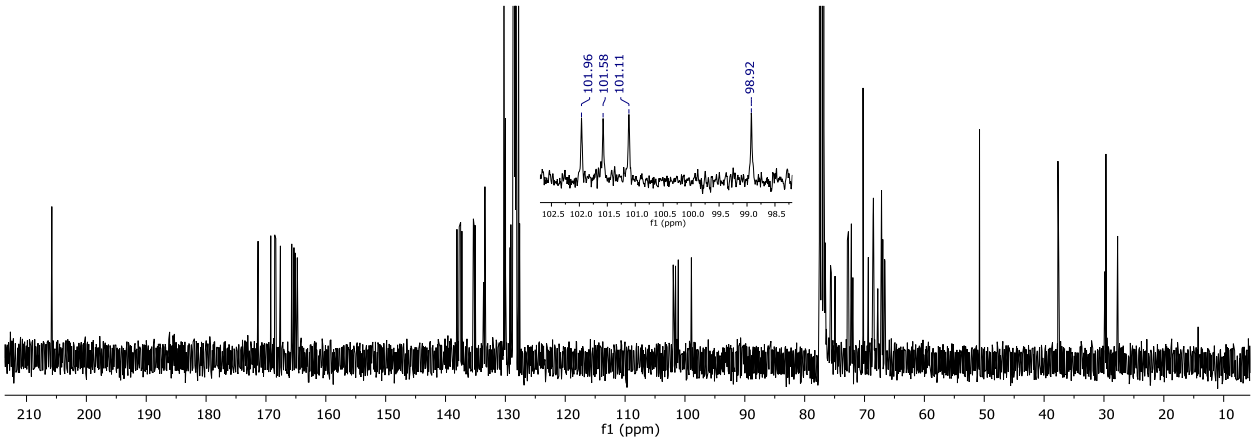
101.96
101.58
101.11
98.92
102.5 102.0 101.5 101.0 100.5 100.0 99.5 99.0 98.5
f1 (ppm)
210 200 190 180 170 160 150 140 130 120 110 100 90 80 70 60 50 40 30 20 10
f1 (ppm)

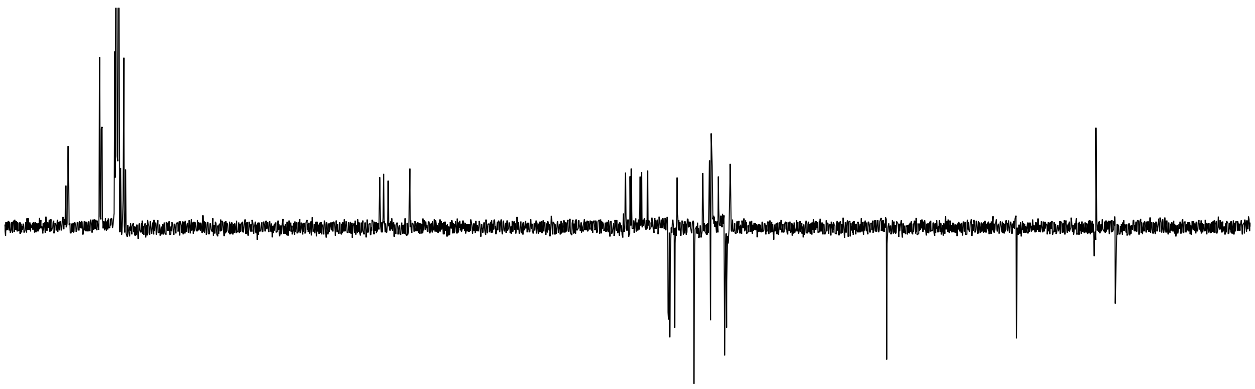

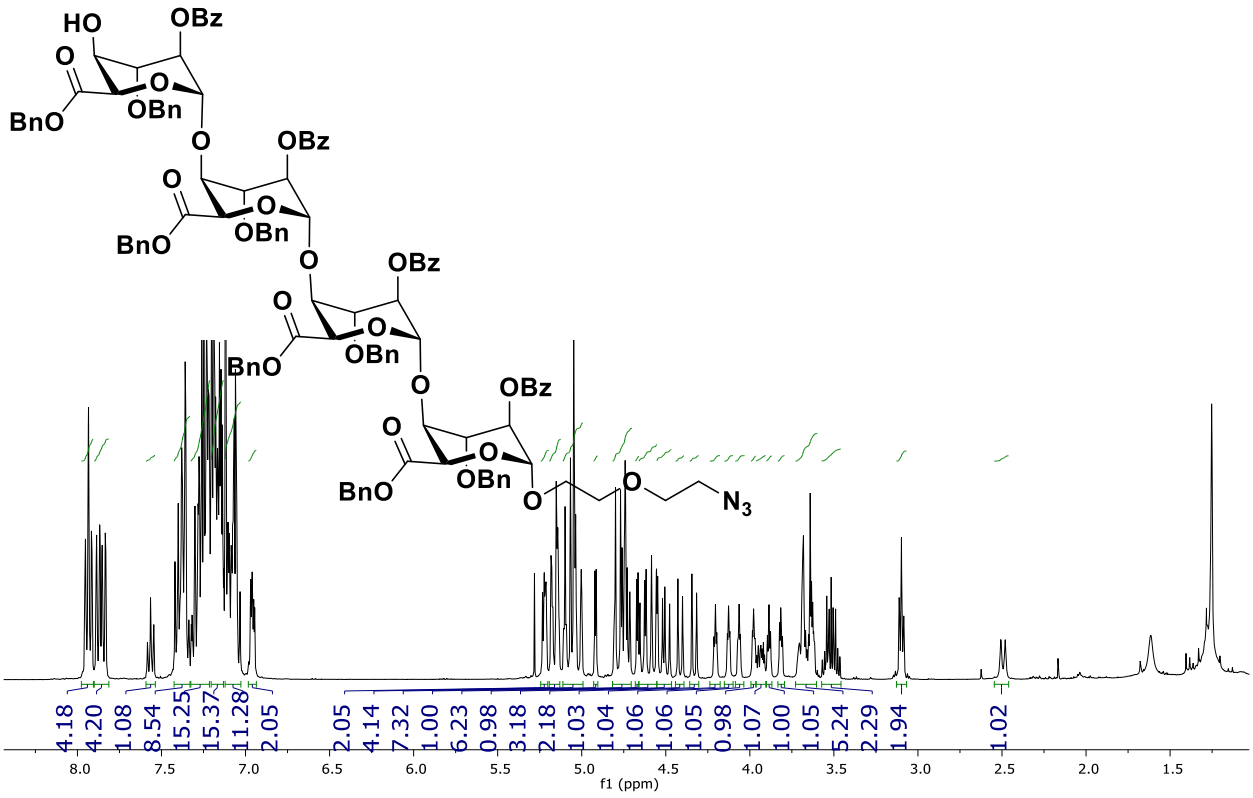
HO
OBz
O
BnO
OBn
O
N3
4.18 4.20 1.08 8.54 15.25 15.37 11.28 2.05 2.05 4.14 7.32 1.00 6.23 0.98 3.18 2.18 1.03 1.04 1.06 1.06 1.05 0.98 1.07 1.00 1.05 5.24 2.29 1.94 1.02
f1 (ppm)

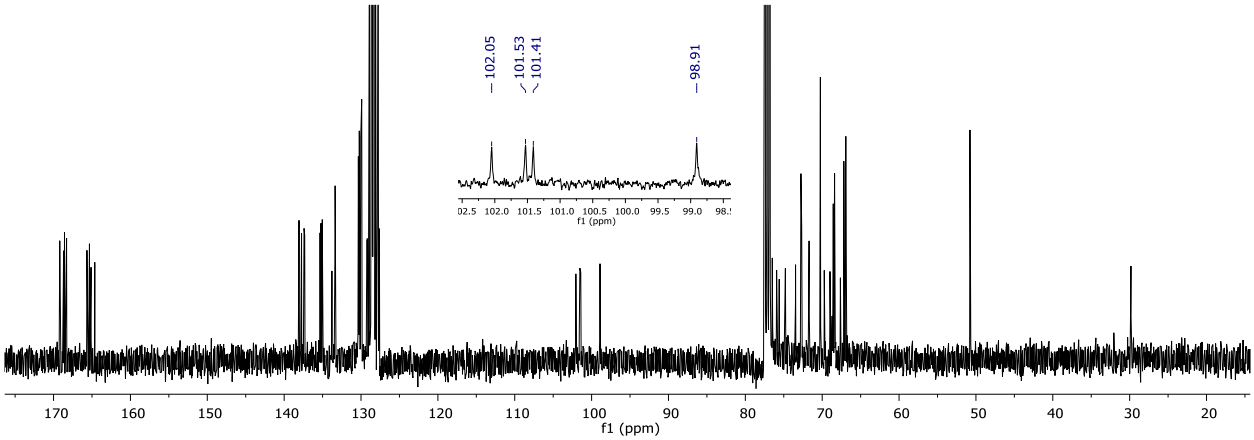
102.05
101.53
101.41
98.91
f1 (ppm)

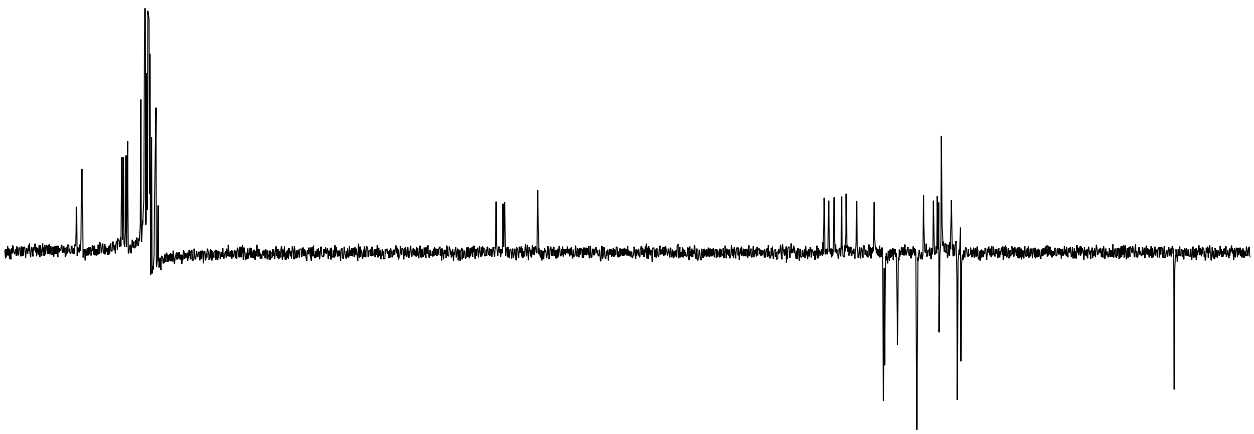

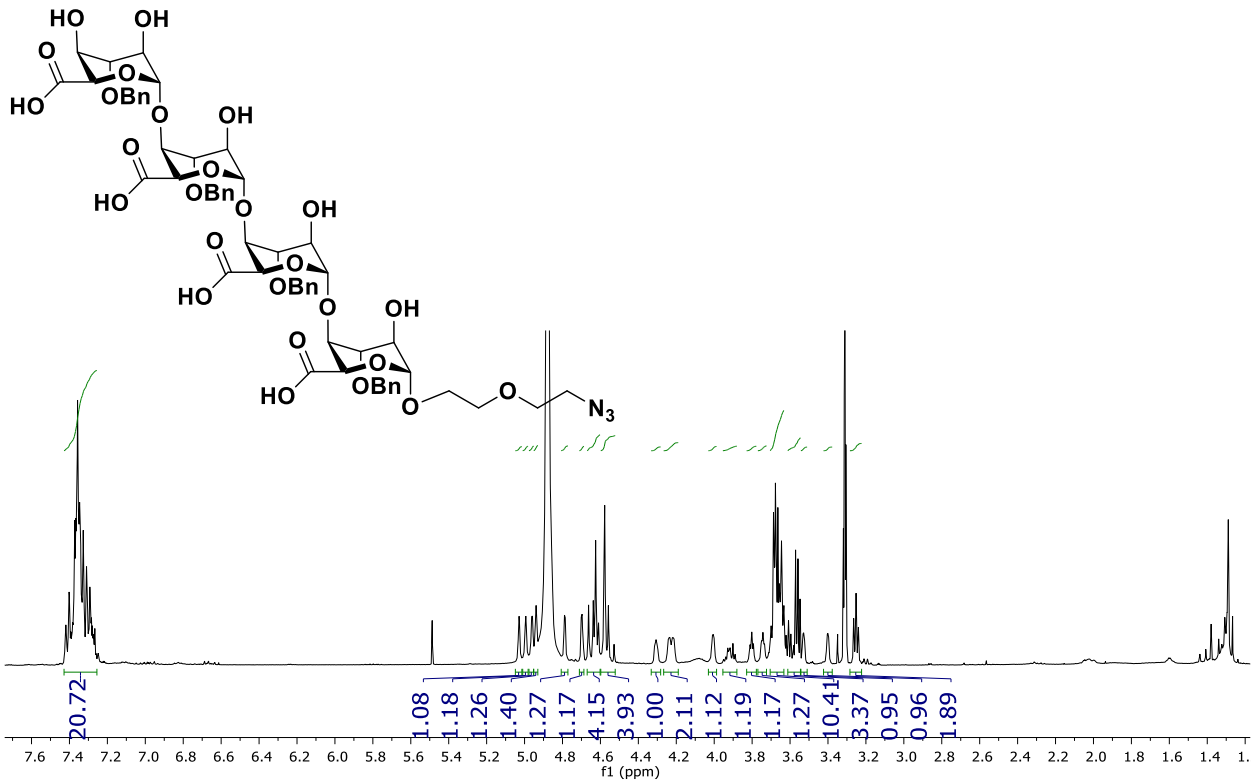
HO
OH
O
HO
OBn
O
OH
O
HO
OBn
O
OH
O
HO
OBn
O
OH
O
HO
OBn
O
O
N3
20.72
1.08
1.18
1.26
1.40
1.27
1.17
4.15
3.93
1.00
2.11
1.12
1.19
1.17
1.27
10.41
3.37
0.95
0.96
1.89
7.6 7.4 7.2 7.0 6.8 6.6 6.4 6.2 6.0 5.8 5.6 5.4 5.2 5.0 4.8 4.6 4.4 4.2 4.0 3.8 3.6 3.4 3.2 3.0 2.8 2.6 2.4 2.2 2.0 1.8 1.6 1.4
f1 (ppm)

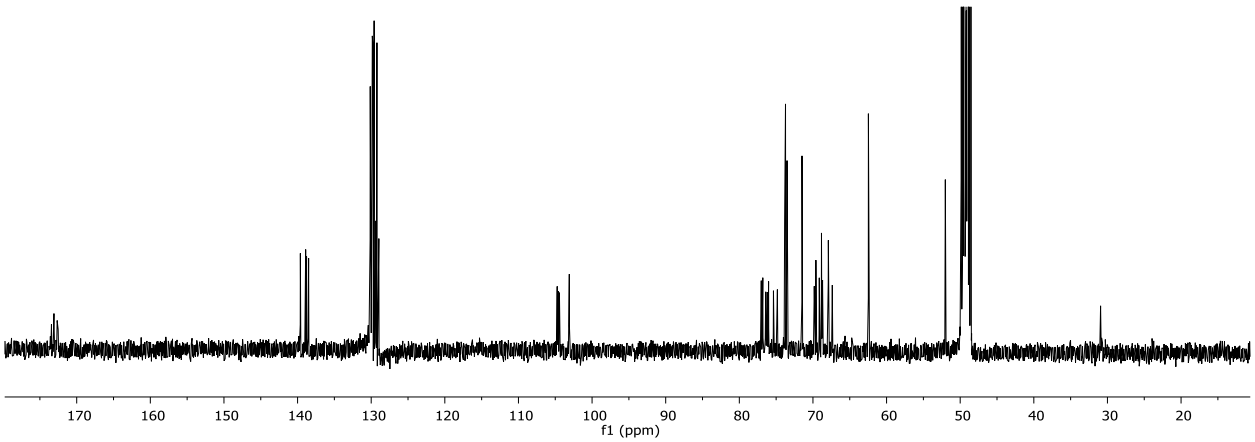
170 160 150 140 130 120 110 100 90 80 70 60 50 40 30 20
f1 (ppm)

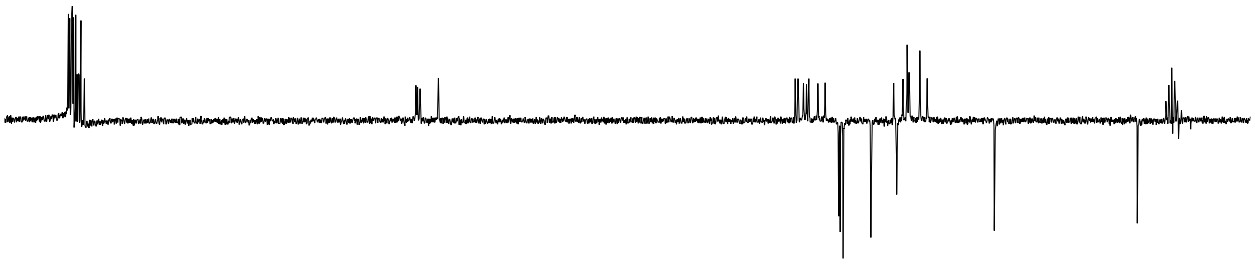

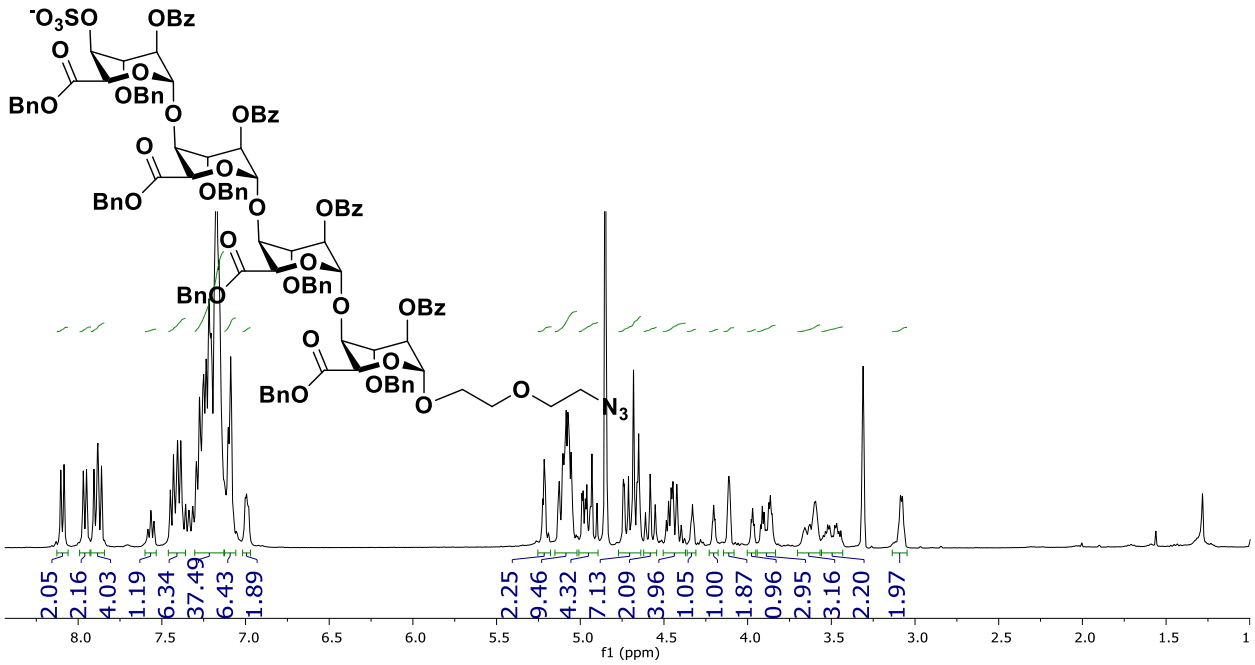
-O3SO
OBz
O
BnO
OBn
N3
2.05
2.16
4.03
1.19
6.34
37.49
6.43
1.89
2.25
9.46
4.32
7.13
2.09
3.96
1.05
1.00
1.87
0.96
2.95
3.16
2.20
1.97
f1 (ppm)

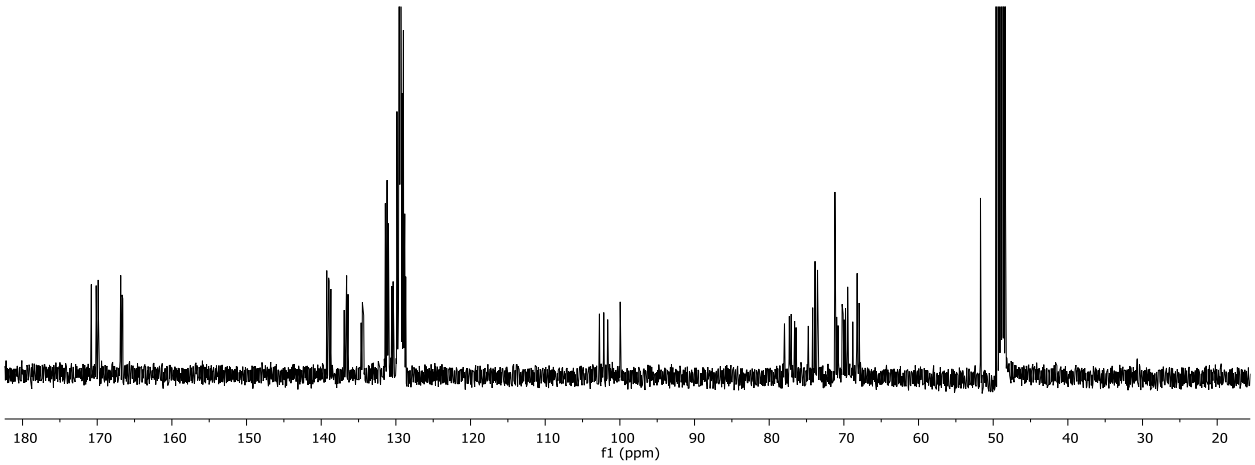
f1 (ppm)

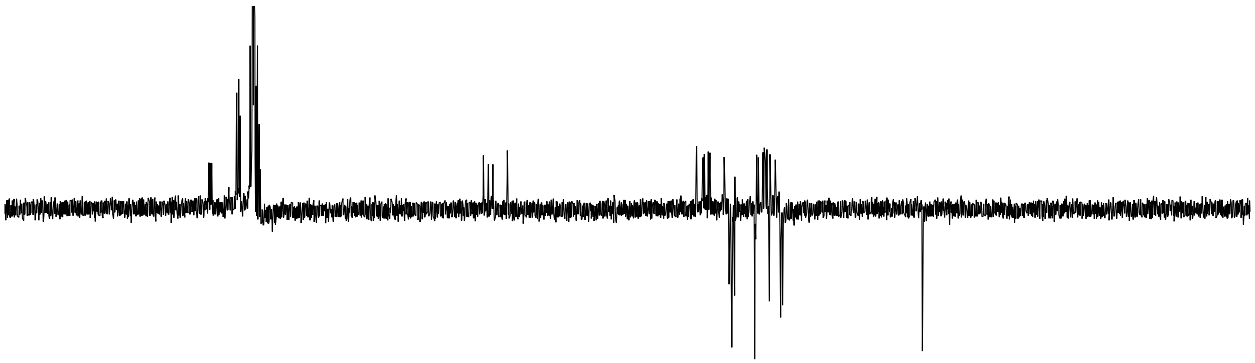

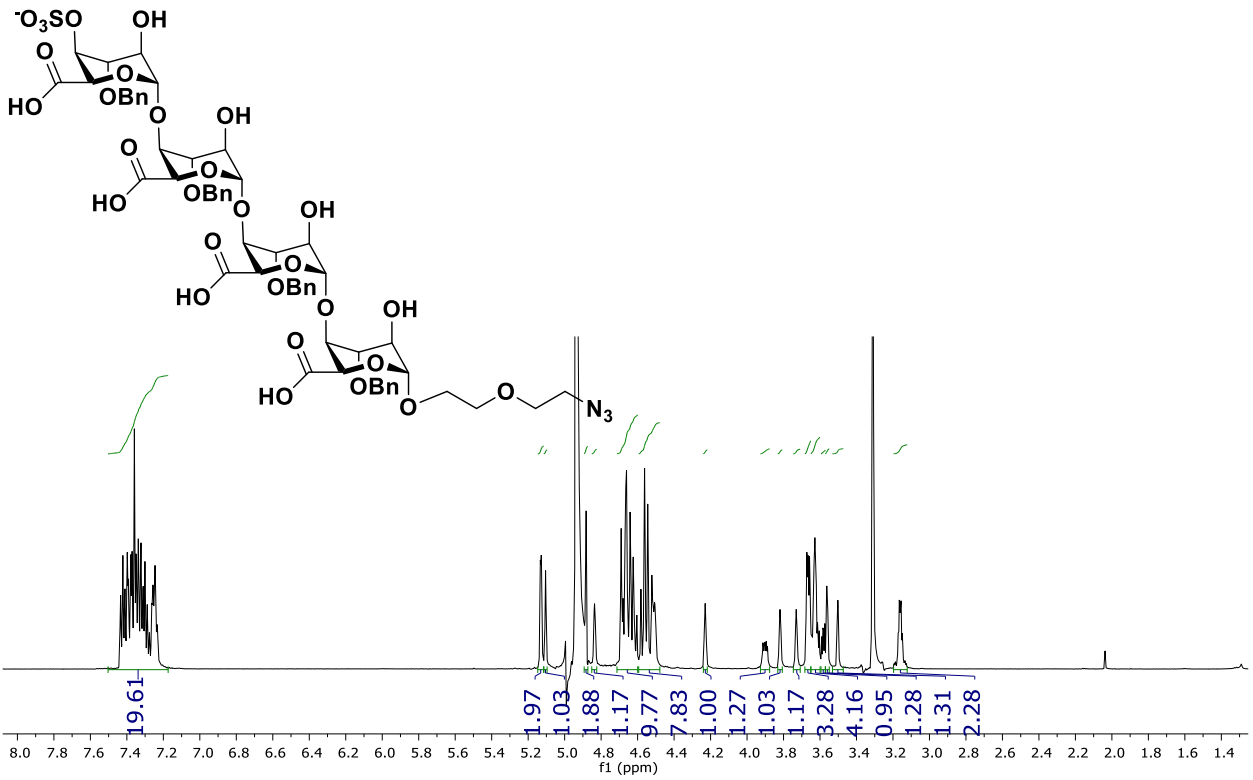
-O3SO
OH
O
HO
O
OBn
O
OH
O
HO
O
OBn
O
OH
O
HO
O
OBn
O
OH
O
HO
O
OBn
O
O
N3
19.61
1.97
1.03
1.88
1.17
9.77
7.83
1.00
1.27
1.03
1.17
3.28
4.16
0.95
1.28
1.31
2.28
f1 (ppm)

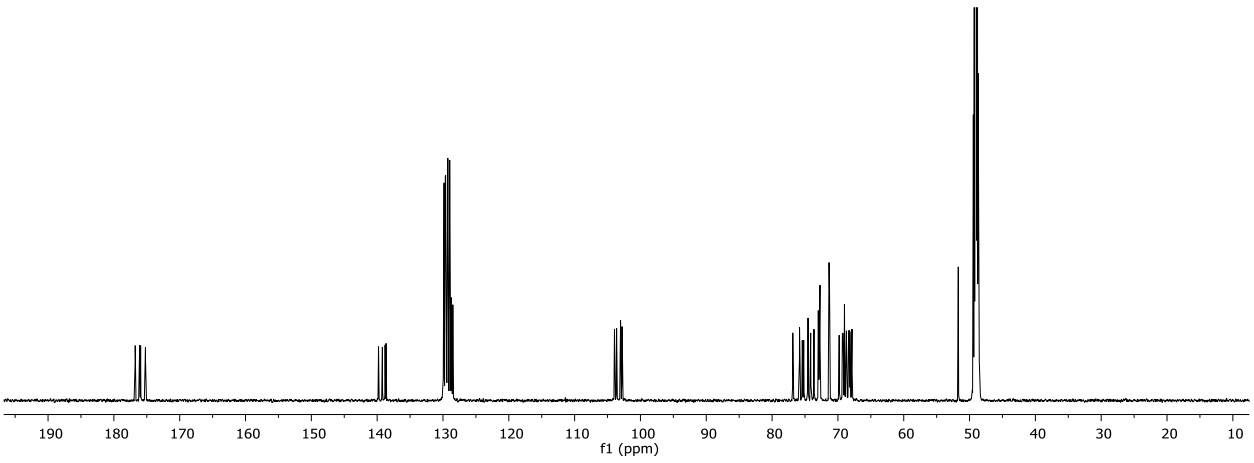
f1 (ppm)

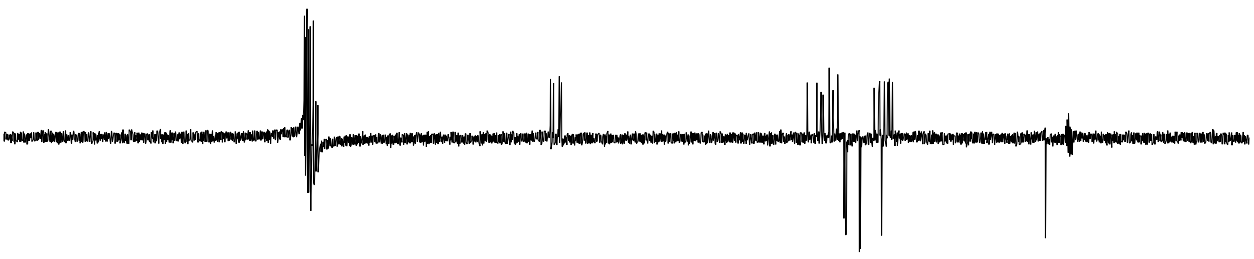

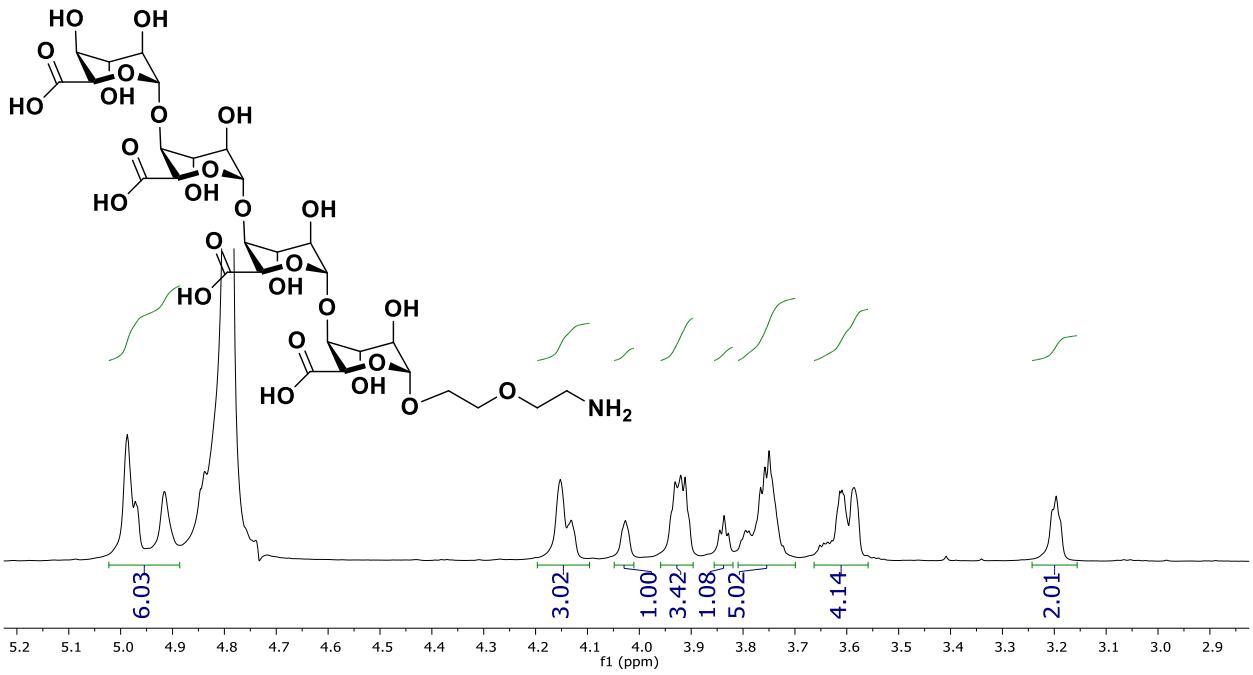
HO
OH
O
HO
OH
O
OH
HO
OH
O
OH
HO
OH
O
OH
HO
OH
O
O
NH2
6.03
3.02
1.00
3.42
1.08
5.02
4.14
2.01
5.2 5.1 5.0 4.9 4.8 4.7 4.6 4.5 4.4 4.3 4.2 4.1 4.0 3.9 3.8 3.7 3.6 3.5 3.4 3.3 3.2 3.1 3.0 2.9
f1 (ppm)

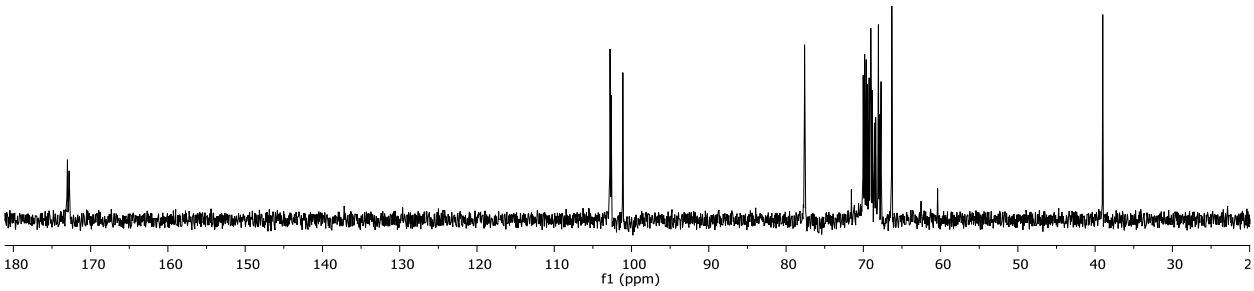
180 170 160 150 140 130 120 110 100 90 80 70 60 50 40 30 2
f1 (ppm)

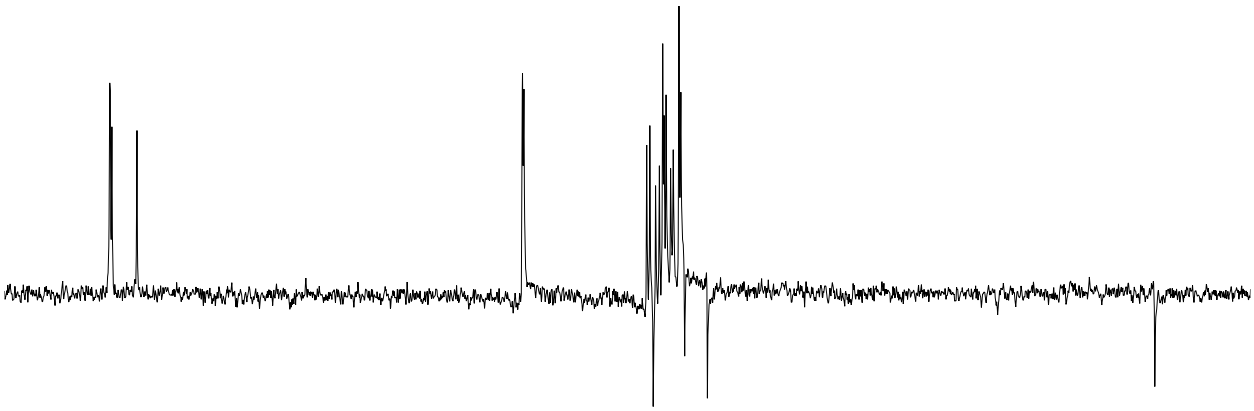

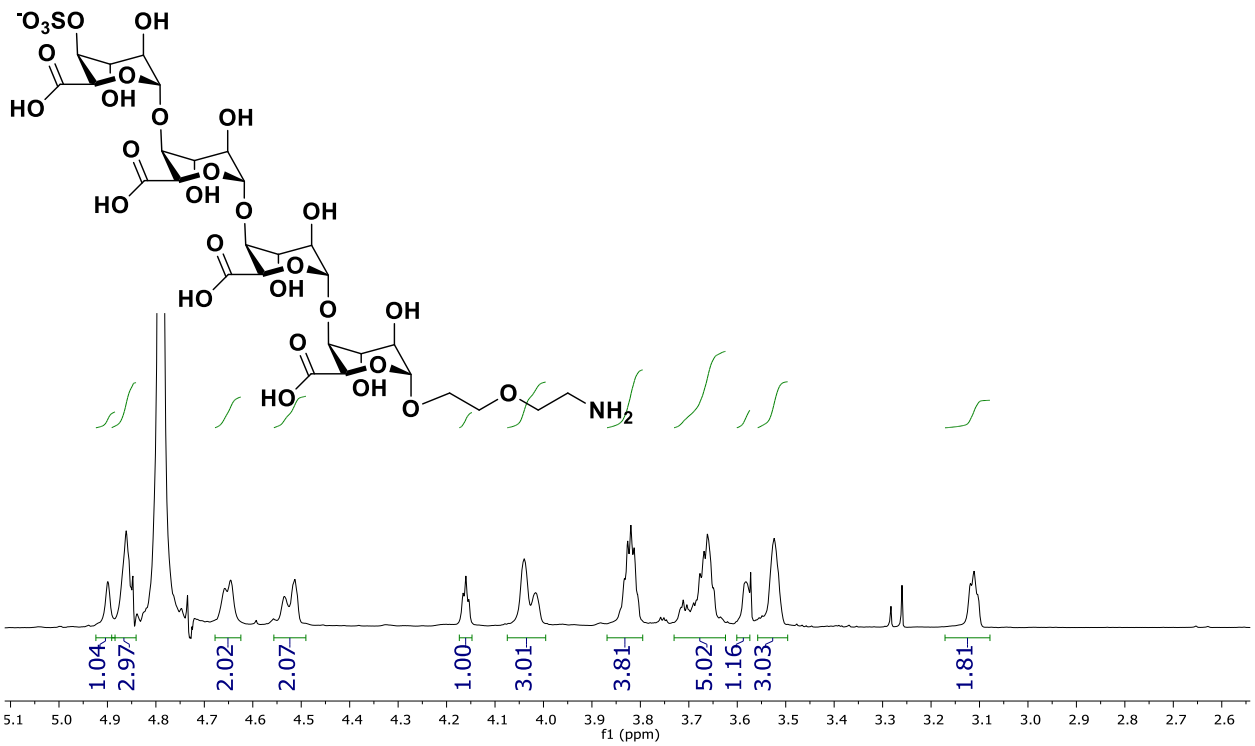
-O3SO
OH
O
HO
OH
O
OH
NH2
1.04
2.97
2.02
2.07
1.00
3.01
3.81
5.02
1.16
3.03
1.81
f1 (ppm)

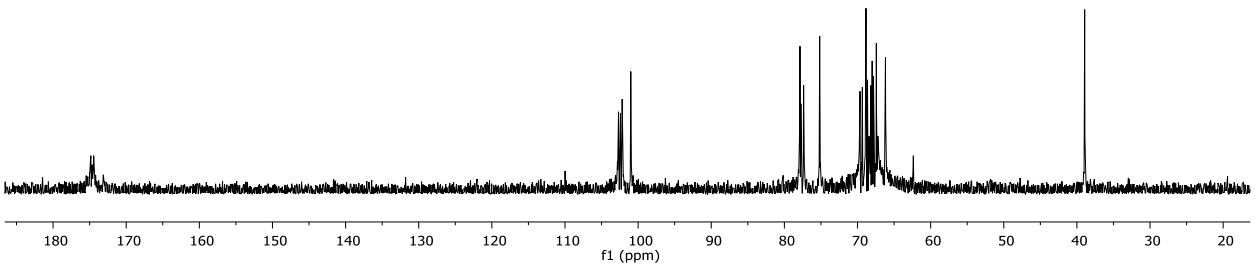
f1 (ppm)

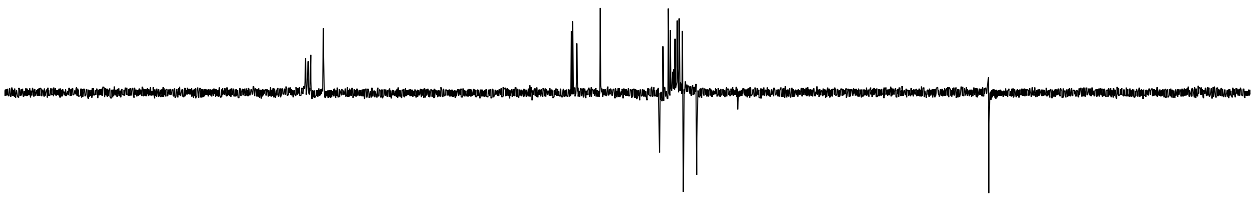

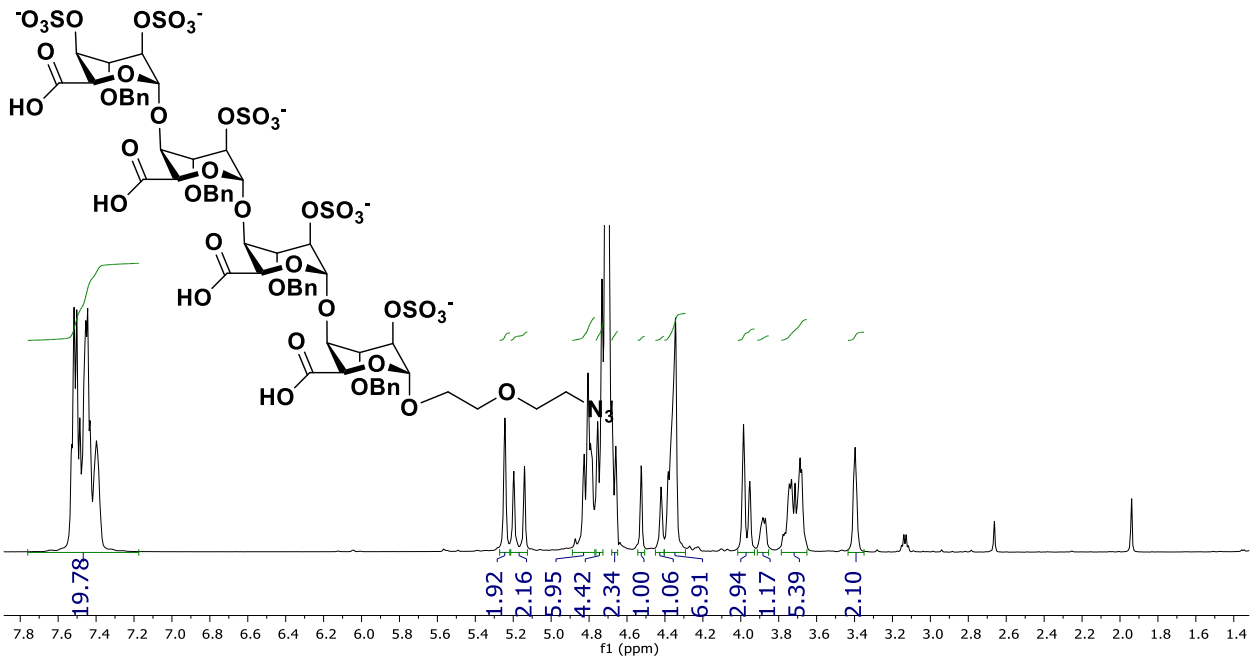
-O3SO
OSO3-
HO
OBn
N3
19.78
1.92
2.16
5.95
4.42
2.34
1.00
1.06
6.91
2.94
1.17
5.39
2.10
f1 (ppm)

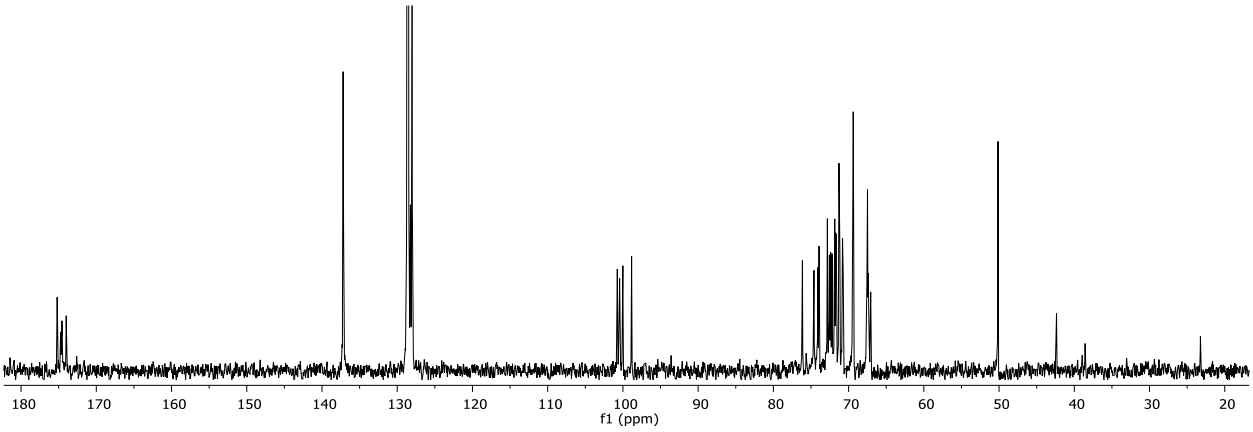
f1 (ppm)

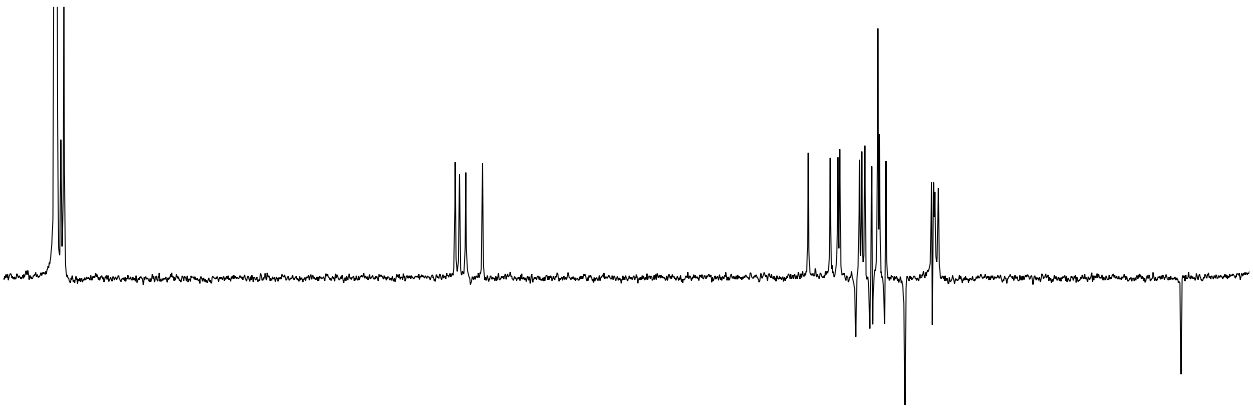

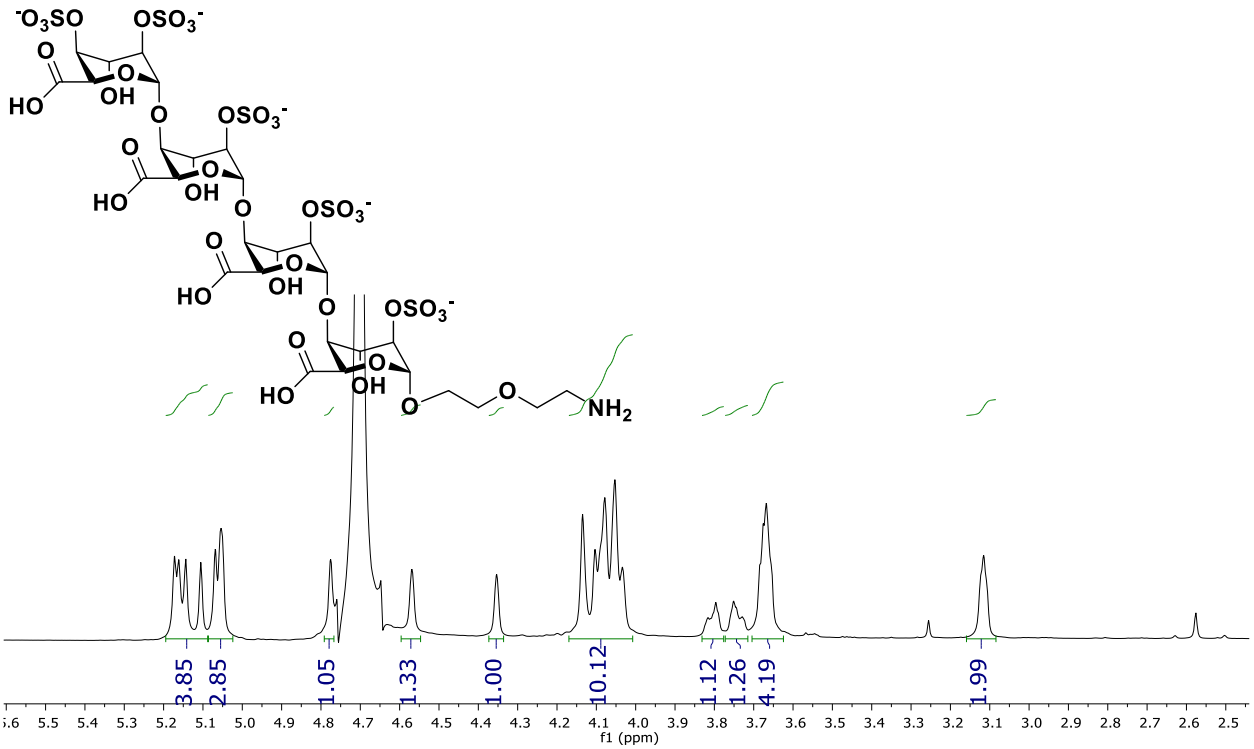
-O3SO
OSO3-
HO
OH
NH2
3.85
2.85
1.05
1.33
1.00
10.12
1.12
1.26
4.19
1.99
f1 (ppm)

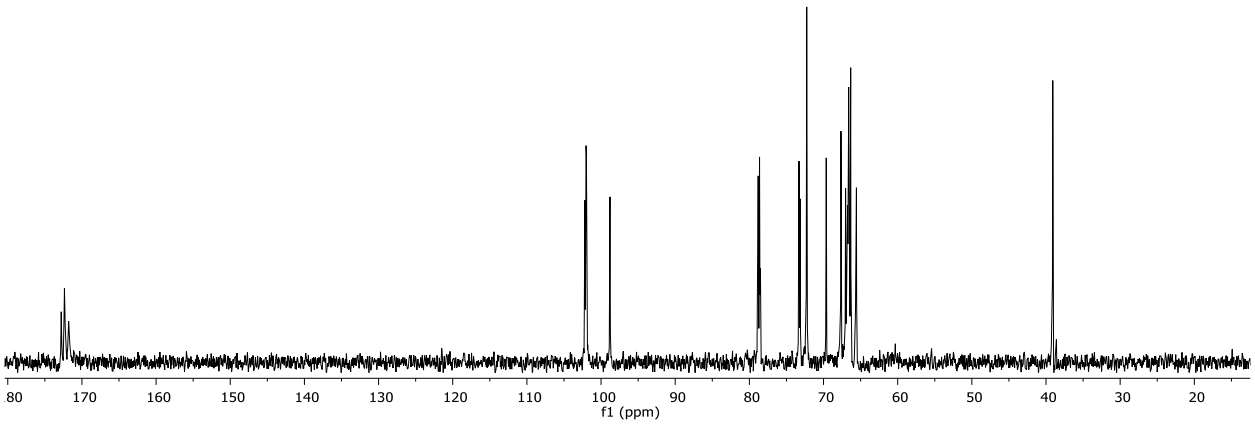
f1 (ppm)

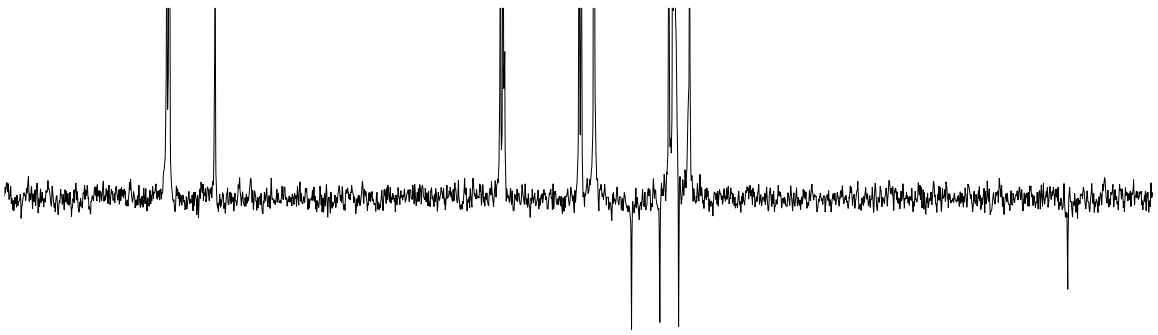

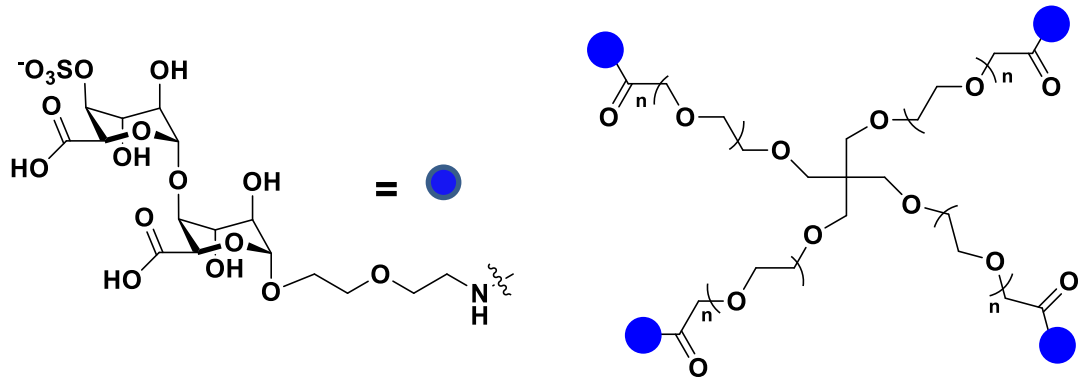

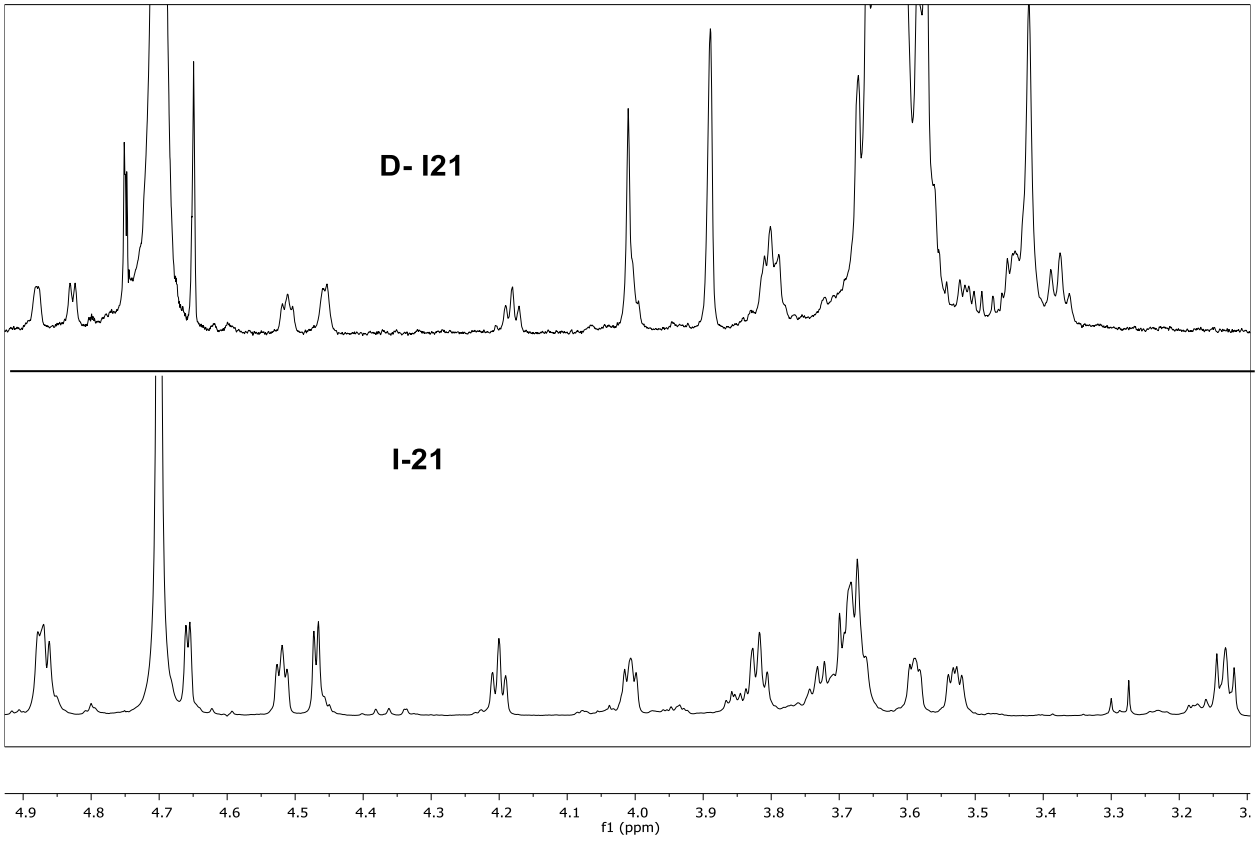
D- I21
I-21
4.9
4.8
4.7
4.6
4.5
4.4
4.3
4.2
4.1
4.0
3.9
3.8
3.7
3.6
3.5
3.4
3.3
3.2
f1 (ppm)

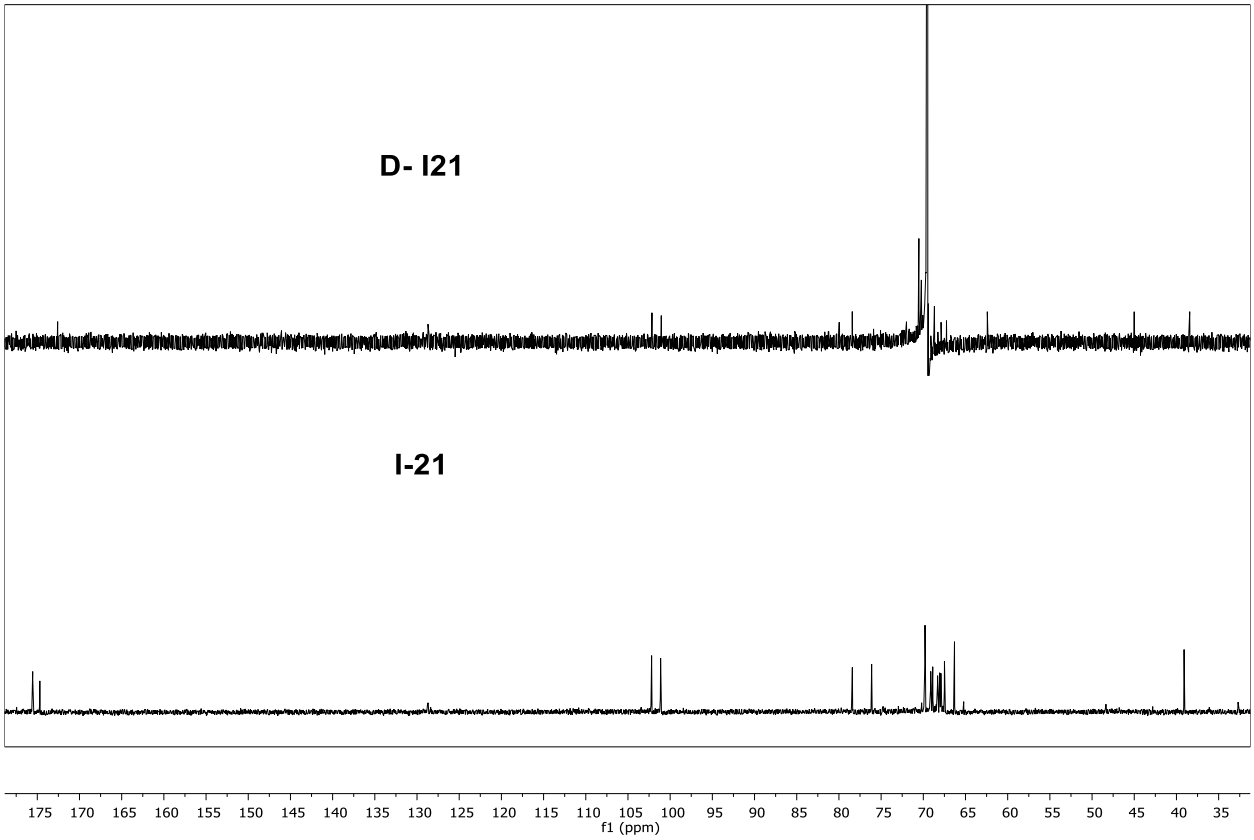
D- I21
I-21
175 170 165 160 155 150 145 140 135 130 125 120 115 110 105 100 95 90 85 80 75 70 65 60 55 50 45 40 35
f1 (ppm)

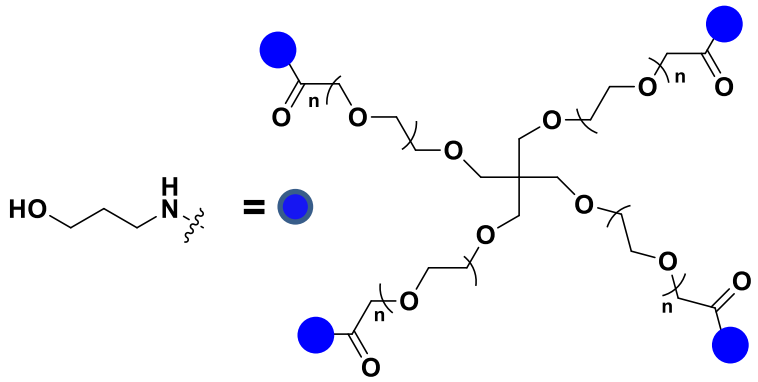
HO
H
N
=
O
n
O
O
O
O
O
O
O
O
n
O
O
n
O
O
n
O

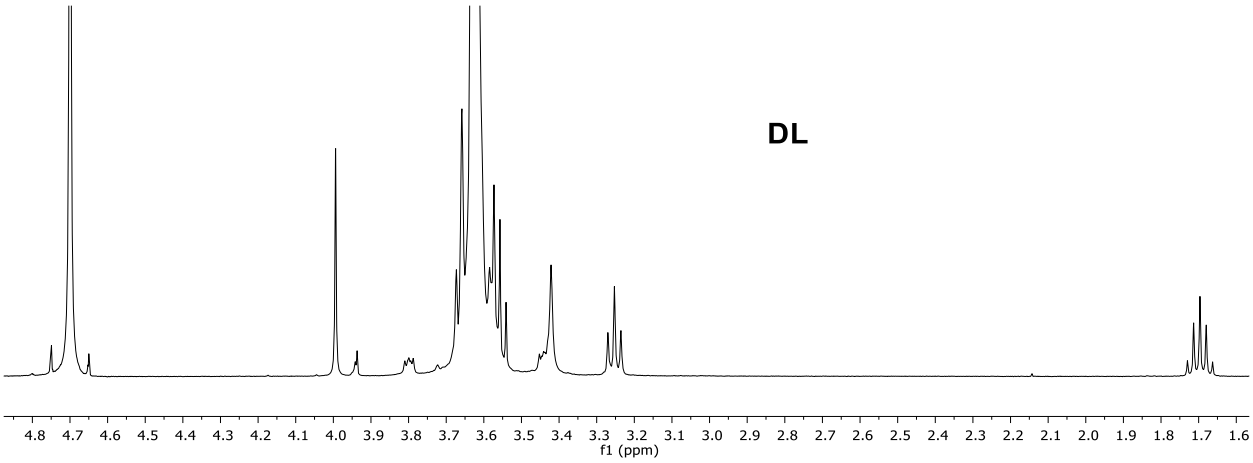
DL
4.8 4.7 4.6 4.5 4.4 4.3 4.2 4.1 4.0 3.9 3.8 3.7 3.6 3.5 3.4 3.3 3.2 3.1 3.0 2.9 2.8 2.7 2.6 2.5 2.4 2.3 2.2 2.1 2.0 1.9 1.8 1.7 1.6
f1 (ppm)

CHAPTER 4

Heparan Sulfate Mimics Unravel Structure-Activity Relationship of Homologus Chemokines and thereby Attenuate Cancer Development

Abstract

Achieving selective inhibition of chemokines activity by structurally well-defined heparan sulfate (HS) or HS mimic molecules can provide important insights into their roles in individual physiological and pathological cellular processes. Herein, we report novel tailor-made HS mimics, which furnish an exclusive iduronic acid (IdoA) scaffold with different sulfation patterns and oligosaccharide chain lengths as potential ligands to target chemokines. Notably, highly sulfated-IdoA tetrasaccharide **(I-45)** exhibited strong binding to CCL2 chemokine and thereby blocking CCL2/CCR2 mediated in vitro cancer cell invasion and metastasis. Taken together, IdoA-based HS mimics offer an alternative HS substrate to generate selective and efficient inhibitors for chemokines and pave the way to a wide range of new therapeutic applications in cancer biology and immunology.

4.1 Introduction

Chemokines are a family of small proteins that have become a focus of extensive research due to their diverse roles in numerous physiological and pathological processes[1-3] including cell trafficking, angiogenesis, embryonic development, neurodegenerative diseases and cancer.[4-10] Thus, the selective inhibition of chemokines can be beneficial in controlling inflammation, viral entry and cancer progression.[11,12] Despite two decades of research in this area, only two antagonists for chemokine receptors have successfully passed clinical trials.[13-15] Hence, there is an urgent need for new approaches in controlling chemokine activity. It has been shown that chemokines utilize the highly sulfated glycosaminoglycan (GAG) heparan sulfate (HS), as a co-receptor to oligomerize and activate their cell surface receptors.[16-22] As a result, identifying the core HS structures responsible for specific chemokine activity is an attractive target for medicinal applications.

HS is composed of α(1,4) linked disaccharide units of D-glucosamine and a hexuronic acid, which can be either D-glucuronic acid (GlcA) or L-iduronic acid (IdoA) with different sulfate modification.[23-29] Theoretically, HS tetrasaccharides can be arranged into 1,024 combinations, highlighting the structural diversity of HS for molecular recognition. The pioneering work of Linhardt, Seeberger, Boons, Hung, Hsieh-Wilson, Desai, Turnbull, Jian and Garnierintroduced reliable chemical and chemoenzymatic protocols to synthesize HS libraries in order to decipher the sulfation codes and oligosaccharide sequences essential for chemokines and other heparan sulfate binding proteins (HSBPs).[30-47] However, it was noted that most chemokines could bind to more than one HS sequence, and the same HS sequence may interact with more than one chemokine or HSBPs. Consequently, the discovery of a specific HS structural domain to modulate individual chemokines has been highly challenging.

Alternatively, HS mimics can be synthesized using the essential structural features of native HS that are responsible for its performance. These features can be incorporated on simplified chemical structure to modulate specificity in chemokine recognition. A broad range of HS mimics have been reported in the literature.[48,49] However, these HS mimics are featureless in terms of conformation plasticity and sulfation patterns, which are key properties of HS used in fine-tuning the binding affinities of HSBPs. Here we report a new set of tailor-made HS mimics **(Fig. 1)** which can use their sulfation

patterns, conformation plasticity, and oligosaccharide chain length to modulate their binding affinities to homologous chemokines. Candidates with high affinities to specific chemokines were identified by microarray screening and further utilized in cancer therapy.

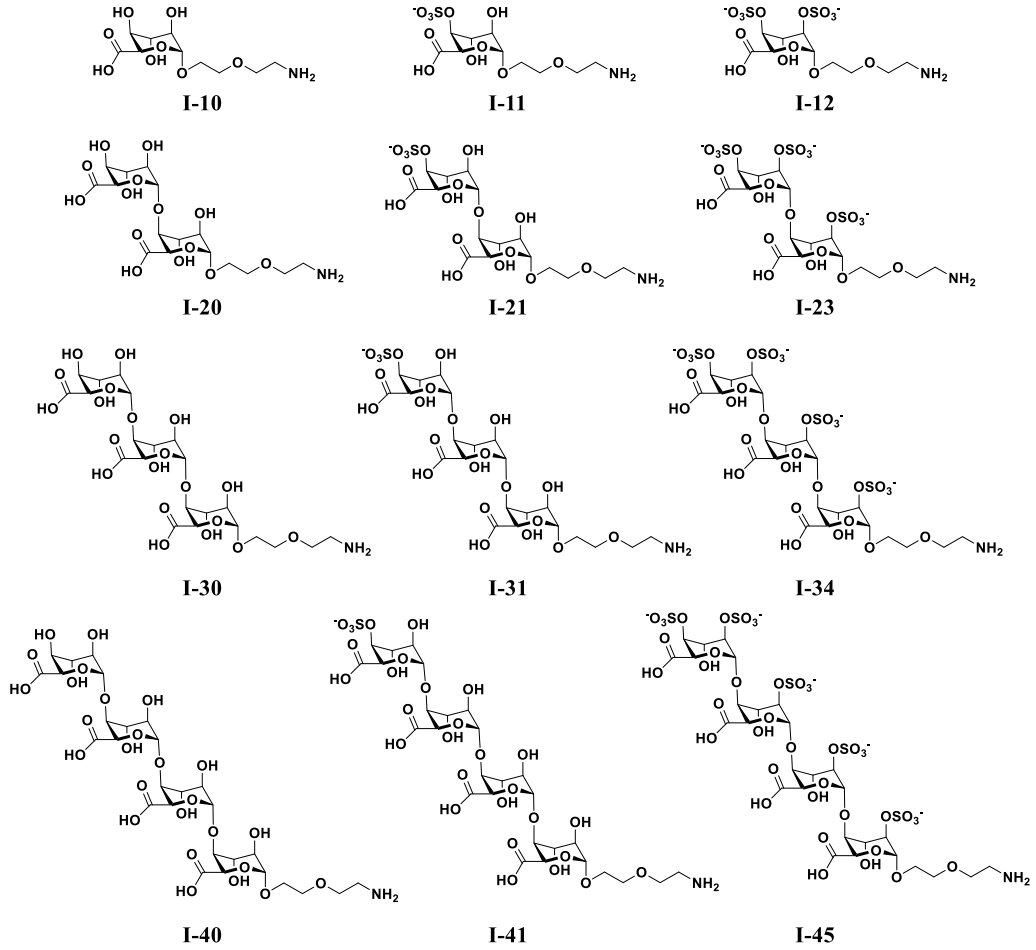

Figure 1: Heparan sulfate Mimics: Iduronic Acid Analogues

4.2 Results and discussion

4.2.1 Synthesis of Iduronic Acid Oligosaccharide

The synthesis of sulfated iduronic acid homo-oligosaccharides is not straightforward, as L-iduronic acid is not commercially available and controlling the α-glycosidic linkages between the successive IdoA residues is difficult. We have reported previously a new linear approach to synthesize oligo-IdoA. Our core building blocks 1,6-anhydro-β-L-idopyranosyl 4-alcohol (**1)** and iduronic acid-thiophenol (L-1**)** were synthesized from 1,2:5,6-di-*O*- isopropylidene-α-D-glucofuranose by six and nine-step reactions,

using described procedures,[50] with a total yield of 0.27% and 0.31% respectively. Using **1** and **L-1** as acceptor and donor, respectively, successive IdoA residue were installed by five step linear reactions (**Scheme 1**).[50] Briefly, **1** and **L-1** were reacted in the presence of NIS and TMSOTf promotor, followed by acetolysis of the anhydro-ring, in the presence of copper (II) trifluoromethanesulfonate [$Cu(OTf)_2$] and acetic anhydride. Then, successive thioglycosylation, mild deacetylation, one-pot TEMPO oxidation, and benzyl esterification yielded the di-IdoA donor. Glycosylation of di-IdoA donor with an azide-linker yielded fully protected di-IdoA intermediate (**L-2**). Similar reaction conditions with di or tri-IdoA donor (**L-2** and **L-3**) and **1** acceptor yielded tri and tetra-IdoA precursor (**L-3**&**L-4**). Global deprotection of these precursors yielded desired non-sulfate IdoA ligands (**I-10**, **I-20**, **I-30** and **I-40**). For IdoA(4S) ligands (**I-11**, **I-21**, **I-31** and **I-41**), IdoA precursors were subjected to selective lev deprotection and sulfation, followed by global deprotection. Highly sulfated-IdoA oligosaccharide series (**I-12**, **I-23**, **I-34** and **I-45**) were obtained by de-esterification, followed by sulfation and hydrogenolysis. All final compounds were purified by ion-exchange resin chromatography, followed by bond elute column. Their structures and purity were confirmed by standard NMR and mass spectrometry techniques.

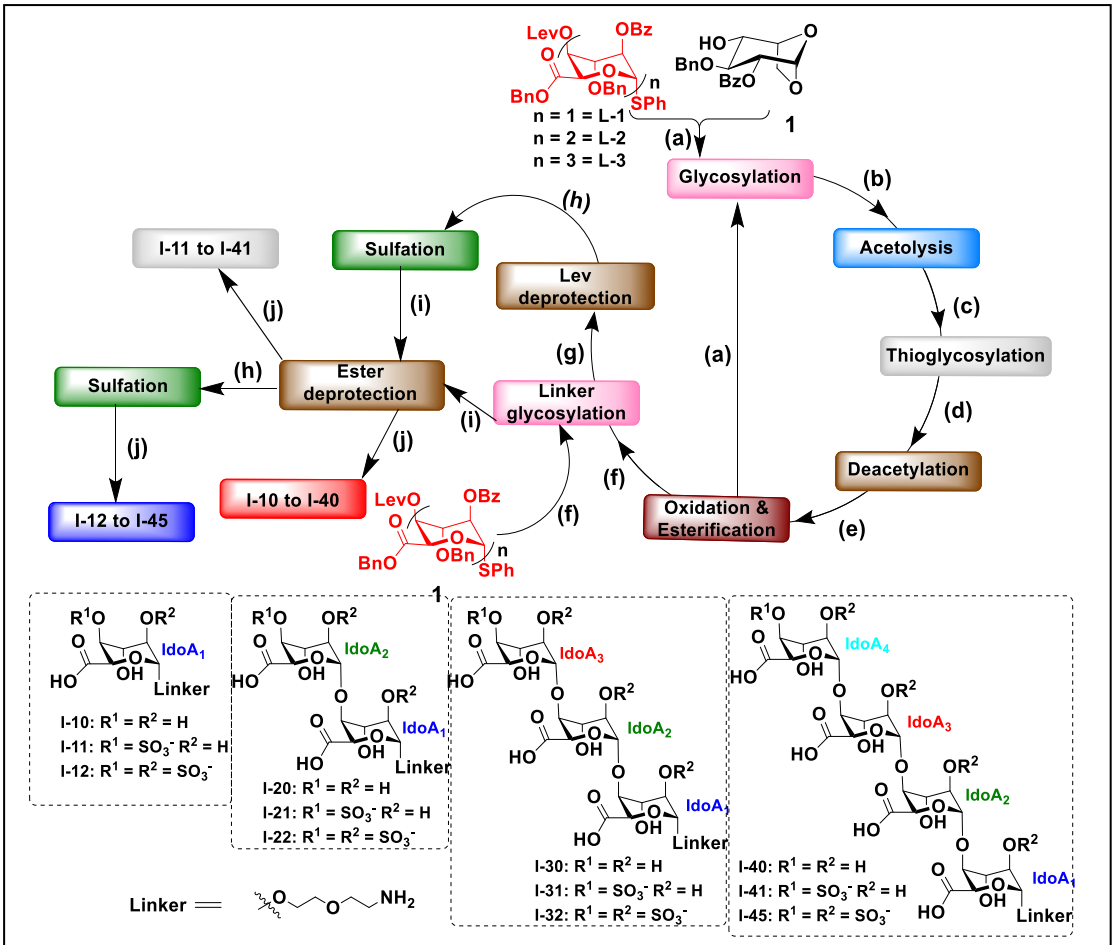

Scheme 1. Synthesis of sulfated-IdoA ranging from monosaccharides to tetrasaccharides. Reagents and conditions: (a) **1** and **2**, NIS, TMSOTf, CH_2Cl_2, 4 Å M.S, –10 °C; (b) $Cu(OTf)_2$, Ac_2O, 0 °C; (c) TMSSPh, ZnI_2, CH_2Cl_2, RT; (d) *P*-TsOH, CH_2Cl_2/MeOH(1:1); (e) TEMPO, BAIB, CH_2Cl_2/H_2O (1:1); BnBr, TBAI, $NaHCO_3$, DMF, 60 °C; (f) azidoethoxyethanol, NIS, TfOH, 4 Å M.S, –5 °C; (g) $H_2NNH_2{\cdot}H_2O$, AcOH, DCM/MeOH (4:1); (h) $SO_3.Et_3N$, DCM 60 °C; (i) LiOH, THF/MeOH/H_2O (4:2:1); (j) $Pd(OH)_2$, MeOH.

4.3 Microarray Analysis

To identify hidden HS-binding active site on chemokines, we constructed a microarray platform of HS mimics. The synthetic HS mimics were printed onto epoxide-functionalized microarray slides replicates of four, as described in the experimental section[10] and tested on three homeostatic chemokines (CCL28, CXCL12 and CCL12) and six inflammatory chemokines (CXCL8 (IL-8), CXCL10 (IP-10), CCL2 (MCP-1), CCL7 (MCP-3), CCL13 (MCP-4) and CCL5 (RANTES)). The rationale of selecting the chemokines is based on their structural and functional homologs, particularly CCL2, CCL7 and CCL13 share high sequence homology.[51] Identifying active HS

ligand for these chemokines is important to monitor their specific activity. To validate the binding order of HS mimics with chemokines, we ranked each glycan based on their percentage of relative fluorescent intensity against optimal fluorescent signal.[52-53] Based on the binding patterns, we further divided them into four distinct groups (**Fig. 2**). In group A, we found that CCL13 (MCP-4), an inflammatory chemokine and CCL28, homeostatic chemokine showed broad-spectrum of moderate and strong binding affinity with HS mimics, indicating that these two chemokines display promiscuous HS binding sites and reinforced the hypothesis that sulfation group is not a key structure feature for these chemokines binding. Furthermore, these results suggesting that group A chemokines may require native HS synthetic analogues to establish selectivity.

In group B, we found that the homeostatic chemokines CXCL12 and CCL21 displayed weak or moderate binding with non-sulfated IdoA ligands (ranked 38-66% for **I-10** to **I-40**) and strong binding to sulfated HS mimics. Both homeostatic chemokines displayed a systematic enhancement in affinity with increasing length of oligosaccharides (**I-11** to **I-31-** ranked 64%, 79% and 92% with CXCL12, 62%, 71% and 83% with CCL21; **I-12** to **I-23** ranked 75% and 98% with CXCL12 and 79% and 86% with CCL21). Surprisingly, they both displayed a weak binding with the tetrasaccharide **I-41** whereas **I-45** had strong binding to CXCL12, (ranked 91%), but not by CCL21. These findings demonstrated that optimal homo-oligosaccharide chain length and sulfation code is critical for molecular-level interaction.

Finally, we compared the binding profile of five inflammatory chemokines, CXCL10 (IP-10), CCL7 (MCP-3), CXCL8 (IL-8), CCL5 (RANTES)and CCL2 (MCP-1). Based on their binding patterns, we classified them into group C and D. In group C, chemokines CXCL10, CCL7 and CXCL8 displayed strong binding affinity with mono and highly sulfated IdoA analogues and weak binding with non-sulfate IdoA analogues, indicating that sulfate groups are key regulator in inflammatory chemokines. Unlike group C, chemokines CCL5 and CCL2 showed exclusive strong binding affinity to high-sulfated HS mimics, no binding to non-sulfated mimics and weak binding with mono-sulfated ligand. Among high-sulfate ligands, **I-23** and **I-45** revealed strong binding to group D chemokines, indicating that sulfation code, even number of IdoA units and absolute $^{1}C_{4}$-IdoA conformation[54] are critical of CCL2 and CCL5 activation.

Overall, the microarray analysis revealed a strong interaction between **I-45** with CCL2, CCL5, CXCL8, CXCL10 and CXCL12 (ranked 88%, 91%, 87% and 91%).

Sulfation	ID	CCL13	CCL28	CXCL12	CCL21	CXCL10	CCL7	CXCL8	CCL5	CCL2
None	I-10	74	46	62	52	47	30	17	2	4
	I-20	82	58	66	63	45	30	12	2	2
	I-30	69	72	38	46	24	17	5	1	0
	I-40	67	56	56	48	44	33	12	2	2
Mono-4-O-Sulfate	I-11	81	80	64	62	57	58	62	15	23
	I-21	94	84	79	71	67	55	73	38	25
	I-31	86	80	92	83	78	75	63	30	36
	I-41	72	54	45	60	23	12	13	10	0
Di-2,4-O-Sulfate	I-12	53	51	75	79	82	94	71	75	66
	I-23	88	76	98	86	96	87	83	86	69
	I-34	67	84	82	80	74	79	95	80	67
	I-45	70	72	91	50	87	80	96	91	88
	Group	A		B		C			D	

%
100
75
50
25
0

Figure 2. Chemokine glycan microarray binding assay. Binding was tested at 3 serial dilutions, then detected with the relevant biotinylated secondary antibody (1 µg/ml) followed by Cy3-Strepavidin (1.5 µg/ml) (Fig S3). Arrays were scanned, relative fluorescent units (RFU) obtained for each chemokine, and mean rank between the 3 dilutions was calculated for glycans printed at 100 µM concentration. For this purpose, the binding RFU's per dilution per glycan were determined, then maximum RFU in each detection was determined and set as 100% binding and all other glycans were calculated as ratio of max (percent). The Rank for each glycan was averaged between the three dilutions for each detection and SEM was calculated. This analysis allowed to compare the glycans binding patterns across chemokines. The mean rank is shown as a heatmap of all the examined binding assays together (red highest, blue lowest and white 50th percentile of ranking).

4.4 SPR Analysis

To quantitatively evaluate the binding affinity between **I-45** and chemokines, SPR experiment was performed using five different chemokines (CCL2, CCL5, CXCL8, CXCL10 and CXCL12), which showed strong selective and sensitive binding in microarray experiments. The equilibrium binding constants (K_D) measured from steady state fits. **I-45** revealed strong binding to CCL2 chemokine (1.6 µM) as compared to other chemokines (CCL5: 5.72 µM; CXCL10: 19.54 µM; CXCL8: 9.34 µM and CXCL12: 18.78 µM respectively) **(Fig. 3a-3c & Fig. 5**), indicating **I-45** is ideal ligand to target CCL2 activity. To date, CCL2 is only the second chemokine shown to

specifically recognize Iduronic acid scaffold. The **I-12** (2,4-disulfated IdoA)-CCL20 chemokine was the first example of the specific interaction mediated by IdoA scaffold.[7b]

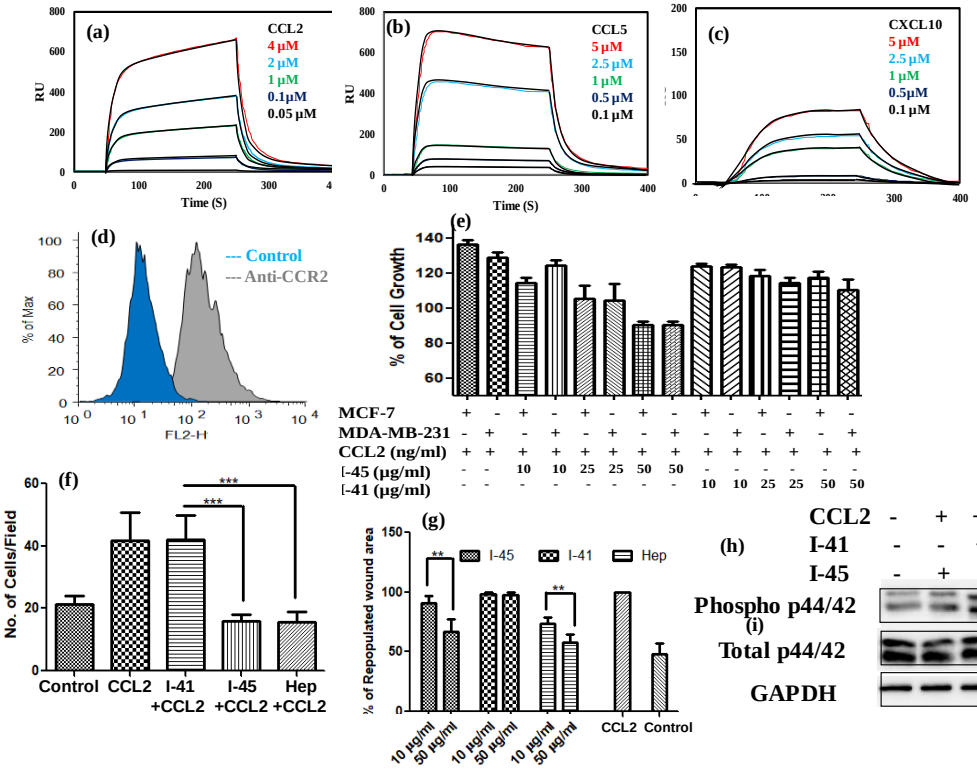

Figure 3. (a) SPR binding analysis of the interaction between CCL2 (0.05–4 µM) and **I-45**, A global fit according to a 1:1 binding model was applied (black curves), resulting dissociation constant (K_D) of 1.67 ± 0.3 µM, k_{on} of $1.26 \pm 0.08 \times 10^5\ M^{-1}\ s^{-1}$, and k_{off} of $2.1 \pm 0.5 \times 10^{-1}\ s^{-1}$; (b) SPR binding analysis between CCL5 (0.1–5µM) and **I-45**: (K_D) of 5.72 ± 0.24 µM, k_{on} of $4.2 \pm 0.46 \times 10^4\ M^{-1}\ s^{-1}$, and k_{off} of $2.4 \pm 0.38 \times 10^{-1}\ s^{-1}$; (c) ($K_D$) of CXCL10 (0.1–5 µM) with **I-45** is 19.54 ± 0.3 µM, k_{on} of $1.29 \pm 0.26 \times 10^4\ M^{-1}\ s^{-1}$, and k_{off} of $2.52 \pm 0.61 \times 10^{-1}\ s^{-1}$; (d) FACS histograph analysis of CCR2 expression level by MCF-7 cells; (e) WST assay for MCF-7 and MDA-MB-231 cells proliferation after 48 h treatment of ligand and chemokines. The bar graphs indicated percentage of cell growth; (f) Wound healing assay: Area repopulated in 5 h. Data expressed as mean ± SD (n=3; **P<0.01); (g) Inhibition of CCL2-mediated cell migrationg through metrigel monolayer containing **I-45**, **I-41** and **Hep** (50 µg/ml) and CCL2 (50 ng). Data expressed as mean ± SD (n=3; ***P<0.001); (h) MAPK pathway analysis: MCF-7 Cells were serum starved overnight and treated with **CCL2** (50 ng/ml) with and without **I-45** and **I-41** ligands (50 µg/ml) and cell lysate after 30 min were quantified for P-p44/42 and Total p44/42.

4.5 Cell Proliferation Assay

CCL2 and its CCR2 receptors are highly expressed in several breast cancer cells and play a pivotal role in cancer cells invasion and metastasis.[55-56] Therefore, inhibiting CCL2 singling offers opportunities for drug discovery to target triple negative breast cancer (TNBC). Here, we selected MCF-7 and MDA-MB-231 breast cancer cells to target CCR2/CCL2 activity, which is known to express high level of CCR2 and at the same time low level of autocrine CCL2 chemokines, ideal condition to test external CCL2 mediated cellular activity.[55-56] The expression of CCR2 on MCF-7 and MDA-MB-231 was further confirmed by flow cytometry (**Fig. 3d** & **Fig. 6**).

Next, cancer cell proliferation assay was performed with **I-45** with CCL2. **I-41** and native heparin were used as a negative and positive controls, respectively, and cell proliferation was evaluated using WST assay. Interestingly, addition of **I-45** to CCL2 treated cells showed ~40-50% reduction in cell proliferation after 48 h (**Fig. 3e**) as compared to **I-41**, confirming that **I-45** is a potential ligand to inhibit the CCL2 mediated cell proliferation.

4.6 Cell Migration Wound Healing Assay

Next, we tested whether **I-45** caninhibit CCR2/CCL2 mediated cell migration using wound healing assay (**Fig. 3f**). Cancer cells were grown to monolayer in 24-well plates and wounds were generated by using sterile tip. The bright field images were recorded, quantified and monitored for several hours.[57] CCL2 (50 ng) induced complete wound closure after 5 h (considered as 100% migration). However, addition of **I-45** (50µg/ml) with CCL2 (50 ng) showed 34% reduction in the cell migration, **I-41** had no effect, and natural heparin showed 42% reduction in the cell migration **(Fig 4f)**. These results clearly illustrate the **I-45** is a potential small molecule to target CCL2. Finally, we performed cell invasiveness by Boyden chamber assay in the presence of **I-41** and **I-45** (**Fig 3g & Fig. 7**). The results correlate to the cell migration assay, where **I-45** significantly reduces cell invasiveness. To further investigate the invasiveness mechanism, we analysed expression level of MAP kinase. Western blot analysis of p42/44 showed that MCF-7 cells treated with **I-45**/CCL2 expressed low level of MAPK compared to CCL2 or **I-41**/CCL2 treated cells (**Fig. 3h**). Overall, these results suggest that **I-45** can be considered as a potential ligand to modulate CCL2 activity and anticancer therapy.

4.7 Conclusion

In conclusion, we have demonstrated the key role of IdoA scaffold in chemokine interactions and thereby unraveled the unique structural requirement to modulate sequence homologous chemokines affinity. To our knowledge, CCL2 is the only second chemokine currently known in the literature to recognize IdoA scaffolds selectively. These finding lay the foundations for developing IdoA based drug molecules for cancer and immunotherapy.

4.8 Experimental Section

4.8.1 Materials

PBSx10 was purchased from Hy-labs, ethanolamine from Fisher, ovalbumin (Grade V), sodium phosphate monobasic monohydrate, sodium phosphate dibasic heptahydrate, Tween-20 and Tris/HCl were purchased from Sigma-Aldrich. Antibodies were purchased from Peprotech: Human SD1α CXCL12, human IL8 CXCL8 72 aa, human exodus-2 CCL21, human MCP-3 CCL7, human MCP-4 CCL13, human IP-10 CXCL10, human MEC CCL28, human RANTES CCL5, human MCP-1/MCAF CCL2, biotinylated antigen affinity-purified goat-anti-murine SDF-1α, biotinylated-rabbit-anti-human IL8 CXCL8, biotinylated-rabbit-anti-human Exodus-2 CCL21, biotinylated goat-anti-human MCP-3, biotinylated anti-H-MCP-4, biotinylated rabbit-anti-human IP-10, biotinylated anti-human MEC, biotinylated-rabbit-anti-human MCAF/MCP-1. Biotinylated anti-Rantes was purchased from R&D. Cy3-sterptavidin (Cy3-SA) was purchased from Jackson ImmunoResearch.

4.9 Glycan microarray

4.9.1 Heparin-Saccharide Microarray Fabrication

Arrays were fabricated with NanoPrint LM-60 Microarray Printer (Arrayit) on epoxide-derivatized slides (PolyAn 2D) with 16 sub-array blocks on each slide. Glycoconjugates were distributed into 384-well source plates using 4 replicate wells per sample and 7 µl per well. Each glycoconjugate diluted into 50 and 100 µM in an optimized printing buffer (300 mM phosphate buffer, pH 8.4 Version VrHI.01. To monitor printing Alexaflour-555-hydraside (Invitrogen, at 1 ng/µl in 178 mM phosphate buffer, pH 5.5)

was used for each printing run. The arrays were printed with four 946MP3 pins (5 µm tip, 0.25 µl sample channel, ~100 µm spot diameter; Arrayit). The humidity level in the arraying chamber was maintained at about 70% during printing. Printed slides were left on arrayer deck over-night, allowing humidity to drop to ambient levels (40-45%). Next, slides were packed, vacuum-sealed and stored at room temperature (RT) until used.

4.9.2 Heparin-Saccharide Microarray Binding Assay

Slides were developed and analyzed as previously described with some modifications.[55-56] Slides were rehydrated with dH_2O and incubated for 30 min in a staining dish with 50°C pre-warmed ethanolamine (0.05 M) in Tris-HCl (0.1 M, pH 9.0) to block the remaining reactive epoxy groups on the slide surface, then washed with 50 °C pre-warmed dH_2O. Slides were centrifuged at 200×*g* for three min then fitted with ProPlate™ Multi-Array 16-well slide module (Grace Bio-lab P37001) to divide into the sub-arrays (blocks). Slides were washed with PBST (0.1% Tween 20), aspirated and blocked with 200 µl/sub-array of blocking buffer (PBS pH 7.3 + 1% w/v ovalbumin) for 1 hour at RT with gentle shaking. Next, the blocking solution was aspirated and 100 µl/block of primary detection proteins (for each detection, 3 serially decreasing concentrations were used, see Table 1) diluted in PBS pH 7.3 + 1% w/v ovalbumin, were incubated with gentle shaking for 2 hours at RT. Slides were washed 4 times with PBST, then with PBS (without Tween-20) for 2 min. Bound antibodies were detected by incubating with biotinylated secondary detections (1 ng/µl, see Table 1) diluted in PBS, 200 µl/block at RT for 1 hour. Slides were washed 4 times with PBST, then with PBS (without Tween-20) for 2 min and biotinylated antibodies were detected with Cy3-SA (1.2µg/ml). Slides were washed 4 times with PBST, then with PBS for 10 min followed by removal from ProPlate™ Multi-Array slide module and immediately dipping in a staining dish with dH_2O for 10 min with shaking. Slide then were centrifuged at 200×*g* for 3 min. and the dry slides immediately scanned.

Table 1. Primary and secondary antibodies and detection concentrations used on the array

Primary Detection	Concentrasions used (ng/µl)	Secondary Detection
Human SD1α (CXCL12)	20, 10, 5	Biotinylated antigen affinity-purified goat-anti-murine SDF-1α
Human IL8 (CXCL8) 72 aa	20, 10, 5	Biotinylated-rabbit-anti-human IL8 (CXCL8)
Human Exodus-2 (CCL21)	20, 10, 5	Biotinylated-rabbit-anti-human Exodus-2 (CCL21)
Human MCP-3 (CCL7)	20, 10, 5	Biotinylated-goat-anti-human MCP-3
Human MCP-4 (CCL13)	20, 10, 5	Biotinylated anti-human MCP-4
Human IP-10 (CXCL10)	10, 5, 2.5	Biotinylated-rabbit-anti-human IP-10
Human BCA-1 (CXCL13)	10, 5, 2.5	Biotinylated-rabbit-anti-human BCA-1
Human MEC (CCL28)	10, 5, 2.5	Biotinylated-anti-human MEC
Human RANTES (CCL5)	2, 1, 0.5	Biotinylated anti-Rantes
Human MCP-1/MCAF (CCL2)	2, 1, 0.5	Biotinylated-rabbit-anti-human MCAF/MCP-1

4.9.3 Array Slide Processing

Processed slides were scanned and analyzed as described at 10 µm resolution with a Genepix 4000B microarray scanner (Molecular Devices) using 350 gain. Image analysis was carried out with Genepix Pro 4.0 analysis software (Molecular Devices). Spots were defined as circular features with a variable radius as determined by the Genepix scanning software. Local background subtraction was performed. RFU from each spot was calculated and ranking was used to compare the data between detections; each detection was tested at 3 dilutions. For each dilution, the binding RFU's of the glycans were listed, maximum RFU was determined and was set to be the 100% binding so all the others were calculated as ratio to it (percent). Then, the rank for each glycan was averaged between the three dilutions and SEM was calculated.

4.9.4 Glycan Microarray Analysis of Binding Assay

Binding was tested at 3 serial dilutions, then detected with the relevant biotinylated secondary antibody (1 µg/ml) followed by Cy3-strepavidin (1.5 µg/ml), as in Table 1. Arrays were scanned and relative fluorescent units (RFU) calculated of chemokines binding to 100 µM glycans printed at four replicates. Rank binding of chemokines (each at three dilutions) to glycans printed at four replicates each was calculated. For each binding assay per printed block, the maximum RFU was determined and set as 100%

binding. Then binding to all the other glycans in the same block was ranked in comparison to the maximal binding, and average rank binding (and SEM) for each glycan across the three examined concentrations of each chemokines was calculated. This analysis allowed to compare the glycan binding profiles of the different g chemokines and dissect their binding preferences.

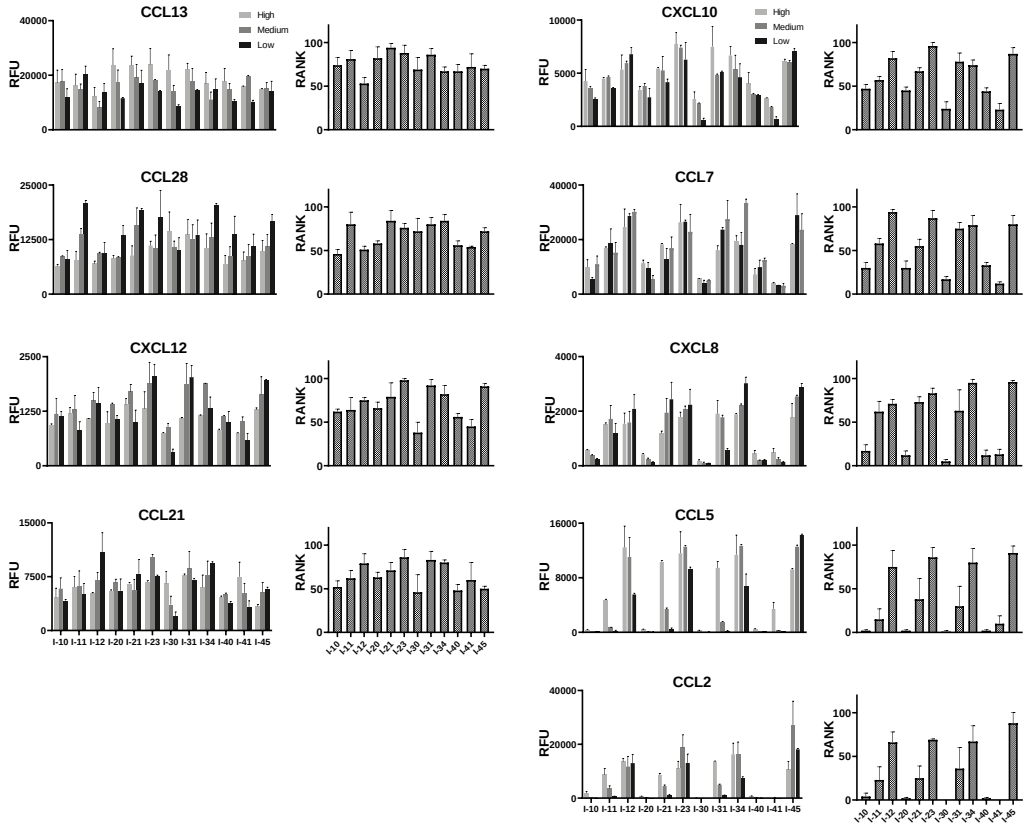

Figure 4. Binding RFU's for each chemokine at 3 serially decreasing dilutions (high, medium and low). Binding was detected with specific biotinylated anti each protein antibody (1 µg/mL) followed by Cy3-Strepavidin (1.5 µg/mL). The arrays then were scanned and relative fluorescent units (RFUs) were calculated. The data presented is for 100µM glycan only. For each chemokine, mean rank between the 3 dilutions was calculated; the binding RFU's for each dilution were listed, maximum RFU was determined and set to be the 100% binding so all the others were calculated as ratio to it (percent). Now the Rank for each glycan was averaged between the three dilutions and SEM was calculated as well.

4.10 Surface Plasmon Resonance Binding Kinetics

I-45 was covalently immobilized on sensor chip via coupling reaction. At first, the dextran matrix on CM5 chip was activated with NHS (0.02 M) and EDC coupling reagent (0.2 M) at a flow rate of 5 µL min^{-1} for 15 min before activating with 50 µL of **1-45** (0.5 mM) in HBS-EP buffer. In the negative control cell after EDC and NHS activation, 0.5 mM of ethanol amine solution was flowed. The positive RU response on 1-45 confirmed immobilization of the HS ligand on CM5 chips. Then, different chemokines at a flow rate of 50 µL/min and 25 °C in HBS-EP buffer without chemokines was then flowed over the sensor surface for 3 min to enable association/dissociation. Kinetic analysis was performed using the BIA evaluation software for T100. Association and dissociation phase data were globally fitted to a simple 1:1 interaction model.

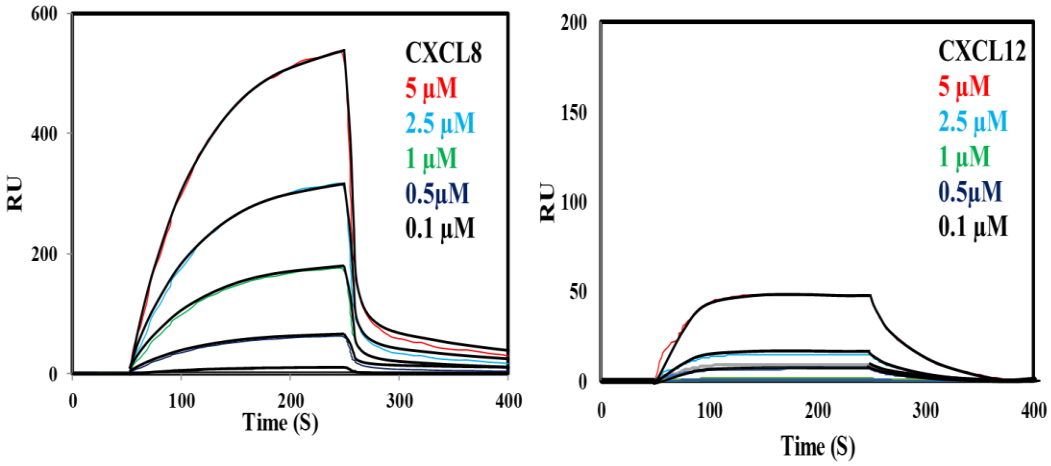

Figure 5. SPR binding analysis of the interaction between CXCL8 (0.05–5 µM) and **I-45**, A global fit according to a 1:1 binding model was applied (black curves), resulting dissociation constant (K_D) of 9.34 ± 0.21 µM, k_{on} of 3.16 ± 0.08 × 10^5 M^{-1} s^{-1}, and k_{off} of 2.96 ± 0.1 × 10^{-1} s^{-1}; (b) SPR binding analysis between CXCL12 (0.1–5µM) and **I-45**: (K_D) of 18.78 ± 0.44 µM, k_{on} of 1.1 ± 0.46 × 10^4 M^{-1} s^{-1}, and k_{off} of 2.1 ± 0.78 × 10^{-1} s^{-1};

4.11 Cell Proliferation Assay

MCF-7 or MDA-MB-231 (approximately 10^4) were plated on 96 well plates in a RPMI-1640 medium in 1% FBS without growth supplements. Cells were incubated for 4 hr before the experiments. First HS biomimetics (**I-45** and **I-41**, 10 or 50 µg/ml) and native heparin (10 or 50 µg/ml) were preincubated with CCL2 (50 ng/ml) and added to the cells. After 48 h of incubation, cells were washed and fixed with paraformaldehyde.

Cell were stained with 4% sulforhodamine B in 1% acetic acid for 30 min and washed with 1% acetic acid solution. Cell proliferation was determined with 2-(4-iodophenyl)-3-(4-nitrophenyl)-5-(2,4-disulfophenyl)- 2H-tetrazolium monosodium salt at 450 nm.

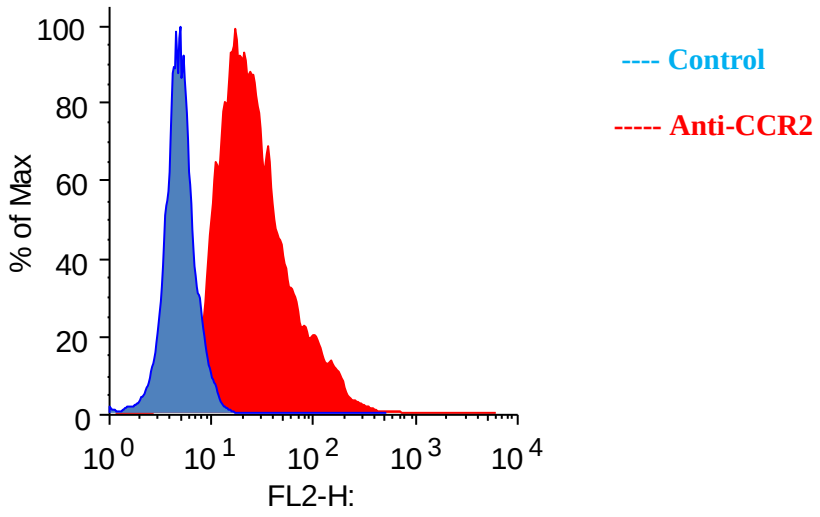

Figure 6. FACS histograph analysis of CCR2 expression level by MDA-MB-231 cells;

4.12 Cell-Division Cycle Analysis

MCF-7 cells were treated with chemokines and HS mimics as mentioned above after 72 h, cells were harvested and fixed overnight in 70 % ethanol at -20 °C. The fixed cells were incubated with propidium iodide (5 µg/mL) and RNase (10 µg/mL) for 30 min at 37 °C. The stained cells were analyzed with a flow cytometer. The DNA content in the G0/G1, S and G2/M phases was quantified by using ModFitLT version 3.0 software.

4.13 Wound Healing Assay

MCF-7 cells were cultured on 24-well plates in RPMI-1640 medium. After monolayer formation, cells were starved with serum free medium for 24 h. Then, wound was created by scratching the monolayer with 1000 µl pipette tip. Cells were treated with heparin and its mimics (**I-45**, **I-41** 10 or 50 µg/ml) with CCL2 (50 ng). After 8 h, CCL2 treated monolayer showed complete wound healing. At that point, % of cell migration distance of heparin mimics treated cells were quantified.

4.14 Cell Invasion Assay

Cell invasion assay was performed in 24-well boyden chamber inserts with 8 µM pore. Upper chamber of transwell inserts were coated with Matrigel. The bottom chamber contained 600 µL RPMI-1640 medium supplemented with 1 % FBS and CCL2 (50 ng/ml) with heparin mimics (I-45, I-41 and heparin). MCF-7 cells were added to the upper chamber. After 24 h incubation at 37 °C, non-invading cells were removed and cells migrated through the membrane to the lower surface were fixed and stained with 0.5 % crystal violet for 30 min and quantified by bright field imaging.

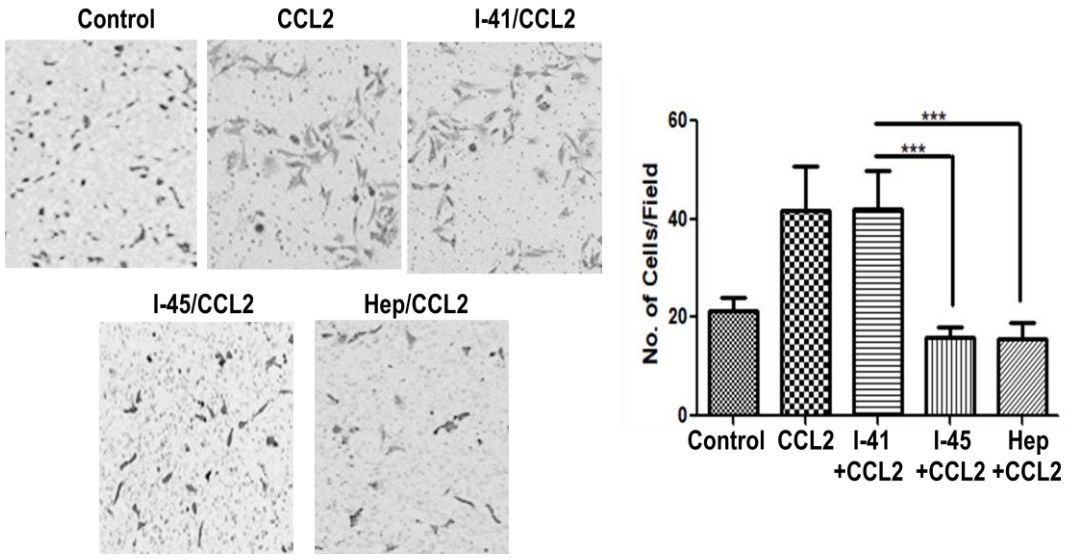

Figure 7. Bright field images of cell invasion assay and quantification.

4.15 Western Blot Analysis

MCF-7 cells were grown in 100 mm Petri dishes and treated with CCL2 (50 ng) and heparin mimics (50 µg) for half hr. The cells were pelleted, and treated with protease inhibitors before treating with lysis buffer containing 150 mM NaCl, 1% NP-40, 0.25% sodium dodecyl sulfate (SDS), 1 mM ethylenediaminetetraacetic acid (EDTA), and 1 mM phenylmethane sulfonyl fluoride (PMSF) in 50 mM Tris-Cl (pH 7.4). After 1 h, the supernatant was collected by centrifugation (14000 rpm) for 15 min and stored in aliquots. The protein content was quantified using the Bradford method. The protein (35 µg) was loaded on SDS-polyacrylamide gel electrophoresis (10%) and transferred onto a polyvinylidene fluoride (PVDF) membrane. The membrane was incubated for 2 h with specific antibodies corresponding to MAPK. The membranes were incubated

with horse radish peroxidase (HRP)-conjugated secondary antibody for 1 h at room temperature, and visualization was done using an Immobilon Western Chemiluminescent HRP substrate kit (Millipore Corporation, MA, USA) with GAPDH as internal standard. BioRad's Protein Ladder (Thermo, EU) was used to determine the molecular weights of the protein bands.

4.16 References

1. Luster, A.D. Chemokines—chemotactic cytokines that mediate inflammation. *N. Engl. J. Med.***338**, 436-445 (1998).
2. Charo, I.F. & Ransohoff, R.M. The many roles of chemokines and chemokine receptors in inflammation. *N. Engl. J. Med.***354**, 610-621 (2006).
3. Brylka, L.J. & Schinke, T. Chemokines in Physiological and Pathological Bone Remodeling. *Front. Immunol.***10**, 2182 (2019).
4. Schall, T.J. & Proudfoot, A.E. Overcoming hurdles in developing successful drugs targeting chemokine receptors. *Nat. Rev. Immunol.***11**, 355-363 (2011).
5. Koenen, R.R. & Weber, C. Therapeutic targeting of chemokine interactions in atherosclerosis. *Nat. Rev. Drug Discov.***9**, 141-153 (2010).
6. Lacotte, S., Brun, S., Muller, S. & Dumortier, H. CXCR3, inflammation, and autoimmune diseases. *Ann. N. Y. Acad. Sci.* **1173**, 310-317 (2009).
7. Fuchs, J.A., Brunner, C., Schineis, P., Hiss, J.A. & Schneider, G. Identification of Chemokine Ligands by Biochemical Fragmentation and Simulated Peptide Evolution. *Angew. Chem. Int. Ed.***58**, 7138-7142 (2019).
8. Fernandez, A., Thompson, E.J., Pollard, J.W., Kitamura, T. & Vendrell, M. A Fluorescent Activatable AND-Gate Chemokine CCL2 Enables In Vivo Detection of Metastasis-Associated Macrophages. *Angew. Chem. Int. Ed.* **58**, 16894-16898 (2019).
9. Korniejewska, A., McKnight, A.J., Johnson, Z., Watson, M.L. & Ward, S.G. Expression and agonist responsiveness of CXCR3 variants in human T lymphocytes. *Immunology***132**, 503-515 (2011).
10. Raman, D., Sobolik-Delmaire, T. & Richmond, A. Chemokines in health and disease. *Exp. Cell Res.***317**, 575-589 (2011).

11. van Kasteren, S.I., Neefjes, J. & Ovaa, H. Creating molecules that modulate immune responses. *Nat. Rev. Chem.***2**, 184-193 (2018).
12. Roskoski Jr, R. A historical overview of protein kinases and their targeted small molecule inhibitors. *Pharmacol. Res.***100**, 1-23 (2015).
13. Andrews, S.P. & Cox, R.J. Small molecule CXCR3 antagonists. *J. Med. Chem.***59**, 2894-2917 (2016).
14. De Clercq, E. The AMD3100 story: the path to the discovery of a stem cell mobilizer (Mozobil). *Biochem. Pharmacol.* **77**, 1655-1664 (2009).
15. Perry, C. Maraviroc. A review of its use in the management of CCR5-tropic HIV-1 infection (vol 70, pg 1189, 2010). *Drugs***70**, 1961-1961 (2010).
16. Lortat-Jacob, H. The molecular basis and functional implications of chemokine interactions with heparan sulphate. *Curr. Opin. Struct. Biol.***19**, 543-548 (2009).
17. Johnson, Z., Proudfoot, A. & Handel, T. Interaction of chemokines and glycosaminoglycans: a new twist in the regulation of chemokine function with opportunities for therapeutic intervention. *Cytokine Growth Factor Rev.* **16**, 625-636 (2005).
18. Handel, T. *et al.* Regulation of protein function by glycosaminoglycans—as exemplified by chemokines. *Annu. Rev. Biochem.***74**, 385-410 (2005).
19. Kufareva, I., Salanga, C.L. & Handel, T.M. Chemokine and chemokine receptor structure and interactions: implications for therapeutic strategies. *Immunol. Cell. Biol.* **93**, 372-383 (2015).
20. Xu, D. & Esko, J.D. Demystifying heparan sulfate–protein interactions. *Annu. Rev. Biochem.***83**, 129-157 (2014).
21. Gandhi, N.S. & Mancera, R.L. The structure of glycosaminoglycans and their interactions with proteins. *Chem. Biol. Drug Des.***72**, 455-482 (2008).
22. Proudfoot, A.E. *et al.* Glycosaminoglycan binding and oligomerization are essential for the in vivo activity of certain chemokines. *Proc. Natl. Acad. Sci.***100**, 1885-1890 (2003).
23. Shi, X. & Zaia, J. Organ-specific heparan sulfate structural phenotypes. *J. Biol. Chem.***284**, 11806-11814 (2009).
24. Feyzi, E., Saldeen, T., Larsson, E., Lindahl, U. & Salmivirta, M. Age-dependent modulation of heparan sulfate structure and function. *J. Biol. Chem.***273**, 13395-13398 (1998).

25. Brickman, Y.G. *et al.* Structural modification of fibroblast growth factor-binding heparan sulfate at a determinative stage of neural development. *J. Biol. Chem.***273**, 4350-4359 (1998).
26. Lindahl, U. & Kjellén, L. Pathophysiology of heparan sulphate: many diseases, few drugs. *J. Intern. Med.* **273**, 555-571 (2013).
27. Nadanaka, S. & Kitagawa, H. Heparan sulphate biosynthesis and disease. *J. Biochem.***144**, 7-14 (2008).
28. Petitou, M. & van Boeckel, C.A. A synthetic antithrombin III binding pentasaccharide is now a drug! What comes next? *Angew. Chem. Int. Ed.***43**, 3118-3133 (2004).
29. Gama, C.I. & Hsieh-Wilson, L.C. Chemical approaches to deciphering the glycosaminoglycan code. *Curr. Opin. Chem. Biol.***9**, 609-619 (2005).
30. de Paz, J.L. *et al.* Profiling heparin–chemokine interactions using synthetic tools. *ACS Chem. Biol.***2**, 735-744 (2007).
31. Nonaka, M. *et al.* Synthetic di-sulfated iduronic acid attenuates asthmatic response by blocking T-cell recruitment to inflammatory sites. *Proc. Natl. Acad. Sci.***111**, 8173-8178 (2014).
32. Lu, W. *et al.* Controlled chemoenzymatic synthesis of heparan sulfate oligosaccharides. *Angew. Chem.***130**, 5438-5442 (2018).
33. de Paz, J.L., Noti, C. & Seeberger, P.H. Microarrays of synthetic heparin oligosaccharides. *J. Am. Chem. Soc.***128**, 2766-2767 (2006).
34. Yoshida, K. *et al.* Chemical Synthesis of Syndecan-3 Glycopeptides Bearing Two Heparan Sulfate Glycan Chains. *Angew. Chem.***126**, 9197-9204 (2014).
35. Sankaranarayanan, N.V. *et al.* A hexasaccharide containing rare 2-O-sulfate-glucuronic acid residues selectively activates heparin cofactor II. *Angew. Chem. Int. Ed.***56**, 2312-2317 (2017).
36. Arungundram, S. *et al.* Modular synthesis of heparan sulfate oligosaccharides for structure− activity relationship studies. *J. Am. Chem. Soc.***131**, 17394-17405 (2009).
37. Zong, C. *et al.* Heparan sulfate microarray reveals that heparan sulfate–protein binding exhibits different ligand requirements. *J. Am. Chem. Soc***139**, 9534-9543 (2017).
38. Zhang, X., Lin, L., Huang, H. & Linhardt, R.J. Chemoenzymatic synthesis of glycosaminoglycans. *Acc. Chem. Res.***53**, 335-346 (2019).

39. Jayson, G.C. *et al.* Synthetic heparan sulfate dodecasaccharides reveal single sulfation site interconverts CXCL8 and CXCL12 chemokine biology. *Chem Commun.***51**, 13846-13849 (2015).
40. Sepuru, K.M., Nagarajan, B., Desai, U.R. & Rajarathnam, K. Molecular basis of chemokine CXCL5-glycosaminoglycan interactions. *J. Biol. Chem.***291**, 20539-20550 (2016).
41. Sepuru, K.M., Nagarajan, B., Desai, U.R. & Rajarathnam, K. Structural basis, stoichiometry, and thermodynamics of binding of the chemokines KC and MIP2 to the glycosaminoglycan heparin. *J. Biol. Chem.***293**, 17817-17828 (2018).
42. Sepuru, K.M., Nagarajan, B., Desai, U.R. & Rajarathnam, K. Structural basis, stoichiometry, and thermodynamics of binding of the chemokines KC and MIP2 to the glycosaminoglycan heparin. *J. Biol. Chem.***293**, 17817-17828 (2018).
43. Griffin, M.E. & Hsieh-Wilson, L.C. Synthetic probes of glycosaminoglycan function. *Curr. Opin. Chem. Biol.* **17**, 1014-1022 (2013).
44. Ziarek, J.J. *et al.* Heparin oligosaccharides inhibit chemokine (CXC motif) ligand 12 (CXCL12) cardioprotection by binding orthogonal to the dimerization interface, promoting oligomerization, and competing with the chemokine (CXC motif) receptor 4 (CXCR4) N terminus. *J. Biol. Chem.***288**, 737-746 (2013).
45. Peterson, F.C. *et al.* Identification and characterization of a glycosaminoglycan recognition element of the C chemokine lymphotactin. *J. Biol. Chem.***279**, 12598-12604 (2004).
46. Sheng, G.J., Oh, Y.I., Chang, S.-K. & Hsieh-Wilson, L.C. Tunable heparan sulfate mimetics for modulating chemokine activity. *J. Am. Chem. Soc.***135**, 10898-10901 (2013).
47. Pawar, N.J. *et al.* Expedient Synthesis of Core Disaccharide Building Blocks from Natural Polysaccharides for Heparan Sulfate Oligosaccharide Assembly. *Angew. Chem. Int. Ed.***58**, 18577-18583 (2019).
48. Bendersky, V., Yang, Y. & Brennan, T.V. Immunomodulatory Activities of the Heparan Sulfate Mimetic PG545, in *Heparanase* 461-470 (Springer, 2020).
49. Chhabra, M. & Ferro, V. PI-88 and related heparan sulfate mimetics, in *Heparanase* 473-491 (Springer, 2020).
50. Shanthamurthy, C.D. & Kikkeri, R. Linear Synthesis of De novo Oligo-Iduronic Acid. *Eur. J. Org. Chem.***2019**, 2950-2953 (2019).

51. Deshmane, S.L., Kremlev, S., Amini, S. & Sawaya, B.E. Monocyte chemoattractant protein-1 (MCP-1): an overview. *J. Interferon Cytokine Res.* **29**, 313-326 (2009).
52. Padler-Karavani, V. *et al.* Cross-comparison of protein recognition of sialic acid diversity on two novel sialoglycan microarrays. *J. Biol. Chem.***287**, 22593-22608 (2012).
53. Ben-Arye, S.L., Yu, H., Chen, X. & Padler-Karavani, V. Profiling anti-Neu5Gc IgG in human sera with a sialoglycan microarray assay. *J. Vis. Exp.*, e56094 (2017).
54. Haasnoot, C.A., de Gelder, R., Kooijman, H. & Kellenbach, E.R. The conformation of the idopyranose ring revisited: How subtle O-substituent induced changes can be deduced from vicinal 1H-NMR coupling constants. *Carbohydr. Res.***496**, 108052 (2020).
55. Lu, Y. *et al.* CCR2 expression correlates with prostate cancer progression. *J Cell. Biochem.***101**, 676-685 (2007).
56. Dutta, P., Sarkissyan, M., Paico, K., Wu, Y. & Vadgama, J.V. MCP-1 is overexpressed in triple-negative breast cancers and drives cancer invasiveness and metastasis. *Breast Cancer Res. Treat.* **170**, 477-486 (2018).
57. Sangabathuni, S. *et al.* Modeling Glyco-Collagen Conjugates Using a Host–Guest Strategy To Alter Phenotypic Cell Migration and in Vivo Wound Healing. *ACS Nano***11**, 11969-11977 (2017).

CHAPTER 5

Discovery of Antiviral Heparan Sulfate Mimics

Abstract

Emerging evidence suggests that a highly sulfated form of glycosaminoglycan (GAG) heparan sulfate (HS) is a co-receptor for the spike protein of SARS-CoV-2 to exert viral infection. Consequently, the inhibition of HS-spike protein interaction with structurally well-defined HS mimics has become a critical pharmaceutical target. Herein, we describe the synthesis of HS mimic amphiphiles, bearing sulfated L-Idose/L-iduronic acid with different oligosaccharide chain length to develop potent SARS-CoV-2 inhibitor. The 5 linear synergistic steps of oligosaccharide synthesis, followed by sulfation yielded a wide range of HS mimics amphiphiles in excellent yield. With these HS mimics were tested for their anti-viral activity, our preliminary data revealed micromolar range inhibition of SARS-CoV-2 viral infection by IDC-3, confirming the structural importance of L-idose moiety in the designing of SARS-CoV-2 drug.

5.1 Introduction

Severe acute respiratory syndrome coronavirus-2 (SARS-CoV-2) is a disease of dysregulation of the respiratory system that results in a massive body complication such as cardiac, kidney injury, and multiple organ failure causing death.[1–3] This virus infects more than 48 million people worldwide, and at least 1.2 million people died this year.[4]There is no treatment for SARS-CoV-2 infection and no vaccine is available. At present, antiviral drugs such as lopinavir, ritonavir remdesivir, favipiravir etc., which have been used for the treatment of viral diseases like flu, hepatitis, HIV are used against Covid-19.[5–12] Alternatively, several immunomodulatory drugs, such as chloroquine, hydroxychloroquine, colchicines, were also recommended to treat SARS-CoV-2.[13–18]However, clinical results of these molecules are inconclusive, and several lethal side-effects stop further usage of these drugs.[19,20] Hence, new approaches for the control of Covid-19 infection are urgently needed. Studies of Covid-19 virus pathogenesis have revealed that the binding of virus spike protein to glycosaminoglycan of heparan sulfate (HS) and angiotensin-converting enzyme-2 (ACE2) cell surface receptor is a critical factor in pathogenicity.[21–23]Hence, considerable effort has been made to deduce HS binding sequence to SARS-CoV-2 active sites.

Structurally, HS is a highly sulfated polysaccharide composed repeating units of α(1-4) linked glucosamine and uronic acid disaccharides, with various *O*-sulfate and *N*-sulfate/*N*-acetate on the uronic acid and glucosamine modifications respectively.[24–30] This modification results 1024 combinations of HS tetrasaccharides. Hence, identify the specific HS ligands for spike protein is challenging. Previously, Boons et al. and Zhongping et al. used a limited HS library to derive the active HS ligand for RBD using microarray and SPR.[23,31] These studies suggested that sulfation patterns and iduronic acid composition in the form of IdoA2S-GlcNS6S turned up to be a potential ligand that modulates SARS-CoV-2 activity.

Furthermore, Linhardt et al. reported that ultrafraction heparin (UFH) and enoxaparin and -6S-desulfate UFH displayed strong inhibition of SAR-CoV-2 binding to epithelial cells.[32,33]Further intranasal administration of these drugs displayed poor toxicity and bioavailability in blood, indicating potential drug molecules for SARS-CoV-2

infection.[34] On the other hand, Desai et al. used computation modelling to identify critical sulfation patterns essential to target spike protein.[35] Their studies confirmed the structural importance of 3-*O*-sulfation of HS in spike proteins recognition and viral inhibition. Although these studies provide insight into how to spike protein reads the native HS ligands, structural complexity and synthetic challenges hindered the discovery of potential HS ligands for spike protein. Alternatively, HS mimics and HS binding peptides showed potential therapeutic molecules to target SARS-CoV-2 infection.[21,36,37] Previously, Turnbull et al. showed that PG545 could be used as a potential ligand to target SARS-CoV-2.[38]

We report herein the design and synthesis of well-defined HS mimics from the linear synthetic strategy to target spike protein. To demonstrate L-hexose's significance with different oligosaccharide chain length in SARS-CoV-2 inhibition, sixmolecules of sulfated HS mimics, equipped with L-idose and L-iduronic acid with cholestenol linker at the reducing end have been synthesized. These HS mimics are expected to determine how to spike protein recognizes L-hexoses. Importantly, this study provides a clear picture of optimal sulfate L-hexose essential for spike protein recognition, thereby inhibiting viral infection.

5.2 Results and Discussion:

5.2.2 Synthesis of Cholestanol Conjugated Iduronic Acid Disaccaride

The synthesis of **IAC-2** started with glycosylating 1,6-anhydro-β-L-idopyranosyl 4-alcohol (**1)** and iduronic acid-thiophenol (**4),** which generate homo-IdoA oligosaccharide**5** precursor as reported previously.[39] Then, compound **5** was subjected to five linear synthetic steps to give desire di-IdoA-cholesterol derivative **10.** Briefly, Compound **5**was treated withcopper (II) trifluoromethanesulfonate [$Cu(OTf)_2$] and acetic anhydride to give **6**, which was thioglycosylated, followed by coupling with cholesterol upon activating by using NIS/TfOH. Then cholesterol derivative **8** was converted to di-IdoA-cholesterol derivative **10**by selective removal of the 6-*O*-acetate with *p*-toulene sulfonic acid, followed by oxidation and esterification. Compound **10** was then subjected to base-catalyzed saponification and sulfation in the presence of $SO_3.Et_3N$ and hydrogenolysis yielded **IAC-2 (Scheme 1).**

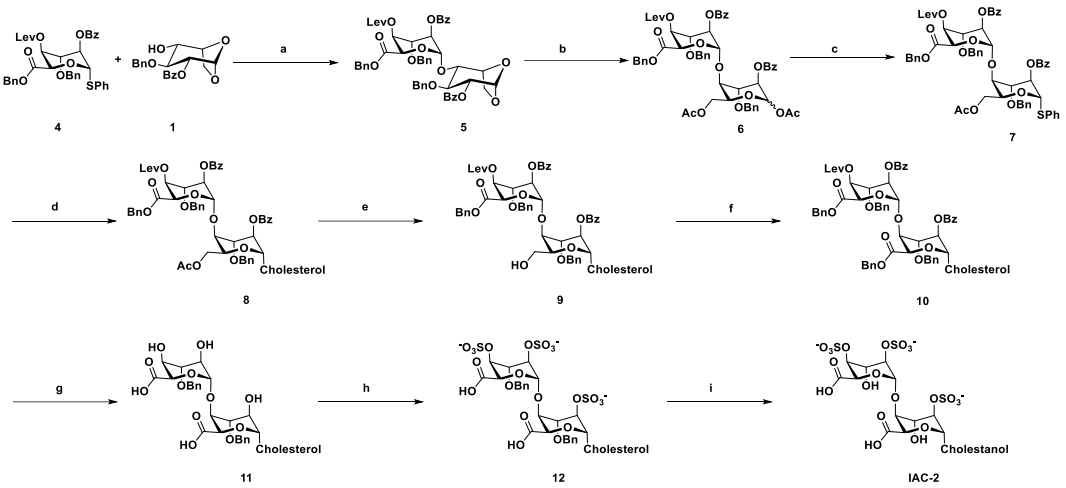

Scheme 1: Synthesis of IAC-2: Reagents and conditions: a) NIS, TMSOTf, CH_2Cl_2, 4 Å M.S, -10 °C, 70%; b) $Cu(OTf)_2$, Ac_2O, 0 °C, 96%; c) TMSSPh, ZnI_2, CH_2Cl_2, RT, 89% ; d) Cholesterol, NIS, TfOH, CH_2Cl_2, 4 Å M.S, -10 °C, 70%; e) *P*-TsOH, CH_2Cl_2/MeOH(1/1), 92%; f) TEMPO, BAIB, CH_2Cl_2/H_2O (1/1); BnBr, TBAI, $NaHCO_3$, DMF, 60 °C, 75%; g) LiOH, THF/MeOH/H_2O(4//2/1), 70%; h)$SO_3.Et_3N$, DMF, 60 °C, 70%, i) H_2, $Pd(OH)_2$ MeOH, 80%.

5.2.3 Synthesis of Cholestanol Conjugated Iduronic Acid Tri- and Tetrasaccaride

In the case of tri and tetrasaccharide iduronic acid amphiphiles (IAC-3 and IAC-4), the L-idopyranose donor **7** and **17** and conventional acceptor **1** was glycosylated and then subjected to the reaction sequence similar to **IAC-2**. Briefly, the glycosylatedproduct **13** and **23** was subjected to selective acetolysis, thioglycosylation using trimethyl(phenylthio)-silane and zinc iodide yielded **17** and **27** respectively. Finally, thiophenylglycosylated tri and tetra-IdoA precursor was treated with cholesterol in the presence of NIS/TfOH yielded 80% of tri and tetraiduronic acid respectively. Saponification of **20** and **30** followed by sulfatedreaction was carried out by using $SO_3.Et_3N$at 60 °C yielded fully sulfated product **22** and **33** respectively. In order to obtain target **IAC-3** and **IAC-4**by subjecting sulfated compound for Hydrogenolysis **(Scheme 2)**. ^{1}H-NMR of HS mimics was fully assigned at RT and high-temperature. We assigned ^{13}C-NMR of the final compound by 2D-HSQC NMR spectra. Finally, the high-resolution mass spectra confirm the molecular weight of the compounds.

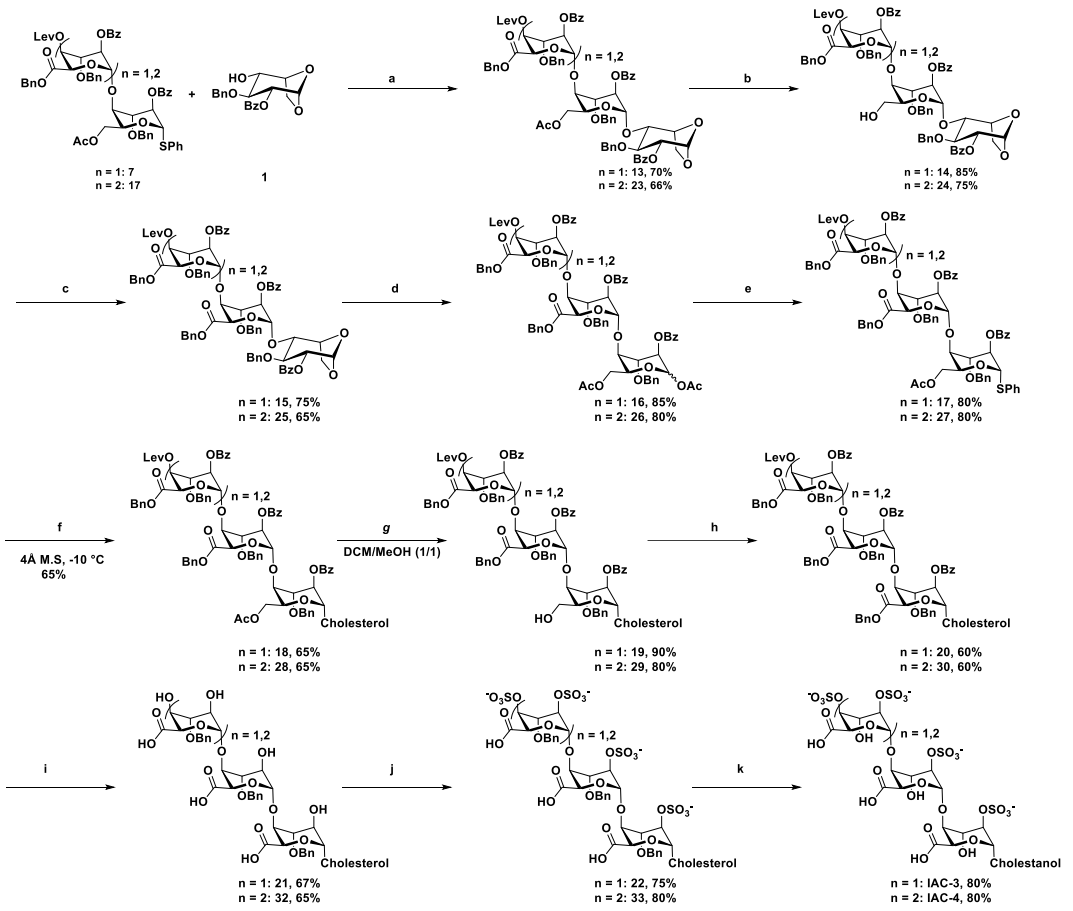

Scheme 2: Synthesis of IAC-3 and IAC-4: Reagents and conditions: a) NIS, TMSOTf, CH_2Cl_2, 4 Å M.S, -10 °C, 13(70%) and 23(66%); b) *P*-TsOH, CH_2Cl_2/MeOH(1/1), 14(85%) and 24(75%); c) TEMPO, BAIB, CH_2Cl_2/H_2O (1/1); BnBr, TBAI, $NaHCO_3$, DMF, 60 °C, 15(75%) and 25(65%); d) $Cu(OTf)_2$, Ac_2O, 0 °C, 16(85%) and 26(80%) ; e) TMSSPh, ZnI_2, CH_2Cl_2, 17(80%) and 27(80); f) Cholesterol, NIS, TfOH, CH_2Cl_2, 4 Å M.S, -10 °C, 18(65%) and 28(65%); g) *P*-TsOH, CH_2Cl_2/MeOH(1/1), 19(90%) and 29(80%); h) TEMPO, BAIB, CH_2Cl_2/H_2O (1/1); BnBr, TBAI, $NaHCO_3$, DMF, 60 °C, 20(60%) and 30 (60%); i) LiOH, THF/MeOH/H_2O(4//2/1), 21(67%) and 32(65%); j)SO_3.Et_3N, DMF, 60 °C, 22(75%) and 33(80%), k) H_2, $Pd(OH)_2$ MeOH, IAC-3(80%) and IAC-4(80%).

5.2.4 Synthesis of Cholestanol Conjugated Idose Di-, Tri- and Tetrasaccharide

To obtain the Idose base HS mimics amphiphiles, L-idose Building blocks **1** was converted to thiophenol L-Idose donor by treating with a mixture of acetic acid and copper (II) trifluoromethanesulfonate [$Cu(OTf)_2$] for anhydro-ring opening, followed by thiophenol glycosylation. The L-idose donor **34** was glycosylated with **1** using TfOH and NIS as an activator to yield 56% of disaccharide precursor. Compound **35** was converted disaccharide donor **37** by treating with [$Cu(OTf)_2$] and acetic acid and thioglycosylation. Compound **37** and cholesterol was coupled by using NIS and TfOH and subjected to deprotection of esters under basic condition and sulfation in the presence of SO3.Et_3N yielded 69% of compound **40**. Finally, the hydrogenation of the benzyl ethers protection over $Pd(OH)_2/C$ gave the target compound **IDC-2**. In the case of tri and tetrasaccharides (**IDC-3** and **IDC-4**), the reaction sequences are similar to **IDC-2 (Scheme 3).** The 1H-NMR of idose HS mimics amphiphiles were fully assigned by 1D and 2D-NMR. The anomeric protons resonate at 5.39, 5.32, 5.26 and 5.23ppm respectively for of cholestanol conjugated sulfated tetrasaccharide was confirmed by HSQC NMR study and the respected ^{13}C peaks are resonate at 96.93, 100.02, 100.88 and 100.56ppm respectively. The molecular weight of the final compound was confirmed by HRMS.

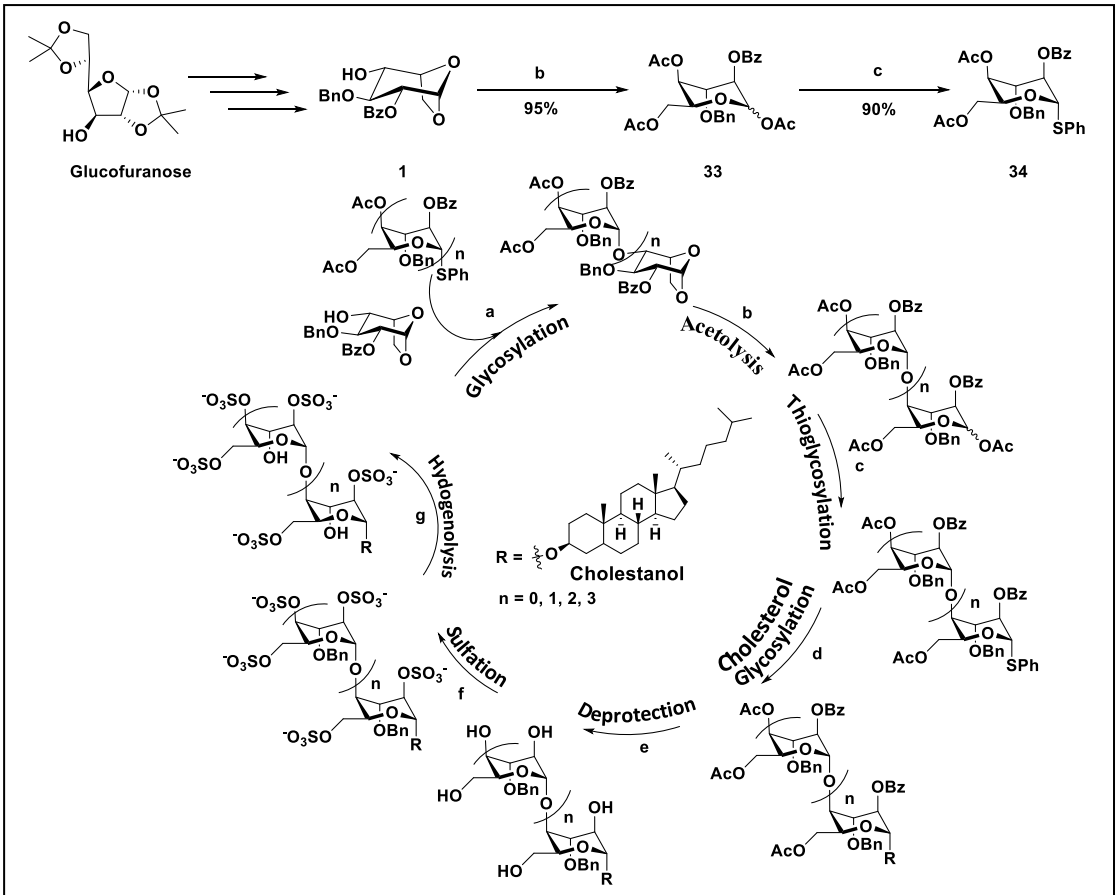

Scheme 3: Synthesis of IDC-2, IDC-3 and IDC-4: Reagents and conditions: a) NIS, TMSOTf, CH_2Cl_2, 4 Å M.S, -10 °C; b) $Cu(OTf)_2$, Ac_2O, 0 °C; c) TMSSPh, ZnI_2, CH_2Cl_2; d) Cholesterol, NIS, TfOH, CH_2Cl_2, 4 Å M.S, -10 °C; e) NaOMe, MeOH/CH_2Cl_2(2/1), f) $SO_3.Et_3N$, DMF, 60 °C; g) H_2, $Pd(OH)_2$ MeOH.

5.3 Antiviral Effects of HS Mimics Amphiphiles in Live Virus Assays

To address the antiviral activity of HS amphiphiles, we performed inhibition studies SARS-CoV-2 infection of Vero Cells in the presence of HS mimics amphiphiles and quantitative binding avidity was measured as the IC_{50} value. As expected, all HS amphiphiles exhibited strong inhibition of SARS-CoV-2 infection. Among the L-iduronic acid series, we observed IAC-2 displayed poor inhibition, whereas IAC-3 displayed strong inhibition of 69 µM as compared to IAC-4 89 µM. In contrast, L-idose analogues showed nearly the same range of SARS-CoV-2 inhibition (60-70 µM). Among them, IDC-3 displayed strong inhibition at ~ 57 µM, in comparison to IDC-4 of 69 µM. These results are comparable to PG545 of 66 µM. These results confirmed

that the trisaccharides scaffold is optimal sugar length essential to inhibit the SARS-CoV-2 infection.

5.4 Conclusions

In conclusion, a library of HS amphiphiles composed of sulfated L-iduronic acid and L-idose were prepared and their binding to SARS-CoV-2 spike protein and antiviral activity were studied. The interrelationship between-hexose and the optimal sugar length essential for targeting SARS-CoV-2 was examined. Our results highlight the fact that highly sulfated L-idose based amphiphilies had a major impact on antiviral activity.

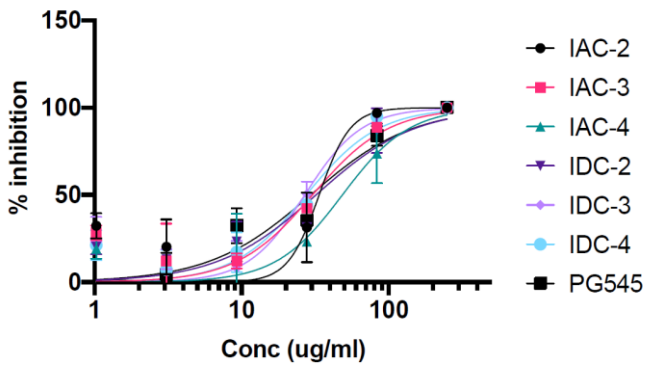

(ug/ml)

	IC50	
	Value	SEM
IAC-2	33.695	9.361
IAC-3	30.358	6.465
IAC-4	48.503	9.189
IDC-2	32.092	7.071
IDC-3	26.912	4.998
IDC-4	27.511	4.553
PG545	29.558	5.240

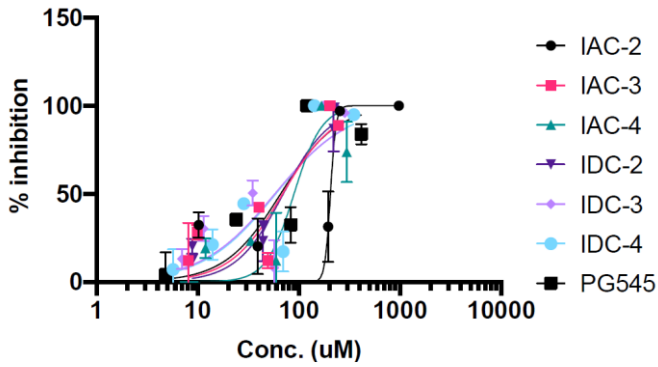

(uM)

	IC50	
	Value	SEM
IAC-2	205.526	12.909
IAC-3	69.122	16.712
IAC-4	89.696	20.732
IDC-2	70.216	10.464
IDC-3	57.996	20.400
IDC-4	59.130	19.055
PG545	66.113	17.819

Figure 1: HS amphiphiles inhibits attachment and invasion of Vero cells by live SARS-CoV-2 virus isolates.

5.5 Experimental Section

5.5.1 General Instructions

All chemicals were reagent grade and used as supplied except where noted. Analytical thin layer chromatography (TLC) was performed on Merck silica gel 60 F254 plates (0.25 mmol). Compounds were visualized by UV irradiation or dipping the plate in CAM/ninhydrin solution followed by heating. Column chromatography was carried out using force flow of the indicated solvent on Flukab Kieselgel 60 (230–400 mesh). ^{1}H and ^{13}C NMR spectra were recorded on Jeol 400 MHz, with cryo probe using residual solvents signals as an internal reference ($CDCl_3$ δ_H, 7.26 ppm, δ_C 77.3 ppm and CD_3OD δ_H 3.31 ppm, δ_C 49.0 ppm). The chemical shifts (δ) are reported in ppm and coupling constants (*J*) in Hz.

5.5.2 Synthetic Procedure

General Procedure for Esters Deprotection

Compound was dissolved in THF/MeOH/H_20 water mixture (4/2/1). 50eq. of $LiOH{\cdot}H_2O$ was added. Allowed the reaction flask stirred for 2-3 days. After completion of reaction quench with amberlite IR120 acidic resin (If the compound is sulfated quench with Dowex 50WX8 H^+ resin) filtered reaction mixture and evaporate under reduced pressure, purified using silica column chromatography using DCM and MeOH as eluent to deprotected compounds.

General Procedure for *O*-Sulfation

Compound was dissolved in dry, DMF (6 mL). $SO_3.Et_3N$ (OH 5 eq per OH group) was added. Allowed the reaction flask stirred for 3 days at 60°C. After completion of reaction cool to room temperature add the aqueous solution of NaHCO3 (10 eq per OH group) and kept it for another 16 h. Filtered the reaction mixture using what's man filter and wash with DCM/MeOH (1/1, 10 mL), solvents were evaporated under reduced pressure and the resulting residue was purified by using C-18 bond elute column eluting with increasing acetonitrile concentration in water, and pass-through sodium (Na+) resin column using water as eluent. The product fraction was lyophilized to afford sulfated compounds as a white powder**.**

General Procedure for Hydrogenolysis

Compound was dissolved in dry methanol, 20% Pd(OH)2 on carbon (0.025 g per one benzyl group) and purged with a hydrogen gas. The reaction mixture was stirred at room temperature for 2-3 days. The mixture was filtered through celite, and the filtrate was evaporated under reduced pressure. The residue was purified through bond elute C-18 column eluted with water. Sulfated compound pass through sodium (Na+) resin. The product fraction was lyophilized to afford sulfated compounds as a white powder**.**

5.5.3 Synthesis of Iduronic Acid Acceptor and Donor

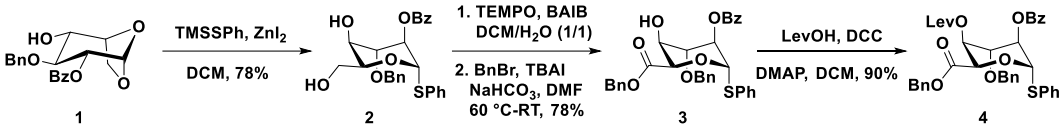

Scheme S5. Synthesis of Monosaccharides Building Block.

Thiophenyl (2-O-benzoyl-3-O-benzyl)-α-L-idopyranoside

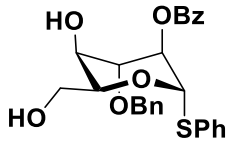

Compound **1** (9.9 g, 27.81 mmol), ZnI_2 (18.64 g, 58.39 mmol) and trimethyl(phenylthio)-silane (16.33 mL, 86.21 mmol) were dissolved in dry DCM (140 mL) under the nitrogen atmosphere and stirred at room temperature for 16 h. The reaction mixture was filtered through celite and diluted with 4N HCl, Dioxane, and water [1/1/1 (v/v/v), 60mL] mixture and stirred for 20 min. The organic layer was separated, washed with saturated $NaHCO_3$ and brine solution, dried over Na_2SO_4 and concentrated under reduced pressure. The residue was purified by flash column chromatography (EtOAc/Hexane = 1/1) to afford **2 (9.8 g, 78%)** as syrup. ^{1}H NMR (400 MHz, Chloroform-*d*) δ 8.01 (dd, *J* = 8.3, 1.2 Hz, 3H), 7.61 – 7.55 (m, 3H), 7.47 – 7.26 (m, 10H), 5.64 (s, 1H), 5.54 (dt, *J* = 2.6, 1.3 Hz, 1H), 4.92 (d, *J* = 11.8 Hz, 1H), 4.80 (t, *J* = 5.2 Hz, 1H), 4.67 (d, *J* = 11.8 Hz, 1H), 3.99 (dd, *J* = 11.9, 6.2 Hz, 1H), 3.91 – 3.85 (m, 3H), 2.90 (d, *J* = 9.8 Hz, 1H), 2.15 (bs, 1H). ^{13}C NMR (101 MHz, Chloroform-*d*) δ 165.13, 137.33, 135.77, 133.86, 132.11, 129.86, 129.24, 128.81, 128.69, 128.19, 127.94, 127.85, 86.88, 74.11, 72.52, 70.00, 68.53, 68.33, 63.51. HRMS m/z calculated for $C_{26}H_{26}O_6SNa$:489.1348; found: 489.1342.

Benzyl (1-thiophenyl-2-O-benzoyl-3-O-benzyl)-α-L-idopyranoside uronate 3

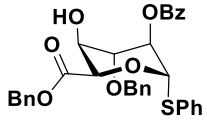

Compound **2** (9.5 g, 20.38 mmol) and [Bis(acetoxy)iodo]benzene (BAIB, 16.41 g, 50.96 mmol) were dissolved in mixture of water and DCM [1/1 (v/v), 180mL]. After 15 mins, 2,2,6,6-tetramethyl-1-piperidinyloxyl free radical (TEMPO, 0.64 g, 4.07 mmol) was added at room temperature and stirred at RT for 6 h. The organic layer was washed with saturated $NH_4Cl_{(aq)}$, dried over Na_2SO_4, filtered, and concentrated under reduced pressure. The dried crude compound (9.7 g, 20.2 mmol) was dissolved in dry DMF (55 mL), benzyl bromide (4.79 mL, 40.41 mmol), tetrabutylammonium iodide (TBAI, 3.73 g, 10.10 mmol), $NaHCO_3$ (2.54 g, 30.31 mmol) were added. The reaction mixture was heated at 60°C for 4 h. Then organic layer was washed with brine solution (3x20mL), dried over Na_2SO_4, filtered, and concentrated under reduced pressure. The residue was purified by flash column chromatography (EtOAc/Hexane = 1/4) to afford **3 (9.3 g, 80%)** as syrup. ^{1}H NMR (400 MHz, Chloroform-*d*) δ 7.98 (dd, *J* = 8.3, 1.2 Hz, 2H), 7.61 – 7.53 (m, 3H), 7.46 – 7.42 (m, 4H), 7.40 – 7.26 (m, 11H), 5.75 (s, 1H), 5.51 (dt, *J* = 2.6, 1.2 Hz, 1H), 5.46 (d, *J* = 1.7 Hz, 1H), 5.36 (d, *J* = 12.3 Hz, 1H), 5.23 (d, *J* = 12.3 Hz, 1H), 4.92 (d, *J* = 11.8 Hz, 1H), 4.69 (d, *J* = 11.8 Hz, 1H), 4.21 – 4.17 (m, 1H), 3.95 (td, *J* = 2.9, 1.2 Hz, 1H), 2.87 (d, *J* = 11.7 Hz, 1H).^{13}C NMR (101 MHz, Chloroform-*d*) δ 169.04, 164.95, 136.95, 135.46, 135.31, 133.81, 131.52, 129.78, 129.10, 128.86, 128.67, 128.63, 128.59, 128.44, 128.26, 128.15, 127.91, 127.70, 86.82, 73.70, 72.56, 69.66, 69.00, 68.25, 67.10.HRMS m/z calculated for $C_{33}H_{30}O_7SNa$:593.1610; found: 593.1604.

Benzyl (1-thiophenyl-2-O-benzoyl-3-O-benzyl-4-O-levulinoyl)-α-L-idopyranoside urinate 4

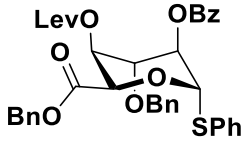

Compound **3** (8.5 g, 14.91 mmol) was dissolved in dry DCM (80 mL), levulinic acid (1.66 mL, 17.89 mmol), *N*,*N*-dicycohexylcarbodiimide (5.37 g, 26.09 mmol) and catalytic amount of 4- dimethylaminopyridine (0.91 g, 0.45 mmol) were added. The reaction mixture was stirred at room temperature for 4 h. The reaction mixture was filtered through celite and washed with saturated $NaHCO_3$ and brine solution respectively. The organic layer was dried over Na_2SO_4, filtered, and concentrated under reduced pressure.

The residue was purified by flash column chromatography (EtOAc/Hexane = 1/3) to afford **4 (8.9 g, 90%)** as syrup. ^{1}H NMR (400 MHz, Chloroform-*d*) δ 8.05 (dd, *J* = 8.4, 1.3 Hz, 2H), 7.58 – 7.52 (m, 3H), 7.47 – 7.43 (m, 3H), 7.41 – 7.34 (m, 8H), 7.33 – 7.22 (m, 5H), 5.78 (s, 1H), 5.50 (d, *J* = 2.0 Hz, 1H), 5.41 (dt, *J* = 2.4, 1.1 Hz, 2H), 5.35 – 5.32 (m, 2H), 5.15 (d, *J* = 12.0 Hz, 1H), 4.91 (d, *J* = 11.7 Hz, 1H), 4.78 (d, *J* = 11.7 Hz, 1H), 3.96 (td, *J* = 2.8, 1.1 Hz, 2H), 2.47 (t, *J* = 6.4 Hz, 2H), 2.33 – 2.25 (m, 1H), 2.23 – 2.155 (m, 1H),), 2.05 (s, 3H). ^{13}C NMR (101 MHz, Chloroform-*d*) δ 205.90, 171.63, 168.12, 165.30, 137.09, 135.59, 135.37, 133.72, 131.48, 130.01, 129.39, 129.18, 129.01, 128.71, 128.63, 128.53, 128.14, 127.81, 127.69, 86.45, 73.03, 71.94, 68.89, 67.95, 67.37, 66.99, 37.78, 29.73, 27.85. HRMS m/z calculated for $C_{38}H_{36}O_9SNa$:691.1978; found: 691.1972.

5.5.4 Synthesis of Cholestanol Conjugated Iduronic Acid Disaccharide (IAC-2):

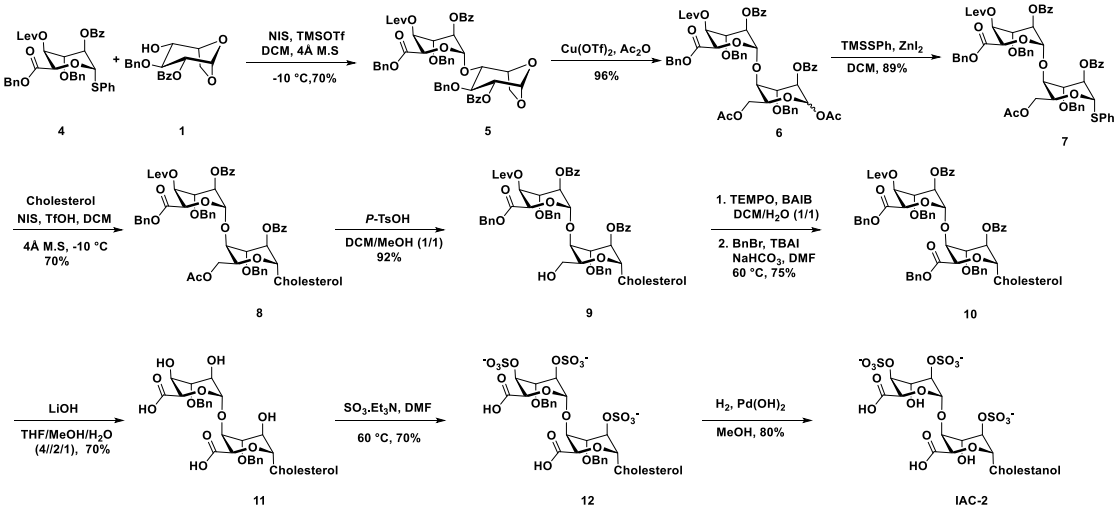

Scheme S6. Synthesis of Iduronic Acid Sulfated Disaccharide.

Benzyl (2-O-benzoyl-3-O-benzyl-4-O-levulinoyl)-α-L-idopyranosyluronate-α(1→4) (2-O-benzoyl-3-O-benzyl-1,6-anhydro)-β-L-idopyranose 5

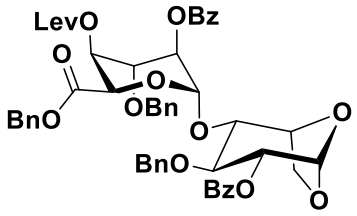

Compound **4** (6.2 g, 9.28 mmol), Compound **1** (3.63 g, 10.21 mmol) and freshly dried 4 Å molecular sieves were dissolved in dry DCM (70 mL) and stirring at RT for 1 h. Then the reaction mixture was cooled to -10 °C and *N*-Iodosuccinimide (3.13 g, 13.92 mmol), TMSOTf (0.35 mL, 1.85 mmol) were added and monitored the reaction by using TLC. After the completion of reaction, quenched with triethylamine and diluted with DCM. The molecular sieves were filtered using celite and organic layer was washed with $Na_2S_2O_3$, followed by $NaHCO_3$, brine solution and dried over Na_2SO_4, then filtered and concentrated under reduced pressure. The residue was purified by column chromatography (EtOAc/Hexane = 1/4) to afford **5 (5.9 g, 70%)** as syrup. ^{1}H NMR (400 MHz, Chloroform-*d*) δ 8.05 – 7.98 (m, 4H), 7.60 – 7.55 (m, 2H), 7.45 – 7.41 (m, 6H), 7.38 – 7.26 (m, 8H), 7.04 – 6.98 (m, 5H), 5.53 (d, *J* = 1.8 Hz, 1H), 5.31 (s, 1H), 5.22 (d, *J* = 11.9 Hz, 2H), 5.12 (dt, *J* = 2.5, 1.1 Hz, 1H), 5.10 (d, *J* = 2.3 Hz, 1H), 5.04 (dd, *J* = 8.3, 1.8 Hz, 1H), 4.83 – 4.76 (m, 3H), 4.64 (t, *J* = 4.5 Hz, 1H), 4.52 (d, *J* = 10.9 Hz, 1H), 4.44 (d, *J* = 10.9 Hz, 1H), 4.25 (dd, *J* = 8.5, 4.0 Hz, 1H), 4.20 (d, *J* = 7.8 Hz, 1H), 3.94 – 3.93 (m, 1H), 3.89 (t, *J* = 8.4 Hz, 1H), 3.78 (dd, *J* = 7.4, 5.4 Hz, 1H), 2.52 – 2.39 (m, 2H), 2.35 – 2.27 (m, 1H), 2.21 – 2.09 (m, 1H), 2.05 (s, 3H). ^{13}C NMR (101 MHz, Chloroform-*d*) δ 205.87, 171.64, 167.88, 165.72, 165.45, 137.66, 137.28, 135.39, 133.83, 133.42, 129.90, 129.48, 129.16, 128.80, 128.59, 128.50, 128.43, 128.25, 128.20, 127.89, 127.52, 99.45, 95.35, 78.14, 75.08, 74.09, 72.96, 72.71, 71.92, 67.92, 67.10, 66.98, 66.15, 65.59, 37.68, 29.69, 27.77. HRMS m/z calculated for $C_{52}H_{50}O_{15}Na$:937.3047; found: 937.3042.

Benzyl (2-O-benzoyl-3-O-benzyl-4-O-levulinoyl)-α-L-idopyranosyl uronate-α(1→4) (1,6-O-diacetyl-2-O-benzoyl-3-O-benzyl)-α/β-L-idopyranoside 6

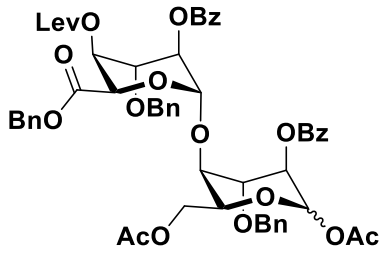

Compound **5** (5.6 g, 6.12 mmol) and copper trifluromethanesulfonate (0.02 g, 0.61 mmol) were dissolved in acetic anhydride (56 mL) at 0 °C. The temperature of the reaction mixture was slowly increased to RT and stirred for another 16 h. Then, EtOAc (50 mL) was added and organic layer was washed with $NaHCO_3$ and brine

solution, dried over Na_2SO_4 and concentrated under reduced pressure. The residue was purified by flash column chromatography (EtOAc/Hexane = 1/4) to afford anomeric mixture **6** (**5.9 g, 96%, α:β = 1:1)** as syrup. ^{1}H NMR (400 MHz, Chloroform-*d*) δ 7.97 (ddd, *J* = 9.7, 7.7, 1.3 Hz, 6H), 7.86 (dd, *J* = 8.2, 1.1 Hz, 2H), 7.55 – 7.50 (m, 2H), 7.45 – 7.43 (m, 1H), 7.41 – 7.36 (m, 7H), 7.32 – 7.24 (m, 18H), 7.23 – 7.14 (m, 16H), 6.16 – 6.15 (m, 2H), 5.29 (dd, *J* = 4.5, 2.2 Hz, 1H), 5.26 – 5.19 (m, 3H), 5.16 – 5.11 (m, 3H), 5.07 (t, *J* = 2.9 Hz, 1H), 4.98 (t, *J* = 3.3 Hz, 1H), 4.92 (t, *J* = 3.2 Hz, 1H), 4.87 (d, *J* = 3.1 Hz, 1H), 4.84 – 4.78 (m, 3H), 4.76 – 4.71 (m, 2H), 4.69 (d, *J* = 2.0 Hz, 1H), 4.64 – 4.56 (m, 5H), 4.48 (td, *J* = 6.7, 2.2 Hz, 1H), 4.40 – 4.28 (m, 5H), 4.19 (t, *J* = 4.4 Hz, 1H), 4.06 (t, *J* = 2.7 Hz, 1H), 3.91 (q, *J* = 4.3, 3.3 Hz, 2H), 3.82 (t, *J* = 3.2 Hz, 1H), 3.79 (t, *J* = 3.4 Hz, 1H), 2.45 – 2.38 (m, 4H), 2.35 – 2.21 (m, 2H), 2.13 – 2.07 (m, 2H), 2.05 (s, 3H), 2.01 (s, 6H), 2.00 (s, 6H). ^{13}C NMR (101 MHz, CHLOROFORM-*D*) δ 205.82, 205.78, 171.44, 171.40, 170.67, 170.60, 169.08, 168.95, 167.96, 167.85, 165.91, 165.49, 165.18, 165.16, 137.82, 137.39, 137.19, 137.15, 135.19, 135.16, 133.64, 133.52, 133.41, 130.09, 129.89, 129.30, 129.26, 128.86, 128.80, 128.64, 128.61, 128.56, 128.53, 128.48, 128.42, 128.40, 128.17, 128.12, 127.99, 127.95, 127.91, 127.80, 127.63, 101.16, 100.12, 91.63, 90.63, 75.74, 75.31, 74.94, 74.21, 73.75, 73.62, 73.24, 72.78, 72.70, 68.41, 68.32, 67.81, 67.75, 67.32, 67.21, 67.18, 66.93, 66.78, 62.72, 62.15, 37.63, 29.71, 27.68, 21.08, 21.02, 20.88, 20.87.HRMS m/z calculated for $C_{56}H_{56}O_{18}Na$:1039.3364; found: 1039.3359.

Benzyl (2-O-benzoyl-3-O-benzyl-4-O-levulinoyl)-α-L-idopyranosyluronate-α(1→4) 1-thiophenyl-(6-O-acetyl-2-O-benzoyl-3-O-benzyl)-α-L-idopyranoside 7

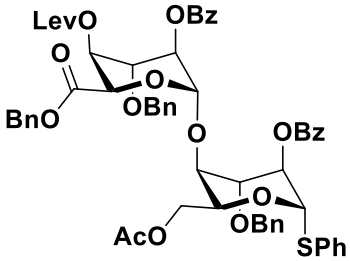

Compound **6** (5.7 g, 5.61 mmol), ZnI_2 (3.76 g, 11.78 mmol) and trimethyl(phenylthio)-silane (3.29 mL, 17.39mmol) were dissolved in dry DCM (80 mL) under the nitrogen atmosphere and stirred at room temperature for 16 h. The reaction mixture was filtered through celite and diluted with 4N HCl, Dioxane, and water [1/1/1 (v/v/v), 40mL] mixture and stirred for 20 min. The organic layer was separated, washed with saturated $NaHCO_3$ and brine solution, dried over Na_2SO_4 and concentrated under reduced pressure. The residue was purified by flash column chromatography (EtOAc/Hexane = 1/1) to afford **7 (5.3 g, 89%)** as solid. ^{1}H NMR (400 MHz, Chloroform-*d*) δ 8.03 (d, *J* = 7.4 Hz, 2H), 7.96 (d, *J* = 7.3 Hz, 2H), 7.59 – 7.56 (m, 3H), 7.45 – 7.41 (m, 5H), 7.36 – 7.30 (m, 9H), 7.29 –

7.21 (m, 9H), 5.55 (s, 1H), 5.47 (s, 1H), 5.28 (d, *J* = 3.3 Hz, 1H), 5.18 (d, *J* = 12.0 Hz, 1H), 5.15 (t, *J* = 3.4 Hz, 1H), 4.99 (t, *J* = 3.7 Hz, 1H), 4.95 (td, *J* = 6.6, 1.9 Hz, 1H), 4.89 (d, *J* = 12.0 Hz, 1H), 4.86 – 4.82 (m, 2H), 4.75 (d, *J* = 11.5 Hz, 1H), 4.65 (d, *J* = 5.2 Hz, 1H), 4.62 (d, *J* = 5.2 Hz, 1H), 4.42 – 4.34 (m, 2H), 4.13 (t, *J* = 2.4 Hz, 1H), 3.92 (s, 1H), 3.86 (t, *J* = 3.7 Hz, 1H), 2.53 – 2.39 (m, 2H), 2.36 – 2.28 (m, 1H), 2.23 – 2.21 (m, 1H), 2.07 (s, 3H), 2.02 (s, 3H). ^{13}C NMR (101 MHz, Chloroform-*d*) δ 205.84, 171.43, 170.61, 168.01, 165.74, 165.21, 137.61, 137.23, 135.88, 135.20, 133.64, 133.43, 131.86, 130.09, 129.94, 129.34, 129.28, 129.00, 128.85, 128.69, 128.59, 128.48, 128.18, 128.04, 127.89, 127.59, 101.17, 86.08, 76.35, 74.15, 73.74, 73.09, 72.81, 69.20, 68.65, 67.99, 67.23, 65.93, 62.72, 37.67, 29.76, 27.72, 20.91. HRMS m/z calculated for $C_{60}H_{58}O_{16}SNa$:1089.3343; found:1089.3338.

Cholestanyl-O-((benzyl (2-O-benzoyl-3-O-benzyl-4-O-levulinoyl))-α-L-idopyranosyluronate-α(1→4) (6-O-acetyl-2-O-benzoyl-3-O-benzyl))-α-L-idopyranoside 8

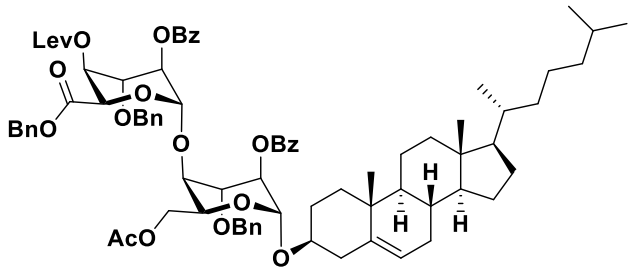

Compound **7** (5.1 g, 4.78 mmol), Cholesterol (2.21 g, 5.74 mmol) and freshly dried 4 Å molecular sieves were dissolved in dry DCM (50 mL) and stirred at RT for 1 h. Then *N*-iodosuccinimide (1.61 g, 7.17 mmol), TfOH (0.085 mL, 0.956 mmol) were added at -10°C and stirred for 30 min. After the completion of reaction, the reaction mixture was quenched with triethylamine and filtered through celite. The organic layer was washed with $Na_2S_2O_3$ followed by $NaHCO_3$, brine solution and dried over Na_2SO_4, then filtered and concentrated under reduced pressure. The residue was purified by column chromatography (EtOAc/Hexane = 1/4) to afford **8 (3.7 g, 70%)** as syrup. ^{1}H NMR (400 MHz, Chloroform-*d*) δ 8.06 – 8.04 (m, 2H), 7.96 (dd, *J* = 8.4, 1.4 Hz, 2H), 7.61 – 7.56 (m, 1H), 7.47 – 7.42 (m, 5H), 7.36 – 7.22 (m, 15H), 5.36 (dt, *J* = 5.8, 1.8 Hz, 1H), 5.27 (d, *J* = 2.5 Hz, 1H), 5.24 (t, *J* = 2.6 Hz, 1H), 5.20 – 5.17 (m, 2H), 5.09 (d, *J* = 2.0 Hz, 1H), 5.03 (t, *J* = 3.3 Hz, 1H), 4.93 (d, *J* = 2.8 Hz, 1H), 4.83 (d, *J* = 11.8 Hz, 2H), 4.79 (d, *J* = 11.5 Hz, 1H), 4.69 (d, *J* = 11.4 Hz, 1H), 4.58 (d, *J* = 11.6 Hz, 1H), 4.57 – 4.53 (m, 1H), 4.43 (dd, *J* = 11.2, 7.2 Hz, 1H), 4.32 (dd, *J* = 11.2, 6.0 Hz, 1H), 4.03 (t, *J* = 3.3 Hz, 1H), 3.93 (t, *J* = 3.2 Hz, 1H), 3.90 (t, *J* = 3.2 Hz, 1H), 3.56 (tt, *J* = 11.2, 4.6 Hz, 1H), 2.53 – 2.44 (m, 2H), 2.42 – 2.23 (m, 3H), 2.16 (dt, *J* = 17.2, 6.4 Hz,

1H), 2.07 (s, 3H), 2.04 (s, 3H), 2.00 – 1.82 (m, 3H), 1.73 – 1.66 (m, 2H), 1.64 – 1.45 (m, 6H), 1.44 – 1.24 (m, 6H), 1.22 – 1.08 (m, 7H), 1.04 (s, 4H), 0.94 (d, *J* = 6.5 Hz, 4H), 0.89 (dd, *J* = 6.6, 1.7 Hz, 6H), 0.70 (s, 3H). ^{13}C NMR (101 MHz, $CDCl_3$) δ 205.83, 171.50, 170.65, 167.92, 165.77, 165.23, 140.62, 138.23, 137.28, 135.27, 133.63, 133.30, 130.03, 129.93, 129.42, 129.39, 128.80, 128.62, 128.56, 128.51, 128.39, 128.26, 128.06, 127.76, 127.58, 122.00, 100.81, 96.64, 77.74, 76.51, 75.09, 73.28, 72.81, 72.48, 68.78, 68.44, 67.85, 67.25, 67.15, 65.21, 62.64, 56.87, 56.27, 50.33, 42.45, 39.90, 39.64, 38.58, 37.69, 37.55, 36.91, 36.31, 35.91, 32.07, 32.01, 29.74, 29.60, 28.36, 28.14, 27.76, 24.41, 23.94, 22.95, 22.69, 21.20, 20.95, 19.52, 18.85, 11.99. HRMS m/z calculated for $C_{81}H_{98}O_{17}Na$:1365.6702; found: 1365.6700.

Cholestanyl-O-)(benzyl (2-O-benzoyl-3-O-benzyl-4-O-levulinoyl))-α-L-idopyranosyluronate-α(1→4) (2-O-benzoyl-3-O-benzyl))-α-L-idopyranoside 9

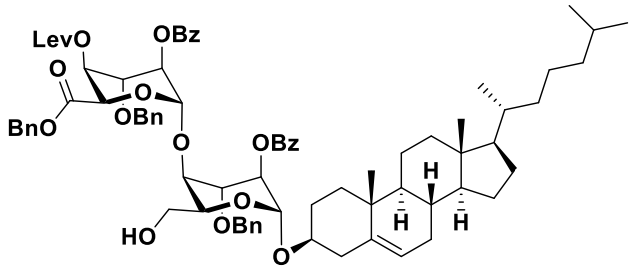

Compound **8** (3.5 g, 2.61 mmol) and *p*-toluenesulfonicacid (1.39 g, 8.08 mmol) was dissolved in equal ratio of mixture of dry DCM (25 mL) and methanol (25 mL) and stirred at RT for 3 days. The reaction mixture was quenched with triethylamine. Solvents were evaporated under reduced pressure, extracted with EtOAc and $NaHCO_3$ and water respectively. The combined organic layer washed with brine solution, dried over Na_2SO_4 and concentrated under reduced pressure. The residue was purified by column chromatography (EtOAc/Hexane = 1/3) to afford **9 (3.21 g, 92%)** as syrup. ^{1}H NMR (400 MHz, Chloroform-*d*) δ 8.03 – 8.01 (m, 2H), 7.97 – 7.94 (m, 2H), 7.59 – 7.55 (m, 1H), 7.45 – 7.40 (m, 5H), 7.33 – 7.18 (m, 15H), 5.33 (dt, *J* = 5.7, 1.9 Hz, 1H), 5.27 (d, *J* = 2.1 Hz, 1H), 5.23 (dd, *J* = 3.5, 2.2 Hz, 1H), 5.16 (d, *J* = 12.1 Hz, 1H), 5.13 (t, *J* = 2.1 Hz, 2H), 5.11 (d, *J* = 1.9 Hz, 1H), 5.03 (t, *J* = 3.1 Hz, 1H), 4.93 (d, *J* = 2.6 Hz, 1H), 4.83 – 4.77 (m, 2H), 4.76 – 4.68 (m, 2H), 4.59 (d, *J* = 11.4 Hz, 1H), 4.42 (td, *J* = 6.2, 2.6 Hz, 1H), 4.03 (t, *J* = 3.7 Hz, 1H), 3.99 (t, *J* = 3.3 Hz, 1H), 3.96 – 3.84 (m, 3H), 3.55 (tt, *J* = 11.1, 4.6 Hz, 1H), 2.55 – 2.42 (m, 2H), 2.40 – 2.33 (m, 2H), 2.32 – 2.25 (m, 2H), 2.20 – 2.12 (m, 1H), 2.07 (s, 3H), 2.04 – 1.92 (m, 3H), 1.89 – 1.78 (m, 2H), 1.72 – 1.64 (m, 2H), 1.56 – 1.43 (m, 6H), 1.37 – 1.34 (m, 3H), 1.27 (s, 3H), 1.17 – 1.08 (m, 6H), 1.01 (s, 3H), 0.92 (d, *J* = 6.5 Hz, 3H), 0.87 (dd, *J* = 6.6, 1.8 Hz, 6H),

0.68 (s, 3H). ^{13}C NMR (101 MHz, CHLOROFORM-*D*) δ 205.99, 171.58, 167.87, 165.75, 165.66, 140.67, 138.24, 137.10, 135.27, 133.80, 133.29, 130.00, 129.96, 129.44, 129.20, 128.82, 128.62, 128.60, 128.57, 128.50, 128.38, 128.34, 128.23, 128.20, 127.69, 127.51, 121.97, 100.65, 96.69, 75.41, 72.98, 72.83, 72.42, 69.49, 68.09, 67.81, 67.42, 67.14, 66.89, 61.82, 56.85, 56.23, 50.24, 42.43, 39.88, 39.63, 38.54, 37.66, 37.43, 36.89, 36.30, 35.90, 32.06, 31.98, 29.83, 29.77, 29.63, 28.36, 28.14, 27.75, 24.41, 23.93, 22.96, 22.70, 21.16, 19.51, 18.84, 11.97. HRMS m/z calculated for $C_{79}H_{96}O_{16}Na$:1323.6596; found: 1323.6591.

Cholestanyl-O-((benzyl (2-O-benzoyl-3-O-benzyl-4-O-levulinoyl)-α-L-idopyranosyluronate-α(1→4) (benzyl (2-O-benzoyl-3-O-benzyl)))-α-L-idopyranoside uronate 10

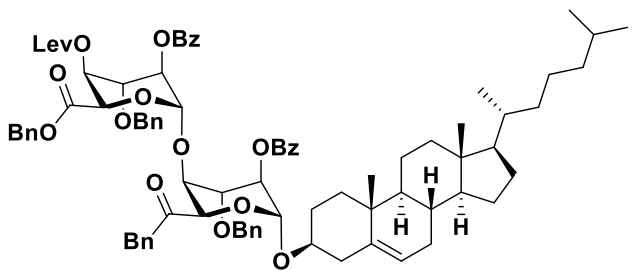

Compound **9**(3.02 g, 2.32 mmol) and [Bis(acetoxy)iodo]benzene (BAIB, 1.87 g, 5.81 mmol) were dissolved in mixture of water and DCM [1/1 (v/v), 60mL]. After 15 mins, 2,2,6,6-tetramethyl-1-piperidinyloxyl free radical (TEMPO, 0.07 g, 0.46 mmol) was added at room temperature and stirred at RT for 6 h. The organic layer was washed with saturated $NH_4Cl_{(aq),}$ dried over Na_2SO_4, filtered, and concentrated under reduced pressure. The dried crude compound (3.05 g, 2.32 mmol) was dissolved in dry DMF (15 mL), benzyl bromide (0.69 mL, 5.81 mmol), tetrabutylammonium iodide (TBAI, 1.71 g, 4.64 mmol), $NaHCO_3$(0.29 g, 3.48 mmol) were added. The reaction mixture was heated at 60°C for 4 h. Then organic layer was washed with brine solution (3x10mL), dried over Na_2SO_4, filtered, and concentrated under reduced pressure. The residue was purified by flash column chromatography (EtOAc/Hexane = 1/4) to afford **10 (2.5 g, 75%)** as syrup. ^{1}H NMR (400 MHz, Chloroform-*d*) δ 8.02 – 7.99 (m, 2H), 7.92 – 7.90 (m, 2H), 7.59 – 7.54 (m, 1H), 7.44 – 7.39 (m, 5H), 7.33 – 7.27 (m, 8H), 7.24 – 7.16 (m, 12H), 5.34 (d, *J* = 3.1 Hz, 1H), 5.29 (dt, *J* = 6.5, 1.9 Hz, 1H), 5.25 – 5.17 (m, 4H), 5.13 (d, *J* = 12.1 Hz, 1H), 5.11 – 5.08 (m, 1H), 4.96 (dd, *J* = 7.4, 3.3 Hz, 2H), 4.92 (d, *J* = 2.3 Hz, 1H), 4.79 – 4.68 (m, 3H), 4.61 (d, *J* = 11.3 Hz, 1H), 4.51 (d, *J* = 11.3 Hz, 1H), 4.26 (t, *J* = 4.0 Hz, 1H), 4.01 (t, *J* = 4.0 Hz, 1H), 3.83 – 3.81 (m, 1H), 3.63 – 3.55 (m, 1H), 2.39 – 2.32 (m, 3H), 2.25 – 2.16 (m, 2H), 2.09 (dt, *J* = 17.3, 6.7 Hz, 1H), 2.01 (s, 3H), 1.96

– 1.92 (m, 1H), 1.85 – 1.78 (m, 1H), 1.58 – 1.54 (m, 4H), 1.52 – 1.45 (m, 4H), 1.42 – 1.33 (m, 4H), 1.25 (d, *J* = 6.3 Hz, 2H), 1.17 – 1.10 (m, 4H), 1.08 – 0.99 (m, 4H), 0.97 (s, 3H), 0.92 (d, *J* = 6.5 Hz, 4H), 0.87 (dd, *J* = 6.6, 1.8 Hz, 6H), 0.67 (s, 3H). ^{13}C NMR (101 MHz, $CDCl_3$) δ 205.79, 171.45, 169.50, 167.72, 165.71, 164.93, 140.52, 137.98, 137.20, 135.28, 133.67, 133.34, 130.04, 130.03, 129.43, 129.30, 128.75, 128.65, 128.60, 128.52, 128.47, 128.43, 128.39, 128.26, 128.11, 127.86, 127.62, 122.06, 100.97, 97.38, 78.66, 75.79, 72.88, 72.49, 72.39, 69.42, 69.09, 68.38, 67.21, 67.14, 66.63, 66.59, 56.90, 56.29, 50.26, 42.47, 39.93, 39.67, 38.80, 37.72, 37.34, 36.84, 36.34, 35.93, 32.09, 32.02, 29.69, 29.58, 28.38, 28.16, 27.79, 24.44, 23.97, 22.97, 22.71, 21.20, 19.51, 18.87, 12.00. HRMS m/z calculated for $C_{86}H_{100}O_{17}Na$:1427.6858; found: 1427.6853.

Cholestanyl-O-((3-O-benzyl)-α-L-idopyranosyl uronic acide-α(1→4) (3-O-benzyl))-α-L-idopyranosideuronic acide 11

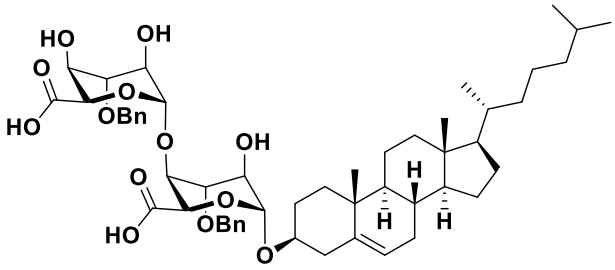

Compound **10**(0.11 g, 0.78 mmol) was dissolved in mixture of THF, MeOH and water [4/2/1 (v/v), 6 mL] and lithium hydroxide (0.16 g, 3.91 mmol) was added. After stirring for 2 days the mixture was neutralized with amberlite® IR 120 acid resin, filtered, and concentrated under reduced pressure. The residue was purified by flash column chromatography (MeOH/DCM = 1/9) to afford **11 (0.05 g, 70%)** as a solid. ^{1}H NMR (400 MHz, Methanol-d_4) δ 7.41 – 7.39 (m, 2H), 7.37 – 7.25 (m, 8H), 5.37 (dt, *J* = 5.8, 1.9 Hz, 1H), 5.09 – 5.05 (m, 2H), 4.82 (dd, *J* = 9.7, 2.3 Hz, 2H), 4.65 – 4.57 (m, 4H), 4.25 (t, *J* = 3.6 Hz, 1H), 4.04 (dd, *J* = 3.5, 1.7 Hz, 1H), 3.77 – 3.73 (m, 2H), 3.66 (td, *J* = 3.5, 1.2 Hz, 1H), 3.56 – 3.50 (m, 2H), 2.40 (ddd, *J* = 14.0, 5.1, 2.2 Hz, 1H), 2.29 – 2.21 (m, 1H), 2.07 – 1.83 (m, 5H), 1.65 – 1.45 (m, 7H), 1.44 – 1.34 (m, 4H), 1.32 – 1.25 (m, 2H), 1.23 – 1.08 (m, 7H), 1.03 (s, 4H), 0.95 (d, *J* = 6.5 Hz, 4H), 0.88 (dd, *J* = 6.6, 1.5 Hz, 6H), 0.72 (s, 3H). ^{13}C NMR (101 MHz, MeOD) δ 173.08, 141.73, 139.42, 138.87, 129.53, 129.50, 129.29, 129.01, 128.91, 128.65, 122.85, 103.68, 101.19, 79.58, 76.93, 76.56, 76.03, 73.25, 73.09, 69.58, 69.38, 69.15, 69.03, 67.08, 58.14, 57.58, 51.64, 43.51, 41.15, 40.71, 39.84, 38.54, 37.85, 37.42, 37.14, 33.23, 33.08, 30.74,

29.37, 29.15, 25.37, 25.00, 23.28, 23.03, 22.22, 19.93, 19.37, 12.46. HRMS m/z calculated for $C_{53}H_{74}O_{13}Na$:941.5027 found:941.5022.

Cholestanyl-O-((2,4-O-disulfonato-3-O-benzyl)-α-L-idopyranosyl uronic acide-α(1→4) (2-O-sulfonato-3-O-benzyl))-α-L-idopyranosideuronic acide 12

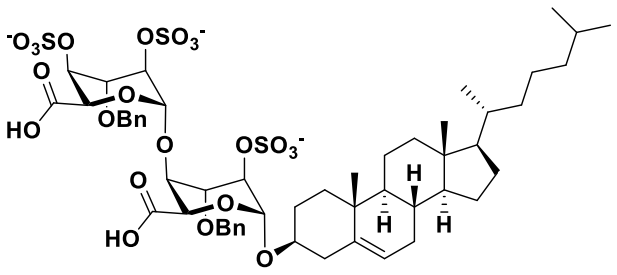

Compound **11** (0.04 g, 0.044 mmol) and $SO_3{\cdot}Et_3N$ (0.12 g, 0.65 mmol) was dissolved in dry, DMF (2 mL). Allowed the reaction flask stirred for 3 days at 60°C. After completion of reaction cool to room temperature add the aqueous solution of $NaHCO_3$ (0.11 g, 1.31 mmol) and kept it for another 16 h. Filtered the reaction mixture using what's man filter and wash with DCM/MeOH (1/1, 10 mL), solvents were evaporated under reduced pressure and the resulting residue was purified by bond elute C-18 column eluted with mixture of solvent (water and acetonitrile). The product fraction was lyophilized to afford sulfated compounds **12 (0.035 g, 70%)** as a white powder. ^{1}H NMR (400 MHz, Deuterium Oxide, temperature at 358K) δ 8.07 (d, *J* = 7.4 Hz, 2H), 7.97 (t, *J* = 7.4 Hz, 4H), 7.92 – 7.82 (m, 3H), 7.75 (t, *J* = 7.5 Hz, 1H), 5.90 (s, 1H), 5.80 (d, *J* = 31.2 Hz, 2H), 5.38 – 5.34 (m, 3H), 5.31 – 5.16 (m, 3H), 4.98 – 4.80 (m, 6H), 4.54 (s, 1H), 4.11 – 4.01 (m, 1H), 2.98 – 293 (m, 1H), 2.73 (q, *J* = 12.1, 10.4 Hz, 1H), 2.53 – 2.28 (m, 5H), 2.15 – 2.00 (m, 5H), 1.99 – 1.88 (m, 5H), 1.86 – 1.77 (m, 3H), 1.75 – 1.63 (m, 5H), 1.61 – 1.55 (m, 2H), 1.52 (s, 3H), 1.47 (d, *J* = 6.2 Hz, 2H), 1.43 – 1.40 (m, 7H), 1.22 (s, 3H). HRMS m/z calculated for $C_{53}H_{71}O_{22}S_3^{3-}$:1155.3616 found (m/z + 3H): 386.1280.

Cholesteryl-O-((2,4-O-disulfonato)-α-L-idopyranosyl uronic acide-α(1→4) (2-O-sulfonato))-α-L-idopyranosideuronic acide IAC-2

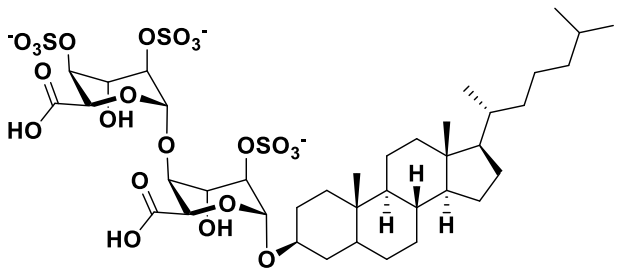

The compound **12** (0.03 g, 0.026 mmol) was dissolved in dry methanol (2 mL), 20% $Pd(OH)_2$ on carbon (0.011 g, 0.078 mmol) was added and purged with hydrogen gas, and the mixture was stirred at room temperature for 24 h. The residue was filtered and the filtrate was evaporated under reduced pressure and purified through a bond

elute C-18 column eluted with water. The product fraction was lyophilized to afford compound **IAC-2 (0.02 g, 80%).** ^{1}H NMR (400 MHz, Deuterium Oxide) δ 5.15 (dd, *J* = 35.1, 23.4 Hz, 2H), 4.88 (s, 1H), 4.47 (d, *J* = 17.9 Hz, 1H), 4.19 – 3.95 (m, 4H), 3.57 (t, *J* = 6.1 Hz, 1H), 3.00 (q, *J* = 7.0 Hz, 2H), 1.88 (dd, *J* = 11.3, 5.5 Hz, 1H), 1.77 – 1.53 (m, 5H), 1.49 – 1.38 (m, 3H), 1.32 – 1.15 (m, 11H), 1.09 – 0.90 (m, 9H), 0.84 – 0.73 (m, 14H), 0.58 (s, 3H). HRMS m/z calculated for $C_{39}H_{61}O_{22}S_3^{3-}$:977.2833 found (m/z + 3H): 326.7687

5.5.5 Synthesis of Cholestanol Conjugated Iduronic Acid Trisaccharide (IAC-3)

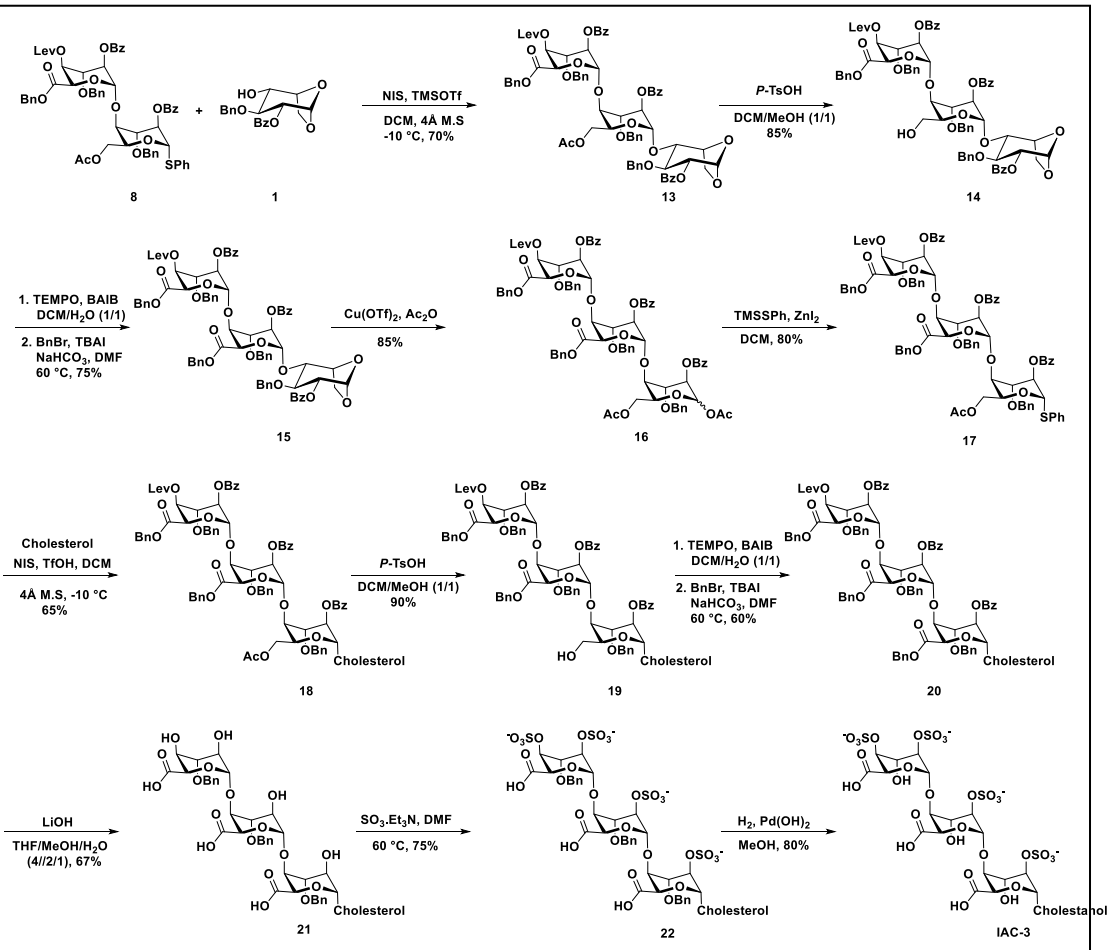

Scheme S7. Synthesis of Iduronic Acid Sulfated Trisaccharide.

Benzyl (2-O-benzoyl-3-O-benzyl-4-O-levulinoyl)-α-L-idopyranosyl uronate-α(1→4)-(6-O-acetyl-2-O-benzoyl-3-O-benzyl)-α-L-idopyranosyl-α(1→4)(2-O-benzoyl-3-O-benzyl-1,6-anhydro)-β-L-idopyranose13

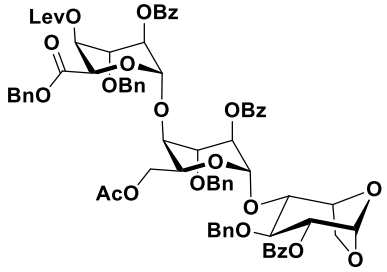

Glycosylation: The synthetic procedure for the preparation of compound **5** was followed to obtain compound **13 (70%)** from compound **8** and **1**as syrup. ^{1}H NMR (400 MHz, Chloroform-*d*) δ 8.07 (dd, *J* = 8.4, 1.4 Hz, 2H), 7.96 (ddd, *J* = 8.5, 3.3, 1.4 Hz, 4H), 7.59 (dtt, *J* = 8.3, 6.9, 1.3 Hz, 2H), 7.50 – 7.41 (m, 8H), 7.34 – 7.30 (m, 7H), 7.29 – 7.24 (m, 7H), 7.12 – 7.05 (m, 5H), 5.53 (d, *J* = 1.8 Hz, 1H), 5.29 (d, *J* = 2.7 Hz, 1H), 5.23 – 5.18 (m, 3H), 5.10 (dd, *J* = 4.9, 2.5 Hz, 2H), 5.03 (dd, *J* = 8.3, 1.8 Hz, 1H), 4.97 (d, *J* = 2.9 Hz, 1H), 4.89 (d, *J* = 12.0 Hz, 1H), 4.83 (d, *J* = 11.4 Hz, 1H), 4.75 – 4.72 (m, 2H), 4.69 – 4.63 (m, 3H), 4.59 (td, *J* = 7.2, 6.5, 2.6 Hz, 1H), 4.53 (d, *J* = 11.4 Hz, 1H), 4.35 – 4.26 (m, 2H), 4.21 (ddd, *J* = 8.4, 4.1, 1.1 Hz, 1H), 4.16 (d, *J* = 7.7 Hz, 1H), 4.06 (t, *J* = 3.8 Hz, 1H), 3.98 (t, *J* = 3.3 Hz, 1H), 3.93 – 3.91 (m, 1H), 3.89 (d, *J* = 8.3 Hz, 1H), 3.68 (ddd, *J* = 7.9, 5.1, 1.1 Hz, 1H), 2.56 – 2.42 (m, 2H), 2.39 – 2.32 (m, 1H), 2.23 – 2.16 (m, 1H), 2.08 (s, 3H), 1.99 (s, 3H). ^{13}C NMR (101 MHz, $CDCl_3$) δ 205.79, 171.47, 170.68, 167.90, 165.84, 165.73, 165.20, 138.13, 137.61, 137.15, 135.18, 133.66, 133.55, 133.31, 129.92, 129.89, 129.50, 129.27, 128.99, 128.75, 128.60, 128.56, 128.51, 128.49, 128.47, 128.41, 128.39, 128.20, 128.08, 127.92, 127.90, 127.39, 100.44, 99.39, 95.56, 77.80, 76.67, 75.64, 75.17, 75.00, 74.84, 73.36, 73.33, 72.86, 72.02, 68.89, 68.33, 67.93, 67.33, 67.17, 65.89, 65.49, 62.14, 37.63, 29.69, 27.71, 20.88. HRMS m/z calculated for $C_{74}H_{72}O_{22}Na$:1335.4413; found: 1335.4413.

Benzyl (2-O-benzoyl-3-O-benzyl-4-O-levulinoyl)-α-L-idopyranosyl uronate-α(1→4) benzyl (2-O-benzoyl-3-O-benzyl)-α-L-idopyranosyl-α(1→4)(2-O-benzoyl-3-O-benzyl-1,6-anhydro)-β-L-idopyranose 14

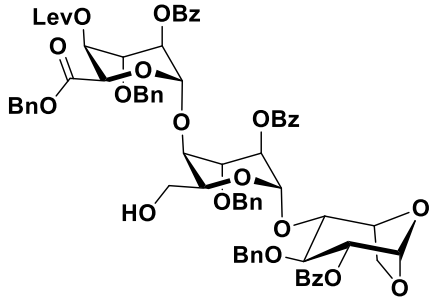

Selective Acetate Deprotection: The synthetic procedure for the preparation of compound **9** was followed to obtain compound **14 (85%)** from compound **13** as syrup. ^{1}H NMR (400 MHz, Chloroform-*d*) δ 8.05 (ddd, *J* = 8.5, 5.8, 1.4 Hz, 4H), 7.95 (d,*J* = 7.4 Hz, 2H), 7.62 – 7.57 (m, 2H), 7.48 – 7.40 (m, 9H), 7.37 – 7.29 (m, 7H), 7.28 – 7.23 (m, 6H), 7.19 – 7.16 i(m, 3H), 7.10 (dd, *J* = 6.7, 3.0 Hz, 2H), 5.56 (d, *J* = 1.7 Hz, 1H), 5.27 (d, *J* = 2.4 Hz, 1H), 5.23 (t, *J* = 2.3 Hz, 1H), 5.19 (d, *J* = 12.1 Hz, 1H), 5.16 (t, *J* = 2.6 Hz, 1H), 5.08 (td, *J* = 7.7, 7.2, 2.5 Hz, 3H), 4.94 (d, *J* = 2.7 Hz, 1H), 4.88 (d, *J* = 12.0 Hz, 1H), 4.79 (dd, *J* = 13.6, 11.3 Hz, 2H), 4.71 (d, *J* = 1.7 Hz, 1H), 4.68 (d, *J* = 1.3 Hz, 1H), 4.62 (t, *J* = 4.6 Hz, 1H), 4.58 (d, *J* = 1.9 Hz, 2H), 4.36 (td, *J* = 6.4, 2.2 Hz, 1H), 4.24 (t, *J* = 4.2 Hz, 1H), 4.22 (s, 1H), 4.07 (t, *J* = 3.3 Hz, 1H), 3.94 (t, *J* = 8.4 Hz, 1H), 3.90 (t, *J* = 3.1 Hz, 2H), 3.78 – 3.75 (m, 1H), 3.65 (dt, *J* = 11.3, 5.5 Hz, 1H), 3.53 (dt, *J* = 11.9, 6.5 Hz, 1H), 2.55 – 2.41 (m, 2H), 2.37 – 2.29 (m, 1H), 2.24 – 2.12 (m, 1H), 2.08 (s, 3H). ^{13}C NMR (101 MHz, $CDCl_3$) δ 205.85, 171.46, 167.91, 165.88, 165.79, 165.34, 137.95, 137.91, 137.14, 135.22, 133.70, 133.52, 133.44, 129.97, 129.93, 129.92, 129.52, 129.31, 129.01, 128.74, 128.61, 128.56, 128.53, 128.51, 128.49, 128.47, 128.44, 128.35, 128.29, 128.24, 128.16, 128.11, 127.94, 127.85, 100.97, 99.43, 96.06, 78.43, 77.01, 76.16, 75.32, 75.18, 74.14, 73.16, 73.01, 72.84, 72.19, 68.64, 68.39, 67.82, 67.16, 67.12, 65.67, 61.40, 37.66, 29.71, 27.74. HRMS m/z calculated for $C_{72}H_{71}O_{21}Na$:1293.4307; found: 1293.4298.

Benzyl (2-O-benzoyl-3-O-benzyl-4-O-levulinoyl)-α-L-idopyranosyl uronate-α(1→4) benzyl (2-O-benzoyl-3-O-benzyl)-α-L-idopyranosyl uronate-α(1→4)(2-O-benzoyl-3-O-benzyl-1,6-anhydro)-β-L-idopyranose 15

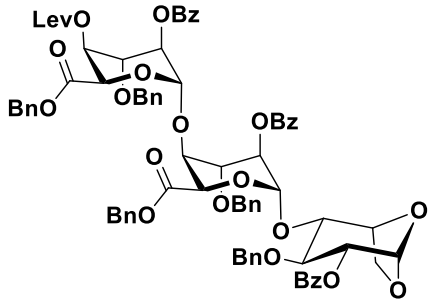

Oxidation and Esterification: The synthetic procedure for the preparation of compound **10** was followed to obtain compound **15 (75%)** from compound **14** as solid. ^{1}H NMR (400 MHz, Chloroform-*d*) δ 8.02 (ddd, *J* = 15.0, 8.4, 1.5 Hz, 4H), 7.92 (dd, *J* = 7.5, 2.3 Hz, 2H), 7.63 – 7.57 (m, 2H), 7.49 – 7.41 (m, 7H), 7.35 – 7.31 (m, 5H), 7.28 – 7.17 (m, 15H), 7.08 (s, 5H), 5.52 (d, *J* = 1.7 Hz, 1H), 5.43 (d, *J* = 3.5 Hz, 1H), 5.31 – 5.30 (m, 1H), 5.23 (t, *J* = 4.0 Hz, 1H), 5.20 – 5.14 (m, 3H), 5.11 – 5.02 (m, 4H), 4.98 (d, *J* = 4.0 Hz, 1H), 4.82 (dd, *J* = 12.2, 1.4 Hz, 1H), 4.76 (d, *J* = 11.1 Hz, 1H), 4.70 – 4.62 (m, 4H), 4.59 – 4.53 (m, 2H), 4.32 (t, *J* = 4.5 Hz, 1H), 4.27 (dd, *J* = 8.4, 4.1 Hz, 1H), 4.10 – 4.65 (m, 2H), 3.92 – 3.86 (m, 2H), 3.53 (dd, *J* = 7.8, 5.2 Hz, 1H), 2.41 (t, *J* = 6.7 Hz, 2H), 2.27 – 2.09 (m, 2H), 2.04 (s, 3H). ^{13}C NMR (101 MHz, CHLOROFORM-*D*) δ 205.78, 171.41, 168.99, 167.72, 165.79, 165.54, 164.79, 137.87, 137.46, 137.04, 135.17, 134.98, 133.67, 133.62, 133.37, 129.95, 129.93, 129.87, 129.48, 129.29, 128.76, 128.71, 128.61, 128.56, 128.50, 128.46, 128.38, 128.34, 128.21, 128.18, 128.12, 127.92, 127.85, 127.51, 100.24, 99.34, 96.46, 77.74, 76.62, 75.71, 75.65, 74.92, 73.73, 72.55, 72.26, 69.46, 69.09, 68.24, 67.28, 67.16, 66.46, 66.40, 65.35, 37.64, 29.64, 27.70. HRMS m/z calculated for $C_{79}H_{74}O_{22}Na$:1397.4569; found: 1397.4564.

Benzyl (2-O-benzoyl-3-O-benzyl-4-O-levulinoyl)-α-L-idopyranosyl uronate-α(1→4) benzyl (2-O-benzoyl-3-O-benzyl)-α-L-idopyranosyl uronate-α(1→4)(1,6-O-diacetyl-2-O-benzoyl-3-O-benzyl)-α/β-L-idopyranoside 16

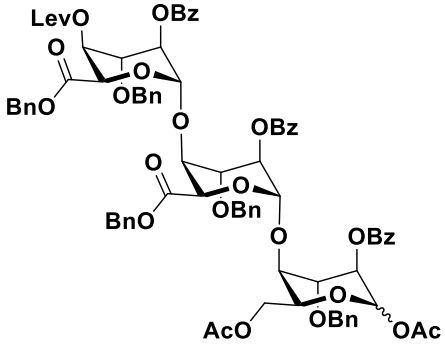

Acetolysis: The synthetic procedure for the preparation of compound **6** was followed to obtain compound **16 (85%, α:β = 1:1)** from compound **15** as solid. ^{1}H NMR (400 MHz, Chloroform-*d*) δ 8.05 – 8.03 (m, 2H), 7.98 – 7.93 (m, 10H), 7.56 (t, *J* = 7.4 Hz, 2H), 7.42 (tt, *J* = 16.4, 8.0 Hz, 13H), 7.34 – 7.27 (m, 23H), 7.26 – 711 (m, 29H), 6.17 (s, 1H), 6.15 (d, *J* = 1.8 Hz, 1H), 5.30 (t, *J* = –4.3 Hz, 3H), 5.25 – 5.16 (m, 4H), 5.13 – 5.01 (m, 12H), 4.94 (dd, *J* = 10.0, 2.2 Hz, 2H), 4.78 – 4.72 (m, 5H), 4.69 – 4.60 (m, 6H), 4.55 (d, *J* = 12.0 Hz, 1H), 4.46– 4.41 (m, 3H), 4.35 (t, *J* = 3.6 Hz, 1H), 4.22 (ddd, *J* = 23.8, 14.2, 6.0 Hz, 4H), 4.03 (dtd, *J* = 21.3, 11.4, 5.1 Hz, 3H), 3.92 (dq, *J* = 13.2, 4.6 Hz, 3H), 3.82 – 3.79 (m, 4H), 2.35 (q, *J* = 6.4, 5.9 Hz, 4H), 2.22 – 2.14 (m, 2H), 2.08 (s, 4H), 2.02 (s, 3H), 2.01 (s, 3H), 2.00 (s, 2H), 1.93 (s, 2H), 1.91 (s, 3H). ^{13}C NMR (101 MHz, Chloroform-*d*) δ 205.80, 205.75, 171.46, 170.45, 169.13, 169.03, 168.95, 167.55, 167.49, 166.81, 166.03, 165.60, 165.34, 165.30,164.88, 164.83, 138.15, 137.70, 137.48, 137.45, 137.19, 137.15, 135.21, 135.08, 135.02, 133.72, 133.51, 133.49, 133.37, 130.21, 130.16, 129.98, 128.71, 128.66, 128.60, 128.53, 128.48, 128.42, 128.38, 128.31, 128.28, 128.21, 128.15, 128.11, 127.97, 127.87, 127.78, 127.58, 101.31, 100.65, 100.58, 91.81, 90.68, 76.51 , 76.38 , 75.66 , 75.33 , 75.07 , 73.46 , 73.29 , 73.20 , 73.15 , 72.75 , 72.62 , 72.53 , 72.41 , 71.12 , 71.01, 70.29, 70.19, 68.1, 67.97, 67.35, 67.30, 67.22, 67.11, 67.03, 66.73, 66.58, 66.50, 66.43, 66.38, 63.17, 62.66, 37.67, 29.83, 29.68, 27.71, 21.14, 21.06, 20.82. HRMS m/z calculated for $C_{83}H_{80}O_{25}Na$:1499.4886; found: 1499.4883.

Benzyl (2-O-benzoyl-3-O-benzyl-4-O-levulinoyl)-α-L-idopyranosyl uronate-α(1→4) benzyl (2-O-benzoyl-3-O-benzyl)-α-L-idopyranosyl uronate-α(1→4)1-thiophenyl (6-O-acetyl-2-O-benzoyl-3-O-benzyl)-α-L-idopyranoside 17

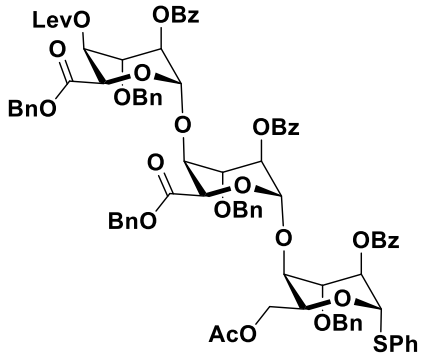

Thioglycosylation: The preparation of the thioglycosylated compound **17 (80%)** was carried out from compound **16** according to the procedure used for synthesizing compound **7.** ^{1}H NMR (400 MHz, Chloroform-*d*) δ 8.04 – 7.99 (m, 6H), 7.61 – 7.56 (m, 3H), 7.52 – 7.41 (m, 8H), 7.39 – 7.33 (m, 5H), 7.32 – 7.24 (m, 13H), 7.21 – 7.13 (m, 10H), 5.56 (s, 1H), 5.45 – 5.44 (m, 1H), 5.36 (d, *J* = 5.7 Hz, 1H), 5.29 (d, *J* = 12.2 Hz, 1H), 5.17 (dd, *J* = 5.8, 3.7 Hz, 1H), 5.10 (ddd, *J* = 16.2, 12.9, 5.0 Hz, 5H), 5.00 (d, *J* = 2.1 Hz, 1H), 4.90 – 4.84 (m, 2H), 4.80 – 4.73 (m, 3H), 4.70 – 4.69 (m, 1H), 4.62(dd, *J* = 19.0, 11.6 Hz, 2H), 4.46 (d, *J* = 11.2 Hz, 1H), 4.32 (d, *J* = 3.1 Hz, 1H), 4.23 (dd, *J* = 11.4, 8.1 Hz, 1H), 4.04 (t, *J* = 4.9 Hz, 1H), 3.99 (dd, *J* = 11.5, 4.5 Hz, 1H), 3.94 (dd, *J* = 5.0, 3.7 Hz, 1H), 3.84 (dd, *J* = 6.8, 3.8 Hz, 2H), 2.38 (t, *J* = 6.4 Hz, 2H), 2.22 (dt, *J* = 17.3, 7.0 Hz, 1H), 2.11 – 2.05 (m, 1H), 2.03 (s, 3H), 1.92 (s, 3H). ^{13}C NMR (101 MHz, Chloroform-*d*) δ 205.77, 171.49, 170.28, 169.13, 167.48, 165.78, 165.27, 164.89, 137.93, 137.49, 137.13, 136.28, 135.24, 135.10, 133.74, 133.48, 133.38, 131.81, 130.13, 130.00, 129.98, 129.52, 129.27, 129.07, 128.91, 128.71, 128.68, 128.59, 128.55, 128.50, 128.46, 128.29, 128.17, 128.14, 127.81, 127.72, 127.44, 101.02, 100.38, 86.01, 76.49, 76.12, 73.57, 73.33, 72.82, 72.76, 72.47, 71.31, 71.27, 69.00, 67.97, 67.33, 67.03, 66.44, 66.27, 65.81, 63.29, 37.67, 29.68, 27.69, 20.81. HRMS m/z calculated for $C_{87}H_{82}O_{23}SNa$:1549.4865; found: 1549.4862.

Cholestanyl-O-((benzyl (2-O-benzoyl-3-O-benzyl-4-O-levulinoyl))-α-L-idopyranosyl uronate-α(1→4) benzyl (2-O-benzoyl-3-O-benzyl)-α-L-idopyranosyl uronate-α(1→4) (6-O-acetyl-2-O-benzoyl-3-O-benzyl))-α-L-idopyranoside 18

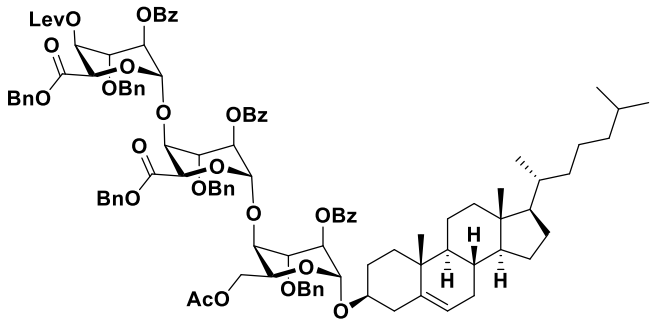

Glycosylation: The cholesterol conjugated product **18 (65%)** was obtained from the compound **17** using synthetic procedure **8.** ^{1}H NMR (400 MHz, Chloroform-*d*) δ 7.99 – 7.92 (m, 6H), 7.57 (tt, *J* = 7.1, 1.3 Hz, 1H), 7.46 – 7.35 (m, 9H), 7.28 (ddd, *J* = 7.2, 3.9, 1.6 Hz, 7H), 7.25 – 7.20 (m, 8H), 7.18 – 7.12 (m, 9H), 5.33 (d, *J* = 5.3 Hz, 1H), 5.31 (d, *J* = 4.6 Hz, 1H), 5.20 – 5.18 (m, 2H), 5.14 (d, *J* = 12.2 Hz, 1H), 5.11 – 5.06 (m, 4H), 5.02 (dd, *J* = 4.6, 1.9 Hz, 2H), 4.93 (d, *J* = 2.1 Hz, 1H), 4.80 (d, *J* = 11.6 Hz, 1H), 4.73 (d, *J* = 11.5 Hz, 1H), 4.69 (d, *J* = 4.1 Hz, 1H), 4.65 (dd, *J* = 11.7, 2.8 Hz, 2H), 4.58 (d, *J* = 11.7 Hz, 1H), 4.49 – 4.43 (m, 2H), 4.25 (dd, *J* = 11.3, 7.7 Hz, 1H), 4.17 – 4.15 (m, 1H), 4.05 (dd, *J* = 11.3, 5.3 Hz, 1H), 3.99 (t, *J* = 4.4 Hz, 1H), 3.93 – 3.91 (m, 1H), 380 – 3.79 (m, 2H), 3.54 (td, *J* = 11.3, 5.5 Hz, 1H), 2.39 – 2.33 (m, 3H), 2.29 – 2.22 (m, 1H), 2.17 (dt, *J* = 17.2, 6.9 Hz, 1H), 2.10 – 2.03 (m, 1H), 2.01 (s, 3H), 2.00 – 1.93 (m, 3H), 1.90 (s, 3H), 1.88 – 1.78 (m, 2H), 1.74 – 1.61 (m, 3H), 1.58 – 1.43 (m, 6H), 1.40 - 132 (m, 3H), 1.27 (m, 2H), 1.22 – 1.06 (m, 7H), 1.02 (s, 3H), 0.92 (d, *J* = 6.5 Hz, 4H), 0.87 (dd, *J* = 6.6, 1.8 Hz, 6H), 0.68 (s, 3H). ^{13}C NMR (101 MHz, $CDCl_3$) δ 205.74, 171.43, 170.42, 168.98, 167.58, 165.84, 165.37, 164.82, 140.66, 138.54, 137.52, 137.11, 135.24, 135.07, 133.68, 133.41, 133.28, 130.10, 130.01, 129.97, 129.60, 129.33, 129.09, 128.69, 128.62, 128.59, 128.54, 128.51, 128.47, 128.44, 128.43, 128.42, 128.38, 128.35, 128.31, 128.26, 128.25, 128.10, 127.75, 127.67, 127.51, 121.95, 101.04, 100.56, 96.53, 76.50, 76.43, 76.38, 74.43, 73.35, 72.60, 72.35, 72.14, 70.24, 70.17, 68.21, 68.11, 67.24, 67.08, 66.46, 66.41, 64.95, 63.03, 56.87, 56.27, 50.34, 42.45, 39.91, 39.65, 38.55, 37.68, 37.60, 36.90, 36.31, 35.91, 32.07, 32.02, 29.66, 29.58, 28.36, 28.14, 27.73, 24.41, 23.95, 22.96, 22.70, 21.20, 20.83, 19.53, 18.85, 11.99.

Cholestanyl-O-((benzyl (2-O-benzoyl-3-O-benzyl-4-O-levulinoyl))-α-L-idopyranosyl uronate-α(1→4) benzyl (2-O-benzoyl-3-O-benzyl)-α-L-idopyranosyl uronate-α(1→4) (2-O-benzoyl-3-O-benzyl))-α-L-idopyranoside 19

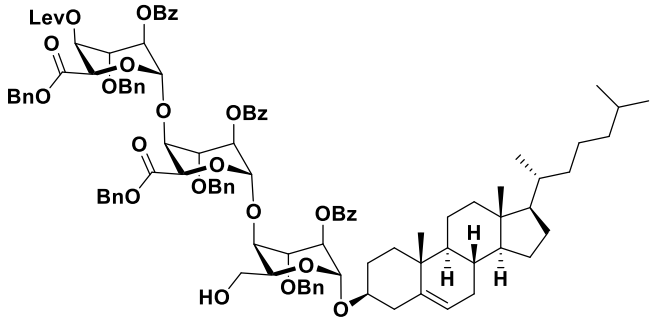

Selective Acetate Deprotection: The synthetic procedure for the preparation of compound **9** was followed to obtain compound **19 (90%)** from compound **18** as syrup. ^{1}H NMR (400 MHz, Chloroform-*d*) δ 8.01 (ddd, *J* = 8.5, 3.5, 1.4 Hz, 4H), 7.97 – 7.94 (m, 2H), 7.61 – 7.57 (m, 1H), 7.48 – 7.39 (m, 8H), 7.32 – 7.14 (m, 25H), 5.34 (d, *J* = 5.1 Hz, 1H), 5.32 (d, *J* = 4.4 Hz, 1H), 5.22 (t, *J* = 2.1 Hz, 1H), 5.20 – 5.17 (m, 1H), 5.15 – 5.06 (m, 7H), 5.01 (d, *J* = 2.3 Hz, 1H), 4.84 – 4.734(m, 3H), 4.72 – 4.63 (m, 4H), 4.51 (d, *J* = 11.2 Hz, 1H), 4.39 – 4.35 (m, 1H), 4.21 (t, *J* = 3.2 Hz, 1H), 4.06 (t, *J* = 4.3 Hz, 1H), 3.94 (t, *J* = 3.8 Hz, 1H), 3.88 (t, *J* = 2.8 Hz, 1H), 3.85 (t, *J* = 2.9 Hz, 1H), 3.78 (dd, *J* = 11.3, 7.4 Hz, 1H), 3.62 – 3.52 (m, 2H), 2.43 – 2.38 (m, 3H), 2.31 – 2.17 (m, 2H), 2.14 – 2.08 (m, 1H), 2.04 (s, 3H), 2.00 – 1.95 (m, 2H), 1.91 – 1.81 (m, 2H), 1.74 – 1.65 (m, 2H), 1.60 – 1.45 (m, 6H), 1.41 – 1.34 (m, 3H), 1.29 (s, 3H), 1.21 – 1.07 (m, 8H), 1.04 (s, 3H), 0.95 (d, *J* = 6.5 Hz, 4H), 0.89 (dd, *J* = 6.6, 1.8 Hz, 6H), 0.70 (s, 3H). ^{13}C NMR (101 MHz, $CDCl_3$) δ 205.75, 171.45, 168.92, 167.60, 165.85, 165.68, 164.85, 140.71, 138.62, 137.44, 137.03, 135.19, 135.07, 133.70, 133.56, 133.22, 130.09, 129.98, 129.94, 129.67, 129.31, 128.99, 128.65, 128.61, 128.58, 128.55, 128.52, 128.49, 128.45, 128.43, 128.38, 128.37, 128.33, 128.26, 128.22, 128.14, 127.85, 127.59, 127.44, 121.92, 100.94, 100.91, 96.42, 77.36, 76.61, 76.52, 74.62, 73.23, 72.62, 72.37, 72.07, 70.46, 70.29, 68.62, 68.24, 67.24, 67.18, 67.09, 66.48, 66.46, 61.97, 56.87, 56.26, 50.26, 42.45, 39.91, 39.65, 38.52, 37.68, 37.46, 36.91, 36.32, 35.91, 32.07, 32.06, 32.01, 29.83, 29.66, 29.63, 28.37, 28.14, 27.73, 24.42, 23.94, 22.95, 22.70, 21.18, 19.52, 18.85, 11.98.

Cholestanyl-O-((benzyl (2-O-benzoyl-3-O-benzyl-4-O-levulinoyl))-α-L-idopyranosyl uronate-α(1→4) benzyl (2-O-benzoyl-3-O-benzyl)-α-L-idopyranosyl uronate-α(1→4) benzyl (2-O-benzoyl-3-O-benzyl))-α-L-idopyranoside uronate 20

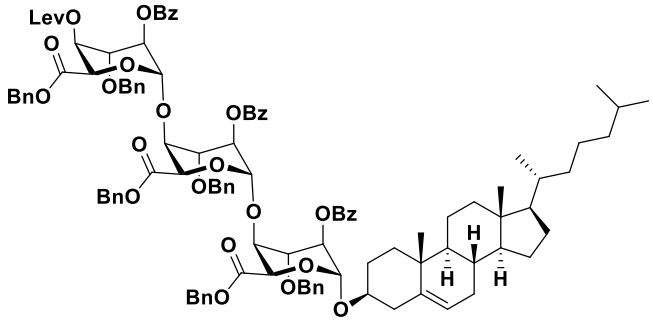

Oxidation and Esterification: The synthetic procedure for the preparation of compound **10** was followed to obtain compound **20 (60%)** from compound **19** as solid. ^{1}H NMR (400 MHz, Chloroform-*d*) δ 7.97 – 7.88 (m, 6H), 7.58 – 7.53 (m, 1H), 7.40 (qd, *J* = 5.4, 4.4, 1.8 Hz, 6H), 7.35 – 7.27 (m, 9H), 7.24 – 7.14 (m, 18H), 7.12 – 7.07 (m, 5H), 5.31 – 5.30 (m, 3H), 5.18 (dt, *J* = 5.8, 2.8 Hz, 2H), 5.11 – 5.08 (m, 2H), 5.04 – 4.95 (m, 6H), 4.89 – 4.88 (m, 1H), 4.78 (t, *J* = 2.4 Hz, 2H), 4.76 – 4.70 (m, 4H), 4.59 (d, *J* = 11.5 Hz, 1H), 4.49 (dd, *J* = 11.2, 2.2 Hz, 2H), 4.26 (t, *J* = 3.4 Hz, 1H), 4.14 (t, *J* = 3.4 Hz, 1H), 3.92 (dq, *J* = 6.7, 3.6 Hz, 2H), 3.75 (t, *J* = 2.7 Hz, 1H), 3.59 (tt, *J* = 10.6, 4.6 Hz, 1H), 2.40 – 2.33 (m, 3H), 2.29 – 2.20 (m, 1H), 2.18 – 2.03 (m, 3H), 2.00 (s, 3H), 1.97 – 1.90 (m, 2H), 1.88 – 1.77 (m, 2H), 1.64 – 1.51 (m, 5H), 1.49 – 1.39 (m, 3H), 1.40 – 1.31 (m, 4H), 1.31 – 1.23 (m, 3H), 1.17 – 1.01 (m, 8H), 0.98 (s, 3H), 0.92 (d, *J* = 6.5 Hz, 3H), 0.87 (dd, *J* = 6.6, 1.8 Hz, 6H), 0.68 (s, 3H). ^{13}C NMR (101 MHz, $CDCl_3$) δ 205.76, 171.34, 169.35, 168.57, 167.63, 165.75, 165.22, 164.75, 140.54, 138.23, 137.44, 137.23, 135.37, 135.22, 135.02, 133.61, 133.41, 133.31, 130.23, 130.10, 129.98, 129.39, 129.35, 129.04, 128.68, 128.63, 128.59, 128.55, 128.48, 128.44, 128.41, 128.36, 128.33, 128.29, 128.28, 128.22, 128.08, 127.86, 127.73, 127.54, 122.00, 101.42, 101.33, 97.40, 78.58, 77.36, 75.56, 75.27, 72.96, 72.50, 72.33, 72.14, 68.93, 68.83, 68.70, 68.50, 68.28, 67.15, 67.11, 66.93, 66.64, 66.57, 56.89, 56.27, 50.24, 42.45, 39.92, 39.65, 38.77, 37.69, 37.33, 36.81, 36.32, 35.92, 32.08, 32.00, 29.83, 29.66, 29.58, 28.37, 28.15, 27.74, 24.43, 23.95, 22.96, 22.70, 21.18, 19.50, 18.86, 11.99.

Cholestanyl-O-((3-O-benzyl-)-α-L-idopyranosyl uronate-α(1→4)(3-O-benzyl)-α-L-idopyranosyl uronate-α(1→4)(3-O-benzyl))-α-L-idopyranoside uronate 19

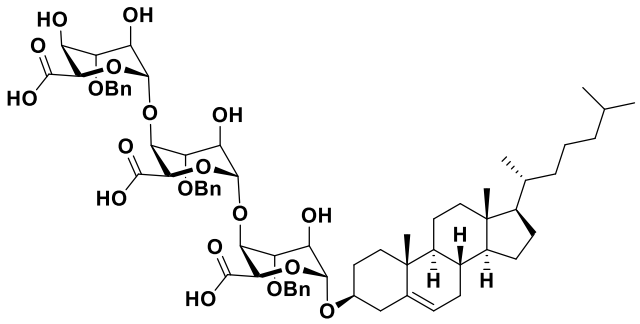

Deprotection: Esters deprotection was carried out for the compound **20** by following synthetic procedure **11** to obtain the compound **21 (67%) .**^{1}H NMR (400 MHz, Methanol-d_4) δ 7.40 – 7.24 (m, 15H), 5.38 (dt, *J* = 4.6, 1.9 Hz, 1H), 5.11 (d, *J* = 2.8 Hz, 1H), 5.00 (d, *J* = 3.9 Hz, 2H), 4.79 (d, *J* = 2.8 Hz, 1H), 4.72 (d, *J* = 1.9 Hz, 1H), 4.67 (d, *J* = 11.5 Hz, 1H), 4.63 – 4.55 (m, 5H), 4.27 – 4.23 (m, 2H), 4.01 (dt, *J* = 3.4, 1.6 Hz, 1H), 3.78 (t, *J* = 4.3 Hz, 1H), 3.70 (t, *J* = 3.2 Hz, 1H), 3.64 (ddt, *J* = 7.4, 5.2, 2.3 Hz, 2H), 3.61 – 3.47 (m, 3H), 2.42 (ddd, *J* = 13.4, 5.0, 2.1 Hz, 1H), 2.29 – 2.22 (m, 1H), 2.07 – 1.82 (m, 5H), 1.66 – 1.46 (m, 7H), 1.45 – 1.25 (m, 6H), 1.23 – 1.08(m, 7), 1.06 – 1.01 (m, 4H), 0.95 (d, *J* = 6.4 Hz, 3H), 0.88 (dd, *J* = 6.7, 1.5 Hz, 6H), 0.72 (s, 3H). ^{13}C NMR (101 MHz, MeOD) δ 173.27, 172.93, 172.61, 141.78, 139.53, 138.71, 138.50, 129.83, 129.64, 129.58, 129.54, 129.33, 129.31, 129.18, 129.11, 128.90, 128.66, 122.86, 104.36, 103.78, 101.19, 79.64, 77.23, 76.53, 76.22, 75.81, 74.92, 73.40, 73.26, 69.67, 69.19, 68.97, 68.49, 67.57, 67.19, 58.16, 57.57, 51.69, 43.51, 41.16, 40.69, 39.83, 38.54, 37.87, 37.38, 37.13, 33.25, 33.06, 30.75, 29.34, 29.16, 25.32, 24.95, 23.20, 22.95, 22.19, 19.85, 19.26, 12.34.

Cholestanyl-O-((2,4-O-disulfonato-3-O-benzyl-)-α-L-idopyranosyl uronate-α(1→4)(2-O-sulfonato-3-O-benzyl)-α-L-idopyranosyl uronate-α(1→4)(2-O-sulfonato-3-O-benzyl))-α-L-idopyranoside uronate 22

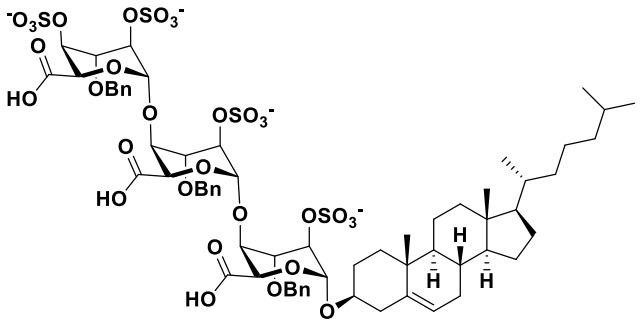

Sulfation: The sulfated compound **22 (75%)** obtained from the compound **21** by following the synthetic procedure **12.** ^{1}H NMR (400 MHz, Deuterium Oxide, Temperature at 358 K) δ 8.13 – 7.86 (m, 15H), 5.99 (s, 1H), 5.92 – 5.82 (m, 3H), 5.47 – 5.29 (m, 8H), 5.24 (d, *J* = 14.4 Hz, 2H), 5.03 – 4.96 (m, 5H), 4.87 (s, 1H), 4.59 (d, *J* = 23.0 Hz, 2H), 4.13 (tt, *J* = 11.0,

4.9 Hz, 1H), 3.02 (d, *J* = 13.1 Hz, 1H), 2.80 (t, *J* = 12.2 Hz, 1H), 2.64 – 2.53 (m, 2H), 2.46 – 2.38 (m, 3H), 2.18 – 1.85 (m, 11H), 1.78 – 1.68 (m, 6H), 1.65 – 1.57 (s, 6H), 1.54 (d, *J* = 6.1 Hz, 4H), 1.46 (d, *J* = 6.5 Hz, 6H), 1.30 (s, 3H).

Cholesteryl-O-((2,4-O-disulfonato-3-O-benzyl-)-α-L-idopyranosyl uronate-α(1→4)(2-O-sulfonato-3-O-benzyl)-α-L-idopyranosyl uronate-α(1→4)(2-O-sulfonato-3-O-benzyl))-α-L-idopyranosideuronate IAC-3

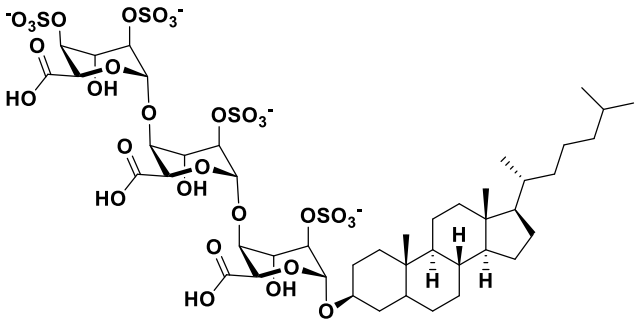

Hydrogenolysis: The compound **IAC-3 (80%)** wasobtainedfrom the compound **22** by following synthetic procedure **IAC-2.** ^{1}H NMR (400 MHz, Deuterium Oxide) δ 5.14 (dd, *J* = 21.1, 11.3 Hz, 3H), 4.87 (d, *J* = 8.9 Hz, 1H), 4.58 (s, 1H), 4.40 (s, 1H), 4.04 (dd, *J* = 39.0, 26.3 Hz, 6H), 3.65 – 3.53 (m, 1H), 2.98 (d, *J* = 7.7 Hz, 2H), 1.92 – 1.87 (m, 1H), 1.75 – 1.55 (m, 5H), 1.50 – 1.38 (m, 2H), 1.34 – 1.15 (m, 11H), 1.10 – 0.90 (m, 9H), 0.83 – 0.72 (m, 12H), 0.58 (s, 3H).

5.5.6 Synthesis of Cholestanol Conjugated Iduronic Acid Disaccharide (IAC-4)

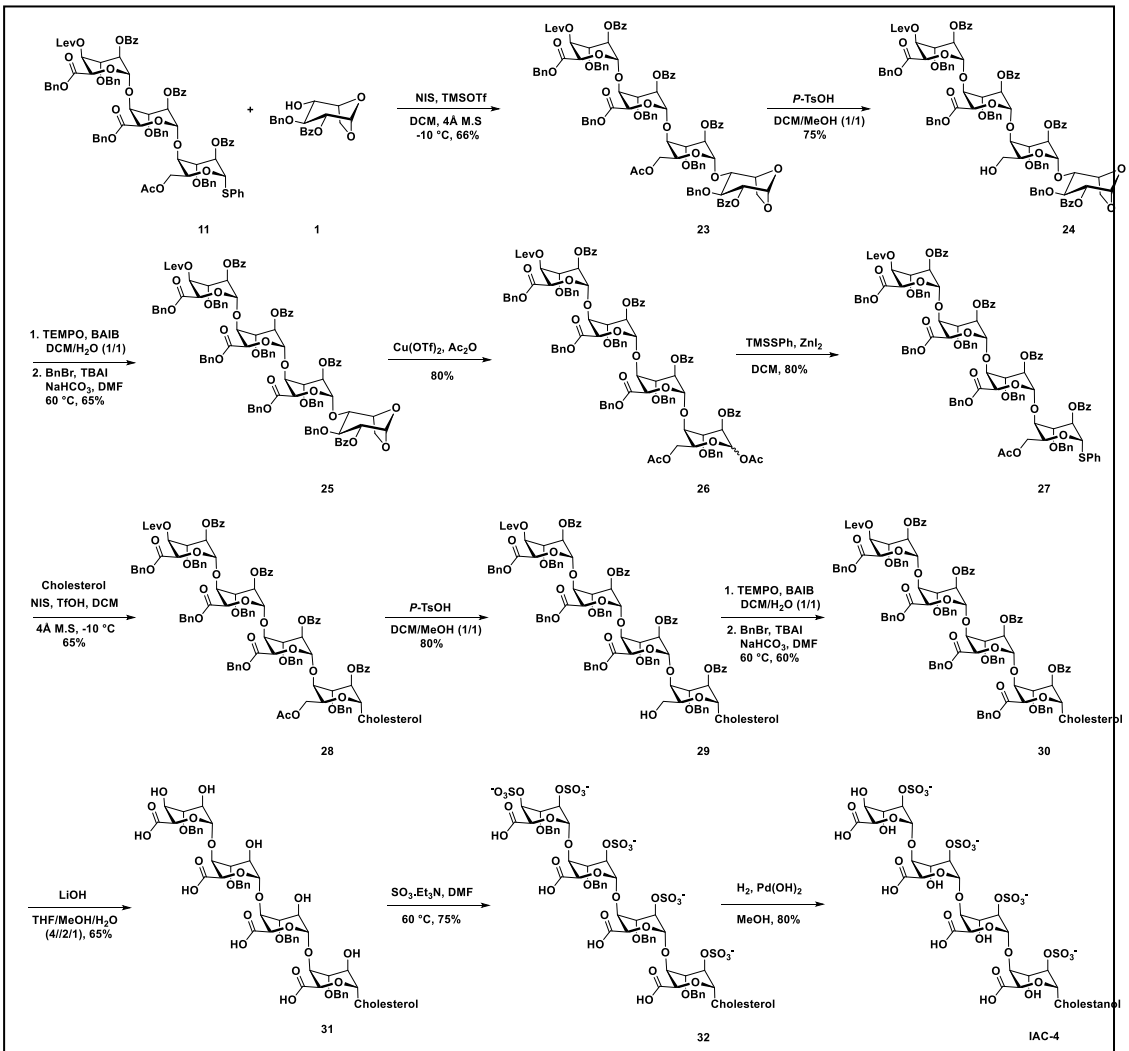

Scheme S8. Synthesis of Iduronic Acid Sulfated Tetrasaccharide.

Benzyl (2-O-benzoyl-3-O-benzyl-4-O-levulinoyl)-α-L-idopyranosyl uronate-α(1→4) benzyl (2-O-benzoyl-3-O-benzyl)-α-L-idopyranosyl uronate-α(1→4)(6-O-acetyl-2-O-benzoyl-3-O-benzyl)-α-L-idopyranosyl-α(1→4)(2-O-benzoyl-3-O-benzyl-1,6-anhydro)-β-L-idopyranose 23

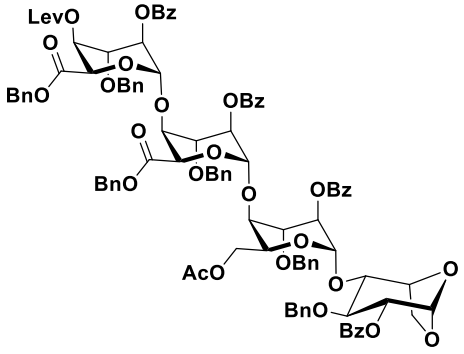

Glycosylation: The synthetic procedure for the preparation of compound **5** was followed to obtain compound **23 (66%)** from compound **11** and **1** as solid. ^{1}H NMR (400 MHz, Chloroform-*d*) δ 7.99– 7.96 (m, 5H), 7.95 – 7.90 (m, 3H), 7.59 – 7.53 (m, 2H), 7.48 – 7.38 (m, 8H), 7.34 – 7.27 (m, 11H), 7.24 – 7.11 (m, 16H), 7.06 – 6.99 (m, 5H), 5.50 (s, 1H), 5.34 (d, *J* = 4.6 Hz, 1H), 5.21 – 5.16 (m, 3H), 5.11 (dd, *J* = 12.1, 3.8 Hz, 3H), 5.07 – 5.03 (m, 3H), 4.99 – 4.95 (m, 2H), 4.76 – 4.72 (m, 3H), 4.69 – 4.62 (m, 6H), 4.49 (d, *J* = 11.4 Hz, 3H), 4.20 – 4.13 (m, 4H), 4.07 – 4.02 (m, 2H), 3.95 (t, *J* = 3.9 Hz, 1H), 3.88 – 3.81 (m, 3H), 3.71 – 3.68 (m, 1H), 2.37 (t, *J* = 6.8 Hz, 2H), 2.23 – 2.15 (m, 1H), 2.10 – 2.04 (m, 1H), 2.02 (s, 3H), 1.88 (s, 3H). ^{13}C NMR (101 MHz, CHLOROFORM-*D*) δ 205.80, 171.43, 170.51, 168.96, 167.56, 165.88, 165.85, 165.37, 164.81, 138.23, 137.87, 137.42, 137.06, 135.17, 134.99, 133.71, 133.55, 133.51, 133.30, 130.04, 129.95, 129.50, 129.25, 129.15, 128.94, 128.70, 128.60, 128.58, 128.54, 128.51, 128.46, 128.42, 128.38, 128.32, 128.24, 128.20, 128.15, 128.08, 127.91, 127.81, 127.36, 100.82, 100.53, 99.39, 95.34, 77.74, 76.63, 76.50, 76.30, 75.82, 74.97, 74.62, 73.41, 73.10, 72.58, 72.25, 71.96, 70.24, 68.21, 68.13, 67.28, 67.10, 66.42, 66.40, 65.77, 65.54, 62.70, 37.65, 29.67, 27.68, 20.82. HRMS m/z calculated for $C_{101}H_{96}O_{29}Na$:1795.5935; found: 1795.5930.

Benzyl (2-O-benzoyl-3-O-benzyl-4-O-levulinoyl)-α-L-idopyranosyl uronatel-α(1→4) benzyl (2-O-benzoyl-3-O-benzyl)-α-L-idopyranosyl uronate-α(1→4)(2-O-benzoyl-3-O-benzyl)-α-L-idopyranosyl-α(1→4)(2-O-benzoyl-3-O-benzyl-1,6-anhydro)-β-L-idopyranose 24

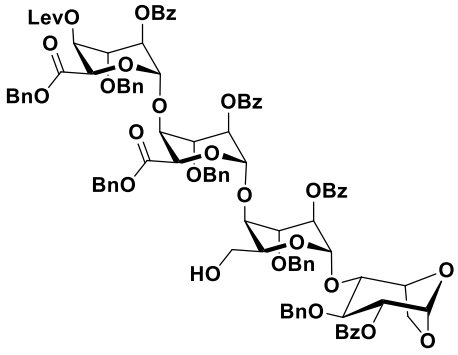

Selective Acetate Deprotection: The synthetic procedure for the preparation of compound **9** was followed to obtain compound **24 (75%)** from compound **23** as syrup. ^{1}H NMR (400 MHz, Chloroform-*d*) δ 799 – 7.93 (m, 8H), 7.55 (t, *J* = 7.4 Hz, 2H), 7.46 – 7.37 (m, 10H), 7.34 – 7.26 (m, 8H), 7.24 – 7.10 (m, 17H), 7.08 – 7.01 (m, 5H), 5.51 (d, *J* = 1.7 Hz, 1H), 5.32 (d, *J* = 4.7 Hz, 1H), 5.18 – 5.14 (m, 3H), 5.10 – 5.06 (m, 3H), 5.04 – 5.01 (m, 3H), 5.00 – 4.99 (m, 1H), 4.93 (d, *J* = 2.1 Hz, 1H), 4.79 – 4.70 (m, 4H), 4.68 (s, 1H), 4.63 (d, *J* = 12.5 Hz, 2H), 4.59 (t, *J* = 4.5 Hz, 1H), 4.53 (s, 2H), 4.47 (d, *J* = 11.2 Hz, 1H), 4.27 (t, *J* = 6.8 Hz, 1H), 4.22 – 4.19 (m, 2H), 4.19 – 4.16 (m, 1H), 4.05 (t, *J* = 4.3 Hz, 1H), 3.91 – 3.87 (m, 2H), 3.81 (s, 1H), 3.76 (dt, *J* = 14.0, 3.8 Hz, 2H), 3.47 (dd, *J* = 11.3, 6.9 Hz, 1H), 3.26 (dd, *J* = 11.3, 6.1 Hz, 1H), 2.35 (t, *J* = 6.8 Hz, 2H), 2.17 (dt, *J* = 17.2, 7.0 Hz, 1H), 2.09 – 2.01 (m, 1H), 2.00 (s, 3H). ^{13}C NMR (101 MHz, CHLOROFORM-*D*) δ 205.80, 171.40, 168.96, 167.54, 165.98, 165.79, 165.46, 164.81, 138.20, 137.93, 137.41, 137.06, 135.15, 135.02, 133.71, 133.55, 133.47, 133.42, 130.06, 129.94, 129.50, 129.23, 129.21, 128.99, 128.67, 128.58, 128.50, 128.44, 128.39, 128.31, 128.23, 128.21, 128.07, 127.91, 127.82, 127.76, 101.03, 100.82, 99.40, 95.79, 78.37, 77.36, 76.95, 76.70, 76.58, 75.80, 75.13, 74.68, 73.97, 73.18, 72.77, 72.39, 72.15, 71.92, 70.49, 70.43, 67.23, 67.09, 66.98, 66.38, 66.35, 65.68, 61.49, 37.64, 29.66, 27.67. HRMS m/z calculated for $C_{99}H_{94}O_{28}Na$:1753.5829; found: 1753.5825.

Benzyl (2-O-benzoyl-3-O-benzyl-4-O-levulinoyl)-α-L-idopyranosyl uronate-α(1→4) benzyl (2-O-benzoyl-3-O-benzyl)-α-L-idopyranosyl uronate-α(1→4)benzyl (2-O-benzoyl-3-O-benzyl)-α-L-idopyranosyl uronate-α(1→4)(2-O-benzoyl-3-O-benzyl-1,6-anhydro)-β-L-idopyranose 25

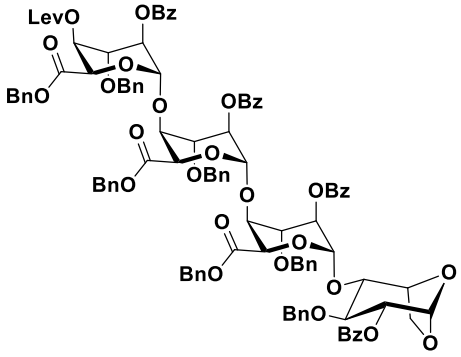

Oxidation and Esterification: The synthetic procedure for the preparation of compound **10** was followed to obtain compound **25 (65%)** from compound **24** as solid. ^{1}H NMR (400 MHz, Chloroform-*d*) δ 7.97 – 7.88 (m, 8H), 7.55 (td, *J* = 7.3, 1.4 Hz, 2H), 7.44 – 7.37 (m, 8H), 7.32 – 7.28 (m, 7H), 7.25 – 7.07 (m, 25H), 7.02 – 6.96 (m, 5H), 5.49 (d, *J* = 1.6 Hz, 1H), 5.32 (t, *J* = 2.6 Hz, 2H), 5.17 – 5.16 (m, 2H), 5.11 – 5.08 (m, 2H), 5.04 (d, *J* = 12.3 Hz, 1H), 5.00 (d, *J* = 2.7 Hz, 3H), 4.97 – 4.96 (m, 1H), 4.94 – 4.856 (m, 3H), 4.81 (d, *J* = 3.1 Hz, 1H), 4.76 – 474 (m, 3H), 4.70 (d, *J* = 5.6 Hz, 1H), 4.65 (d, *J* = 9.0 Hz, 1H), 4.62 (d, *J* = 4.4 Hz, 1H), 4.60 – 4.55 (m, 3H), 4.49 (s, 1H), 4.46 (d, *J* = 1.7 Hz, 1H), 4.28 (t, *J* = 3.8 Hz, 1H), 4.23 (dd, *J* = 8.4, 4.1 Hz, 1H), 4.17 (t, *J* = 3.9 Hz, 1H), 4.06 (d, *J* = 7.7 Hz, 1H), 3.97 (t, *J* = 3.4 Hz, 1H), 3.92 (t, *J* = 3.2 Hz, 1H), 3.85 (t, *J* = 8.4 Hz, 1H), 3.75 (d, *J* = 2.9 Hz, 1H), 3.57 – 3.54 (m, 1H), 2.35 (t, *J* = 6.7 Hz, 2H), 2.19 – 2.02 (m, 2H), 2.00 (s, 3H). ^{13}C NMR (101 MHz, $CDCl_3$) δ 205.74, 171.32, 168.80, 168.56, 167.60, 165.81, 165.66, 165.17, 164.75, 137.92, 137.77, 137.36, 137.23, 135.18, 135.13, 134.98, 133.62, 133.58, 133.46, 133.34, 130.21, 129.99, 129.96, 129.57, 129.35, 128.98, 128.97, 128.69, 128.58, 128.54, 128.49, 128.46, 128.35, 128.25, 128.16, 128.10, 127.90, 127.83, 127.46, 101.30, 100.91, 99.38, 96.33, 77.85, 76.78, 76.72, 75.87, 75.59, 75.43, 75.34, 74.91, 73.39, 73.06, 72.33, 72.24, 72.17, 69.00, 68.89, 68.46, 68.31, 67.19, 67.13, 67.03, 66.68, 66.64, 65.44, 37.66, 29.65, 27.70. HRMS m/z calculated for $C_{106}H_{98}O_{29}Na$:1834.6194; found: 1834.6189.

Benzyl (2-O-benzoyl-3-O-benzyl-4-O-levulinoyl)-α-L-idopyranosyl uronate-α(1→4) benzyl (2-O-benzoyl-3-O-benzyl)-α-L-idopyranosyl uronate-α(1→4) benzyl (2-O-benzoyl-3-O-benzyl)-α-L-idopyranosyl uronate-α(1→4)(1,6-O-diacetyl-2-O-benzoyl-3-O-benzyl)-α/β-L-idopyranoside 26

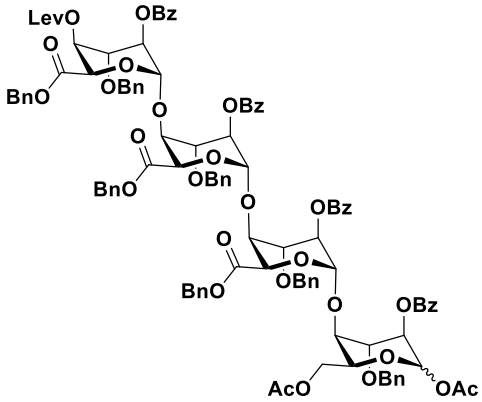

Acetolysis: The synthetic procedure for the preparation of compound **6** was followed to obtain compound **26 (80%, α:β = 1:1)** from compound **25** as solid. ^{1}H NMR (400 MHz, Chloroform-*d*) δ 8.03 – 7.86 (m, 20H), 7.78 – 7.52 (m, 3H), 7.46 – 7.34 (m, 17H), 7.33 – 7.18 (m, 57H), 7.117 - 713 (m, 20H), 7.12 (s, 7H), 7.11 – 7.05 (m, 10H), 6.16 (s, 1H), 6.14 (d, *J* = 2.0 Hz, 1H), 5.28 (dd, *J* = 4.0, 2.0 Hz, 1H), 5.26 (d, *J* = 4.0 Hz, 2H), 5.19 – 5.09 (m, 12H), 5.04 (d, *J* = 19.4 Hz, 2H), 4.98 (dt, *J* = 9.2, 3.8 Hz, 5H), 4.93 (d, *J* = 1.6 Hz, 2H), 4.90 – 4.85 (m, 7H), 4.80 (d, *J* = 3.1 Hz, 2H), 4.76 (t, *J* = 2.3 Hz, 2H), 4.74 – 4.71 (m, 4H), 4.70 – 4.67 (m, 5H), 4.65 – 4.52 (m, 13H), 4.45 – 4.41 (m, 4H), 4.33 (t, *J* = 3.7 Hz, 1H), 4.30 – 4.21 (m, 5H), 4.14 – 4.10 (m, 2H), 4.05 (dq, *J* = 13.9, 3.9 Hz, 6H), 3.97 (t, *J* = 4.1 Hz, 1H), 3.91 (q, *J* = 3.5 Hz, 2H), 3.82 (q, *J* = 3.2 Hz, 2H), 3.74 (dt, *J* = 3.3, 1.8 Hz, 2H), 2.34 (td, *J* = 6.8, 1.5 Hz, 5H), 2.17 – 2.08 (m, 4H), 2.07 (s, 3H), 2.04 (dd, *J* = 3.8, 1.9 Hz, 1H), 2.02 (s, 3H), 2.00 (s, 6H), 1.95 (s, 3H), 1.93 (s, 3H). ^{13}C NMR (101 MHz, $CDCl_3$) δ 205.76, 171.32, 170.49, 170.47, 169.11, 169.02, 168.93, 168.75, 168.42, 168.37, 167.61, 166.04, 165.60, 165.41, 165.38, 165.22, 165.18, 164.77, 138.16, 137.75, 137.72, 137.70, 137.45, 137.44, 135.19, 135.12, 135.08, 134.99, 134.96, 133.64, 133.49, 133.46, 133.43, 133.33, 130.20, 130.13, 130.03, 129.99, 129.46, 129.38, 129.20, 129.15, 129.03, 128.96, 128.91, 128.70, 128.64, 128.59, 128.56, 128.49, 128.43, 128.41, 128.38, 128.37, 128.34, 128.31, 128.29, 128.21, 128.20, 128.14, 128.06, 127.92, 127.89, 127.85, 127.80, 127.73, 127.65, 127.55, 101.56, 101.40, 101.02, 101.00, 100.74, 100.54, 91.81, 90.72, 76.73, 76.63, 76.42, 76.23, 76.01, 75.78, 75.70, 75.41, 75.17, 73.69, 73.32, 73.18, 73.10, 73.07, 73.04, 72.53, 72.37, 72.30, 72.23, 72.14, 70.70, 70.55, 69.91, 69.76, 69.02, 68.90, 68.54, 68.52, 68.40, 67.30, 67.13, 67.11, 66.79, 66.78, 66.73, 66.51, 63.03, 62.57, 37.68, 29.69, 29.67, 27.71, 21.06, 20.86, 20.84. HRMS m/z calculated for $C_{110}H_{104}O_{32}Na$:1959.6408; found: 1959.6398.

Benzyl (2-O-benzoyl-3-O-benzyl-4-O-levulinoyl)-α-L-idopyranosyl uronate-α(1→4) benzyl (2-O-benzoyl-3-O-benzyl)-α-L-idopyranosyl uronate-α(1→4) benzyl (2-O-benzoyl-3-O-benzyl)-α-L-idopyranosyl uronate-α(1→4) 1-thiophenyl (6-O-acetyl-2-O-benzoyl, 3-O-benzyl)-α-L-idopyranoside 27

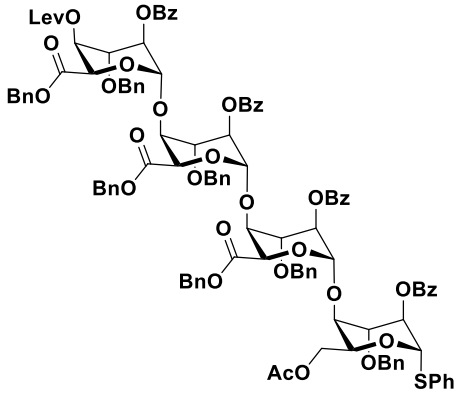

Thioglycosylation: The preparation of the thioglycosylated compound **27 (80%)** was carried out from compound **26** according to the procedure used for synthesizing compound **7**as syrup.^{1}H NMR (400 MHz, Chloroform-*d*) δ 7.96 (ddd, *J* = 6.8, 6.0, 1.5 Hz, 6H), 7.86 (dd, *J* = 8.3, 1.1 Hz, 2H), 7.58 – 7.53 (m, 3H), 7.47 – 7.43 (m, 1H), 7.42 – 7.36 (m, 7H), 7.34 – 7.27 (m, 12H), 7.25 – 7.04 (m, 29H), 5.53 (s, 1H), 5.40 (dt, *J* = 2.4, 1.1 Hz, 1H), 5.29 (d, *J* = 5.2 Hz, 1H), 5.17 – 5.12 (m, 4H), 5.07 (dd, *J* = 16.1, 12.1 Hz, 2H), 4.98 – 4.97 (m, 1H), 4.96 – 4.90 (m, 2H), 4.87 – 4.84 (m, 4H), 4.79 – 4.67 (m, 6H), 4.59 (ddd, *J* = 15.8, 11.4, 4.1 Hz, 4H), 4.42 (d, *J* = 11.3 Hz, 1H), 4.26 – 4.21 (m, 2H), 4.06 – 4.02 (m, 4H), 3.93 (t, *J* = 3.2 Hz, 1H), 3.79 (t, *J* = 2.5 Hz, 1H), 3.74 (td, *J* = 3.3, 0.9 Hz, 1H), 2.34 (t, *J* = 6.8 Hz, 2H), 2.17 – 2.02 (m, 2H), 1.99 (s, 3H), 1.91 (s, 3H).^{13}C NMR (101 MHz, $CDCl_3$) δ 205.76, 171.33, 170.33, 168.96, 168.33, 167.63, 165.81, 165.36, 165.24, 164.77, 137.93, 137.74, 137.41, 137.26, 136.29, 135.18, 135.12, 134.97, 133.64, 133.52, 133.45, 133.35, 131.76, 130.20, 130.11, 130.02, 129.99, 129.45, 129.39, 129.19, 128.91, 128.88, 128.71, 128.63, 128.59, 128.56, 128.48, 128.44, 128.40, 128.34, 128.26, 128.17, 128.10, 127.96, 127.79, 127.75, 127.67, 127.41, 101.56, 101.29, 100.82, 86.10, 76.74, 76.30, 76.28, 75.58, 73.76, 73.18, 72.84, 72.36, 72.26, 70.89, 69.06, 68.70, 68.55, 68.11, 67.15, 67.11, 66.82, 66.76, 65.85, 63.18, 37.68, 29.67, 27.72, 20.83. HRMS m/z calculated for $C_{114}H_{106}O_{30}SNa$:2009.6387; found: 2009.6379.

Cholestanyl-O-((benzyl (2-O-benzoyl-3-O-benzyl-4-O-levulinoyl))-α-L-idopyranosyl uronate-α(1→4) benzyl (2-O-benzoyl-3-O-benzyl)-α-L-idopyranosyl uronate-α(1→4) benzyl (2-O-benzoyl-3-O-benzyl)-α-L-idopyranosyl uronate-α(1→4) (6-O-acetyl-2-O-benzoyl, 3-O-benzyl))-α-L-idopyranoside 28

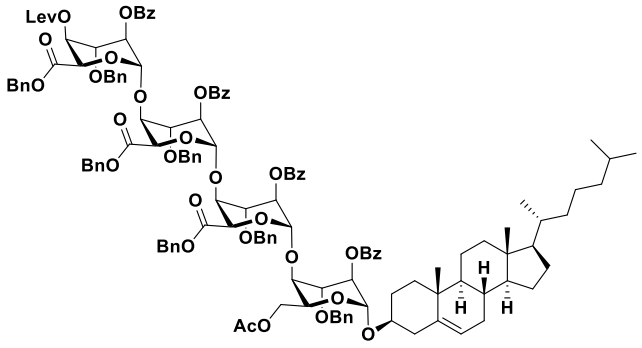

Glycosylation: The cholesterol conjugated product **28 (65%)** was obtained from the compound **27** using synthetic procedure **8** as solid. ^{1}H NMR (400 MHz, Chloroform-*d*) δ 7.97 – 7.93 (m, 6H), 7.89 – 7.87 (m, 2H), 7.56 (tt, *J* = 7.1, 1.3 Hz, 1H), 7.45 – 7.37 (m, 7H), 7.34 – 7.21 (m, 21H), 7.20 – 7.07 (m, 23H), 5.33 (d, *J* = 4.6 Hz, 1H), 5.27 (d, *J* = 4.0 Hz, 1H), 5.19 – 5.16 (m, 3H), 5.13 (t, *J* = 2.8 Hz, 1H), 5.09 (dd, *J* = 16.9, 4.8 Hz, 3H), 5.01 – 4.98 (m, 2H), 4.94 (s, 1H), 4.91 (s, 2H), 4.86 – 4.85 (m, 1H), 4.82 (d, *J* = 3.0 Hz, 1H), 4.76 (d, *J* = 2.4 Hz, 1H), 4.74 – 4.65 (m, 6H), 4.58 (d, *J* = 11.5 Hz, 1H), 4.54 – 4.44 (m, 4H), 4.29 (dd, *J* = 11.2, 7.6 Hz, 1H), 4.13 – 4.08 (m, 3H), 4.02 (q, *J* = 3.5, 2.9 Hz, 2H), 3.91 (t, *J* = 3.1 Hz, 1H), 3.80 (s, 1H), 3.74 (t, *J* = 3.0 Hz, 1H), 3.57 – 3.48 (m, 1H), 2.39 – 2.33 (m, 3H), 2.28 – 2.22 (m, 1H), 2.18 – 2.07 (m, 2H), 2.04 (dd, *J* = 10.4, 4.0 Hz, 1H), 2.00 (s, 3H), 1.92 (s, 3H), 1.88 – 1.80 (m, 2H), 1.65 (d, *J* = 6.3 Hz, 2H), 1.59 – 1.43 (m, 6H), 1.41 – 1.32 (m, 4H), 1.29 – 1.25 (m, 3H), 1.19 – 1.06 (m, 7H), 1.02 (s, 3H), 0.92 (d, *J* = 6.5 Hz, 4H), 0.88 (d, *J* = 1.8 Hz, 3H), 0.86 (d, *J* = 1.7 Hz, 3H), 0.68 (s, 3H). ^{13}C NMR (101 MHz, CHLOROFORM-*D*) δ 205.76, 171.31, 170.48, 168.80, 168.43, 167.61, 165.85, 165.43, 165.17, 164.75, 140.67, 138.52, 137.77, 137.38, 137.24, 135.18, 135.11, 134.98, 133.63, 133.46, 133.37, 133.24, 130.20, 130.05, 129.98, 129.48, 129.36, 129.21, 128.93, 128.70, 128.64, 128.56, 128.48, 128.44, 128.40, 128.34, 128.28, 128.20, 128.10, 127.89, 127.69, 127.64, 127.47, 121.94, 101.46, 101.24, 100.96, 96.52, 77.36, 76.52, 76.24, 75.96, 75.57, 74.59, 73.14, 73.01, 72.27, 72.13, 72.08, 69.76, 68.91, 68.52, 68.21, 67.11, 67.04, 66.73, 66.65, 64.97, 62.95, 56.86, 56.25, 50.32, 42.44, 39.89, 39.64, 38.54, 37.66, 37.58, 36.90, 36.31, 35.91, 32.06, 32.00, 31.71, 29.66, 29.57, 28.36, 28.14, 27.70, 24.41, 23.94, 22.95, 22.69, 21.19, 20.86, 19.52, 18.84, 11.98.

Cholestanyl-O-((benzyl (2-O-benzoyl-3-O-benzyl-4-O-levulinoyl))-α-L-idopyranosyl uronate-α(1→4) benzyl (2-O-benzoyl-3-O-benzyl)-α-L-idopyranosyl uronate-α(1→4) benzyl (2-O-benzoyl-3-O-benzyl)-α-L-idopyranosyl uronate-α(1→4) (2-O-benzoyl, 3-O-benzyl))-α-L-idopyranoside 29

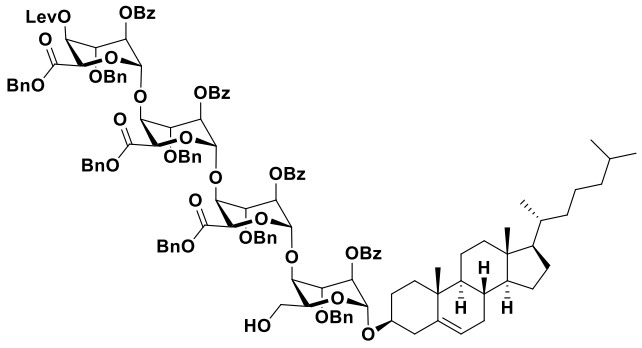

Selective Acetate Deprotection: The synthetic procedure for the preparation of compound **9** was followed to obtain compound **29 (80%)** from compound **28** as syrup. ^{1}H NMR (400 MHz, Chloroform-*d*) δ 7.95 (ddt, *J* = 8.4, 3.5, 1.3 Hz, 6H), 7.90 – 7.87 (m, 2H), 7.58 – 7.53 (m, 1H), 7.44 – 7.37 (m, 7H), 7.33 – 7.05 (m, 44H), 5.31 (dd, *J* = 4.9, 2.7 Hz, 1H), 5.25 (d, *J* = 4.0 Hz, 1H), 5.21 (d, *J* = 3.1 Hz, 1H), 5.17 (t, *J* = 2.2 Hz, 1H), 5.14 (t, *J* = 3.1 Hz, 1H), 5.12 – 5.10 (m, 2H), 5.10 – 5.07 (m, 2H), 5.00 – 4.92 (m, 3H), 4.89 – 4.86 (m, 3H), 4.85 (d, *J* = 3.2 Hz, 1H), 4.78 (d, *J* = 2.5 Hz, 1H), 4.74 – 4.68 (m, 5H), 4.67 – 4.58 (m, 2H), 4.54 (d, *J* = 4.7 Hz, 1H), 4.51 (d, *J* = 4.2 Hz, 1H), 4.48 (d, *J* = 11.4 Hz, 1H), 4.34 (td, *J* = 6.2, 2.1 Hz, 1H), 4.13 (t, *J* = 3.2 Hz, 1H), 4.06 (dq, *J* = 7.8, 3.9 Hz, 3H), 3.93 (t, *J* = 3.4 Hz, 1H), 3.86 (t, *J* = 2.9 Hz, 1H), 3.80 – 3.74 (m, 2H), 3.63 (q, *J* = 8.9, 7.9 Hz, 1H), 3.53 (td, *J* = 11.3, 5.6 Hz, 1H), 2.39 – 2.33 (m, 3H), 2.24 (t, *J* = 12.0 Hz, 1H), 2.18 – 2.05 (m, 3H), 2.00 (s, 3H), 1.97 – 1.92 (m, 2H), 1.88 – 1.78 (m, 2H), 1.67 – 1.63 (m, 1H), 1.60 (s, 3H), 1.55 – 1.47 (m, 5H), 1.43 (t, *J* = 5.5 Hz, 1H), 1.35 – 1.31 (m, 3H), 1.26 (s, 3H), 1.16 – 1.10 (m, 5H), 1.08 – 1.05 (m, 2H), 1.01 (s, 3H), 0.92 (d, *J* = 6.5 Hz, 3H), 0.87 (d, *J* = 1.7 Hz, 2H), 0.86 (d, *J* = 1.7 Hz, 2H), 0.67 (s, 3H). ^{13}C NMR (101 MHz, $CDCl_3$) δ 205.77, 171.34, 168.77, 168.49, 167.62, 165.86, 165.81, 165.26, 164.79, 140.75, 138.63, 137.73, 137.35, 137.26, 135.20, 135.12, 134.99, 133.66, 133.55, 133.51, 133.21, 130.23, 130.06, 130.00, 129.61, 129.38, 129.13, 128.96, 128.71, 128.64, 128.60, 128.58, 128.56, 128.52, 128.50, 128.48, 128.43, 128.39, 128.36, 128.22, 128.20, 128.14, 127.93, 127.80, 127.58, 127.41, 101.32, 101.21, 101.08, 96.46, 77.36, 76.28, 76.19, 75.69, 74.87, 73.13, 73.02, 72.33, 72.14, 72.09, 70.18, 70.01, 69.10, 68.80, 68.50, 68.49, 67.26, 67.15, 67.05, 66.77, 66.73, 61.96, 56.89, 56.28, 50.28, 42.46, 39.93, 39.67, 38.53, 37.69, 37.48, 36.93, 36.33, 35.93, 32.09, 32.03, 29.85, 29.68, 29.64, 28.38, 28.16, 27.72, 24.43, 23.96, 22.97, 22.71, 21.19, 19.54, 18.86, 12.00.

Cholestanyl-O-((benzyl (2-O-benzoyl-3-O-benzyl-4-O-levulinoyl))-α-L-idopyranosyl uronate-α(1→4) benzyl (2-O-benzoyl-3-O-benzyl)-α-L-idopyranosyl uronate-α(1→4) benzyl (2-O-benzoyl-3-O-benzyl)-α-L-idopyranosyl uronate-α(1→4) benzyl(2-O-benzoyl, 3-O-benzyl))-α-L-idopyranoside uronate30

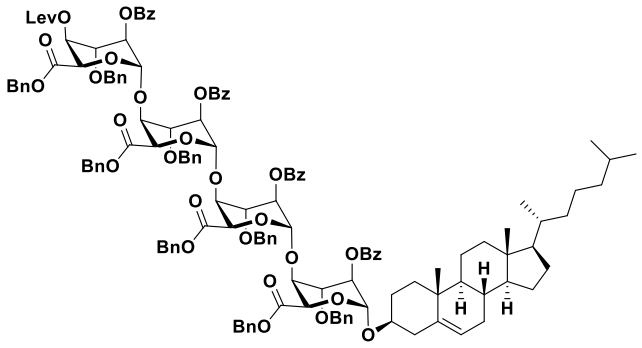

Oxidation and Esterification: The synthetic procedure for the preparation of compound **10** was followed to obtain compound **30 (60%)** from compound **29** as solid. ^{1}H NMR (400 MHz, Chloroform-*d*) δ 7.91 (dtd, *J* = 18.2, 8.3, 1.4 Hz, 8H), 7.57 – 7.53 (m, 1H), 7.41 – 7.27 (m, 16H), 7.24 – 7.07 (m, 33H), 7.00 (dd, *J* = 6.8, 2.9 Hz, 2H), 5.30 – 5.29 (m, 2H), 5.24 (d, *J* = 2.5 Hz, 1H), 5.20 (d, *J* = 3.5 Hz, 1H), 5.14 (t, *J* = 2.9 Hz, 1H), 5.11 – 4.99 (m, 7H), 4.96 (t, *J* = 2.1 Hz, 1H), 4.94 (d, *J* = 3.3 Hz, 1H), 4.85 – 4.84 (m, 2H), 4.80 (d, *J* = 2.9 Hz, 1H), 4.75 (d, *J* = 2.4 Hz, 1H), 4.73 – 4.67 (m, 4H), 4.67 – 4.56 (m, 4H), 4.47 (dd, *J* = 11.1, 7.0 Hz, 2H), 4.38 (d, *J* = 11.5 Hz, 1H), 4.22 (t, *J* = 3.7 Hz, 1H), 4.08 (q, *J* = 3.6 Hz, 2H), 3.96 (t, *J* = 3.4 Hz, 1H), 3.86 (dt, *J* = 12.0, 3.9 Hz, 2H), 3.72 (t, *J* = 3.3 Hz, 1H), 3.57 (td, *J* = 11.4, 5.5 Hz, 1H), 2.34 (t, *J* = 6.8 Hz, 3H), 2.23 (d, *J* = 12.1 Hz, 1H), 2.16 – 2.01 (m, 3H), 1.99 (s, 3H), 1.95 – 1.93 (m, 1H), 1.87 – 1.76 (m, 2H), 1.61 (s, 3H), 1.54 – 1.38 (m, 6H), 1.36 – 1.31(m, 1H), 1.26 (s, 2H), 1.12 (td, *J* = 14.1, 13.6, 6.7 Hz, 5H), 1.06 – 1.00 (m, 3H), 0.97 (s, 3H), 0.92 (d, *J* = 6.5 Hz, 3H), 0.87 (d, *J* = 1.8 Hz, 3H), 0.86 (d, *J* = 1.8 Hz, 3H), 0.67 (s, 3H). ^{13}C NMR (101 MHz, $CDCl_3$) δ 205.79, 171.33, 169.41, 168.53, 168.41, 167.59, 165.76, 165.29, 165.10, 164.76, 140.55, 138.22, 137.73, 137.48, 137.26, 135.37, 135.23, 135.11, 135.03, 133.64, 133.41, 133.29, 130.25, 130.05, 129.99, 129.38, 129.28, 129.23, 129.08, 128.69, 128.65, 128.59, 128.58, 128.57, 128.54, 128.51, 128.48, 128.45, 128.41, 128.39, 128.37, 128.35, 128.33, 128.31, 128.27, 128.23, 128.19, 128.12, 127.85, 127.79, 127.73, 127.51, 122.00, 101.56, 101.49, 101.12, 97.35, 78.54, 77.36, 77.03, 76.61, 76.53, 75.61, 75.51, 74.93, 72.86, 72.81, 72.53, 72.21, 71.95, 69.28, 69.05, 68.90, 68.59, 68.52, 67.91, 67.13, 67.10, 67.03, 66.94, 66.63, 66.56, 56.89, 56.28, 50.24, 42.46, 39.93, 39.66, 38.77, 37.69, 37.33, 36.82, 36.33, 35.93, 32.08, 32.01, 29.67, 29.58, 28.38, 28.16, 27.72, 24.43, 23.96, 22.97, 22.71, 21.19, 19.50, 18.86, 11.99.

Cholestanyl-O-((3-O-benzyl)-α-L-idopyranosyl uronate-α(1→4) (3-O-benzyl)-α-L-idopyranosyl uronate-α(1→4) (3-O-benzyl)-α-L-idopyranosyl uronate-α(1→4) (3-O-benzyl))-α-L-idopyranoside uronate31

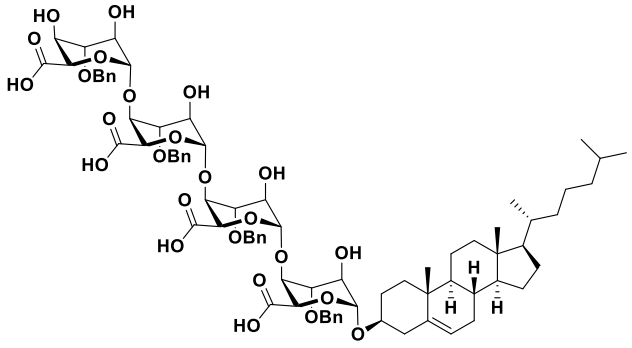

Deprotection: Esters deprotection was carried out for the compound **30** by following synthetic procedure **11** to obtain the compound **31 (65%)** as sticky solid. ^{1}H NMR (600 MHz, Methanol-d_4) δ 7.44 – 7.22 (m, 20H), 5.38 (dt, *J* = 5.0, 2.1 Hz, 1H), 5.12 (d, *J* = 2.8 Hz, 1H), 5.02 (d, *J* = 21.0 Hz, 2H), 4.94 (s, 1H), 4.80 – 4.79 (m, 2H), 4.69 (m, 1H), 4.67 – 4.53 (m, 8H), 4.25 (dt, *J* = 25.5, 4.7 Hz, 3H), 4.01 – 4.00 (m, 1H), 3.78 (t, *J* = 4.4 Hz, 1H), 3.74 (d, *J* = 3.2 Hz, 1H), 3.68 – 3.63 (m, 3H), 3.60 – 3.52 (m, 3H), 3.40 (s, 1H), 3.20 (q, *J* = 7.3 Hz, 1H), 2.41 (ddd, *J* = 13.5, 4.8, 2.2 Hz, 1H), 2.28 – 2.23 (m, 1H), 2.05 (dt, *J* = 12.6, 3.5 Hz, 1H), 2.01 – 1.96 (m, 1H), 1.93 – 1.83 (m, 3H), 1.62 (dtd, *J* = 13.9, 7.0, 3.4 Hz, 2H), 1.58 – 1.47 (m, 5H), 1.43 – 1.36 (m, 3H), 1.33 – 1.29 (m, 4H), 1.22 – 1.08 (m, 7H), 1.04 (s, 3H), 0.95 (d, *J* = 6.5 Hz, 3H), 0.88 (dd, *J* = 6.6, 2.3 Hz, 6H), 0.72 (s, 3H). ^{13}C NMR (151 MHz, MeOD) δ 173.37, 172.95, 172.57, 172.38, 141.77, 139.51, 138.69, 138.60, 138.30, 129.92, 129.82, 129.68, 129.63, 129.60, 129.55, 129.31, 129.28, 129.17, 129.12, 128.91, 128.66, 122.87, 104.50, 104.38, 103.81, 101.18, 79.63, 77.22, 76.56, 76.24, 75.98, 75.81, 75.17, 74.62, 73.61, 73.55, 73.38, 73.29, 69.63, 69.21, 68.93, 68.50, 67.71, 67.62, 67.17, 58.16, 57.57, 51.69, 49.57, 47.92, 43.51, 41.16, 40.69, 39.83, 38.54, 37.87, 37.38, 37.13, 33.25, 33.06, 30.74, 29.34, 29.16, 25.33, 24.95, 23.20, 22.95, 22.19, 19.85, 19.26, 12.33, 9.21.

Cholestanyl-O-((2,4-O-disulfonato-3-O-benzyl)-α-L-idopyranosyl uronate-α(1→4) (2-O-sulfonato-3-O-benzyl)-α-L-idopyranosyl uronate-α(1→4) (2-Osulfonato-3-O-benzyl)-α-L-idopyranosyl uronate-α(1→4) (2-Osulfonato-3-O-benzyl))-α-L-idopyranoside uronate32

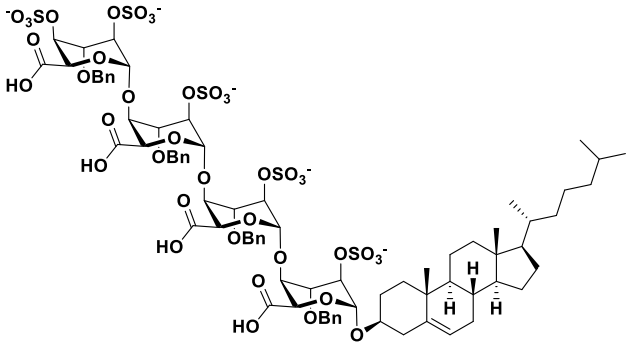

Sulfation: The sulfated compound **32 (75%)** obtained from the compound **31** by following the synthetic procedure **12**. ^{1}H NMR (400 MHz, Deuterium Oxide) δ 8.14 – 7.83 (m, 20H), 5.99 – 5.80 (m, 5H), 5.63 – 5.51 (m, 3H), 5.42 – 5.28 (m, 10H), 5.06 – 4.92 (m, 5H), 4.69 (s, 1H), 4.59 (s, 1H), 4.18 – 4.08 (m, 1H), 3.04 (d, *J* = 13.4 Hz, 1H), 2.84 – 2.78 (m, 1H), 2.58 – 2.37 (m, 5H), 2.17 – 2.06 (s, 6H), 1.99 – 1.83 (m, 7H), 1.80 – 1.67 (s, 6H), 1.60 – 1.52 (m, 9H), 1.44 (d, *J* = 7.1 Hz, 6H), 1.28 (s, 3H).

Cholesteryl-O-((2,4-O-disulfonato)-α-L-idopyranosyl uronate-α(1→4) (2-O-sulfonato)-α-L-idopyranosyl uronate-α(1→4) (2-Osulfonato)-α-L-idopyranosyl uronate-α(1→4) (2-Osulfonato))-α-L-idopyranoside uronate IAC-4

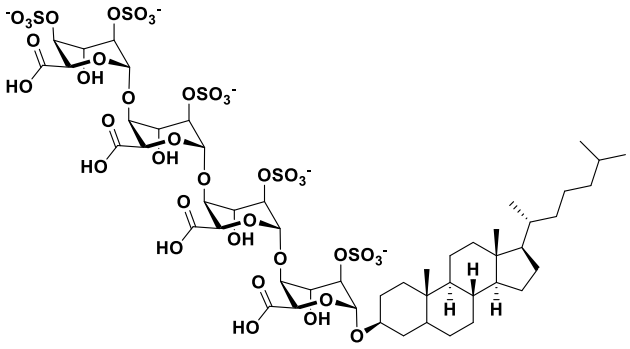

Hydrogenolysis: The compound **IAC-4 (80%)** wasobtainedfrom the compound **32** by following synthetic procedure **IAC-2.** ^{1}H NMR (400 MHz, Deuterium Oxide) δ 4.96 (t, *J* = 12.1 Hz, 4H), 4.65 (s, 2H), 4.43 – 4.26 (m, 2H), 4.00 – 3.81 (m, 9H), 3.49 – 3.38 (d, *J* = 22.3 Hz, 1H), 2.85 – 2.79 (m, 2H), 1.73 (d, *J* = 12.0 Hz, 1H), 1.62 – 1.39 (s, 5H), 1.36 -1.22 (m, 4H), 1.17 – 0.96 (m, 13H), 0.94 – 0.75 (m, 8H), 0.86 – 0.57 (m, 12H), 0.43 (s, 3H).

5.5.7 Synthesis of Idose Acceptor and Donor

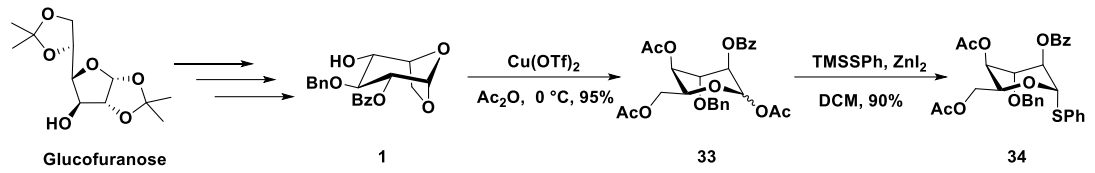

Scheme S1. Synthesis of Monosaccharides Building Block.

(1,3,6-O-triacetyl-2-O-benzoyl-3-O-benzyl)-α-L-idopyranoside 33

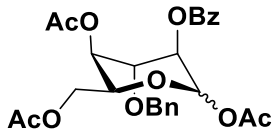

Compound **1** (9.7 g, 27.25 mmol) was dissolved in acetic anhydride (100 mL) and stirred for few 15 min at 0 °C, under nitrogen atmosphere, copper trifluromethanesulfonate (0.99 g, 2.72 mmol) was added. Allow the reaction flask to stir for 16 h, quench the reaction with $NaHCO_3$ and residue was extracted with EtOAc and the organic layer washed with water and brine solution, dried over Na_2SO_4 and concentrated under reduced pressure. The residue was purified by flash column chromatography (EtOAc/Hexane = 1/4) to afford anomeric mixture **33 (13 g, 95%)** as a solid. HRMS m/z calculated for $C_{26}H_{28}O_{10}Na$: 523.1580 found: 523.1577.

Thiophenyl-(4,6-O-diacetyl-2-O-benzoyl-3-O-benzyl)-α-L-idopyranoside34

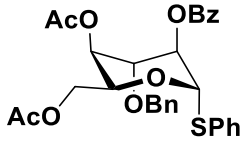

Compound **3** (12.6 g, 25.20 mmol), ZnI_2 (16.89 g, 52.92 mmol) and trimethyl(phenylthio)-silane (14.79 mL, 78.12 mmol) were dissolved in dry DCM (150 mL) under the nitrogen atmosphere and stirred at room temperature. After 16 h, reaction mixture was filtered through celite. The organic layer was washed with 0.1N HCl and $NaHCO_3$ followed by brine solution, dried over Na_2SO_4 and concentrated under reduced pressure. The residue was purified by flash column chromatography (EtOAc/Hexane = 1/1) to afford **4 (12.5 g, 90%)** as a sticky liquid. ^{1}H NMR (400 MHz, Chloroform-*d*) δ 8.08 – 8.05 (m, 2H), 7.59 – 7.55 (m, 3H), 7.48 – 7.37 (m, 6H), 7.34 – 7.25 (m, 4H), 5.62 (s, 1H), 5.45 – 5.45 (m, 1H), 5.10 (ddd, *J* = 7.3, 5.0, 1.6 Hz, 1H), 4.98 (t, *J* = 2.1 Hz, 1H), 4.92 (d, *J* = 11.8 Hz, 1H), 4.76 (d, *J* = 11.8 Hz, 1H), 4.27 (qd, *J* = 11.5, 6.4 Hz, 2H), 3.91 (dt, *J* = 3.6, 1.7 Hz, 1H), 2.04 (s, 3H), 1.95 (s, 3H). ^{13}C NMR (101 MHz, $CDCl_3$) δ 170.58, 170.05, 165.08, 137.13, 135.80, 133.61, 131.80, 129.84, 129.40, 128.95, 128.53, 128.46, 128.03,

127.72, 127.61, 86.06, 72.74, 71.74, 68.84, 67.04, 64.64, 62.96, 20.78, 20.75. HRMS m/z calculated for $C_{30}H_{30}O_8SNa$: 573.1559 found: 573.1554.

5.5.8 Synthesis of Cholestanol Conjugated Idose Disaccharide (IDC-2)

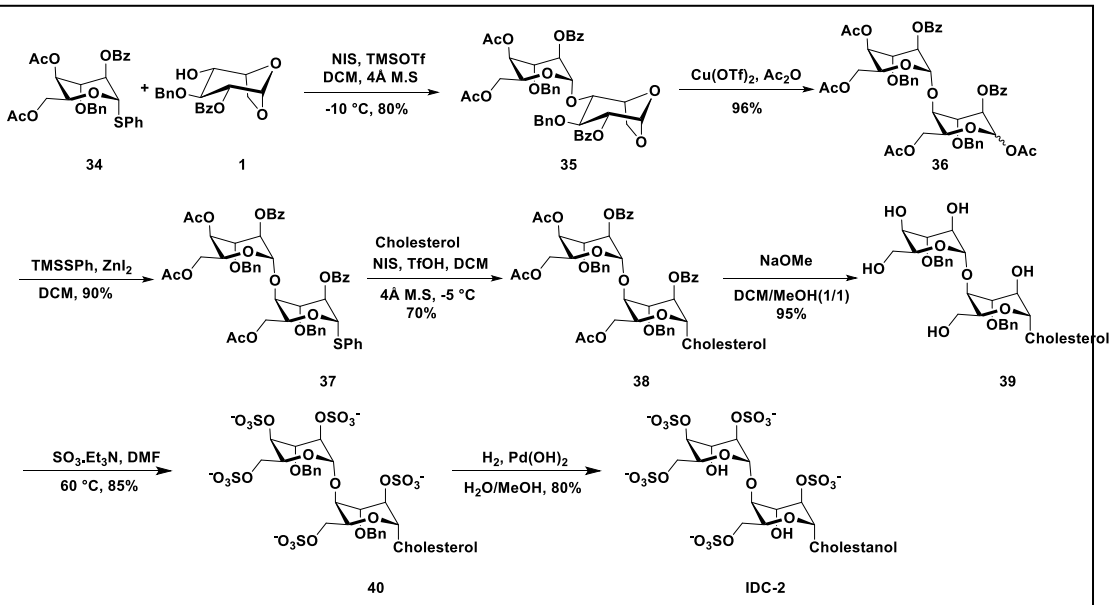

Scheme S2. Synthesis of Sulfated Disaccharide.

(4, 6-O-diacetyl-2-O-benzoyl-3-O-benzyl)-α-L-idopyrnosyl-α(1→4) (2-O-benzoyl-3-O-benzyl-1,6-anhydro)-β-L-idopyranose35

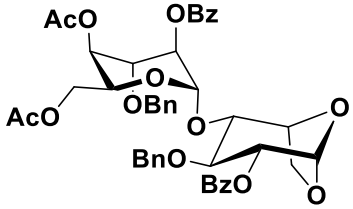

Compound **34** (12.23 g, 22.24 mmol), Compound **1** (8.71 g, 24.46 mmol), was dissolved in dry DCM (125 mL), and freshly dried 4 Å molecular sieves, were added under anhydrous conditions. After stirring for 1hr at RT, the reaction mixture was cooled to -10°C. *N*-Iodosuccinimide (7.51 g, 33.35 mmol) and TMSOTf (2.02 mL, 11.12 mmol) was added and monitored the reaction using TLC. After the completion of reaction, quenched with triethylamine and diluted with DCM. Filtered the molecular sieves using celite filter and washed with $NaHCO_3$, dried over Na_2SO_4, filtered and concentrated under reduced pressure. The residue was purified by column chromatography (EtOAc/Hexane = 1/4) to afford **35 (14 g, 70%)** as a sticky solid. ^{1}H NMR (400 MHz, Chloroform-*d*) δ 8.07 – 8.05 (m, 2H), 7.98 – 7.95 (m, 2H),

7.63 – 7.55 (m, 2H), 7.48 – 7.29 (m, 9H), 7.09 (dt, *J* = 4.5, 2.8 Hz, 3H), 7.03 (dd, *J* = 6.6, 3.0 Hz, 2H), 5.54 (d, *J* = 1.8 Hz, 1H), 5.16 (dt, *J* = 2.4, 1.0 Hz, 1H), 5.13 (s, 1H), 5.03 (dd, *J* = 8.3, 1.8 Hz, 1H), 4.90 (t, *J* = 2.2 Hz, 1H), 4.84 – 4.75 (m, 2H), 4.65 (t, *J* = 4.5 Hz, 2H), 4.61 – 4.49 (m, 2H), 4.24 – 4.20 (m, 2H), 4.04 – 4.02 (m, 2H), 3.91 (t, *J* = 8.4 Hz, 1H), 3.87 – 3.85 (m, 1H), 3.80 (ddd, *J* = 7.8, 5.0, 1.2 Hz, 1H), 2.00 (s, 3H), 1.97 (s, 3H). ^{13}C NMR (101 MHz, $CDCl_3$) δ 170.71, 170.22, 165.87, 165.40, 138.05, 137.37, 133.86, 133.43, 129.94, 129.88, 129.50, 129.32, 128.65, 128.62, 128.50, 128.23, 128.14, 127.91, 127.56, 99.48, 95.11, 78.04, 76.95, 75.16, 74.08, 72.78, 71.90, 67.33, 67.02, 65.66, 64.10, 62.65, 20.91, 20.86. HRMS m/z calculated for $C_{44}H_{44}O_{14}Na$: 819.2629 found: 819.2628.

(4,6-O-diacetyl-2-benzoyl-3-O-benzyl)-α-L-idopyranosyl-α(1→4) (1,6-O-diacetyl-2-O-benzoyl-3-O-benzyl)-α/β -L-idopyranoside 36

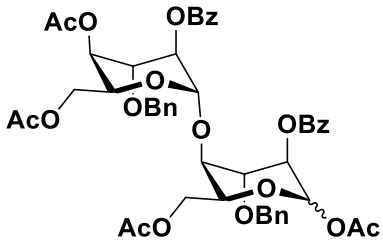

Compound **35** (13.67 g, 17.17 mmol) was dissolved in acetic anhydride (130 mL) and stirred for few min at 0 °C, under nitrogen atmosphere. After 15 min copper trifluromethanesulfonate (0.62 g, 1.72 mmol) was added. Allow the reaction flask to stir for another 16 h, quench the reaction with $NaHCO_3$ and residue was extracted with EtOAc and the organic layer washed with water and brine solution, dried over Na_2SO_4 and concentrated under reduced pressure. The residue was purified by flash column chromatography (EtOAc/Hexane = 1/2) to afford anomeric mixture **36 (14.9 g, 82%, α:β = 1:1)** as a white solid. ^{1}H NMR (400 MHz, Chloroform-*d*) δ 8.07 – 8.00 (m, 4H), 7.90 – 7.87 (m, 2H), 7.65 – 7.57 (m, 4H), 7.52 – 7.44 (m, 6H), 7.42 – 7.21 (m, 16H), 6.29 (s, 1H), 6.25 (d, *J* = 2.3 Hz, 1H), 5.52 (dd, *J* = 4.4, 2.3 Hz, 1H), 5.44 (d, *J* = 2.1 Hz, 1H), 5.30 – 5.22 (m, 2H), 5.07 (d, *J* = 14.0 Hz, 2H), 4.94 – 4.87 (m, 3H), 4.80 – 4.69 (m, 4H), 4.61 – 4.51 (m, 3H), 4.49 – 4.42 (m, 5H), 4.34 (t, *J* = 4.2 Hz, 1H), 4.21 – 4.24 (m, 1H), 3.93 – 3.81 (m, 5H), 3.57 (dd, *J* = 11.7, 4.2 Hz, 1H), 3.38 (dd, *J* = 11.7, 4.0 Hz, 1H), 2.14 (s, 4H), 2.09 (s, 6H), 1.99 (d, *J* = 1.3 Hz, 8H), 1.94 (s, 2H). ^{13}C NMR (101 MHz, $CDCl_3$) δ 170.70, 170.62, 170.58, 169.93, 169.03, 168.91, 165.98, 165.39, 165.10, 165.07, 137.68, 137.25, 137.21, 137.19, 133.68, 133.66, 133.53, 133.40, 130.14, 129.80, 129.78, 129.37, 129.34, 129.18, 128.80, 128.55, 128.54, 128.52, 128.50, 128.46, 128.41, 128.40, 128.28, 128.20, 128.18, 128.12, 128.00, 127.96, 127.84, 127.47, 101.81, 100.86, 91.80, 90.67, 76.62, 76.03, 75.36, 74.38, 73.58, 72.88,

72.65, 72.57, 72.47, 72.33, 67.68, 67.49, 67.33, 66.98, 66.78, 66.51, 66.49, 64.37, 64.03, 63.09, 62.96, 62.75, 62.32, 21.06, 20.97, 20.88, 20.85, 20.81, 20.61. HRMS m/z calculated for $C_{48}H_{50}O_{17}Na$: 921.2946 found: 921.2939.

Thiophenyl-((4,6-O-diacetyl-2-benzoyl-3-O-benzyl)-α-L-idopyranosyl-α(1→4) (6-O-acetyl-2-benzoyl-3-O-benzyl))-α-L-idopyranoside 37

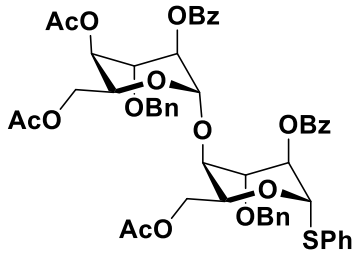

Compound **36** (14.73 g, 16.40 mmol), ZnI_2 (10.99 g, 34.45mmol) and trimethyl(phenylthio)-silane (9.63 mL, 50.85 mmol) were dissolved in dry DCM (170 mL) under the nitrogen atmosphere and stirred at room temperature. After 16 h, reaction mixture was filtered through celite. The organic layer was washed with 0.1N HCl and $NaHCO_3$ followed by brine solution, dried over Na_2SO_4 and concentrated under reduced pressure. The residue was purified by flash column chromatography (EtOAc/Hexane = 1/1) to afford **37 (14 g, 90%).** ^{1}H NMR (400 MHz, Chloroform-*d*) δ 8.04 – 8.01 (m, 2H), 7.94 – 7.91 (m, 2H), 7.58 (td, *J* = 7.4, 1.7 Hz, 3H), 7.50 – 7.42 (m, 7H), 7.37 – 7.20 (m, 11H), 5.64 (s, 1H), 5.60 (d, *J* = 3.0 Hz, 1H), 5.23 (s, 1H), 5.04 (s, 1H), 5.00 – 4.93 (m, 2H), 4.84 (dd, *J* = 11.3, 2.1 Hz, 1H), 4.68 (ddd, *J* = 20.8, 11.6, 2.4 Hz, 2H), 4.49 – 4.39 (m, 4H), 4.18 (d, *J* = 3.1 Hz, 1H), 3.82 (dp, *J* = 9.0, 2.5 Hz, 3H), 3.45 (dt, *J* = 12.0, 3.8 Hz, 1H), 2.03 (d, *J* = 1.3 Hz, 3H), 1.96 (d, *J* = 1.5 Hz, 3H), 1.91 (d, *J* = 1.7 Hz, 3H). ^{13}C NMR (101 MHz, $CDCl_3$) δ 170.62, 170.57, 169.91, 165.58, 165.11, 137.42, 137.22, 135.75, 133.65, 133.43, 131.71, 130.13, 129.80, 129.36, 129.14, 128.99, 128.55, 128.51, 128.46, 128.38, 128.27, 128.06, 127.99, 127.68, 127.57, 101.81, 86.10, 77.33, 74.34, 72.84, 72.60, 72.46, 68.73, 67.75, 66.95, 65.99, 64.33, 62.81, 62.78, 20.87, 20.81, 20.58. HRMS m/z calculated for $C_{52}H_{52}O_{15}SNa$: 971.2925 found: 971.2923.

Cholestanyl-O-((4,6-O-diacetyl-2-benzoyl-3-O-benzyl)-α-L-idopyranosyl-α(1→4) (6-O-acetyl-2-benzoyl-3-O-benzyl))-α-L-idopyranoside 38

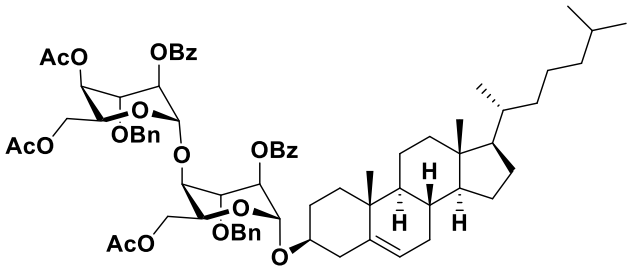

Compound **37** (1.87 g, 1.97 mmol), Cholesterol (0.83 g, 2.16 mmol) and freshly dried 4 Å molecular sieves were dissolved in dry DCM (20 mL) and stirred at RT for 1 h. Then *N*-iodosuccinimide (0.67 g, 2.96 mmol), TfOH (0.052 mL, 0.59 mmol) were added at -5°C and stirred for 30 min. After the completion of reaction, the reaction mixture was quenched with triethylamine and filtered through celite. The organic layer was washed with $Na_2S_2O_3$ followed by $NaHCO_3$, brine solution and dried over Na_2SO_4, then filtered and concentrated under reduced pressure. The residue was purified by column chromatography (EtOAc/Hexane = 1/4) to afford **38 (1.7 g, 70%)** as a sticky liquid. ^{1}H NMR (400 MHz, Chloroform-*d*) δ 8.04 – 8.01 (m, 2H), 7.91 – 7.89 (m, 2H), 7.60 – 7.53 (m, 3H), 7.45 (dt, *J* = 13.1, 7.5 Hz, 3H), 7.37 – 7.20 (m, 10H), 5.36 (q, *J* = 2.4 Hz, 2H), 5.23 – 5.22 (m, 1H), 5.12 (d, *J* = 1.9 Hz, 1H), 5.04 (s, 1H), 4.89 (t, *J* = 11.1 Hz, 2H), 4.66 (dd, *J* = 13.3, 11.4 Hz, 2H), 4.56 (td, *J* = 6.6, 2.3 Hz, 1H), 4.50 – 4.43 (m, 3H), 4.36 (dd, *J* = 11.2, 6.1 Hz, 1H), 4.09 (t, *J* = 3.2 Hz, 1H), 3.86 – 3.81 (m, 3H), 3.58 (tt, *J* = 11.1, 4.6 Hz, 1H), 3.44 (dd, *J* = 11.6, 4.2 Hz, 1H), 2.40 (ddd, *J* = 13.3, 4.7, 2.1 Hz, 1H), 2.31 – 2.24 (m, 1H), 2.04 (s, 3H), 1.95 (d, *J* = 1.5 Hz, 6H), 1.73 – 1.66 (m, 2H), 1.59 – 1.45 (m, 6H), 1.39 – 1.30 (m, 3H), 1.18 – 1.08 (m, 4H), 1.03 (s, 3H), 0.92 (d, *J* = 6.4 Hz, 3H), 0.87 (dd, *J* = 6.7, 1.8 Hz, 7H), 0.68 (s, 3H). ^{13}C NMR (101 MHz, $CDCl_3$) δ 170.75, 170.73, 170.04, 165.68, 165.18, 140.61, 138.16, 137.36, 133.68, 133.35, 130.12, 129.86, 129.47, 129.41, 128.56, 128.54, 128.40, 128.38, 128.12, 127.75, 127.66, 122.07, 101.34, 96.70, 77.68, 75.17, 72.56, 72.51, 72.35, 68.32, 67.64, 66.80, 65.20, 64.08, 63.05, 62.81, 56.87, 56.27, 50.34, 42.45, 39.90, 39.64, 38.62, 37.57, 36.93, 36.31, 35.91, 32.08, 32.02, 29.65, 28.36, 28.14, 24.42, 23.94, 22.95, 22.69, 21.21, 20.98, 20.88, 20.70, 19.53, 18.85, 11.99. HRMS m/z calculated for $C_{73}H_{92}O_{16}Na$: 1247.6283 found: 1247.6279.

Cholestanyl-O-(3-O-benzyl)-α-L-idopyranosyl-α(1→4)(3-O-benzyl))-α-L-idopyranoside 39

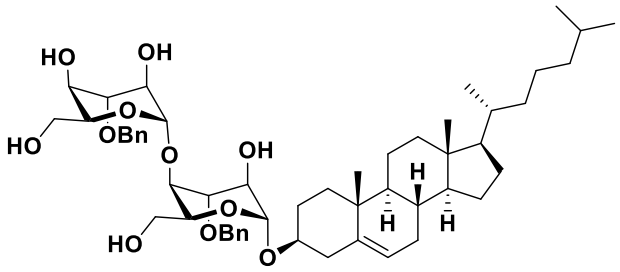

Compound **38** (0.64 g, 0.52 mmol) was dissolved in dry methanol (8 mL) and dry DCM (4 mL). NaOMe (0.14 g, 2.61 mmol) was added, under nitrogen atmosphere. After the completion of reaction, the reaction mixture neutralized with amberlite® IR 120 acid resin, filtered, and concentrated under reduced pressure. The residue was purified by flash column chromatography (EtOAc/Hexane = 1/1) to afford **39 (0.35 g, 95%)** as a white solid. ^{1}H NMR (400 MHz, Chloroform-*d*) δ 7.32 – 7.19 (m, 10H), 5.28 (d, *J* = 4.9 Hz, 1H), 4.87 (d, *J* = 3.0 Hz, 2H), 4.66 (d, *J* = 11.8 Hz, 1H), 4.53 – 4.43 (m, 4H), 4.25 (t, *J* = 6.7 Hz, 1H), 4.09 (d, *J* = 3.6 Hz, 1H), 3.91 – 3.80 (m, 3H), 3.73 – 3.49 (m, 11H), 3.42 (dq, *J* = 10.9, 5.5, 4.5 Hz, 1H), 2.31 (dt, *J* = 13.5, 3.0 Hz, 1H), 2.20 – 2.13 (m, 1H), 1.97 – 1.72 (m, 7H), 1.59 – 1.36 (m, 7H), 1.31 – 1.23 (m, 2H), 1.19 (s, 3H), 1.10 – 0.98 (m, 6H), 0.95 (s, 3H), 0.85 (d, *J* = 6.4 Hz, 3H), 0.80 (dd, *J* = 6.7, 1.8 Hz, 6H), 0.61 (s, 3H). ^{13}C NMR (101 MHz, $CDCl_3$) δ 140.81, 138.20, 137.25, 128.66, 128.50, 128.47, 128.30, 127.83, 127.72, 121.94, 103.26, 99.48, 77.23, 74.56, 74.26, 74.11, 72.71, 72.37, 71.11, 70.27, 66.81, 66.46, 66.19, 64.81, 61.85, 56.88, 56.29, 50.29, 42.46, 39.92, 39.65, 38.69, 37.52, 36.94, 36.33, 35.93, 32.10, 32.04, 29.83, 29.80, 28.38, 28.15, 24.44, 23.97, 22.96, 22.70, 21.21, 19.55, 18.87, 12.00. HRMS m/z calculated for $C_{53}H_{78}O_{11}Na$: 913.5442 found: 913.5438.

Cholestanyl-O-((2,4,6-O-trisulfonato-3-O-benzyl)-α-L-idopyranosyl-α(1→4) (2,6-O-disulfonato-3-O-benzyl))-α-L-idopyranoside 40

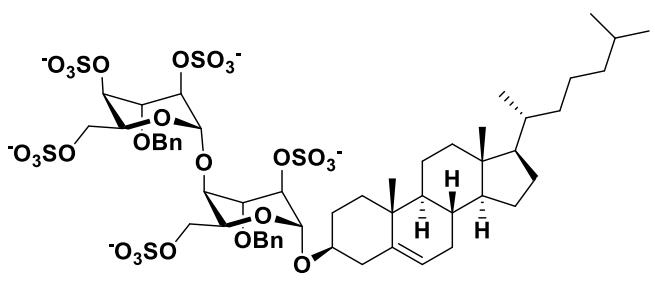

Compound **39** (0.12 g, 0.135 mmol) and $SO_3{\cdot}Et_3N$ (0.61 g, 3.37 mmol) was dissolved in dry, DMF (5 mL). Allowed the reaction flask stirred for 3 days at 60°C. After completion of reaction cool to room temperature add the aqueous solution of $NaHCO_3$ (0.57 g, 6.74 mmol) and kept it for another 16 h. Filtered the reaction mixture using what's man filter and wash with

DCM/MeOH (1/1, 10 mL), solvents were evaporated under reduced pressure and the resulting residue was purified by bond elute C-18 column eluted with mixture of solvent (water and acetonitrile). The product fraction was lyophilized to afford sulfated compounds **40 (0.15 g, 85%)** as a white powder. ^{1}H NMR (400 MHz, Deuterium Oxide, Temperature at 338) δ 7.94 – 7.70 (m, 10H), 5.82 (t, *J* = 20.4 Hz, 2H), 5.64 – 5.53 (m, 3H), 5.27 – 5.06 (m, 6H), 4.98 – 4.90 (m, 2H), 4.68 – 4.55 (m, 4H), 4.43 (s, 1H), 4.30 (dd, *J* = 14.8, 5.4 Hz, 1H), 4.30 – 3.94 (m,1H), 2.90 – 2.56 (m, 4H), 2.43 – 2.14 (s, 6H), 2.06 – 1.67 (m, 11H), 1.63 – 1.43 (m, 10), 1.36 – 1.25 (m, 9H), 1.11 (s, 3H). HRMS m/z calculated for $C_{53}H_{73}O_{26}S_5^{5-}$: 1285.3021 found (m/z + 5H): 258.0662.

Cholestanyl-O-((2,4,6-O-trisulfonato)-α-L-idopyranosyl-α(1→4) (2,6-O-disulfonato))-α-L-idopyranoside IDC-2

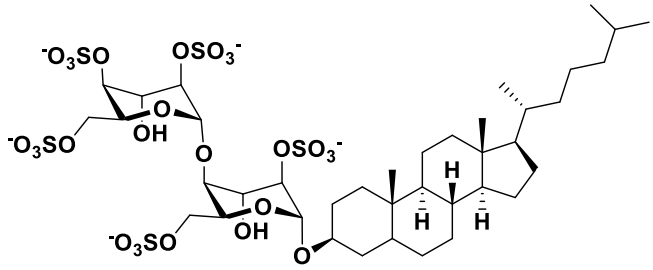

The compound **40** (0.05 g, 0.039 mmol) was dissolved in dry methanol (2 mL), 20% $Pd(OH)_2$ on carbon (0.11 g, 0.017 mmol) was added and purged with hydrogen gas, and the mixture was stirred at room temperature for 24 h. The residue was filtered and the filtrate was evaporated under reduced pressure and purified through a bond elute C-18 column eluted with water. The product fraction was lyophilized to afford compound **IDC-2 (**0.035 g, 57%). HRMS m/z calculated for $C_{39}H_{63}O_{26}S_5^{5-}$: 1107.2239 found: 222.4540.

5.5.9 Synthesis of Cholestanol Conjugated Idose Trisaccharide (IDC-3)

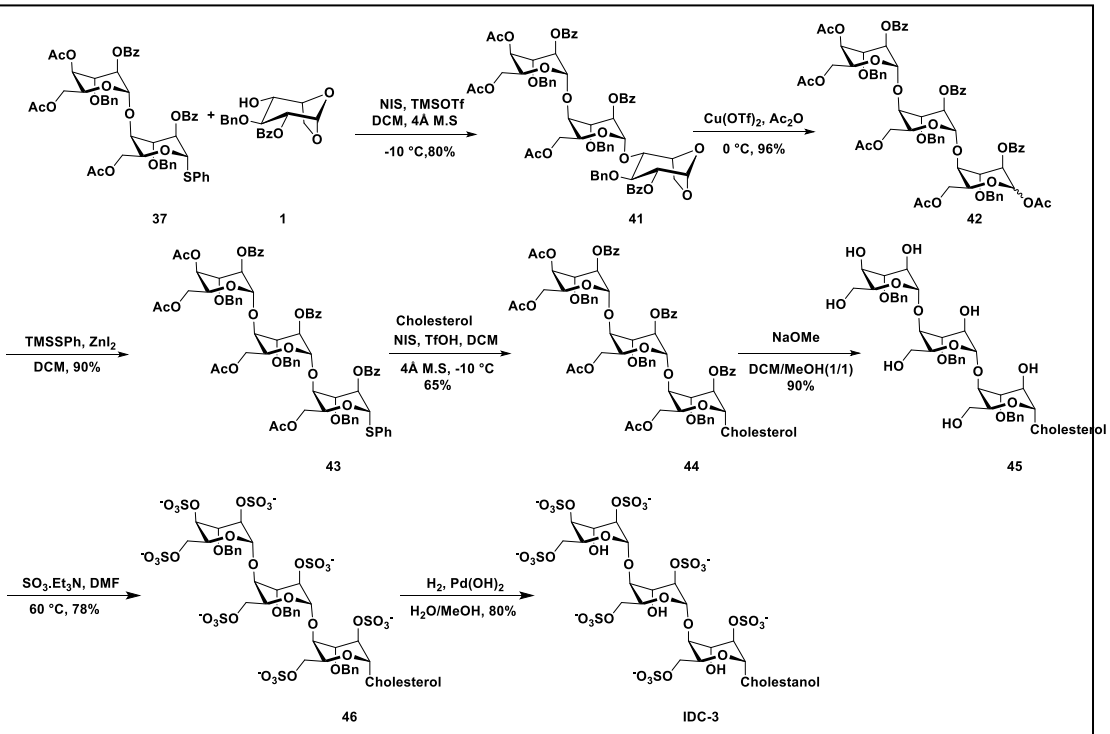

Scheme S3. Synthesis of Sulfated Trisaccharide.

(4, 6-O-diacetyl-2-O-benzoyl-3-O-benzyl)-α-L-idopyrnosyl-α(1→4) (6-O-acetyl-2-O-benzoyl-3-O-benzyl)-α-L-idopyrnosyl- α(1→4) (2-O-benzoyl-3-O-benzyl-1,6-anhydro)-β-L-idopyranose41

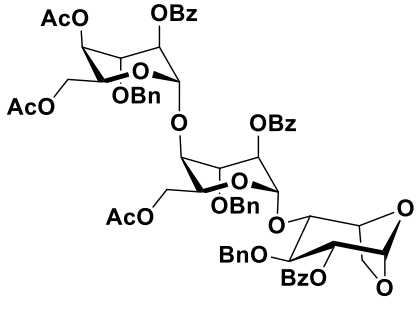

Glycosylation: The synthetic procedure for the preparation of compound **35** was followed to obtain compound **41 (80%)** from compound **37** and compound **1**. ^{1}H NMR (400 MHz, Chloroform-*d*) δ 8.08 – 8.05 (m, 2H), 7.95 (ddd, *J* = 15.5, 8.2, 1.4 Hz, 4H), 7.64 – 7.50 (m, 5H), 7.46 (dt, *J* = 15.7, 7.8 Hz, 4H), 7.35 (td, *J* = 9.3, 8.1, 2.7 Hz, 4H), 7.31 – 7.25 (m, 6H), 7.11 – 7.06 (m, 5H), 5.55 (d, *J* = 1.7 Hz, 1H), 5.38 (t, *J* = 2.4 Hz, 1H), 5.25 – 5.24 (m, 1H), 5.15 (s, 1H), 5.07 – 5.04 (m, 2H), 4.89 (dd, *J* = 17.6, 11.3 Hz, 2H), 4.77 – 4.67 (m, 4H), 4.63 (td, *J* = 6.4, 2.0 Hz, 1H), 4.59 (t, *J* = 2.1 Hz, 1H), 4.54 (d, *J* = 11.6 Hz, 1H), 4.51 – 4.48 (m, 1H), 4.37 (d, *J* = 6.4 Hz, 2H), 4.28 (dd, *J* = 8.4, 4.0 Hz, 1H), 4.19 (d, *J* = 7.8 Hz, 1H), 4.14

(t, *J* = 2.9 Hz, 1H), 3.94 – 3.86 (m, 4H), 3.74 – 3.71 (m, 1H), 3.55 (dd, *J* = 11.7, 4.5 Hz, 1H), 2.02 (s, 3H), 2.00 (s, 3H), 1.94 (s, 3H). ^{13}C NMR (101 MHz, $CDCl_3$) δ 170.74, 170.58, 169.99, 165.82, 165.65, 165.12, 138.13, 137.55, 137.25, 133.70, 133.60, 133.32, 130.05, 129.92, 129.82, 129.49, 129.37, 128.96, 128.54, 128.51, 128.50, 128.48, 128.41, 128.33, 128.14, 128.07, 127.86, 127.39, 101.15, 99.43, 95.64, 77.84, 76.68, 76.58, 75.18, 75.03, 74.53, 73.11, 72.62, 72.47, 71.96, 68.26, 67.50, 66.70, 65.79, 65.53, 64.10, 62.90, 62.40, 20.91, 20.84, 20.60. HRMS m/z calculated for $C_{66}H_{66}O_{21}Na$: 1217.3994 found: 1217.1989.

(4, 6-O-diacetyl-2-O-benzoyl-3-O-benzyl)-α-L-idopyrnosyl-α(1→4) (6-O-acetyl-2-O-benzoyl-3-O-benzyl)-α-L-idopyrnosyl- α(1→4) (1,6-diacetyl-2-O-benzoyl-3-O-benzyl)-α/β-L-idopyranose42

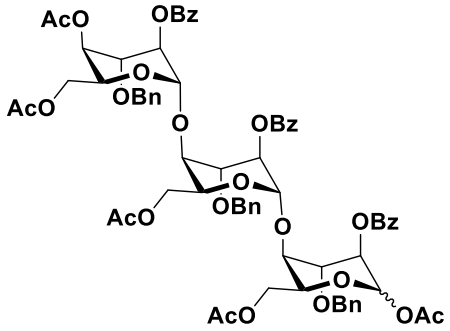

Acetolysis: Using synthetic procedure **36**, the compound **41** was kept for acetolysis, to obtained anomeric mixture of compound **42 (96%)**. ^{1}H NMR (400 MHz, Chloroform-*d*) δ 8.05 – 8.03 (m, 6H), 7.96 – 7.93 (m, 6H), 7.61 (t, *J* = 7.4 Hz, 2H), 7.53 – 7.43 (m, 12H), 7.42 – 7.2 (m, 32H), 6.25 – 6.23 (m, 2H), 5.44 (dd, *J* = 4.5, 2.3 Hz, 1H), 5.40 (t, *J* = 3.1 Hz, 1H), 5.36 – 5.33 (m, 2H), 5.15 (dt, *J* = 4.5, 2.0 Hz, 2H), 5.04 (d, *J* = 2.3 Hz, 2H), 4.87 (ddd, *J* = 19.7, 14.2, 10.4 Hz, 7H), 4.77 (dd, *J* = 7.8, 4.0 Hz, 2H), 4.74 – 4.60 (m, 6H), 4.55 (td, *J* = 6.6, 2.1 Hz, 1H), 4.47 (ddt, *J* = 8.2, 4.4, 1.7 Hz, 2H), 4.43 – 4.34 (m, 5H), 4.32 – 4.25 (m, 2H), 4.21 – 4.10 (m, 4H), 4.04 (dq, *J* = 9.0, 4.8, 4.4 Hz, 3H), 3.92 – 3.83 (m, 7H), 3.58 (ddd, *J* = 11.6, 4.5, 1.4 Hz, 3H), 3.45 (t, *J* = 3.4 Hz, 1H), 2.13 (s, 3H), 2.07 (s, 2H), 2.06 (s, 1H), 2.00 (s, 3H), 1.99 (s, 3H), 1.97 (d, *J* = 3.1 Hz, 5H), 1.93 – 1.92 (m, 8H), 1.90 (s, 2H). ^{13}C NMR (101 MHz, $CDCl_3$) δ 170.56, 170.54, 170.51, 170.48, 170.47, 170.42, 169.94, 169.93, 169.02, 168.90, 165.90, 165.45, 165.34, 165.30, 165.03, 165.00, 137.69, 137.47, 137.43, 137.31, 137.22, 133.66, 133.41, 133.38, 133.26, 133.20, 130.23, 130.20, 129.99, 129.77, 129.34, 129.31, 129.09, 129.04, 128.70, 128.53, 128.50, 128.44, 128.42, 128.38, 128.35, 128.28, 128.23, 128.21, 128.07, 128.04, 128.01, 127.94, 127.83, 127.53, 101.52, 100.69, 100.52, 91.71, 90.65, 76.72, 76.68, 75.85, 75.32, 75.28, 75.03, 74.88, 73.73, 73.37, 72.97, 72.94, 72.59, 72.53, 72.48, 72.41, 72.35, 68.63, 68.04, 67.49, 67.39, 67.29, 66.83, 66.78, 66.72, 66.50, 66.46, 66.02, 64.15, 64.09, 62.90, 62.79, 62.75, 62.33, 62.28, 60.41, 21.08, 21.04, 20.96,

20.78, 20.75, 20.71, 20.66, 20.59, 20.56.HRMS m/z calculated for $C_{70}H_{72}O_{24}Na$: 1319.4311 found: 1319.4307.

Thiophenyl-((4,6-O-diacetyl-2-benzoyl-3-O-benzyl)-α-L-idopyranosyl-α(1→4) (6-O-acetyl-2-benzoyl-3-O-benzyl)-α-L-idopyranosyl-α(1→4) (6-O-acetyl-2-benzoyl-3-O-benzyl))-α-L-idopyranoside 43

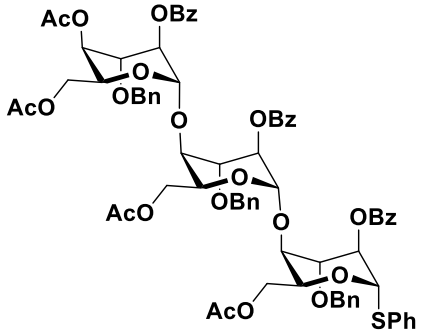

Thioglycosylation: The preparation of the thioglycosylated compound **43 (90%)** was carried out from compound **42** according to the procedure used for synthesizing compound **37.** ^{1}H NMR (400 MHz, Chloroform-*d*) δ 8.04 (ddd, *J* = 15.2, 8.3, 1.4 Hz, 4H), 7.96 – 7.94 (m, 2H), 7.64 – 7.60 (m, 3H), 7.55 – 7.43 (m, 9H), 7.40 – 7.26 (m, 15H), 7.24 – 7.18 (m, 3H), 5.59 (dd, *J* = 5.2, 2.8 Hz, 2H), 5.36 (t, *J* = 3.8 Hz, 1H), 5.16 – 5.15 (m, 1H), 5.04 (d, *J* = 3.4 Hz, 1H), 5.00 – 4.95 (m, 2H), 4.91 (s, 1H), 4.79 (ddd, *J* = 34.8, 15.4, 11.4 Hz, 4H), 4.66 – 4.63 (m, 2H), 4.52 – 4.48 (m, 1H), 4.42 – 4.35 (m, 2H), 4.29 (ddd, *J* = 10.5, 5.7, 3.0 Hz, 1H), 4.21 (d, *J* = 2.8 Hz, 1H), 4.16 (dd, *J* = 11.6, 7.5 Hz, 1H), 4.00 (dt, *J* = 13.5, 5.1 Hz, 2H), 3.91 – 3.84 (m, 2H), 3.81 (t, *J* = 2.5 Hz, 1H), 3.62 (dd, *J* = 11.6, 4.6 Hz, 1H), 3.55 (t, *J* = 3.8 Hz, 1H), 1.98 (d, *J* = 3.2 Hz, 6H), 1.91 (d, *J* = 3.6 Hz, 6H). ^{13}C NMR (101 MHz, $CDCl_3$) δ 170.55, 170.42, 170.37, 169.94, 165.64, 165.28, 165.01, 137.47, 137.43, 137.17, 135.82, 133.65, 133.35, 133.16, 131.72, 130.17, 129.97, 129.76, 129.39, 129.31, 129.12, 128.91, 128.54, 128.49, 128.45, 128.38, 128.30, 128.28, 128.18, 128.10, 128.07, 127.97, 127.82, 127.73, 127.48, 101.25, 100.17, 86.01, 76.50, 76.43, 75.30, 73.64, 73.01, 72.59, 72.44, 68.97, 68.69, 67.34, 66.75, 66.62, 65.99, 64.05, 62.85, 62.74, 61.93, 20.78, 20.74, 20.64, 20.58. HRMS m/z calculated for $C_{74}H_{74}O_{22}SNa$: 1369.4290 found: 1369.4286.

Cholestanyl-O-((4,6-O-diacetyl-2-benzoyl-3-O-benzyl)-α-L-idopyranosyl-α(1→4) (6-O-acetyl-2-benzoyl-3-O-benzyl)-α-L-idopyranosyl-α(1→4) (6-O-acetyl-2-benzoyl-3-O-benzyl))-α-L-idopyranoside 44

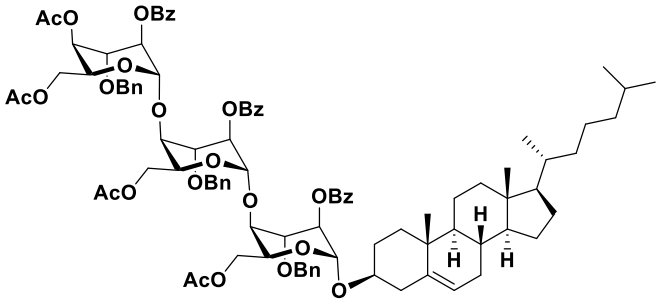

Glycosylation: The cholesterol conjugated product **44 (65%)** was obtained from the compound **43** using synthetic procedure **38.** ^{1}H NMR (400 MHz, Chloroform-*d*) δ 8.05 – 8.03 (m, 2H), 7.99 – 7.96 (m, 2H), 7.94 – 7.91 (m, 2H), 7.63 – 7.59 (m, 1H), 7.48 (pd, *J* = 8.1, 7.3, 3.0 Hz, 6H), 7.39 (dt, *J* = 7.9, 1.5 Hz, 4H), 7.34 – 7.21 (m, 13H), 5.39 – 5.35 (m, 2H), 5.30 (t, *J* = 2.4 Hz, 1H), 5.14 (t, *J* = 1.9 Hz, 1H), 5.11 (d, *J* = 1.9 Hz, 1H), 5.03 (d, *J* = 2.7 Hz, 1H), 4.92 (d, *J* = 11.3 Hz, 2H), 4.86 (dd, *J* = 11.3, 4.4 Hz, 2H), 4.71 (d, *J* = 2.0 Hz, 1H), 4.69 – 4.65 (m, 2H), 4.59 (t, *J* = 2.2 Hz, 1H), 4.55 (ddd, *J* = 7.8, 5.7, 2.2 Hz, 1H), 4.49 – 4.45 (m, 1H), 4.40 (dd, *J* = 11.4, 7.4 Hz, 1H), 4.34 – 4.27 (m, 2H), 4.14 (dd, *J* = 11.5, 7.7 Hz, 1H), 4.09 (t, *J* = 3.4 Hz, 1H), 4.04 (t, *J* = 3.9 Hz, 1H), 3.97 (dd, *J* = 11.6, 5.3 Hz, 1H), 3.89 – 3.81 (m, 3H), 3.60 – 3.51 (m, 3H), 2.39 (ddd, *J* = 13.5, 4.9, 2.1 Hz, 1H), 2.31 – 2.24 (m, 1H), 1.97 (d, *J* = 5.3 Hz, 8H), 1.91 (s, 6H), 1.68 (q, *J* = 7.4, 4.1 Hz, 3H), 1.61 – 1.45 (m, 7H), 1.40 – 1.34 (m, 3H), 1.30 – 1.27 (m, 2H), 1.22 – 1.08 (m, 8H), 1.04 (s, 3H), 0.94 (d, *J* = 6.5 Hz, 4H), 0.90 (d, *J* = 1.7 Hz, 3H), 0.88 (d, *J* = 1.7 Hz, 3H), 0.70 (s, 3H). ^{13}C NMR (101 MHz, $CDCl_3$) δ 170.69, 170.62, 170.56, 170.03, 165.76, 165.45, 165.09, 140.64, 138.21, 137.61, 137.29, 133.72, 133.43, 133.12, 130.23, 130.10, 129.87, 129.66, 129.44, 129.22, 128.58, 128.53, 128.45, 128.39, 128.33, 128.31, 128.30, 128.14, 127.97, 127.73, 122.02, 101.00, 100.74, 96.66, 77.75, 77.36, 76.45, 75.17, 74.66, 73.04, 72.62, 72.46, 72.21, 68.37, 68.35, 67.56, 66.77, 66.11, 65.32, 64.16, 62.91, 62.82, 62.32, 56.88, 56.28, 50.34, 42.46, 39.91, 39.65, 38.63, 37.58, 36.92, 36.32, 35.92, 32.08, 32.03, 29.64, 28.37, 28.15, 24.43, 23.96, 22.96, 22.70, 21.21, 20.89, 20.76, 20.68, 19.53, 18.86, 11.99. HRMS m/z calculated for $C_{95}H_{114}O_{23}Na$: 1645.7649 found: 1645.7643.

Cholestanyl-O-((3-O-benzyl)-α-L-idopyranosyl-α(1→4) (3-O-benzyl)-α-L-idopyranosyl-α(1→4) (3-O-benzyl))-α-L-idopyranoside 45

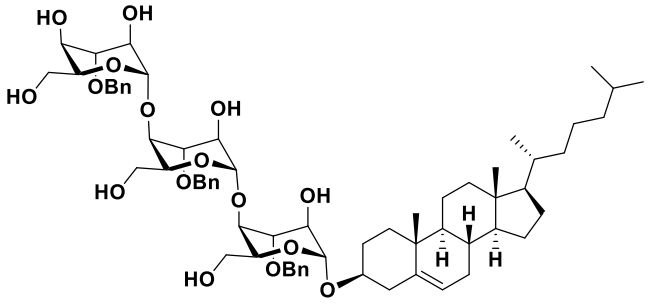

Deprotection: Esters deprotection was carried out for the compound **44** by following synthetic procedure **39** to obtain the compound **45 (90%)**. ^{1}H NMR (400 MHz, Chloroform-*d*) δ 7.32 (d, *J* = 7.0 Hz, 2H), 7.29 – 7.19 (m, 14H), 5.28 (d, *J* = 4.9 Hz, 1H), 4.91 (s, 1H), 4.83 (s, 1H), 4.71 – 4.67 (m, 2H), 4.53 (s, 2H), 4.46 (d, *J* = 12.6 Hz, 4H), 4.30 (p, *J* = 7.9, 6.9 Hz, 3H), 4.07 (dd, *J* = 15.3, 11.7 Hz, 2H), 3.93 (d, *J* = 3.7 Hz, 1H), 3.81 – 3.69 (m, 6H), 3.59 – 3.37 (m, 11H), 3.00 (s, 1H), 2.82 (s, 1H), 2.32 (ddd, *J* = 13.3, 4.8, 2.0 Hz, 1H), 2.21 – 2.08 (m, 4H), 1.97 – 1.73 (m, 5H), 1.62 – 1.36 (m, 7H), 1.34 – 1.26 (m, 3H), 1.19 (s, 2H), 1.11 – 1.01 (m, 6H), 0.95 (s, 3H), 0.85 (d, *J* = 6.4 Hz, 3H), 0.80 (dd, *J* = 6.6, 1.8 Hz, 6H), 0.61 (s, 3H). ^{13}C NMR (101 MHz, $CDCl_3$) δ 140.78, 138.33, 137.19, 137.15, 128.70, 128.68, 128.45, 128.35, 127.79, 127.66, 121.95, 103.17, 103.13, 99.36, 77.36, 74.87, 74.30, 74.15, 73.29, 72.79, 72.76, 72.00, 71.33, 70.08, 66.91, 66.88, 66.61, 66.45, 66.38, 66.20, 64.63, 62.20, 61.29, 56.87, 56.28, 50.28, 42.46, 39.91, 39.65, 38.67, 37.51, 36.94, 36.33, 35.93, 32.09, 32.03, 29.80, 28.37, 28.15, 24.43, 23.97, 22.96, 22.70, 21.20, 19.54, 18.86, 11.99. HRMS m/z calculated for $C_{66}H_{94}O_{16}Na$: 1165.6440 found: 1165.6438.

Cholestanyl-O-((2,4,6-O-trisulfonato-3-O-benzyl)-α-L-idopyranosyl-α(1→4) (2,6-O-disulfonato-3-O-benzyl)-α-L-idopyranosyl-α(1→4) (2,6-O-disulfonato-3-O-benzyl))-α-L-idopyranoside 46

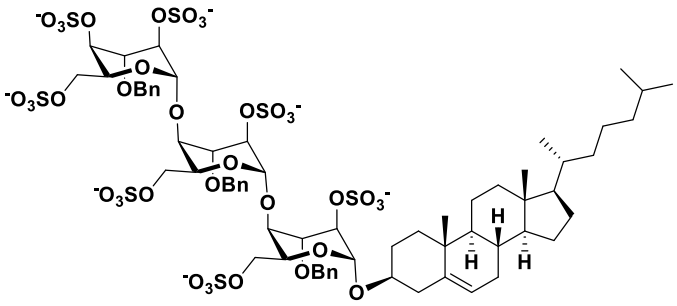

Sulfation: The sulfated compound **46 (78%)** obtained from the compound **45** by following the synthetic procedure **40.** ^{1}H NMR (400 MHz, Deuterium Oxide, Temperature at 318K) δ 7.58 – 7.35 (m, 15H), 5.49 (s, 1H), 5.27 (s, 1H), 5.14 (s, 1H), 5.02 (s, 1H), 4.89 – 4.73 (m, 7H), 4.50 – 4.42 (m, 4H), 4.31 – 4.11 (m, 9H), 3.82 (d, *J*

= 20.8 Hz, 2H), 3.65 – 3.59 (m, 1H), 2.48 (d, *J* = 13.0 Hz, 1H), 2.29 (t, *J* = 13.5 Hz, 1H), 2.04 – 1.91 (m, 5H), 1.63 – 1.31 (m, 11H), 1.22 – 1.03 (m, 12H), 0.97 (d, *J* = 6.3 Hz, 4H), 0.87 (d, *J* = 6.6 Hz, 6H), 0.74 (s, 3H). HRMS m/z calculated for $C_{66}H_{87}O_{37}S_7^{7-}$: 1695.3010 found: 242.1850.

Cholestanyl-O-((2,4,6-O-trisulfonato)-α-L-idopyranosyl-α(1→4) (2,6-O-disulfonato)-α-L-idopyranosyl-α(1→4) (2,6-O-disulfonato))-α-L-idopyranoside IDC-3

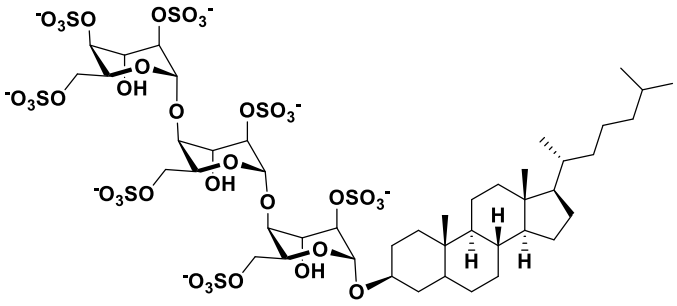

Hydrogenolysis: The compound **IDC-3 (80%)** was obtained from the compound **46** by following synthetic procedure **IDC-2.** ^{1}H NMR (400 MHz, Deuterium Oxide) δ 5.40 (d, *J* = 11.5 Hz, 1H), 5.18 (s, 2H), 5.00 – 4.85 (m, 2H), 4.60 – 4.41 (m, 6H), 4.35 – 4.13 (m, 3H), 4.05 (d, *J* = 15.4 Hz, 3H), 3.98 – 3.72 (m, 3H), 2.24 (bs, 1H), 2.16 – 1.90 (m, 5H), 1.83 – 1.73 (m, 4H), 1.62 – 1.50 (m, 9H), 1.40 – 1.25 (m, 10H), 1.19 – 1.18 (m, 4H), 1.13 (d, *J* = 6.0 Hz, 6H), 1.07 (s, 3H), 0.93 (s, 3H). HRMS m/z calculated for $C_{45}H_{71}O_{37}S_7^{7-}$: 1427.1758 found: 203.8819.

5.5.10 Synthesis of Cholestanol Conjugated Idose Tetrasaccharide (IDC-4):

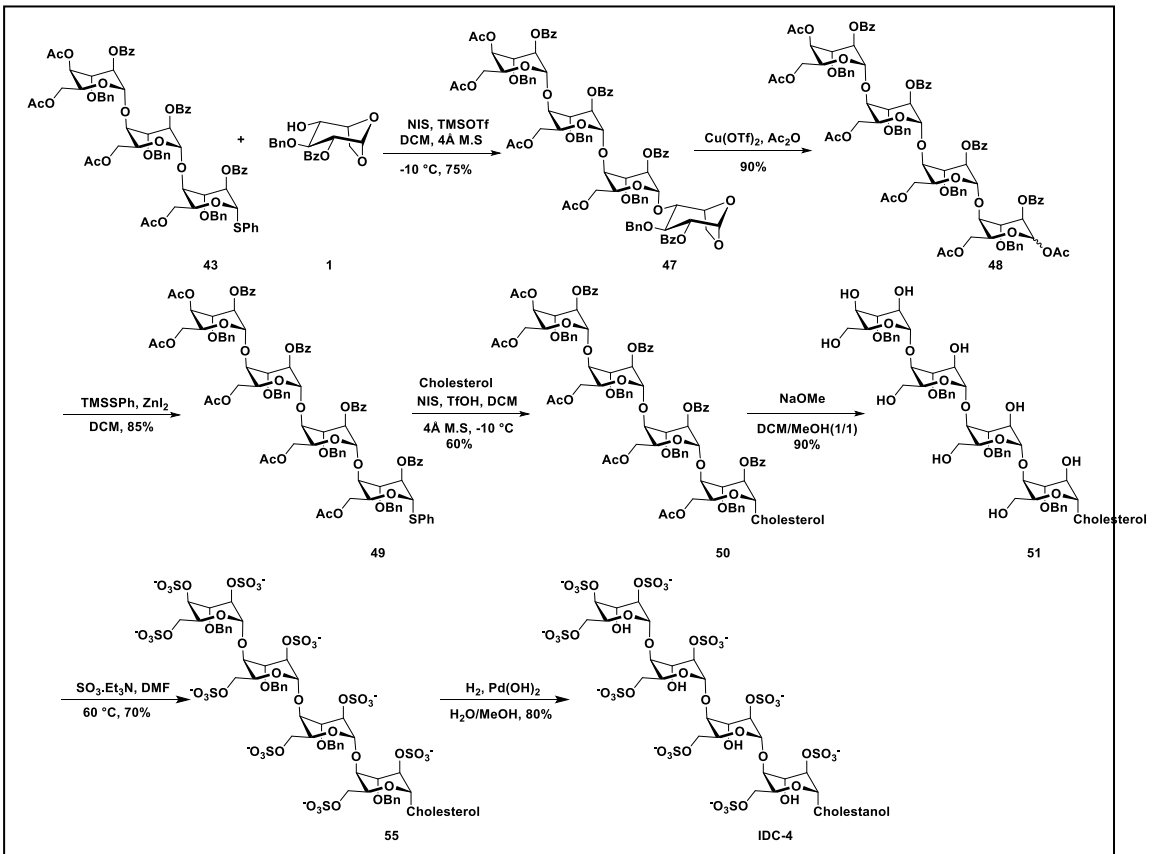

Scheme S4. Synthesis of Sulfated Tetrasaccharide.

(4, 6-O-diacetyl-2-O-benzoyl-3-O-benzyl)-α-L-idopyrnosyl-α(1→4) (6-O-acetyl-2-O-benzoyl-3-O-benzyl)-α-L-idopyrnosyl-α(1→4) (6-O-acetyl-2-O-benzoyl-3-O-benzyl)-α-L-idopyrnosyl- α(1→4) (2-O-benzoyl-3-O-benzyl-1,6-anhydro)-β-L-idopyranose47

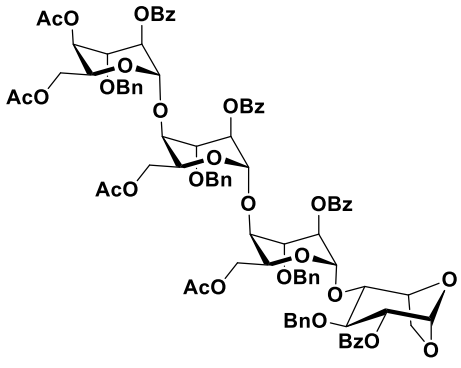

Glycosylation: The synthetic procedure for the preparation of compound **35** was followed to obtain compound **47 (75%)** from compound **43** and compound **1**. ^{1}H NMR (400 MHz, Chloroform-*d*) δ 8.02 (dd, *J* = 8.2, 1.5 Hz, 2H), 7.95 – 7.91 (m, 6H), 7.62 – 7.54 (m, 2H), 7.52 – 7.41 (m, 8H), 7.39 – 7.32 (m, 4H), 7.31 – 7.20 (m, 14H), 7.07 (s, 4H), 5.51 (d, *J* = 1.7 Hz, 1H), 5.36 (t, *J* = 2.9 Hz, 1H), 5.28 (t, *J* =

2.6 Hz, 1H), 5.15 – 5.14 (m, 1H), 5.10 (s, 1H), 5.02 – 4.99 (m, 2H), 4.91 (s, 1H), 4.87 – 4.81 (m, 3H), 4.77 – 4.62 (m, 5H), 4.59 – 4.52 (m, 3H), 4.47 – 4.44 (m, 1H), 4.34 (tt, *J* = 6.6, 3.2 Hz, 1H), 4.24 (ddd, *J* = 21.1, 8.1, 4.6 Hz, 3H), 4.16 – 4.08 (m, 3H), 4.04 (t, *J* = 3.7 Hz, 1H), 3.99 (dd, *J* = 11.6, 5.4 Hz, 1H), 3.91 – 3.81 (m, 4H), 3.69 – 3.66 (m, 1H), 3.56 (td, *J* = 6.3, 5.1, 3.3 Hz, 2H), 1.95 (s, 3H), 1.91 (d, *J* = 5.6 Hz, 6H), 1.85 (s, 3H). ^{13}C NMR (101 MHz, $CDCl_3$) δ 170.56, 170.53, 170.41, 169.92, 165.78, 165.66, 165.35, 165.00, 138.13, 137.52, 137.42, 137.19, 133.64, 133.39, 133.30, 133.25, 130.08, 130.04, 130.00, 129.87, 129.78, 129.75, 129.44, 129.30, 129.11, 129.04, 128.47, 128.42, 128.37, 128.34, 128.25, 128.21, 128.18, 128.03, 127.99, 127.92, 127.84, 127.78, 127.41, 127.34, 100.85, 100.73, 99.35, 95.50, 77.73, 77.29, 76.66, 76.60, 75.86, 74.97, 74.94, 74.63, 74.61, 72.97, 72.82, 72.52, 72.40, 71.92, 68.21, 68.11, 67.47, 66.72, 65.99, 65.94, 65.45, 64.13, 62.76, 62.37, 62.14, 20.77, 20.59, 20.57. HRMS m/z calculated for $C_{88}H_{88}O_{28}Na$: 1615.5360 found: 1615.5358.

(4, 6-O-diacetyl-2-O-benzoyl-3-O-benzyl)-α-L-idopyrnosyl-α(1→4) (6-O-acetyl-2-O-benzoyl-3-O-benzyl)-α-L-idopyrnosyl-α(1→4) (6-O-acetyl-2-O-benzoyl-3-O-benzyl)-α-L-idopyrnosyl- α(1→4) (1,6-O-diacetoxy-2-O-benzoyl-3-O-benzyl)-β-L-idopyranose47

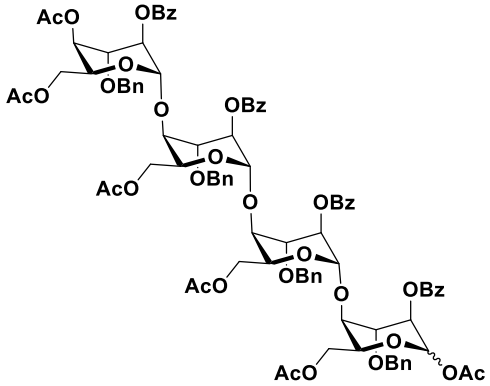

Acetolysis: Using synthetic procedure **36**, the compound **47** was kept for acetolysis, to obtained anomeric mixture of compound **48 (90%)**. ^{1}H NMR (400 MHz, Chloroform-*d*) δ 8.05 (dd, *J* = 6.7, 1.6 Hz, 6H), 7.99 – 7.91 (m, 9H), 7.62 (t, *J* = 7.6 Hz, 2H), 7.53 – 7.45 (m, 15H), 7.41 – 7.18 (m, 48H), 6.24 – 6.22 (m, 2H), 5.43 (dd, *J* = 4.6, 2.3 Hz, 1H), 5.35 – 5.24 (m, 5H), 5.17 – 5.16 (m, 2H), 5.08 – 5.00 (m, 2H), 4.91 (d, *J* = 11.1 Hz, 3H), 4.87 (d, *J* = 3.1 Hz, 2H), 4.84 – 4.81 (m, 3H), 4.79 – 4.75 (m, 3H), 4.73 – 4.59 (m, 9H), 4.52 (qd, *J* = 7.6, 7.1, 3.0 Hz, 2H), 4.47 – 4.24 (m, 12H), 4.19 – 3.94 (m, 11H), 3.90 – 3.78 (m, 7H), 3.60 – 3.53 (m, 4H), 3.44 (t, *J* = 3.5 Hz, 1H), 2.12 (s, 3H), 2.11 (s, 1H), 2.07 (s, 2H), 2.02 – 2.00 (m, 6H), 1.99 – 1.95 (m, 8H), 1.91 (d, *J* = 1.9 Hz, 5H), 1.88 (s, 3H), 1.85 (s, 6H). ^{13}C NMR (101 MHz, $CDCl_3$) δ 170.62, 170.54, 170.52, 170.50, 170.40, 170.37, 169.99, 169.83, 169.11, 169.00, 165.99, 165.51, 165.46, 165.41, 165.37, 165.09, 137.79, 137.57, 137.55, 137.51, 137.40, 137.34, 137.27, 134.03, 133.73, 133.46, 133.34, 133.27, 133.25,

133.23, 130.29, 130.22, 130.15, 130.08, 129.85, 129.44, 129.38, 129.36, 129.18, 129.14, 129.12, 128.77, 128.57, 128.52, 128.48, 128.45, 128.41, 128.39, 128.36, 128.33, 128.27, 128.18, 128.13, 128.10, 128.03, 127.96, 127.93, 127.89, 127.86, 127.69, 127.57, 101.43, 100.80, 100.67, 100.54, 100.39, 100.29, 91.76, 90.72, 77.36, 76.63, 76.61, 76.02, 75.97, 75.85, 75.39, 75.15, 75.08, 74.83, 74.53, 73.89, 73.43, 73.03, 72.90, 72.66, 72.62, 72.57, 72.48, 72.45, 68.61, 68.40, 68.28, 68.09, 67.59, 67.35, 66.98, 66.96, 66.91, 66.82, 66.60, 66.56, 66.24, 66.13, 66.05, 65.97, 64.33, 64.28, 64.23, 62.93, 62.88, 62.87, 62.81, 62.79, 62.39, 62.19, 21.14, 21.11, 21.04, 20.85, 20.82, 20.77, 20.73, 20.69, 20.67, 20.64. HRMS m/z calculated for $C_{92}H_{94}O_{31}Na$: 1717.5677 found: 1717.5669.

Thiophenyl-((4, 6-O-diacetyl-2-O-benzoyl-3-O-benzyl)-α-L-idopyrnosyl-α(1→4) (6-O-acetyl-2-O-benzoyl-3-O-benzyl)-α-L-idopyrnosyl-α(1→4) (6-O-acetyl-2-O-benzoyl-3-O-benzyl)-α-L-idopyrnosyl- α(1→4) (6-O-acetoxy-2-O-benzoyl-3-O-benzyl))-α-L-idopyranose49

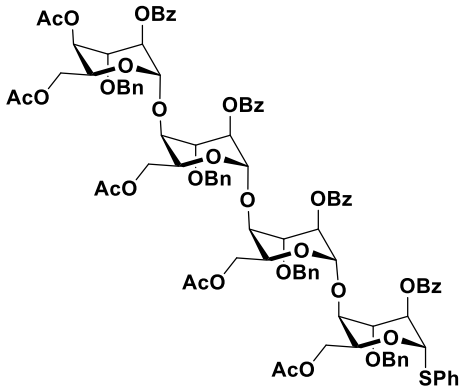

Thioglycosylation: The preparation of the thioglycosylated compound **49 (85%)** was carried out from compound **48** according to the procedure used for synthesizing compound **37.** ^{1}H NMR (400 MHz, Chloroform-*d*) δ 7.93 (td, *J* = 8.3, 1.4 Hz, 4H), 7.84 (ddd, *J* = 16.4, 8.2, 1.4 Hz, 4H), 7.53 – 7.47 (m, 3H), 7.43 – 7.34 (m, 9H), 7.27 – 7.14 (m, 20H), 7.12 – 7.04 (m, 5H), 5.47 – 5.45 (m, 2H), 5.19 (dt, *J* = 7.6, 3.3 Hz, 2H), 5.07 (t, *J* = 2.0 Hz, 1H), 4.89 (d, *J* = 3.5 Hz, 1H), 4.85 (d, *J* = 11.6 Hz, 3H), 4.79 – 4.71 (m, 3H), 4.69 – 4.55 (m, 5H), 4.48 (t, *J* = 2.3 Hz, 1H), 4.34 (ddd, *J* = 7.2, 4.7, 1.8 Hz, 1H), 4.30 – 4.21 (m, 3H), 4.17 (ddd, *J* = 8.0, 6.2, 2.8 Hz, 1H), 4.09 (d, *J* = 3.1 Hz, 1H), 4.03 – 3.93 (m, 4H), 3.88 (t, *J* = 4.5 Hz, 1H), 3.83 – 3.75 (m, 2H), 3.72 (t, *J* = 3.1 Hz, 1H), 3.68 (t, *J* = 2.6 Hz, 1H), 3.50 (t, *J* = 3.3 Hz, 1H), 3.45 – 3.42 (m, 2H), 1.87 (d, *J* = 1.5 Hz, 6H), 1.80 (s, 3H), 1.75 (s, 3H), 1.72 (s, 3H). ^{13}C NMR (101 MHz, $CDCl_3$) δ 170.63, 170.54, 170.50, 170.36, 170.00, 165.72, 165.42, 165.10, 137.59, 137.54, 137.49, 137.28, 135.91, 133.73, 133.48, 133.27, 133.22, 131.82, 130.26, 130.14, 130.09, 129.85, 129.49, 129.39, 129.12, 128.98, 128.59, 128.58, 128.52, 128.45, 128.39, 128.37, 128.34, 128.21, 128.18, 128.13, 128.01, 127.86, 127.79, 127.55, 101.25, 100.93, 100.02, 86.09, 77.36,

76.69, 76.49, 75.87, 75.04, 74.92, 73.80, 73.02, 72.97, 72.70, 72.57, 72.49, 68.96, 68.80, 68.16, 67.61, 66.84, 66.71, 66.06, 65.97, 64.25, 62.92, 62.82, 62.28, 62.02, 20.86, 20.84, 20.72, 20.64 HRMS m/z calculated for C96H96O29Na: 1767.5656 found: 1767.5655.

Cholestanyl-O-((4, 6-O-diacetyl-2-O-benzoyl-3-O-benzyl)-α-L-idopyrnosyl-α(1→4) (6-O-acetyl-2-O-benzoyl-3-O-benzyl)-α-L-idopyrnosyl-α(1→4) (6-O-acetyl-2-O-benzoyl-3-O-benzyl)-α-L-idopyrnosyl- α(1→4) (6-O-acetoxy-2-O-benzoyl-3-O-benzyl))-α-L-idopyranose50

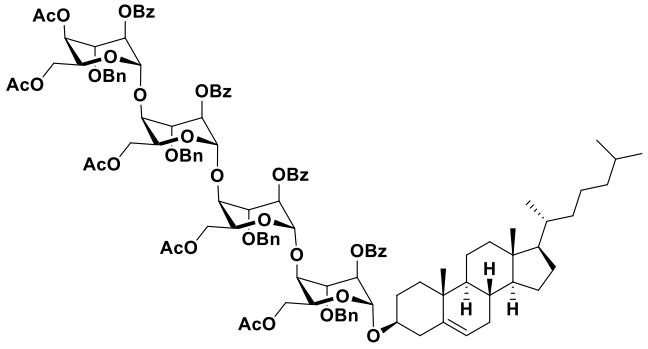

Glycosylation: The cholesterol conjugated product **50 (60%)** was obtained from the compound **49** using synthetic procedure **38.** ^{1}H NMR (400 MHz, Chloroform-*d*) δ 7.95 – 7.93 (m, 2H), 7.90 – 7.781 (m, 6H), 7.54 – 7.49 (m, 1H), 7.43 – 7.35 (m, 7H), 7.29 – 7.08 (m, 25H), 5.26 (d, *J* = 4.8 Hz, 1H), 5.20 (dt, *J* = 6.1, 3.0 Hz, 3H), 5.06 (t, *J* = 2.0 Hz, 1H), 5.00 (d, *J* = 1.9 Hz, 1H), 4.90 (d, *J* = 2.7 Hz, 1H), 4.82 – 4.79 (m, 3H), 4.73 (dd, *J* = 11.4, 5.8 Hz, 3H), 4.62 – 4.53 (m, 4H), 4.49 (t, *J* = 2.3 Hz, 1H), 4.43 (ddd, *J* = 7.8, 5.8, 2.3 Hz, 1H), 4.32 (ddd, *J* = 18.4, 9.4, 6.0 Hz, 2H), 4.26 – 4.15 (m, 3H), 4.00 (ddd, *J* = 12.0, 7.6, 4.8 Hz, 3H), 3.93 (dd, *J* = 7.2, 4.5 Hz, 3H), 3.81 – 3.75 (m, 2H), 3.72 (q, *J* = 3.0 Hz, 2H), 3.50 – 3.41 (m, 4H), 2.29 (ddd, *J* = 13.2, 4.9, 2.1 Hz, 1H), 2.20 – 2.14 (m, 1H), 1.87 (d, *J* = 7.4 Hz, 7H), 1.81 (s, 3H), 1.76 (s, 3H), 1.75 (s, 3H), 1.63 – 1.61 (m, 3H), 1.53 – 1.35 (m, 6H), 1.32 – 1.16 (m, 5H), 1.013 – 0.98 (m, 8H), 0.93 (s, 4H), 0.84 (d, *J* = 6.5 Hz, 4H), 0.79 (dd, *J* = 6.7, 1.7 Hz, 7H), 0.60 (s, 3H). ^{13}C NMR (101 MHz, $CDCl_3$) δ 170.65, 170.58, 170.53, 170.46, 170.01, 165.75, 165.50, 165.40, 165.10, 140.63, 138.23, 137.65, 137.52, 137.29, 133.73, 133.46, 133.19, 133.13, 130.22, 130.18, 130.10, 129.86, 129.67, 129.42, 129.40, 129.16, 128.58, 128.53, 128.45, 128.43, 128.35, 128.33, 128.29, 128.26, 128.22, 128.14, 127.98, 127.92, 127.80, 127.70, 121.99, 100.87, 100.84, 100.43, 96.63, 77.72, 77.36, 76.73, 76.41, 76.08, 75.04, 74.69, 73.01, 72.87, 72.57, 72.48, 72.20, 68.36, 68.22, 67.62, 66.87, 66.15, 66.07, 65.30, 64.27, 62.31, 62.83, 62.28, 56.87, 56.27, 50.32, 42.44, 39.90, 39.64, 38.61, 37.57, 36.90, 36.31, 35.91, 32.07, 32.01, 29.62, 28.36,

28.14, 24.41, 23.94, 22.95, 22.69, 21.20, 20.90, 20.87, 20.72, 20.66, 19.52, 18.85, 11.98. HRMS m/z calculated for $C_{117}H_{136}O_{30}Na$: 2043.9014 found: 2043.9010.

Cholestanyl-O-((3-O-benzyl)-α-L-idopyrnosyl-α(1→4) (3-O-benzyl)-α-L-idopyrnosyl-α(1→4) (3-O-benzyl)-α-L-idopyrnosyl- α(1→4) (3-O-benzyl))-α-L-idopyranose51

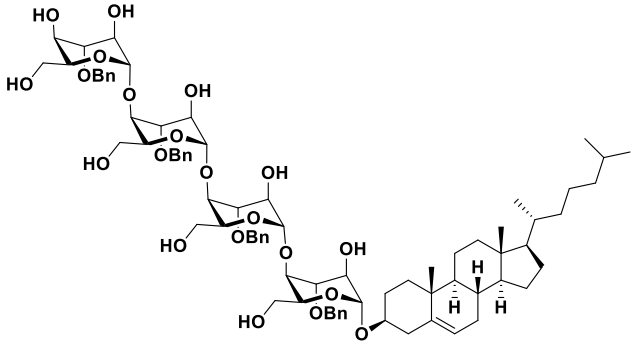

Deprotection: Esters deprotection was carried out for the compound **50** by following synthetic procedure **39** to obtain the compound **51 (90%).** ^{1}H NMR (600 MHz, Chloroform-*d*) δ 7.43 – 7.29 (m, 20H), 5.38 (dd, *J* = 5.1, 2.6 Hz, 1H), 5.01 (s, 1H), 4.87 (d, *J* = 17.1 Hz, 2H), 4.79 (d, *J* = 11.7 Hz, 1H), 4.74 (s, 1H), 4.68 – 4.61 (m, 2H), 4.58 – 4.52 (m, 6H), 4.42 (t, *J* = 8.6 Hz, 3H), 4.38 – 4.36 (m, 2H), 4.24 (t, *J* = 6.7 Hz, 1H), 4.14 (d, *J* = 11.9 Hz, 2H), 3.96 (dt, *J* = 28.2, 3.1 Hz, 2H), 3.86 (d, *J* = 3.9 Hz, 3H), 3.82 – 3.77 (m, 4H), 3.71 – 3.49 (m,12H), 3.44 – 3.39 (m, 2H), 3.06 (s, 1H), 2.82 (t, *J* = 20.4 Hz, 1H), 2.44 – 2.37 (m, 2H), 2.29 – 2.25 (m, 2H), 2.08 – 1.95 (m, 7H), 1.87 (tdd, *J* = 19.1, 10.0, 6.3 Hz, 2H), 1.71 – 1.64 (m, 1H), 1.62 – 1.44 (m, 6H), 1.41 – 1.25 (m, 5H), 1.21 – 1.07 (m, 7H), 1.04 (s, 3H), 1.02 – 1.00 (m, 2H), 0.94 (d, *J* = 6.5 Hz, 3H), 0.89 (dd, *J* = 6.6, 2.8 Hz, 6H), 0.70 (s, 3H). ^{13}C NMR (151 MHz, $CDCl_3$) δ 140.77, 138.34, 137.31, 137.07, 137.01, 128.72, 128.68, 128.49, 128.44, 128.40, 128.37, 127.76, 127.61, 121.95, 103.11, 103.06, 103.00, 99.37, 77.10, 74.75, 74.21, 73.88, 73.86, 73.09, 72.94, 72.68, 72.42, 72.37, 71.84, 71.26, 70.08, 67.06, 66.84, 66.82, 66.66, 66.47, 66.29, 66.26, 66.00, 64.67, 62.04, 61.90, 61.03, 56.82, 56.20, 50.21, 42.42, 39.86, 39.62, 38.61, 37.47, 36.92, 36.29, 35.92, 32.07, 31.98, 29.77, 28.38, 28.15, 24.42, 23.94, 22.98, 22.71, 21.17, 19.55, 18.84, 11.98. HRMS m/z calculated for $C_{79}H_{110}O_{21}Na$: 1417.7437 found: 1417.7434.

Cholestanyl-O-((2,4,6-O-trisulfonato-3-O-benzyl)-α-L-idopyrnosyl-α(1→4) (2,6-O-disulfonato-3-O-benzyl 3-O-benzyl)-α-L-idopyrnosyl-α(1→4) (2,6-O-disulfonato-3-O-benzyl)-α-L-idopyrnosyl- α(1→4) (2,6-O-disulfonato-3-O-benzyl))-α-L-idopyranose52

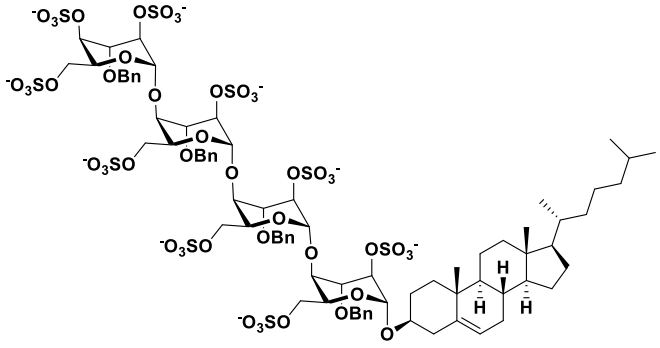

Sulfation: The sulfated compound **52 (70%)** obtained from the compound **51** by following the synthetic procedure **40.** ^{1}H NMR (400 MHz, Deuterium Oxide, Temperature at 328K) δ 7.85 – 7.65 (m, 20H), 5.78 (s, 1H), 5.56 (s, 1H), 5.46 (s, 1H), 5.34 (d, *J* = 15.2 Hz, 2H), 5.10 (h, *J* = 11.8 Hz, 10H), 4.94 – 4.84 (m, 5H), 4.73 (s, 3H), 4.66 – 4.36 (m, 11H), 4.22 (s, 1H), 4.07 (d, *J* = 10.5 Hz, 2H), 3.96 – 3.85 (m, 1H), 2.78 (d, *J* = 13.3 Hz, 1H), 2.58 (t, *J* = 13.0 Hz, 1H), 2.34 – 2.10 (m, 5H), 2.01 – 1.75 (m, 7H), 1.73 – 1.58 (m, 4H), 1.55 – 1.33 (m, 12H), 1.26 (d, *J* = 6.2 Hz, 4H), 1.16 (d, *J* = 6.5 Hz, 6H), 1.03 (s, 3H). HRMS m/z calculated for $C_{79}H_{101}O_{48}S_9^{9-}$: 2105.2889 found: 233.9220.

Cholesteryl-O-((2,4,6-O-trisulfonato)-α-L-idopyrnosyl-α(1→4) (2,6-O-disulfonato-3-O-benzyl 3)-α-L-idopyrnosyl-α(1→4) (2,6-O-disulfonato)-α-L-idopyrnosyl-α(1→4) (2,6-O-disulfonato))-α-L-idopyranose IDC-4

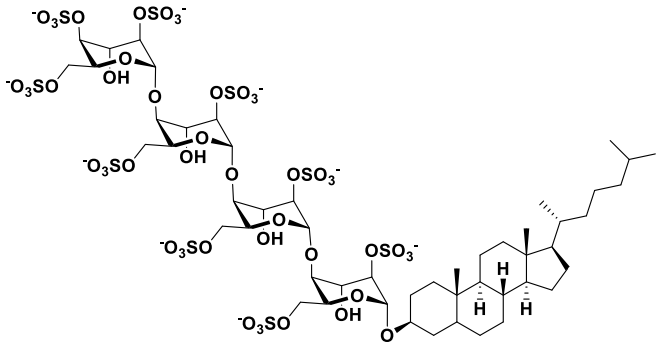

Hydrogenolysis: The compound **IDC-4 (80%)** wasobtainedfrom the compound **52** by following synthetic procedure **IDC-2.** ^{1}H NMR (400 MHz, Deuterium Oxide) δ 5.20 – 5.12 (m, 1H), 5.01 – 4.88 (m, 3H), 4.70 – 4.58 (m, 2H), 4.53 – 4.41 (m, 2H), 4.29 (s, 8H), 4.16 – 4.06 (m, 2H), 4.01 – 3.90 (m, 3H), 3.88 – 3.80 (m, 3H), 3.78 – 3.68 (m, 3H), 3.58 – 3.48 (m, 1H), 2.05 – 1.84 (m, 3H), 1.78 – 1.52 (m, 7H), 1.48 – 1.28 (m, 8H), 1.22 – 1.10 (m, 6H), 1.06 – 0.82 (m, 16H), 0.71 (s, 3H). HRMS m/z calculated for $C_{51}H_{79}O_{48}S_9^{9-}$: 1747.1277 found: 194.1250.

5.6 Plaque Reduction Neutralization Test (PRNT)

SARS-CoV-2 isolates generated from infected patients in Queensland, Australia were used for the PRNT assay, QLD02/2020 – 30/1/2020 (GISAID accession EPI_ISL_407896. Virus were passaged three times in Vero E6 cells and titrated by focus-forming assay on Vero E6 cells. Serial dilutions of compounds were incubated with ~6000 focus-forming units per ml of SARS-CoV-2 for 1 h at 37°C. Serum-virus mixtures were added to Vero E6 cell monolayers (pre-seeded at 40,000 cells/well in 96-well plates and incubated overnight) and incubated at 37°C for 30 min. Subsequently, cells were overlaid with 1% (w/v) medium viscosity carboxymethyl cellulose in M199 (Gibco) supplemented with 2% heat-inactivated fetal bovine serum supplemented with 1% Penicillin-Streptomycin (Sigma-Aldrich) and incubated at 37oC in 5% CO2 for 14 h. After incubation, overlay was removed and cells fixed with 80% cold-acetone in PBS for 30 min at -20°C. Plates were then dried, blocked with blocking buffer (1xKPL in 0.1% PBS-Tween 20) for 1 h and then incubated with 1 µg/ml of CR3022 anti-S mAb and 0.2 µg/ml IR-Dye800-conjugated goat anti-human IgG (LI-COR) in blocking buffer. Plates were washed 3 times after antibody incubations by submerging in PBS with 0.1% Tween-20. Plates were then dried prior to visualising using Odyssey (LI-COR).

5.7 References

1. Q., L. *et al.* Early transmission dynamics in Wuhan, China, of novel coronavirus-infected pneumonia. *New England Journal of Medicine* vol. 382 1199–1207 (2020).

2. Wang, W., Tang, J. & Wei, F. Updated understanding of the outbreak of 2019 novel coronavirus (2019-nCoV) in Wuhan, China. *J. Med. Virol.***92**, 441–447 (2020).

3. Yang, Y. *et al.* The Deadly Coronaviruses: The 2003 SARS Pandemic and The 2020 Novel Coronavirus Epidemic in China , The Company' s Public News and Information. *J. Autoimmun.***109**, 102487 (2020).

4. (OMS), W. H. O. COVID-19 Weekly Epidemiological Update. 1;4 (2020).

5. Li, Y. *et al.* Efficacy and Safety of Lopinavir/Ritonavir or Arbidol in Adult Patients with Mild/Moderate COVID-19: An Exploratory Randomized Controlled Trial. *Med* (2020) doi:10.1016/j.medj.2020.04.001.

6. Mentré, F. *et al.* Dose regimen of favipiravir for Ebola virus disease. *Lancet Infect. Dis.***15**, 150–151 (2015).

7. Wang, M. *et al.* Remdesivir and chloroquine effectively inhibit the recently emerged novel coronavirus (2019-nCoV) in vitro. *Cell Res.***30**, 269–271 (2020).

8. de Wit, E. *et al.* Prophylactic and therapeutic remdesivir (GS-5734) treatment in the rhesus macaque model of MERS-CoV infection. *Proc. Natl. Acad. Sci. U. S. A.***117**, 6771–6776 (2020).

9. Deeks, E. D. Darunavir/Cobicistat/Emtricitabine/Tenofovir Alafenamide: A Review in HIV-1 Infection. *Drugs***78**, 1013–1024 (2018).

10. Arabi, Y. M. *et al.* Treatment of Middle East respiratory syndrome with a combination of lopinavir/ritonavir and interferon-β1b (MIRACLE trial): Statistical analysis plan for a recursive two-stage group sequential randomized controlled trial. *Trials***21**, 1–8 (2020).

11. Sheahan, T. P. *et al.* Comparative therapeutic efficacy of remdesivir and combination lopinavir, ritonavir, and interferon beta against MERS-CoV. *Nat. Commun.***11**, (2020).

12. Yao, T. T., Qian, J. D., Zhu, W. Y., Wang, Y. & Wang, G. Q. A systematic review of lopinavir therapy for SARS coronavirus and MERS coronavirus—A possible reference for coronavirus disease-19 treatment option. *J. Med. Virol.***92**, 556–563 (2020).

13. Gao, J., Tian, Z. & Yang, X. Breakthrough: Chloroquine phosphate has shown apparent efficacy in treatment of COVID-19 associated pneumonia in clinical studies. *Biosci. Trends***14**, 1–2 (2020).

14. Xu, X. *et al.* Effective treatment of severe COVID-19 patients with tocilizumab. *Proc. Natl. Acad. Sci. U. S. A.***117**, 10970–10975 (2020).

15. Deftereos, S. *et al.* Colchicine and the heart: Pushing the envelope. *J. Am. Coll. Cardiol.***62**, 1817–1825 (2013).

16. Devaux, C. A., Rolain, J. M., Colson, P. & Raoult, D. New insights on the antiviral effects of chloroquine against coronavirus: what to expect for COVID-19? *Int. J. Antimicrob. Agents***55**, (2020).

17. Mauthe, M. *et al.* Chloroquine inhibits autophagic flux by decreasing autophagosome-lysosome fusion. *Autophagy***14**, 1435–1455 (2018).

18. Scott, L. J. Tocilizumab: A Review in Rheumatoid Arthritis. *Drugs***77**, 1865–1879 (2017).

19. Cao, B. *et al.* A Trial of Lopinavir–Ritonavir in Adults Hospitalized with Severe Covid-19. *N. Engl. J. Med.***382**, 1787–1799 (2020).

20. Dong, L., Hu, S. & Gao, J. Discovering drugs to treat coronavirus disease 2019 (COVID-19). *Drug Discov. Ther.***14**, 58–60 (2020).

21. Clausen, T. M. *et al.* SARS-CoV-2 Infection Depends on Cellular Heparan Sulfate and ACE2. *Cell***183**, 1043-1057 (2020).

22. Kim, S. Y. *et al.* Characterization of heparin and severe acute respiratory

syndrome-related coronavirus 2 (SARS-CoV-2) spike glycoprotein binding interactions. *Antiviral Res.***181**, (2020).

23. Hao, W. *et al.* Binding of the SARS-CoV-2 Spike Protein to Glycans. **2019**, (2020).

24. Noti, C. & Seeberger, P. H. Chemical approaches to define the structure-activity relationship of heparin-like glycosaminoglycans. *Chem. Biol.***12**, 731–756 (2005).

25. Dulaney, S. B. *et al.* Divergent Synthesis of Heparan Sulfate Oligosaccharides. *J. Org. Chem.***80**, 12265–12279 (2015).

26. Cram, D. J. International Edition in English. *Angew. Chemie Int. Ed. English***24**, 799–810 (1985).

27. Hu, Y.-P. *et al.* Divergent Synthesis of 48 Heparan Sulfate-Based Disaccharides and Probing the Specific Sugar–Fibroblast Growth Factor-1 Interaction. *J. Am. Chem. Soc.***134**, 20722–20727 (2012).

28. Zong, C. *et al.* Heparan Sulfate Microarray Reveals That Heparan Sulfate-Protein Binding Exhibits Different Ligand Requirements. *J. Am. Chem. Soc.***139**, 9534–9543 (2017).

29. Lu, N. D. *et al.* Synthesis of 48 disaccharide building blocks for the assembly of a heparin and heparan sulfate oligosaccharide library. *Org. Lett.***8**, 5995–5998 (2006).

30. Petitou, M. & Van Boeckel, C. A. A. A synthetic antithrombin III binding pentasaccharide is now a drug! What comes next? *Angew. Chemie - Int. Ed.***43**, 3118–3133 (2004).

31. Boons, B., J. *et al.* Heparan sulfate proteoglycans as attachment factor for SARS-CoV-2. https://doi.org/10.1101/2020.05.10.087288

32. Linhardt, R., J. *et al*. Characterization of heparin and severe acute respiratory syndrome-relatedcoronavirus 2 (SARS-CoV-2) spike glycoprotein binding interactions. *Antiviral Res.* **181**, 104873(2020).

33. Tandon, R. *et al.* Effective Inhibition of SARS-CoV-2 Entry by Heparin and Enoxaparin Derivative. https://doi.org/10.1101/2020.06.08.140236

34. Nitulescu, G. M. *et al.* Comprehensive analysis of drugs to treat SARS-CoV-2 infection: Mechanistic insights into current COVID-19 therapies (Review). *Int. J. Mol. Med.***46**, 467–488 (2020).

35. Tiwari, V., Beer, J. C., Sankaranarayanan, N. V., Swanson-mungerson, M. & Desai, U. R. Discovering small-molecule therapeutics against SARS-CoV-2. *Drug Discov. Today***25**, 1535-1544 (2020).

36. Knight. R. *et al.* Bacterial modification of the host glycosaminoglycan heparan sulfate modulates SARSCoV-2 infectivity. https://doi.org/10.1101/2020.08.17.238444.

37. Zhang, Q. *et al.* Heparan sulfate assists SARS-CoV-2 in cell entry and can be targeted by approved drugs in vitro. *Cell Discov.***6**, (2020).

38. Guimond, S. E. *et al.* Pixatimod (PG545), a clinical-stage heparan sulfate mimetic, is a potent inhibitor of the SARS-CoV-2 virus. *bioRxiv***44**, https://doi.org/10.1101/2020.06.24.169334.

39. Shanthamurthy, C. D. & Kikkeri, R. Linear Synthesis of De novo Oligo-Iduronic Acid. *European J. Org. Chem.***2019**, 2950–2953 (2019).

5.8 Spectral Data

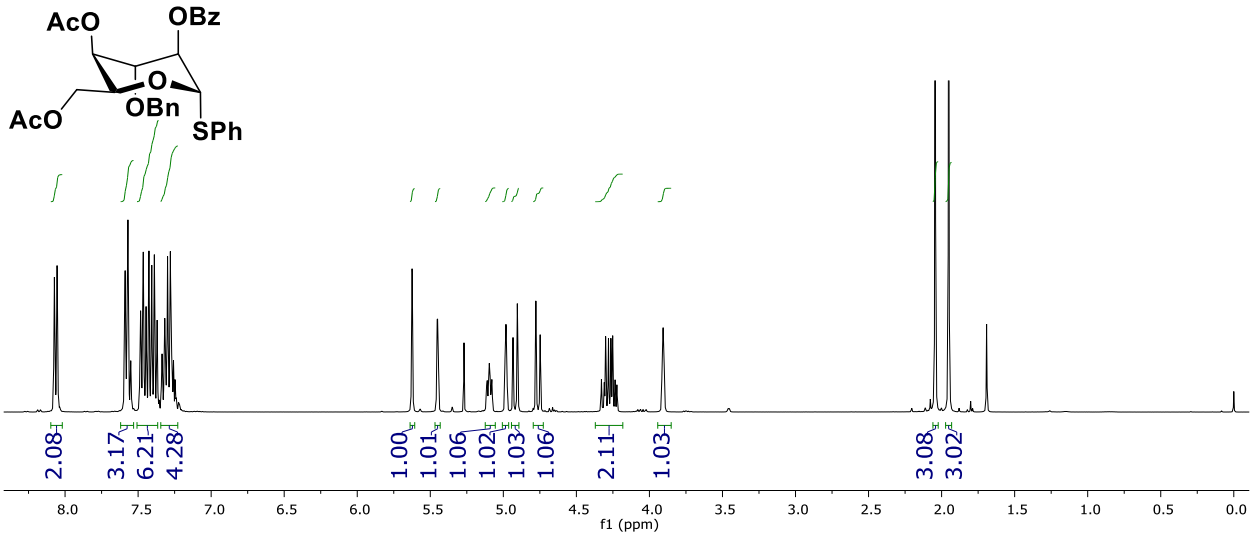

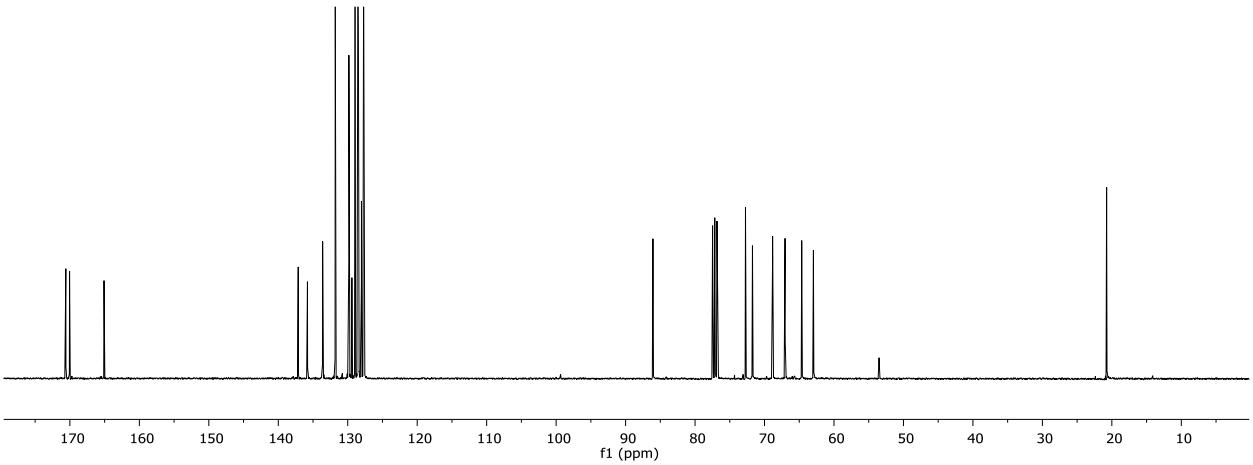

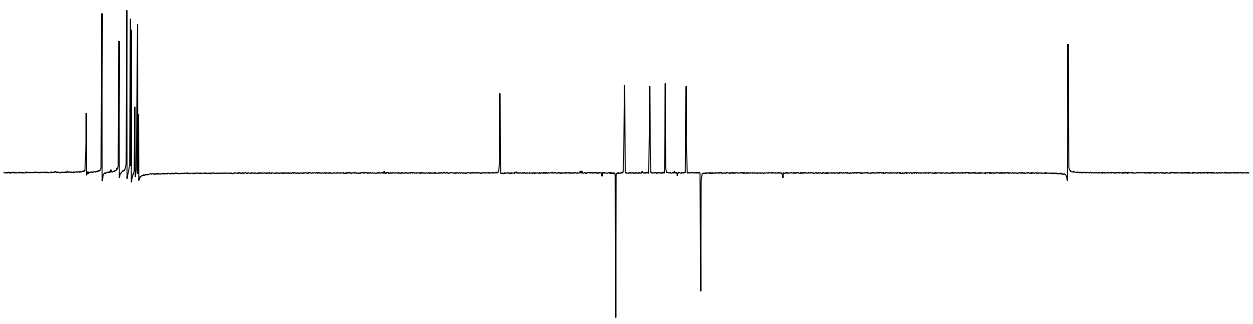

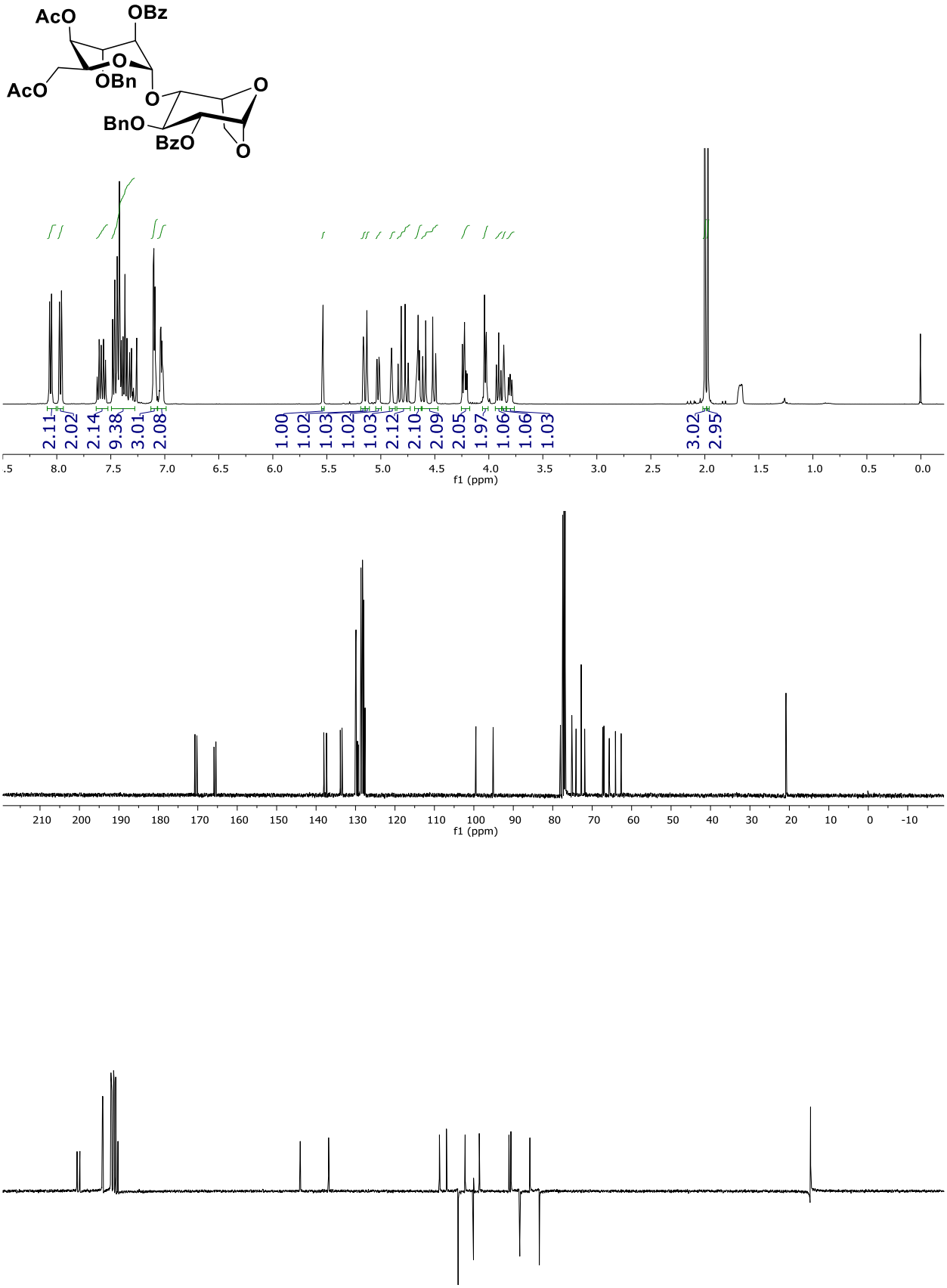
AcO
OBz
O
OBn
AcO
O
BnO
BzO
O
2.11
2.02
2.14
9.38
3.01
2.08
1.00
1.02
1.03
1.02
1.03
2.12
2.10
2.09
2.05
1.97
1.06
1.06
1.03
3.02
2.95
f1 (ppm)
f1 (ppm)

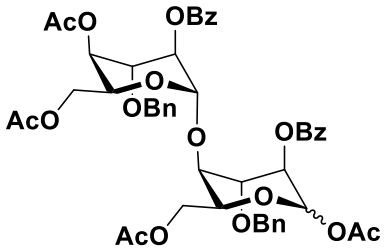
AcO
OBz
O
OBn
AcO
O
OBz
O
OBn
AcO
OAc

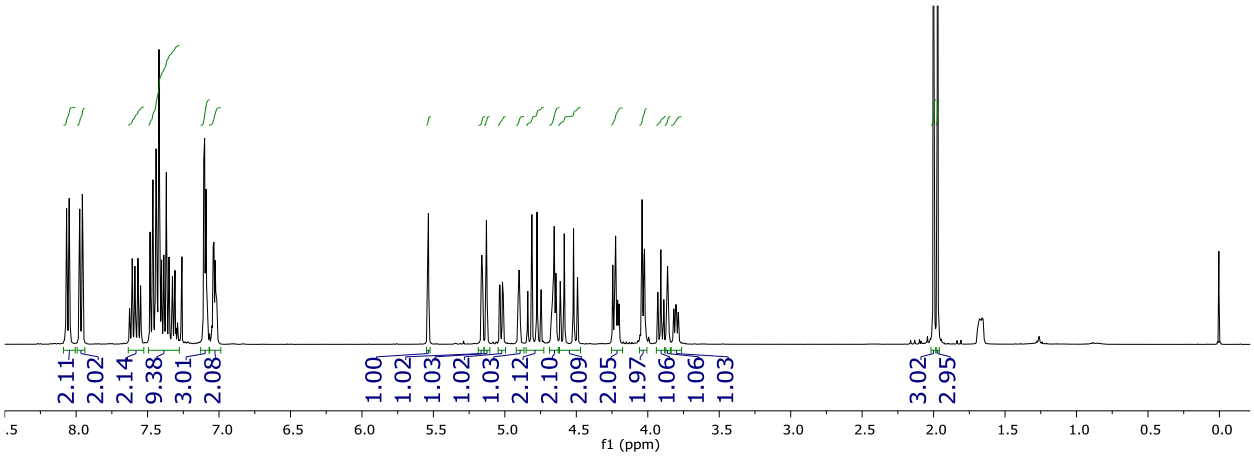
2.11
2.02
2.14
9.38
3.01
2.08
1.00
1.02
1.03
1.02
1.03
2.12
2.10
2.09
2.05
1.97
1.06
1.06
1.03
3.02
2.95
f1 (ppm)

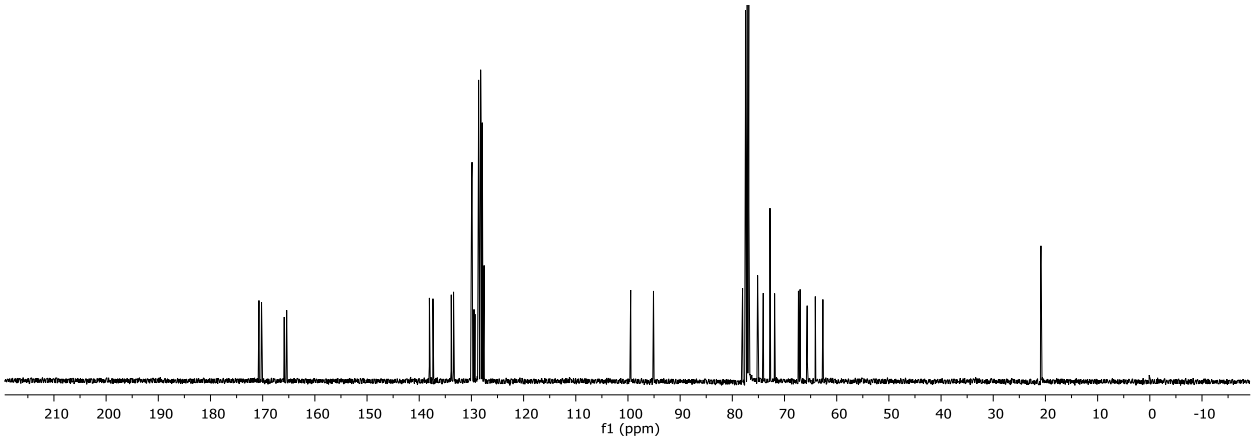
f1 (ppm)

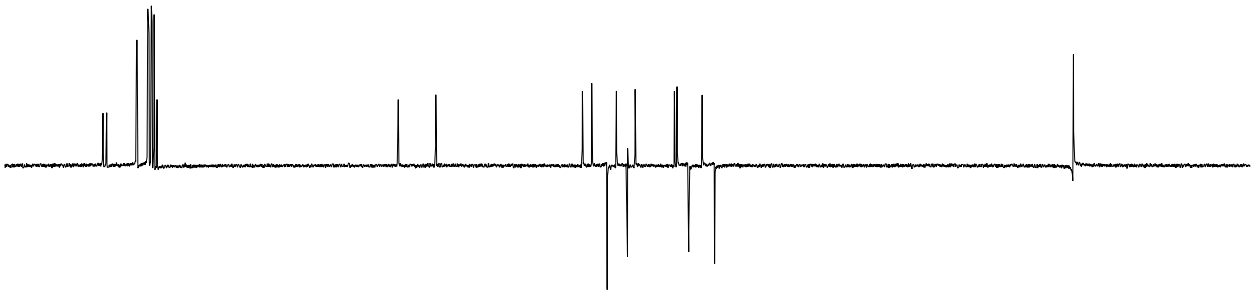

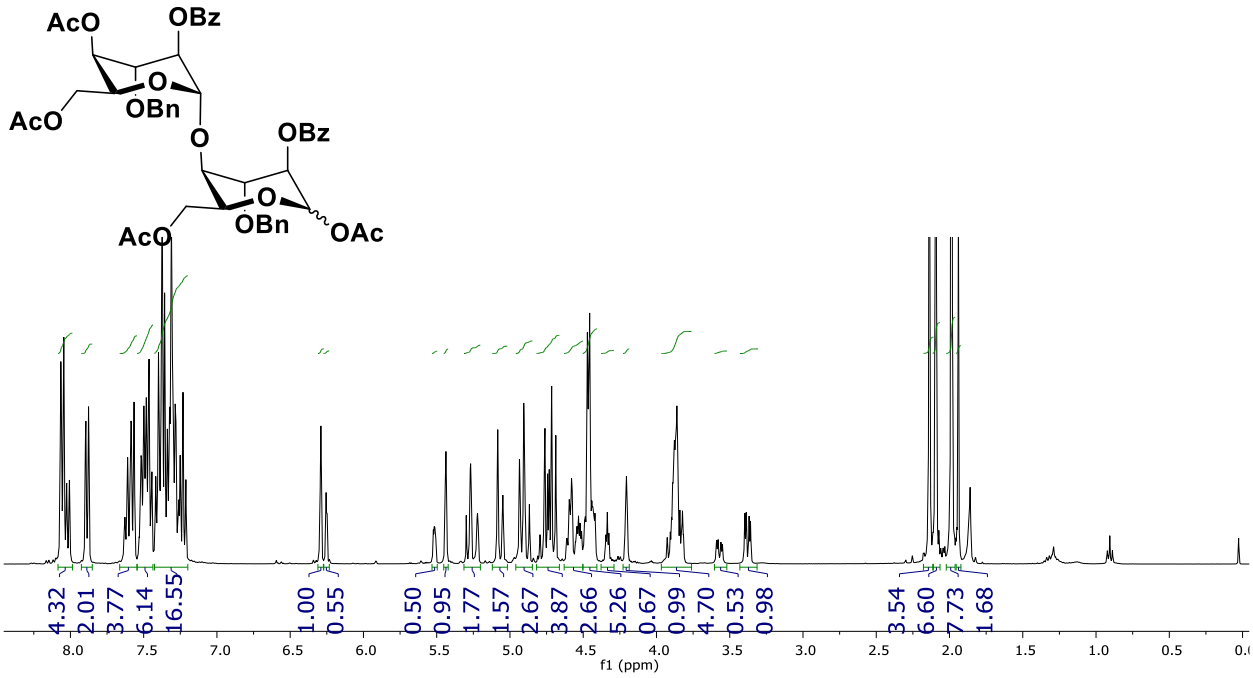
AcO
OBz
O
OBn
AcO
O
OBz
O
OBn
AcO
OAc
4.32
2.01
3.77
6.14
16.55
1.00
0.55
0.50
0.95
1.77
1.57
2.67
3.87
2.66
5.26
0.67
0.99
4.70
0.53
0.98
3.54
6.60
7.73
1.68
f1 (ppm)

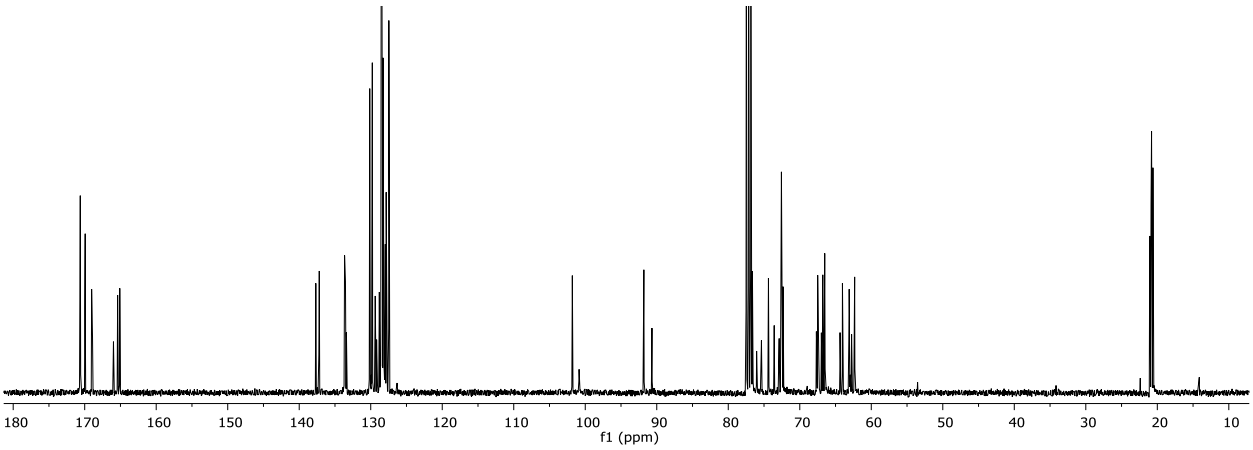
f1 (ppm)

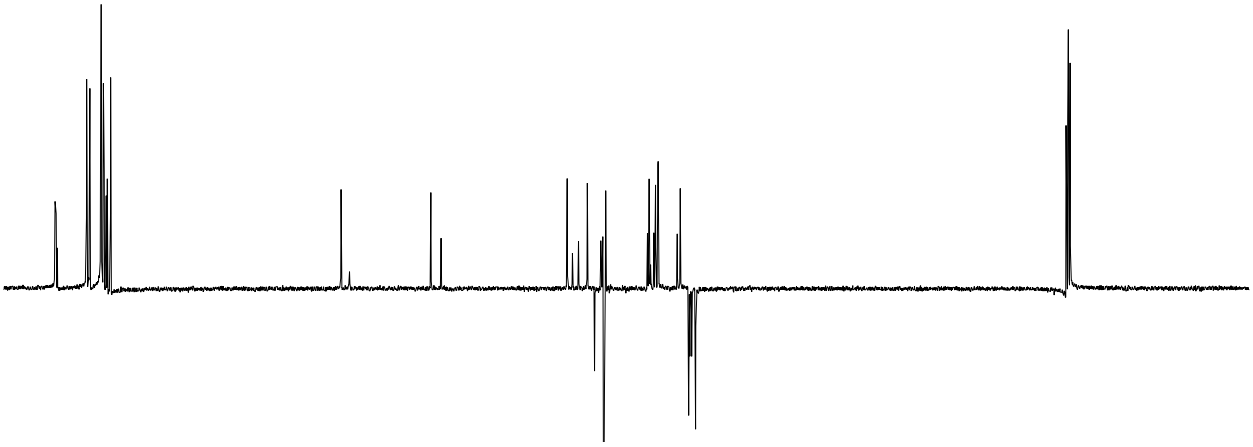

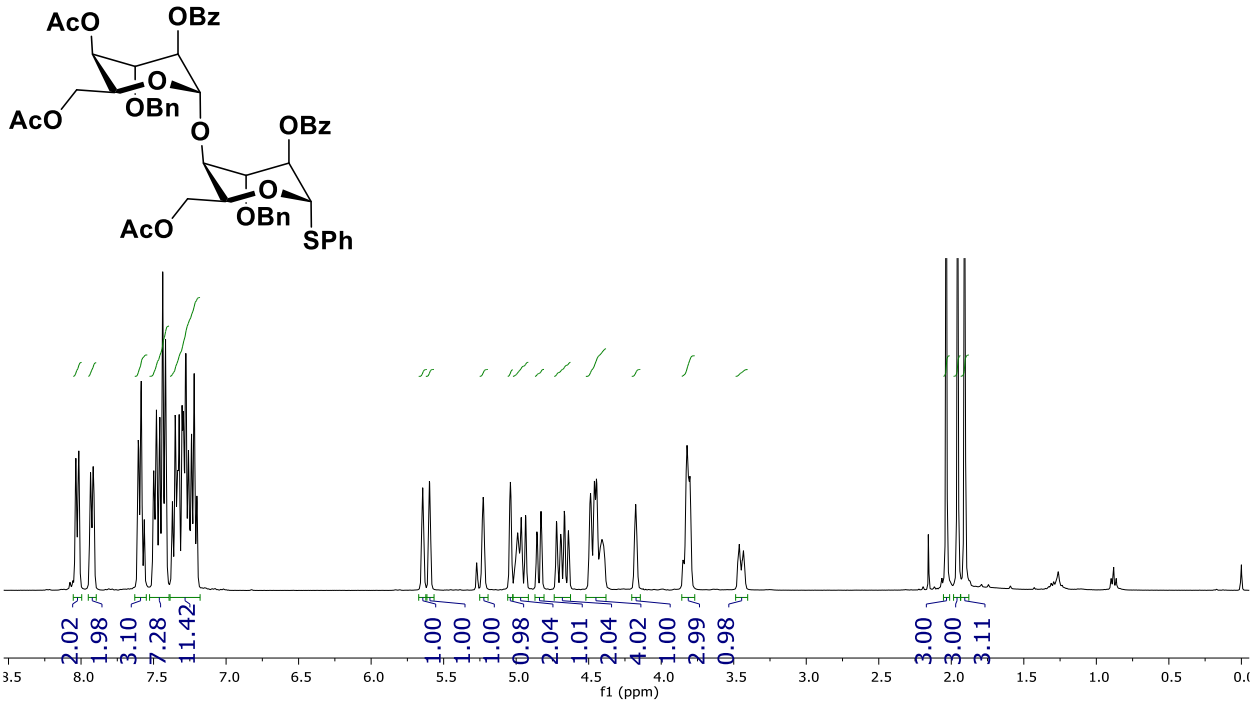
AcO
OBz
O
OBn
AcO
O
OBz
O
OBn
AcO
SPh
2.02
1.98
3.10
7.28
11.42
1.00
1.00
1.00
0.98
2.04
1.01
2.04
4.02
1.00
2.99
0.98
3.00
3.00
3.11
f1 (ppm)

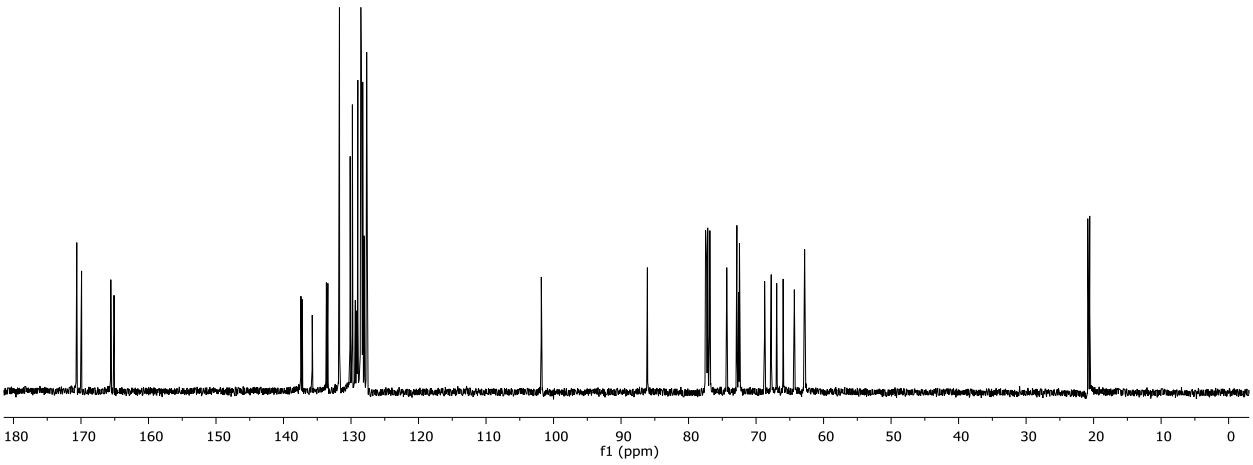
f1 (ppm)

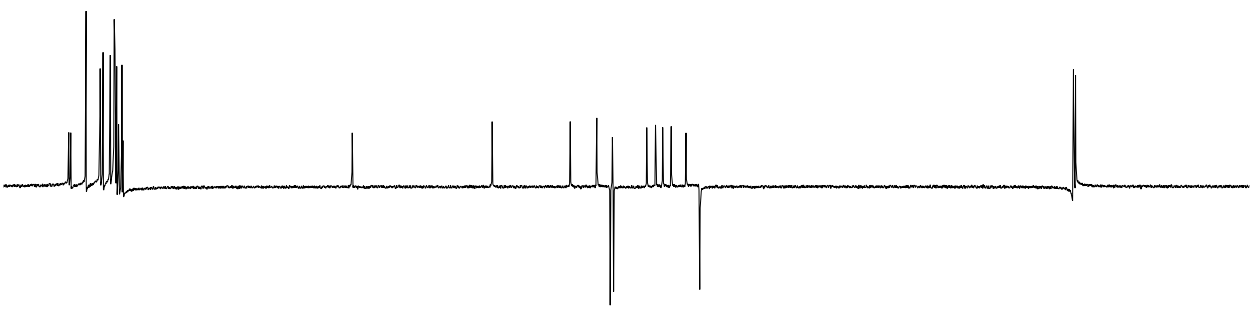

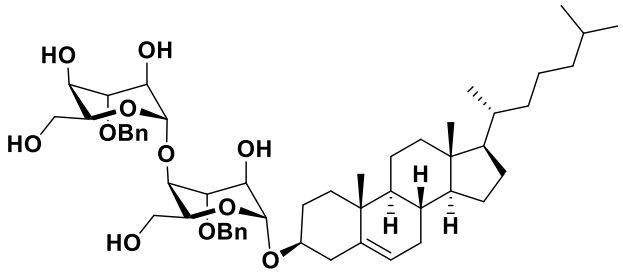
HO
OH
O
OBn
HO
O
OH
O
OBn
HO
O
H
H
H

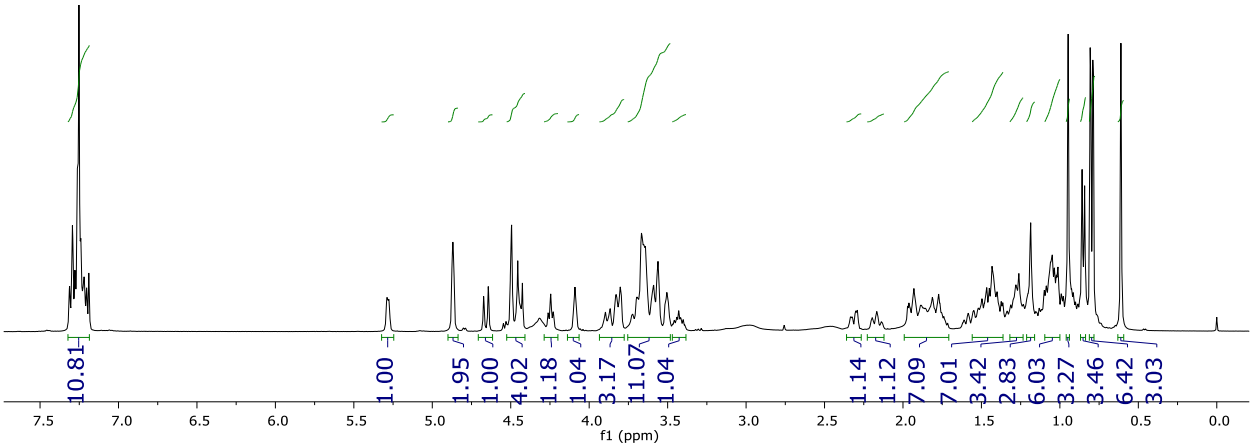
10.81
1.00
1.95
1.00
4.02
1.18
1.04
3.17
11.07
1.04
1.14
1.12
7.09
7.01
3.42
2.83
6.03
3.27
3.46
6.42
3.03
f1 (ppm)

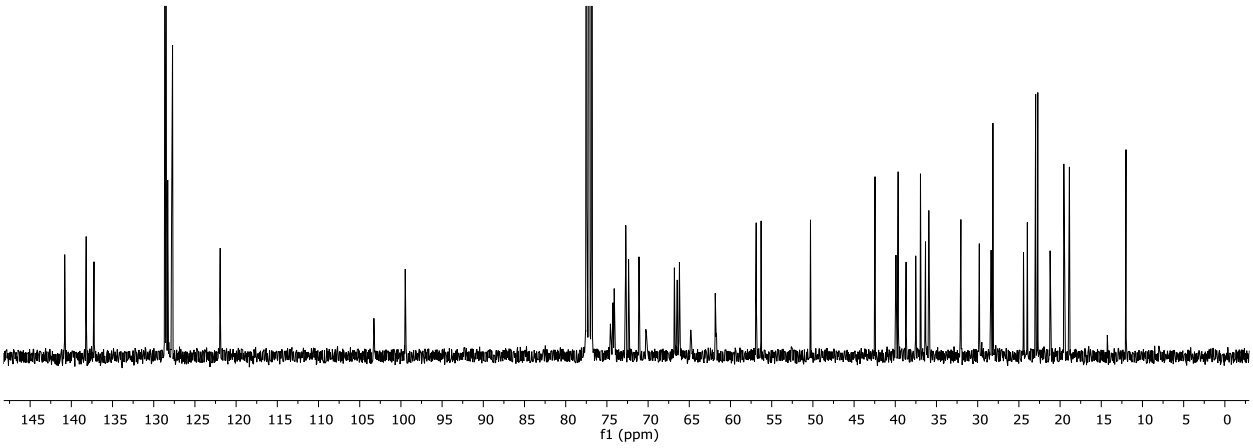
f1 (ppm)

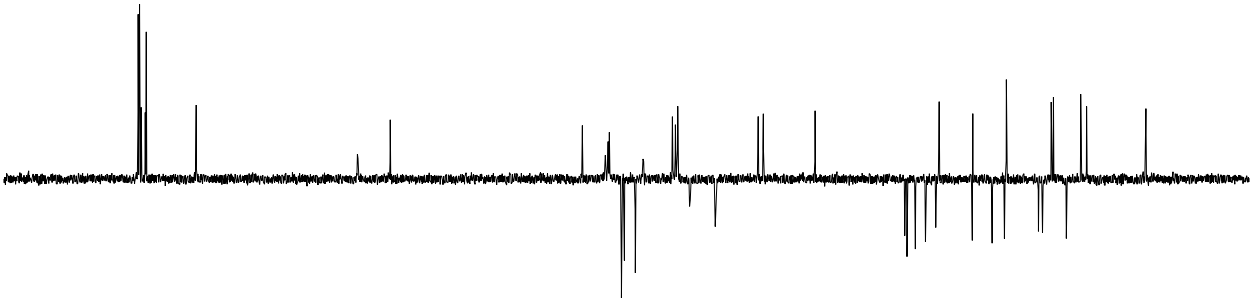

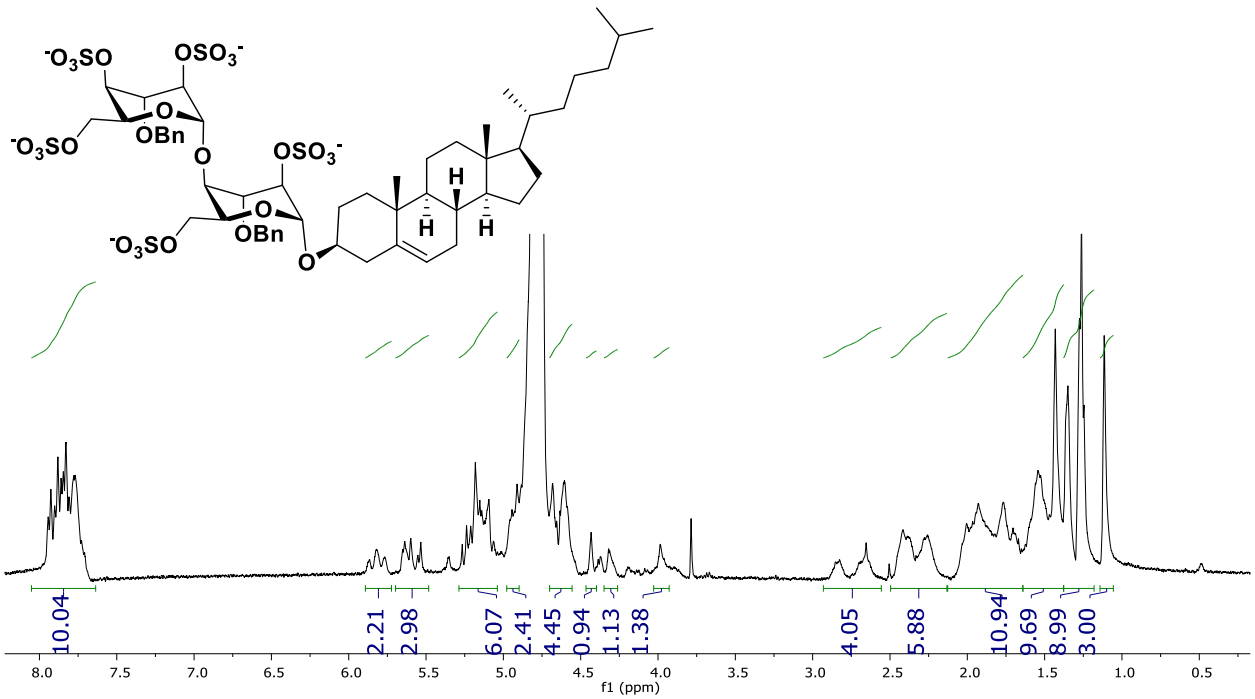
-O3SO
OSO3-
O
OBn
-O3SO
OSO3-
O
OBn
-O3SO
O
H
H
H
10.04
2.21
2.98
6.07
2.41
4.45
0.94
1.13
1.38
4.05
5.88
10.94
9.69
8.99
3.00
f1 (ppm)

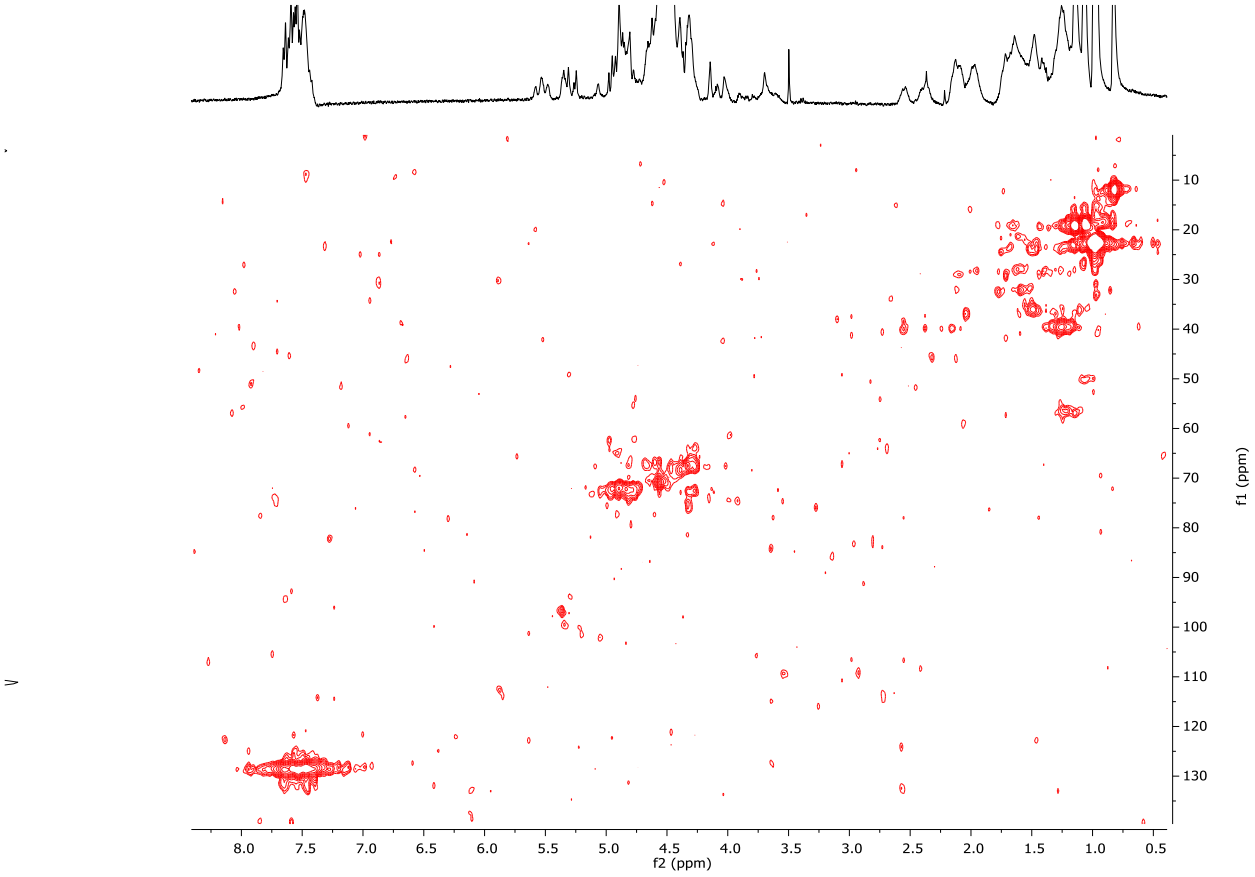
f2 (ppm)
f1 (ppm)

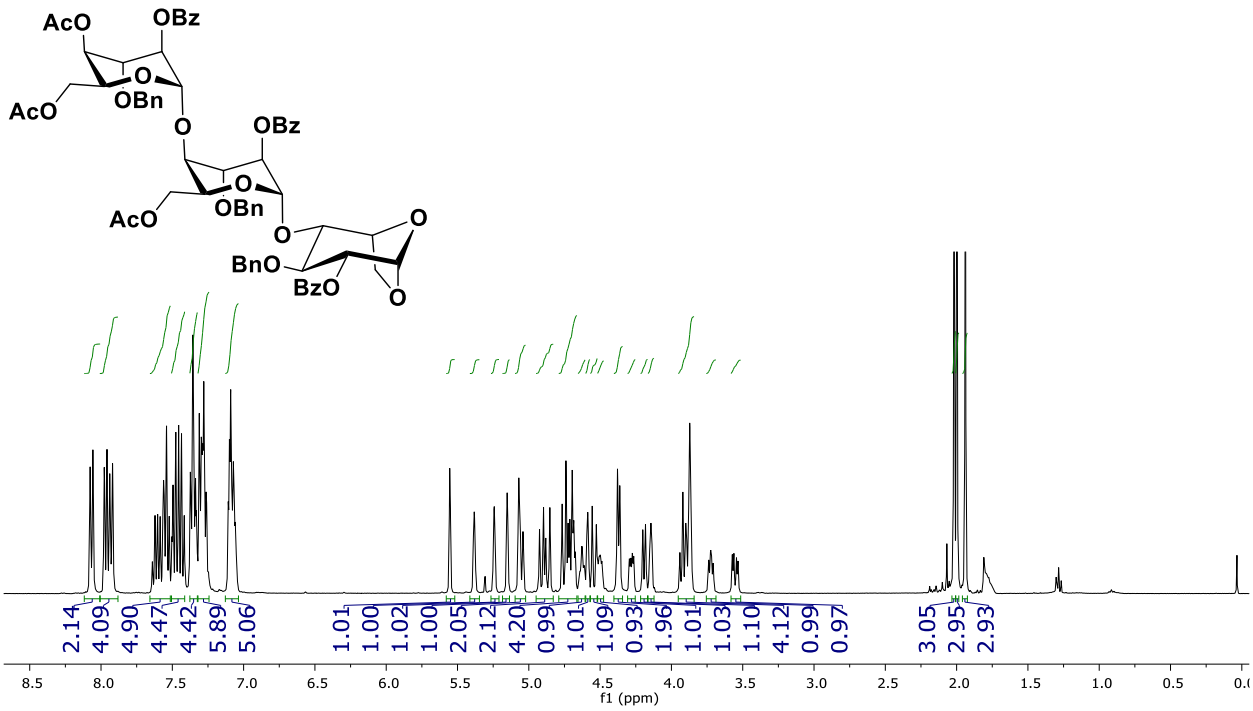
AcO
OBz
O
OBn
AcO
O
OBz
O
OBn
AcO
O
BnO
BzO
O
2.14
4.09
4.90
4.47
4.42
5.89
5.06
1.01
1.00
1.02
1.00
2.05
2.12
4.20
0.99
1.01
1.09
0.93
1.96
1.01
1.03
1.10
4.12
0.99
0.97
3.05
2.95
2.93
f1 (ppm)

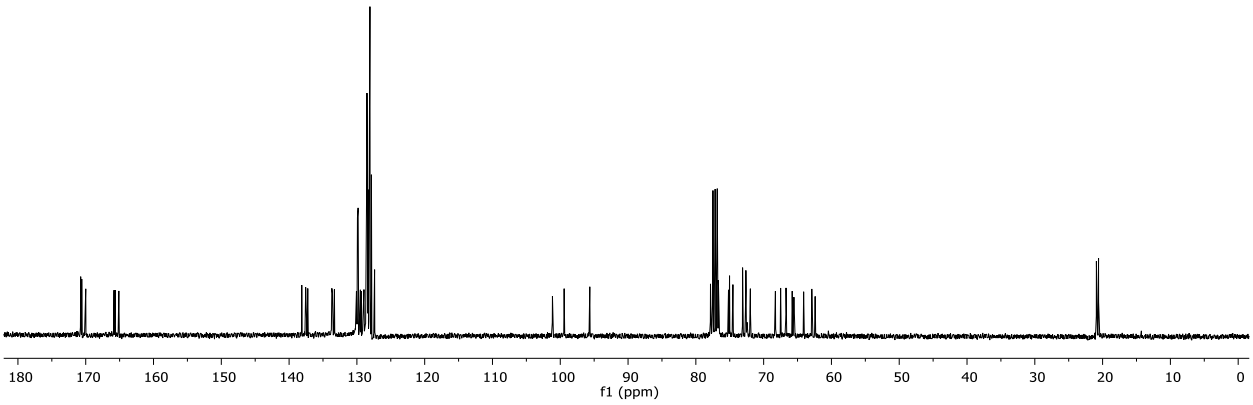
f1 (ppm)

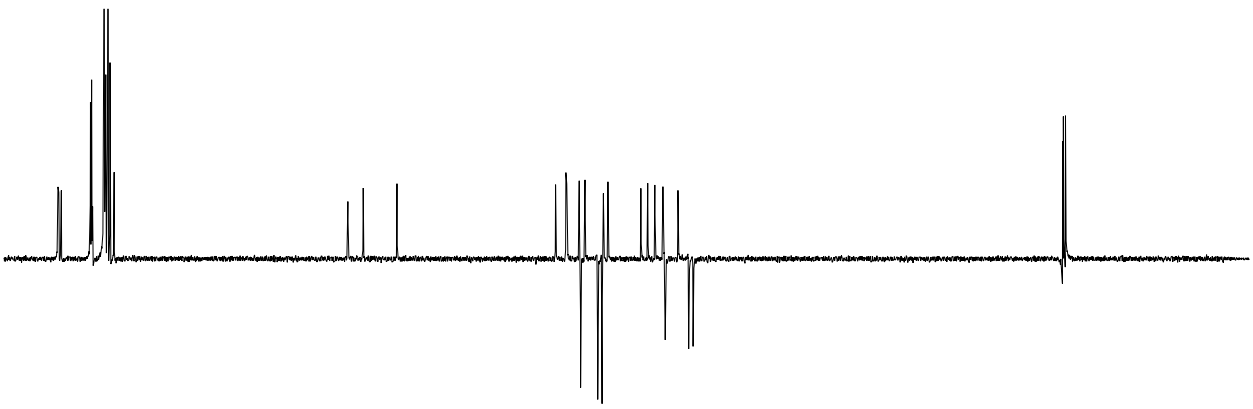

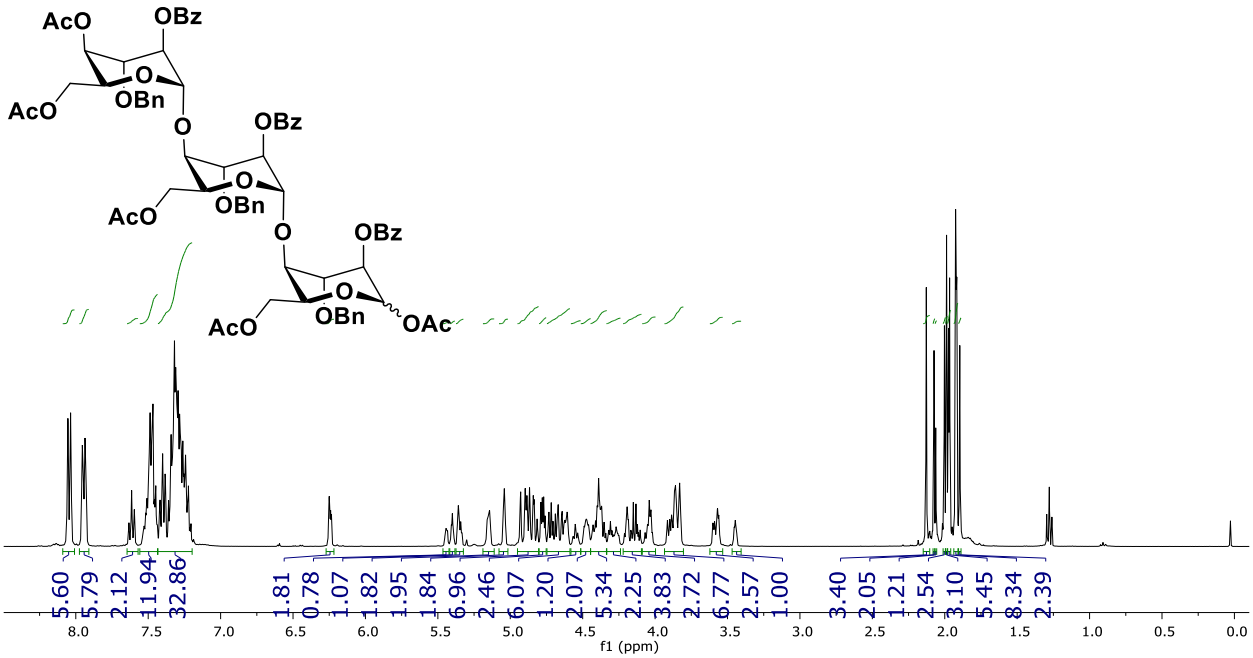
AcO
OBz
O
OBn
AcO
O
OBz
O
OBn
AcO
O
OBz
O
OBn
AcO
OAc
5.60
5.79
2.12
11.94
32.86
1.81
0.78
1.07
1.82
1.95
1.84
6.96
2.46
6.07
1.20
2.07
5.34
2.25
3.83
2.72
6.77
2.57
1.00
3.40
2.05
1.21
2.54
3.10
5.45
8.34
2.39
f1 (ppm)

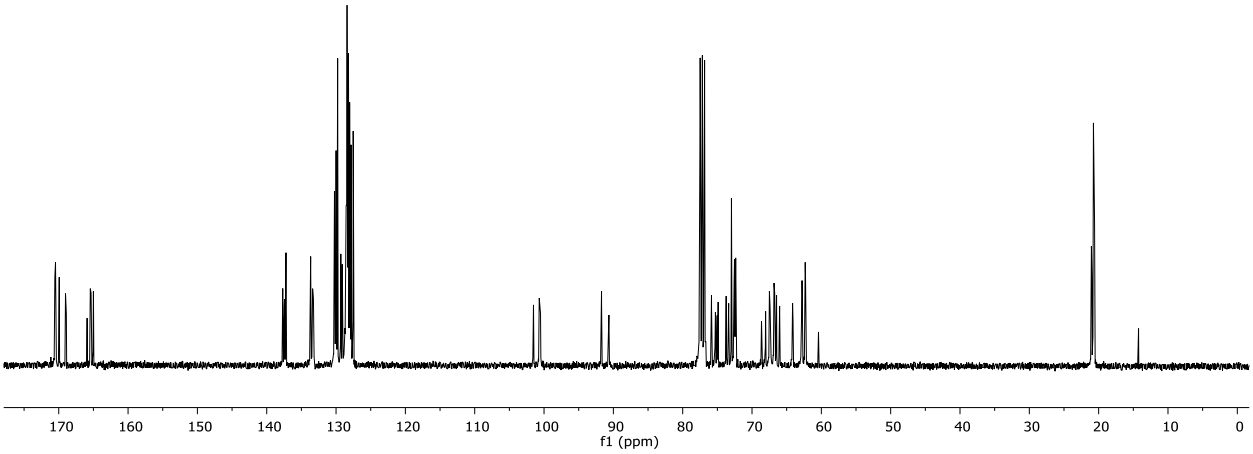
f1 (ppm)

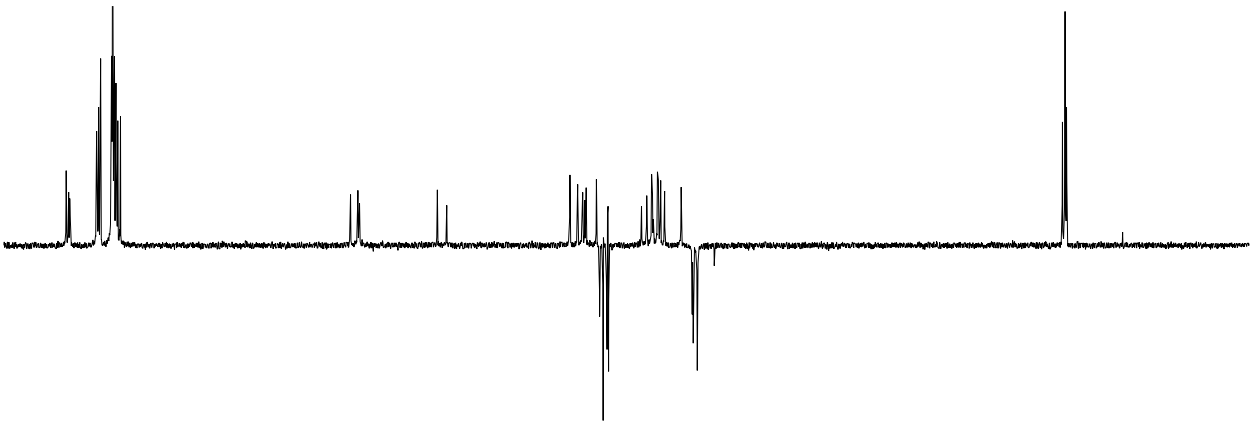

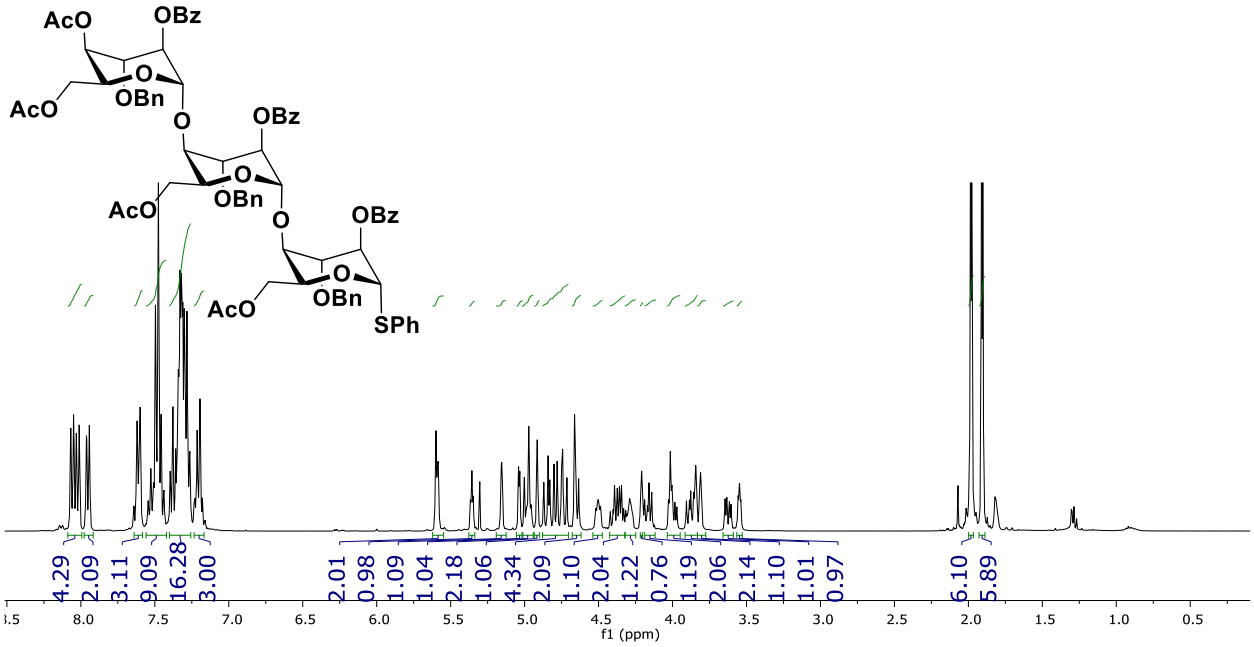
AcO
OBz
O
OBn
AcO
O
OBz
O
OBn
AcO
O
OBz
O
OBn
AcO
SPh
4.29
2.09
3.11
9.09
16.28
3.00
2.01
0.98
1.09
1.04
2.18
1.06
4.34
2.09
1.10
2.04
1.22
0.76
1.19
2.06
2.14
1.10
1.01
0.97
6.10
5.89
f1 (ppm)

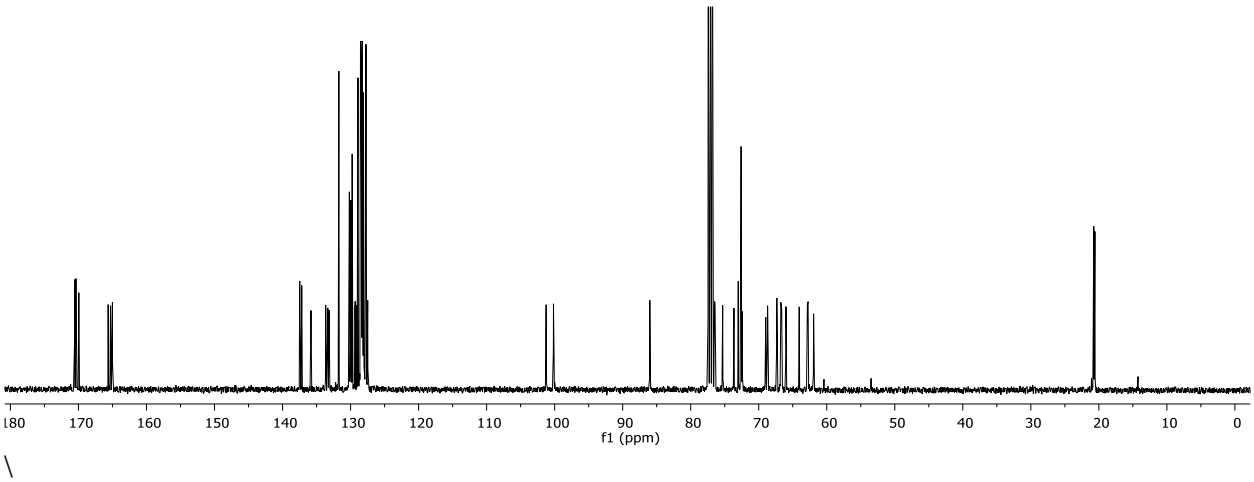
f1 (ppm)

\

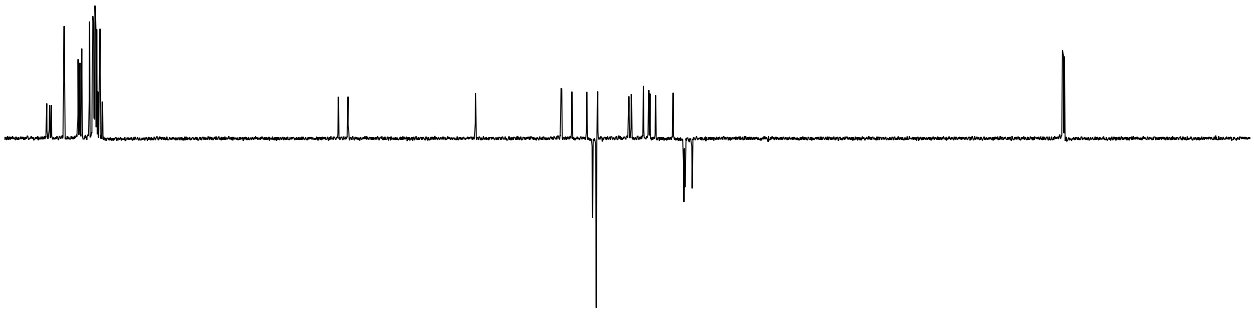

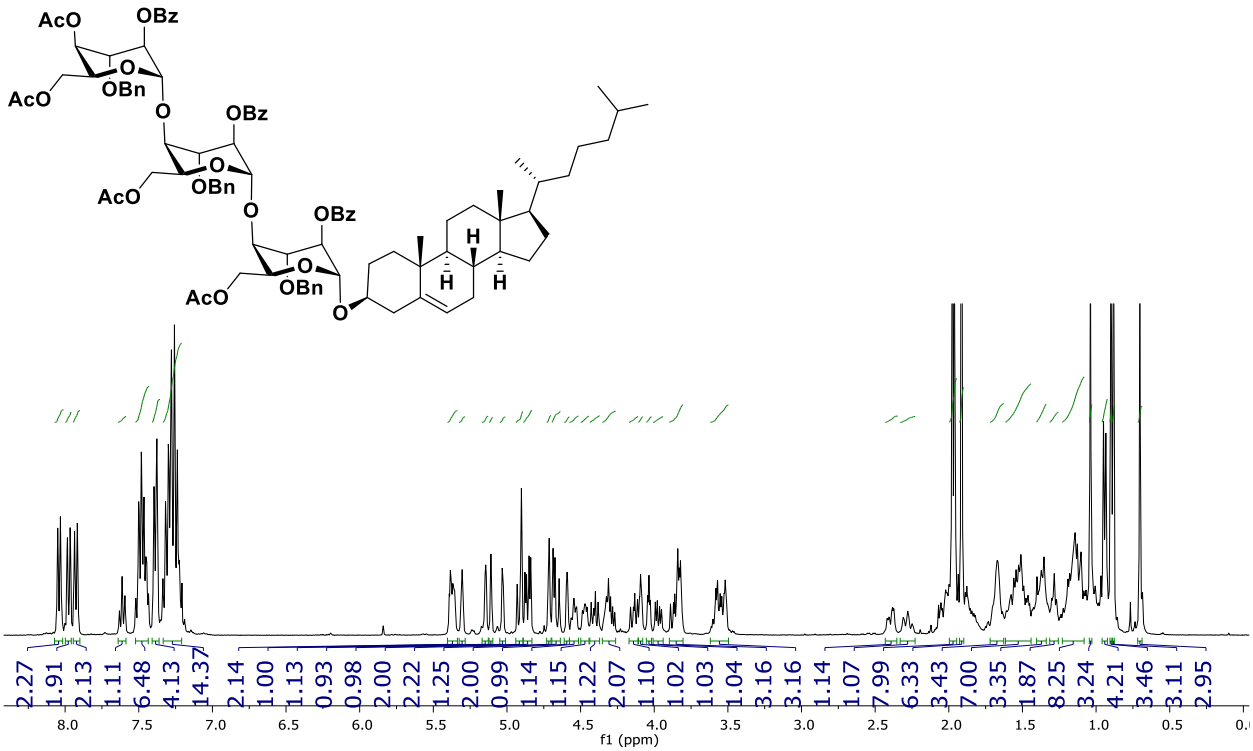
AcO
OBz
O
OBn
AcO
O
OBz
O
OBn
AcO
O
OBz
O
OBn
AcO
O
H
H
H
2.27 1.91 2.13 1.11 6.48 4.13 14.37 2.14 1.00 1.13 0.93 0.98 2.00 2.22 1.25 2.00 0.99 1.14 1.15 1.22 2.07 1.10 1.02 1.03 1.04 3.16 3.16 1.14 1.07 7.99 6.33 3.43 7.00 3.35 1.87 8.25 3.24 4.21 3.46 3.11 2.95
8.0 7.5 7.0 6.5 6.0 5.5 5.0 4.5 4.0 3.5 3.0 2.5 2.0 1.5 1.0 0.5
f1 (ppm)

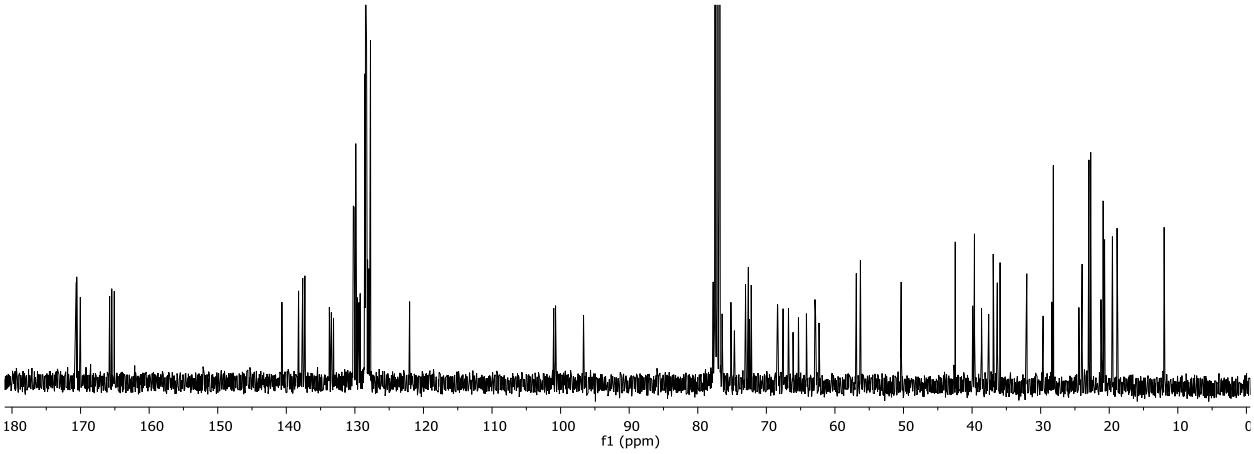
180 170 160 150 140 130 120 110 100 90 80 70 60 50 40 30 20 10
f1 (ppm)

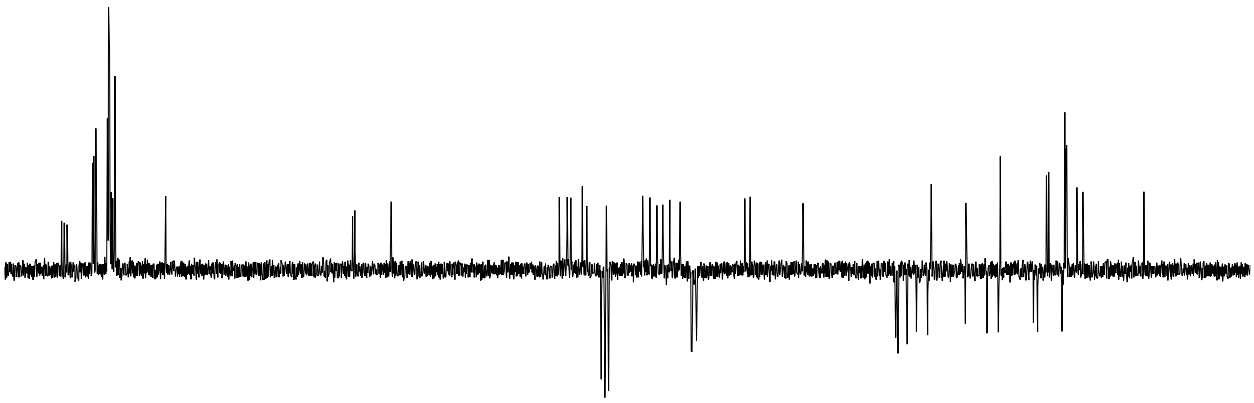

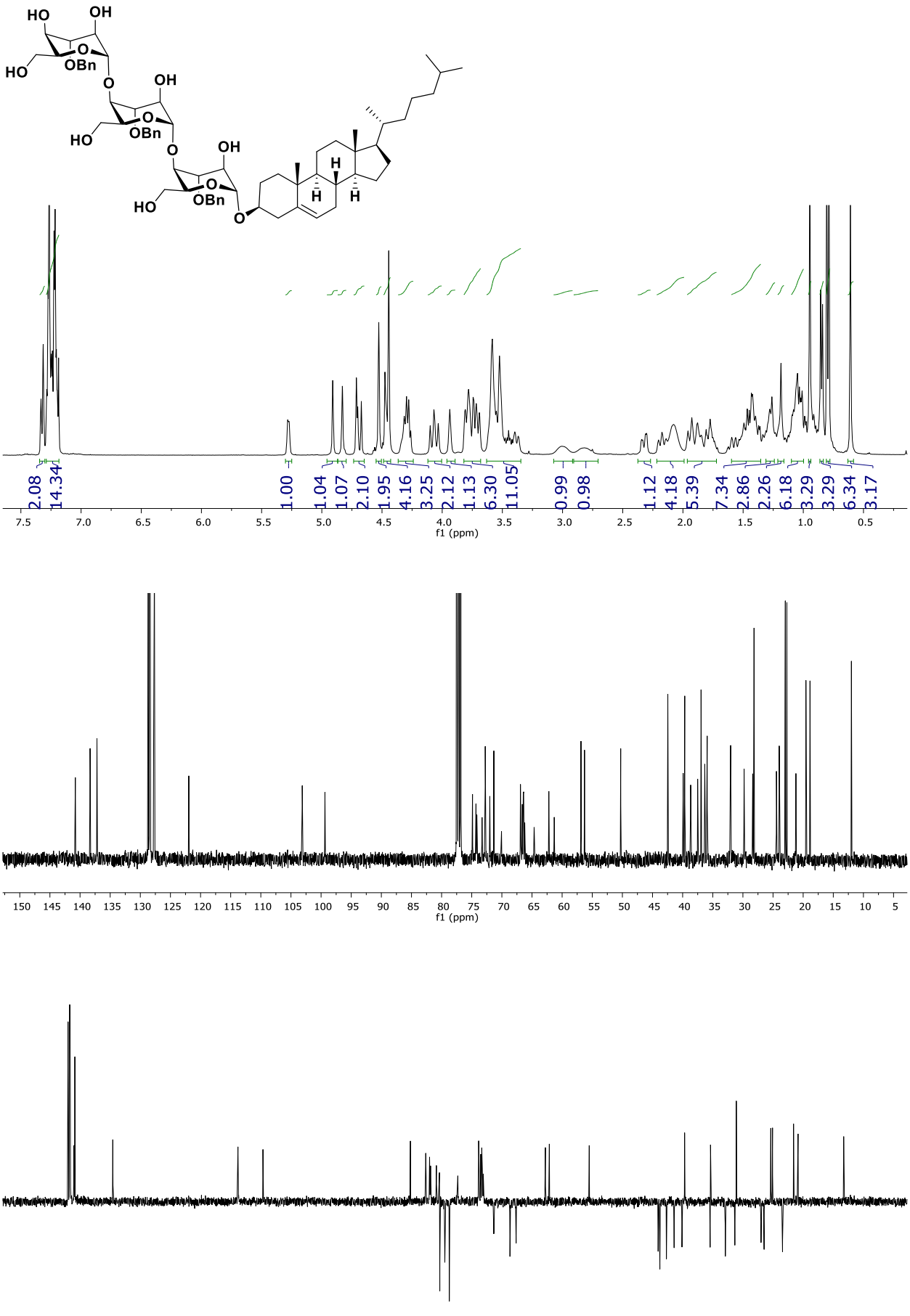
HO
OH
O
OBn
HO
O
OH
O
OBn
HO
O
OH
O
OBn
HO
O
H
H
H
2.08
14.34
1.00
1.04
1.07
2.10
1.95
4.16
3.25
2.12
1.13
6.30
11.05
0.99
0.98
1.12
4.18
5.39
7.34
2.86
2.26
6.18
3.29
3.29
6.34
3.17
7.5
7.0
6.5
6.0
5.5
5.0
4.5
4.0
3.5
3.0
2.5
2.0
1.5
1.0
0.5
f1 (ppm)
150
145
140
135
130
125
120
115
110
105
100
95
90
85
80
75
70
65
60
55
50
45
40
35
30
25
20
15
10
5
f1 (ppm)

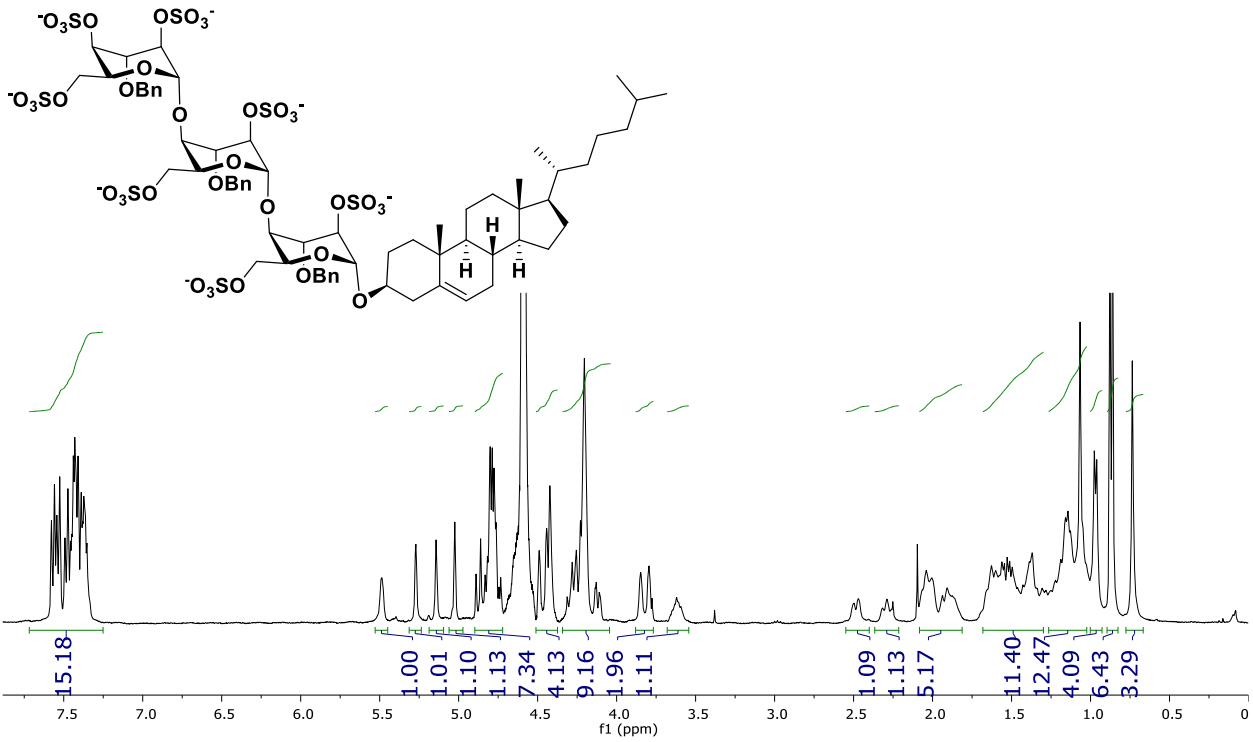
15.18
1.00
1.01
1.10
1.13
7.34
4.13
9.16
1.96
1.11
1.09
1.13
5.17
11.40
12.47
4.09
6.43
3.29
f1 (ppm)

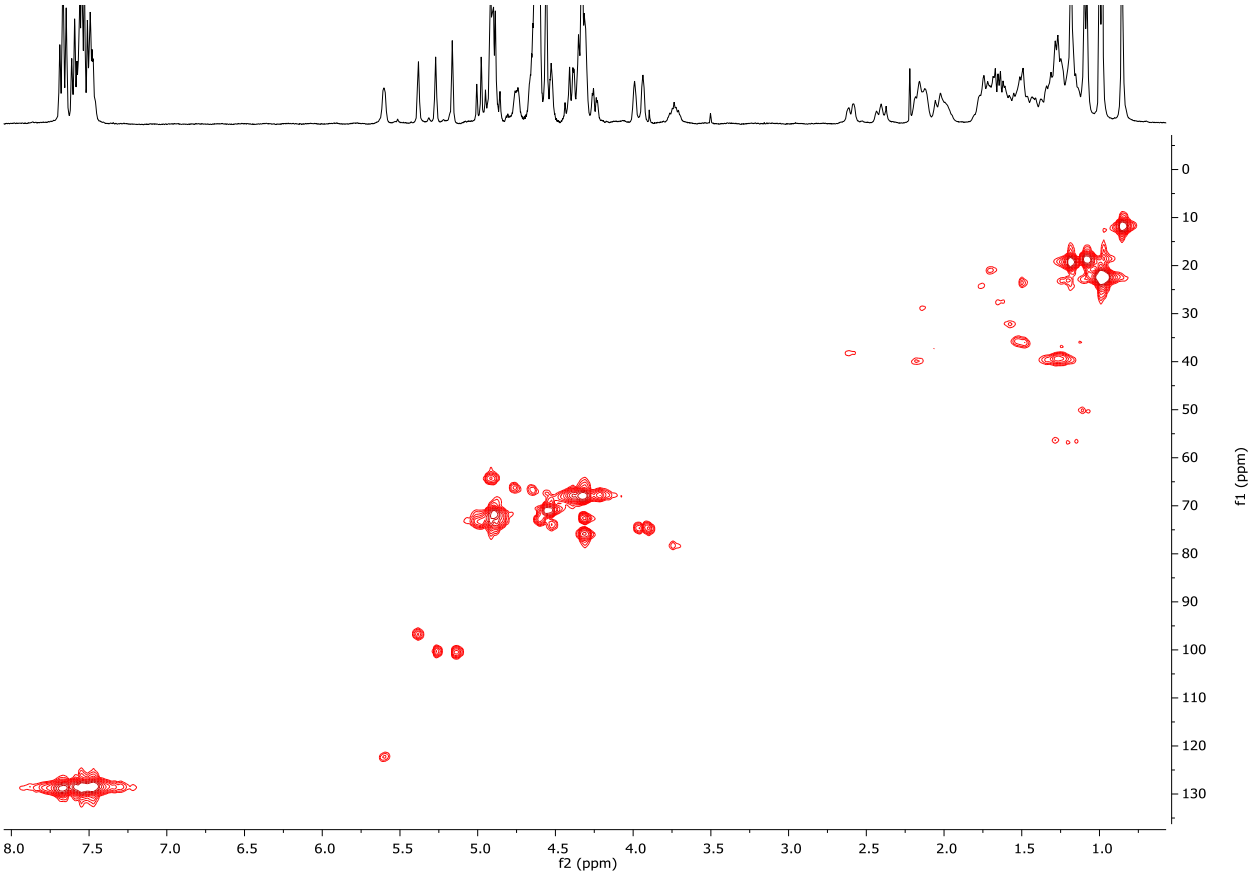
f2 (ppm)
f1 (ppm)

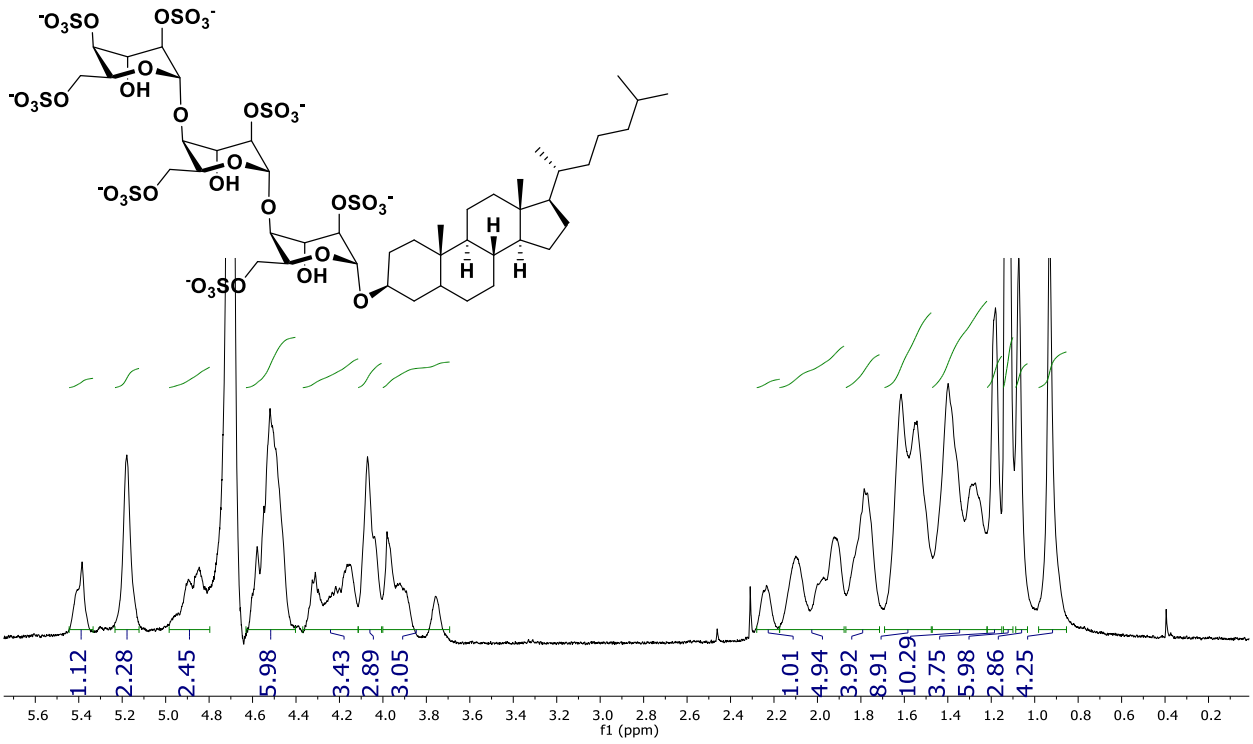
1.12
2.28
2.45
5.98
3.43
2.89
3.05
1.01
4.94
3.92
8.91
10.29
3.75
5.98
2.86
4.25
f1 (ppm)

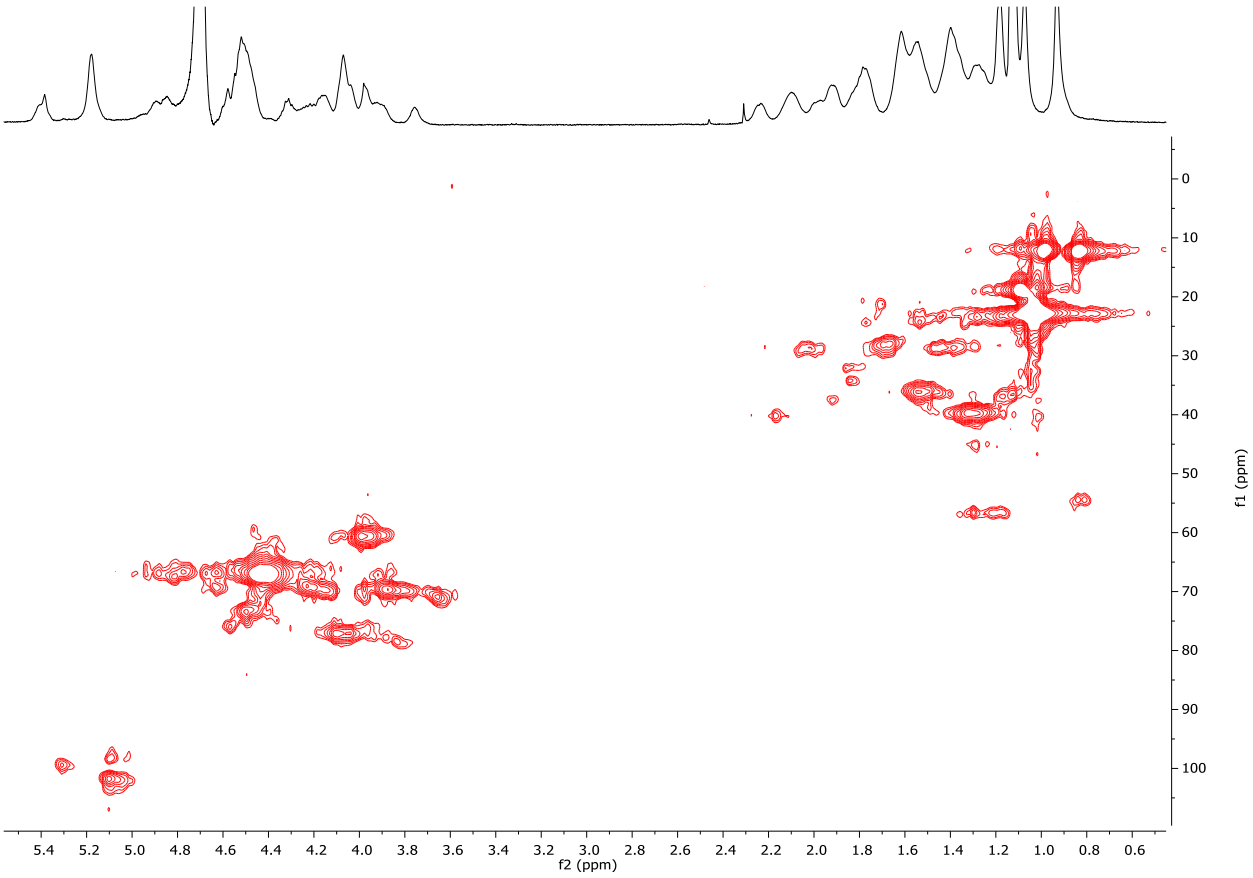
f2 (ppm)
f1 (ppm)

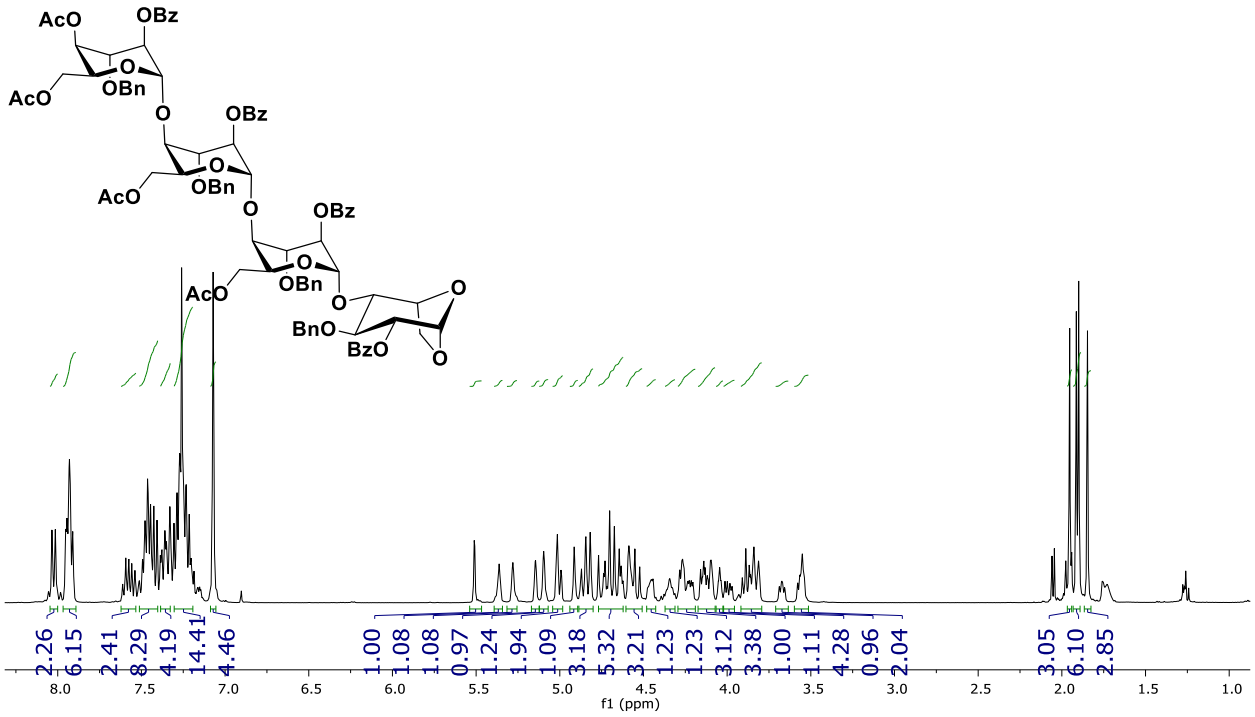
AcO
OBz
O
OBn
AcO
O
OBz
O
OBn
AcO
O
OBz
O
OBn
AcO
O
BnO
BzO
O
O
2.26 6.15 2.41 8.29 4.19 14.41 4.46 1.00 1.08 1.08 0.97 1.24 1.94 1.09 3.18 5.32 3.21 1.23 1.23 3.12 3.38 1.00 1.11 4.28 0.96 2.04 3.05 6.10 2.85
8.0 7.5 7.0 6.5 6.0 5.5 5.0 4.5 4.0 3.5 3.0 2.5 2.0 1.5 1.0
f1 (ppm)

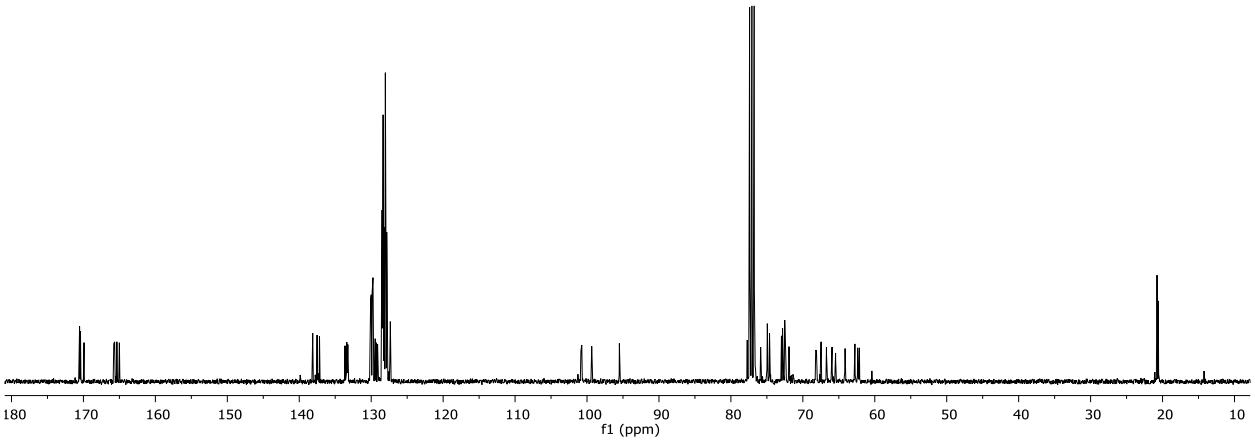
180 170 160 150 140 130 120 110 100 90 80 70 60 50 40 30 20 10
f1 (ppm)

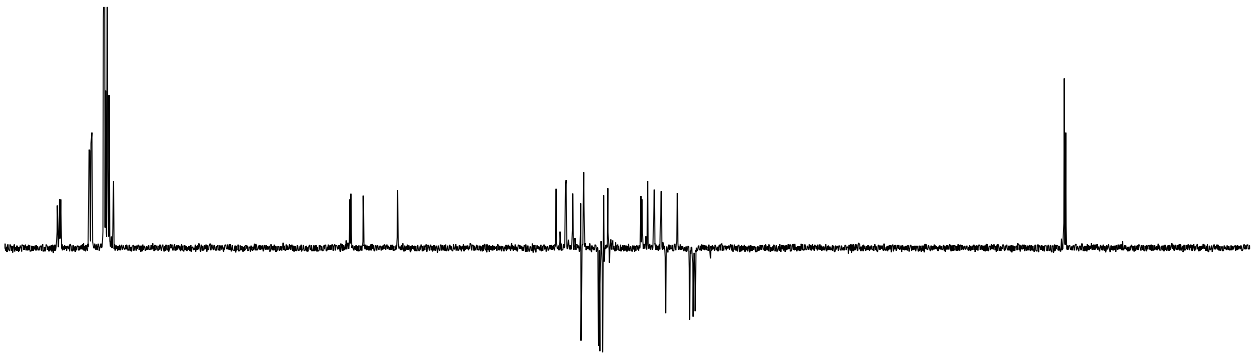

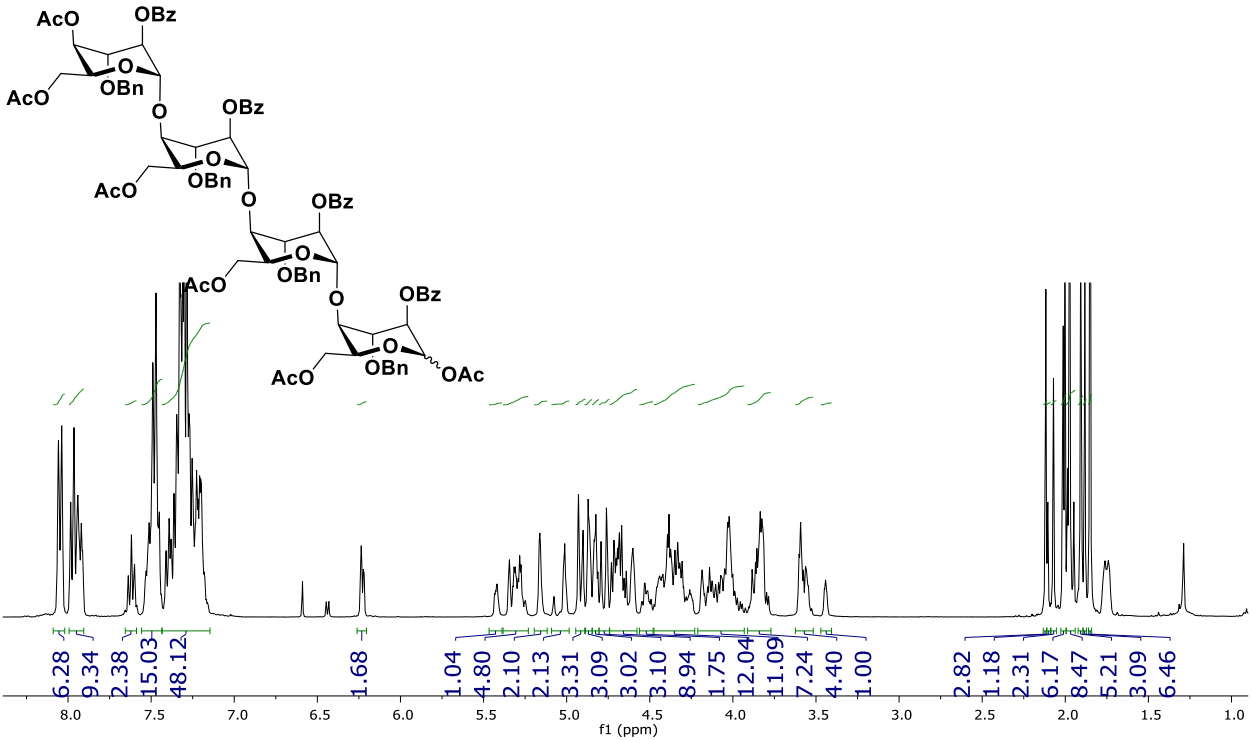
AcO
OBz
O
OBn
AcO
OBz
O
OBn
AcO
OBz
O
OBn
AcO
OBz
O
OBn
OAc
6.28
9.34
2.38
15.03
48.12
1.68
1.04
4.80
2.10
2.13
3.31
3.09
3.02
3.10
8.94
1.75
12.04
11.09
7.24
4.40
1.00
2.82
1.18
2.31
6.17
8.47
5.21
3.09
6.46
f1 (ppm)

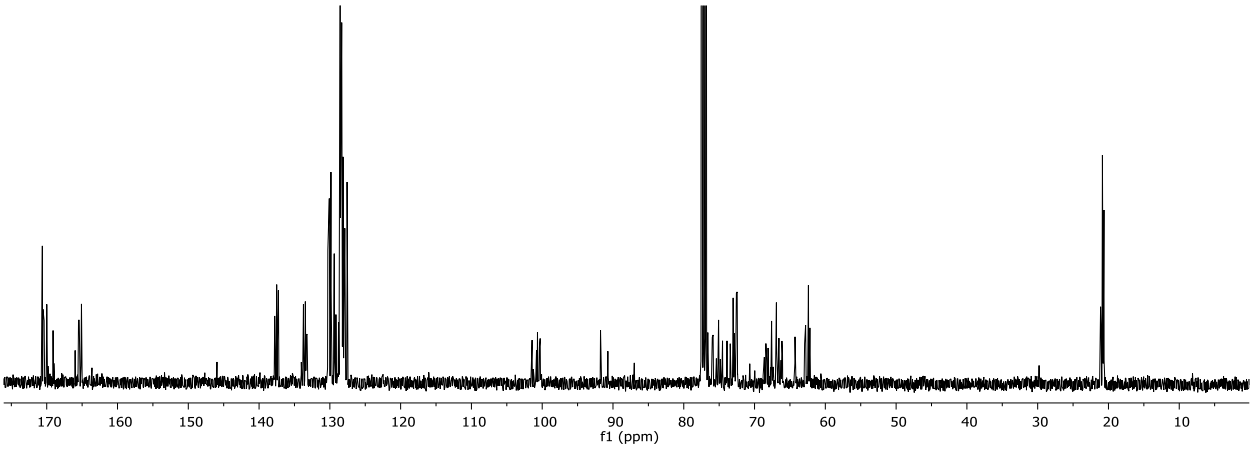
f1 (ppm)

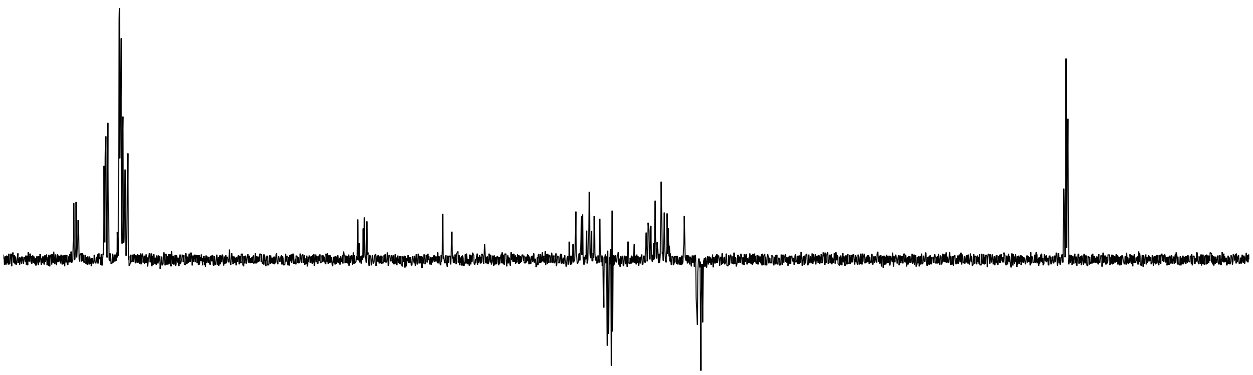

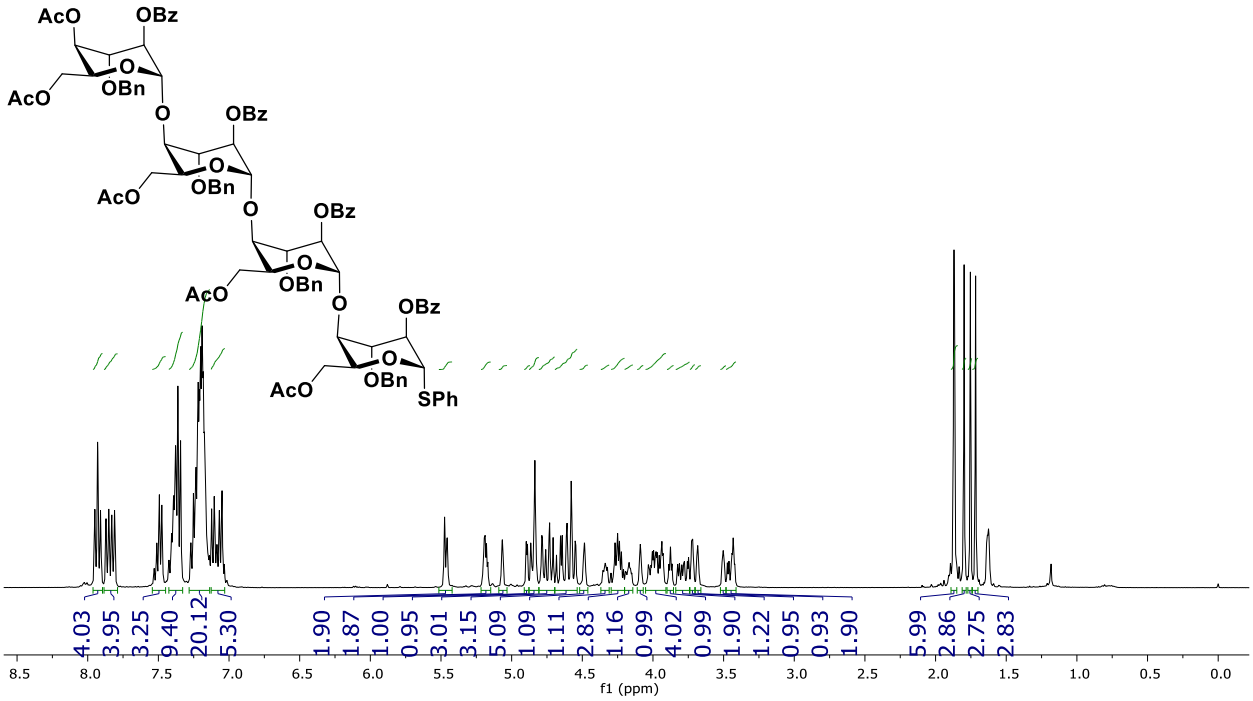
AcO
OBz
O
OBn
AcO
OBz
O
OBn
AcO
OBz
O
OBn
AcO
OBz
O
OBn
SPh
4.03
3.95
3.25
9.40
20.12
5.30
1.90
1.87
1.00
0.95
3.01
3.15
5.09
1.09
1.11
2.83
1.16
0.99
4.02
0.99
1.90
1.22
0.95
0.93
1.90
5.99
2.86
2.75
2.83
f1 (ppm)

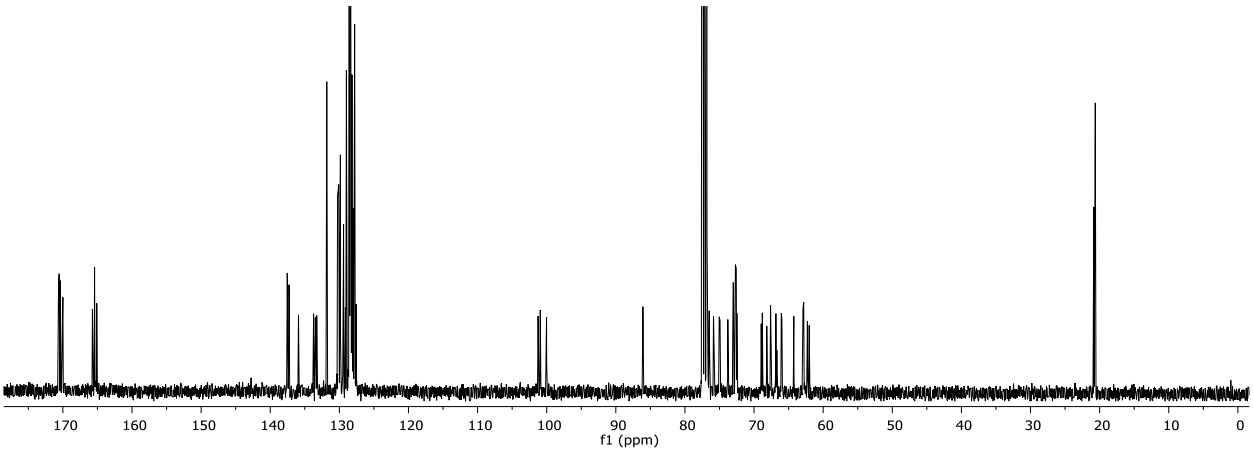
f1 (ppm)

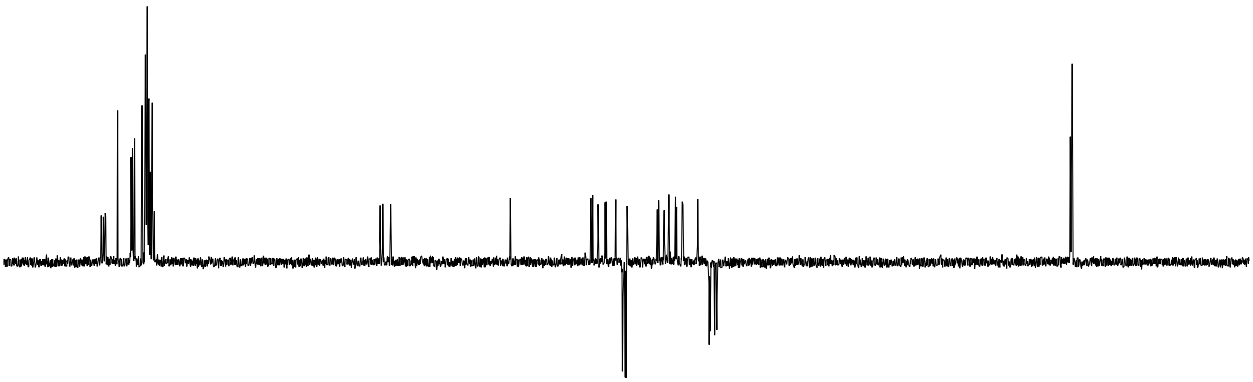

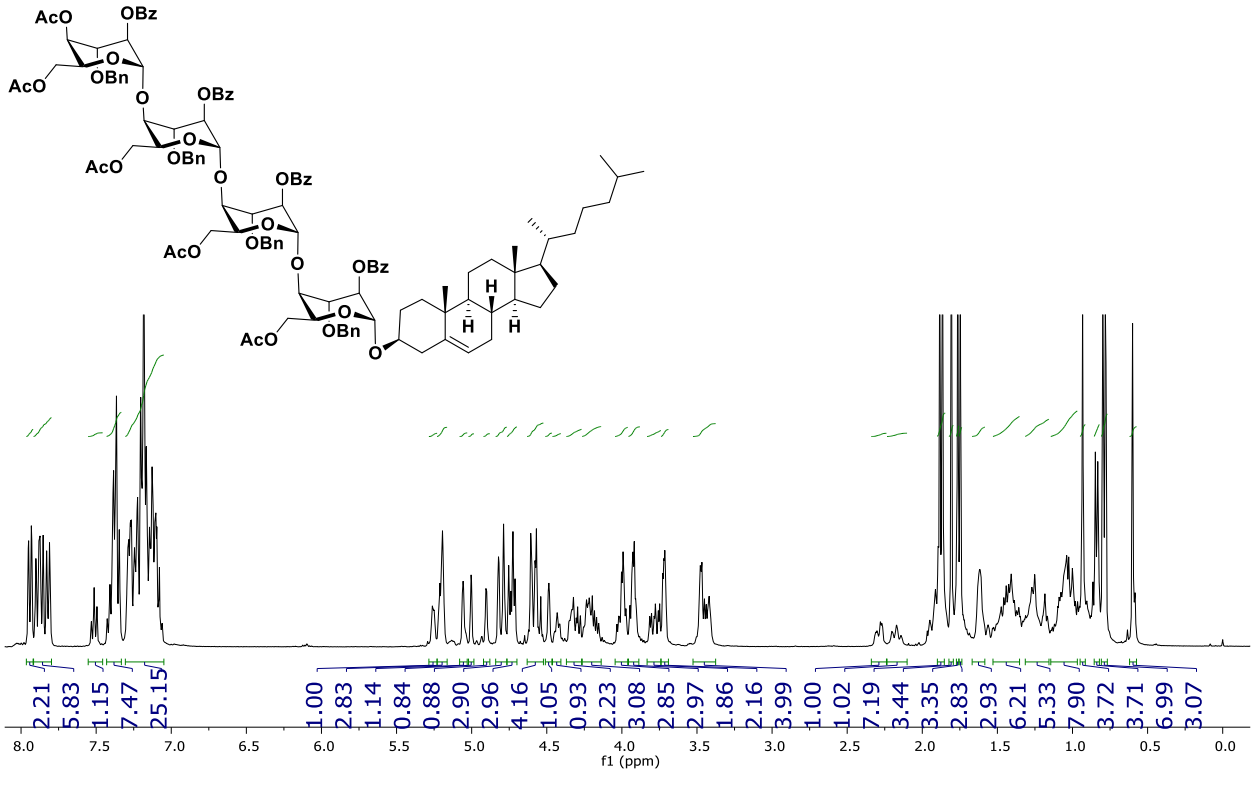
AcO
OBz
OBn
O
H
2.21 5.83 1.15 7.47 25.15 1.00 2.83 1.14 0.84 0.88 2.90 2.96 4.16 1.05 0.93 2.23 3.08 2.85 2.97 1.86 2.16 3.99 1.00 1.02 7.19 3.44 3.35 2.83 2.93 6.21 5.33 7.90 3.72 3.71 6.99 3.07
8.0 7.5 7.0 6.5 6.0 5.5 5.0 4.5 4.0 3.5 3.0 2.5 2.0 1.5 1.0 0.5 0.0
f1 (ppm)

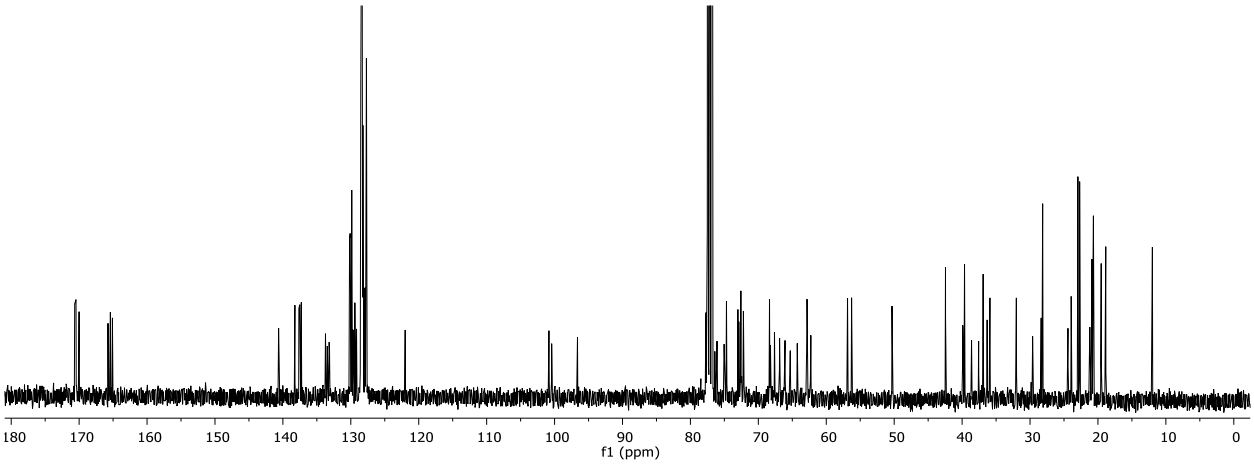
180 170 160 150 140 130 120 110 100 90 80 70 60 50 40 30 20 10 0
f1 (ppm)

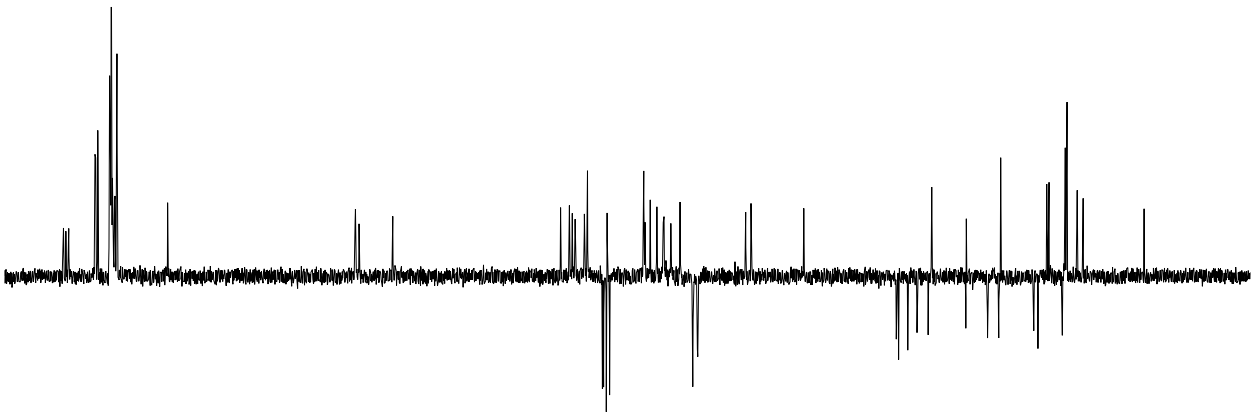

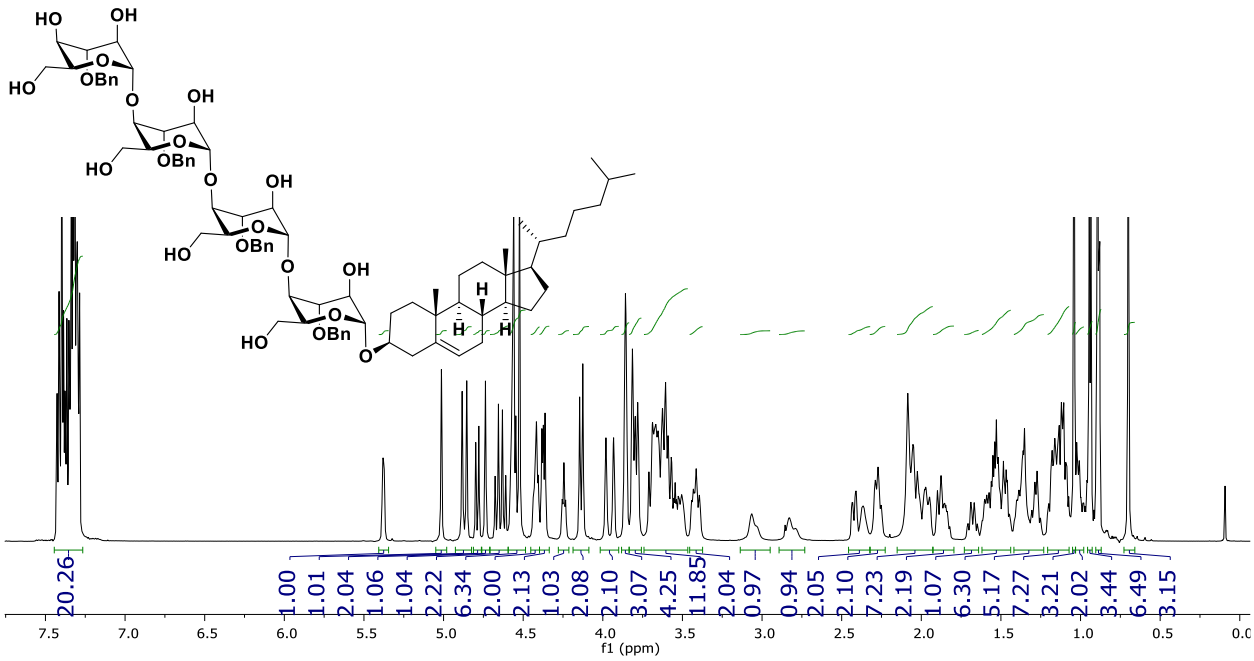
HO
OH
O
OBn
HO
OH
O
OBn
HO
OH
O
OBn
HO
OH
O
OBn
H
H
H
O
20.26
1.00
1.01
2.04
1.06
1.04
2.22
6.34
2.00
2.13
1.03
2.08
2.10
3.07
4.25
11.85
2.04
0.97
0.94
2.05
2.10
7.23
2.19
1.07
6.30
5.17
7.27
3.21
2.02
3.44
6.49
3.15
7.5
7.0
6.5
6.0
5.5
5.0
4.5
4.0
3.5
3.0
2.5
2.0
1.5
1.0
0.5
f1 (ppm)

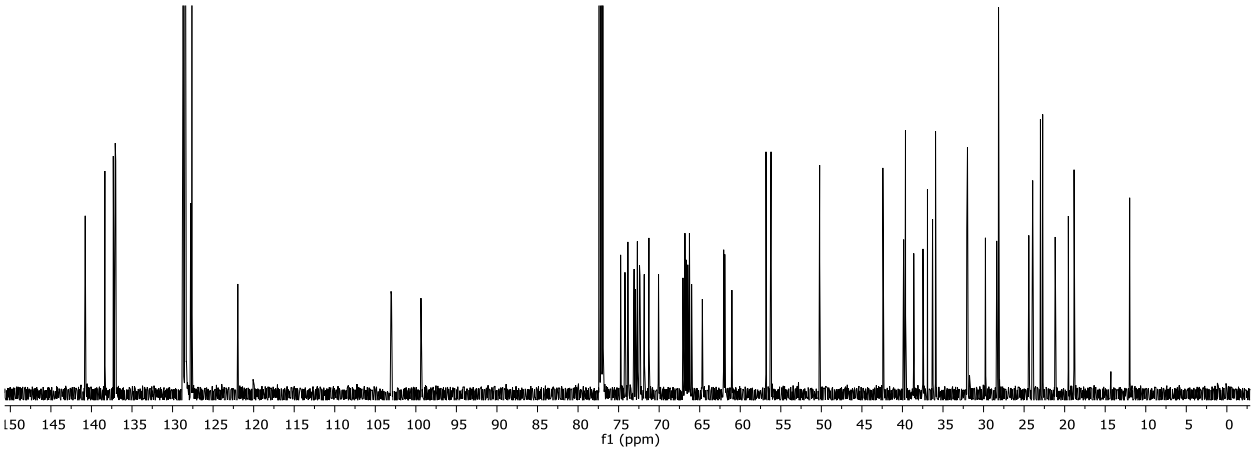
150 145 140 135 130 125 120 115 110 105 100 95 90 85 80 75 70 65 60 55 50 45 40 35 30 25 20 15 10 5 0
f1 (ppm)

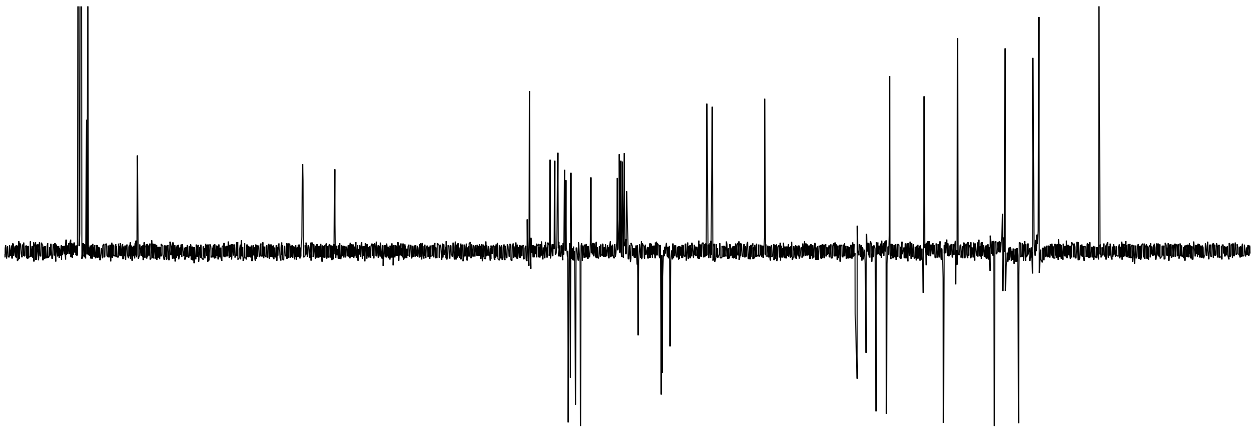

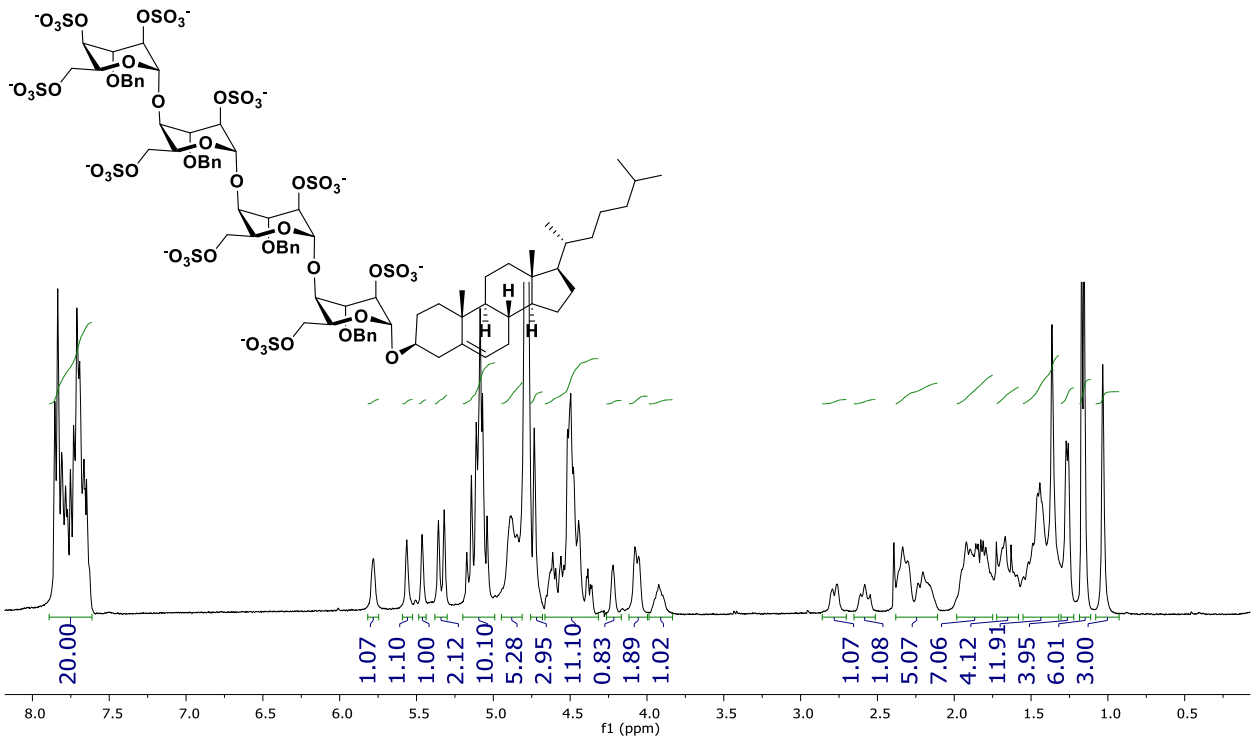
20.00
1.07
1.10
1.00
2.12
10.10
5.28
2.95
11.10
0.83
1.89
1.02
1.07
1.08
5.07
7.06
4.12
11.91
3.95
6.01
3.00
f1 (ppm)

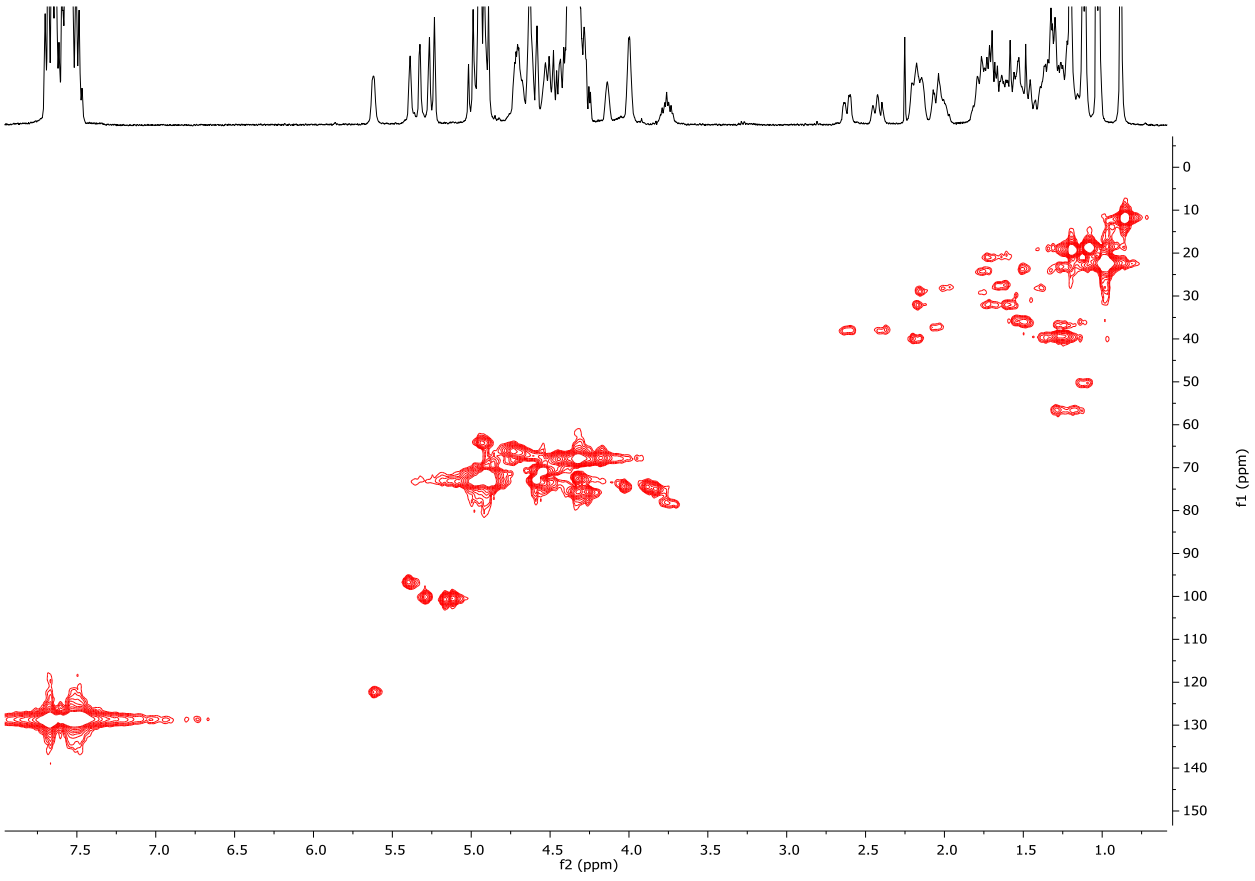
f2 (ppm)
f1 (ppm)

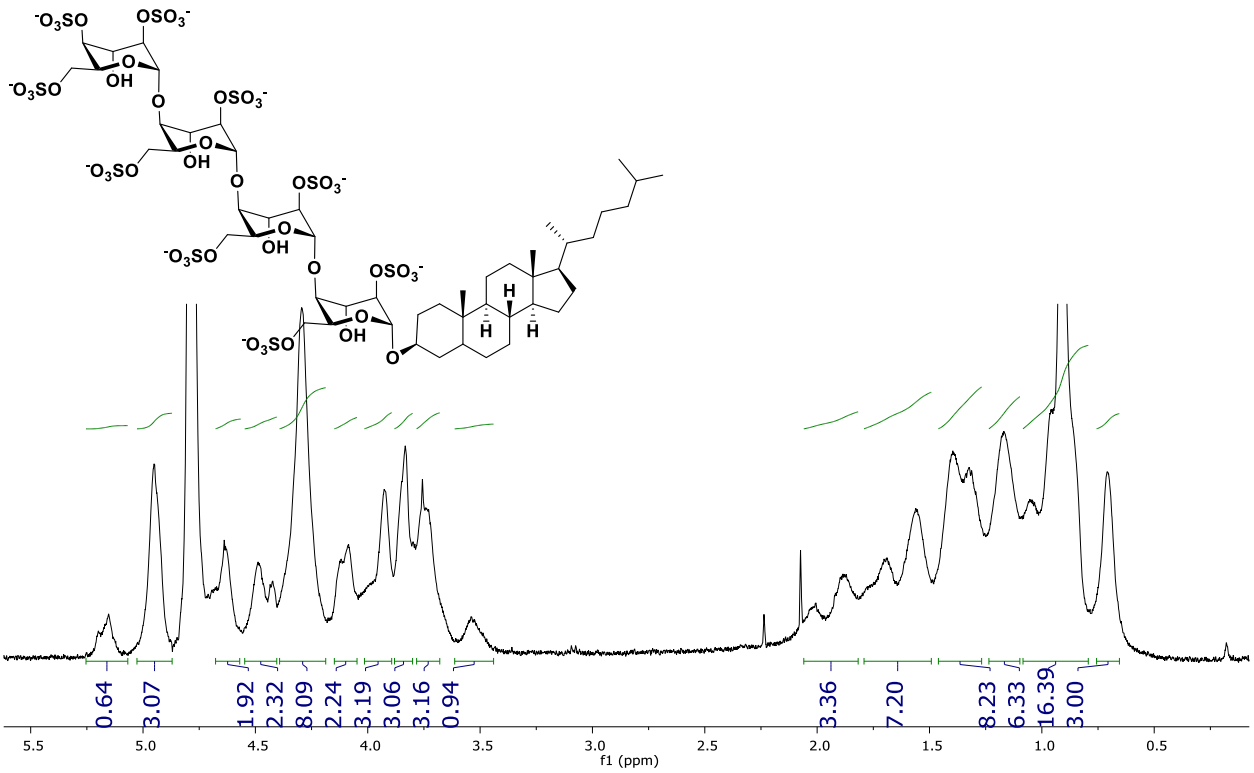
0.64
3.07
1.92
2.32
8.09
2.24
3.19
3.06
3.16
0.94
3.36
7.20
8.23
6.33
16.39
3.00
f1 (ppm)

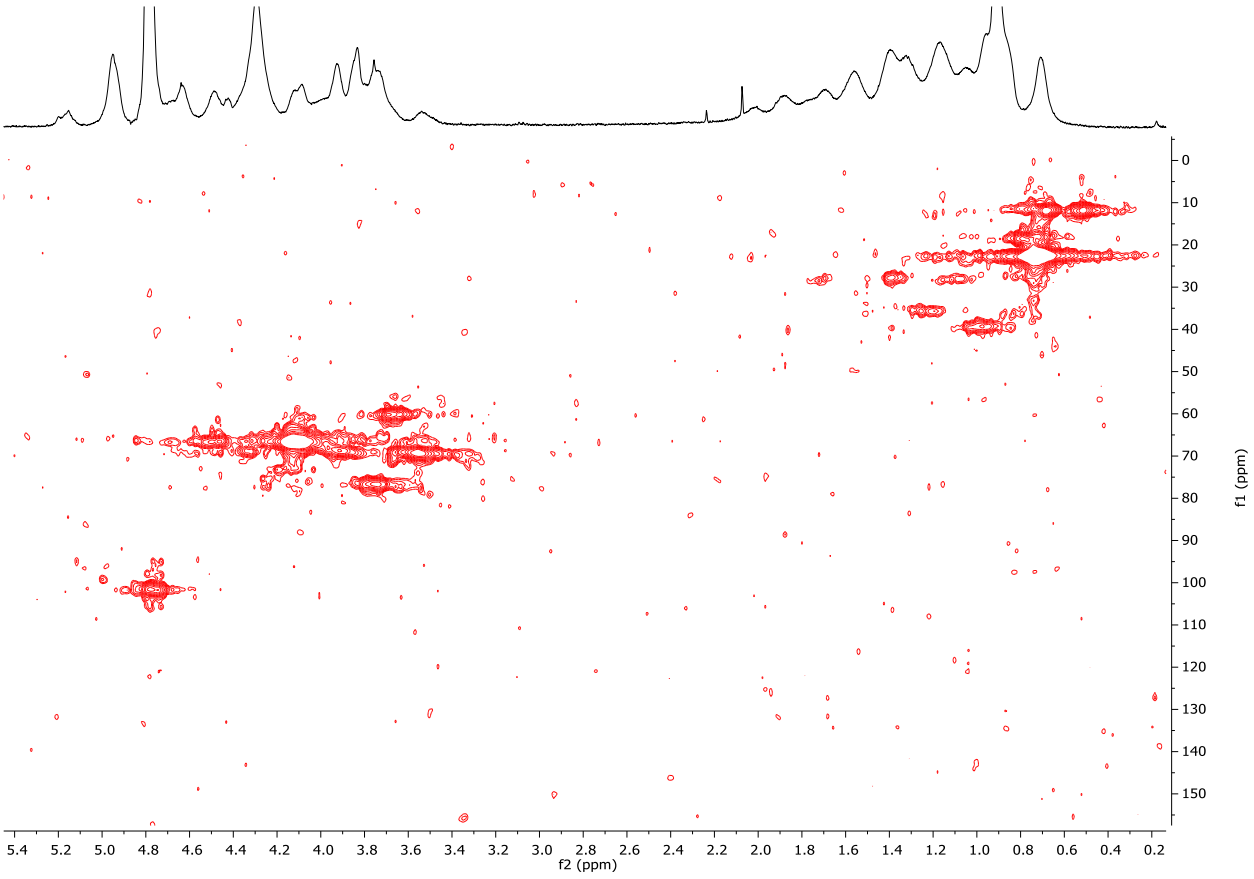
f2 (ppm)
f1 (ppm)

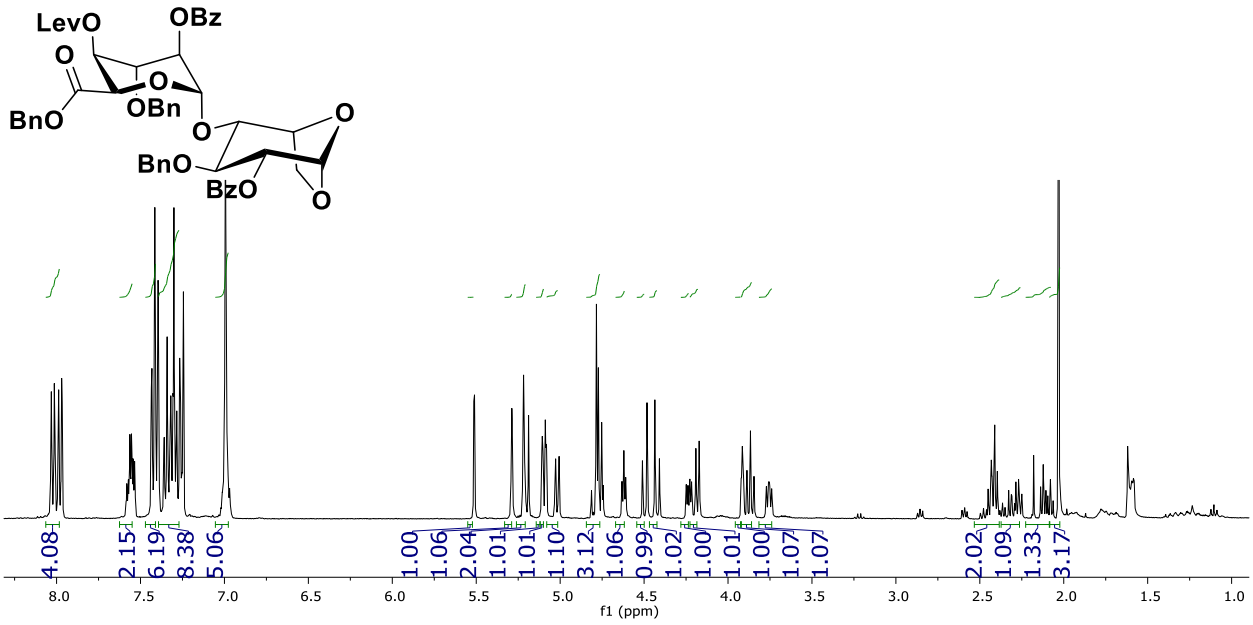
LevO
OBz
O
O
BnO
OBn
O
O
BnO
BzO
O
4.08
2.15
6.19
8.38
5.06
1.00
1.06
2.04
1.01
1.01
1.10
3.12
1.06
0.99
1.02
1.00
1.01
1.00
1.07
1.07
2.02
1.09
1.33
3.17
8.0
7.5
7.0
6.5
6.0
5.5
5.0
4.5
4.0
3.5
3.0
2.5
2.0
1.5
1.0
f1 (ppm)

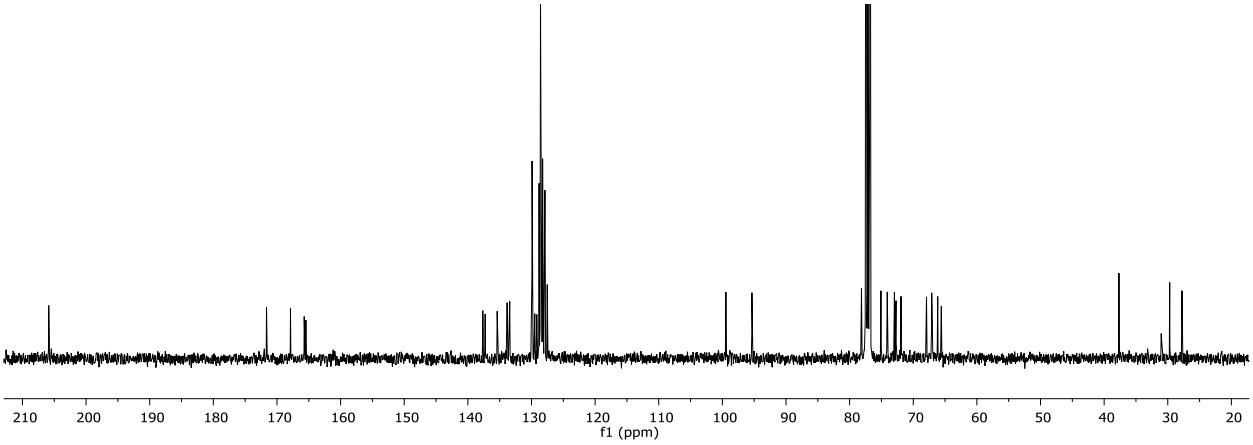
210
200
190
180
170
160
150
140
130
120
110
100
90
80
70
60
50
40
30
20
f1 (ppm)

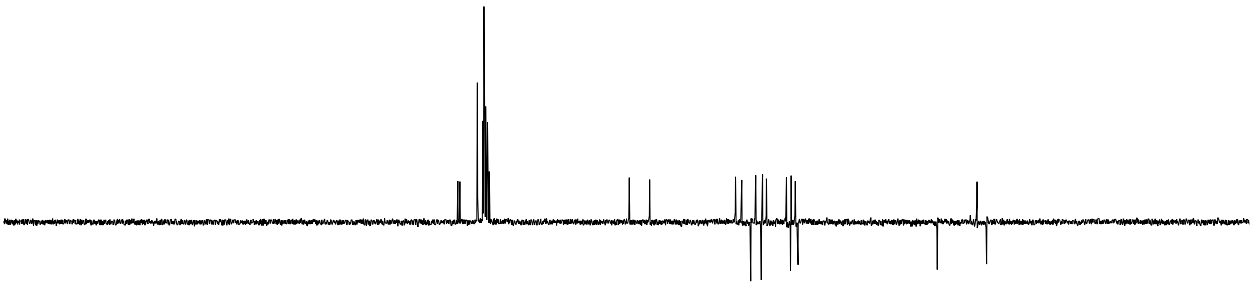

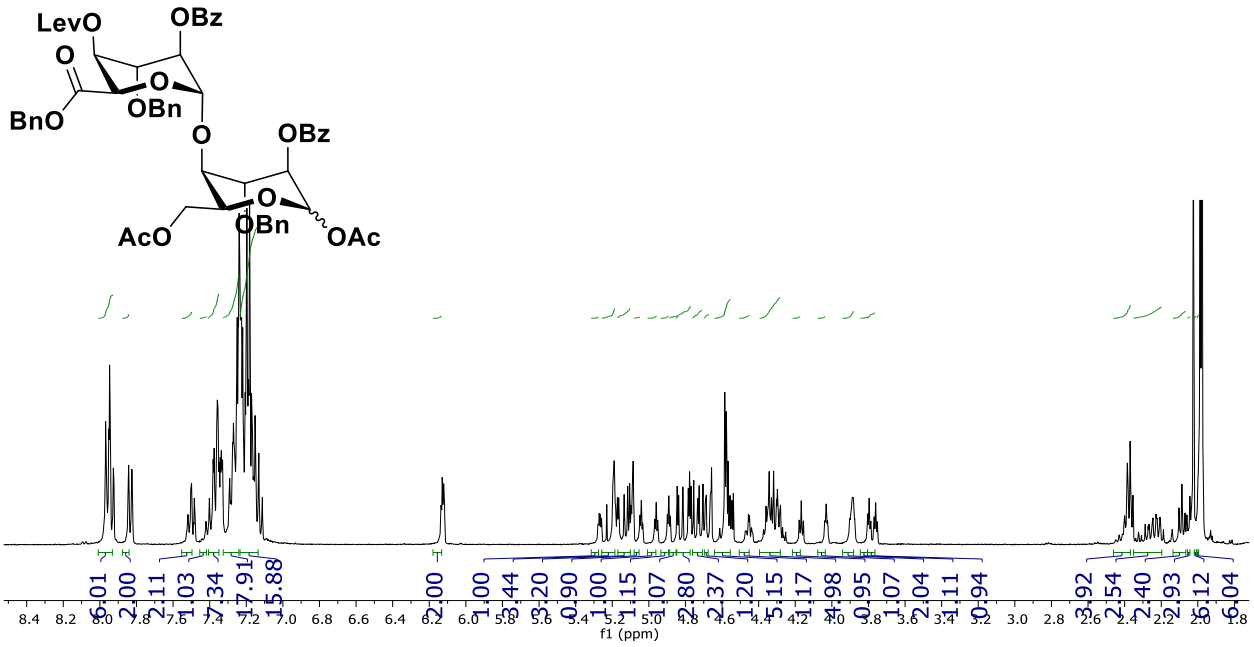
LevO
OBz
O
O
OBn
BnO
O
OBz
O
OBn
AcO
OAc
6.01 2.00 2.11 1.03 7.34 17.91 15.88 2.00 1.00 3.44 3.20 0.90 1.00 1.15 1.07 2.80 2.37 1.20 5.15 1.17 4.98 0.95 1.07 2.04 1.11 0.94 3.92 2.54 2.40 2.93 6.12 6.04
f1 (ppm)

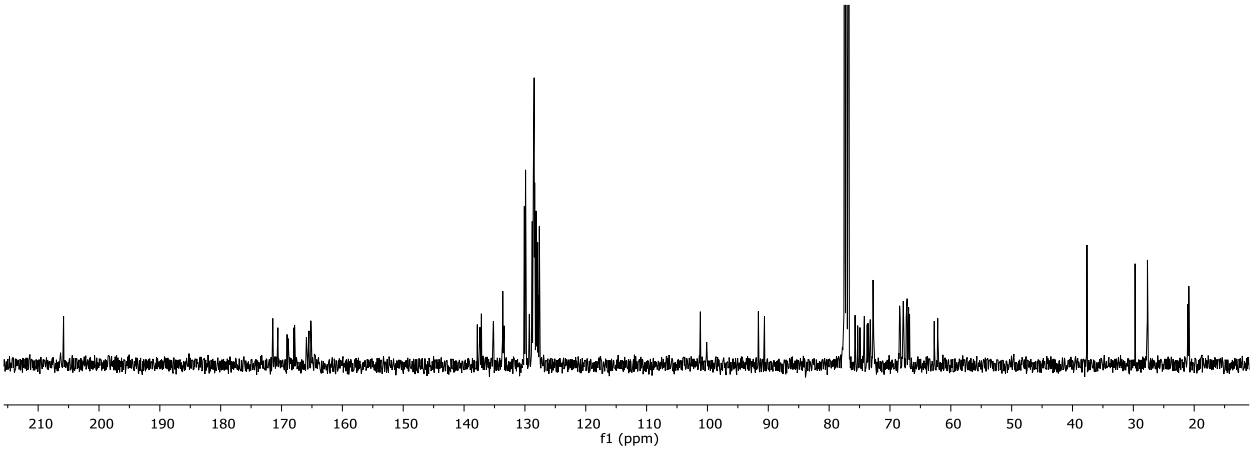
f1 (ppm)

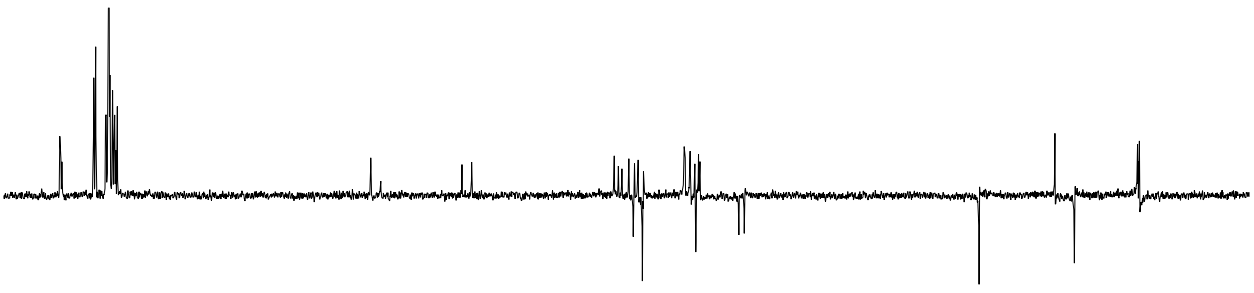

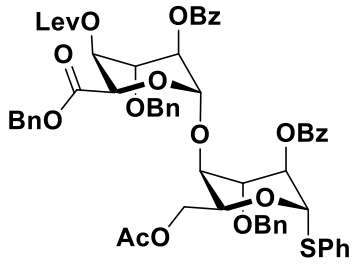
LevO
OBz
O
O
BnO
OBn
O
OBz
O
OBn
AcO
SPh

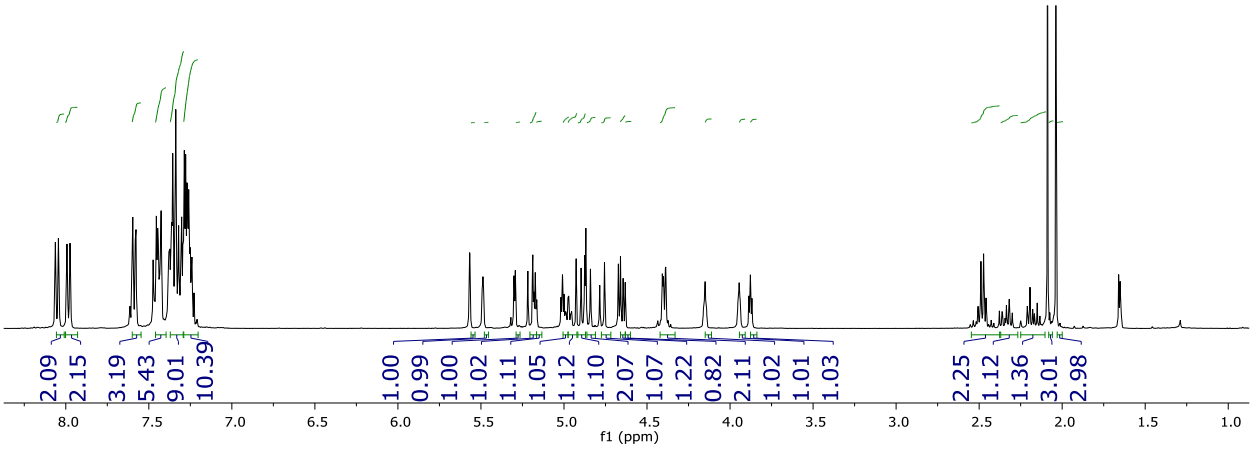
2.09
2.15
3.19
5.43
9.01
10.39
1.00
0.99
1.00
1.02
1.11
1.05
1.12
1.10
2.07
1.07
1.22
0.82
2.11
1.02
1.01
1.03
2.25
1.12
1.36
3.01
2.98
f1 (ppm)

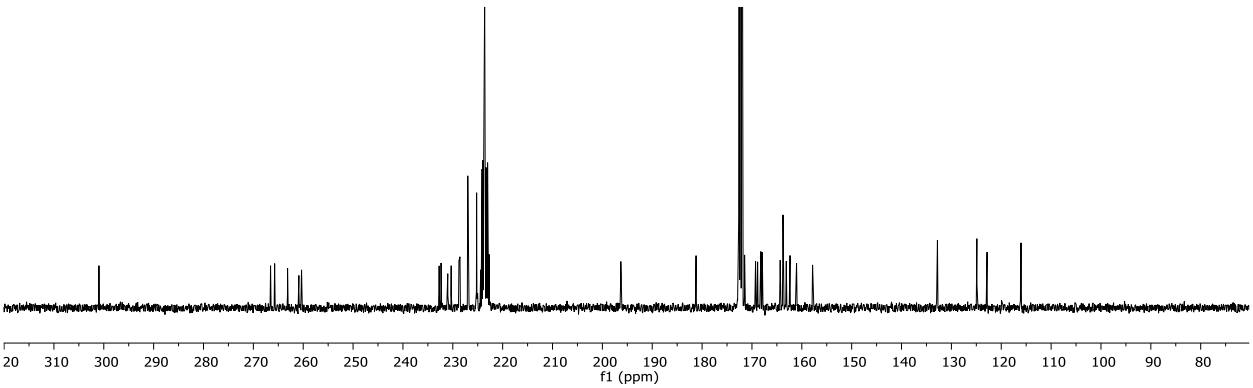
f1 (ppm)

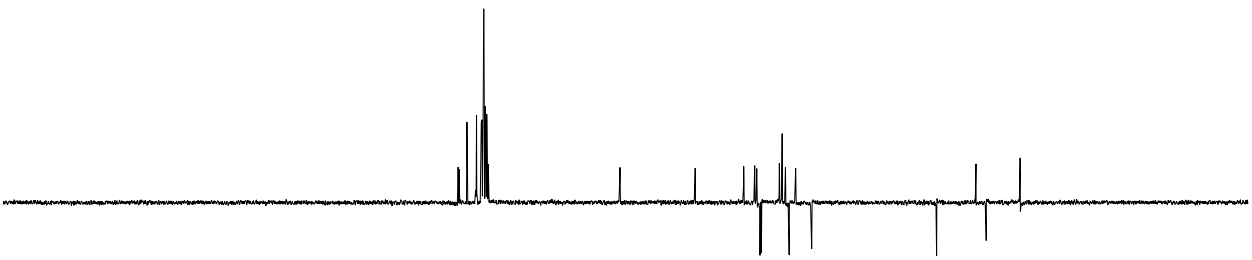

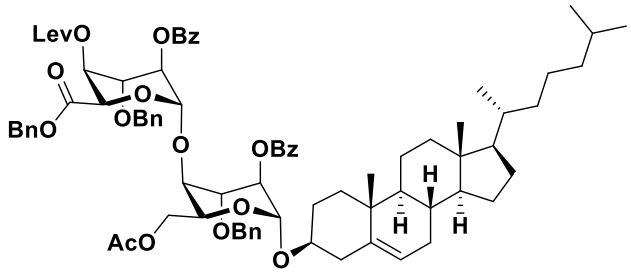
LevO
OBz
O
O
OBn
BnO
O
OBz
O
OBn
AcO
O
H
H
H

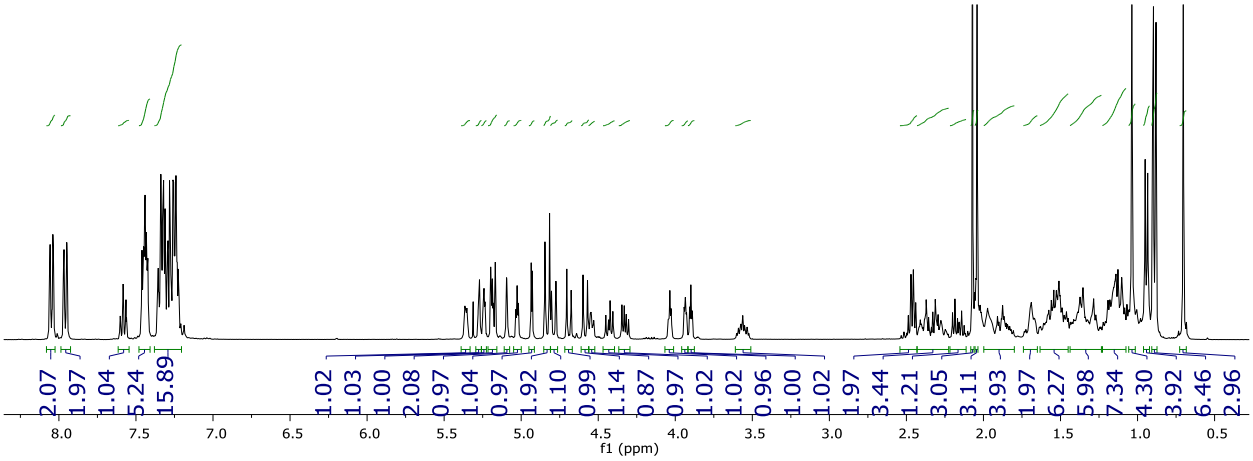
2.07 1.97 1.04 5.24 15.89 1.02 1.03 1.00 2.08 0.97 1.04 0.97 1.92 1.10 0.99 1.14 0.87 0.97 1.02 1.02 0.96 1.00 1.02 1.97 3.44 1.21 3.05 3.11 3.93 1.97 6.27 5.98 7.34 4.30 3.92 6.46 2.96
8.0 7.5 7.0 6.5 6.0 5.5 5.0 4.5 4.0 3.5 3.0 2.5 2.0 1.5 1.0 0.5
f1 (ppm)

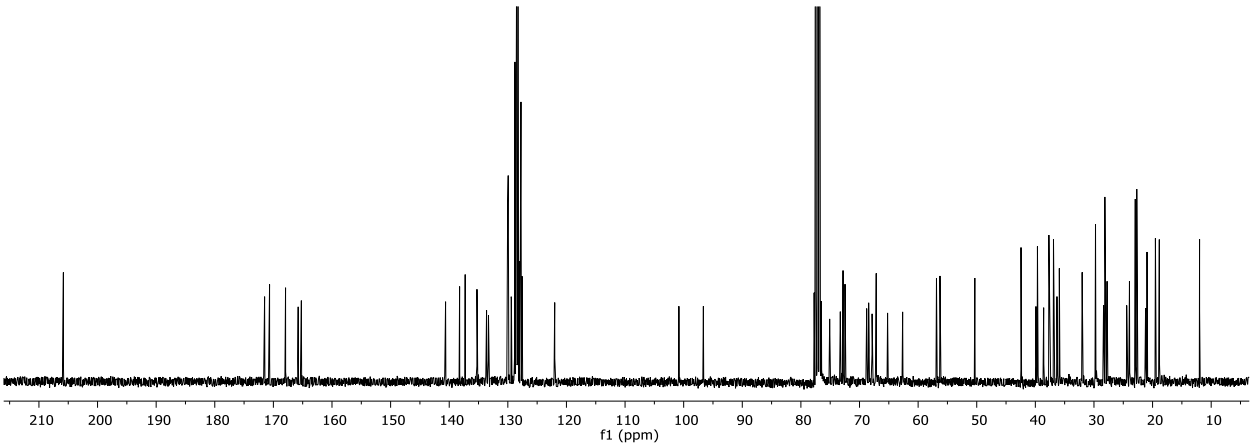
210 200 190 180 170 160 150 140 130 120 110 100 90 80 70 60 50 40 30 20 10
f1 (ppm)

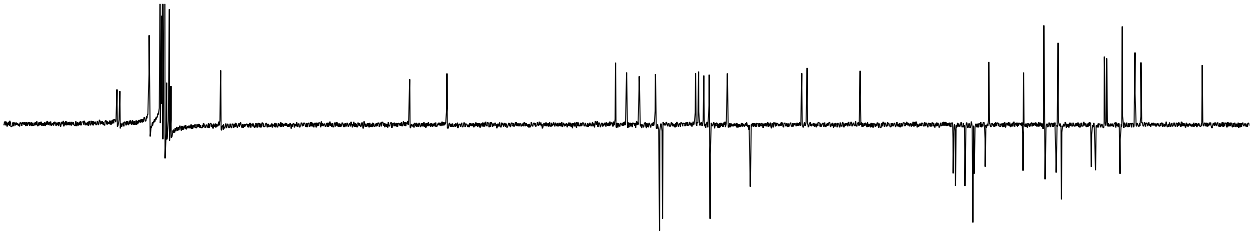

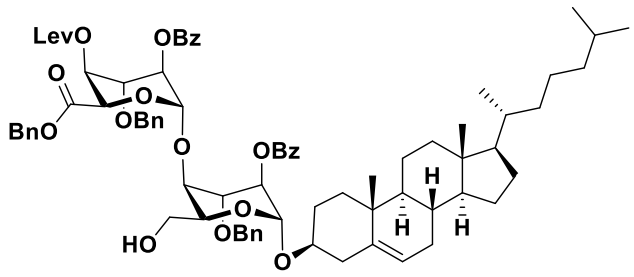
LevO
OBz
O
O
OBn
BnO
O
OBz
H
O
OBn
HO
O
H
H

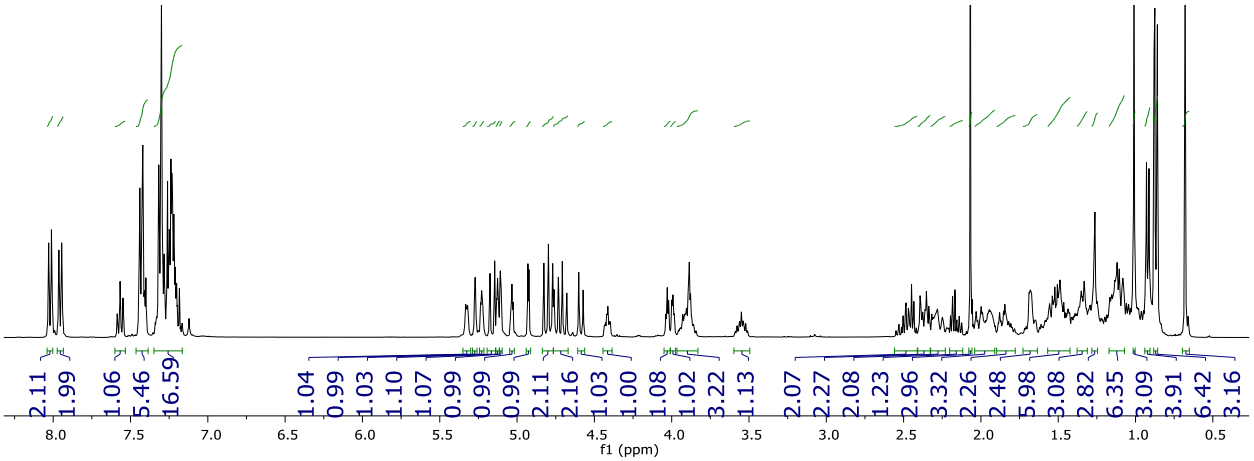
2.11 1.99 1.06 5.46 16.59 1.04 0.99 1.03 1.10 1.07 0.99 0.99 0.99 2.11 2.16 1.03 1.00 1.08 1.02 3.22 1.13 2.07 2.27 2.08 1.23 2.96 3.32 2.26 2.48 5.98 3.08 2.82 6.35 3.09 3.91 6.42 3.16
8.0 7.5 7.0 6.5 6.0 5.5 5.0 4.5 4.0 3.5 3.0 2.5 2.0 1.5 1.0 0.5
f1 (ppm)

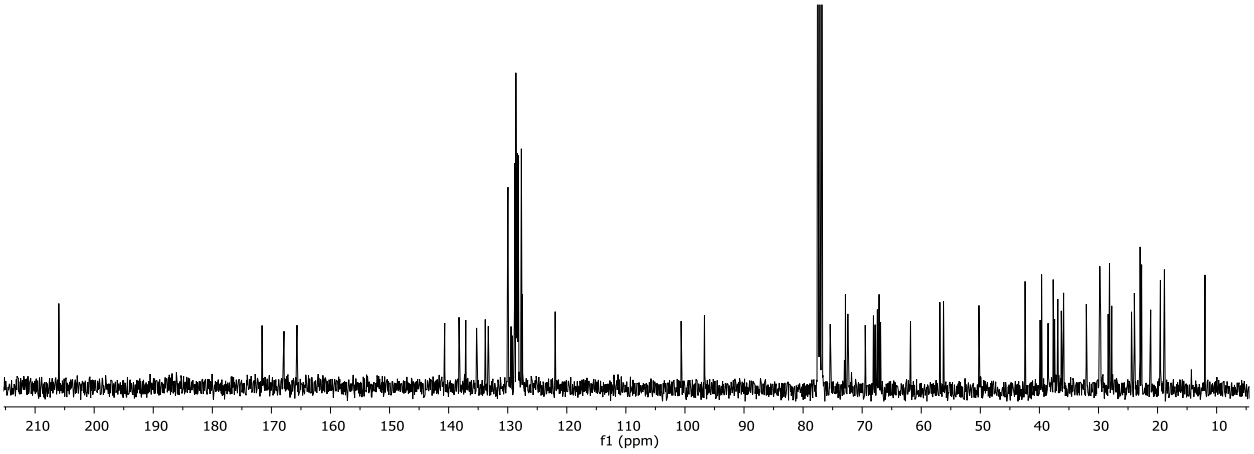
210 200 190 180 170 160 150 140 130 120 110 100 90 80 70 60 50 40 30 20 10
f1 (ppm)

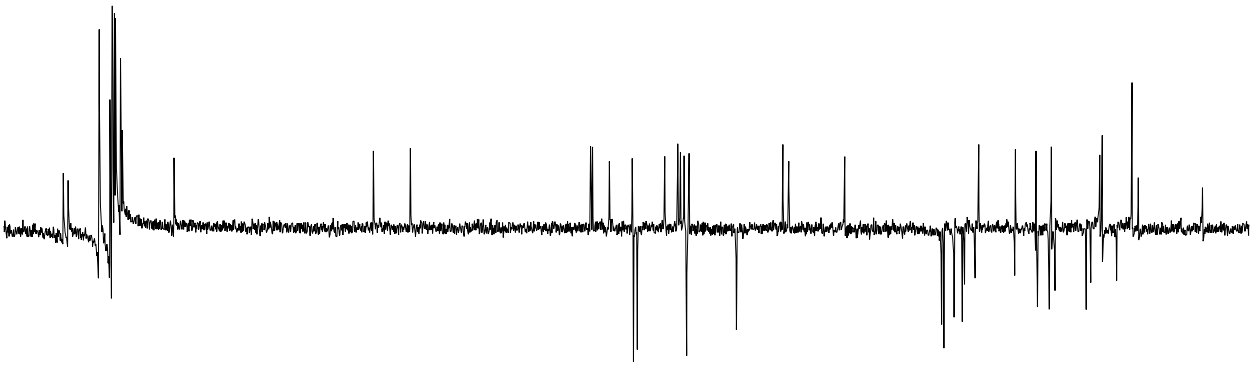

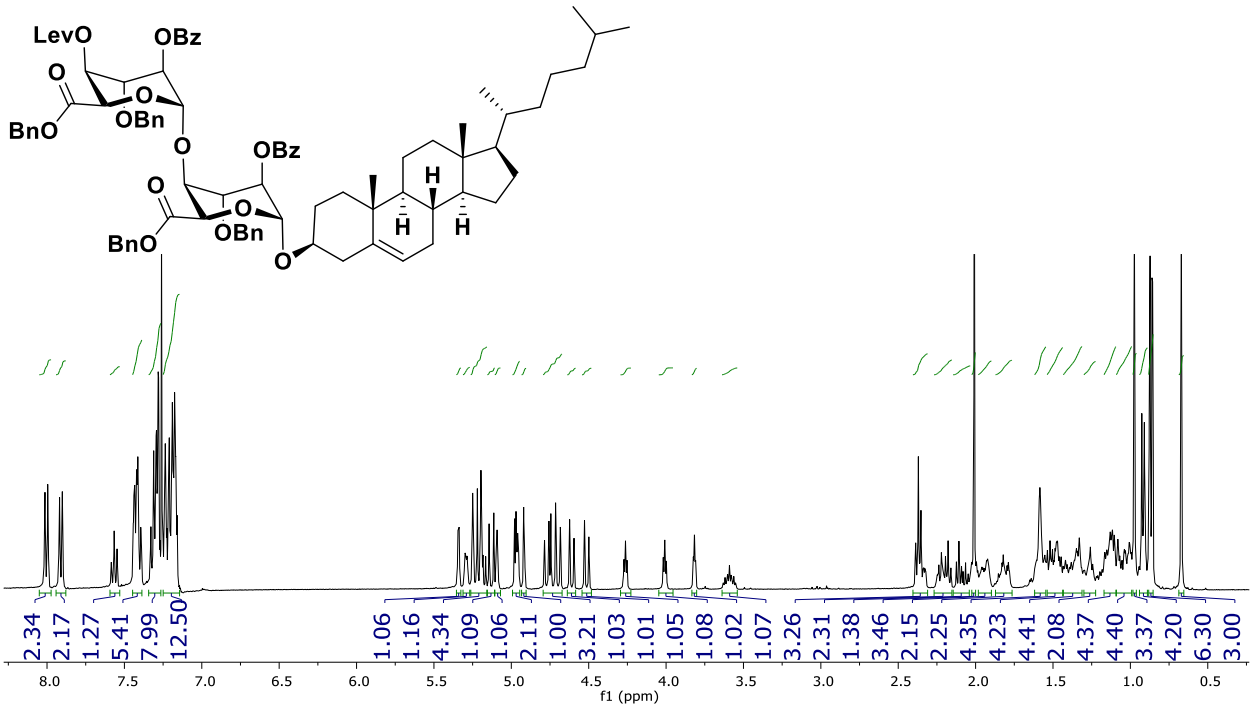
LevO
OBz
O
BnO
O
OBn
O
OBz
O
BnO
O
OBn
O
H
H
H
2.34 2.17 1.27 5.41 7.99 12.50 1.06 1.16 4.34 1.09 1.06 2.11 1.00 3.21 1.03 1.01 1.05 1.08 1.02 1.07 3.26 2.31 1.38 3.46 2.15 2.25 4.35 4.23 4.41 2.08 4.37 4.40 3.37 4.20 6.30 3.00
8.0 7.5 7.0 6.5 6.0 5.5 5.0 4.5 4.0 3.5 3.0 2.5 2.0 1.5 1.0 0.5
f1 (ppm)

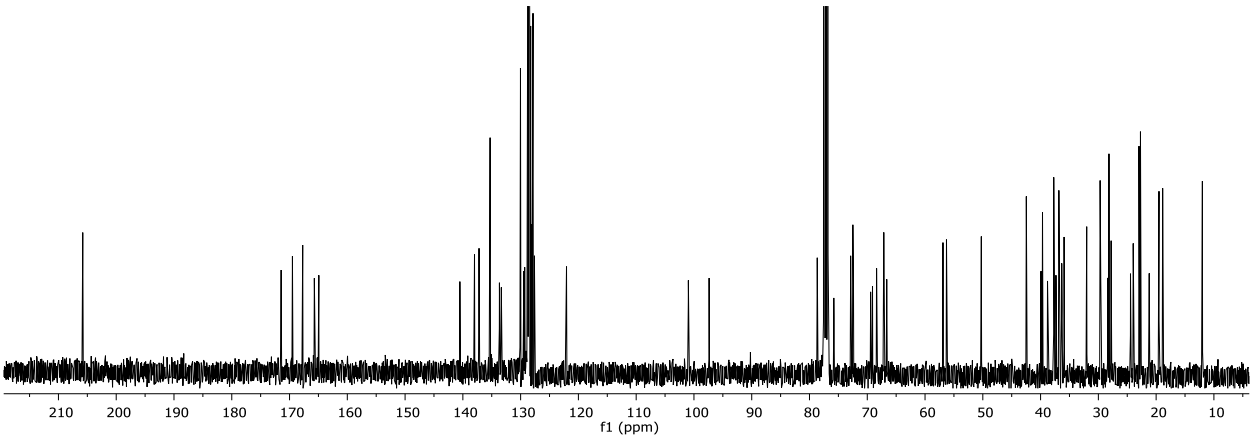
210 200 190 180 170 160 150 140 130 120 110 100 90 80 70 60 50 40 30 20 10
f1 (ppm)

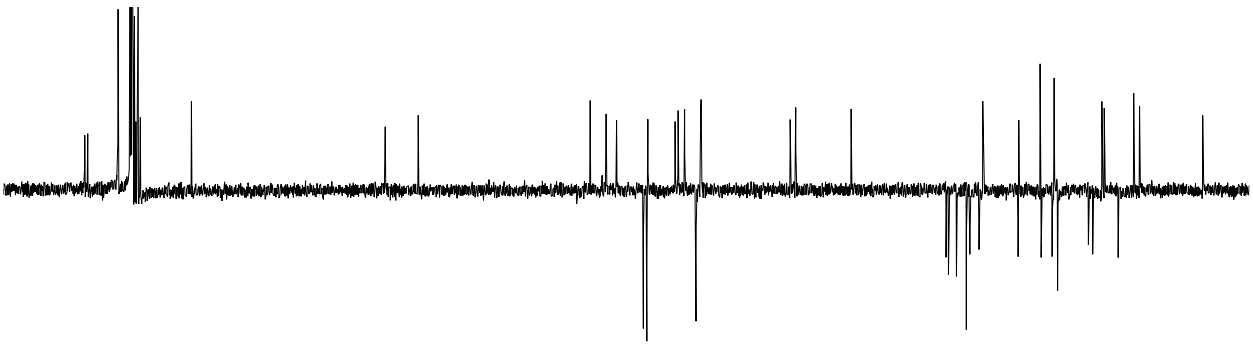

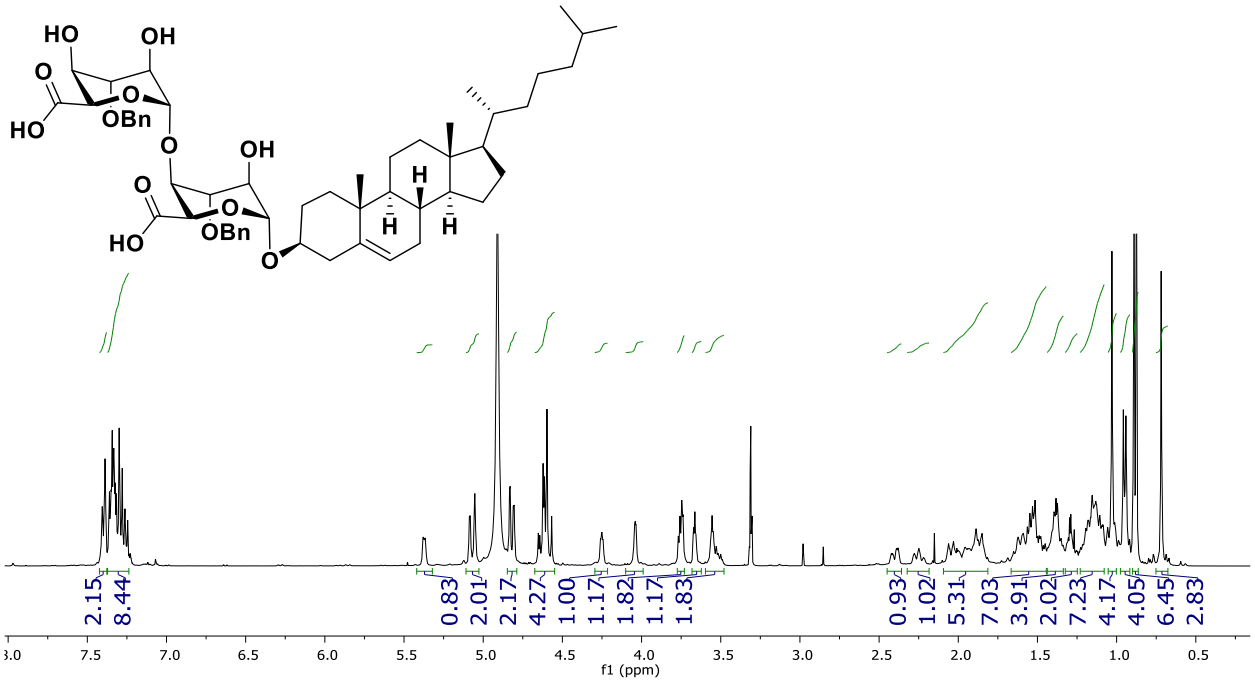
HO
OH
O
HO
O
OBn
O
OH
O
HO
O
OBn
O
H
H
H
2.15
8.44
0.83
2.01
2.17
4.27
1.00
1.17
1.82
1.17
1.83
0.93
1.02
5.31
7.03
3.91
2.02
7.23
4.17
4.05
6.45
2.83
f1 (ppm)

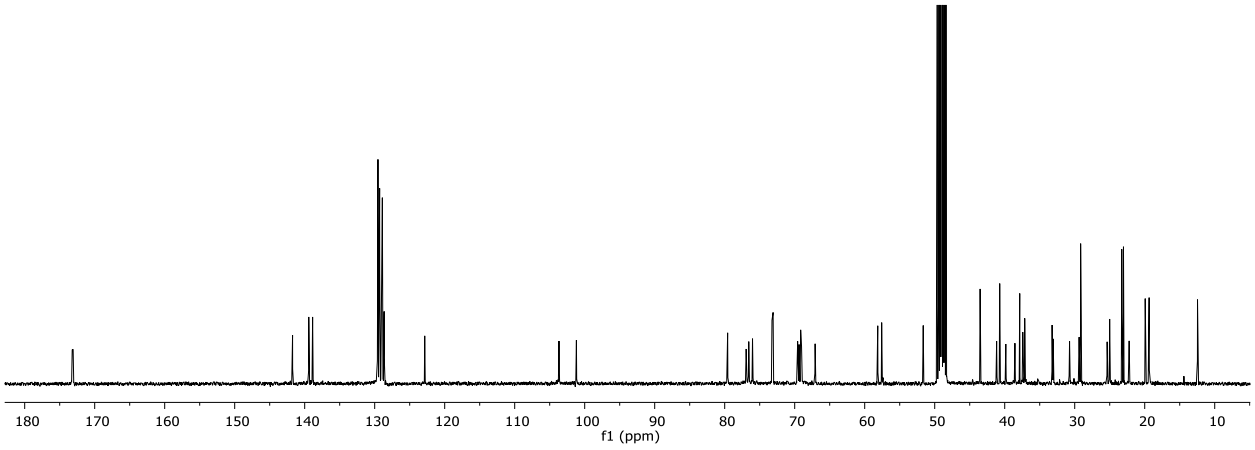
f1 (ppm)

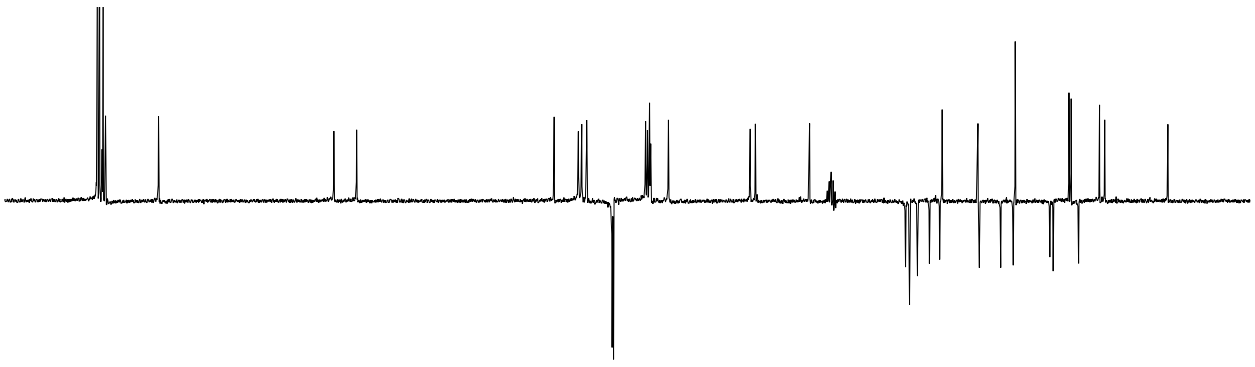

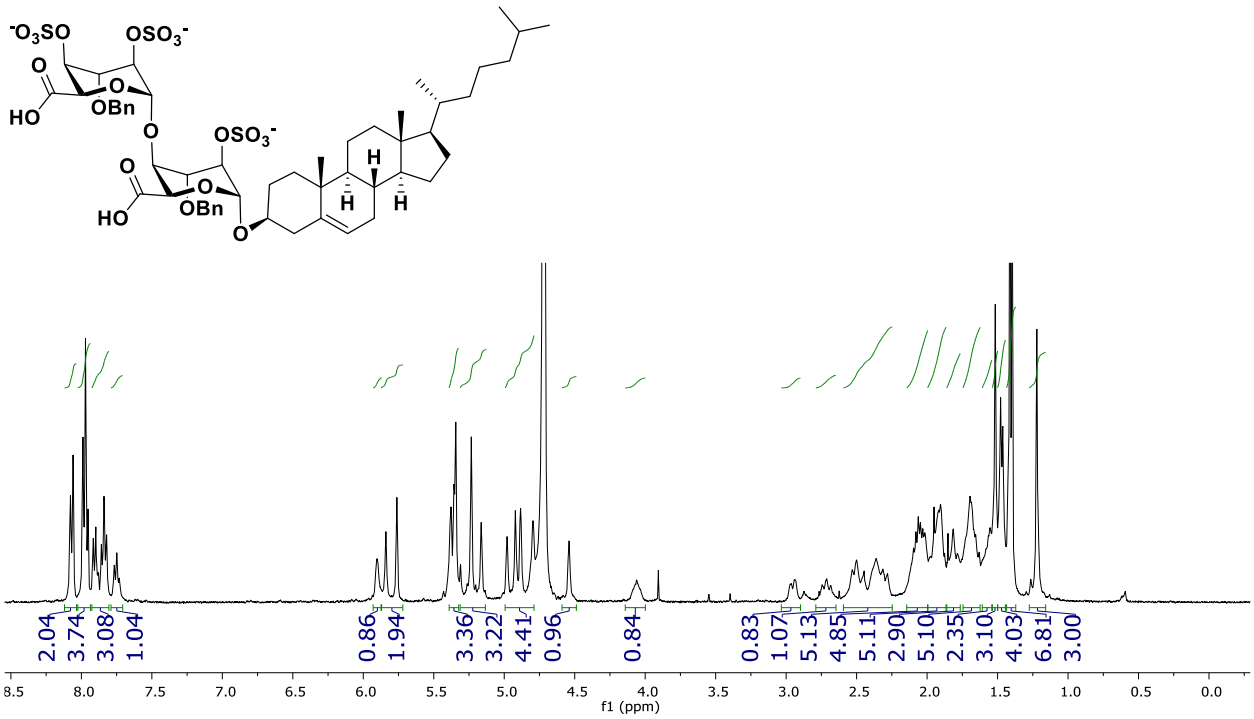
2.04
3.74
3.08
1.04
0.86
1.94
3.36
3.22
4.41
0.96
0.84
0.83
1.07
5.13
4.85
5.11
2.90
5.10
2.35
3.10
4.03
6.81
3.00
f1 (ppm)

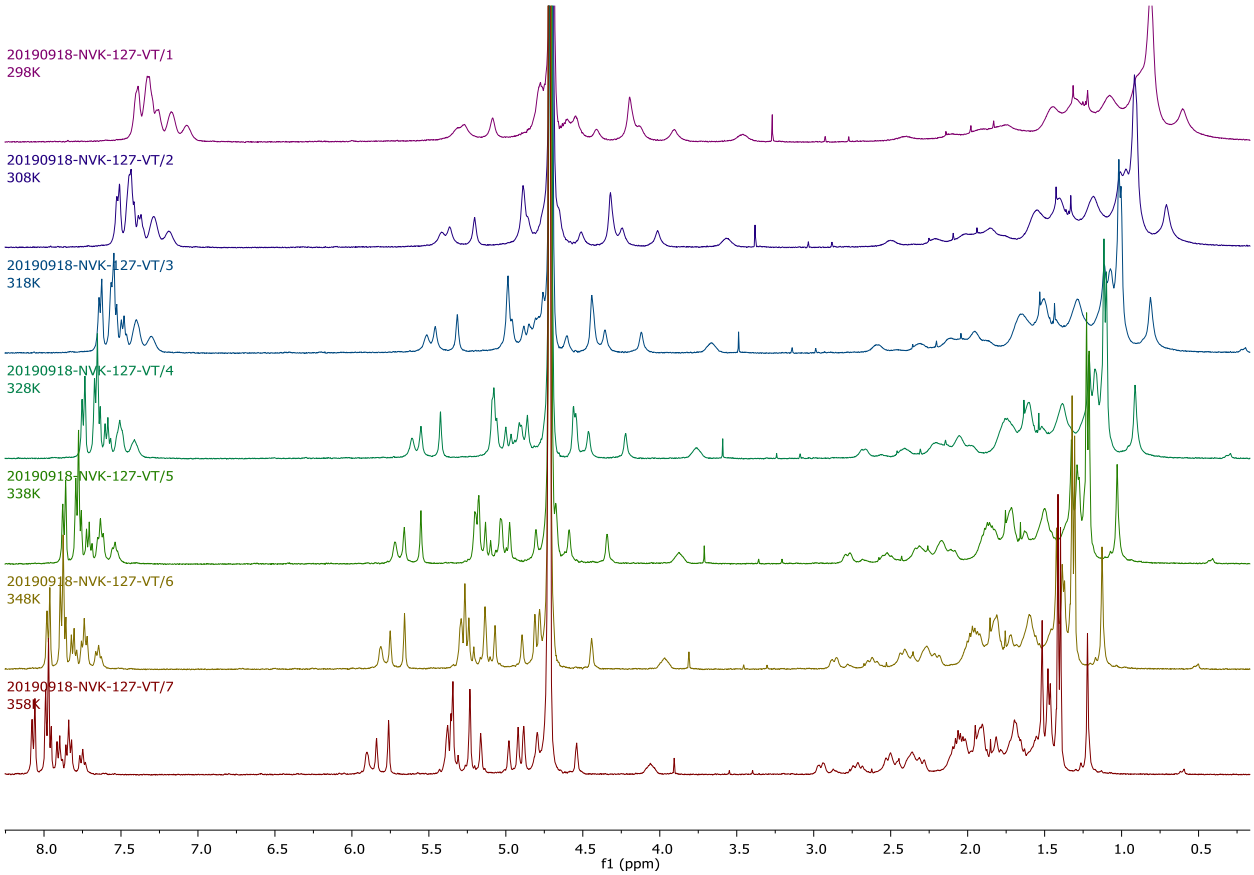
20190918-NVK-127-VT/1
298K
20190918-NVK-127-VT/2
308K
20190918-NVK-127-VT/3
318K
20190918-NVK-127-VT/4
328K
20190918-NVK-127-VT/5
338K
20190918-NVK-127-VT/6
348K
20190918-NVK-127-VT/7
358K
f1 (ppm)

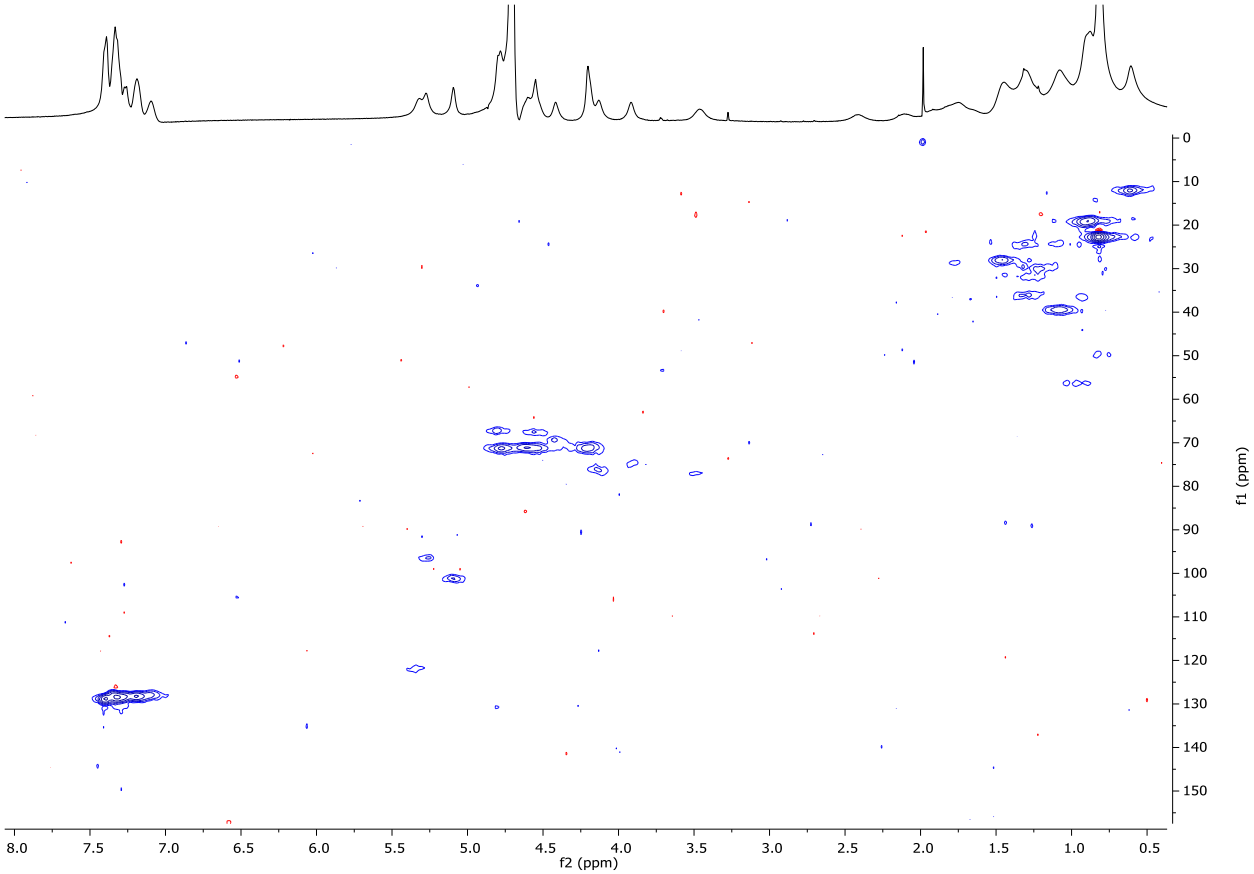
0
10
20
30
40
50
60
70
80
90
100
110
120
130
140
150
f1 (ppm)
8.0
7.5
7.0
6.5
6.0
5.5
5.0
4.5
4.0
3.5
3.0
2.5
2.0
1.5
1.0
0.5
f2 (ppm)

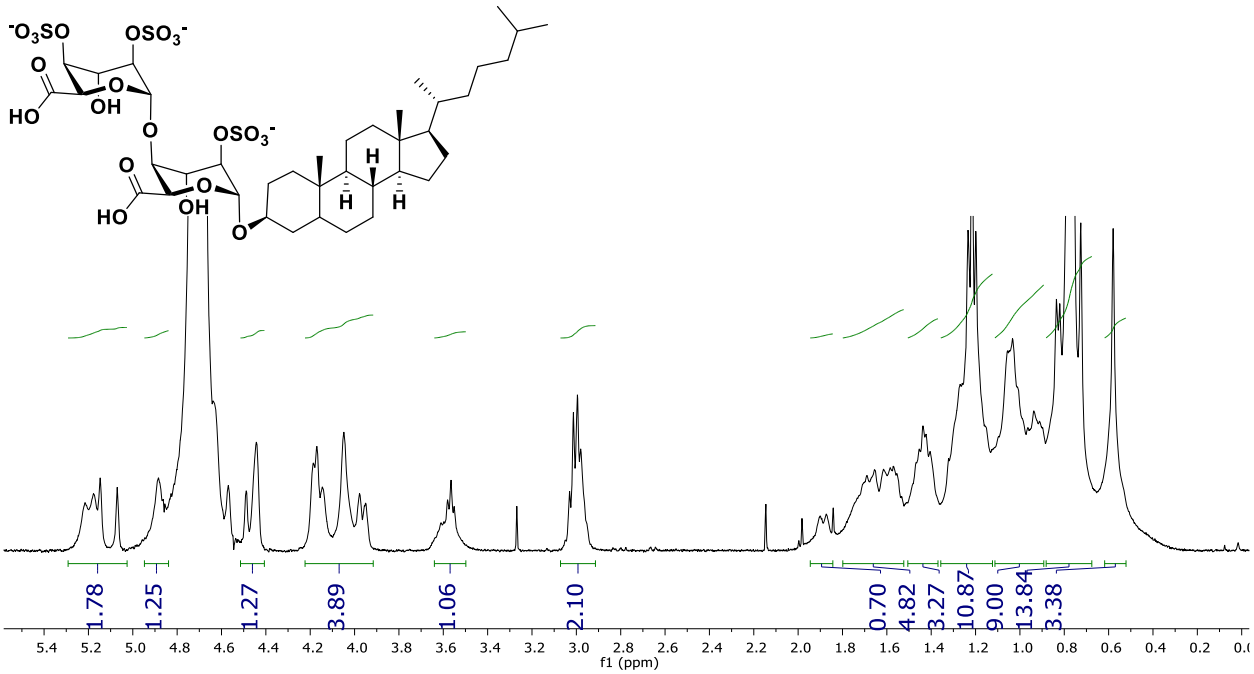
$^{-}O_3SO$
OSO_3^-
HO
OH
O
OSO_3^-
HO
OH
H
H
H
1.78
1.25
1.27
3.89
1.06
2.10
0.70
4.82
3.27
10.87
9.00
13.84
3.38
f1 (ppm)

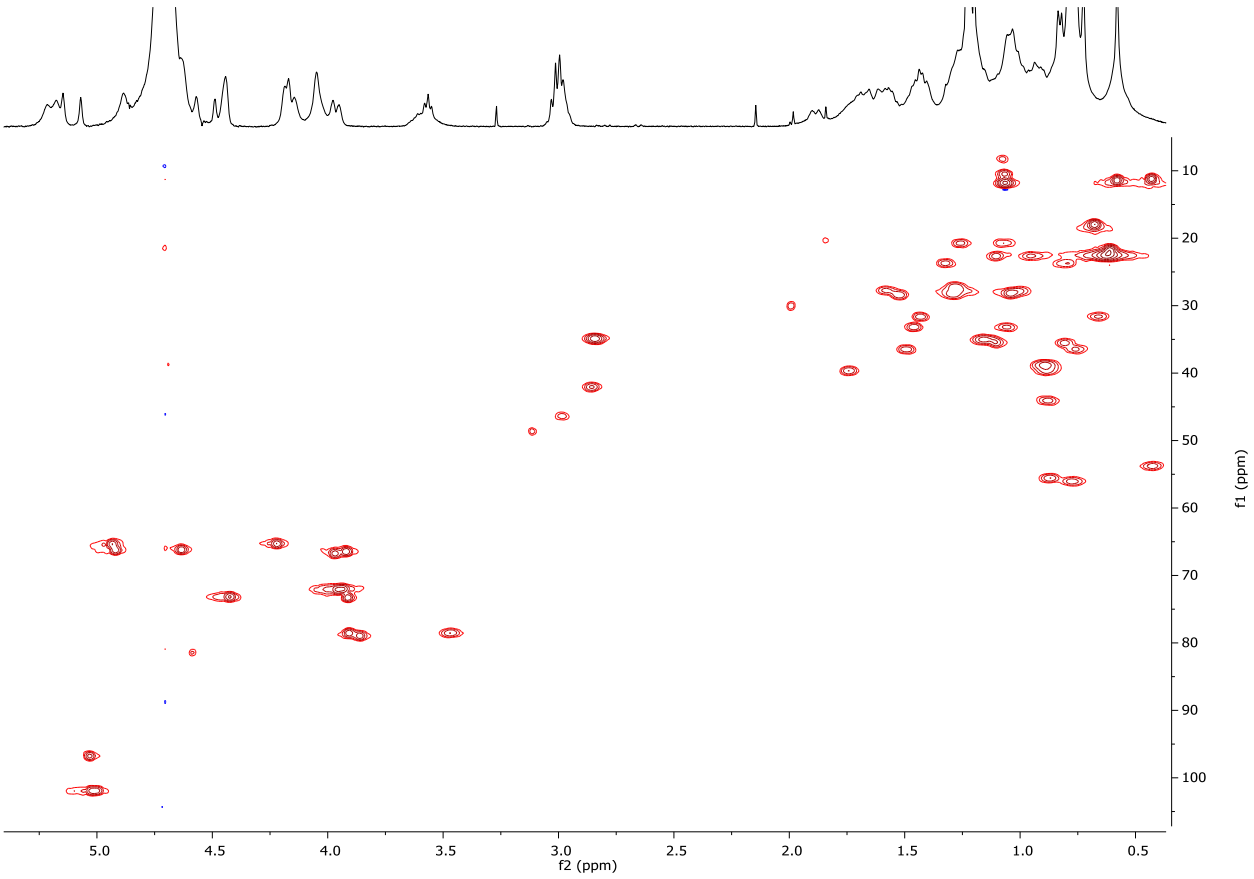
f2 (ppm)
f1 (ppm)

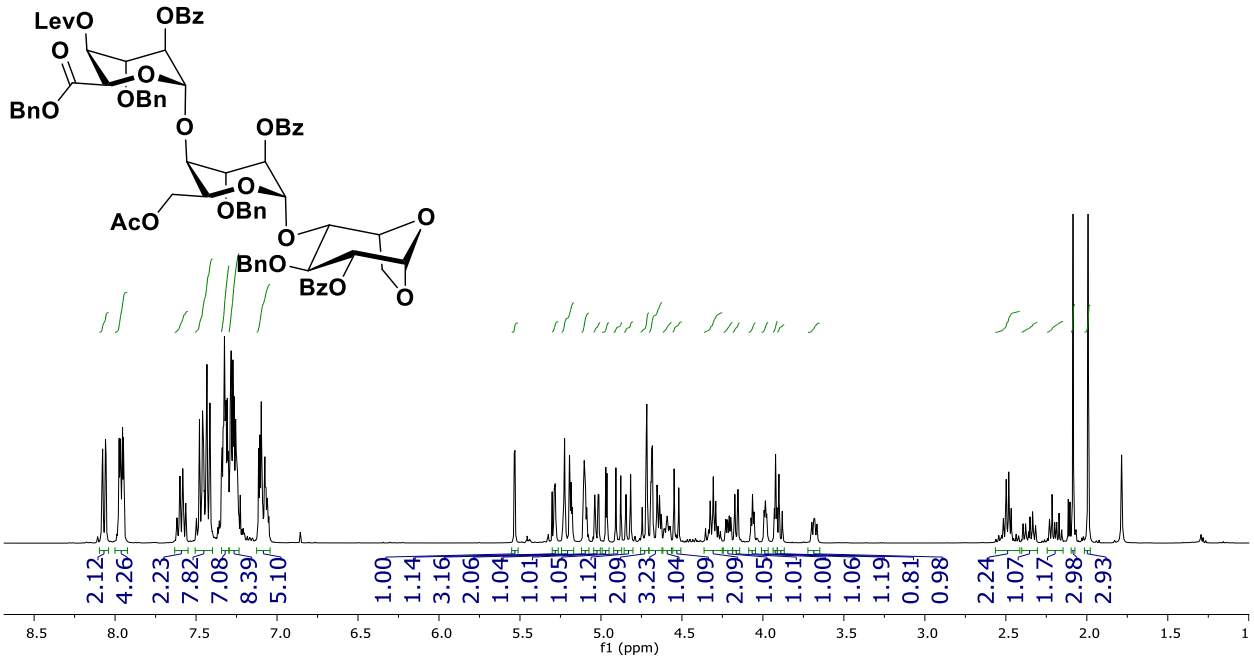
LevO
OBz
O
O
OBn
BnO
O
OBz
O
OBn
AcO
O
BnO
BzO
O
2.12
4.26
2.23
7.82
7.08
8.39
5.10
1.00
1.14
3.16
2.06
1.04
1.01
1.05
1.12
2.09
3.23
1.04
1.09
2.09
1.05
1.01
1.00
1.06
1.19
0.81
0.98
2.24
1.07
1.17
2.98
2.93
f1 (ppm)

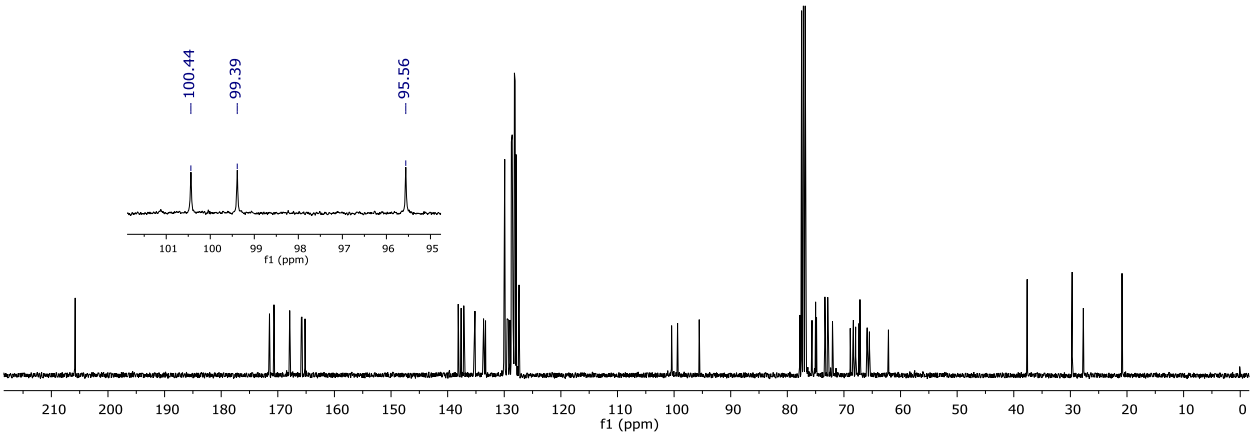
100.44
99.39
95.56
f1 (ppm)

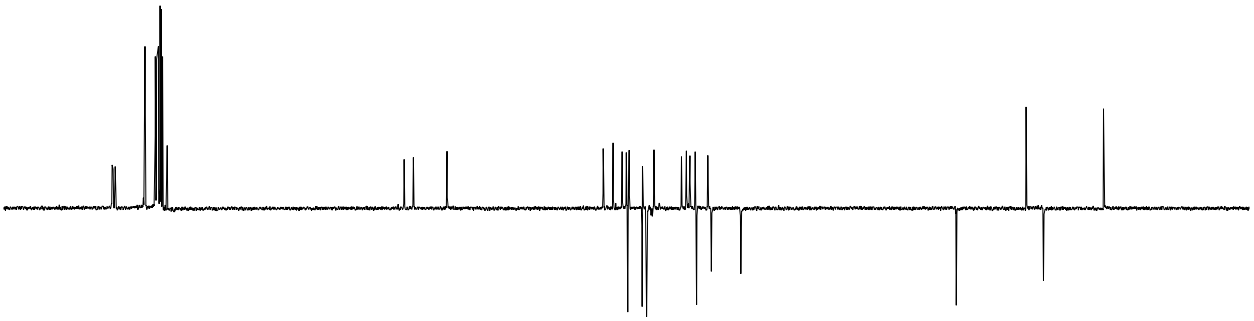

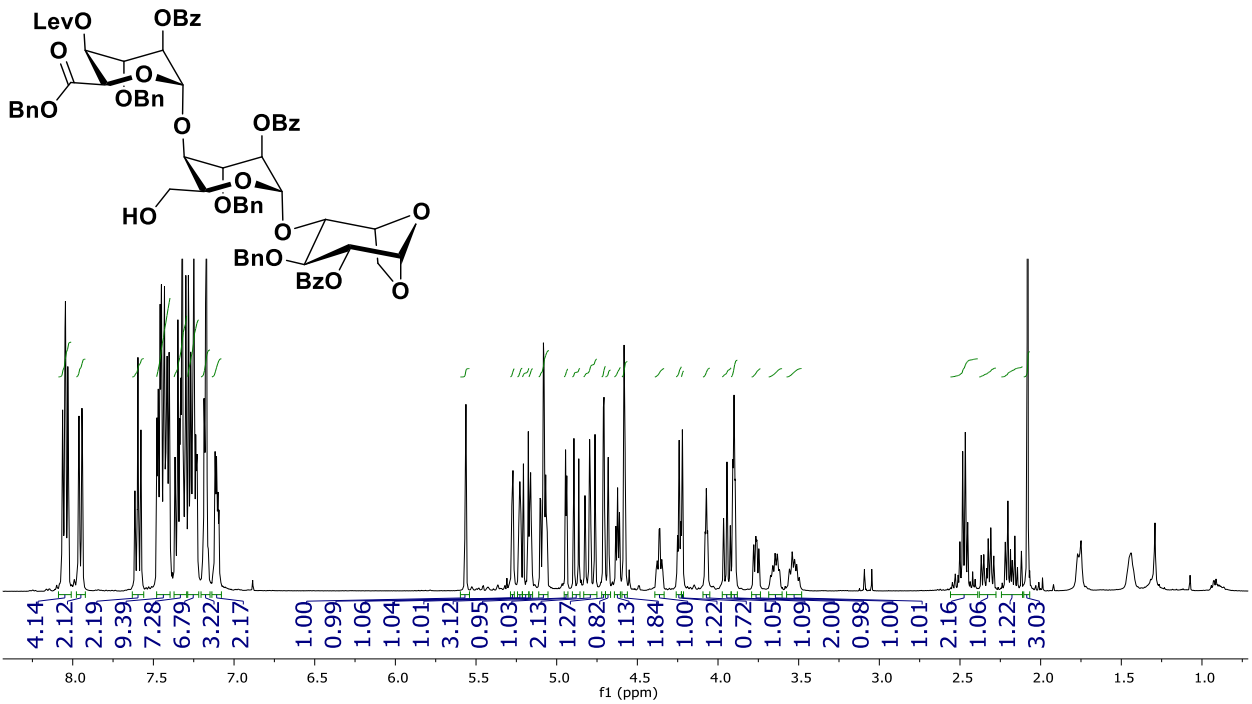
LevO
OBz
O
O
BnO
OBn
O
OBz
O
HO
OBn
O
O
BnO
BzO
O
4.14
2.12
2.19
9.39
7.28
6.79
3.22
2.17
1.00
0.99
1.06
1.04
1.01
3.12
0.95
1.03
2.13
1.27
0.82
1.13
1.84
1.00
1.22
0.72
1.05
1.09
2.00
0.98
1.00
1.01
2.16
1.06
1.22
3.03
8.0
7.5
7.0
6.5
6.0
5.5
5.0
4.5
4.0
3.5
3.0
2.5
2.0
1.5
1.0
f1 (ppm)

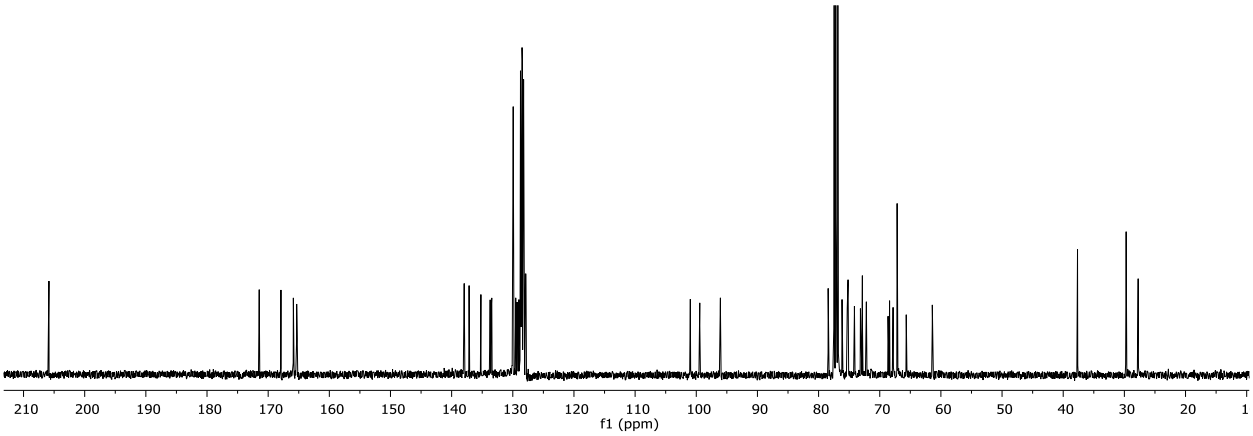
210
200
190
180
170
160
150
140
130
120
110
100
90
80
70
60
50
40
30
20
1
f1 (ppm)

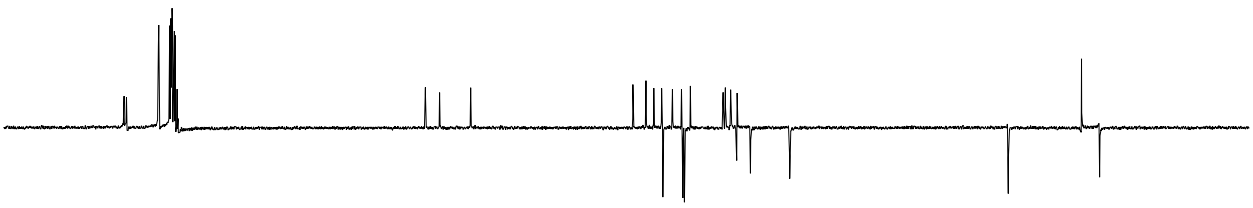

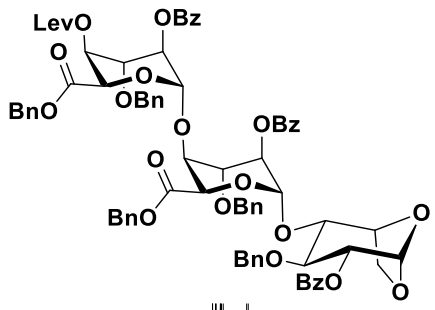
LevO
OBz
O
O
OBn
BnO
O
OBz
O
O
OBn
BnO
O
BnO
BzO
O
O

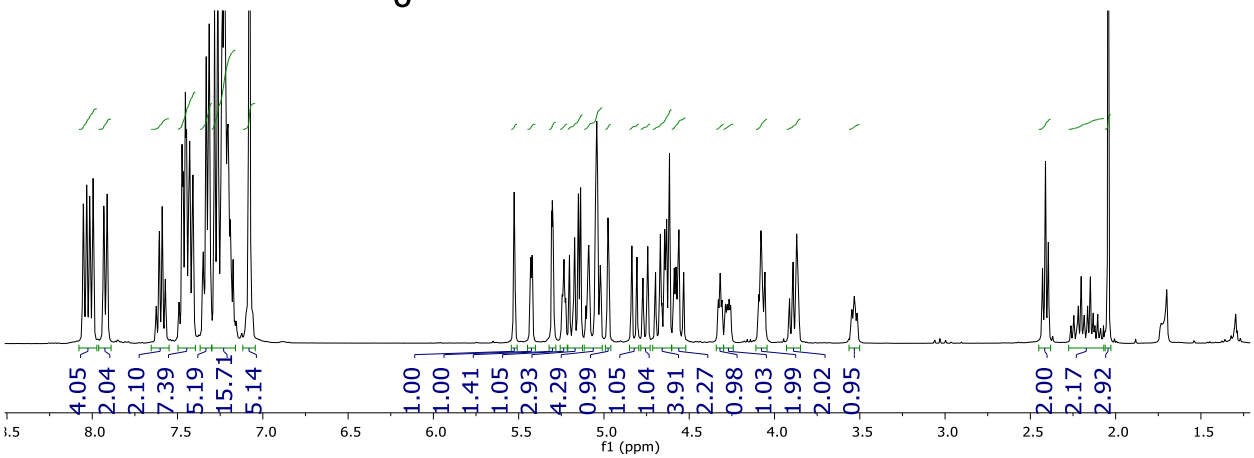
4.05
2.04
2.10
7.39
5.19
15.71
5.14
1.00
1.00
1.41
1.05
2.93
4.29
0.99
1.05
1.04
3.91
2.27
0.98
1.03
1.99
2.02
0.95
2.00
2.17
2.92
f1 (ppm)

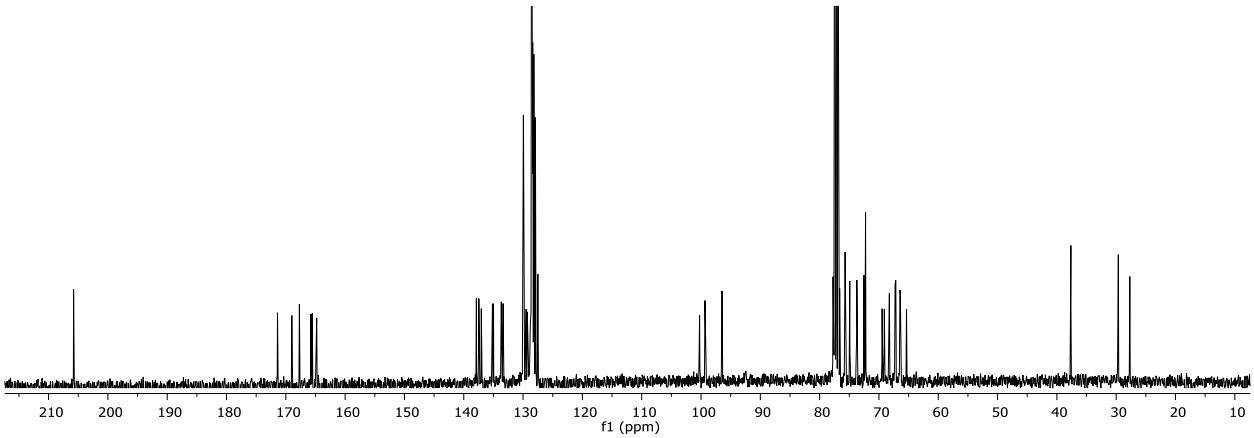
f1 (ppm)

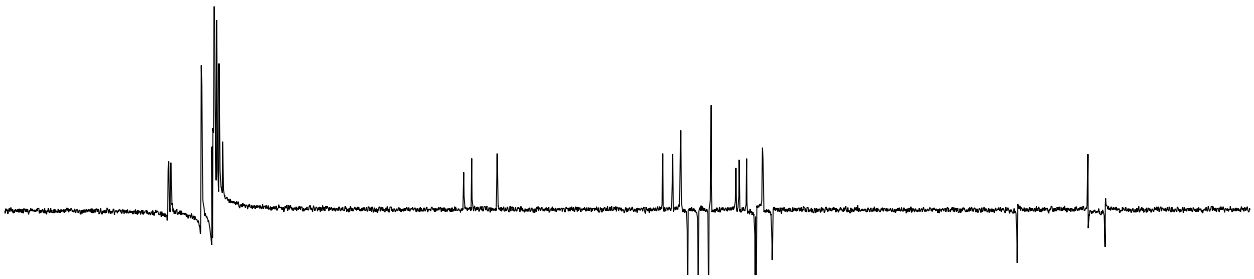

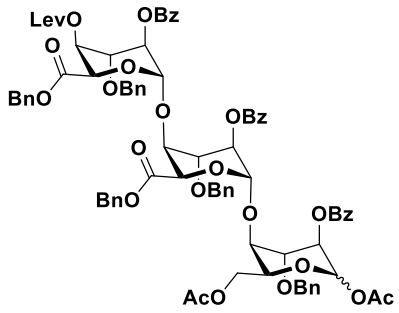
LevO
OBz
O
O
OBn
BnO
O
OBz
O
O
OBn
BnO
O
OBz
O
OBn
AcO
OAc

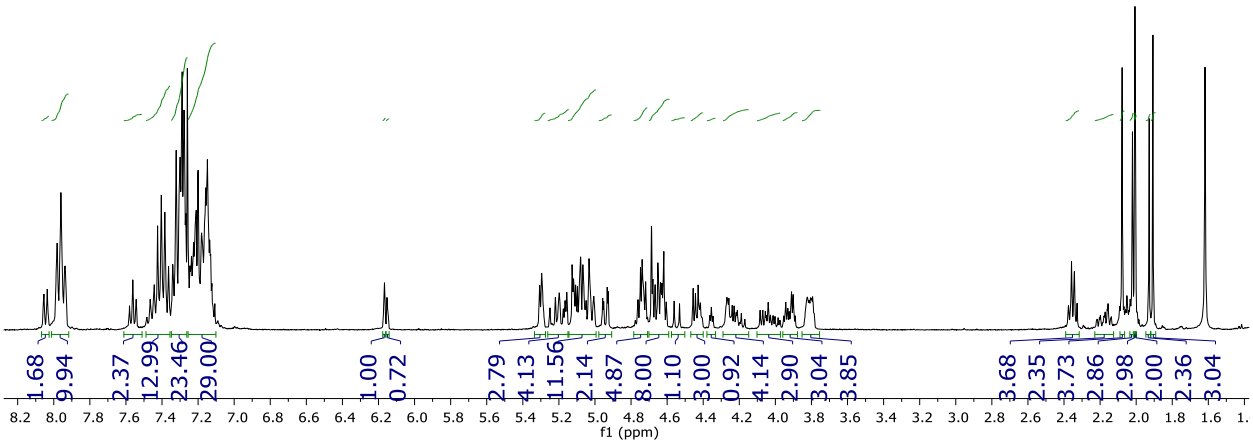
1.68
9.94
2.37
12.99
23.46
29.00
1.00
0.72
2.79
4.13
11.56
2.14
4.87
8.00
1.10
3.00
0.92
4.14
2.90
3.04
3.85
3.68
2.35
3.73
2.86
2.98
2.00
2.36
3.04
f1 (ppm)

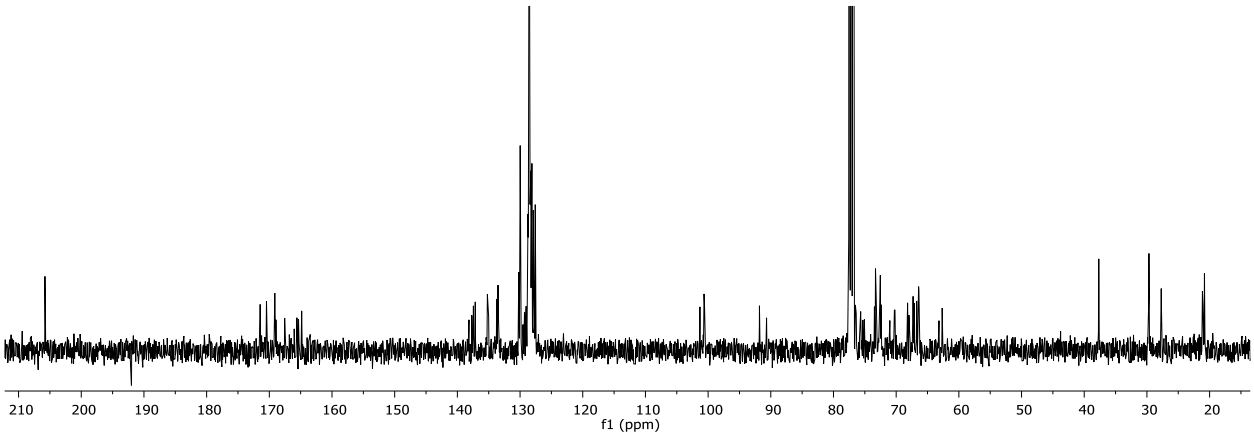
f1 (ppm)

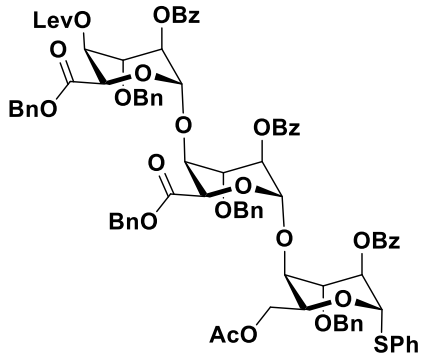
LevO
OBz
O
O
BnO
OBn
O
OBz
O
O
BnO
OBn
O
OBz
O
AcO
OBn
SPh

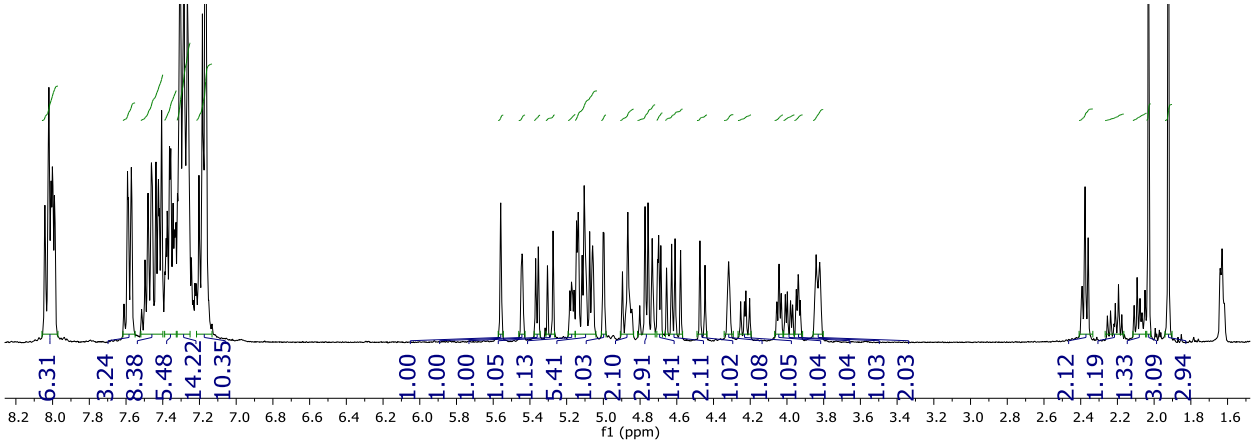
6.31
3.24
8.38
5.48
14.22
10.35
1.00
1.00
1.00
1.05
1.13
5.41
1.03
2.10
2.91
1.41
2.11
1.02
1.08
1.05
1.04
1.04
1.03
2.03
2.12
1.19
1.33
3.09
2.94
f1 (ppm)

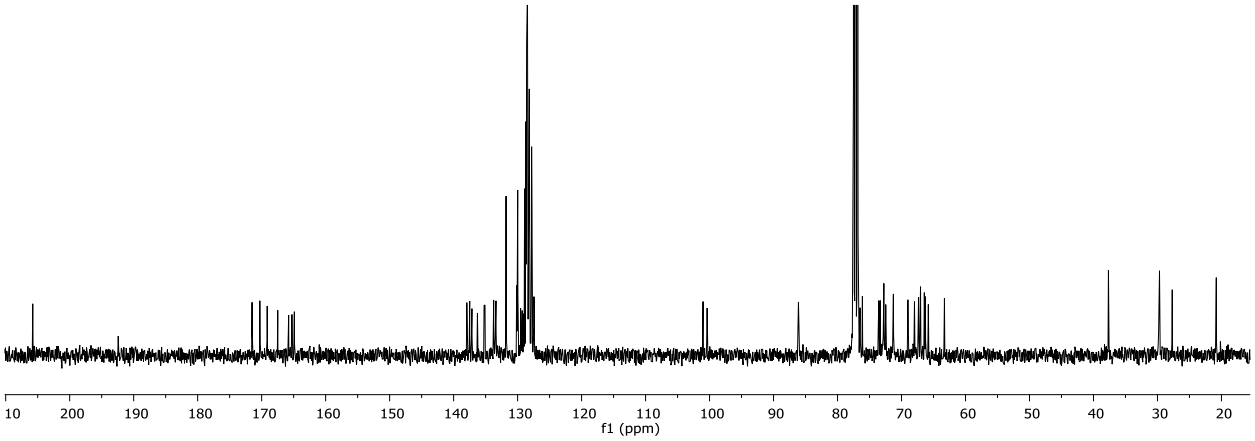
f1 (ppm)

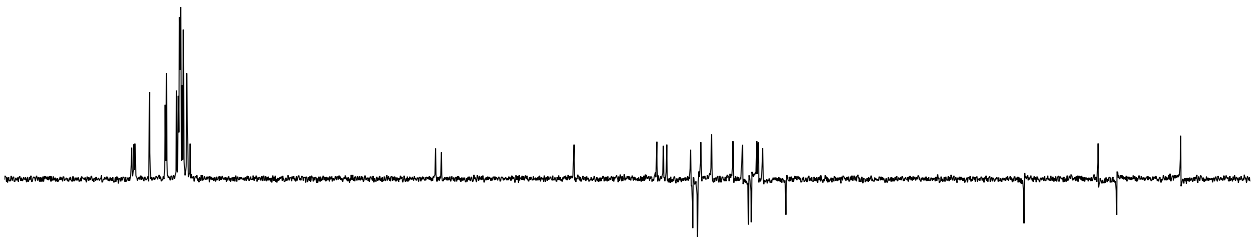

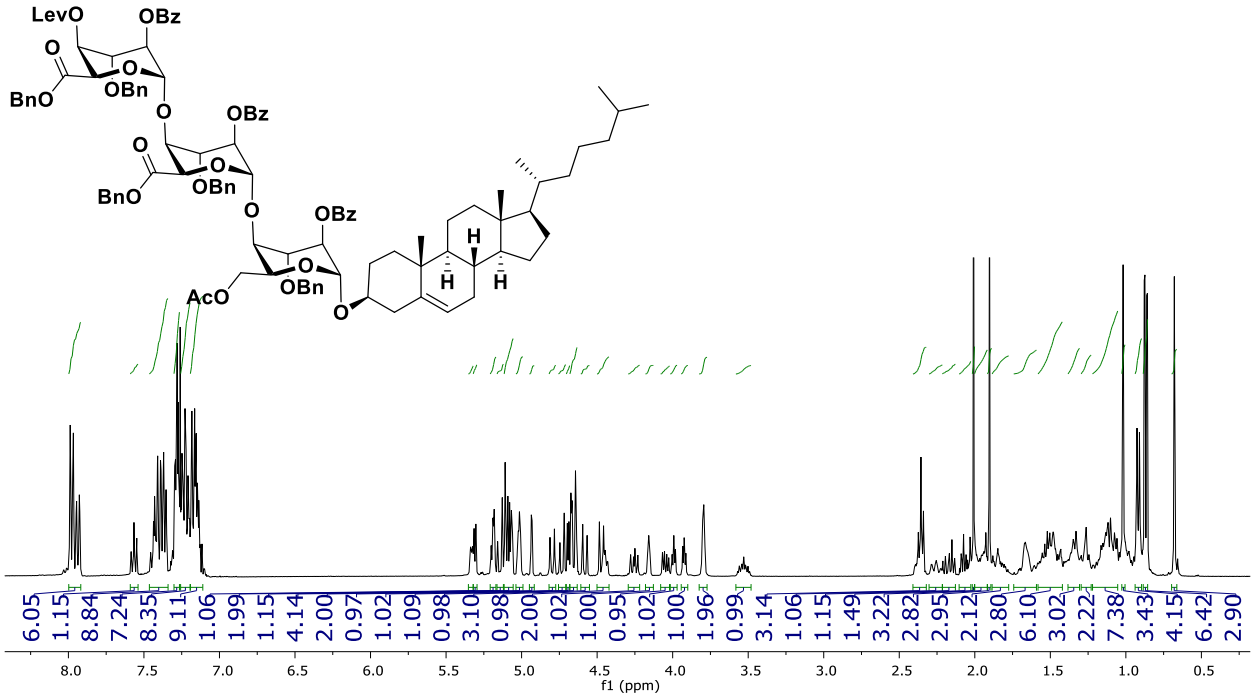
LevO
OBz
O
BnO
OBn
O
OBz
O
BnO
OBn
O
OBz
AcO
OBn
O
H
H
H
6.05 1.15 8.84 7.24 8.35 9.11 1.06 1.99 1.15 4.14 2.00 0.97 1.02 1.09 0.98 3.10 0.98 2.00 1.02 1.00 0.95 1.02 1.00 1.96 0.99 3.14 1.06 1.15 1.49 3.22 2.82 2.95 2.12 2.80 6.10 3.02 2.22 7.38 3.43 4.15 6.42 2.90
8.0 7.5 7.0 6.5 6.0 5.5 5.0 4.5 4.0 3.5 3.0 2.5 2.0 1.5 1.0 0.5
f1 (ppm)

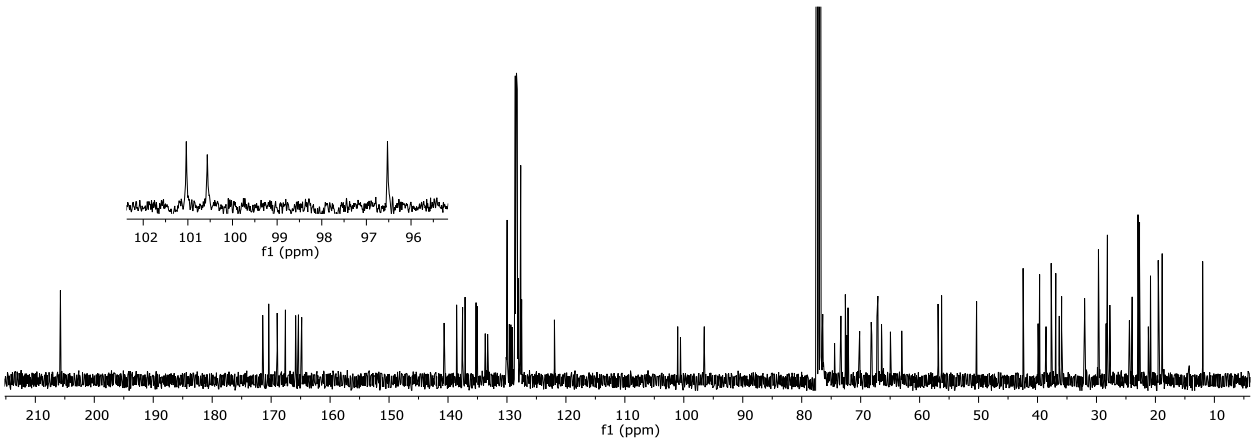
102 101 100 99 98 97 96
f1 (ppm)
210 200 190 180 170 160 150 140 130 120 110 100 90 80 70 60 50 40 30 20 10
f1 (ppm)

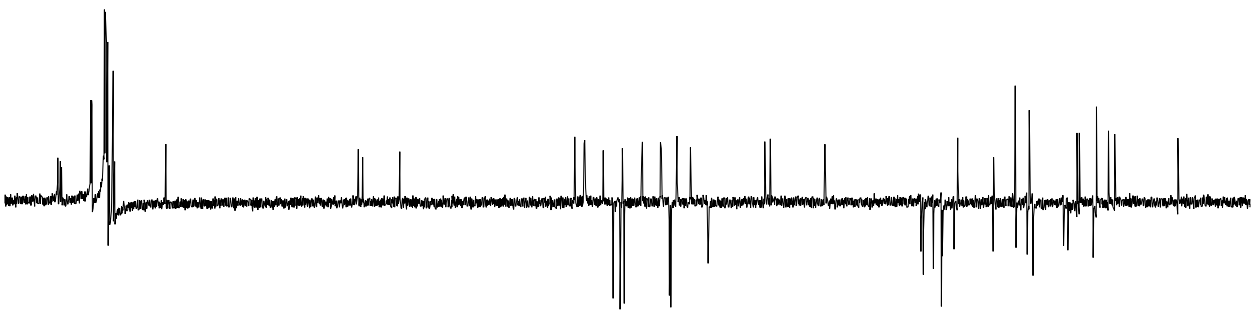

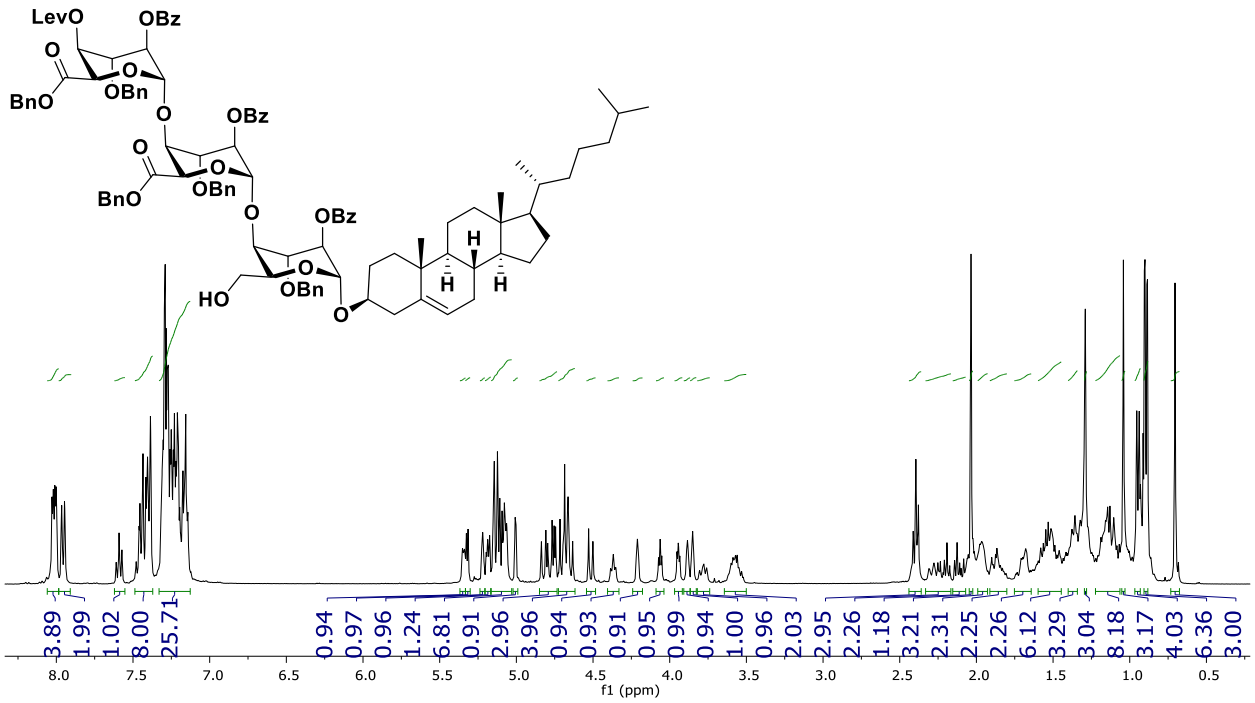
LevO
OBz
BnO
OBn
HO
H
3.89 1.99 1.02 8.00 25.71 0.94 0.97 0.96 1.24 6.81 0.91 2.96 3.96 0.94 0.93 0.91 0.95 0.99 0.94 1.00 0.96 2.03 2.95 2.26 1.18 3.21 2.31 2.25 2.26 6.12 3.29 3.04 8.18 3.17 4.03 6.36 3.00
f1 (ppm)

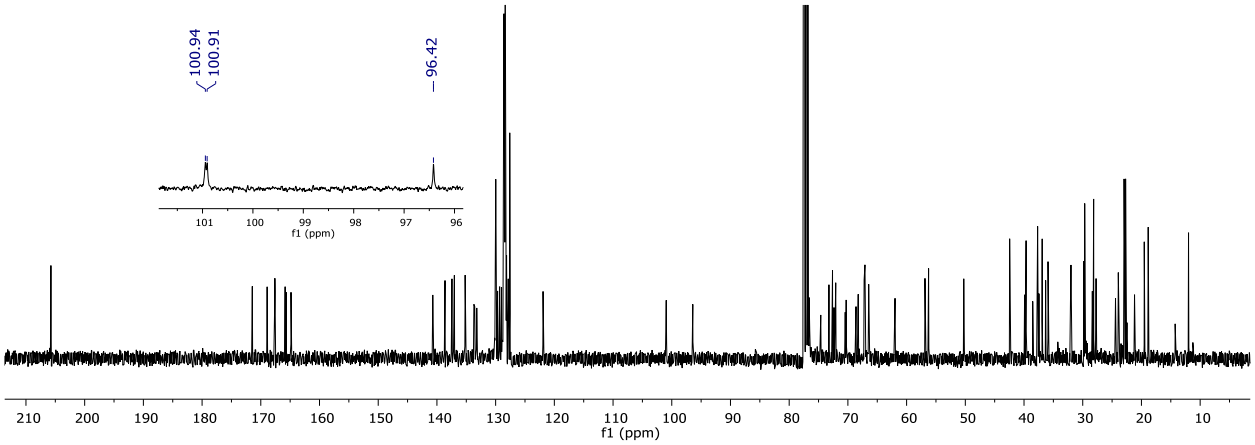
100.94
100.91
96.42
f1 (ppm)

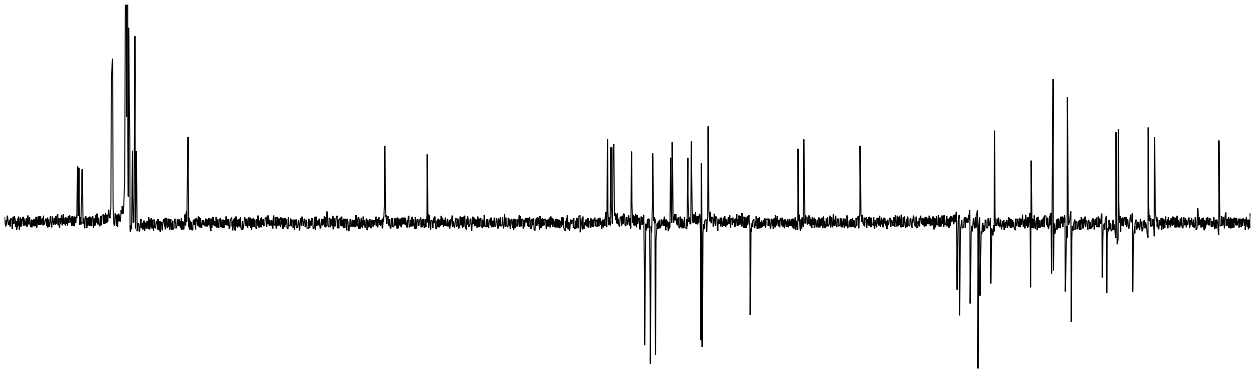

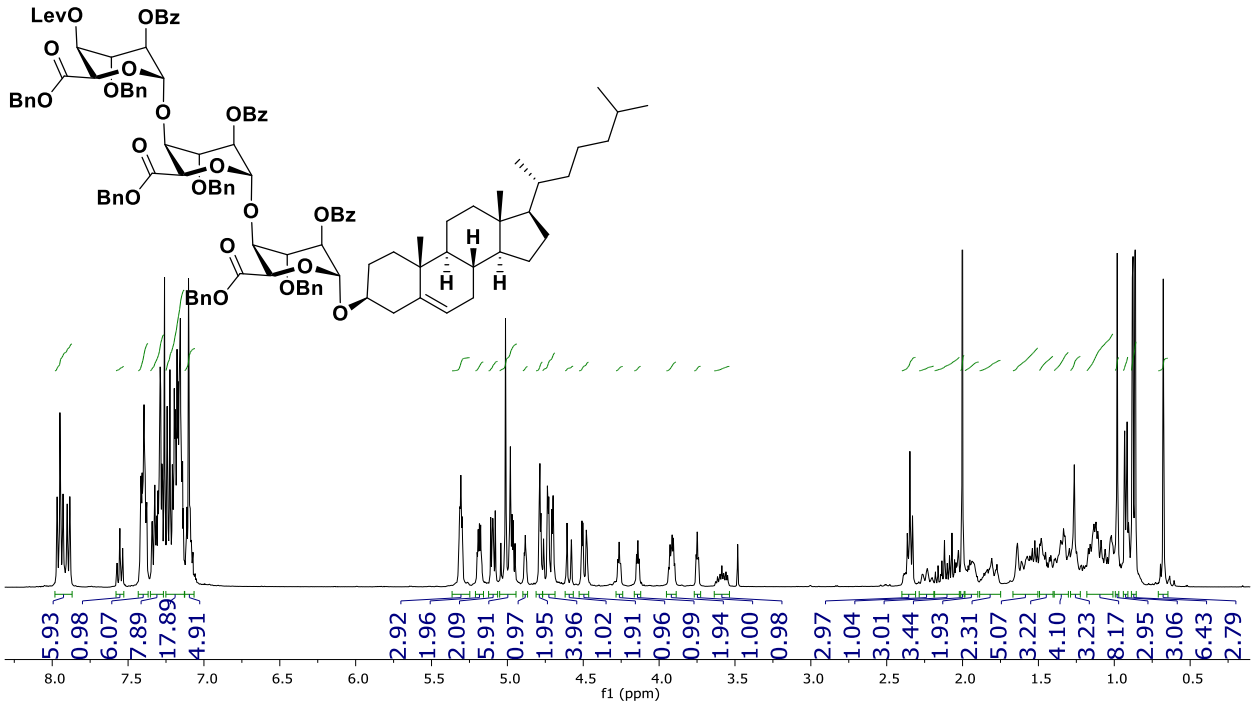
LevO
OBz
BnO
OBn
H
5.93 0.98 6.07 7.89 17.89 4.91 2.92 1.96 2.09 5.91 0.97 1.95 3.96 1.02 1.91 0.96 0.99 1.94 1.00 0.98 2.97 1.04 3.01 3.44 1.93 2.31 5.07 3.22 4.10 3.23 8.17 2.95 3.06 6.43 2.79
f1 (ppm)

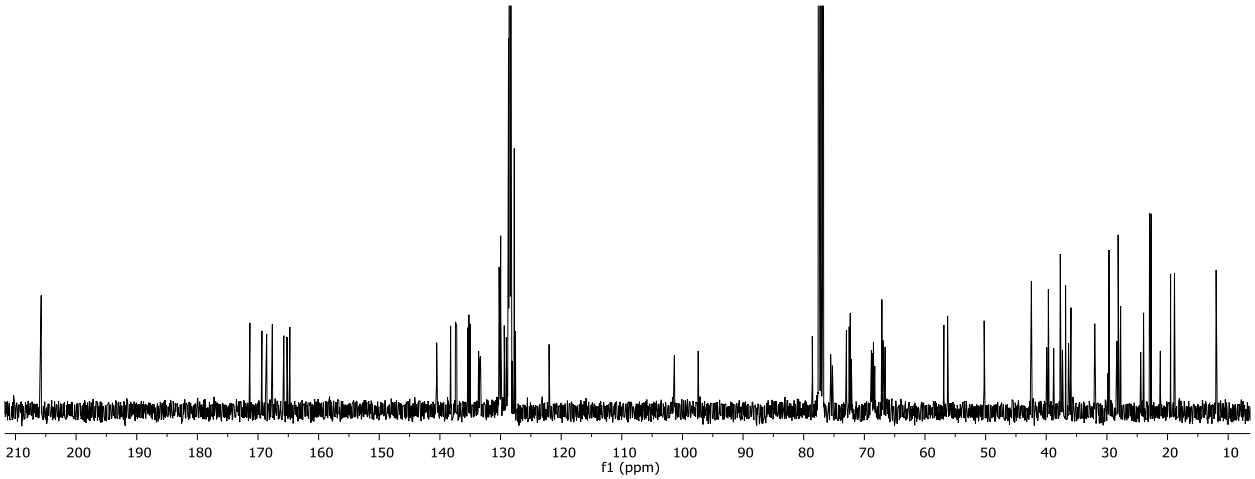
f1 (ppm)

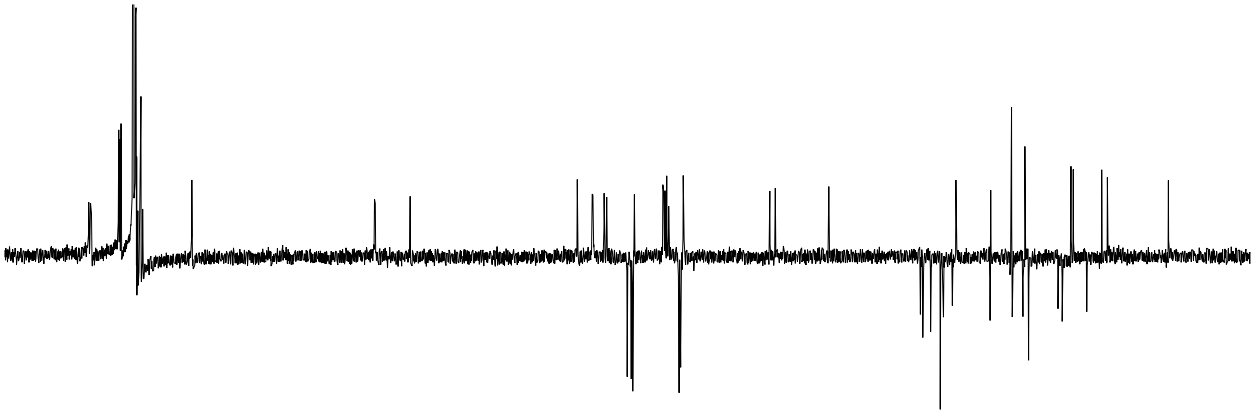

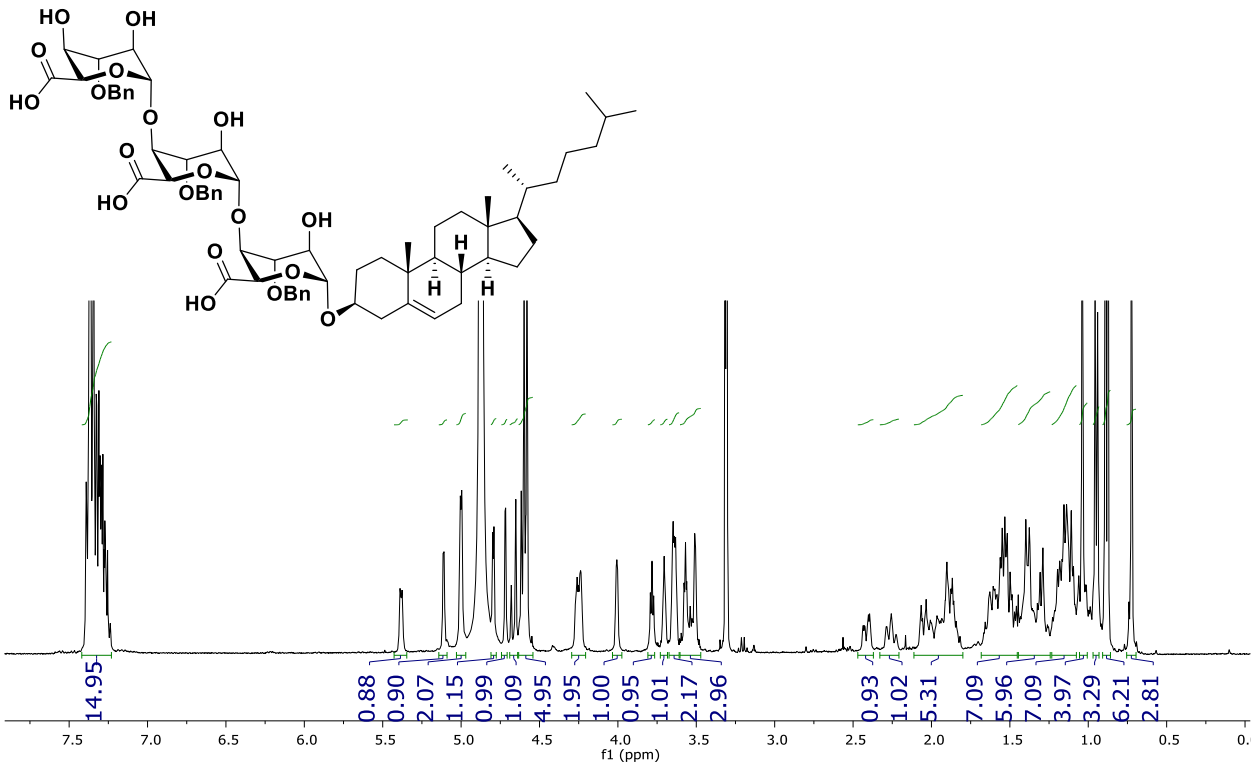
HO
OH
O
HO
OBn
O
OH
O
HO
OBn
O
OH
O
HO
OBn
O
H
H
H
14.95
0.88
0.90
2.07
1.15
0.99
1.09
4.95
1.95
1.00
0.95
1.01
2.17
2.96
0.93
1.02
5.31
7.09
5.96
7.09
3.97
3.29
6.21
2.81
f1 (ppm)

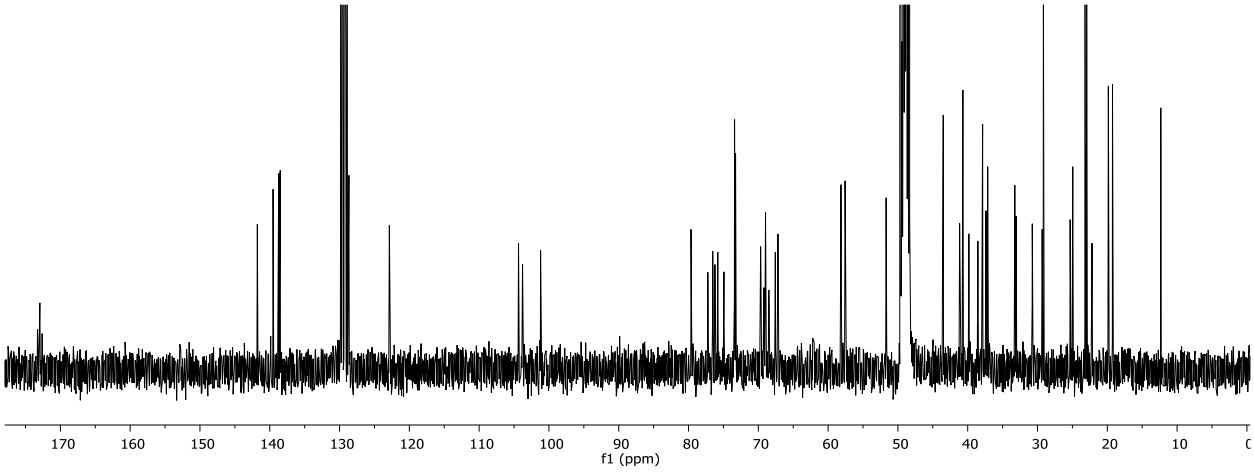
f1 (ppm)

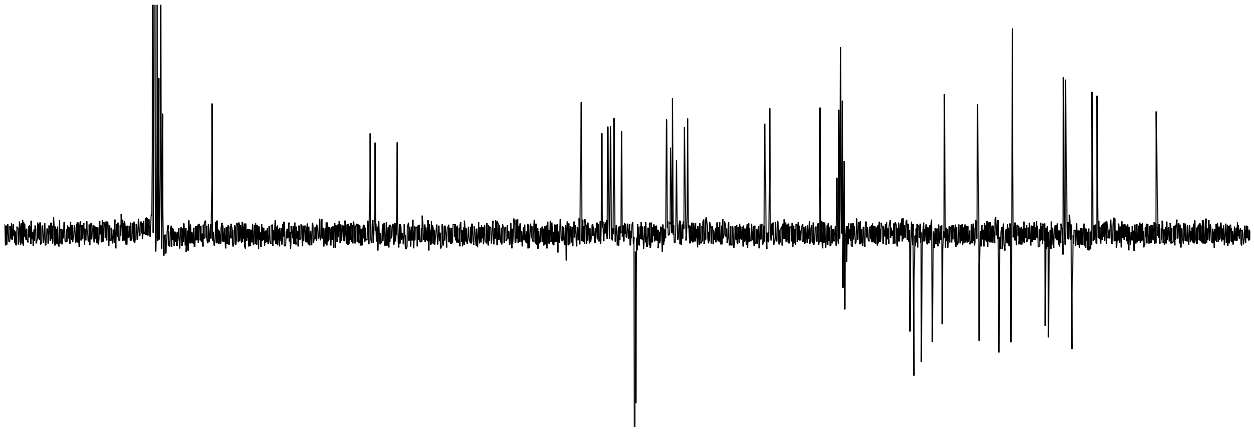

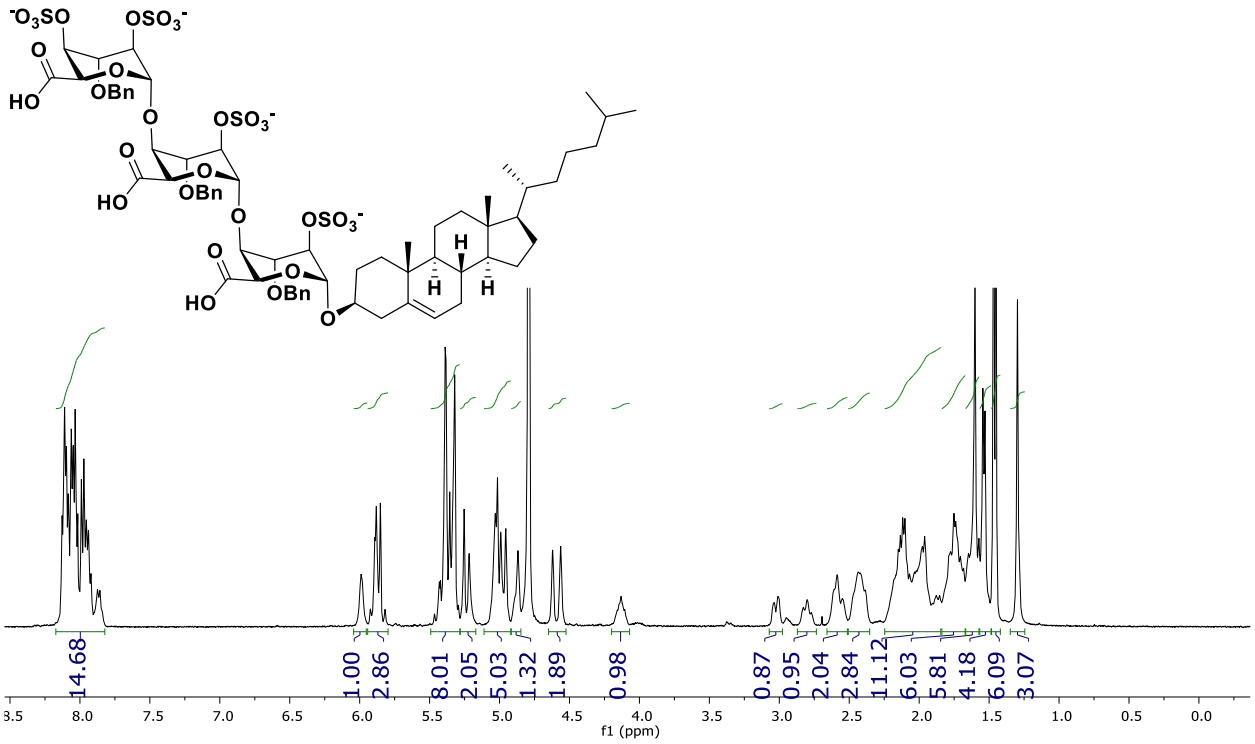
14.68
1.00
2.86
8.01
2.05
5.03
1.32
1.89
0.98
0.87
0.95
2.04
2.84
11.12
6.03
5.81
4.18
6.09
3.07
f1 (ppm)

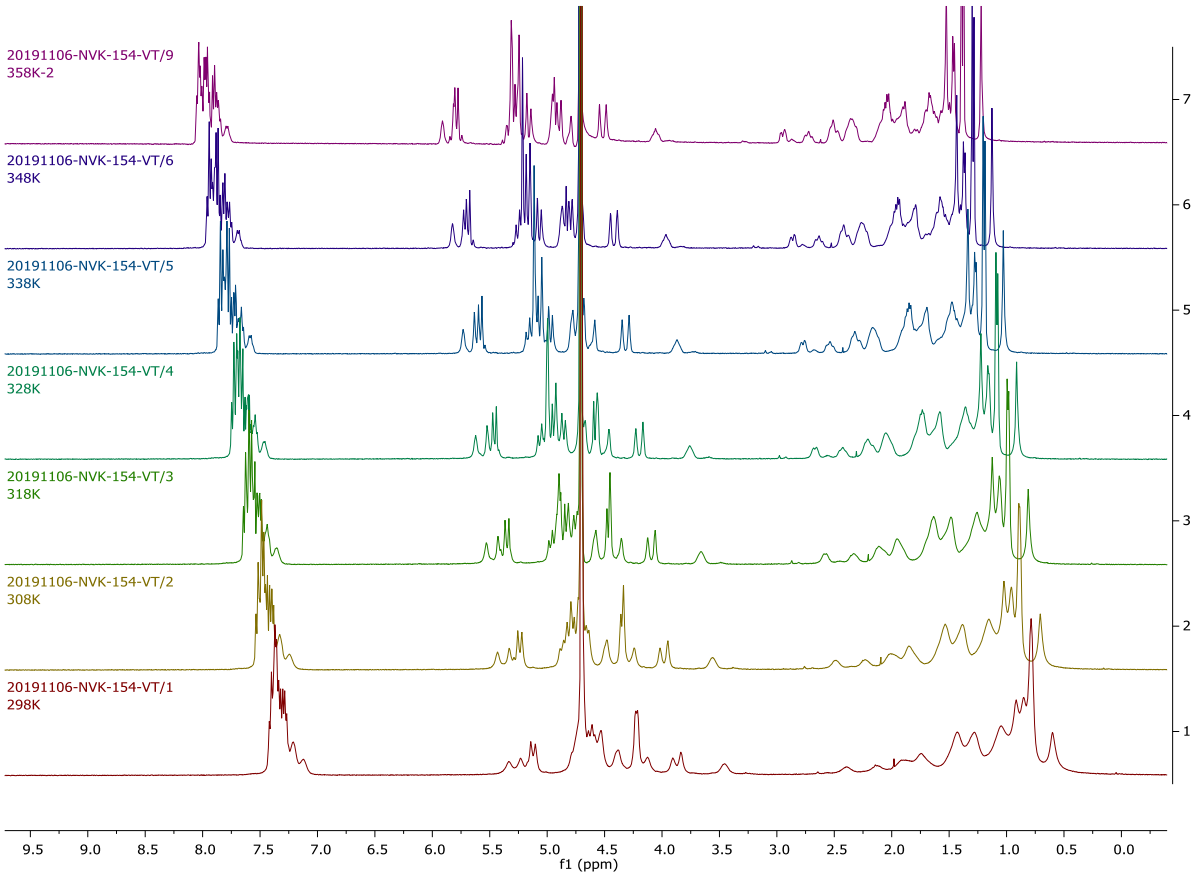
20191106-NVK-154-VT/9
358K-2
20191106-NVK-154-VT/6
348K
20191106-NVK-154-VT/5
338K
20191106-NVK-154-VT/4
328K
20191106-NVK-154-VT/3
318K
20191106-NVK-154-VT/2
308K
20191106-NVK-154-VT/1
298K
f1 (ppm)

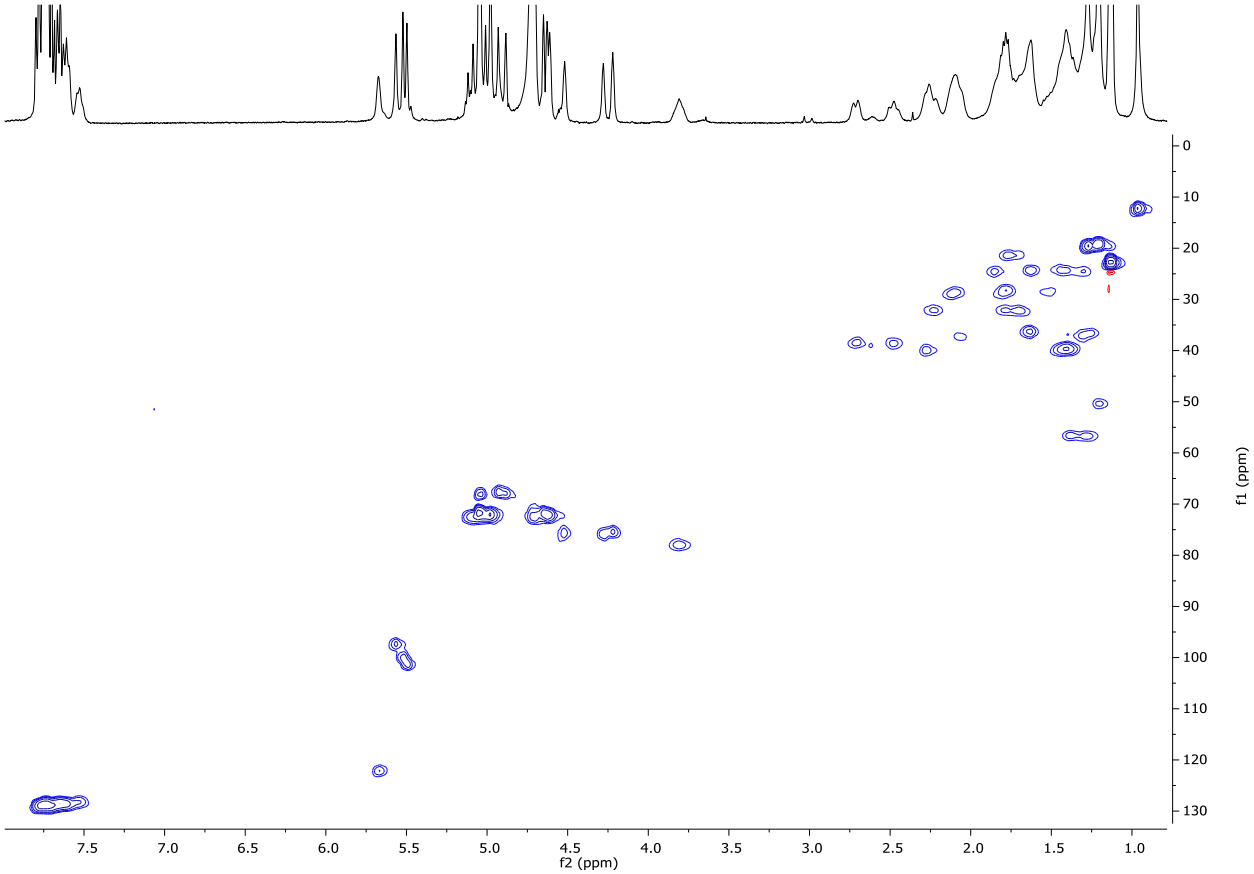
0
10
20
30
40
50
60
70
80
90
100
110
120
130
f1 (ppm)
7.5
7.0
6.5
6.0
5.5
5.0
4.5
4.0
3.5
3.0
2.5
2.0
1.5
1.0
f2 (ppm)

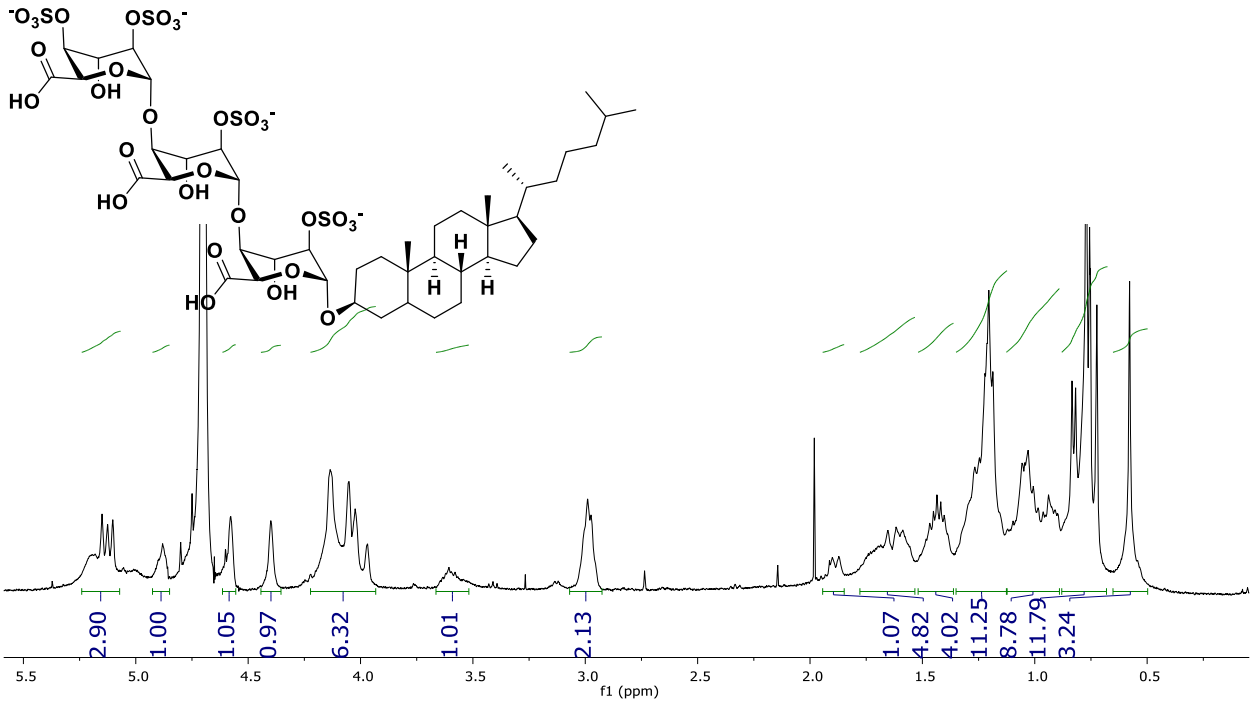
-O3SO
OSO3-
HO
OH
O
H
2.90
1.00
1.05
0.97
6.32
1.01
2.13
1.07
4.82
4.02
11.25
8.78
11.79
3.24
f1 (ppm)

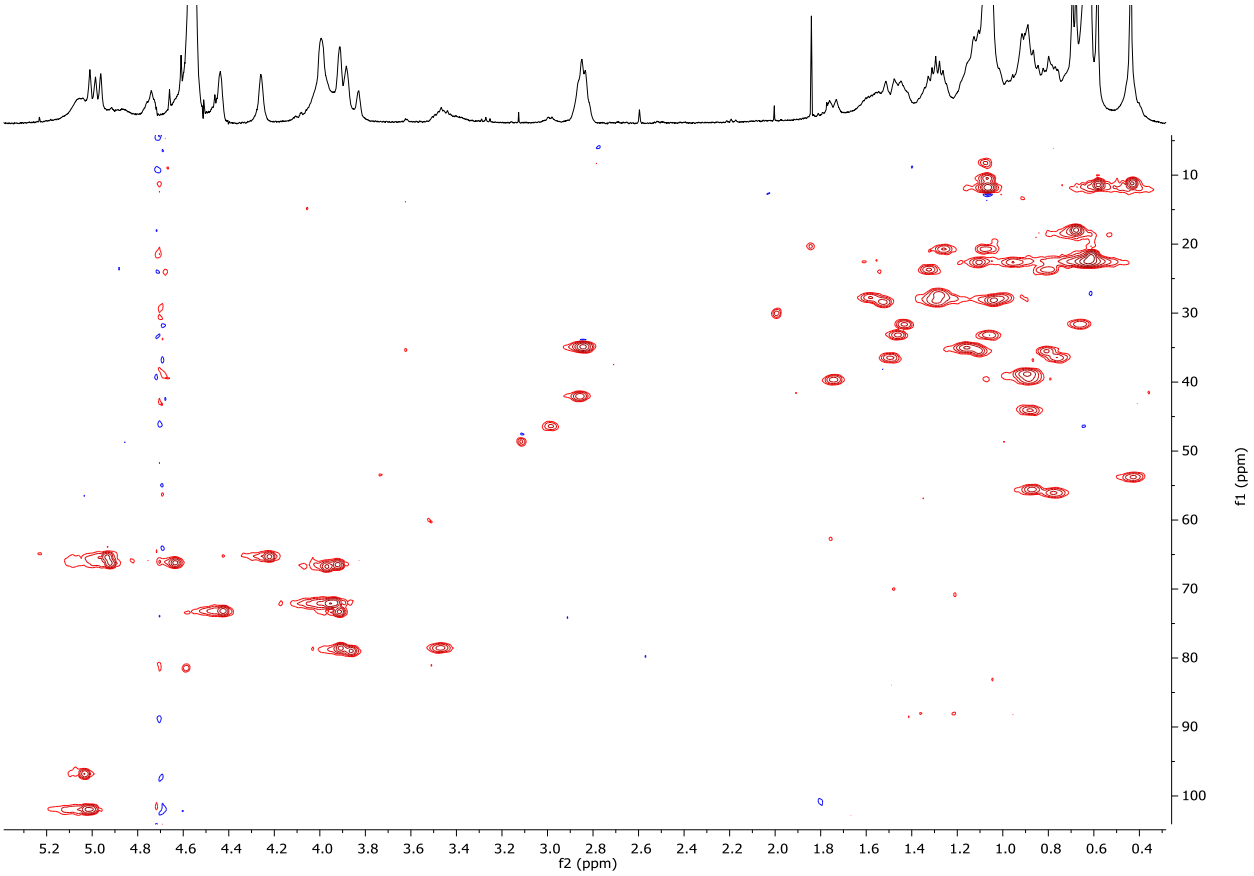
f2 (ppm)
f1 (ppm)

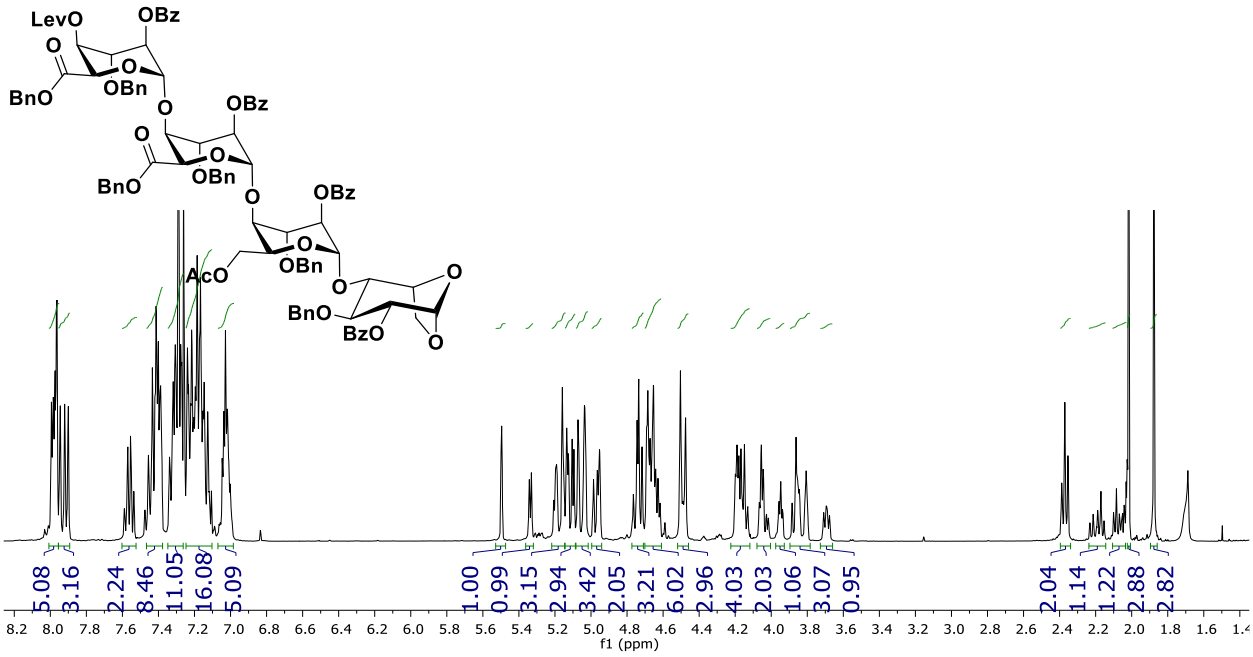
LevO
OBz
BnO
OBn
AcO
BzO
5.08
3.16
2.24
8.46
11.05
16.08
5.09
1.00
0.99
3.15
2.94
3.42
2.05
3.21
6.02
2.96
4.03
2.03
1.06
3.07
0.95
2.04
1.14
1.22
2.88
2.82
f1 (ppm)

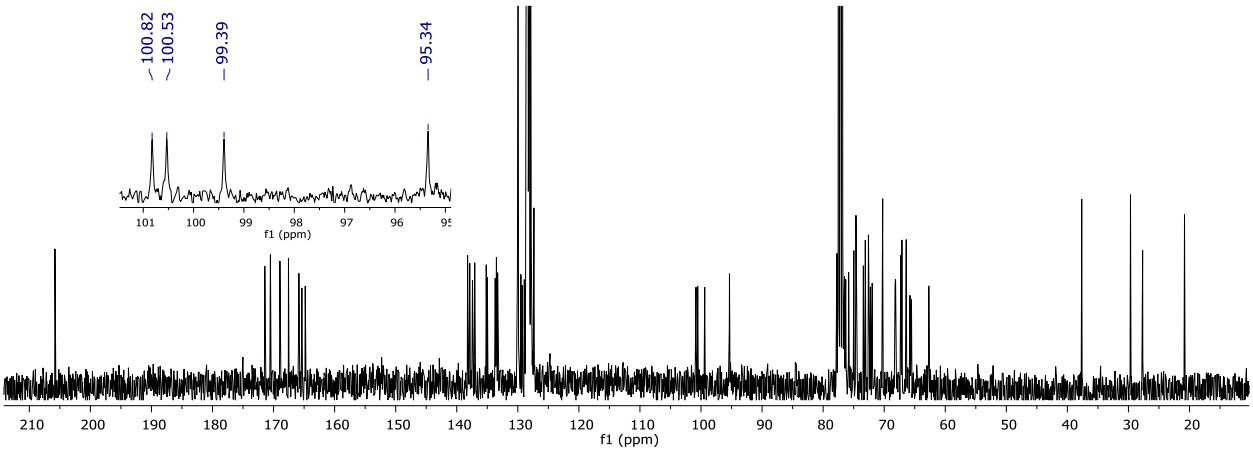
100.82
100.53
99.39
95.34
f1 (ppm)

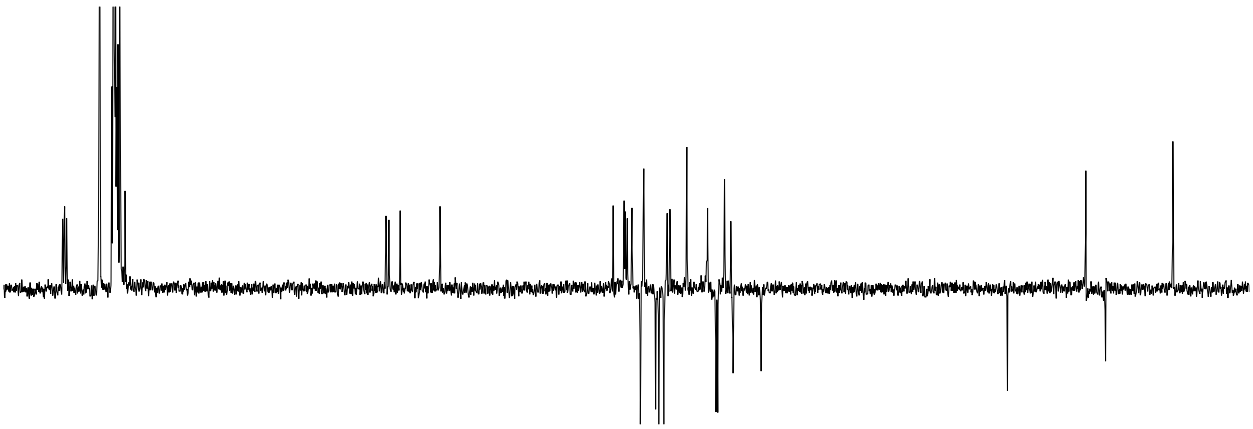

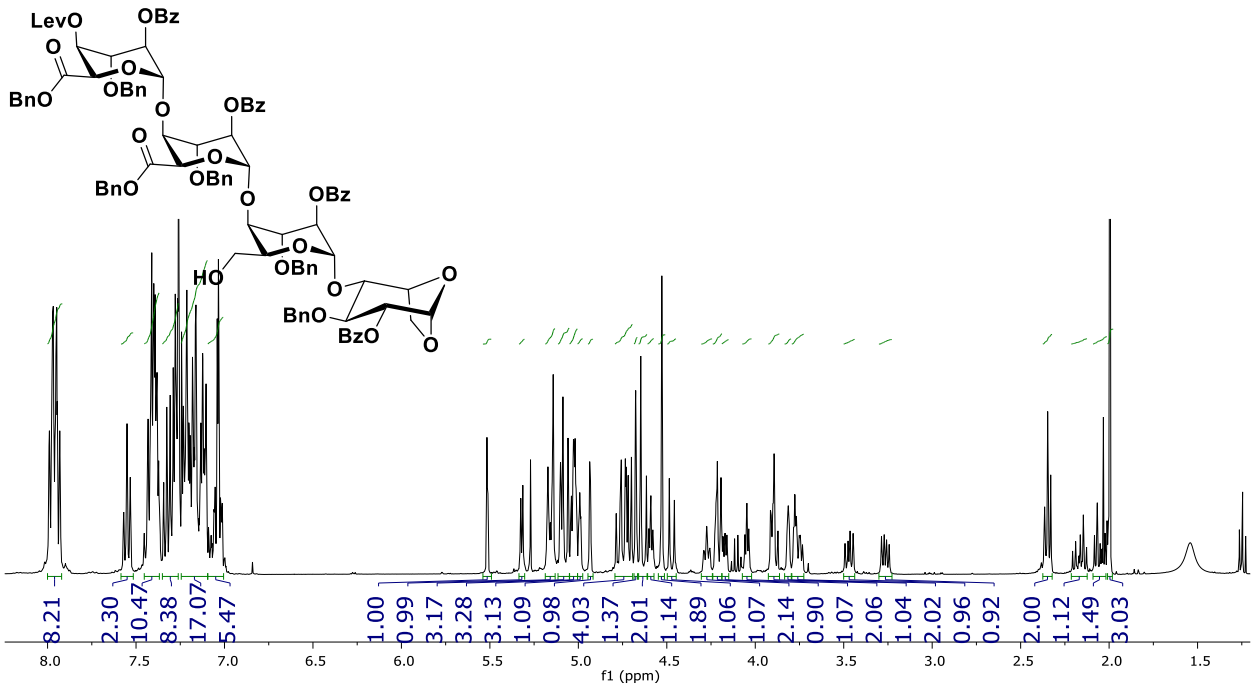
LevO
OBz
BnO
OBn
HO
BzO
8.21
2.30
10.47
8.38
17.07
5.47
1.00
0.99
3.17
3.28
3.13
1.09
0.98
4.03
1.37
2.01
1.14
1.89
1.06
1.07
2.14
0.90
1.07
2.06
1.04
2.02
0.96
0.92
2.00
1.12
1.49
3.03
f1 (ppm)

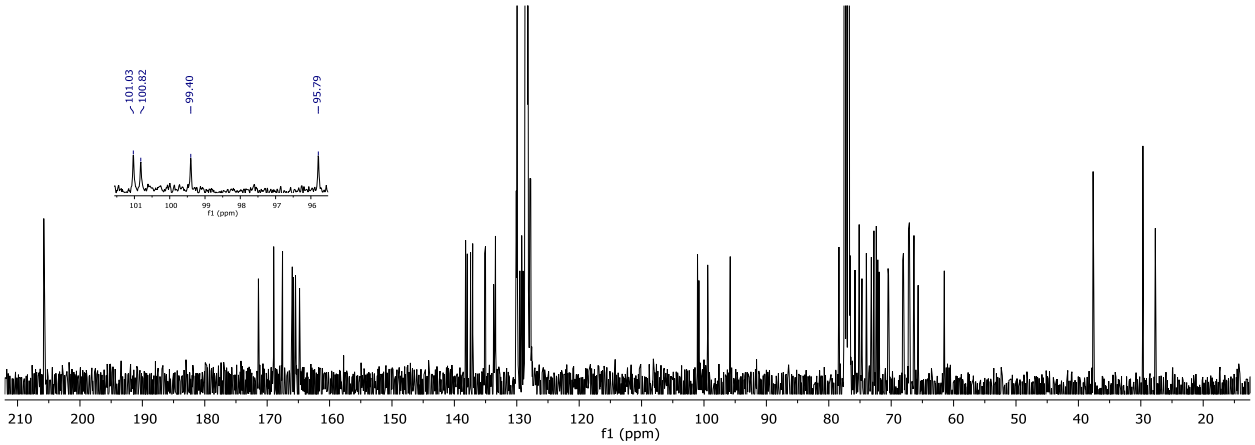
101.03
100.82
99.40
95.79
f1 (ppm)

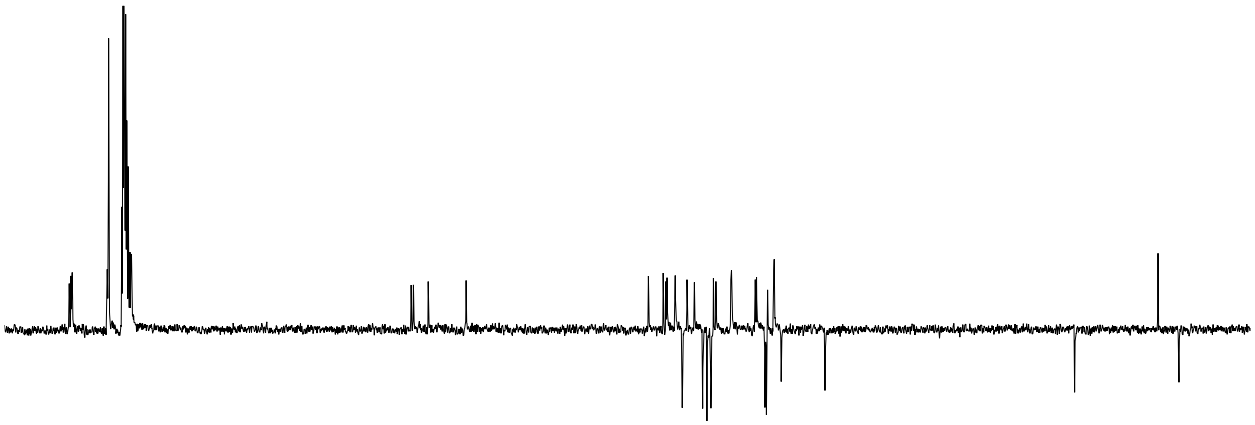

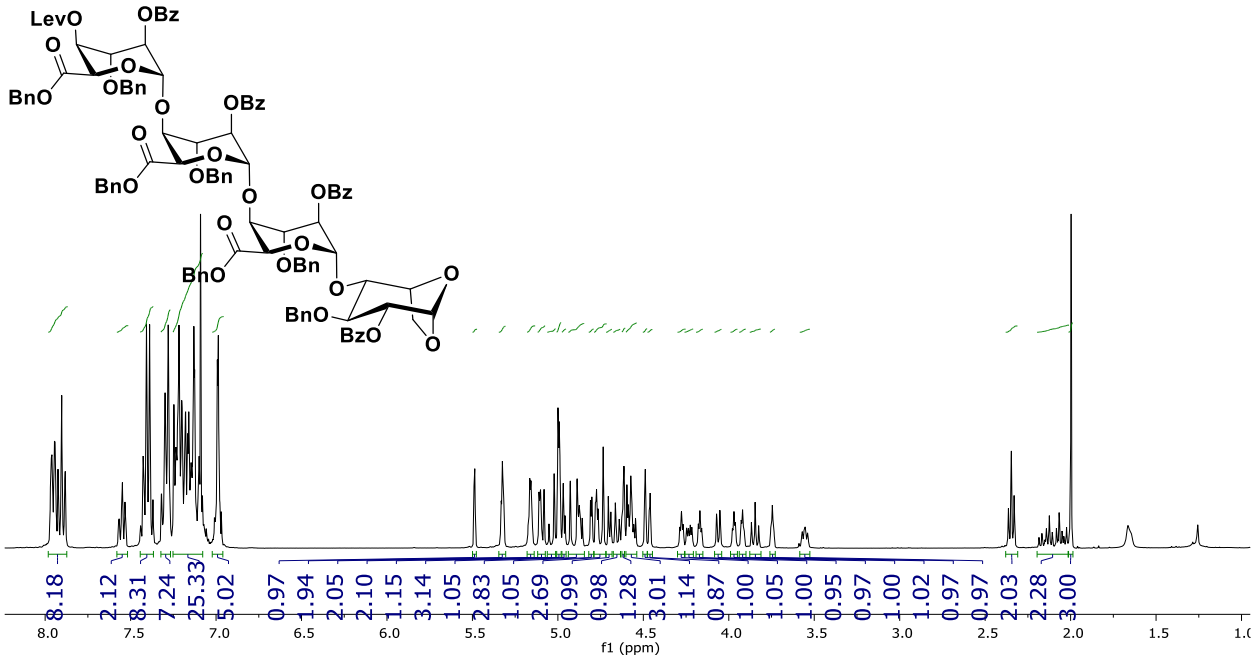
LevO
OBz
BnO
OBn
O
OBz
BnO
OBn
O
OBz
BnO
OBn
O
BnO
BzO
O
8.18
2.12
8.31
7.24
25.33
5.02
0.97
1.94
2.05
2.10
1.15
3.14
1.05
2.83
1.05
2.69
0.99
0.98
1.28
3.01
1.14
0.87
1.00
1.05
1.00
0.95
0.97
1.00
1.02
0.97
0.97
2.03
2.28
3.00
f1 (ppm)

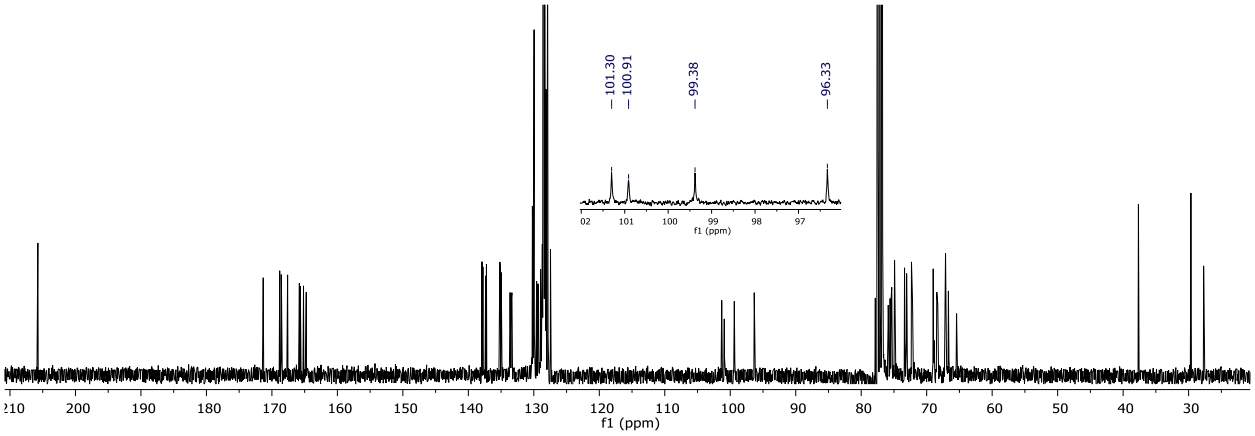
101.30
100.91
99.38
96.33
f1 (ppm)

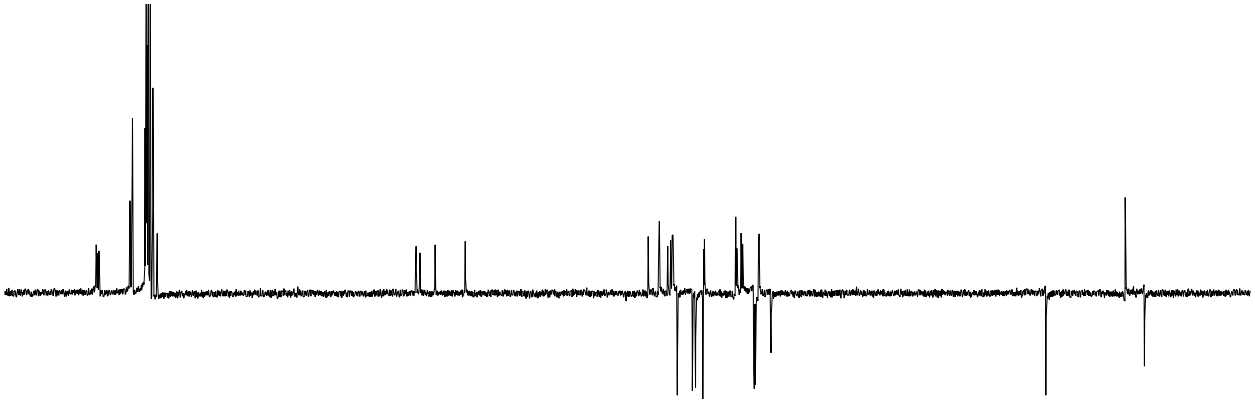

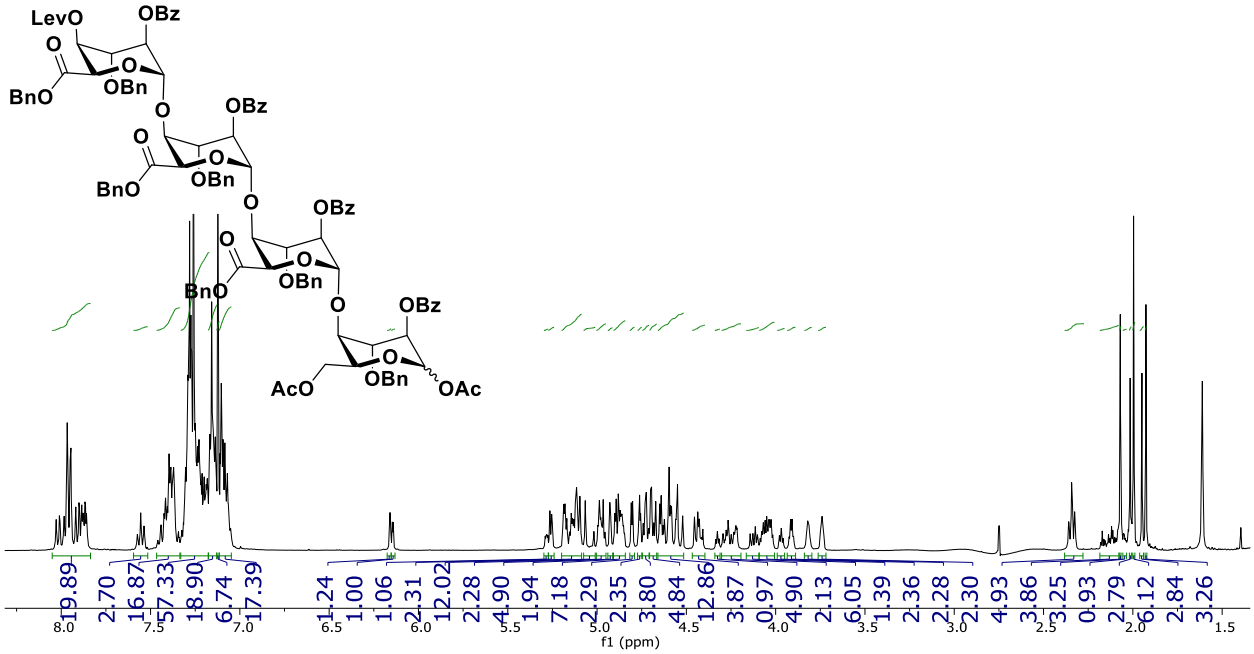
LevO
OBz
BnO
OBn
AcO
OAc
19.89
2.70
16.87
57.33
18.90
6.74
17.39
1.24
1.00
1.06
2.31
12.02
2.28
4.90
1.94
7.18
2.29
2.35
3.80
4.84
12.86
3.87
0.97
4.90
2.13
6.05
1.39
2.36
2.28
2.30
4.93
3.86
3.25
0.93
2.79
6.12
2.84
3.26
f1 (ppm)

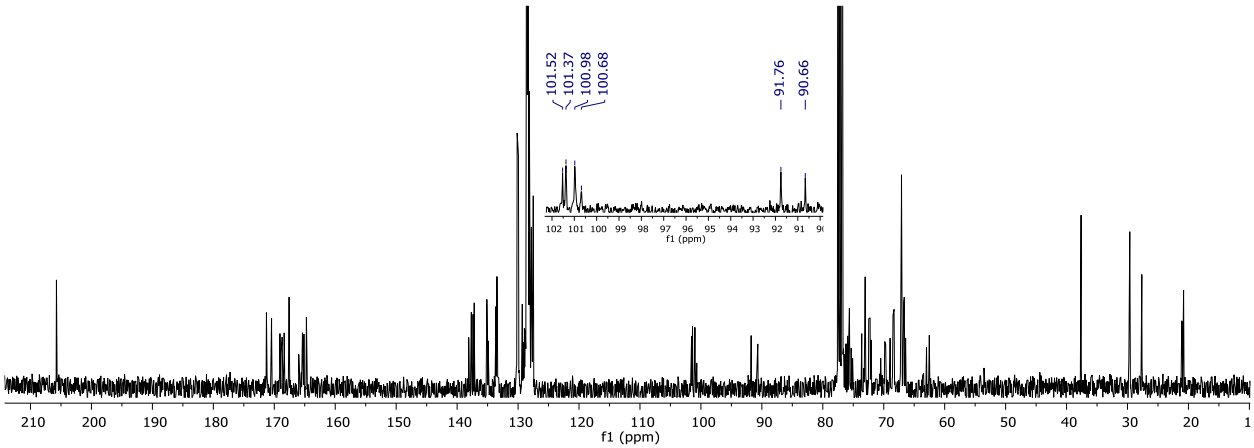
101.52
101.37
100.98
100.68
91.76
90.66
f1 (ppm)

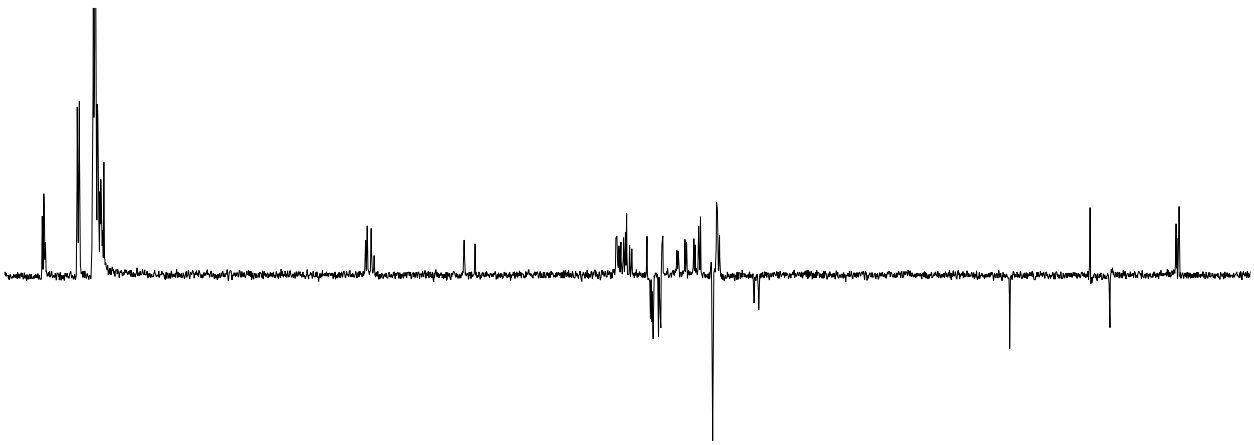

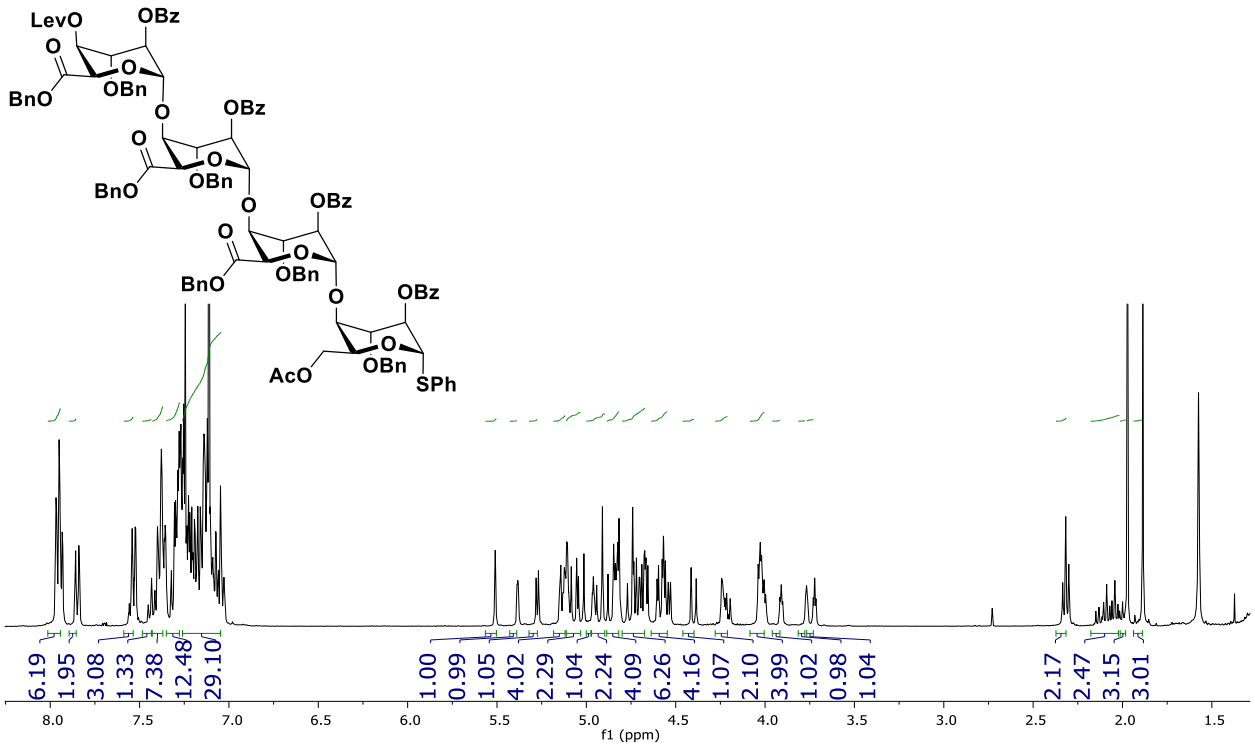
LevO
OBz
O
BnO
OBn
AcO
SPh
6.19
1.95
3.08
1.33
7.38
12.48
29.10
1.00
0.99
1.05
4.02
2.29
1.04
2.24
4.09
6.26
4.16
1.07
2.10
3.99
1.02
0.98
1.04
2.17
2.47
3.15
3.01
f1 (ppm)

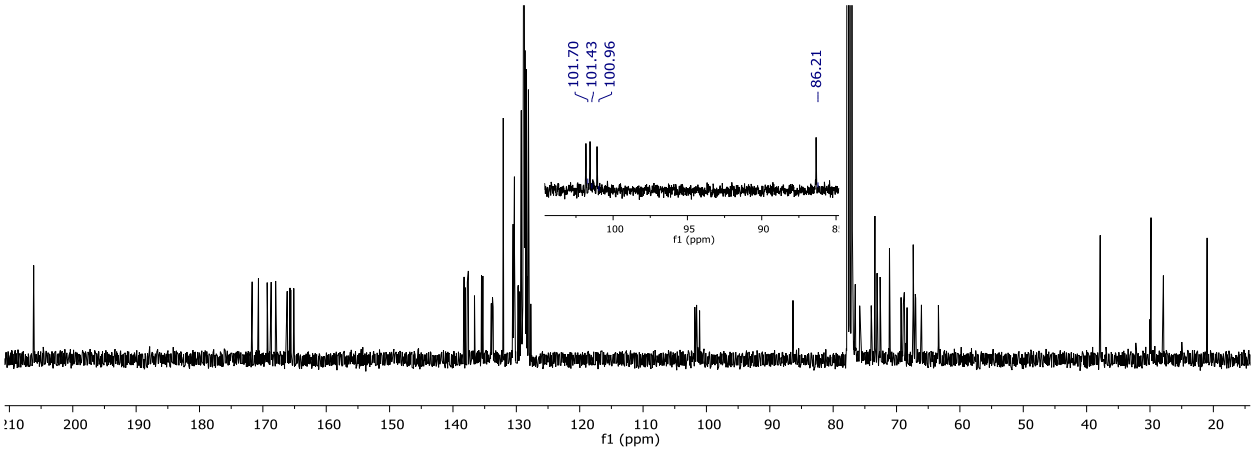
101.70
101.43
100.96
86.21
f1 (ppm)

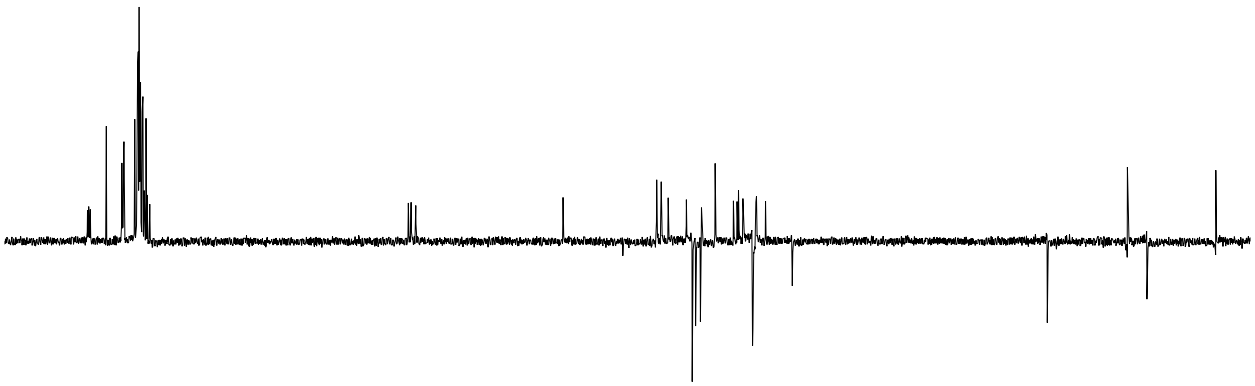

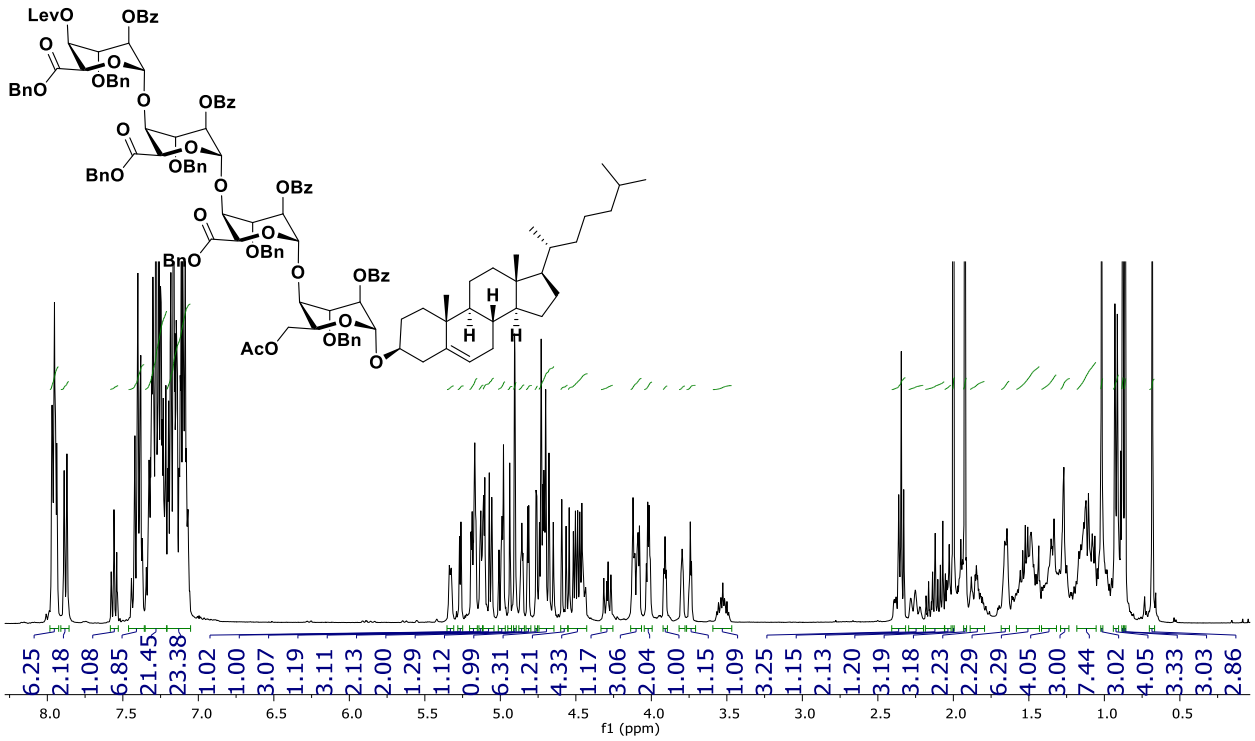
LevO
OBz
BnO
OBn
AcO
H
6.25 2.18 1.08 6.85 21.45 23.38 1.02 1.00 3.07 1.19 3.11 2.13 2.00 1.29 1.12 0.99 6.31 1.21 4.33 1.17 3.06 2.04 1.00 1.15 1.09 3.25 1.15 2.13 1.20 3.19 3.18 2.23 2.29 6.29 4.05 3.00 7.44 3.02 4.05 3.33 3.03 2.86
8.0 7.5 7.0 6.5 6.0 5.5 5.0 4.5 4.0 3.5 3.0 2.5 2.0 1.5 1.0 0.5
f1 (ppm)

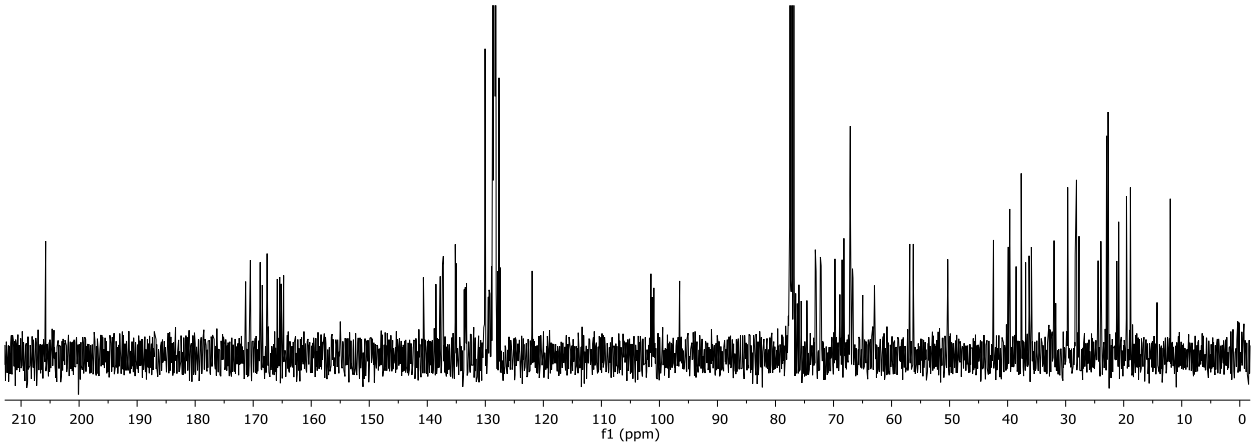
210 200 190 180 170 160 150 140 130 120 110 100 90 80 70 60 50 40 30 20 10 0
f1 (ppm)

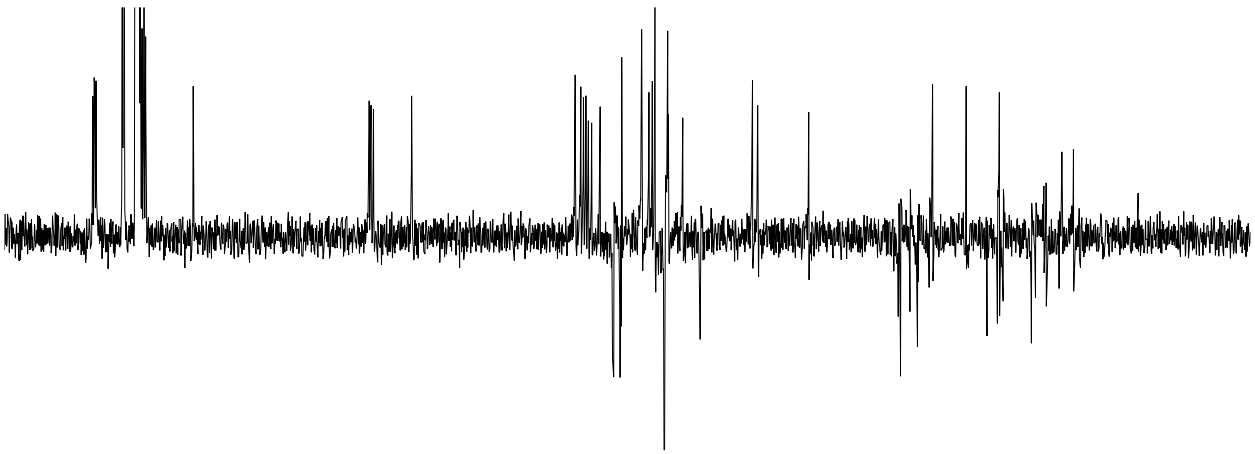

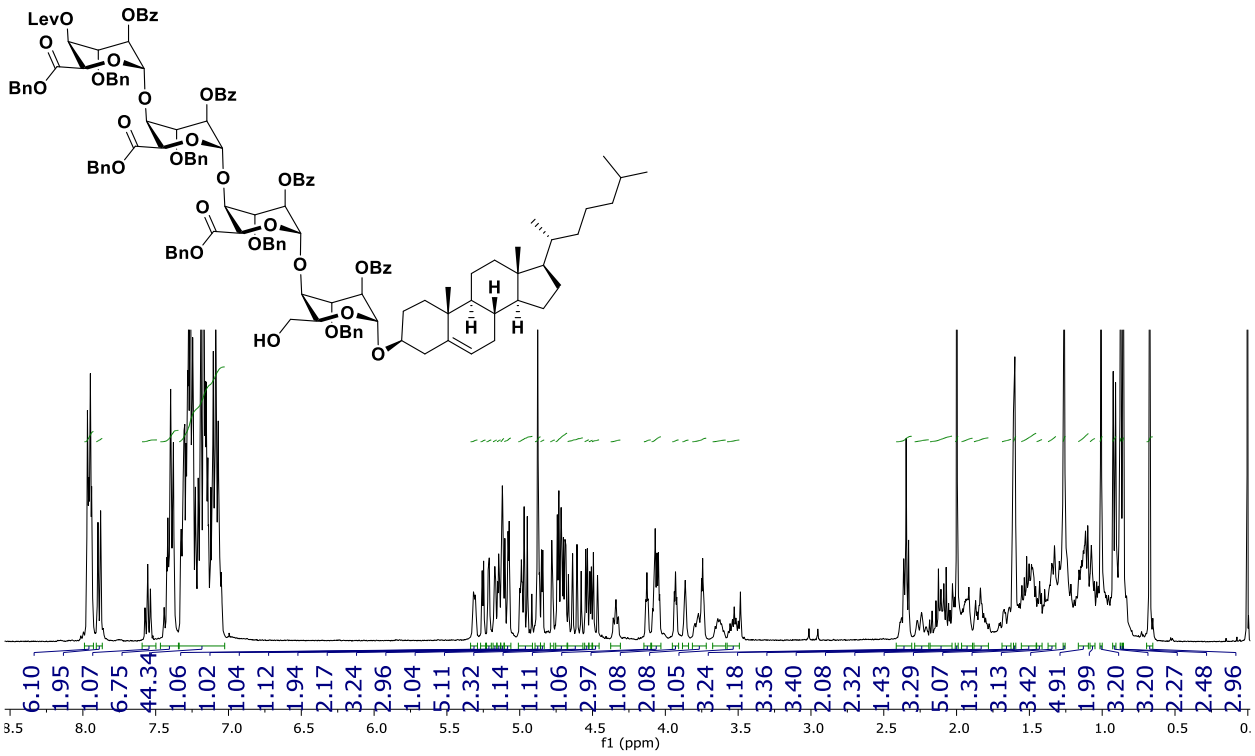
LevO
OBz
BnO
OBn
HO
H
6.10 1.95 1.07 6.75 44.34 1.06 1.02 1.04 1.12 1.94 2.17 3.24 2.96 1.04 5.11 2.32 1.14 1.11 1.06 2.97 1.08 2.08 1.05 3.24 1.18 3.36 3.40 2.08 2.32 1.43 3.29 5.07 1.31 3.13 3.42 4.91 1.99 3.20 3.20 2.27 2.48 2.96
f1 (ppm)

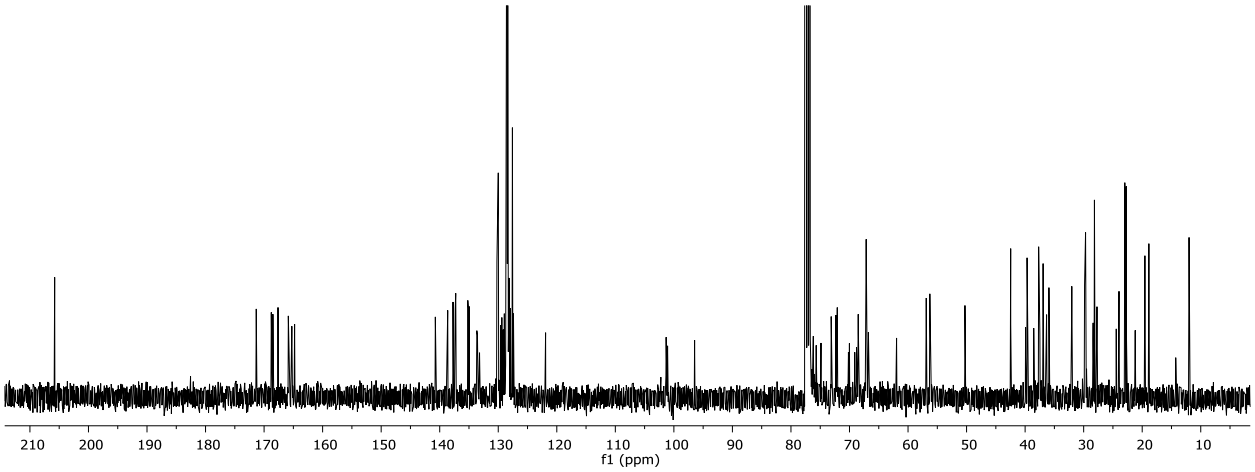
f1 (ppm)

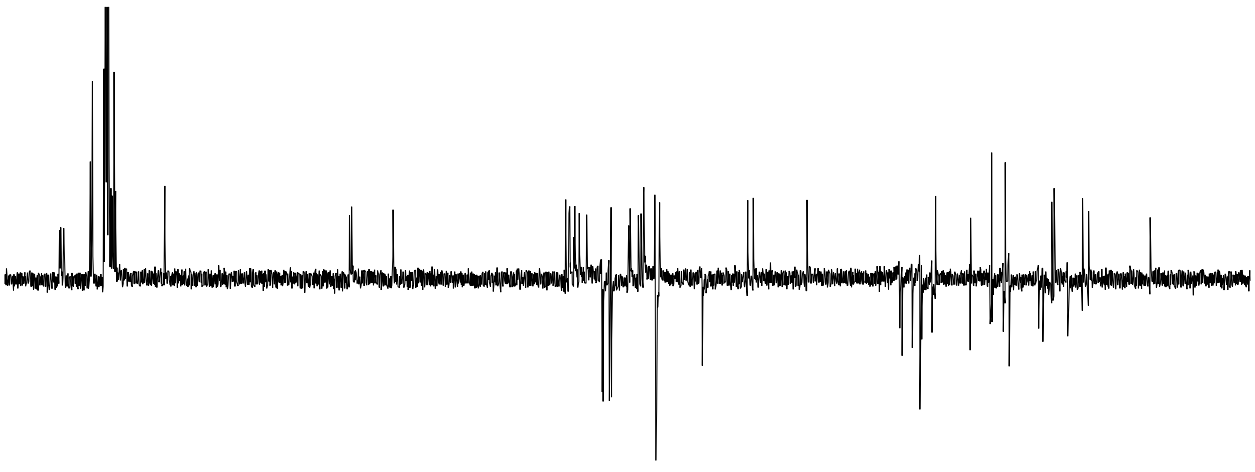

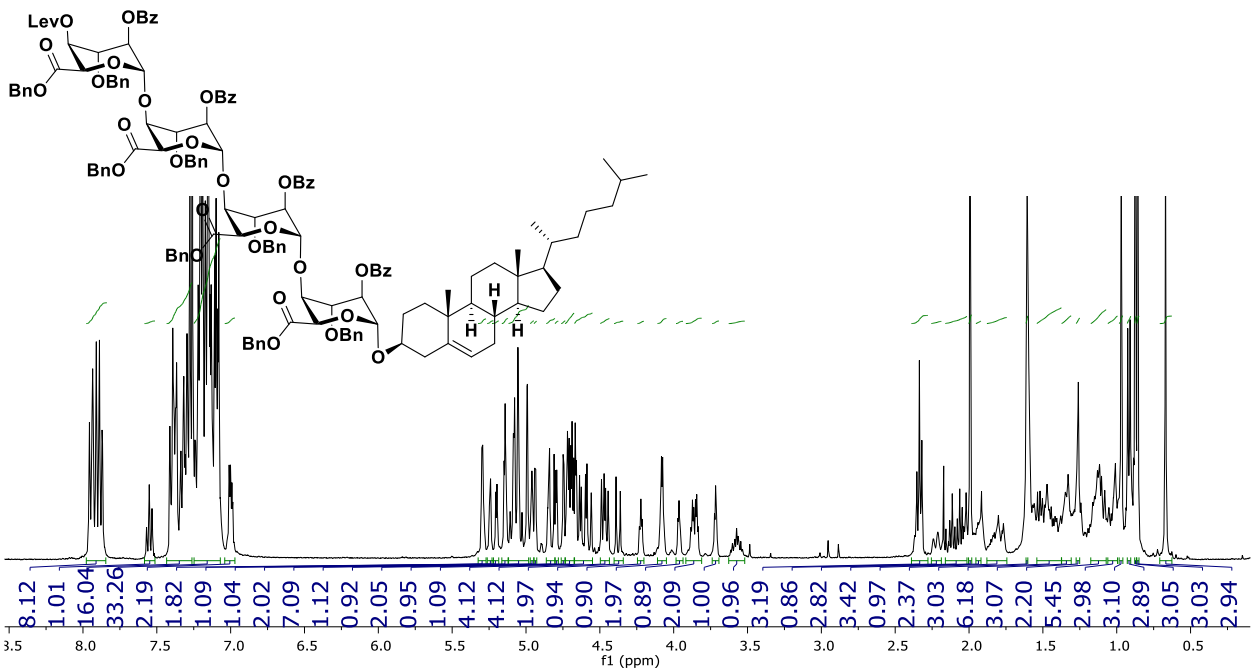
LevO
OBz
BnO
OBn
O
H
8.12 1.01 16.04 33.26 2.19 1.82 1.09 1.04 2.02 7.09 1.12 0.92 2.05 0.95 1.09 4.12 4.12 1.97 0.94 0.90 1.97 0.89 2.09 1.00 0.96 3.19 0.86 2.82 3.42 0.97 2.37 3.03 6.18 3.07 2.20 5.45 2.98 3.10 2.89 3.05 3.03 2.94
f1 (ppm)

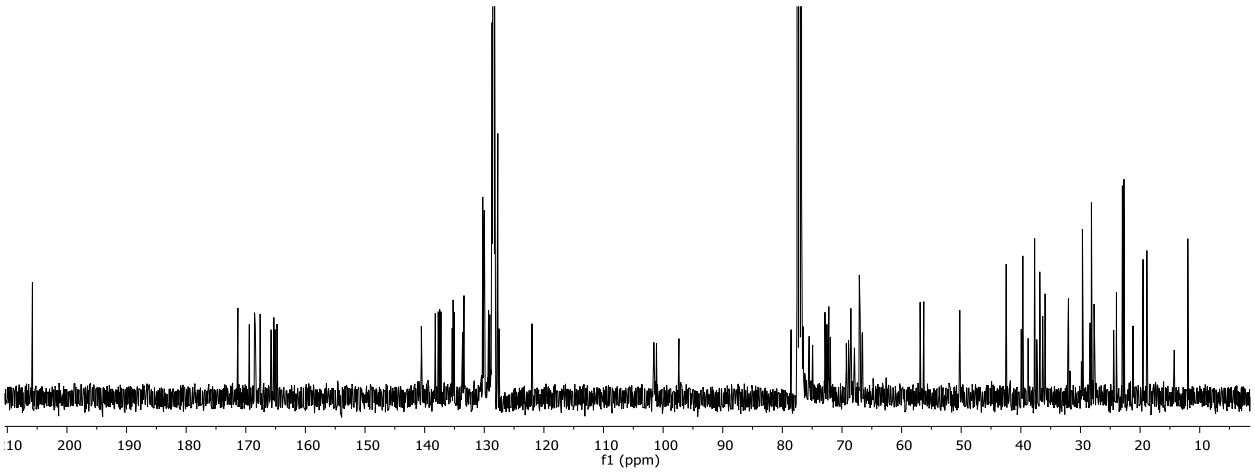
f1 (ppm)

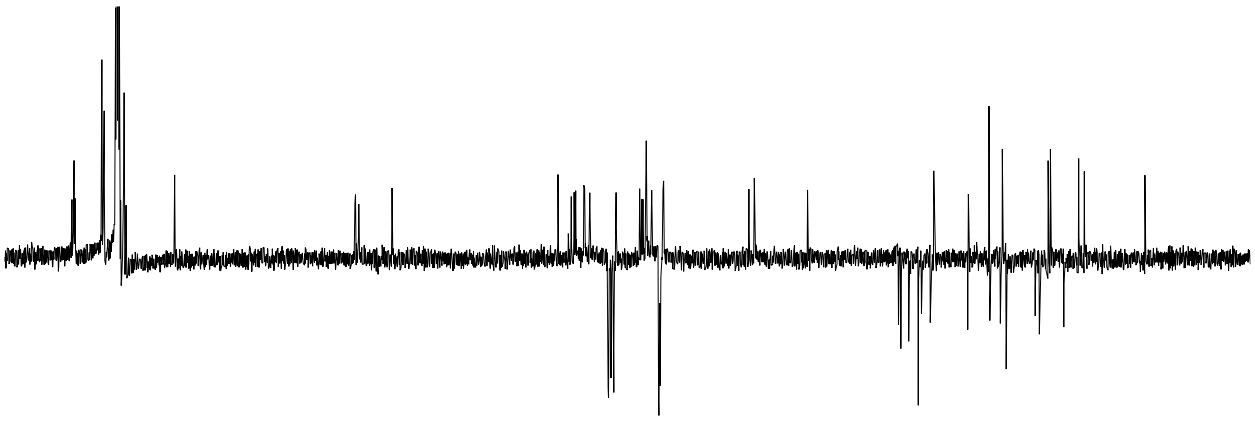

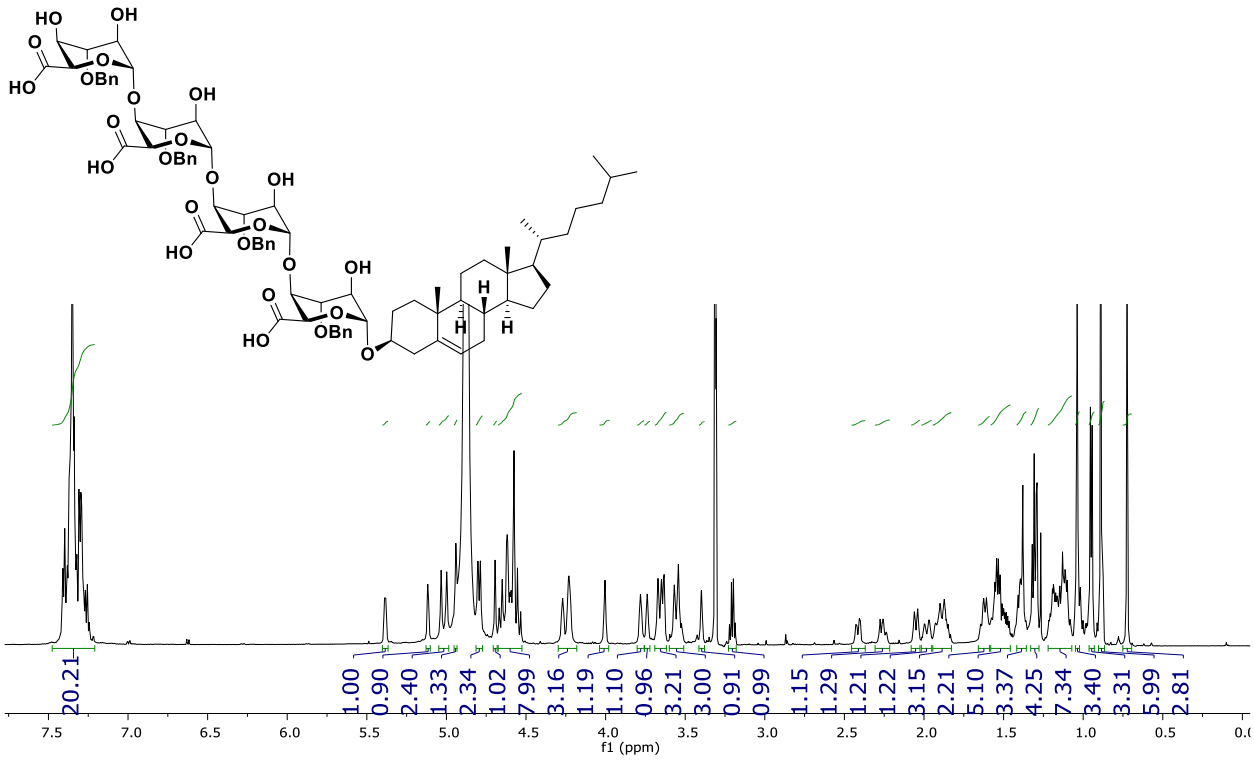
HO
OH
O
OBn
HO
H
20.21
1.00
0.90
2.40
1.33
2.34
1.02
7.99
3.16
1.19
1.10
0.96
3.21
3.00
0.91
0.99
1.15
1.29
1.21
1.22
3.15
2.21
5.10
3.37
4.25
7.34
3.40
3.31
5.99
2.81
f1 (ppm)

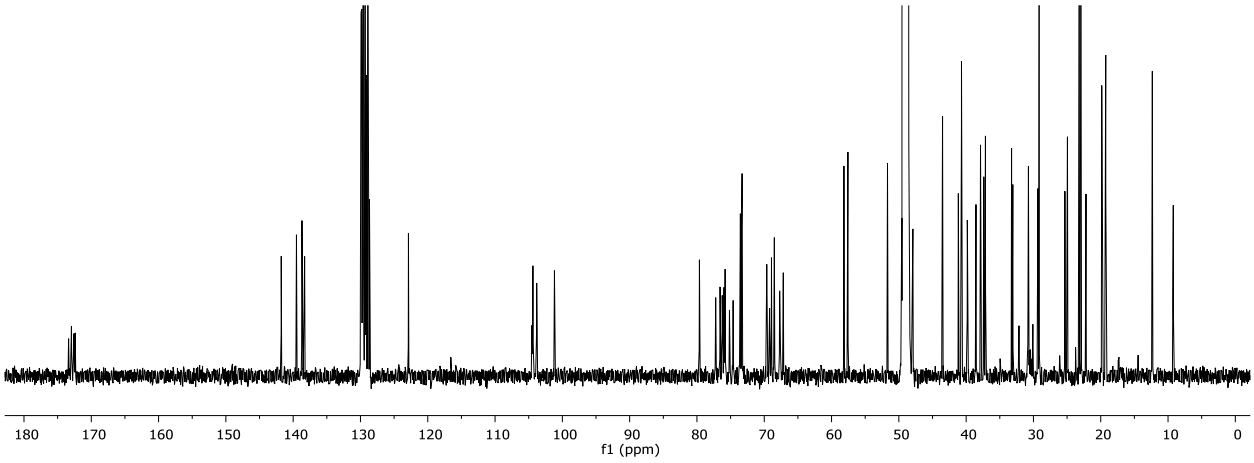
f1 (ppm)

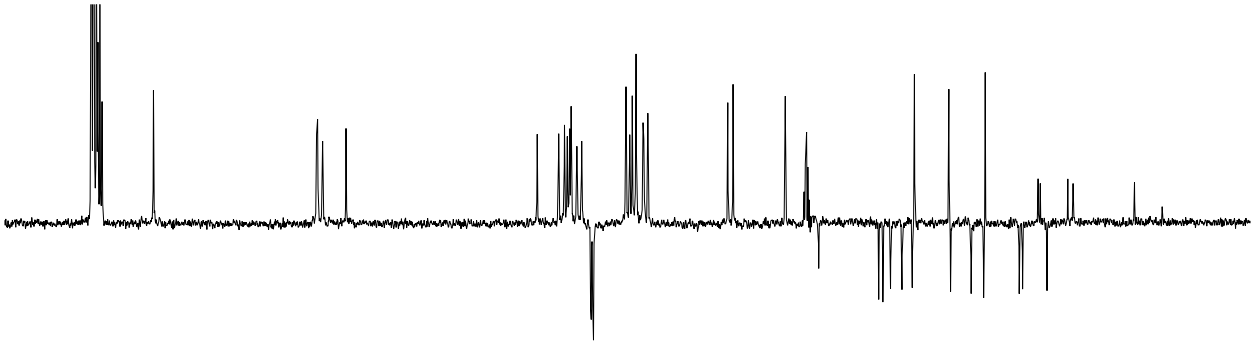

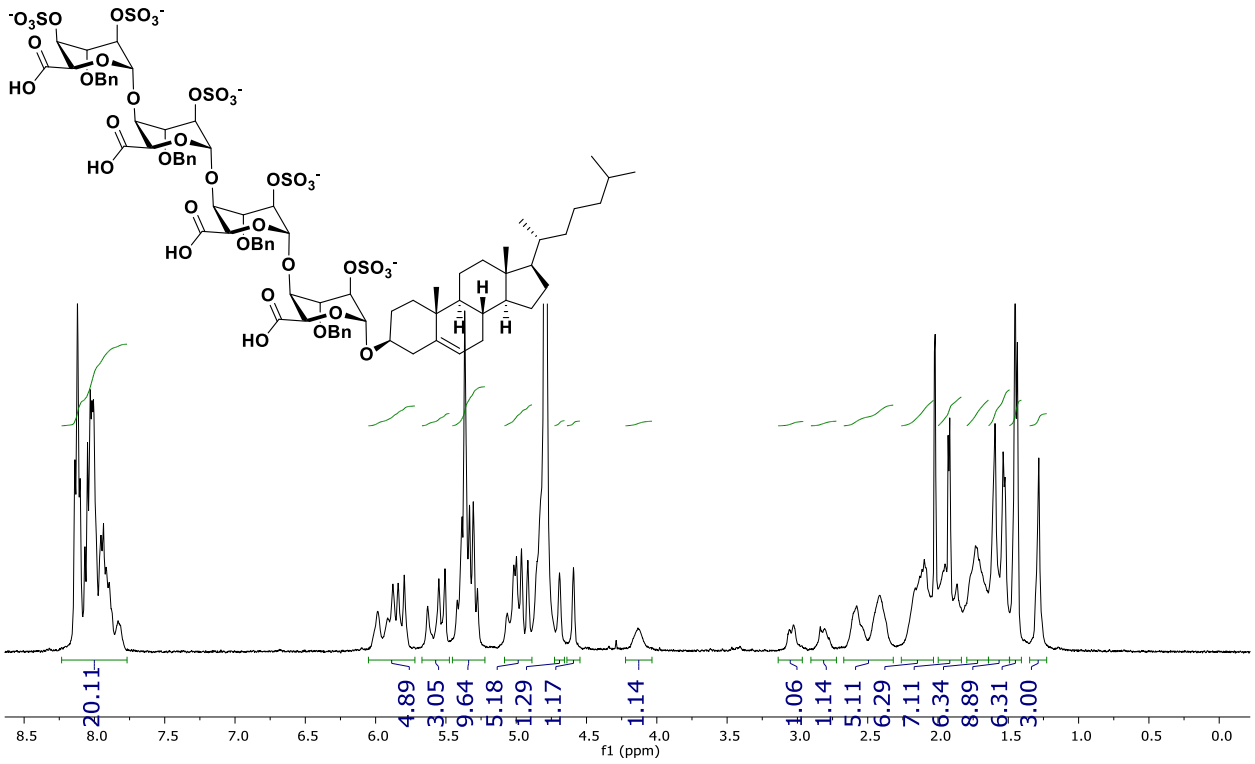
20.11
4.89
3.05
9.64
5.18
1.29
1.17
1.14
1.06
1.14
5.11
6.29
7.11
6.34
8.89
6.31
3.00
f1 (ppm)

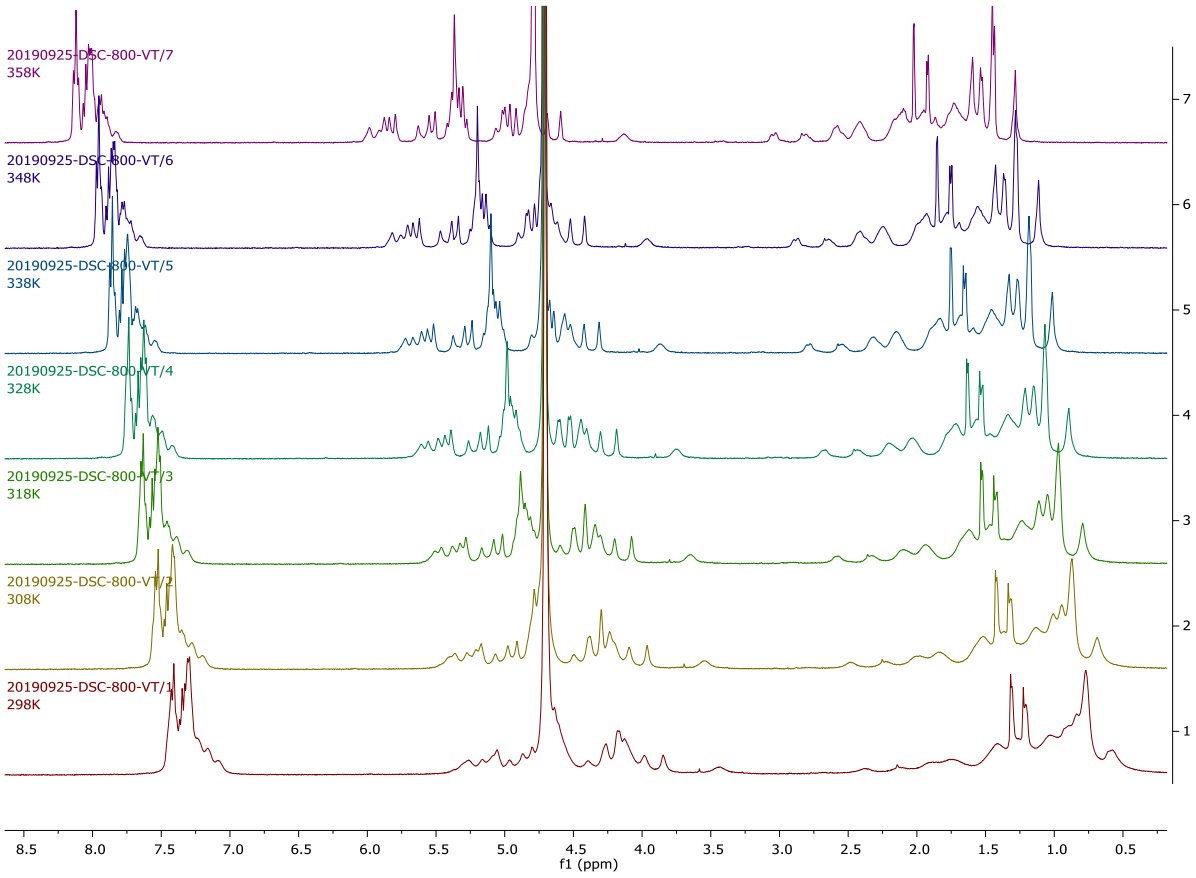
20190925-DSC-800-VT/7
358K
20190925-DSC-800-VT/6
348K
20190925-DSC-800-VT/5
338K
20190925-DSC-800-VT/4
328K
20190925-DSC-800-VT/3
318K
20190925-DSC-800-VT/2
308K
20190925-DSC-800-VT/1
298K
f1 (ppm)

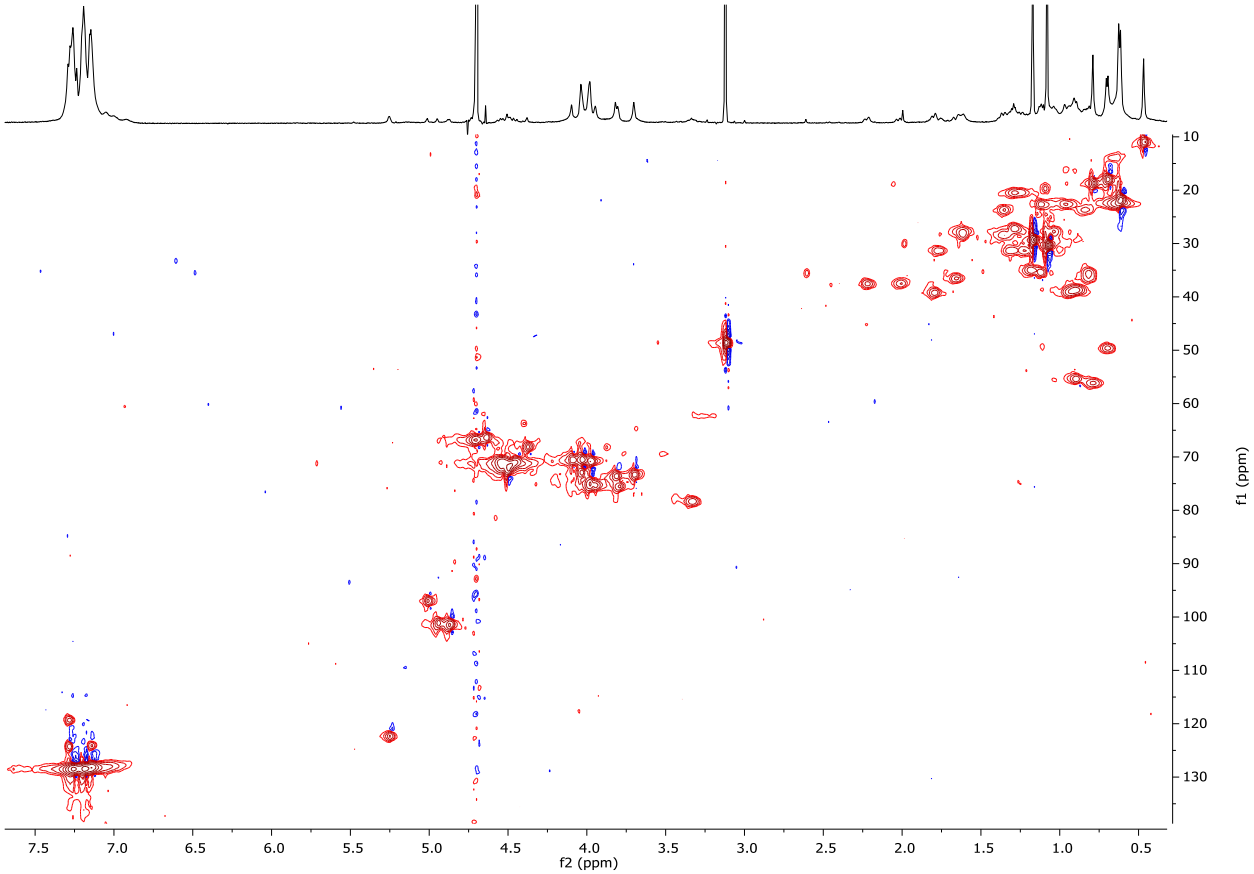
10
20
30
40
50
60
70
80
90
100
110
120
130
f1 (ppm)
7.5
7.0
6.5
6.0
5.5
5.0
4.5
4.0
3.5
3.0
2.5
2.0
1.5
1.0
0.5
f2 (ppm)

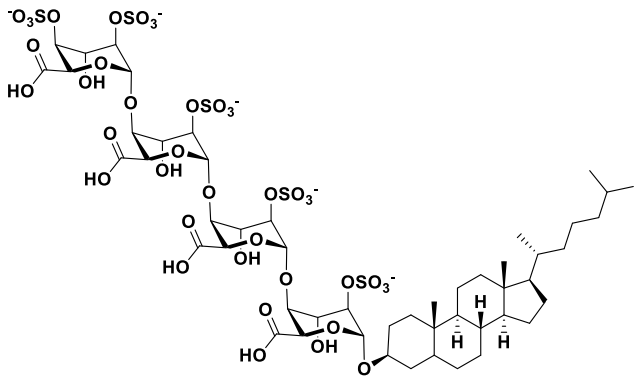
$^{-}O_3SO$
OSO_3^-
HO
OH
O
H
H
H

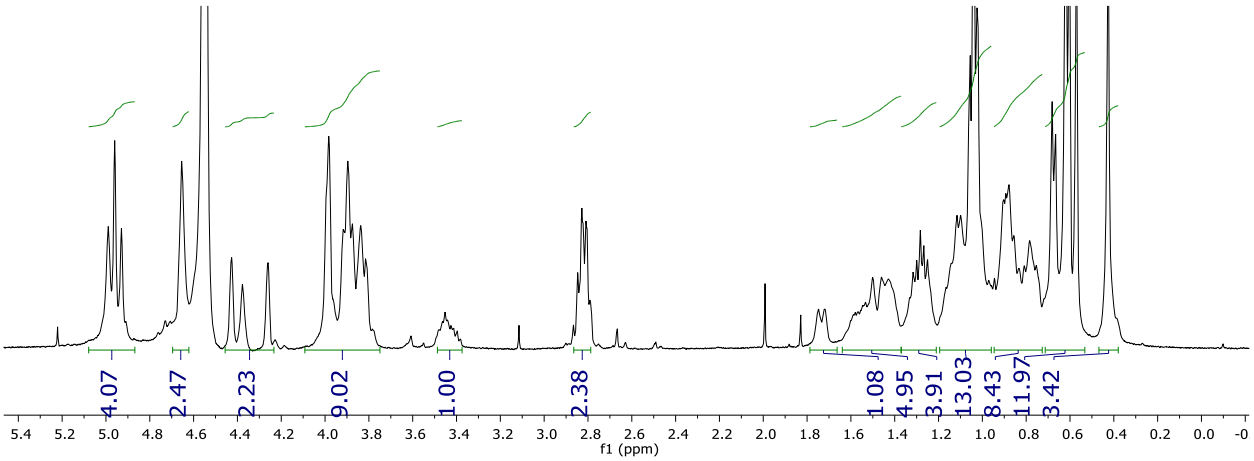
4.07
2.47
2.23
9.02
1.00
2.38
1.08
4.95
3.91
13.03
8.43
11.97
3.42
f1 (ppm)

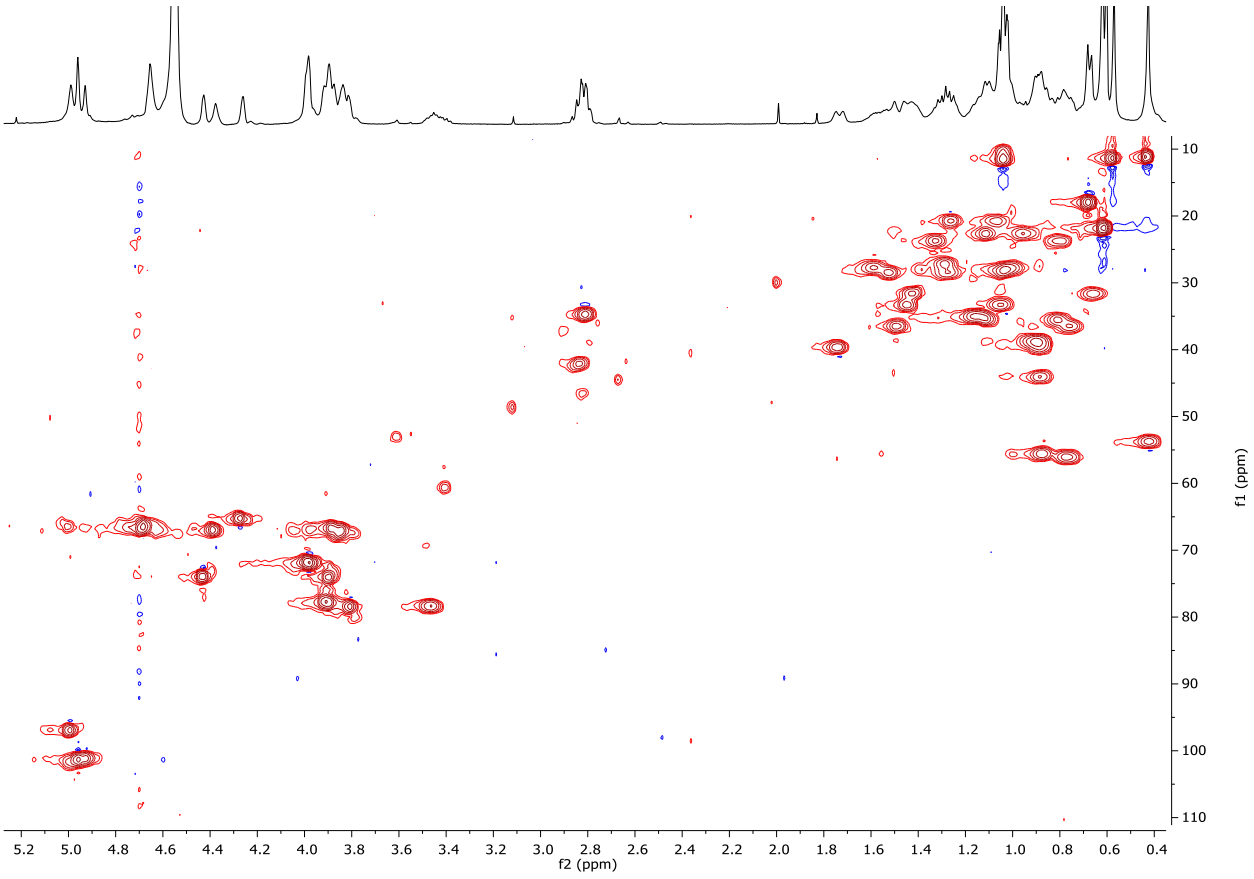
f2 (ppm)
f1 (ppm)